



CHARLES PANKOW
FOUNDATION

Building Innovation through Research

Reinforced Concrete Coupling Beams with High-Strength Steel Bars

Alexander S. Weber-Kamin

Shahedreen Ameen

Rémy D. Lequesne

Andrés Lepage

Department of Civil, Environmental & Architectural Engineering

The University of Kansas

Lawrence, Kansas, USA



December 2019

**Reinforced Concrete Coupling Beams
With High-Strength Steel Bars**

CPF Research Grant Agreement #03-17
CHARLES PANKOW FOUNDATION
1390 Chain Bridge Road, Suite 700
McLean, Virginia 22101

Principal Investigators: Dr. Andrés Lepage
Dr. Rémy D. Lequesne

Graduate Research Assistants: Alexander S. Weber-Kamin
Shahedreen Ameen

Industry Support:
Industry Champions: David Fields, MKA
Ramón Gilsanz, GMS
Advisory Panel: Dominic Kelly, SGH
Conrad Paulson, WJE

ABSTRACT

The use of high-strength steel bars in reinforced concrete coupling beams is expected to reduce reinforcement congestion. A series of tests was conducted to investigate the effects of high-strength reinforcement on coupling beam behavior. This document summarizes the test program and test data.

Eleven large-scale coupling beam specimens were tested under fully reversed cyclic displacements of increasing magnitude. The main variables of the test program included: yield stress of the primary longitudinal reinforcement (Grade 80, 100, and 120 [550, 690, and 830]), span-to-depth (aspect) ratio (1.5, 2.5, and 3.5), and layout of the primary longitudinal reinforcement (diagonal [D] and parallel [P]). All beams had the same nominal concrete compressive strength (8,000 psi [55 MPa]) and cross-sectional dimensions (12 by 18 in. [310 by 460 mm]). Beams were designed for target shear stresses of $8\sqrt{f'_c}$ psi ($0.67\sqrt{f'_c}$ MPa) for D-type beams and $6\sqrt{f'_c}$ psi ($0.5\sqrt{f'_c}$ MPa) for P-type beams. Transverse reinforcement was Grade 80 (550) in all but one beam, which had Grade 120 (830) reinforcement.

The test program is documented by presenting the details of specimen construction, test setup, instrumentation, and loading protocol. Documentation of test data includes material properties, cyclic force-deformation response, progression of damage, calculated and measured strengths, initial stiffness, and measured reinforcement strains.

ACKNOWLEDGMENTS

Primary financial support for the experimental program was provided by the Charles Pankow Foundation, the Concrete Reinforcing Steel Institute, and the ACI Foundation's Concrete Research Council. Additional support was provided by Commercial Metals Company, MMFX Technologies Corporation, Harris Rebar, Midwest Concrete Materials, Nucor Corporation, and The University of Kansas through the Department of Civil, Environmental and Architectural Engineering and the School of Engineering.

Grateful acknowledgment is made to the Industry Champions, David Fields (principal at MKA, Seattle) and Ramón Gilsanz (partner at GMS, New York) and the Advisory Panel, Dominic Kelly (principal at SGH, Boston) and Conrad Paulson (principal at WJE, Los Angeles), for their ideas and constructive criticism.

Appreciation is due to the multitude of dedicated students and technicians who were involved in the construction, instrumentation, and testing of specimens.

TABLE OF CONTENTS

ABSTRACT.....	i
ACKNOWLEDGMENTS	ii
LIST OF TABLES	v
LIST OF FIGURES	vi
CHAPTER 1: INTRODUCTION.....	1
1.1 Background and Motivation	1
1.2 Research Objectives	2
CHAPTER 2: EXPERIMENTAL PROGRAM.....	4
2.1 Specimens.....	4
2.1.1 Design and Detailing.....	4
2.1.2 Materials.....	9
2.1.3 Construction	10
2.2 Test Setup	10
2.3 Instrumentation.....	11
2.3.1 Linear Variable Differential Transformers (LVDTs)	11
2.3.2 Infrared Non-Contact Position Measurement System.....	11
2.3.3 Strain Gauges	12
2.4 Loading Protocol	12
CHAPTER 3: EXPERIMENTAL RESULTS.....	14
3.1 Measured Shear versus Chord Rotation	14
3.2 Specimen Response and Observations	15
3.2.1 D80-1.5	16
3.2.2 D100-1.5	17
3.2.3 D120-1.5	17
3.2.4 D80-2.5	18
3.2.5 D100-2.5	18
3.2.6 D120-2.5	18
3.2.7 D80-3.5	19
3.2.8 D100-3.5	19
3.2.9 D120-3.5	20

3.2.10 P80-2.5	20
3.2.11 P100-2.5	21
3.3 ASCE 41 Envelopes	21
3.4 Progression of Damage.....	23
3.5 Calculated and Measured Strengths of Specimens.....	26
3.6 Stiffness	27
3.7 Measured Reinforcement Strains	30
3.7.1 Diagonal Reinforcement	32
3.7.2 Parallel Primary Reinforcement.....	33
3.7.3 Parallel Secondary Reinforcement.....	34
3.7.4 Transverse Reinforcement	34
CHAPTER 4: CONCLUDING REMARKS	36
REFERENCES.....	39
TABLES.....	41
FIGURES.....	56
APPENDIX A: NOTATION.....	A-1
APPENDIX B: SELECTED PHOTOS OF SPECIMENS DURING CONSTRUCTION.....	B-1
APPENDIX C: SELECTED PHOTOS OF SPECIMENS DURING TESTING.....	C-1

LIST OF TABLES

Table 1 – Design data for coupling beam specimens	42
Table 2 – Measured compressive and tensile strengths of concrete	43
Table 3 – Concrete mixture proportions	44
Table 4 – Reinforcing steel properties	45
Table 5 – Specimen and actuator nominal elevations relative to strong floor.....	45
Table 6 – List of strain gauges on primary and secondary longitudinal reinforcement	46
Table 7 – List of strain gauges on transverse reinforcement	47
Table 8 – Loading protocol.....	48
Table 9 – Coupling beam maximum shear stress and deformation capacity.....	49
Table 10 – Force-deformation envelope for D-type coupling beams with aspect ratio of 1.5	50
Table 11 – Force-deformation envelope for D-type coupling beams with aspect ratio of 2.5	51
Table 12 – Force-deformation envelope for D-type coupling beams with aspect ratio of 3.5	52
Table 13 – Force-deformation envelope for P-type coupling beams with aspect ratio of 2.5.....	53
Table 14 – Coupling beam measured and calculated strengths	54
Table 15 – Summary of test data	55

LIST OF FIGURES

Figure 1 – Reinforcement layout types, parallel (P) and diagonal (D).....	57
Figure 2 – Elevation view of D80-1.5	58
Figure 3 – Reinforcement details of D80-1.5	59
Figure 4 – Elevation view of D100-1.5	60
Figure 5 – Reinforcement details of D100-1.5	61
Figure 6 – Elevation view of D120-1.5	62
Figure 7 – Reinforcement details of D120-1.5	63
Figure 8 – Elevation view of D80-2.5	64
Figure 9 – Reinforcement details of D80-2.5	65
Figure 10 – Elevation view of D100-2.5	66
Figure 11 – Reinforcement details of D100-2.5	67
Figure 12 – Elevation view of D120-2.5	68
Figure 13 – Reinforcement details of D120-2.5	69
Figure 14 – Elevation view of D80-3.5	70
Figure 15 – Reinforcement details of D80-3.5	71
Figure 16 – Elevation view of D100-3.5	72
Figure 17 – Reinforcement details of D100-3.5	73
Figure 18 – Elevation view of D120-3.5	74
Figure 19 – Reinforcement details of D120-3.5	75
Figure 20 – Elevation view of P80-2.5	76
Figure 21 – Reinforcement details of P80-2.5	77
Figure 22 – Elevation view of P100-2.5	78
Figure 23 – Reinforcement details of P100-2.5	79
Figure 24 – Measured stress versus strain for reinforcement	80
Figure 25 – Test setup, view from northeast.....	81
Figure 26 – Test setup, view from northwest	81
Figure 27 – Test setup, plan view	82
Figure 28 – Test setup for coupling beams with aspect ratio of 1.5	83
Figure 29 – Test setup for coupling beams with aspect ratio of 2.5	83
Figure 30 – Test setup for coupling beams with aspect ratio of 3.5	84

Figure 31 – LVDT locations	85
Figure 32 – Infrared marker positions	85
Figure 33 – Strain gauge layout (view from north), D-type specimens.....	86
Figure 34 – Strain gauge layout (view from north), P-type specimens	87
Figure 35 – Loading protocol	88
Figure 36 – General deformed shape of specimen, view from north.....	88
Figure 37 – Shear versus chord rotation for D80-1.5	89
Figure 38 – Shear versus chord rotation for D100-1.5	89
Figure 39 – Shear versus chord rotation for D120-1.5	90
Figure 40 – Shear versus chord rotation for D80-2.5	90
Figure 41 – Shear versus chord rotation for D100-2.5	91
Figure 42 – Shear versus chord rotation for D120-2.5	91
Figure 43 – Shear versus chord rotation for D80-3.5	92
Figure 44 – Shear versus chord rotation for D100-3.5	92
Figure 45 – Shear versus chord rotation for D120-3.5	93
Figure 46 – Shear versus chord rotation for P80-2.5	94
Figure 47 – Shear versus chord rotation for P100-2.5.....	94
Figure 48 – Shear versus chord rotation envelope for D80-1.5.....	95
Figure 49 – Shear versus chord rotation envelope for D100-1.5.....	95
Figure 50 – Shear versus chord rotation envelope for D120-1.5.....	96
Figure 51 – Shear versus chord rotation envelope for D80-2.5.....	96
Figure 52 – Shear versus chord rotation envelope for D100-2.5.....	97
Figure 53 – Shear versus chord rotation envelope for D120-2.5.....	97
Figure 54 – Shear versus chord rotation envelope for D80-3.5.....	98
Figure 55 – Shear versus chord rotation envelope for D100-3.5.....	98
Figure 56 – Shear versus chord rotation envelope for D120-3.5.....	99
Figure 57 – Shear versus chord rotation envelope for P80-2.5.....	100
Figure 58 – Shear versus chord rotation envelope for P100-2.5.....	100
Figure 59 – Chord rotation capacity versus primary reinforcement grade for D-type coupling beams	101
Figure 60 – Shear versus chord rotation envelopes for D80-1.5, D100-1.5, and D120-1.5	102

Figure 61 – Shear versus chord rotation envelopes for D80-2.5, D100-2.5, and D120-2.5	102
Figure 62 – Shear versus chord rotation envelopes for D80-3.5, D100-3.5, and D120-3.5	103
Figure 63 – Shear versus chord rotation envelopes for P80-2.5 and P100-2.5.....	104
Figure 64 – Normalized shear versus chord rotation envelopes for P80-2.5 and P100-2.5	104
Figure 65 – Generalized force-deformation relationship for diagonally-reinforced concrete coupling beams	105
Figure 66 – Reinforcing bar fracture locations, D80-1.5.....	106
Figure 67 – Reinforcing bar fracture locations, D100-1.5.....	106
Figure 68 – Reinforcing bar fracture locations, D120-1.5.....	107
Figure 69 – Reinforcing bar fracture locations, D80-2.5.....	107
Figure 70 – Reinforcing bar fracture locations, D100-2.5.....	108
Figure 71 – Reinforcing bar fracture locations, D120-2.5.....	108
Figure 72 – Reinforcing bar fracture locations, D80-3.5.....	109
Figure 73 – Reinforcing bar fracture locations, D100-3.5.....	109
Figure 74 – Reinforcing bar fracture locations, D120-3.5.....	110
Figure 75 – Reinforcing bar fracture locations, P80-2.5	111
Figure 76 – Reinforcing bar fracture locations, P100-2.5	111
Figure 77 – Shear versus chord rotation envelopes for D80-1.5, D100-1.5, and D120-1.5	112
Figure 78 – Shear versus chord rotation envelopes for D80-2.5, D100-2.5, and D120-2.5	112
Figure 79 – Shear versus chord rotation envelopes for D80-3.5, D100-3.5, and D120-3.5	113
Figure 80 – Shear versus chord rotation envelopes for P80-2.5 and P100-2.5.....	113
Figure 81 – Effective moment of inertia, I_{eff} , normalized by gross moment of inertia, I_g	114
Figure 82 – Effective moment of inertia, I_{eff} , normalized by transformed uncracked moment of inertia, I_{tr}	114
Figure 83 – Measured strain in diagonal bar of D80-1.5, strain gauge D1.....	115
Figure 84 – Measured strain in diagonal bar of D80-1.5, strain gauge D2.....	115
Figure 85 – Measured strain in diagonal bar of D80-1.5, strain gauge D3.....	116
Figure 86 – Measured strain in diagonal bar of D80-1.5, strain gauge D4.....	116
Figure 87 – Measured strain in diagonal bar of D80-1.5, strain gauge D5.....	117
Figure 88 – Measured strain in diagonal bar of D80-1.5, strain gauge D6.....	117

Figure 89 – Measured strain in diagonal bar of D80-1.5, strain gauge D7.....	118
Figure 90 – Measured strain in diagonal bar of D80-1.5, strain gauge D8.....	118
Figure 91 – Measured strain in diagonal bar of D80-1.5, strain gauge D9.....	119
Figure 92 – Measured strain in diagonal bar of D80-1.5, strain gauge D10.....	119
Figure 93 – Measured strain in diagonal bar of D80-1.5, strain gauge D11.....	120
Figure 94 – Measured strain in diagonal bar of D80-1.5, strain gauge D12.....	120
Figure 95 – Measured strain in diagonal bar of D80-1.5, strain gauge D13.....	121
Figure 96 – Measured strain in diagonal bar of D80-1.5, strain gauge D14.....	121
Figure 97 – Measured strain in closed stirrup of D80-1.5, strain gauge S1	122
Figure 98 – Measured strain in closed stirrup of D80-1.5, strain gauge S2	122
Figure 99 – Measured strain in closed stirrup of D80-1.5, strain gauge S3	123
Figure 100 – Measured strain in closed stirrup of D80-1.5, strain gauge S4	123
Figure 101 – Measured strain in closed stirrup of D80-1.5, strain gauge S5	124
Figure 102 – Measured strain in closed stirrup of D80-1.5, strain gauge S6	124
Figure 103 – Measured strain in closed stirrup of D80-1.5, strain gauge S7	125
Figure 104 – Measured strain in closed stirrup of D80-1.5, strain gauge S8	125
Figure 105 – Measured strain in closed stirrup of D80-1.5, strain gauge S9	126
Figure 106 – Measured strain in parallel bar of D80-1.5, strain gauge H1	127
Figure 107 – Measured strain in parallel bar of D80-1.5, strain gauge H2	127
Figure 108 – Measured strain in parallel bar of D80-1.5, strain gauge H3	128
Figure 109 – Measured strain in parallel bar of D80-1.5, strain gauge H4	128
Figure 110 – Measured strain in parallel bar of D80-1.5, strain gauge H5	129
Figure 111 – Measured strain in parallel bar of D80-1.5, strain gauge H6	129
Figure 112 – Measured strain in parallel bar of D80-1.5, strain gauge H9	130
Figure 113 – Measured strain in parallel bar of D80-1.5, strain gauge H11	131
Figure 114 – Measured strain in parallel bar of D80-1.5, strain gauge H12	131
Figure 115 – Measured strain in parallel bar of D80-1.5, strain gauge H13	132
Figure 116 – Measured strain in parallel bar of D80-1.5, strain gauge H14	132
Figure 117 – Measured strain in crosstie of D80-1.5, strain gauge T1.....	133
Figure 118 – Measured strain in crosstie of D80-1.5, strain gauge T2.....	133
Figure 119 – Measured strain in crosstie of D80-1.5, strain gauge T3.....	134

Figure 120 – Measured strain in crosstie of D80-1.5, strain gauge T4.....	134
Figure 121 – Measured strain in diagonal bar of D100-1.5, strain gauge D1.....	135
Figure 122 – Measured strain in diagonal bar of D100-1.5, strain gauge D2.....	135
Figure 123 – Measured strain in diagonal bar of D100-1.5, strain gauge D3.....	136
Figure 124 – Measured strain in diagonal bar of D100-1.5, strain gauge D4.....	136
Figure 125 – Measured strain in diagonal bar of D100-1.5, strain gauge D5.....	137
Figure 126 – Measured strain in diagonal bar of D100-1.5, strain gauge D6.....	137
Figure 127 – Measured strain in diagonal bar of D100-1.5, strain gauge D7.....	138
Figure 128 – Measured strain in diagonal bar of D100-1.5, strain gauge D8.....	138
Figure 129 – Measured strain in diagonal bar of D100-1.5, strain gauge D9.....	139
Figure 130 – Measured strain in diagonal bar of D100-1.5, strain gauge D10.....	139
Figure 131 – Measured strain in diagonal bar of D100-1.5, strain gauge D11.....	140
Figure 132 – Measured strain in diagonal bar of D100-1.5, strain gauge D12.....	140
Figure 133 – Measured strain in diagonal bar of D100-1.5, strain gauge D13.....	141
Figure 134 – Measured strain in diagonal bar of D100-1.5, strain gauge D14.....	141
Figure 135 – Measured strain in closed stirrup of D100-1.5, strain gauge S1	142
Figure 136 – Measured strain in closed stirrup of D100-1.5, strain gauge S2	142
Figure 137 – Measured strain in closed stirrup of D100-1.5, strain gauge S3	143
Figure 138 – Measured strain in closed stirrup of D100-1.5, strain gauge S4	143
Figure 139 – Measured strain in closed stirrup of D100-1.5, strain gauge S5	144
Figure 140 – Measured strain in closed stirrup of D100-1.5, strain gauge S6	144
Figure 141 – Measured strain in closed stirrup of D100-1.5, strain gauge S7	145
Figure 142 – Measured strain in closed stirrup of D100-1.5, strain gauge S8	145
Figure 143 – Measured strain in closed stirrup of D100-1.5, strain gauge S9	146
Figure 144 – Measured strain in parallel bar of D100-1.5, strain gauge H1	147
Figure 145 – Measured strain in parallel bar of D100-1.5, strain gauge H2	147
Figure 146 – Measured strain in parallel bar of D100-1.5, strain gauge H3	148
Figure 147 – Measured strain in parallel bar of D100-1.5, strain gauge H4	148
Figure 148 – Measured strain in parallel bar of D100-1.5, strain gauge H5	149
Figure 149 – Measured strain in parallel bar of D100-1.5, strain gauge H6	149
Figure 150 – Measured strain in parallel bar of D100-1.5, strain gauge H7	150

Figure 151 – Measured strain in parallel bar of D100-1.5, strain gauge H8	150
Figure 152 – Measured strain in parallel bar of D100-1.5, strain gauge H9	151
Figure 153 – Measured strain in parallel bar of D100-1.5, strain gauge H10	151
Figure 154 – Measured strain in parallel bar of D100-1.5, strain gauge H11	152
Figure 155 – Measured strain in parallel bar of D100-1.5, strain gauge H12	152
Figure 156 – Measured strain in crosstie of D100-1.5, strain gauge T1.....	153
Figure 157 – Measured strain in crosstie of D100-1.5, strain gauge T2.....	153
Figure 158 – Measured strain in crosstie of D100-1.5, strain gauge T3.....	154
Figure 159 – Measured strain in crosstie of D100-1.5, strain gauge T4.....	154
Figure 160 – Measured strain in crosstie of D100-1.5, strain gauge T5.....	155
Figure 161 – Measured strain in diagonal bar of D120-1.5, strain gauge D1.....	156
Figure 162 – Measured strain in diagonal bar of D120-1.5, strain gauge D2.....	156
Figure 163 – Measured strain in diagonal bar of D120-1.5, strain gauge D3.....	157
Figure 164 – Measured strain in diagonal bar of D120-1.5, strain gauge D4.....	157
Figure 165 – Measured strain in diagonal bar of D120-1.5, strain gauge D5.....	158
Figure 166 – Measured strain in diagonal bar of D120-1.5, strain gauge D6.....	158
Figure 167 – Measured strain in diagonal bar of D120-1.5, strain gauge D7.....	159
Figure 168 – Measured strain in diagonal bar of D120-1.5, strain gauge D8.....	159
Figure 169 – Measured strain in diagonal bar of D120-1.5, strain gauge D9.....	160
Figure 170 – Measured strain in diagonal bar of D120-1.5, strain gauge D10.....	160
Figure 171 – Measured strain in diagonal bar of D120-1.5, strain gauge D11.....	161
Figure 172 – Measured strain in diagonal bar of D120-1.5, strain gauge D12.....	161
Figure 173 – Measured strain in diagonal bar of D120-1.5, strain gauge D13.....	162
Figure 174 – Measured strain in diagonal bar of D120-1.5, strain gauge D14.....	162
Figure 175 – Measured strain in closed stirrup of D120-1.5, strain gauge S1	163
Figure 176 – Measured strain in closed stirrup of D120-1.5, strain gauge S2	163
Figure 177 – Measured strain in closed stirrup of D120-1.5, strain gauge S3	164
Figure 178 – Measured strain in closed stirrup of D120-1.5, strain gauge S4	164
Figure 179 – Measured strain in closed stirrup of D120-1.5, strain gauge S5	165
Figure 180 – Measured strain in closed stirrup of D120-1.5, strain gauge S6	165
Figure 181 – Measured strain in closed stirrup of D120-1.5, strain gauge S7	166

Figure 182 – Measured strain in closed stirrup of D120-1.5, strain gauge S8	166
Figure 183 – Measured strain in closed stirrup of D120-1.5, strain gauge S9	167
Figure 184 – Measured strain in parallel bar of D120-1.5, strain gauge H1	168
Figure 185 – Measured strain in parallel bar of D120-1.5, strain gauge H2	168
Figure 186 – Measured strain in parallel bar of D120-1.5, strain gauge H3	169
Figure 187 – Measured strain in parallel bar of D120-1.5, strain gauge H4	169
Figure 188 – Measured strain in parallel bar of D120-1.5, strain gauge H5	170
Figure 189 – Measured strain in parallel bar of D120-1.5, strain gauge H6	170
Figure 190 – Measured strain in parallel bar of D120-1.5, strain gauge H7	171
Figure 191 – Measured strain in parallel bar of D120-1.5, strain gauge H8	171
Figure 192 – Measured strain in parallel bar of D120-1.5, strain gauge H9	172
Figure 193 – Measured strain in parallel bar of D120-1.5, strain gauge H10	172
Figure 194 – Measured strain in parallel bar of D120-1.5, strain gauge H11	173
Figure 195 – Measured strain in crosstie of D120-1.5, strain gauge T1.....	174
Figure 196 – Measured strain in crosstie of D120-1.5, strain gauge T2.....	174
Figure 197 – Measured strain in crosstie of D120-1.5, strain gauge T3.....	175
Figure 198 – Measured strain in crosstie of D120-1.5, strain gauge T4.....	175
Figure 199 – Measured strain in crosstie of D120-1.5, strain gauge T5.....	176
Figure 200 – Measured strain in crosstie of D120-1.5, strain gauge T6.....	176
Figure 201 – Measured strain in diagonal bar of D80-2.5, strain gauge D1.....	177
Figure 202 – Measured strain in diagonal bar of D80-2.5, strain gauge D2.....	177
Figure 203 – Measured strain in diagonal bar of D80-2.5, strain gauge D3.....	178
Figure 204 – Measured strain in diagonal bar of D80-2.5, strain gauge D4.....	178
Figure 205 – Measured strain in diagonal bar of D80-2.5, strain gauge D5.....	179
Figure 206 – Measured strain in diagonal bar of D80-2.5, strain gauge D6.....	179
Figure 207 – Measured strain in diagonal bar of D80-2.5, strain gauge D7.....	180
Figure 208 – Measured strain in diagonal bar of D80-2.5, strain gauge D8.....	180
Figure 209 – Measured strain in diagonal bar of D80-2.5, strain gauge D9.....	181
Figure 210 – Measured strain in diagonal bar of D80-2.5, strain gauge D10.....	181
Figure 211 – Measured strain in diagonal bar of D80-2.5, strain gauge D11.....	182
Figure 212 – Measured strain in diagonal bar of D80-2.5, strain gauge D12.....	182

Figure 213 – Measured strain in diagonal bar of D80-2.5, strain gauge D13.....	183
Figure 214 – Measured strain in diagonal bar of D80-2.5, strain gauge D14.....	183
Figure 215 – Measured strain in closed stirrup of D80-2.5, strain gauge S1	184
Figure 216 – Measured strain in closed stirrup of D80-2.5, strain gauge S2	184
Figure 217 – Measured strain in closed stirrup of D80-2.5, strain gauge S3	185
Figure 218 – Measured strain in closed stirrup of D80-2.5, strain gauge S4	185
Figure 219 – Measured strain in closed stirrup of D80-2.5, strain gauge S5	186
Figure 220 – Measured strain in closed stirrup of D80-2.5, strain gauge S6	186
Figure 221 – Measured strain in closed stirrup of D80-2.5, strain gauge S7	187
Figure 222 – Measured strain in closed stirrup of D80-2.5, strain gauge S8	187
Figure 223 – Measured strain in closed stirrup of D80-2.5, strain gauge S9	188
Figure 224 – Measured strain in parallel bar of D80-2.5, strain gauge H1	189
Figure 225 – Measured strain in parallel bar of D80-2.5, strain gauge H2	189
Figure 226 – Measured strain in parallel bar of D80-2.5, strain gauge H3	190
Figure 227 – Measured strain in parallel bar of D80-2.5, strain gauge H4	190
Figure 228 – Measured strain in parallel bar of D80-2.5, strain gauge H5	191
Figure 229 – Measured strain in crosstie of D80-2.5, strain gauge T1.....	192
Figure 230 – Measured strain in crosstie of D80-2.5, strain gauge T2.....	192
Figure 231 – Measured strain in crosstie of D80-2.5, strain gauge T3.....	193
Figure 232 – Measured strain in diagonal bar of D100-2.5, strain gauge D1.....	194
Figure 233 – Measured strain in diagonal bar of D100-2.5, strain gauge D2.....	194
Figure 234 – Measured strain in diagonal bar of D100-2.5, strain gauge D3.....	195
Figure 235 – Measured strain in diagonal bar of D100-2.5, strain gauge D4.....	195
Figure 236 – Measured strain in diagonal bar of D100-2.5, strain gauge D5.....	196
Figure 237 – Measured strain in diagonal bar of D100-2.5, strain gauge D6.....	196
Figure 238 – Measured strain in diagonal bar of D100-2.5, strain gauge D7.....	197
Figure 239 – Measured strain in diagonal bar of D100-2.5, strain gauge D8.....	197
Figure 240 – Measured strain in diagonal bar of D100-2.5, strain gauge D9.....	198
Figure 241 – Measured strain in diagonal bar of D100-2.5, strain gauge D10.....	198
Figure 242 – Measured strain in diagonal bar of D100-2.5, strain gauge D11.....	199
Figure 243 – Measured strain in diagonal bar of D100-2.5, strain gauge D12.....	199

Figure 244 – Measured strain in diagonal bar of D100-2.5, strain gauge D13.....	200
Figure 245 – Measured strain in diagonal bar of D100-2.5, strain gauge D14.....	200
Figure 246 – Measured strain in closed stirrup of D100-2.5, strain gauge S1	201
Figure 247 – Measured strain in closed stirrup of D100-2.5, strain gauge S2	201
Figure 248 – Measured strain in closed stirrup of D100-2.5, strain gauge S3	202
Figure 249 – Measured strain in closed stirrup of D100-2.5, strain gauge S4	202
Figure 250 – Measured strain in closed stirrup of D100-2.5, strain gauge S5	203
Figure 251 – Measured strain in closed stirrup of D100-2.5, strain gauge S6	203
Figure 252 – Measured strain in closed stirrup of D100-2.5, strain gauge S7	204
Figure 253 – Measured strain in closed stirrup of D100-2.5, strain gauge S8	204
Figure 254 – Measured strain in closed stirrup of D100-2.5, strain gauge S9	205
Figure 255 – Measured strain in parallel bar of D100-2.5, strain gauge H1	206
Figure 256 – Measured strain in parallel bar of D100-2.5, strain gauge H2	206
Figure 257 – Measured strain in parallel bar of D100-2.5, strain gauge H3	207
Figure 258 – Measured strain in parallel bar of D100-2.5, strain gauge H4	207
Figure 259 – Measured strain in parallel bar of D100-2.5, strain gauge H5	208
Figure 260 – Measured strain in parallel bar of D100-2.5, strain gauge H6	208
Figure 261 – Measured strain in crosstie of D100-2.5, strain gauge T1.....	209
Figure 262 – Measured strain in crosstie of D100-2.5, strain gauge T2.....	209
Figure 263 – Measured strain in crosstie of D100-2.5, strain gauge T3.....	210
Figure 264 – Measured strain in diagonal bar of D120-2.5, strain gauge D1.....	211
Figure 265 – Measured strain in diagonal bar of D120-2.5, strain gauge D2.....	211
Figure 266 – Measured strain in diagonal bar of D120-2.5, strain gauge D3.....	212
Figure 267 – Measured strain in diagonal bar of D120-2.5, strain gauge D4.....	212
Figure 268 – Measured strain in diagonal bar of D120-2.5, strain gauge D5.....	213
Figure 269 – Measured strain in diagonal bar of D120-2.5, strain gauge D6.....	213
Figure 270 – Measured strain in diagonal bar of D120-2.5, strain gauge D7.....	214
Figure 271 – Measured strain in diagonal bar of D120-2.5, strain gauge D8.....	214
Figure 272 – Measured strain in diagonal bar of D120-2.5, strain gauge D9.....	215
Figure 273 – Measured strain in diagonal bar of D120-2.5, strain gauge D10.....	215
Figure 274 – Measured strain in diagonal bar of D120-2.5, strain gauge D11.....	216

Figure 275 – Measured strain in diagonal bar of D120-2.5, strain gauge D12.....	216
Figure 276 – Measured strain in diagonal bar of D120-2.5, strain gauge D13.....	217
Figure 277 – Measured strain in diagonal bar of D120-2.5, strain gauge D14.....	217
Figure 278 – Measured strain in closed stirrup of D120-2.5, strain gauge S1	218
Figure 279 – Measured strain in closed stirrup of D120-2.5, strain gauge S2	218
Figure 280 – Measured strain in closed stirrup of D120-2.5, strain gauge S3	219
Figure 281 – Measured strain in closed stirrup of D120-2.5, strain gauge S4	219
Figure 282 – Measured strain in closed stirrup of D120-2.5, strain gauge S5	220
Figure 283 – Measured strain in closed stirrup of D120-2.5, strain gauge S6	220
Figure 284 – Measured strain in closed stirrup of D120-2.5, strain gauge S7	221
Figure 285 – Measured strain in closed stirrup of D120-2.5, strain gauge S8	221
Figure 286 – Measured strain in closed stirrup of D120-2.5, strain gauge S9	222
Figure 287 – Measured strain in closed stirrup of D120-2.5, strain gauge S10	222
Figure 288 – Measured strain in closed stirrup of D120-2.5, strain gauge S11	223
Figure 289 – Measured strain in closed stirrup of D120-2.5, strain gauge S12	223
Figure 290 – Measured strain in closed stirrup of D120-2.5, strain gauge S13	224
Figure 291 – Measured strain in closed stirrup of D120-2.5, strain gauge S14	224
Figure 292 – Measured strain in closed stirrup of D120-2.5, strain gauge S15	225
Figure 293 – Measured strain in closed stirrup of D120-2.5, strain gauge S16	225
Figure 294 – Measured strain in closed stirrup of D120-2.5, strain gauge S17	226
Figure 295 – Measured strain in closed stirrup of D120-2.5, strain gauge S18	226
Figure 296 – Measured strain in parallel bar of D120-2.5, strain gauge H1	227
Figure 297 – Measured strain in parallel bar of D120-2.5, strain gauge H2	227
Figure 298 – Measured strain in parallel bar of D120-2.5, strain gauge H3	228
Figure 299 – Measured strain in parallel bar of D120-2.5, strain gauge H4	228
Figure 300 – Measured strain in parallel bar of D120-2.5, strain gauge H5	229
Figure 301 – Measured strain in parallel bar of D120-2.5, strain gauge H6	229
Figure 302 – Measured strain in crosstie of D120-2.5, strain gauge T1.....	230
Figure 303 – Measured strain in crosstie of D120-2.5, strain gauge T2.....	230
Figure 304 – Measured strain in crosstie of D120-2.5, strain gauge T3.....	231
Figure 305 – Measured strain in diagonal bar of D80-3.5, strain gauge D1.....	232

Figure 306 – Measured strain in diagonal bar of D80-3.5, strain gauge D2.....	232
Figure 307 – Measured strain in diagonal bar of D80-3.5, strain gauge D3.....	233
Figure 308 – Measured strain in diagonal bar of D80-3.5, strain gauge D4.....	233
Figure 309 – Measured strain in diagonal bar of D80-3.5, strain gauge D5.....	234
Figure 310 – Measured strain in diagonal bar of D80-3.5, strain gauge D6.....	234
Figure 311 – Measured strain in diagonal bar of D80-3.5, strain gauge D7.....	235
Figure 312 – Measured strain in diagonal bar of D80-3.5, strain gauge D8.....	235
Figure 313 – Measured strain in diagonal bar of D80-3.5, strain gauge D9.....	236
Figure 314 – Measured strain in diagonal bar of D80-3.5, strain gauge D10.....	236
Figure 315 – Measured strain in diagonal bar of D80-3.5, strain gauge D11.....	237
Figure 316 – Measured strain in diagonal bar of D80-3.5, strain gauge D12.....	237
Figure 317 – Measured strain in diagonal bar of D80-3.5, strain gauge D13.....	238
Figure 318 – Measured strain in diagonal bar of D80-3.5, strain gauge D14.....	238
Figure 319 – Measured strain in closed stirrup of D80-3.5, strain gauge S1	239
Figure 320 – Measured strain in closed stirrup of D80-3.5, strain gauge S2	239
Figure 321 – Measured strain in closed stirrup of D80-3.5, strain gauge S3	240
Figure 322 – Measured strain in closed stirrup of D80-3.5, strain gauge S4	240
Figure 323 – Measured strain in closed stirrup of D80-3.5, strain gauge S5	241
Figure 324 – Measured strain in closed stirrup of D80-3.5, strain gauge S6	241
Figure 325 – Measured strain in closed stirrup of D80-3.5, strain gauge S7	242
Figure 326 – Measured strain in closed stirrup of D80-3.5, strain gauge S8	242
Figure 327 – Measured strain in closed stirrup of D80-3.5, strain gauge S9	243
Figure 328 – Measured strain in parallel bar of D80-3.5, strain gauge H1	244
Figure 329 – Measured strain in parallel bar of D80-3.5, strain gauge H2	244
Figure 330 – Measured strain in parallel bar of D80-3.5, strain gauge H3	245
Figure 331 – Measured strain in parallel bar of D80-3.5, strain gauge H4	245
Figure 332 – Measured strain in parallel bar of D80-3.5, strain gauge H5	246
Figure 333 – Measured strain in parallel bar of D80-3.5, strain gauge H6	246
Figure 334 – Measured strain in parallel bar of D80-3.5, strain gauge H7	247
Figure 335 – Measured strain in parallel bar of D80-3.5, strain gauge H8	247
Figure 336 – Measured strain in crosstie of D80-3.5, strain gauge T1.....	248

Figure 337 – Measured strain in crosstie of D80-3.5, strain gauge T2.....	248
Figure 338 – Measured strain in crosstie of D80-3.5, strain gauge T3.....	249
Figure 339 – Measured strain in diagonal bar of D100-3.5, strain gauge D1.....	250
Figure 340 – Measured strain in diagonal bar of D100-3.5, strain gauge D2.....	250
Figure 341 – Measured strain in diagonal bar of D100-3.5, strain gauge D3.....	251
Figure 342 – Measured strain in diagonal bar of D100-3.5, strain gauge D4.....	251
Figure 343 – Measured strain in diagonal bar of D100-3.5, strain gauge D5.....	252
Figure 344 – Measured strain in diagonal bar of D100-3.5, strain gauge D6.....	252
Figure 345 – Measured strain in diagonal bar of D100-3.5, strain gauge D7.....	253
Figure 346 – Measured strain in diagonal bar of D100-3.5, strain gauge D8.....	253
Figure 347 – Measured strain in diagonal bar of D100-3.5, strain gauge D9.....	254
Figure 348 – Measured strain in diagonal bar of D100-3.5, strain gauge D10.....	254
Figure 349 – Measured strain in diagonal bar of D100-3.5, strain gauge D11.....	255
Figure 350 – Measured strain in diagonal bar of D100-3.5, strain gauge D12.....	255
Figure 351 – Measured strain in diagonal bar of D100-3.5, strain gauge D13.....	256
Figure 352 – Measured strain in diagonal bar of D100-3.5, strain gauge D14.....	256
Figure 353 – Measured strain in closed stirrup of D100-3.5, strain gauge S1	257
Figure 354 – Measured strain in closed stirrup of D100-3.5, strain gauge S2	257
Figure 355 – Measured strain in closed stirrup of D100-3.5, strain gauge S3	258
Figure 356 – Measured strain in closed stirrup of D100-3.5, strain gauge S4	258
Figure 357 – Measured strain in closed stirrup of D100-3.5, strain gauge S5	259
Figure 358 – Measured strain in closed stirrup of D100-3.5, strain gauge S6	259
Figure 359 – Measured strain in closed stirrup of D100-3.5, strain gauge S7	260
Figure 360 – Measured strain in closed stirrup of D100-3.5, strain gauge S8	260
Figure 361 – Measured strain in closed stirrup of D100-3.5, strain gauge S9	261
Figure 362 – Measured strain in parallel bar of D100-3.5, strain gauge H1	262
Figure 363 – Measured strain in parallel bar of D100-3.5, strain gauge H2	262
Figure 364 – Measured strain in parallel bar of D100-3.5, strain gauge H3	263
Figure 365 – Measured strain in parallel bar of D100-3.5, strain gauge H4	263
Figure 366 – Measured strain in parallel bar of D100-3.5, strain gauge H5	264
Figure 367 – Measured strain in parallel bar of D100-3.5, strain gauge H6	264

Figure 368 – Measured strain in parallel bar of D100-3.5, strain gauge H7	265
Figure 369 – Measured strain in crosstie of D100-3.5, strain gauge T1.....	266
Figure 370 – Measured strain in crosstie of D100-3.5, strain gauge T2.....	266
Figure 371 – Measured strain in crosstie of D100-3.5, strain gauge T3.....	267
Figure 372 – Measured strain in diagonal bar of D120-3.5, strain gauge D1.....	268
Figure 373 – Measured strain in diagonal bar of D120-3.5, strain gauge D2.....	268
Figure 374 – Measured strain in diagonal bar of D120-3.5, strain gauge D3.....	269
Figure 375 – Measured strain in diagonal bar of D120-3.5, strain gauge D4.....	269
Figure 376 – Measured strain in diagonal bar of D120-3.5, strain gauge D5.....	270
Figure 377 – Measured strain in diagonal bar of D120-3.5, strain gauge D6.....	270
Figure 378 – Measured strain in diagonal bar of D120-3.5, strain gauge D7.....	271
Figure 379 – Measured strain in diagonal bar of D120-3.5, strain gauge D8.....	271
Figure 380 – Measured strain in diagonal bar of D120-3.5, strain gauge D9.....	272
Figure 381 – Measured strain in diagonal bar of D120-3.5, strain gauge D10.....	272
Figure 382 – Measured strain in diagonal bar of D120-3.5, strain gauge D11.....	273
Figure 383 – Measured strain in diagonal bar of D120-3.5, strain gauge D12.....	273
Figure 384 – Measured strain in diagonal bar of D120-3.5, strain gauge D13.....	274
Figure 385 – Measured strain in diagonal bar of D120-3.5, strain gauge D14.....	274
Figure 386 – Measured strain in closed stirrup of D120-3.5, strain gauge S1	275
Figure 387 – Measured strain in closed stirrup of D120-3.5, strain gauge S2	275
Figure 388 – Measured strain in closed stirrup of D120-3.5, strain gauge S3	276
Figure 389 – Measured strain in closed stirrup of D120-3.5, strain gauge S4	276
Figure 390 – Measured strain in closed stirrup of D120-3.5, strain gauge S5	277
Figure 391 – Measured strain in closed stirrup of D120-3.5, strain gauge S6	277
Figure 392 – Measured strain in closed stirrup of D120-3.5, strain gauge S7	278
Figure 393 – Measured strain in closed stirrup of D120-3.5, strain gauge S8	278
Figure 394 – Measured strain in closed stirrup of D120-3.5, strain gauge S9	279
Figure 395 – Measured strain in parallel bar of D120-3.5, strain gauge H1	280
Figure 396 – Measured strain in parallel bar of D120-3.5, strain gauge H2	280
Figure 397 – Measured strain in parallel bar of D120-3.5, strain gauge H3	281
Figure 398 – Measured strain in parallel bar of D120-3.5, strain gauge H4	281

Figure 399 – Measured strain in parallel bar of D120-3.5, strain gauge H5	282
Figure 400 – Measured strain in crosstie of D120-3.5, strain gauge T1.....	283
Figure 401 – Measured strain in crosstie of D120-3.5, strain gauge T2.....	283
Figure 402 – Measured strain in crosstie of D120-3.5, strain gauge T3.....	284
Figure 403 – Measured strain in parallel bar of P80-2.5, strain gauge P1.....	285
Figure 404 – Measured strain in parallel bar of P80-2.5, strain gauge P2.....	285
Figure 405 – Measured strain in parallel bar of P80-2.5, strain gauge P3.....	286
Figure 406 – Measured strain in parallel bar of P80-2.5, strain gauge P4.....	286
Figure 407 – Measured strain in parallel bar of P80-2.5, strain gauge P5.....	287
Figure 408 – Measured strain in parallel bar of P80-2.5, strain gauge P6.....	287
Figure 409 – Measured strain in parallel bar of P80-2.5, strain gauge P7.....	288
Figure 410 – Measured strain in parallel bar of P80-2.5, strain gauge P8.....	288
Figure 411 – Measured strain in parallel bar of P80-2.5, strain gauge P9.....	289
Figure 412 – Measured strain in parallel bar of P80-2.5, strain gauge P10.....	289
Figure 413 – Measured strain in parallel bar of P80-2.5, strain gauge P11.....	290
Figure 414 – Measured strain in parallel bar of P80-2.5, strain gauge P12.....	290
Figure 415 – Measured strain in closed stirrup of P80-2.5, strain gauge S1	291
Figure 416 – Measured strain in closed stirrup of P80-2.5, strain gauge S2	291
Figure 417 – Measured strain in closed stirrup of P80-2.5, strain gauge S3	292
Figure 418 – Measured strain in closed stirrup of P80-2.5, strain gauge S4	292
Figure 419 – Measured strain in closed stirrup of P80-2.5, strain gauge S5	293
Figure 420 – Measured strain in closed stirrup of P80-2.5, strain gauge S6	293
Figure 421 – Measured strain in closed stirrup of P80-2.5, strain gauge S7	294
Figure 422 – Measured strain in closed stirrup of P80-2.5, strain gauge S8	294
Figure 423 – Measured strain in closed stirrup of P80-2.5, strain gauge S9	295
Figure 424 – Measured strain in crosstie of P80-2.5, strain gauge T1	296
Figure 425 – Measured strain in parallel bar of P100-2.5, strain gauge P1.....	297
Figure 426 – Measured strain in parallel bar of P100-2.5, strain gauge P2.....	297
Figure 427 – Measured strain in parallel bar of P100-2.5, strain gauge P3.....	298
Figure 428 – Measured strain in parallel bar of P100-2.5, strain gauge P4.....	298
Figure 429 – Measured strain in parallel bar of P100-2.5, strain gauge P5.....	299

Figure 430 – Measured strain in parallel bar of P100-2.5, strain gauge P6.....	299
Figure 431 – Measured strain in parallel bar of P100-2.5, strain gauge P7.....	300
Figure 432 – Measured strain in parallel bar of P100-2.5, strain gauge P8.....	300
Figure 433 – Measured strain in parallel bar of P100-2.5, strain gauge P9.....	301
Figure 434 – Measured strain in parallel bar of P100-2.5, strain gauge P10.....	301
Figure 435 – Measured strain in parallel bar of P100-2.5, strain gauge P11.....	302
Figure 436 – Measured strain in parallel bar of P100-2.5, strain gauge P12.....	302
Figure 437 – Measured strain in closed stirrup of P100-2.5, strain gauge S1	303
Figure 438 – Measured strain in closed stirrup of P100-2.5, strain gauge S2	303
Figure 439 – Measured strain in closed stirrup of P100-2.5, strain gauge S3	304
Figure 440 – Measured strain in closed stirrup of P100-2.5, strain gauge S4	304
Figure 441 – Measured strain in closed stirrup of P100-2.5, strain gauge S5	305
Figure 442 – Measured strain in closed stirrup of P100-2.5, strain gauge S6	305
Figure 443 – Measured strain in closed stirrup of P100-2.5, strain gauge S7	306
Figure 444 – Measured strain in closed stirrup of P100-2.5, strain gauge S8	306
Figure 445 – Measured strain in closed stirrup of P100-2.5, strain gauge S9	307
Figure 446 – Measured strain in crosstie of P100-2.5, strain gauge T1	308
Figure 447 – Envelopes of measured strains in diagonal bars of D80-1.5, D strain gauges	309
Figure 448 – Envelopes of measured strains in closed stirrups of D80-1.5, S strain gauges	309
Figure 449 – Envelopes of measured strains in parallel bars of D80-1.5, H strain gauges	310
Figure 450 – Envelopes of measured strains in crossties of D80-1.5, T strain gauges	310
Figure 451 – Envelopes of measured strains in diagonal bars of D100-1.5, D strain gauges	311
Figure 452 – Envelopes of measured strains in closed stirrups of D100-1.5, S strain gauges ...	311
Figure 453 – Envelopes of measured strains in parallel bars of D100-1.5, H strain gauges	312
Figure 454 – Envelopes of measured strains in crossties of D100-1.5, T strain gauges	312
Figure 455 – Envelopes of measured strains in diagonal bars of D120-1.5, D strain gauges	313
Figure 456 – Envelopes of measured strains in closed stirrups of D120-1.5, S strain gauges ...	313
Figure 457 – Envelopes of measured strains in parallel bars of D120-1.5, H strain gauges	314
Figure 458 – Envelopes of measured strains in crossties of D120-1.5, T strain gauges	314
Figure 459 – Envelopes of measured strains in diagonal bars of D80-2.5, D strain gauges	315
Figure 460 – Envelopes of measured strains in closed stirrups of D80-2.5, S strain gauges	315

Figure 461 – Envelopes of measured strains in parallel bars of D80-2.5, H strain gauges	316
Figure 462 – Envelopes of measured strains in crossties of D80-2.5, T strain gauges	316
Figure 463 – Envelopes of measured strains in diagonal bars of D100-2.5, D strain gauges	317
Figure 464 – Envelopes of measured strains in closed stirrups of D100-2.5, S strain gauges ...	317
Figure 465 – Envelopes of measured strains in parallel bars of D100-2.5, H strain gauges	318
Figure 466 – Envelopes of measured strains in crossties of D100-2.5, T strain gauges	318
Figure 467 – Envelopes of measured strains in diagonal bars of D120-2.5, D strain gauges	319
Figure 468 – Envelopes of measured strains in closed stirrups of D120-2.5, S strain gauges ...	319
Figure 469 – Envelopes of measured strains in parallel bars of D120-2.5, H strain gauges	320
Figure 470 – Envelopes of measured strains in crossties of D120-2.5, T strain gauges	320
Figure 471 – Envelopes of measured strains in diagonal bars of D80-3.5, D strain gauges	321
Figure 472 – Envelopes of measured strains in closed stirrups of D80-3.5, S strain gauges	321
Figure 473 – Envelopes of measured strains in parallel bars of D80-3.5, H strain gauges	322
Figure 474 – Envelopes of measured strains in crossties of D80-3.5, T strain gauges	322
Figure 475 – Envelopes of measured strains in diagonal bars of D100-3.5, D strain gauges	323
Figure 476 – Envelopes of measured strains in closed stirrups of D100-3.5, S strain gauges ...	323
Figure 477 – Envelopes of measured strains in parallel bars of D100-3.5, H strain gauges	324
Figure 478 – Envelopes of measured strains in crossties of D100-3.5, T strain gauges	324
Figure 479 – Envelopes of measured strains in diagonal bars of D120-3.5, D strain gauges	325
Figure 480 – Envelopes of measured strains in closed stirrups of D120-3.5, S strain gauges ...	325
Figure 481 – Envelopes of measured strains in parallel bars of D120-3.5, H strain gauges	326
Figure 482 – Envelopes of measured strains in crossties of D120-3.5, T strain gauges	326
Figure 483 – Envelopes of measured strains in parallel bars of P80-2.5, P strain gauges	327
Figure 484 – Envelopes of measured strains in closed stirrups of P80-2.5, S strain gauges.....	327
Figure 485 – Envelopes of measured strains in crossties of P80-2.5, T strain gauges	328
Figure 486 – Envelopes of measured strains in parallel bars of P100-2.5, P strain gauges	329
Figure 487 – Envelopes of measured strains in closed stirrups of P100-2.5, S strain gauges....	329
Figure 488 – Envelopes of measured strains in crossties of P100-2.5, T strain gauges	330
Figure 489 – Envelopes of measured strains in diagonal bars of D-type beams with an aspect ratio of 1.5, D strain gauges.....	331

Figure 490 – Envelopes of measured strains in closed stirrups of D-type beams with an aspect ratio of 1.5, S strain gauges	331
Figure 491 – Envelopes of measured strains in parallel bars of D-type beams with an aspect ratio of 1.5, H strain gauges.....	332
Figure 492 – Envelopes of measured strains in crossties of D-type beams with an aspect ratio of 1.5, T strain gauges	332
Figure 493 – Envelopes of measured strains in diagonal bars of D-type beams with an aspect ratio of 2.5, D strain gauges.....	333
Figure 494 – Envelopes of measured strains in closed stirrups of D-type beams with an aspect ratio of 2.5, S strain gauges	333
Figure 495 – Envelopes of measured strains in parallel bars of D-type beams with an aspect ratio of 2.5, H strain gauges.....	334
Figure 496 – Envelopes of measured strains in crossties of D-type beams with an aspect ratio of 2.5, T strain gauges	334
Figure 497 – Envelopes of measured strains in diagonal bars of D-type beams with an aspect ratio of 3.5, D strain gauges.....	335
Figure 498 – Envelopes of measured strains in closed stirrups of D-type beams with an aspect ratio of 3.5, S strain gauges	335
Figure 499 – Envelopes of measured strains in parallel bars of D-type beams with an aspect ratio of 3.5, H strain gauges.....	336
Figure 500 – Envelopes of measured strains in crossties of D-type beams with an aspect ratio of 3.5, T strain gauges	336
Figure 501 – Envelopes of measured strains in parallel bars of P-type beams with an aspect ratio of 2.5, P strain gauges	337
Figure 502 – Envelopes of measured strains in closed stirrups of P-type beams with an aspect ratio of 2.5, S strain gauges	337
Figure 503 – Envelopes of measured strains in crossties of P-type beams with aspect ratio of 2.5, T strain gauges.....	338
Figure 504 – Maximum strains in D-type beams during loading steps 5 through 9 (1% through 4% chord rotation), D strain gauges.....	339

Figure 505 – Maximum strains in P-type beams during loading steps 5 through 9 (1% through 4% chord rotation), P strain gauges.....	339
Figure B.1 – Coupling beam reinforcement, D120-1.5	B–2
Figure B.2 – Coupling beam reinforcement, D120-2.5	B–2
Figure B.3 – Coupling beam reinforcement, D120-3.5	B–3
Figure B.4 – Coupling beam reinforcement, P100-2.5.....	B–3
Figure B.5 – Base block reinforcement, typical of beams with aspect ratios of 2.5 and 3.5.....	B–4
Figure B.6 –Top block reinforcement, typical of beams with aspect ratios of 2.5 and 3.5	B–4
Figure B.7 – Specimens before casting, D80-1.5, D100-1.5, and D120-1.5 (from left to right)	B–5
Figure B.8 – Specimens after formwork removal, D100-3.5, D80-3.5, P100-2.5, P80-2.5, D100-2.5, and D80-2.5 (from left to right)	B–5
Figure C.1 – D80-1.5 during second cycle to 2% chord rotation	C–2
Figure C.2 – D80-1.5 during second cycle to 6% chord rotation	C–3
Figure C.3 – D80-1.5 at +2% chord rotation, second cycle.....	C–4
Figure C.4 – D80-1.5 at -2% chord rotation, second cycle.....	C–4
Figure C.5 – D80-1.5 at +4% chord rotation, second cycle.....	C–4
Figure C.6 – D80-1.5 at -4% chord rotation, second cycle.....	C–4
Figure C.7 – D80-1.5 at +6% chord rotation, second cycle.....	C–5
Figure C.8 – D80-1.5 at -6% chord rotation, second cycle.....	C–5
Figure C.9 – D80-1.5 at +8% chord rotation, first cycle	C–5
Figure C.10 – D80-1.5 at -8% chord rotation, first cycle	C–5
Figure C.11 – D100-1.5 during second cycle to 2% chord rotation	C–6
Figure C.12 – D100-1.5 during second cycle to 6% chord rotation	C–7
Figure C.13 – D100-1.5 at +2% chord rotation, second cycle.....	C–8
Figure C.14 – D100-1.5 at -2% chord rotation, second cycle.....	C–8
Figure C.15 – D100-1.5 at +4% chord rotation, second cycle.....	C–8
Figure C.16 – D100-1.5 at -4% chord rotation, second cycle.....	C–8
Figure C.17 – D100-1.5 at +6% chord rotation, second cycle.....	C–9
Figure C.18 – D100-1.5 at -6% chord rotation, second cycle.....	C–9
Figure C.19 – D100-1.5 at +8% chord rotation, first cycle	C–9

Figure C.20 – D120-1.5 during second cycle to 2% chord rotation	C-10
Figure C.21 – D120-1.5 during first cycle to 6% chord rotation.....	C-11
Figure C.22 – D120-1.5 at +2% chord rotation, second cycle.....	C-12
Figure C.23 – D120-1.5 at -2% chord rotation, second cycle.....	C-12
Figure C.24 – D120-1.5 at +4% chord rotation, second cycle.....	C-12
Figure C.25 – D120-1.5 at -4% chord rotation, second cycle.....	C-12
Figure C.26 – D120-1.5 at +6% chord rotation, first cycle	C-13
Figure C.27 – D120-1.5 at -6% chord rotation, first cycle	C-13
Figure C.28 – D80-2.5 during second cycle to 2% chord rotation	C-14
Figure C.29 – D80-2.5 during second cycle to 6% chord rotation	C-15
Figure C.30 – D80-2.5 at +2% chord rotation, second cycle.....	C-16
Figure C.31 – D80-2.5 at -2% chord rotation, second cycle.....	C-16
Figure C.32 – D80-2.5 at +4% chord rotation, second cycle.....	C-16
Figure C.33 – D80-2.5 at -4% chord rotation, second cycle.....	C-16
Figure C.34 – D80-2.5 at +6% chord rotation, second cycle.....	C-17
Figure C.35 – D80-2.5 at -6% chord rotation, second cycle.....	C-17
Figure C.36 – D80-2.5 at +8% chord rotation, second cycle.....	C-17
Figure C.37 – D80-2.5 at -8% chord rotation, second cycle.....	C-17
Figure C.38 – D80-2.5 at +10% chord rotation, first cycle	C-18
Figure C.39 – D80-2.5 at -10% chord rotation, first cycle	C-18
Figure C.40 – D100-2.5 during second cycle to 2% chord rotation	C-19
Figure C.41 – D100-2.5 during second cycle to 6% chord rotation	C-20
Figure C.42 – D100-2.5 at +2% chord rotation, second cycle.....	C-21
Figure C.43 – D100-2.5 at -2% chord rotation, second cycle.....	C-21
Figure C.44 – D100-2.5 at +4% chord rotation, second cycle.....	C-21
Figure C.45 – D100-2.5 at -4% chord rotation, second cycle.....	C-21
Figure C.46 – D100-2.5 at +6% chord rotation, second cycle.....	C-22
Figure C.47 – D100-2.5 at -6% chord rotation, second cycle.....	C-22
Figure C.48 – D100-2.5 at +8% chord rotation, first cycle	C-22
Figure C.49 – D100-2.5 at -8% chord rotation, first cycle	C-22
Figure C.50 – D120-2.5 during second cycle to 2% chord rotation	C-23

Figure C.51 – D120-2.5 during second cycle to 6% chord rotation	C-24
Figure C.52 – D120-2.5 at +2% chord rotation, second cycle.....	C-25
Figure C.53 – D120-2.5 at -2% chord rotation, second cycle.....	C-25
Figure C.54 – D120-2.5 at +4% chord rotation, second cycle.....	C-25
Figure C.55 – D120-2.5 at -4% chord rotation, second cycle.....	C-25
Figure C.56 – D120-2.5 at +6% chord rotation, second cycle.....	C-26
Figure C.57 – D120-2.5 at -6% chord rotation, second cycle.....	C-26
Figure C.58 – D120-2.5 at +8% chord rotation, second cycle.....	C-26
Figure C.59 – D120-2.5 at -8% chord rotation, second cycle.....	C-26
Figure C.60 – D80-3.5 during second cycle to 2% chord rotation	C-27
Figure C.61 – D80-3.5 during second cycle to 6% chord rotation	C-29
Figure C.62 – D80-3.5 at +2% chord rotation, second cycle.....	C-30
Figure C.63 – D80-3.5 at -2% chord rotation, second cycle.....	C-30
Figure C.64 – D80-3.5 at +4% chord rotation, second cycle.....	C-30
Figure C.65 – D80-3.5 at -4% chord rotation, second cycle.....	C-30
Figure C.66 – D80-3.5 at +6% chord rotation, second cycle.....	C-31
Figure C.67 – D80-3.5 at -6% chord rotation, second cycle.....	C-31
Figure C.68 – D80-3.5 at +8% chord rotation, second cycle.....	C-31
Figure C.69 – D80-3.5 at -8% chord rotation, second cycle.....	C-31
Figure C.70 – D80-3.5 at +10% chord rotation, first cycle	C-32
Figure C.71 – D80-3.5 at -10% chord rotation, first cycle	C-32
Figure C.72 – D100-3.5 during second cycle to 2% chord rotation	C-33
Figure C.73 – D100-3.5 during second cycle to 6% chord rotation	C-35
Figure C.74 – D100-3.5 at +2% chord rotation, second cycle.....	C-36
Figure C.75 – D100-3.5 at -2% chord rotation, second cycle.....	C-36
Figure C.76 – D100-3.5 at +4% chord rotation, second cycle.....	C-36
Figure C.77 – D100-3.5 at -4% chord rotation, second cycle.....	C-36
Figure C.78 – D100-3.5 at +6% chord rotation, second cycle.....	C-37
Figure C.79 – D100-3.5 at -6% chord rotation, second cycle.....	C-37
Figure C.80 – D100-3.5 at +8% chord rotation, second cycle.....	C-37
Figure C.81 – D100-3.5 at -8% chord rotation, second cycle.....	C-37

Figure C.82 – D100-3.5 at +10% chord rotation, first cycle	C-38
Figure C.83 – D100-3.5 at -10% chord rotation, first cycle	C-38
Figure C.84 – D120-3.5 during second cycle to 2% chord rotation	C-39
Figure C.85 – D120-3.5 during second cycle to 6% chord rotation	C-40
Figure C.86 – D120-3.5 at +2% chord rotation, second cycle.....	C-41
Figure C.87 – D120-3.5 at -2% chord rotation, second cycle.....	C-41
Figure C.88 – D120-3.5 at +4% chord rotation, second cycle.....	C-41
Figure C.89 – D120-3.5 at -4% chord rotation, second cycle.....	C-41
Figure C.90 – D120-3.5 at +6% chord rotation, second cycle.....	C-42
Figure C.91 – D120-3.5 at -6% chord rotation, second cycle.....	C-42
Figure C.92 – D120-3.5 at +8% chord rotation, second cycle.....	C-42
Figure C.93 – D120-3.5 at -8% chord rotation, second cycle.....	C-42
Figure C.94 – P80-2.5 during second cycle to 2% chord rotation.....	C-43
Figure C.95 – P80-2.5 during second cycle to 6% chord rotation.....	C-44
Figure C.96 – P80-2.5 at +2% chord rotation, second cycle	C-45
Figure C.97 – P80-2.5 at -2% chord rotation, second cycle	C-45
Figure C.98 – P80-2.5 at +4% chord rotation, second cycle	C-45
Figure C.99 – P80-2.5 at -4% chord rotation, second cycle	C-45
Figure C.100 – P80-2.5 at +6% chord rotation, second cycle	C-46
Figure C.101 – P80-2.5 at -6% chord rotation, second cycle	C-46
Figure C.102 – P100-2.5 during second cycle to 2% chord rotation.....	C-47
Figure C.103 – P100-2.5 during second cycle to 6% chord rotation.....	C-48
Figure C.104 – P100-2.5 at +2% chord rotation, second cycle	C-49
Figure C.105 – P100-2.5 at -2% chord rotation, second cycle	C-49
Figure C.106 – P100-2.5 at +4% chord rotation, second cycle	C-49
Figure C.107 – P100-2.5 at -4% chord rotation, second cycle	C-49
Figure C.108 – P100-2.5 at +6% chord rotation, second cycle	C-50
Figure C.109 – P100-2.5 at -6% chord rotation, second cycle	C-50

CHAPTER 1: INTRODUCTION

1.1 Background and Motivation

Reinforced concrete structural walls are a common lateral force resisting system used in medium to high-rise construction. Structural walls resist lateral forces and limit building drift during earthquakes or high wind events. Perforations in a structural wall to accommodate windows, doors, and other building components reduce the stiffness and strength of the lateral force resisting system and may lead to the structural wall acting as a series of independent, smaller structural walls. Coupling beams are used to couple the actions of structural walls, restoring much of the lost stiffness and strength while retaining the openings necessary for building use. The transfer of forces between structural wall segments by coupling beams results in wall axial tension and compression forces that form a moment couple in response to overturning loads.

The geometry of the coupled wall system amplifies interstory wall drifts into greater coupling beam deformations. The large shear and deformation demands placed on reinforced concrete coupling beams require special reinforcement detailing. This detailing is aimed at preventing shear strength and stiffness reductions when the coupling beam is subjected to repeated inelastic loading cycles that would compromise the lateral strength and stiffness of the reinforced concrete coupled wall system.

The amount and detailing of reinforcement required in concrete coupling beams typically cause reinforcement congestion and increase construction costs. Reducing the quantity or size of the coupling beam diagonal and transverse reinforcement by using high-strength reinforcement is one way to reduce reinforcement congestion. The ACI Building Code (ACI 318-14)^[1] limits the nominal yield stress of primary longitudinal reinforcement in special seismic systems to 60 ksi

(420 MPa) and transverse confining reinforcement to 100 ksi (690 MPa) because there are limited experimental data from specimens constructed with high-strength reinforcement. Typical problems associated with the use of high-strength steel in reinforced concrete, such as width of cracks, are not a concern in members primarily designed to resist large, inelastic cyclic deformations. Therefore, there is reason to believe high-strength steel reinforcement can function as diagonal reinforcement in coupling beams.

The ACI Building Code^[1] requires the use of diagonal reinforcement in coupling beams with aspect ratios (ℓ_n/h) less than two and nominal shear stresses higher than $4\sqrt{f'_c}$ psi ($0.33\sqrt{f'_c}$ MPa). Coupling beams with aspect ratios not less than four are required to be designed as a beam of a special moment frame. The Code permits coupling beams with aspect ratios between two and four to be designed as either diagonally-reinforced or as special moment frame beams. Diagonal bars in slender beams (with aspect ratios higher than two) have a small angle relative to the horizontal, resulting in a need for large amounts of diagonal reinforcement to resist the shear demand. Slender coupling beams may therefore especially benefit from the use of high-strength reinforcement. The effect of using high-strength steel on the behavior of coupling beams with a representative range of aspect ratios needs to be evaluated.

1.2 Research Objectives

This study was undertaken to investigate the use of high-strength steel as reinforcement in diagonally-reinforced and special moment frame coupling beams. The expected impact of this work is to reduce reinforcement congestion and, as a result, lower construction costs of robust and more efficient reinforced concrete buildings.

The test results presented in this report may be useful as a basis for comparisons between coupling beams reinforced with Grade 80, 100, and 120 (550, 690, and 830) steel bars. They may also be useful for developing and calibrating models for use in design and analysis of systems with high-strength reinforcement.

CHAPTER 2: EXPERIMENTAL PROGRAM

2.1 Specimens

2.1.1 Design and Detailing

Eleven large-scale coupling beam specimens were subjected to pseudo-static cyclic displacements of increasing magnitude. Details of the specimens are listed in Table 1 and shown in Figures 1 through 23. The approximately 1/2-scale specimens had nominally the same beam cross sectional dimensions: a height (h) of 18 in. (460 mm) and a width (b_w) of 12 in. (300 mm); clear span lengths (ℓ_n) of 27, 45, or 63 in. (690, 1140, or 1600 mm), resulting in aspect ratios (ℓ_n/h) of 1.5, 2.5, or 3.5 (which are similar to the range of aspect ratios commonly used in practice); either Grade 80, 100, or 120 (550, 690, or 830) reinforcing bars; and either diagonal (D-type) or moment-frame (P-type) reinforcement.

Each specimen consisted of a coupling beam that framed into top and bottom blocks. The end blocks had dense reinforcement cages near the connection with the coupling beam to emulate structural wall boundary elements. The coupling beams were tested rotated 90 degrees from horizontal for convenience. All reinforcement in the end blocks was Grade 60 (420) except for the coupling beam reinforcement embedded into the end blocks.

Specimens, such as D120-3.5 or P80-2.5, were named using the following rules: the first letter indicates whether it has diagonal (D) or parallel (P) primary longitudinal reinforcement (see Figure 1), followed by a number that represents the reinforcement grade (in ksi), and the last number (separated by a dash) indicates the coupling beam aspect ratio (clear span to overall height, ℓ_n/h).

One D-type coupling beam was constructed for each combination of aspect ratio (1.5, 2.5, or 3.5) and diagonal bar grade (Grade 80, 100, or 120 [550, 690, or 830]), for a total of nine specimens with D-type reinforcement layout. D-type specimens were designed to have a nominal shear stress of approximately $8\sqrt{f'_c}$ psi ($0.67\sqrt{f'_c}$ MPa) based on f'_c of 8,000 psi (55 MPa). The targeted shear stress is near the maximum design stress of $10\sqrt{f'_c}$ psi ($0.71\sqrt{f'_c}$ MPa) permitted by the ACI Building Code^[1] for diagonally-reinforced coupling beams. Beam shear strength (V_n) was calculated using ACI 318-14 Section 18.10.7.4.a^[1] (Equation 2.1) with nominal f_y . The product of yield stress and reinforcement ratio, ρf_y , was approximately constant for a given beam aspect ratio so the amount of diagonal reinforcement was inversely proportional to its yield stress. Transverse reinforcement was provided in accordance with ACI 318-14 Section 18.10.7.4.d^[1] using Equation 2.2, see below for additional details. The transverse reinforcement was Grade 80 (550) for all beams except D120-2.5, which had Grade 120 (830) transverse reinforcement.

$$V_n = 2A_{vd} f_y \sin \alpha \quad \text{Equation 2.1}$$

Two P-type coupling beams were constructed with an aspect ratio of 2.5 and either Grade 80 or 100 (550 or 690) longitudinal reinforcement. The target shear stress for the P-type beams was approximately $6\sqrt{f'_c}$ psi ($0.5\sqrt{f'_c}$ MPa). This shear stress was based on the beam reaching its probable flexural strength at both ends. Probable flexural strength was calculated using a rectangular stress block for concrete in compression with f'_c of 8,000 psi (55 MPa), linear strain distribution, and elasto-plastic stress-strain behavior for the reinforcement with a maximum stress of $1.25f_y$ in the longitudinal tension reinforcement. The maximum design stress permitted by the Code for beams with special moment frame reinforcement is $6\sqrt{f'_c}$ psi ($0.5\sqrt{f'_c}$ MPa). Transverse reinforcement was provided such that 0.75 times the nominal shear strength of a P-type coupling

beam exceeded the shear demand associated with probable flexural strength at both ends of the beam.

The coupling beams described in Table 1 are similar to those tested by Naish et al.^[16], which included diagonally-reinforced beams with aspect ratios of 2.4 and 3.3, Grade 60 (420) reinforcement, and confinement for the entire beam cross section. The similarities between the beams allow the use of those tested by Naish et al. as control beams; the scope of this study was therefore focused on beams with higher-grade reinforcement. However, there were some differences in the designs that caused the beams in this study to be subjected to more demanding conditions. First, the design shear stresses for D-type beams in this study were 10% to 70% higher than the design shear stresses used by Naish et al., where nominal shear stresses of $7.3\sqrt{f'_c}$ psi ($0.61\sqrt{f'_c}$ MPa) and $4.8\sqrt{f'_c}$ psi ($0.40\sqrt{f'_c}$ MPa) were used for diagonally-reinforced beams with aspect ratios of 2.4 and 3.3, respectively; and second, the volumetric ratios of transverse reinforcement for D-type beams in this study were approximately 20% lower (but still compliant with the ACI Building Code^[1]) than those used by Naish et al.

The specimens in this study are also similar to those described in Ameen et al.^[3] and Poudel et al.^[18] which included diagonally-reinforced coupling beams with an aspect ratio of 1.9, Grades 60 and 120 (420 and 830) reinforcement, full-section confinement, and several coupling beams with fully-developed secondary longitudinal reinforcement. However, the design shear stresses in Ameen et al. and Poudel et al. were approximately 10 to $14\sqrt{f'_c}$ psi (0.83 to $1.2\sqrt{f'_c}$ MPa), approximately 20% to 80% higher than the design shear stresses of the D-type beams in this study. Another difference was that coupling beams in this study were free to elongate axially whereas some of the beams tested by Ameen et al. and Poudel et al. were restrained axially. This may have

caused those beams to exhibit somewhat higher shear forces and lower chord rotation capacities. Finally, the beam widths in this study were 12 in. (300 mm) rather than 10 in. (250 mm). The 20% increase in width was not expected to affect results and allowed more options when selecting transverse reinforcement for concrete confinement.

The coupling beams had No. 6 (19) or No. 7 (22) Grade 80, 100, or 120 (550, 690, or 830) steel bars as primary longitudinal reinforcement. D-type specimens were constructed with two bundles of diagonal reinforcing bars that intersected near midspan of the coupling beam with an angle of inclination between 10 and 23 degrees depending on the aspect ratio. P-type specimens were constructed with six parallel reinforcing bars, three near each of the extreme fibers of the beam cross section. The design data in Table 1 include the quantity and minimum straight embedment length (ℓ_e) of the primary longitudinal reinforcement of the coupling beams into the top and bottom blocks. The as-built dimensions of the specimens are shown in Figures 2 through 23.

Transverse reinforcement, in the form of closed hoops and crossties oriented parallel to both strong and weak axes, was used in all D-type beams to provide full-section confinement. For D-type beams, the transverse reinforcement was not considered when calculating the shear strength in accordance with Equation 2.1 following ACI 318-14 Section 18.10.7.4.a^[1]. Instead, it met the requirements of ACI 318-14 Section 18.10.7.4.d^[1] (shown in Equation 2.2). All D-type beams had No. 3 (10) Grade 80 (550) transverse reinforcement except D120-2.5, where No. 3 (10) Grade 120 (830) was used. Each layer of transverse reinforcement in D-type beams consisted of a closed hoop with seismic hooks (135 degrees), one crosstie along the beam depth, and two crossties along the beam width. All crossties had one end with a 135 degree hook and the other with a 90 degree hook, as permitted by ACI 318-14^[1]. Beam cross sections for the D-type beams are shown in Figures 2

through 19. The longitudinal spacing of each layer of transverse reinforcement in the D-type beams was 3 in. (76 mm). For both transverse directions of the cross-sectional area of D-type beams, the amount of transverse reinforcement provided closely match the amount required by Equation 2.2 (based on ACI 318-14 Section 18.10.7.4.d^[1]):

$$A_{sh} \geq [0.09 s b_c f'_c / f_{yt}; 0.3 s b_c \left(\frac{A_g}{A_{ch}} - 1 \right) f'_c / f_{yt}] \quad \text{Equation 2.2}$$

Beam cross sections for P-type beams are shown in Figures 21 and 23, where the transverse reinforcement was designed such that 0.75 times the nominal shear strength exceeded the shear force associated with the probable flexural strength being developed at both ends of the beam. The shear strength attributed to the concrete was zero. The resulting longitudinal spacing of transverse reinforcement for P80-2.5 and P100-2.5 was 3.5 in. (89 mm) and 3 in. (76 mm), respectively. These spacings satisfied ACI 318-14 Section 18.6.4.4^[1].

Following recommendations by NIST GCR 14-917-30^[17], the maximum spacing of transverse reinforcement for both D-type and P-type beams was limited to $5d_b$ for beams with Grade 80 (550) longitudinal reinforcement and $4d_b$ for beams with Grade 100 or 120 (690 or 830) longitudinal reinforcement.

D-type specimens had ten secondary longitudinal No. 3 (10) bars distributed around the perimeter of the beam such that each secondary longitudinal bar was supported by either a crosstie or a corner of a hoop. These bars were Grade 80 (550) for all specimens except for D120-2.5, where all bars were Grade 120 (830). Consistent with the detailing recommended in the ACI Building Code^[1] commentary, the secondary longitudinal reinforcement was terminated 2 in. (51 mm) into the top and bottom blocks for all specimens except D120-2.5. The No. 3 (10)

longitudinal bars in D120-2.5 were extended into the end blocks a length sufficient to develop a stress of $1.25f_y$. This deviation, along with the Grade 120 (830) transverse reinforcement, was done to explore whether developing the secondary longitudinal reinforcement and providing excess transverse reinforcement (by means of higher f_{yt}) would cause improved deformation capacity by inhibiting the concentration of damage at the block-beam interfaces.

2.1.2 Materials

2.1.2.1 Concrete

Ready-mix concrete with a maximum aggregate size of 0.5 in. (13 mm), provided by a local supplier, was used to cast the specimens. The specified compressive strength (f'_c) was 8,000 psi (55 MPa). The measured compressive and tensile strengths of concrete (f_{cm} and f_{ct} in Table 2) were obtained from tests of 6 by 12 in. (150 by 300 mm) standard concrete cylinders following ASTM C39^[9] and C496^[11]. Slump of the plastic concrete was obtained in accordance with ASTM C143^[10]. Slump measurements and concrete mixture proportions are shown in Table 3.

2.1.2.2 Reinforcing Steel

Deformed steel reinforcing bars were used for all reinforcement. Mill certifications for reinforcing bars used as Grade 80 and 100 (550 and 690) showed compliance with ASTM A615^[6] Grades 80 and 100 (550 and 690). Mill certifications for reinforcing bars used as Grade 120 (830) showed compliance with ASTM A1035^[8] Grade 120 (830). Mechanical properties of reinforcing bars (Table 4) used in the beams were obtained from tensile tests in accordance with ASTM A370^[5]. Figure 24 shows sample tensile test results of the six types of reinforcing bars used in the coupling beams.

Reinforcement used to construct the top and bottom blocks was Grade 60 (420) and complied with ASTM A615^[6] Grade 60 (420).

2.1.3 Construction

Photos taken during various stages of specimen construction are shown in Figures B.1 through B.8 of Appendix B. The specimens were cast monolithically with the top and bottom block formwork lying flat on the laboratory floor. The coupling beam concrete was supported with elevated wood formwork because the width of the beams was narrower than the width of the end blocks. Construction of each specimen included the assembly of reinforcing bar cages, installation of strain gauges on relevant reinforcing bars, construction of wooden formwork, and placement of the concrete. After casting, specimens and cylinders were covered with wet burlap and plastic sheets until formwork removal three to five days after casting. Specimens were kept in a climate-controlled laboratory from casting to testing.

2.2 Test Setup

The test setup is shown in Figures 25 through 27. The bottom block of each specimen was bolted to the laboratory strong floor with two unbonded 2.5-in. (64-mm) diameter high-strength threaded rods passing through the bottom block and strong floor. Two hydraulic actuators acting in parallel were used to load the specimens. The actuators each have a stroke length of 40 in. (1020 mm) and a force capacity of 220 kips (980 kN). The two actuators were connected to the strong wall and the specimen by means of vertically oriented HP steel sections. Actuator elevations are indicated in Table 5 and illustrated in Figures 28 through 30. One of the HP sections was connected to the top block of the specimen with two hollow structural steel (HSS) sections (acting as a spacer) transmitting compression when the actuators pushed the specimen and six unbonded

2.25-in. (57-mm) diameter high-strength threaded rods transmitting tension when the actuators pulled the specimen. Additional steel fixtures were used to externally brace the HP section against out-of-plane motions. Mirrored steel (attached to the HP section), nylon pads (attached to the external bracing system), and white lithium grease (between the mirrored steel and nylon pads) were used to minimize friction between the HP section and the external bracing.

2.3 Instrumentation

Several instruments were used to record specimen response during the tests: one linear variable differential transformers (LVDT) and load cell integral to each actuator; two LVDTs attached to the top block; an infrared non-contact position measurement system; and strain gauges attached to reinforcing bars. Actuator load cell data were used to report the applied shear throughout the tests. LVDT data are not reported because they are redundant with data from the infrared position measurement system.

2.3.1 Linear Variable Differential Transformers (LVDTs)

Movement of the top block was recorded with two LVDTs (Figure 31). These results were used to validate the measurements made with the infrared position measurement system. These LVDTs were attached to the top block face opposite to the actuators, horizontally centered with respect to the thickness of the top block. They were located approximately 24 and 36 in. (610 and 910 mm) above the bottom of the top block.

2.3.2 Infrared Non-Contact Position Measurement System

The motion capture system recorded the positions of optical markers attached to the surface of each specimen (63, 83, or 94 markers for beams with aspect ratios of 1.5, 2.5 or 3.5) and three

optical markers attached to a rigid stand on the laboratory floor. The markers emit infrared light pulses that are detected by the infrared camera system. The spatial coordinates of the markers were triangulated and recorded throughout the tests. The markers were arranged in a 4-in. (100-mm) square grid over one face of the coupling beam and part of the top and bottom blocks, as shown in Figure 32.

2.3.3 Strain Gauges

Several 120-ohm electrical resistance strain gauges were applied to selected reinforcing bars prior to casting. D-type specimens were instrumented with at least 31 strain gauges and P-type specimens with at least 22. Figures 33 and 34 generically show locations where a strain gauge was used in at least one specimen. Tables 6 and 7 identify the strain gauge locations for each specimen and indicate which gauges malfunctioned prior to testing. Strain gauges on diagonal reinforcement (D in D-type beams) and developed longitudinal reinforcement (P in P-type beams and H in D120-2.5) were rated for 15% strain (150 millistrains) to allow strain measurements near fracture elongation of reinforcement. The remaining strain gauges were rated for 5% strain.

2.4 Loading Protocol

Specimens were subjected to a series of reversed cyclic displacements following the protocol described in Table 8 and shown in Figure 35, patterned after the protocol recommended in FEMA 461^[14]. Several small cycles were imposed prior to testing (with forces too small to cause cracking) to facilitate tightening of the threaded rods connecting the bottom block to the strong floor and the top block to the actuators. Force-based control was used for the first few cycles of loading before yielding of the reinforcement. Displacement-based control was used starting at 0.5% chord rotation for beams with aspect ratios of 1.5 and 2.5 and 0.75% chord rotation for beams

with an aspect ratio of 3.5. Testing continued until the beam residual strength was nearly 20% of the peak strength, provided instability was not a concern.

The weight of all fixtures (HP sections, spacer sections, steel plates, and actuators) eccentrically attached to the specimen (Figure 25) caused a permanent moment of approximately 42 ft-kips (57 m-kN) prior to loading. At the start of the test, an equal and opposite moment was applied using the actuators.

Applied forces or displacements were selected to minimize the relative rotation between top and bottom blocks (i.e., the difference between the top block rotation and the bottom block rotation). This was done to ensure that double-curvature was imposed on the coupling beam, resulting in an inflection point near beam midspan.

The loading rates are given in Table 8 for coupling beams with aspect ratios of 1.5 and 2.5; coupling beams with an aspect ratio of 3.5 were tested at twice the given rates. Loading rates were periodically increased in increments of 0.01 in./sec (0.25 mm/sec) as chord rotation demands increased.

CHAPTER 3: EXPERIMENTAL RESULTS

3.1 Measured Shear versus Chord Rotation

Chord rotation (CR) of the coupling beam is defined as the displacement of the top block relative to the bottom block divided by the length of the beam clear span and corrected for rotation of the top and bottom blocks:

$$CR = \frac{\delta_{top} - \delta_{bot}}{l_n} - \frac{\theta_{top} + \theta_{bot}}{2} \quad \text{Equation 3.1}$$

Figure 36 shows the generalized deformed shape of a coupling beam with displacement and rotational components identified. The chord rotation represents the average of the relative rotation at each end of the coupling beam. Figure 36 corresponds to a specimen elevation view from laboratory north with the top block displacement (δ_{top}) and bottom block displacement (δ_{bot}) positive when moving eastward (away from the laboratory strong wall). Figure 36 also shows positive top block rotation (θ_{top}) and bottom block rotation (θ_{bot}) as counterclockwise rotation when viewed from laboratory north.

Displacements and rotations were calculated from measurements obtained with the infrared non-contact position measuring system (Section 2.3.1) and checked with data from the redundant LVDTs. The infrared markers were offset from the edges of the top and bottom blocks by approximately 2.5 in. (64 mm) to reduce the probability of losing an end-block marker (due to concrete spalling) during the test. This offset was accounted for in the components of Equation 3.1.

3.2 Specimen Response and Observations

The eleven specimens described in Chapter 2 were subjected to the loading protocol discussed in Section 2.4. Table 9 summarizes the deformation capacity and maximum shear of each coupling beam. Maximum shear stress was normalized by the square root of the concrete compressive strength at the time of testing (f_{cm} in Table 2). General observations during testing of each specimen are summarized in Sections 3.2.1 through 3.2.11.

The measured force-deformation relationships for each coupling beam are plotted in Figures 37 through 47 in terms of shear versus chord rotation and discussed in the following sections. A shear-chord rotation envelope for each coupling beam was developed in accordance with ASCE 41-17 Section 7.6.3.1.1^[4] by connecting the maximum displacement of the first cycle of each loading step. The envelopes thus generated were superimposed on the measured shear-chord rotation data in Figures 48 through 58. Coordinates of the breakpoints for the envelopes are listed in Tables 10 through 13.

Two definitions were used for deformation capacity or chord rotation capacity in Table 9. The first, called Deformation Capacity A, was defined as the average of the maximum chord rotation reached in each loading direction while sustaining 80% of the maximum strength in that loading direction. The second, called Deformation Capacity B, was defined as the average of the chord rotations in each loading direction where the envelope of the shear versus chord rotation curve formed by connecting the maximum chord rotation of the first cycle of each loading step intersects with 80% of the maximum applied shear (in each loading direction).

Both definitions of chord rotation capacity are provided because the distinctions may appeal to designers and researchers differently. Deformation Capacity A is a more stringent

appraisal of chord rotation capacity and represents chord rotations the coupling beam was actually subjected to. Deformation Capacity B, which is based on an envelope drawn according to ASCE 41-17^[4], is based on the assumption that force-deformation relationships are represented by linear interpolations between measured values. Deformation Capacity B is less sensitive to loading protocol than Deformation Capacity A and is also always greater than or equal to Deformation Capacity A. Deformation capacity in this report refers to Deformation Capacity B unless otherwise noted.

The deformation capacity of each D-type beam is shown in Figure 59, organized by aspect ratio (ℓ_n/h) and measured yield stress (f_{ym}) of the diagonal reinforcement. Deformation capacity for D-type beams is positively correlated to aspect ratio and negatively correlated to the yield stress of the diagonal reinforcement. The deformation capacity of D120-2.5 deviates from the trend shown by the beams with aspect ratios of 2.5. This may be attributable to the higher ρf_{yt} and/or the fully-developed secondary longitudinal reinforcement distributing the damage away from the beam-end interfaces.

3.2.1 D80-1.5

Measured shear force is plotted versus chord rotation in Figure 37 for D80-1.5. The coupling beam completed both cycles to 6% chord rotation (Step 10 of the loading protocol in Table 8) before strength notably diminished. The second excursion to -6% reached a shear of approximately 80% of the strength after at least one bar fractured. This resulted in a deformation capacity of 6.9% (as reported in Table 9). One cycle to 8% chord rotation (Step 11 in Table 8) was completed before the test was terminated. Strength loss was initiated by buckling of diagonal bars which fractured in subsequent opposite loading cycles.

3.2.2 D100-1.5

Measured shear force is plotted versus chord rotation in Figure 38 for D100-1.5. This coupling beam completed both cycles to 4% chord rotation (Step 9) before multiple bar fractures occurred during the first cycle to 6% and strength diminished rapidly. This resulted in a deformation capacity of 5.3% (as reported in Table 9). One excursion to +8% chord rotation (Step 11) was attempted but aborted at approximately +6.1% due to stability concerns from the numerous bar fractures during the previous loading cycle (Step 10B). Strength loss was initiated by buckling of the diagonal bars followed by bar fractures in subsequent cycles.

3.2.3 D120-1.5

Measured shear force is plotted versus chord rotation in Figure 39 for D120-1.5. The coupling beam completed both cycles to 3% chord rotation (Step 8) and the first excursion to 4%. However, an exception to the testing protocol occurred during the first excursion to -4% (Step 9). The coupling beam displaced through -4.9% before fracturing all reinforcing bars in one group of diagonal bars near the top end of the beam. The sudden bar fractures caused a large increase in top block rotation, resulting in a large increase in chord rotation to 8.1%. There was no prior evidence of bar buckling or fracture. The test resumed with cycles to 4% and 6% chord rotations (Steps 9 and 10). The deformation capacity was 5.2% based on the definition of Deformation Capacity B (as reported in Table 9).

Reinforcing bar fractures near -5% suggest that the beam would not have completed Step 10 if the exception to the loading protocol had not occurred. Failure was imminent regardless of the testing protocol. It was observed after testing that all four reinforcing bars in one of the diagonal-bar bundles near the top of the coupling beam had fractured.

3.2.4 D80-2.5

Measured shear force is plotted versus chord rotation in Figure 40 for D80-2.5. The coupling beam completed two cycles to 6% chord rotation (Step 10) and half of a cycle to 8% chord rotation before strength diminished by more than 20%. This resulted in a deformation capacity of 7.6% (as reported in Table 9). One cycle to 10% chord rotation (Step 12) was completed before the test was terminated. Strength loss was due to fracture of diagonal bars near the ends of the coupling beam after they were observed to have buckled in a prior cycle.

3.2.5 D100-2.5

Measured shear force is plotted versus chord rotation for D100-2.5 in Figure 41. The coupling beam reached chord rotations of -4.7%^a and +6% in each loading direction before a 20% loss of strength, resulting in a deformation capacity of 6% (as reported in Table 9). Loading continued until nearly two cycles at 8% chord rotation (Step 11) were completed. Strength loss was caused by fracture of one set of diagonal bars near the top end of the coupling beam after they were observed to have buckled in a prior cycle.

3.2.6 D120-2.5

Measured shear force is plotted versus chord rotation for D120-2.5 in Figure 42. The deformation capacity of the coupling beam was 6.9% (as reported in Table 9). Beam strength began to diminish in the first cycle to 6% with bar fractures occurring during the second excursion to +6%. Loading continued until completion of two cycles to 8% (Step 11). Strength loss was associated with hoop opening and bar buckling followed by bar fracture in both diagonal bundles

^a A chord rotation of 4% was targeted.

near the bottom end of the coupling beam. Several longitudinal No. 3 bars also fractured. D120-2.5 had longitudinal No. 3 bars extended into the end blocks for a length sufficient to develop 1.25 times the specified yield stress of the bar at the face of the end blocks. This may have contributed to achieving a maximum shear stress of $15\sqrt{f'_c}$ psi ($1.25\sqrt{f'_c}$ MPa).

3.2.7 D80-3.5

Measured shear force is plotted versus chord rotation in Figure 43 for D80-3.5. The coupling beam completed one cycle to 8% chord rotation (Step 11) before bar fractures occurred during the second excursion to +8% with a strength loss of approximately 30%. This resulted in a deformation capacity of 8.6% (as reported in Table 9). Testing continued through one cycle of 10% (Step 12). A second excursion to +10% chord rotation was attempted but aborted due to numerous bar fractures at approximately +3%. Strength loss was due to buckling followed by fracture of diagonal bars near the ends of the coupling beam.

3.2.8 D100-3.5

Measured shear force is plotted versus chord rotation in Figure 44 for D100-3.5. The coupling beam completed one cycle to 6% chord rotation (Step 10) before bar fractures occurred during the second excursion to +6% with a strength loss of nearly 20%. This resulted in a deformation capacity of 6.8% (as reported in Table 9). Testing continued through one cycle of 10% (Step 12). Strength loss was due to fractures of diagonal bars near the ends of the coupling beam after they were observed to have buckled in previous cycles. Large out-of-plane deformations (2.7% of the beam clear span) occurred during the second cycle to 6% chord rotation.

3.2.9 D120-3.5

Measured shear force is plotted versus chord rotation in Figure 45 for D120-3.5. The coupling beam completed one cycle to 6% chord rotation (Step 10) before bar fractures occurred during the second excursion to +6% with a strength loss of nearly 80%. This resulted in a deformation capacity of 6.7% (as reported in Table 9). Testing continued through two cycles of 8% (Step 11). Strength loss was due to buckling followed by fracture of diagonal bars near the ends of the coupling beam.

Continuous data from the position tracking marker system are unavailable after the second 2% cycle (Step 7) due to a recording error of the primary data acquisition system. However, shear-chord rotation coordinates were also recorded each time the test was paused with independent software that used optical character recognition to capture in real-time the display of the primary data acquisition system. These discrete data are shown in Figure 45 as hollow points connected with dotted lines.

3.2.10 P80-2.5

Test results are plotted for P80-2.5 in terms of measured shear force versus chord rotation in Figure 46. The deformation capacity of the coupling beam was 3.9% (as reported in Table 9). Although strength began to diminish in the second excursion to a chord rotation of -3%, the first excursion to +4% reached a shear that was greater than 80% of the strength in the positive loading direction. Loading continued until two cycles to 6% chord rotation (Step 10) had been completed. No bar fracture was observed during the test. Strength loss was due to shear strength decay, with damage concentrated near the ends of the coupling beam.

3.2.11 P100-2.5

Test results are plotted for P100-2.5 in terms of measured shear force versus chord rotation in Figure 47. The chord rotation capacity of the coupling beam was 4.1% (as reported in Table 9). The first cycle to +3% was the last cycle to exceed 80% of the strength in the positive loading direction. The second excursion to a chord rotation of -3% reached a shear nearly equal to 80% of the strength in the negative loading direction, while the first excursion to -4% exceeded the 80% threshold. Loading continued until two cycles to 6% chord rotation (Step 10) had been completed. No bar fracture was observed after the test. Strength loss was due to shear strength decay associated with damage near the ends of the coupling beam.

3.3 ASCE 41 Envelopes

Figures 60 through 64 show the shear-chord rotation envelopes of the tested beams grouped by aspect ratio (ℓ_n/h of 1.5, 2.5, or 1.5) and reinforcement layout (D- or P-type beams). The plots also include the generalized force-deformation curve for modeling coupling beams as defined in ASCE 41-17 Table 10-19^[4]. The coordinates of points A through E are based on Figure 10-1(b)^[4] (shown in Figure 65), which depend on parameters c , d , and e in Table 10-19^[4]. For D-type beams, Table 10 19^[4] gives $c = 0.8$, $d = 0.03$, and $e = 0.05$. For P-type beams with conforming transverse reinforcement and shear stresses greater than or equal to $6\sqrt{f'_c} b_w d$ psi ($0.5\sqrt{f'_c} b_w d$ MPa), Table 10 19^[4] gives $c = 0.5$, $d = 0.02$, and $e = 0.04$. Parameters c , d , and e correspond, respectively, to the residual strength ratio (or shear at points D and E in relation to point B); the deformation at peak force (or chord rotation at point C); and the maximum deformation before total loss of strength (or chord rotation at point E). In ASCE 41-17^[4], point B is generally associated with the

calculated member strength based on the measured yield strength of reinforcement f_{ym} , whereas point C is generally based on $1.25f_{ym}$.

For D-type beams, the ordinate of point B in Figures 60 through 62 was determined based on the target design shear stress of $8\sqrt{f'_c}$ psi ($0.67\sqrt{f'_c}$ MPa), as indicated by the average v_e in Table 1, and the ordinate of point C was based on $10\sqrt{f'_c}$ psi ($0.83\sqrt{f'_c}$ MPa), or 5/4 of the ordinate of point B.

For P-type beams, the ordinate of point C in Figure 63 was determined based on the target design shear stress of $6\sqrt{f'_c}$ psi ($0.5\sqrt{f'_c}$ MPa), as indicated by the average v_e in Table 1, and the ordinate of point B was based on $4.8\sqrt{f'_c}$ psi ($0.40\sqrt{f'_c}$ MPa), or 4/5 of the ordinate of point C.

The slope from points A to B (initial stiffness) was calculated based on ASCE 41-17 Table 10-5^[4] using a flexural rigidity of $E_c I_{eff}$, where $I_{eff} = 0.3I_g$, and a shear rigidity of $G_c A_{eff}$, where $A_{eff} = 1.0A_w$. The initial slope of the shear versus chord rotation curve (in units of force/rad) is given by

$$K = \frac{1}{\frac{l_n^2}{12E_c I_{eff}} + \frac{1}{G_c A_{eff}}} \quad \text{Equation 3.2}$$

Figures 60 through 63 show Point B was not enclosed by the envelopes of any of the coupling beams, which indicates that the beams had less stiffness than expected based on the ASCE 41-17^[4] provisions. Beam stiffness is discussed in more detail in Section 3.6.

Figures 60 through 63 show that envelopes from the measured test data of each coupling beam exceeded the chord rotation capacity that ASCE 41-17^[4] assigns to coupling beams that are compliant with ACI 318-14^[1].

Figure 63 shows that the shear strength exhibited by P100-2.5 was higher than the shear force at point C though the shear strength of P80-2.5 was not. This can be attributed to the different design strengths of the P-type beams. The design shear stresses of P80-2.5 and P100-2.5 were 5.2 and $6.4\sqrt{f'_c}$ psi (0.43 and $0.53\sqrt{f'_c}$ MPa), respectively. When the shear force applied to each P-type beam is normalized by the shear force associated with the nominal flexural strength (M_{nm}), as shown in Figure 64, both P-type beams exceeded the normalized shear at point B, which is shown as ± 1.0 , indicating that both beams exceeded their nominal strength. However, neither P-type beam reached a peak that exceeded the normalized shear at point C, which is shown as ± 1.25 . This indicates that an acceptable upper bound for the shear demand in P-type coupling beams may be determined using $1.25M_{nm}$.

3.4 Progression of Damage

The condition of the specimens (viewed from the south) during the last cycle to target chord rotations of 2, 4, 6, 8, and 10% are shown in Figures C.1 through C.109 of Appendix C. The locations of necked and fractured bars were recorded after each test, as shown in Figures 66 through 76.

The first flexural cracks in each test were frequently observed during the first cycle to 0.2% chord rotation. Flexural and shear cracks continued to develop until testing ceased but most cracks initiated before 2% chord rotation, after which cracks primarily widened and lengthened.

Horizontal cracking, associated with flexural cracking, was observed on both 12-in. (300-mm) faces of the coupling beam. When these cracks penetrated through the 18-in. (460-mm) depth of the coupling beam, some remained perpendicular to the beam longitudinal axis but they frequently developed into inclined flexure-shear cracks. Horizontal cracks were most likely to become inclined away from the beam ends but toward the nearest support.

All specimens had horizontal cracks extending across the 18-in. (460-mm) beam depth at both ends of the coupling beam early in the tests. These cracks tended to become wide as rotations concentrated near the face of the top and bottom blocks. These concentrated rotations are attributed to elongation and slip of the longitudinal reinforcement inside the end blocks, also referred to as strain penetration.

Inclined (shear) cracks formed along the 18-in. (460-mm) face of the beam, primarily developing from the tips of horizontal (flexural) cracks. Most inclined cracks were oriented at approximately 45 degrees from the beam longitudinal axis. Corner to corner cracks only occurred in the beams with an aspect ratio of 1.5, see cracks on D80-1.5 (Figure C.1) or D120-1.5 (Figure C.20). The spacing of inclined cracks was fairly even near midspan of the beams.

Most of the fractured diagonal reinforcement was observed to buckle in a half-cycle prior to fracturing. For example, buckling of reinforcing bars in the bottom west bar bundle of D80-1.5 was observed at -6% chord rotation (shown in Figure C.8) followed by bar fracture en route to +8% chord rotation (shown in Figure C.9). This type of buckling-induced fracture may be due to the bar exceeding a “critical bending strain” from large curvature demands on the bar during buckling. The testing of Barcley and Kowalsky (2019)^[13] showed that the magnitude of the imposed strain due to buckling influences the tensile strain capacity of reinforcing bars tested

under cyclic loading. No visible buckling, necking, or fracture was observed for the primary longitudinal reinforcement in the P-type beams. However, the primary longitudinal reinforcement was deformed laterally (shown in Figure C.99) near the coupling beam ends as a result of concentrated shear deformations (also referred to as sliding shear).

One beam end exhibited more damage than the other in most specimens. Differences between beam ends were least pronounced in D80-1.5, D80-2.5, D120-2.5, and D80-3.5, which are shown near final loading steps in Figures C.2, C.29, C.51, and C.61. This list consists of the three D-type specimens with Grade 80 (550) primary reinforcement and the single D-type Grade 120 (830) specimen with developed No. 3 (10) secondary longitudinal reinforcement. The more symmetrical behavior in the Grade 80 (550) beams may be due to reduced occurrence of buckling. It is likely that fewer Grade 80 (550) diagonal bars buckled because spacing of transverse reinforcement in all D-type beams was identical (3 in. [76 mm]). The likelihood of buckling for Grade 80 (550) bars was reduced due to lower stress demands (associated with their lower yield stress). In addition, some Grade 80 (550) diagonals used larger diameter bars with lower slenderness ratios.

The development of the No. 3 (10) reinforcement in D120-2.5 likely contributed to the more symmetric observed damage because it forced beam deformations to be less concentrated at the beam ends. During chord rotation cycles to 6%, specimens D100-1.5 and D120-1.5 (Figures C.12 and C.21) with secondary longitudinal reinforcement terminating at 2 in. (51 mm) into the end blocks had damage concentrated near the beam ends. During chord rotation cycles to 6%, D100-2.5 (Figure C.41) had concrete loss due to crushing or spalling extending approximately 3 to 4 in. (76 and 100 mm) away from the end blocks. The damage at the bottom end was primarily localized in the bottom east corner, corresponding to the compression zone for positive chord

rotations. The damage to the top end was distributed across the entire 18-in. (460-mm) beam width. In contrast, D120-2.5 at chord rotations of -6% (Figure C.51) had visible damage to its concrete across the entire 18-in. (460-mm) beam width and extended approximately 8 in. (200 mm) away from the face of the end blocks.

3.5 Calculated and Measured Strengths of Specimens

Table 14 shows the maximum measured and calculated strengths for each specimen and the measured-to-calculated strength ratio. The calculated shear strength of the D-type beams, V_{nm} , was obtained by substituting measured yield stress, f_{ym} , into Equation 2.1, which corresponds to the nominal strength of a diagonally-reinforced coupling beam according to ACI 318-14 Section 18.10.7.4.a^[1]. The developed No. 3 (10) reinforcement in D120-2.5 were not considered in calculations as the ACI equation neglects developed longitudinal reinforcement in diagonally-reinforced coupling beams.

The calculated strength of the P-type beams, V_{nm} , corresponds to the shear stress associated with the nominal flexural strength occurring at both ends of the beam, calculated using a tensile bar stress of $1.0f_{ym}$, a concrete compressive strength of f_{cm} , and including the contribution of reinforcement in compression. Values of f_{cm} and f_{ym} were taken from Tables 2 and 4.

The average ratio of measured-to-calculated strength was 1.48 for D-type beams and 1.15 for P-type beams. The higher average ratio for D-type beams may be because the calculated strength, V_{nm} , depends only on the diagonal reinforcement and neglects the contribution of the concrete and transverse reinforcement. These results are consistent with those from other studies^[3, 15, 16]. The ratios for the D-type beams ranged from 1.28 to 1.68, excluding D120-2.5 which had a

ratio of 1.90 partly due to developing the No. 3 (10) bars (secondary longitudinal reinforcement) into the end blocks. All of the measured-to-calculated strength ratios for D120 beams were higher than those of D80 and D100 beams with the same aspect ratio.

For D-type beams, the measured-to-calculated strength ratio would reduce from 1.48 to 1.18 if the strength is estimated using $1.25f_{ym}$ instead of $1.0f_{ym}$. Alternative calculations based on probable flexural strength (using $1.25f_{ym}$) and accounting for the projected area of steel may also provide additional accuracy. This is further examined in other work^[3, 15, 18].

3.6 Stiffness

Secant stiffness (K_S) refers to the slope of a line drawn from a point at the origin of the force-deformation envelope to any other point on the envelope. Secant stiffness was calculated with Equation 3.3. This definition of stiffness is based on deformations defined using chord rotation times clear span length ($CR l_n$). For each of the coordinates (CR, V) presented in Tables 10 through 13, the corresponding K_S are tabulated.

$$K_S = \frac{V}{CR l_n} \quad \text{Equation 3.3}$$

Shear-chord rotation envelope data, shown in Tables 10 through 13, were used to estimate the initial stiffness (K_e) and the corresponding effective moment of inertia (I_{eff}) for each of the coupling beams. The initial stiffness was defined as the secant stiffness to a notional first yield, which was assumed to occur at a shear equal to $0.75V_{max}$. Two initial stiffness values were determined for each coupling beam, one for each loading direction. This definition of initial stiffness was selected because it is simple and it was observed that tangential stiffness visibly

decreased beyond the assumed notional first yield. Chord rotations (CR_{75}) associated with $0.75 V_{max}$ are listed in Tables 10 through 13 and identified with a diamond in the envelopes of shear versus chord rotation in Figures 77 through 80.

Values of K_e in the positive loading direction ranged from 990 kips/in. (173 kN/mm) in D80-1.5 to 167 kips/in. (29 kN/mm) in D120-3.5. Although similar stiffness values were expected for both loading directions, minor differences were observed. Values of K_e in the negative loading direction were within 7% of its positive loading counterpart for beams with aspect ratios of 2.5 and 3.5 but a difference of up to 22% was observed for beams with aspect ratios of 1.5. The greater difference for beams with aspect ratios of 1.5 was in part due to the smaller displacement associated with the first yield of beams with a clear span of 27 in. (690 mm). Note that a chord rotation of $CR_{75} = -0.55\%$, as seen in Table 10 for D80-1.5, corresponds to a displacement (corrected for relative rotation of the end blocks) of -0.15 in. (3.8 mm).

Values of K_e were negatively correlated to both beam aspect ratio and primary reinforcement grade. The average values of K_e for the D-type beams with an aspect ratio of 1.5, 2.5, and 3.5 were 920, 362, and 206 kips/in. (160, 63, and 36 kN/mm), respectively. For P-type beams with an aspect ratio of 2.5, the average value of K_e was 277 kips/in. (49 kN/mm).

Comparisons among beams grouped by grade of the primary reinforcement show that K_e was inversely proportional to reinforcement grade. This observation is consistent with the coupling beam test data reported by Ameen^[3]. Values of K_e for D80-1.5 were approximately 20% greater than K_e for D100-1.5 and approximately 50% greater than K_e for D120-1.5. A similar trend was observed for D80-3.5 when compared with D100-3.5 and D120-3.5. Values of K_e for P80-2.5 were approximately 20% greater than K_e for P100-2.5.

An effective moment of inertia (I_{eff}) for both loading directions was calculated using Equation 3.4, which attributes all deformations to flexure. Values of I_{eff} are plotted in Figures 81 and 82 as the ratio of I_{eff} to either the gross moment of inertia (I_g) or transformed uncracked moment of inertia (I_{tr}). For D-type beams, the value of I_{tr} accounts for the projected area of the diagonal steel bars and the net area of concrete.

$$I_{eff} = \frac{0.75 V_{max} l_n^2}{12 E_c CR_{75}} \quad \text{Equation 3.4}$$

The effective moments of inertia normalized by I_g and I_{tr} in Figures 81 and 82 have similar trends. Both aspect ratio (l_n/h) and I_{eff}/I_g were positively correlated for D-type beams, with average values of 0.05, 0.09, and 0.14 for l_n/h of 1.5, 2.5, and 3.5, respectively. The average I_{eff}/I_g for P-type beams was approximately 0.07. The positive correlation of I_{eff}/I_g and I_{eff}/I_{tr} to l_n/h may in part be due to the more important role of shear deformations in the behavior of beams with small l_n/h . In other words, I_{eff}/I_g was lower for beams with higher shear deformations than for those with lower shear deformations. The negative correlation between reinforcement grade and both I_{eff}/I_g and I_{eff}/I_{tr} is attributed to the amount of longitudinal reinforcement used in the beams, which was inversely proportional to the steel grade. Beams with l_n/h of 3.5, namely, D80-3.5, D100-3.5, and D120-3.5, had I_{eff}/I_{tr} of 0.13, 0.11, and 0.09, respectively. The trend was less pronounced in D-type beams with l_n/h of 2.5, but this was expected because D120-2.5 had the secondary longitudinal reinforcement developed into the end blocks, which may have increased the cracked stiffness of the beam.

3.7 Measured Reinforcement Strains

Reinforcing bars were instrumented with electrical resistance strain gauges as described in Section 2.3.3 and listed in Tables 6 and 7. All strain gauge data are reported assuming zero strain in the reinforcement at the start of the tests. The layout of strain gauges is shown in Figures 33 and 34. Measured strain data versus chord rotation are shown in Figures 83 through 446 with a sketch of the specimen reinforcement and the location (circled) of the strain gauge providing the plotted data. The figures are sorted by specimen identification followed by strain gauge identification: D for Diagonal bars in D-type beams; P for primary Parallel bars in P-type beams; S for closed Stirrups; H for secondary Horizontal longitudinal bars in D-type beams; and T for Transverse cross-ties. Bars with H gauges were in the horizontal position during casting.

Figures 447 through 488 show the envelope of measured strains at the peak chord rotation of each loading step (Table 8). It is important to note that higher strains may have occurred during a cycle that did not define the peak chord rotation for a loading step (which involves two cycles). Each of these figures contain data from all gauges of one type (D, P, S, H, or T) in a single specimen. For example, Figure 447 shows strain maxima measured with D strain gauges in D80-1.5 at discrete points corresponding to the peak chord rotation of each loading step. The text labels in Figures 447 through 488 identify which strain gauge corresponds to each curve shown. The text labels were vertically translated to avoid overlap. The ends of each curve have an “x” indicating the chord rotation at which the gauge became inoperable and an open circle identifies the overall maximum strain recorded for the reported gauge type. Figures 447 through 488 also include a heavier black line to represent the overall strain envelope for that gauge type in that specimen. To facilitate comparisons among specimens, the overall envelopes are grouped in Figures 489 through 503 based on reinforcement layout (D- or P-type) and aspect ratio (1.5, 2.5,

or 3.5). For example, Figure 489 shows the envelopes of strains measured with D strain gauges in D-type beams with an aspect ratio of 1.5.

In the following sections, strain gauge data are occasionally used as a basis for stating that the reinforcement yielded at a certain point during the test. For the purpose of this discussion, strains in excess of 0.3, 0.4, and 0.5% (3, 4, and 5 millistrains) are taken to be indicative of yielding for Grade 80, 100, and 120 (550, 690, and 830) reinforcement, respectively. More precise statements regarding the initiation of yielding are not made for several reasons: 1) effects of concrete shrinkage on bar strains at the start of the test are neglected, 2) strain gauges measure bar strains at discrete locations that may not coincide with the location of maximum strain, and 3) stress-strain curves for high-strength reinforcement do not generally show a well-defined yield plateau.

A change in slope in the strain versus chord rotation curves is apparent for beams with Grade 80 (550) reinforcement, which shows a well-defined yield plateau in Figure 24. A sharp change in slope is evident in Figures 212 and 214 for gauges D12 and D14 in D80-2.5. However, a more gradual change in slope occurred in Figures 268 and 269 for gauges D5 and D6 in D120-2.5 with Grade 120 (830) reinforcement, which lacked a well-defined yield plateau in Figure 24.

Continuous strain gauge data are not shown for D120-3.5 in Figures 372 through 402 after the second 2% cycle (end of Step 7 in Table 8) due to a recording error that occurred with the position tracking data acquisition system. The plots of strain gauge data versus chord rotation shown in Figures 372 through 402 show the strain for each gauge with the corresponding chord rotation recorded by a backup system based on optical character recognition (OCR) activated each

time the test was paused. The strain data synchronized with the recordings of the OCR system are shown with dashed lines and bounded by open circles.

3.7.1 Diagonal Reinforcement

The strain envelopes in Figures 489, 493, and 497 show the maximum strains measured on the diagonal reinforcement with D gauges in the D-type specimens. The location of the gauges are shown in Figure 33. No consistent patterns are discernible between the maximum strain measured with the D strain gauges and either reinforcement grade or aspect ratio. However, for chord rotations lower than 3%, specimens with Grade 120 (830) reinforcement tended to have lower strains than other specimens, particularly for D120-2.5, which had the secondary longitudinal reinforcement, No. 3 (10) bars developed into the end blocks.

Strain values consistent with yielding were observed in D gauges at both beam-end interfaces. Beams with primary reinforcement of higher grade and higher aspect ratio (l_n/h) experienced yielding at higher chord rotations. Maximum strain values were consistently measured in D gauges located at the beam-end interfaces (D5, D6, D13, and D14, see Figure 33).

Figures 489, 493, and 497 show that the highest strain in diagonal bars exceeded 5% (50 millistrains) in most specimens, and occasionally exceeded 7%. The highest strains generally occurred at chord rotations between 3 and 6%, with the higher chord rotations typically defined by beams with an aspect ratio of 3.5. In loading cycles where beam strength was decreasing, the reported maximum strain in diagonal bars appears to decrease. This is because gauges became inoperable where damage was most severe (and strains were highest). The envelopes (Figures 489, 493, and 497) were therefore based on working gauges where strains were relatively low at high chord rotations.

Figure 504 shows the maximum strain in the diagonal bars of D-type beams during any of the cycles of loading steps 5 through 9 (nominal chord rotations of 1 through 4%, see Table 8). For the limited test data, an upper bound estimate of maximum strain for D-type beams with aspect ratios of 1.5, 2.5, or 3.5 may be defined by $2CR$, which gives 8% strain for $CR = 4\%$.

3.7.2 Parallel Primary Reinforcement

The envelopes of strains measured with P gauges on the primary reinforcement (parallel to the beam longitudinal axis) in P-type specimens, are shown in Figure 501. The overall maximum measured strains were approximately 5% (50 millistrains) for P80-2.5 and 3% for P100-2.5, both considerably higher than the strain associated with yielding. The strains in P80-2.5 were similar in magnitude to the strains measured with D gauges in D-type specimens whereas the maximum strains in P100-2.5 were lower. This may be due to the absence of a yield plateau in the Grade 100 (690) reinforcement of P100-2.5.

The maximum strain measured with P gauges at the beam-end interfaces (P5, P6, P11, and P12, see Figure 34) exceeded 1%, see Figures 483 and 486. Strain gauge P6 in P80-2.5 (Figure 483) recorded the maximum strains throughout the chord rotation history, but gauge P6 malfunctioned in P100-2.5 and P5 became inoperable early in the test (Figure 486). The highest measured strains generally occurred at chord rotations higher than those corresponding to the maximum shear (see open circles at CR_{100} in Figure 501).

Figure 505 shows the maximum strain in the primary longitudinal reinforcement of P-type beams during any of the cycles of loading steps 5 through 9 (nominal chord rotations of 1 through 4%, see Table 8). Based on the limited test data, an upper bound estimate of maximum strain for

P-type beams with an aspect ratio of 2.5 may be defined by $1.5CR$, which gives 4.5% strain for $CR = 3\%$.

3.7.3 Parallel Secondary Reinforcement

Figure 33 shows the location of the H strain gauges on the secondary longitudinal reinforcement (parallel to the beam longitudinal axis) in D-type specimens. The strain envelopes for these gauges are shown in Figures 491, 495, and 499. All of the parallel secondary reinforcement in D-type specimens was Grade 80 (550), and only extended 2 in. (51 mm) into the end blocks, except for the secondary reinforcement in D120-2.5, which was Grade 120 (830) and extended nominally 17 in. (430 mm) into the end blocks.

The maximum strains measured with H gauges in D-type beams were highly variable, with maximum values recorded in gauges located approximately at one-third of the beam span (except for D120-2.5). Beams with an aspect ratio of 1.5 were the only ones with strain maxima (for H gauges) generally below yielding, strain well in excess of yielding was recorded in all other D-type beams.

Strain gauges at the beam-end interfaces of D120-2.5 recorded maximum values near 1.3% (13 millistrains, refer to gauges H1 and H2 in Figure 469), clearly indicating yielding of the reinforcement. High strain demands were expected in the H gauges of D120-2.5 due to the 17-in. (430-mm) embedment of the reinforcement into the end blocks.

3.7.4 Transverse Reinforcement

The strain envelopes for S gauges on the closed stirrups are shown in Figures 490, 494, 498, and 502 and those for T gauges on crossties are shown in Figures 492, 496, 500, and 503. The

locations of S and T gauges are shown in Figures 33 and 34. Grade 80 (550) transverse reinforcement was used in all beams except D120-2.5, which had Grade 120 (830) transverse reinforcement.

The maximum strains recorded by S gauges, for chord rotations lower than 6%, did not exceed 0.3% (3 millistrains) in any of the beams, except D120-2.5. The recorded strain from the closed stirrups in D120-2.5 was higher than D80-2.5 and D100-2.5, which indicates that the developed secondary longitudinal reinforcement had an effect on distributing damage into the beam span, with increased expansion of the concrete core and higher strains in the closed stirrups. However, strains higher than 0.5% were not recorded, indicating that the Grade 120 closed stirrups may not have yielded. Maximum recorded strain exceeded 0.3% in several of the S gauges in D120-2.5. Therefore, providing higher ρf_{yt} than required by ACI 318-14^[1] seemed to be effective and avoided yielding of the transverse reinforcement.

Crossties along both transverse directions were instrumented (T gauges) in D-type beams. The strain versus chord rotation envelopes (Figures 492, 496, 500, and 503) were nearly symmetrical for both loading directions. Maximum strains were generally below 0.3% in the Grade 80 (550) transverse reinforcement except for the single instrumented crosstie (T1) in P80-2.5, which approached 0.4%. No correlation with the grade of the primary longitudinal reinforcement or aspect ratio (l_n/h) was observed.

CHAPTER 4: CONCLUDING REMARKS

Experimental data are reported for eleven large-scale reinforced concrete coupling beams subjected to reversed cyclic displacements. This research was conducted to investigate the use of high-strength reinforcement in diagonally-reinforced (D-type) and moment frame (P-type) coupling beams. Variables included nominal yield stress of the primary longitudinal reinforcement (80, 100, and 120 ksi [550, 690, and 830 MPa]), span-to-depth (aspect) ratio (1.5, 2.5, and 3.5), and layout of primary longitudinal reinforcement (diagonal [D] and parallel [P]). All beams had the same nominal concrete compressive strength (8,000 psi [55 MPa]) and cross-sectional dimensions (12 by 18 in. [300 by 460 mm]). The D-type beams were designed for a target shear strength of $8\sqrt{f'_c} b_w h$ psi ($0.67\sqrt{f'_c} b_w h$ MPa) and the P-type beams for $6\sqrt{f'_c} b_w d$ psi ($0.5\sqrt{f'_c} b_w d$ MPa). All transverse reinforcement was Grade 80 (550) except for one D-type beam that had Grade 120 (830) transverse reinforcement (D120-2.5). A summary of the test data is listed in Table 15. The main findings and observations from this study are summarized as follows:

1. Chord rotation capacities of D-type beams with Grade 100 or Grade 120 (690 or 830) diagonal reinforcement were similar, with average deformation capacities of approximately 5, 6, and 7% for beams with aspect ratios of 1.5, 2.5, and 3.5, respectively. Deformation capacity was based on the average chord rotation (for positive and negative loading directions) corresponding to 20% loss of strength. These deformation capacities exceeded the minimum chord rotation capacities in ASCE 41-17^[4] for diagonally-reinforced coupling beams with shear stresses greater than or equal to $6\sqrt{f'_c}$ psi ($0.5\sqrt{f'_c}$ MPa).
2. D-type beams with Grade 80 (550) diagonal reinforcement exhibited approximately 25% higher chord rotation capacities, on average, than their Grade 100 or Grade 120 (690 or 830)

counterparts. The increased rotation capacity of the beams with Grade 80 (550) diagonal bars may be attributed to their lower ratio of f_y to s/d_b , where f_y is the yield stress of the diagonal bar, d_b is the diameter of the diagonal bar, and s is the spacing of the hoops, which delayed buckling of the Grade 80 (550) diagonal bars during testing.

3. Chord rotation capacities of P-type beams with Grade 80 or Grade 100 (550 or 690) longitudinal reinforcement were similar, with an average chord rotation capacity of approximately 4% for beams with an aspect ratio of 2.5.
4. Measured strength of D-type beams, on average, was nearly 50% higher than the calculated nominal shear strength (V_{nm} for a diagonally-reinforced coupling beam based on f_{ym}). Therefore, the expected strength of diagonally-reinforced coupling beams is generally underestimated when strength is based on only the contribution of the diagonal reinforcement.
5. Measured strength of P-type beams, on average, was approximately 15% higher than the calculated nominal flexural strength (M_{nm} for a moment frame beam based on f_{cm} and f_{ym}). Therefore, the probable flexural strength (based on $1.25f_y$) is generally conservative for determining the required shear reinforcement for these beams.
6. For the coupling beams of this study, the initial stiffness associated with the secant to 75% of the maximum shear (on the ascending branch of the shear-chord rotation envelope) was consistently lower than the recommended value in ASCE 41-17^[4]. The effective moment of inertia (I_{eff}) corresponding to the initial stiffness varied between $0.04I_g$ to $0.17I_g$, with the lower coefficient for beams with aspect ratios of 1.5 and higher for beams with aspect ratios of 3.5. These values of I_{eff} account for the effects of shear deformations and bar slip (or strain penetration into supports). For beams designed to a target strength (with constant ρf_y), the initial stiffness was inversely proportional to the reinforcement grade.

7. The chord rotation capacities of D-type beams with Grade 120 (830) diagonal reinforcement were nearly identical to those with Grade 100 (690) reinforcement, except for D120-2.5, which reached 6.9% compared with 6.0% for D100-2.5. The improved deformation capacity of D120-2.5 was attributed to the combined effects of 1) extending the non-diagonal longitudinal reinforcement into the end blocks to develop $1.25f_y$, which reduced localized damage at the beam-wall interface and 2) using higher grade of transverse reinforcement, Grade 120 (830) instead of 80 (550) with the same area and spacing as in the other D-type beams. Beam D120-2.5 reached a strength of $15\sqrt{f_{cm}}b_w h$ psi ($1.25\sqrt{f_{cm}}b_w h$ MPa) approximately 75% higher than the usable strength (ϕV_n) permitted in ACI 318-14^[1].
8. Strain gauge measurements in diagonal bars of nine D-type beams showed that maximum strains ranged between 3 and 8% at a chord rotation of 4%, with lower maxima occurring in D120-2.5, which had the secondary longitudinal reinforcement extended beyond the beam-wall interface to develop $1.25f_y$. Strain gauge data from the two P-type beams showed that maximum strains in the primary longitudinal bars reached 4.5% at a chord rotation of 3%.

REFERENCES

1. ACI 318 (2014). “Building Code Requirements for Structural Concrete (ACI 318-14) and Commentary (ACI 318R-14).” American Concrete Institute, Farmington Hills, Michigan.
2. ACI 408 (2003). “Bond and Development of Straight Reinforcing Bars in Tension (ACI 408R-03).” American Concrete Institute, Farmington Hills, Michigan.
3. Ameen, S. (2019). “Diagonally-Reinforced Concrete Coupling Beams with High-Strength Steel Bars.” PhD Dissertation, The University of Kansas, Lawrence, Kansas.
4. ASCE 41 (2017). “Seismic Evaluation and Retrofit of Existing Buildings (ASCE 41-17).” American Society of Civil Engineers, Reston, Virginia.
5. ASTM A370 (2017). “Standard Test Methods and Definitions for Mechanical Testing of Steel Products (ASTM A370-17).” ASTM International, West Conshohocken, Pennsylvania.
6. ASTM A615 (2016). “Standard Specification for Deformed and Plain Carbon-Steel Bars for Concrete Reinforcement (A615-16/A615M-16).” ASTM International, West Conshohocken, Pennsylvania.
7. ASTM A706 (2016). “Standard Specification for Deformed and Plain Low-Alloy Steel Bars for Concrete Reinforcement (ASTM A706/A706M-16).” ASTM International, West Conshohocken, Pennsylvania.
8. ASTM A1035 (2016). “Standard Specification for Deformed and Plain, Low-Carbon, Chromium, Steel Bars for Concrete Reinforcement (ASTM A1035/1035M-16b).” ASTM International, West Conshohocken, Pennsylvania.
9. ASTM C39 (2017). “Standard Test Method for Compressive Strength of Cylindrical Concrete Specimens (ASTM C39/C39M-17a).” ASTM International, West Conshohocken, Pennsylvania.
10. ASTM C143 (2015). “Standard Test Method for Slump of Hydraulic-Cement Concrete (ASTM C143/C143M-15a).” ASTM International, West Conshohocken, Pennsylvania.
11. ASTM C496 (2011). “Standard Test Method for Splitting Tensile Strength of Cylindrical Concrete Specimens (ASTM C496/C496M-11).” ASTM International, West Conshohocken, Pennsylvania.
12. ASTM E8 (2016). “Standard Test Methods for Tension Testing of Metallic Materials (ASTM E8/E8M-16a).” ASTM International, West Conshohocken, Pennsylvania.
13. Barclay, L. and Kowalsky, M. (2019). “Critical Bending Strain of Reinforcing Steel and the Buckled Bar Tension Test.” ACI Materials Journal, 116 (3), 53-61.
14. FEMA 461 (2007). “Interim Testing Protocols for Determining the Seismic Performance Characteristics of Structural and Nonstructural Components.” Applied Technology Council, Redwood City, California.

15. Lequesne, R.D. (2011). “Behavior and Design of High-Performance Fiber-Reinforced Concrete Coupling Beams and Coupled-Wall Systems.” PhD Dissertation, University of Michigan, Ann Arbor, Michigan.
16. Naish, D., Fry, A., Klemencic, R., and Wallace, J. (2013). “Reinforced Concrete Coupling Beams – Part I: Testing.” *ACI Structural Journal*, 110 (6), 1057-1066.
17. NIST GCR 14-917-30 (2014). “Use of High-Strength Reinforcement in Earthquake-Resistant Concrete Structures.” National Institute of Standards and Technology, Gaithersburg, Maryland.
18. Poudel, A., Lequesne, R. D., and Lepage, A. (2018). “Diagonally-Reinforced Concrete Coupling Beams: Effects of Axial Restraint.” University of Kansas Center for Research, Inc., Lawrence, Kansas.

TABLES

Table 1 – Design data for coupling beam specimens^a
(1 in. = 25.4 mm, 1 ksi = 1,000 psi = 6.89 MPa)

Coupling Beam ^b				Primary Longitudinal Reinforcement							Transverse Reinforcement			
Id.	v_e	$\frac{\ell_n}{h}$	ℓ_n	f_y	n	d_b	ℓ_e ^c	A_{vd}	α	A_s	Weak Axis ^d	Strong Axis ^e	f_{yt}	s
	$\sqrt{f'_c}$, psi		in.	ksi		in.	in.	in. ²	degrees	in. ²	in. ²	in. ²	ksi	in.
D80-1.5	8.4	1.5	27	80	6	0.75	21	2.64	22.7	-	0.44	0.33	80	3
D100-1.5	8.8	1.5	27	100	5	0.75	27	2.20	22.7	-	0.44	0.33	80	3
D120-1.5	8.4	1.5	27	120	4	0.75	34	1.76	22.7	-	0.44	0.33	80	3
D80-2.5	8.0	2.5	45	80	9	0.75	21	3.96	14.2	-	0.44	0.33	80	3
D100-2.5	7.8	2.5	45	100	7	0.75	27	3.08	14.2	-	0.44	0.33	80	3
D120-2.5	8.0	2.5	45	120	6	0.75	34	2.64	14.2	-	0.44	0.33	120	3
D80-3.5	7.8	3.5	63	80	9	0.875	24	5.40	10.0	-	0.44	0.33	80	3
D100-3.5	7.3	3.5	63	100	9	0.75	27	3.96	10.3	-	0.44	0.33	80	3
D120-3.5	7.8	3.5	63	120	8	0.75	34	3.52	10.3	-	0.44	0.33	80	3
P80-2.5	5.2	2.5	45	80	3	0.75	21	-	-	1.32	0.22	0.33	80	3.5
P100-2.5	6.4	2.5	45	100	3	0.75	27	-	-	1.32	0.22	0.33	80	3

^a For notation and definitions, see APPENDIX A: NOTATION.

^b All specimens have $f'_c = 8,000$ psi, $h = 18$ in., $b_w = 12$ in., and $c_c = 0.75$ in. to No. 3 (10) transverse reinforcement. Specimen Id. starts with D for cases with diagonal reinforcement and P for cases with parallel reinforcement, see Figure 1.

^c Minimum straight embedment length based on ACI 408R-03 Eq. 4.11.a^[2] using $\phi = \omega = \alpha = \beta = \lambda = 1$, $(c + \omega + K_{tr})/d_b = 4$, $1.25f_y$ psi, and $f'_c = 8,000$ psi. Grade 80 (550) No. 3 (10) longitudinal reinforcing bars were terminated approximately 2 in. into the top and bottom blocks consistent with the detailing recommendations in the ACI Building Code^[1] commentary, except for Grade 120 (830) No. 3 (10) longitudinal reinforcing bars in D120-2.5 with a minimum straight embedment length of 17 in. into the top and bottom blocks.

^d Transverse reinforcement along the 12-in. width of the coupling beam; 4 legs of No. 3 (10) bars at spacing s for D-type beams and 2 legs of No. 3 (10) bars for P-type beams.

^e Transverse reinforcement along the 18-in. depth of the coupling beam; 3 legs of No. 3 (10) bars at spacing s .

Table 2 – Measured compressive and tensile strengths of concrete^a (1,000 psi = 6.89 MPa)

Coupling Beam Identification	Cast Date	Test Date	Age (days)	f_{cm} ^b (psi)	f_{ct} ^c (psi)
D80-1.5	3 Nov 17	1 May 18	179	7,600	710
D100-1.5	3 Nov 17	9 Apr 18	157	8,200	720
D120-1.5	3 Nov 17	31 May 18	209	7,600	610
D80-2.5	16 Jun 17	3 Oct 17	109	8,400	620
D100-2.5	30 Jun 17	29 Nov 17	152	8,000	790
D120-2.5	18 Aug 17	6 Mar 18	200	7,800	760
D80-3.5	26 Jul 17	19 Jun 18	328	7,800	660
D100-3.5	26 Jul 17	6 Jul 18	345	7,900	650
D120-3.5	18 Aug 17	25 Jul 18	341	8,200	660
P80-2.5	16 Jun 17	10 Nov 17	147	8,300	790
P100-2.5	30 Jun 17	12 Dec 17	165	7,500	790

^a For notation and definitions, see APPENDIX A: NOTATION.

^b Tested in accordance with ASTM C39^[9], average of two tests of 6 by 12 in. (150 by 300 mm) cylinders.

^c Tested in accordance with ASTM C496^[11], average of two tests of 6 by 12 in. (150 by 300 mm) cylinders.

Table 3 – Concrete mixture proportions (1 lb = 4.45 N, 1 gal = 128 oz = 3.79 L, 1 in. = 25.4 mm, 1 yd³ = 0.764 m³)

Constituent Materials	Unit	Date of Casting				
		16 Jun 17	30 Jun 17	26 Jul 17	18 Aug 17	3 Nov 17
		Coupling Beam Identification				
		D80-2.5, P80-2.5	D100-2.5, P100-2.5	D80-3.5, D100-3.5	D120-2.5, D120-3.5	D80-1.5, D100-1.5, D120-1.5
Water	gal/yd ³	36	36	36	36	36
Cementitious Material (<i>CM</i>)						
Cement	lb/yd ³	647	647	645	668	662
Fly Ash	lb/yd ³	149	158	148	157	149
Fine Aggregate	lb/yd ³	1672	1659	1656	1658	1663
Coarse Aggregate ^a	lb/yd ³	1180	1184	1182	1178	1177
Admixtures ^b						
Set Retarder	oz/yd ³	32	32	32	32	32
Rheology Modifier	oz/yd ³	48	48	48	48	48
Water Reducer	oz/yd ³	56	56	56	56	56
Water/ <i>CM</i>		0.38	0.38	0.38	0.36	0.37
Initial Slump ^c	in.	9.0	10.5	9.0	9.5	9.0

^a Maximum aggregate size of ½ in.

^b Concrete arrived at laboratory with tabulated amounts of admixtures. Supplemental water-reducing admixture was added in the laboratory to achieve a minimum 20-in. spread before casting.

^c Slump measured in accordance with ASTM C143^[10] when concrete arrived at laboratory.

Table 4 – Reinforcing steel properties^a (1 in. = 25.4 mm, 1 ksi = 6.89 MPa)

Coupling Beam Identification	Bar Size No.	Nominal Bar Diameter d_b in.	Yield Stress ^b		Tensile Strength ^b	f_t/f_{ym}	Uniform Elongation ^c	Fracture Elongation ^d
			f_{ym} ksi	f_{ytm} ksi	f_t ksi		ϵ_{su} %	ϵ_{sf} %
D80-1.5	3 (10)	0.375		89	113		9.7	12.9
D80-2.5	6 (19)	0.75	83		110	1.32	9.2	13.3
P80-2.5								
D80-3.5	3 (10)	0.375		89	113		9.7	12.9
	7 (22)	0.875	84		114	1.36	10.0	16.4
D100-1.5	3 (10)	0.375		89	113		9.7	12.9
D100-2.5	6 (19)	0.75	108		125	1.16	6.8	9.8
D100-3.5								
D100-2.5								
D120-1.5	3 (10)	0.375		89	113		9.7	12.9
D120-3.5	6 (19)	0.75	116		163	1.41	5.2	9.9
D120-2.5	3 (10)	0.375	133	133	173	1.30	4.5	6.3
	6 (19)	0.75	116		163	1.41	5.2	9.9

^a For notation and definitions, see APPENDIX A: NOTATION.

^b Tested in accordance with ASTM A370^[5].

^c Corresponds to strain at peak stress, in accordance with ASTM E8^[12], based on 8-in. (203-mm) gauge length.

^d Calculated strain corresponding to zero stress on a line with slope equal to modulus of elasticity and passing through the fracture point, based on 8-in. (203-mm) gauge length.

Table 5 – Specimen and actuator nominal elevations relative to strong floor (1 in. = 25.4 mm)

$\frac{l_n}{h}$	Top of Bottom Block (in.)	Bottom of Top Block (in.)	Actuator A Centerline (in.)	Actuator B Centerline (in.)
1.5	39.5	66.5	21	87
2.5	36.5	81.5	45	87
3.5	36.5	99.5	51	130

Table 6 – List of strain gauges on primary and secondary longitudinal reinforcement

		Coupling Beam Identification												
		D80-1.5	D100-1.5	D120-1.5	D80-2.5	D100-2.5	D120-2.5	D80-3.5	D100-3.5	D120-3.5	P80-2.5	P100-2.5		
Primary Reinforcement	Diagonal	D1	X	X	X	X	X	X	X	X	O	X		
		D2	X	O	X	O	X	X	X	X	X	X		
		D3	X	X	X	X	X	X	X	X	O	X		
		D4	X	X	X	X	X	X	X	X	X	X		
		D5	X	X	X	X	O	X	X	X	X	X		
		D6	X	X	X	X	X	X	X	X	X	X		
		D7	X	X	X	X	X	X	X	X	X	X		
		D8	X	X	X	X	X	X	O	X	X	X		
		D9	O	X	X	O	X	O	X	X	X	X		
		D10	X	X	X	X	X	X	X	X	X	X		
		D11	X	X	X	X	O	X	X	X	X	X		
		D12	X	X	X	X	O	X	X	X	X	X		
		D13	X	X	O	O	X	X	X	X	X	X		
		D14	X	X	X	X	X	X	X	X	X	X		
Primary Reinforcement	Parallel ^a	P1											X	X
		P2											X	O
		P3											X	X
		P4											X	X
		P5											X	X
		P6											X	O
		P7											X	X
		P8											X	O
		P9											X	X
		P10											X	X
		P11											X	X
		P12											X	X
Secondary Reinforcement	Parallel ^b	H1	X	O	O	X	X	X	X	X	X	X		
		H2	X	O	X	X	O	X	O	X	X	X		
		H3	X	X	X	X	O	X	O	X	X	X		
		H4	X	X	X	X	X	X	X	O	X	X		
		H5	X	X	O	X	X	O	X	O	X	X		
		H6	X	X	X		X	O	X	X				
		H7		X	O				O	X				
		H8		O	X				X					
		H9	X	X	X									
		H10		X	X									
		H11	X	O	X									
		H12	X	X										
		H13	X											
		H14	X											

“X” indicates strain gauge is present.

“O” indicates strain gauge is present but data not available due to instrument malfunction.

^a No. 6 (19) reinforcement placed parallel to the longitudinal axis of the P-type beams.

^b No. 3 (10) reinforcement placed parallel to the longitudinal axis of the D-type beams.

Table 7 – List of strain gauges on transverse reinforcement

		Coupling Beam Identification											
		D80-1.5	D100-1.5	D120-1.5	D80-2.5	D100-2.5	D120-2.5	D80-3.5	D100-3.5	D120-3.5	P80-2.5	P100-2.5	
Transverse Reinforcement	Closed Stirrups	S1	O	O	X	O	X	O	O	O	O	X	X
		S2	X	X	X	X	X	X	X	X	X	X	X
		S3	X	X	X	X	X	X	X	X	X	O	X
		S4	X	X	X	X	X	X	X	X	X	O	X
		S5	X	X	X	X	O	X	X	X	X	X	X
		S6	X	O	X	X	X	X	X	X	X	X	X
		S7	X	X	X	X	X	X	X	X	X	X	X
		S8	X	X	X	X	X	X	X	X	X	X	X
		S9	X	X	X	X	X	X	X	O	X	X	X
		S10						X					
		S11						X					
		S12						X					
		S13						X					
		S14						X					
		S15						X					
		S16						X					
		S17						X					
		S18						O					
Transverse Reinforcement	Cross-ties	T1	X	X	O	X	X	X	X	X	X	X	X
		T2	X	X	O	X	X	X	X	X	X		
		T3	X	X	X	O	X	X	X	X	X		
		T4	X	X	X								
		T5		X	X								
		T6			X								

“X” indicates strain gauge is present.

“O” indicates strain gauge is present but data not available due to instrument malfunction.

Table 8 – Loading protocol (1 in. = 25.4 mm)

Step ^a	Chord Rotation ^b %	Loading Rate in./s ^c
1	0.20	0.01
2	0.30	0.01
3	0.50	0.01
4	0.75	0.01
5	1.00	0.02
6	1.50	0.02
7	2.00	0.02
8	3.00	0.03
9	4.00	0.03
10	6.00	0.04
11	8.00	0.04
12	10.00	0.04

^a Two cycles of loading in each step, following recommendations in FEMA 461^[14], see Figure 35.

^b Based on the relative lateral displacement between end blocks divided by the beam clear span (excluding contributions due to sliding of the specimen and rotation of the end blocks).

^c Loading rate of coupling beams with aspect ratios of 1.5 and 2.5. Coupling beams with an aspect ratio of 3.5 were tested at twice these rates.

Table 9 – Coupling beam maximum shear stress and deformation capacity^a
 (1,000 psi = 6.89 MPa, 1 kip = 4.45 kN)

Coupling Beam Id.	Maximum Applied Shear V_{max} kips	Maximum Applied Shear Stress v_{max} $\sqrt{f_{cm}}$, psi	Deformation Capacity A ^b %	Deformation Capacity B ^c %
D80-1.5	254	13.5	6.1	6.9
D100-1.5	257	13.1	4.9	5.3
D120-1.5	264	14.0	4.6	5.2
D80-2.5	220	11.1	7.1	7.6
D100-2.5	220	11.4	5.3	6.0
D120-2.5	286	15.0	6.6	6.9
D80-3.5	219	11.5	8.3	8.6
D100-3.5	196	10.2	6.3	6.8
D120-3.5	216	11.0	6.5	6.7
P80-2.5	91	5.0	3.6	3.9
P100-2.5	110	6.4	3.6	4.1

^a For notation and definitions, see APPENDIX A: NOTATION.

^b The average of the highest chord rotations reached in each loading direction before strength diminished to less than 80% of the maximum applied shear.

^c The average of the chord rotations in each loading direction where the envelope curve formed by connecting the maximum chord rotation of the first cycle of each loading step intersects with 80% of the maximum applied shear.

Table 10 – Force-deformation envelope for D-type coupling beams with aspect ratio of 1.5 (1 kip = 4.45 kN, 1 in. = 25.4 mm)

Target Chord Rot. CR %	D80-1.5				D100-1.5				D120-1.5			
	Actual Chord Rot. CR^a %	Shear V kips	V/V_{max}^b	Secant Stiffness K_S kips / in.	Actual Chord Rot. CR^a %	Shear V kips	V/V_{max}^b	Secant Stiffness K_S kips / in.	Actual Chord Rot. CR^a %	Shear V kips	V/V_{max}^b	Secant Stiffness K_S kips / in.
	-10	-8.23	-31.75	0.13	14	-6.61	-151.45	0.59	85	-8.56	-31.43	0.12
-8	-6.07	-226.30	0.95	138	-4.24	-216.96	0.84	190	-4.88	-237.76	0.91	180
-6	-4.09	-235.70	0.99	213	-3.08	-241.74	0.94	291	-3.20	-261.53	1.00	303
-4	-3.01	-235.67	0.99	290	-2.05	-246.26	0.96	445	-2.06	-254.64	0.97	458
-3	-1.90	-229.89	0.96	448	-1.74	-257.10	1.00	547	-1.60	-246.66	0.94	571
-2	-1.54	-223.37	0.93	537	-1.04	-238.81	0.93	850	-1.05	-209.23	0.80	738
-1.5	-1.44	-228.92	0.96	589	-0.78	-202.63	0.79	962	-0.77	-177.18	0.68	852
-1	-1.12	-238.91	1.00	790	-0.52	-168.44	0.66	1200	-0.52	-138.50	0.53	986
-.75	-0.78	-221.76	0.93	1053	-0.32	-123.83	0.48	1433	-0.31	-92.79	0.35	1109
-.5	-0.51	-171.53	0.72	1246	-0.22	-103.48	0.40	1742	-0.20	-68.89	0.26	1276
-.3	-0.31	-124.27	0.52	1485	0.00	3.83	0.02	0	0.00	2.37	0.01	0
-.2	-0.21	-96.21	0.40	1697	0.22	82.98	0.33	1397	0.21	71.26	0.27	1257
0	0.00	1.37	0.01	0	0.31	99.00	0.39	1183	0.31	91.17	0.35	1089
.2	0.20	80.68	0.32	1494	0.51	142.57	0.57	1035	0.52	120.71	0.46	860
.3	0.30	103.95	0.41	1283	0.77	185.55	0.74	892	0.76	157.36	0.60	767
.5	0.50	150.30	0.59	1113	1.01	223.96	0.89	821	1.02	189.37	0.72	688
.75	0.75	197.28	0.78	974	1.47	251.72	1.00	634	1.52	231.26	0.88	563
1	0.99	229.39	0.90	858	2.03	240.36	0.95	439	2.08	254.60	0.96	453
1.5	1.48	248.17	0.98	621	2.95	241.39	0.96	303	2.99	264.11	1.00	327
2	2.12	254.24	1.00	444	3.99	229.06	0.91	213	4.16	243.43	0.92	217
3	2.69	252.05	0.99	347	5.60	218.95	0.87	145	5.44	192.14	0.73	131
4	2.98	251.50	0.99	313	6.04	185.41	0.74	114	6.09	141.53	0.54	86
6	3.87	248.72	0.98	238	8.30	20.79	0.08	9				
8	6.11	246.22	0.97	149								
10	8.22	170.00	0.67	77								
$-0.75 V_{max}^c$	-0.55	-178.71	0.75	1207	-0.70	-192.11	0.75	1016	-0.93	-195.88	0.75	777
$+0.75 V_{max}^c$	0.71	189.86	0.75	990	0.79	188.08	0.75	887	1.11	197.22	0.75	656

^a The actual chord rotation, CR, associated with the peak force for each loading step. CR is the measured displacement of the top block relative to the bottom block divided by the coupling beam clear span, ℓ_n , and correcting for relative rotation of the end blocks.

^b V_{max} is the maximum measured shear force in the respective loading direction.

^c The interpolated chord rotation at the intersection of $0.75 V_{max}$ (before V_{max}) and the shear-chord rotation envelope.

Table 11 – Force-deformation envelope for D-type coupling beams with aspect ratio of 2.5 (1 kip = 4.45 kN, 1 in. = 25.4 mm)

Target Chord Rot. <i>CR</i> %	D80-2.5				D100-2.5				D120-2.5			
	Actual Chord Rot. <i>CR</i> ^a %	Shear <i>V</i> kips	<i>V/V_{max}</i> ^b	Secant Stiffness <i>K_S</i> kips / in.	Actual Chord Rot. <i>CR</i> ^a %	Shear <i>V</i> kips	<i>V/V_{max}</i> ^b	Secant Stiffness <i>K_S</i> kips / in.	Actual Chord Rot. <i>CR</i> ^a %	Shear <i>V</i> kips	<i>V/V_{max}</i> ^b	Secant Stiffness <i>K_S</i> kips / in.
	-10	-10.01	-20.96	0.10	5	-7.99	-46.15	0.21	13	-8.35	-119.57	0.42
-8	-7.91	-131.70	0.60	37	-6.04	-127.65	0.58	47	-6.42	-243.63	0.86	84
-6	-5.91	-216.84	0.99	82	-4.67	-216.89	0.99	103	-4.30	-283.46	1.00	146
-4	-3.85	-215.74	0.98	125					-3.15	-272.27	0.96	192
-3	-3.11	-220.13	1.00	157					-2.04	-241.03	0.85	263
-2	-2.03	-213.19	0.97	233	-2.48	-220.12	1.00	197	-1.56	-217.28	0.77	310
-1.5	-1.51	-201.65	0.92	297	-0.98	-167.82	0.76	381	-1.00	-162.48	0.57	361
-1	-0.99	-170.95	0.78	384	-0.75	-138.02	0.63	409	-0.74	-134.47	0.47	404
-.75	-0.70	-144.26	0.66	458	-0.50	-101.22	0.46	450	-0.53	-105.53	0.37	442
-.5	-0.47	-108.58	0.49	513	-0.29	-73.03	0.33	560	-0.31	-65.09	0.23	467
-.3	-0.28	-80.44	0.37	638	-0.19	-60.27	0.27	705	-0.20	-40.35	0.14	448
-.2	-0.23	-72.21	0.33	698	0.00	0.00	0.00	0	0.01	2.10	0.01	467
0	0.00	0.00	0.00	0	0.20	58.02	0.27	645	0.20	40.13	0.14	446
.2	0.23	63.45	0.29	613	0.33	76.62	0.36	516	0.31	64.96	0.23	466
.3	0.38	92.87	0.43	543	0.54	102.19	0.48	421	0.61	116.76	0.41	425
.5	0.48	106.54	0.49	493	0.81	144.25	0.67	396	0.77	138.26	0.48	399
.75	0.76	142.91	0.66	418	1.04	170.74	0.80	365	1.01	168.12	0.59	370
1	0.98	166.18	0.76	377	1.45	203.97	0.95	313	1.50	216.83	0.76	321
1.5	1.89	212.34	0.97	250	2.16	214.25	1.00	220	2.10	251.95	0.88	267
2	2.06	193.89	0.89	209	3.06	210.68	0.98	153	3.15	277.43	0.97	196
3	2.92	209.56	0.96	159	4.02	194.51	0.91	108	4.29	285.94	1.00	148
4	3.94	207.45	0.95	117					5.80	271.60	0.95	104
6	6.00	217.95	1.00	81	6.01	191.05	0.89	71	6.68	251.57	0.88	84
8	8.17	180.68	0.83	49	8.12	124.04	0.58	34	9.11	94.56	0.33	23
10												
$-0.75 V_{max}$ ^c	-0.92	-164.28	0.75	398	-0.96	-165.53	0.75	382	-1.50	-211.80	0.75	313
$+0.75 V_{max}$ ^c	0.96	163.85	0.75	380	0.95	160.55	0.75	375	1.47	213.96	0.75	323

^a The actual chord rotation, CR, associated with the peak force for each loading step. CR is the measured displacement of the top block relative to the bottom block divided by the coupling beam clear span, ℓ_n , and correcting for relative rotation of the end blocks.

^b V_{max} is the maximum measured shear force in the respective loading direction.

^c The interpolated chord rotation at the intersection of $0.75 V_{max}$ (before V_{max}) and the shear-chord rotation envelope.

Table 12 – Force-deformation envelope for D-type coupling beams with aspect ratio of 3.5 (1 kip = 4.45 kN, 1 in. = 25.4 mm)

Target Chord Rot. <i>CR</i> %	D80-3.5				D100-3.5				D120-3.5			
	Actual Chord Rot.	Shear		Secant Stiffness	Actual Chord Rot.	Shear		Secant Stiffness	Actual Chord Rot.	Shear		Secant Stiffness
	<i>CR</i> ^a %	<i>V</i> kips	<i>V/V_{max}</i> ^b	<i>K_S</i> kips / in.	<i>CR</i> ^a %	<i>V</i> kips	<i>V/V_{max}</i> ^b	<i>K_S</i> kips / in.	<i>CR</i> ^a %	<i>V</i> kips	<i>V/V_{max}</i> ^b	<i>K_S</i> kips / in.
-10	-10.29	-53.91	0.25	8	-10.25	-38.06	0.20	6	-7.91	-93.00	0.43	19
-8	-8.24	-182.26	0.84	35	-8.09	-102.84	0.54	20	-6.38	-184.10	0.85	46
-6	-6.04	-217.50	1.00	57	-6.35	-180.91	0.94	45	-4.08	-215.70	1.00	84
-4	-4.13	-209.83	0.96	81	-4.12	-186.92	0.97	72	-3.01	-214.54	0.99	113
-3	-3.09	-207.46	0.95	107	-3.10	-191.73	1.00	98	-1.97	-191.87	0.89	155
-2	-2.16	-204.24	0.94	150	-2.11	-189.19	0.99	142	-1.58	-172.44	0.80	173
-1.5	-1.56	-195.04	0.90	198	-1.58	-175.56	0.92	176	-1.03	-129.45	0.60	199
-1	-1.08	-164.62	0.76	242	-1.05	-134.79	0.70	204	-0.77	-105.13	0.49	217
-.75	-0.77	-125.98	0.58	260	-0.76	-106.16	0.55	222	-0.51	-78.48	0.36	244
-.5	-0.51	-95.35	0.44	297	-0.51	-77.91	0.41	242	-0.31	-55.70	0.26	285
-.3	-0.30	-66.42	0.31	351	-0.31	-55.74	0.29	285	-0.20	-40.57	0.19	322
-.2	-0.22	-46.14	0.21	333	-0.22	-45.86	0.24	331	0.00	0.06	0.00	0
0	0.00	-0.16	0.00	0	0.00	1.63	0.01	0	0.23	43.16	0.20	298
.2	0.22	49.87	0.23	360	0.26	52.65	0.27	321	0.33	57.05	0.27	274
.3	0.34	71.92	0.33	336	0.31	57.99	0.30	297	0.53	79.80	0.38	239
.5	0.51	95.47	0.44	297	0.53	86.95	0.44	260	0.78	104.60	0.49	213
.75	0.78	130.92	0.60	266	0.77	114.71	0.59	236	1.02	126.60	0.60	197
1	1.08	166.34	0.76	244	1.02	139.32	0.71	217	1.55	161.65	0.76	166
1.5	1.55	196.19	0.90	201	1.57	177.08	0.90	179	2.07	182.77	0.86	140
2	2.03	206.40	0.95	161	2.02	187.53	0.96	147	3.04	211.46	1.00	110
3	3.13	212.97	0.98	108	3.16	195.99	1.00	98	4.14	212.40	1.00	81
4	4.16	211.81	0.97	81	4.36	189.27	0.97	69	6.53	191.10	0.90	46
6	5.96	219.40	1.00	57	6.20	184.12	0.94	47	8.48	62.12	0.29	12
8	8.28	211.74	0.97	41	8.11	94.05	0.48	18				
10	10.20	84.96	0.39	13	10.25	34.29	0.17	5				
-0.75 <i>V_{max}</i> ^c	-1.07	-163.13	0.75	242	-1.17	-144.06	0.75	195	-1.44	-161.69	0.75	178
+0.75 <i>V_{max}</i> ^c	1.06	164.25	0.75	245	1.14	147.27	0.75	206	1.52	159.46	0.75	167

^a The actual chord rotation, CR, associated with the peak force for each loading step. CR is the measured displacement of the top block relative to the bottom block divided by the coupling beam clear span, ℓ_n , and correcting for relative rotation of the end blocks.

^b V_{max} is the maximum measured shear force in the respective loading direction.

^c The interpolated chord rotation at the intersection of 0.75 V_{max} (before V_{max}) and the shear-chord rotation envelope.

Table 13 – Force-deformation envelope for P-type coupling beams
with aspect ratio of 2.5 (1 kip = 4.45 kN, 1 in. = 25.4 mm)

Target Chord Rot. CR %	P80-2.5				P100-2.5			
	Actual Chord Rot. CR^a %	Shear V kips	V/V_{max}^b	Secant Stiffness K_S kips / in.	Actual Chord Rot. CR^a %	Shear V kips	V/V_{max}^b	Secant Stiffness K_S kips / in.
	-10							
-8								
-6	-6.03	-16.81	0.19	6	-6.53	-29.39	0.27	10
-4	-4.06	-39.15	0.44	21	-4.02	-96.44	0.89	53
-3	-3.04	-77.09	0.86	56	-3.23	-106.60	0.98	73
-2	-1.98	-89.56	1.00	101	-2.05	-108.48	1.00	118
-1.5	-1.50	-87.17	0.97	129	-1.46	-104.53	0.96	159
-1	-1.01	-82.07	0.92	181	-0.99	-95.65	0.88	215
-.75	-0.84	-80.11	0.89	212	-0.73	-82.75	0.76	252
-.5	-0.47	-66.10	0.74	313	-0.50	-67.15	0.62	298
-.3	-0.35	-58.97	0.66	374	-0.29	-50.74	0.47	389
-.2	-0.19	-42.31	0.47	495	-0.23	-44.38	0.41	429
0	0.00	0.00	0.00	0	0.00	0.00	0.00	0
.2	0.18	42.34	0.47	523	0.23	41.34	0.38	399
.3	0.31	52.68	0.58	378	0.35	51.10	0.47	324
.5	0.55	73.64	0.81	298	0.58	63.98	0.58	245
.75	0.82	84.79	0.94	230	0.77	83.49	0.76	241
1	1.00	84.80	0.94	188	1.09	98.78	0.90	201
1.5	1.58	88.92	0.98	125	1.76	109.85	1.00	139
2	1.93	88.61	0.98	102	2.11	107.52	0.98	113
3	2.86	90.58	1.00	70	3.18	106.76	0.97	75
4	4.09	80.15	0.88	44	4.10	76.02	0.69	41
6	7.09	30.53	0.34	10	6.15	48.95	0.45	18
8								
10								
$-0.75 V_{max}^c$	-0.50	-67.17	0.75	299	-0.71	-81.64	0.75	255
$+0.75 V_{max}^c$	0.48	67.94	0.75	311	0.76	82.41	0.75	241

^a The actual chord rotation, CR, associated with the peak force for each loading step. CR is the measured displacement of the top block relative to the bottom block divided by the coupling beam clear span, ℓ_n , and correcting for relative rotation of the end blocks.

^b V_{max} is the maximum measured shear force in the respective loading direction.

^c The interpolated chord rotation at the intersection of $0.75 V_{max}$ (before V_{max}) and the shear-chord rotation envelope.

Table 14 – Coupling beam measured and calculated strengths^a
 (1,000 psi = 6.89 MPa, 1 kip = 4.45 kN)

Coupling Beam Id.	Measured		Calculated			Measured-to-Calculated Ratio ^b
	V_{max} kips	v_{max} $\sqrt{f_{cm}}$, psi	V_{nm} kips	$2M_{nm}/l_n$ kips	v_{nm} $\sqrt{f_{cm}}$, psi	
D80-1.5	254	13.5	169	-	9.0	1.50
D100-1.5	257	13.1	183	-	9.4	1.40
D120-1.5	264	14.0	158	-	8.4	1.68
D80-2.5	220	11.1	161	-	8.1	1.36
D100-2.5	220	11.4	163	-	8.4	1.35
D120-2.5	286	15.0	150	-	7.9	1.90
D80-3.5	219	11.5	158	-	8.3	1.39
D100-3.5	196	10.2	153	-	8.0	1.28
D120-3.5	216	11.0	146	-	7.5	1.48
P80-2.5	91	5.0	-	77	4.3	1.18
P100-2.5	110	6.4	-	99	5.8	1.11

^a For notation and definitions, see APPENDIX A: NOTATION.

^b The average of measured-to-calculated ratios is 1.43 for D-type beams (excluding D120-2.5) and 1.15 for P-type beams.

Table 15 – Summary of test data^a
(1 ksi = 1000 psi = 6.89 MPa)

Coupling Beam Id.	Reinforcement Type	$\frac{\ell_n}{h}$	f_{cm}	f_{ym}	f_{ytm}	v_{max} ^b	v_{nm} ^c	Measured Chord Rotation Capacity ^d	ASCE 41-17 Chord Rotation Capacity ^e
			psi	ksi	ksi	$\sqrt{f_{cm}}$, psi	$\sqrt{f_{cm}}$, psi	%	%
D80-1.5	Diagonal	1.5	7,600	83	89	13.5	9.0	6.9	5.0
D100-1.5	Diagonal	1.5	8,200	108	89	13.1	9.4	5.3	5.0
D120-1.5	Diagonal	1.5	7,600	116	89	14.0	8.4	5.2	5.0
D80-2.5	Diagonal	2.5	8,400	83	89	11.1	8.1	7.6	5.0
D100-2.5	Diagonal	2.5	8,000	108	89	11.4	8.4	6.0	5.0
D120-2.5	Diagonal	2.5	7,800	116	133	15.0	7.9	6.9	5.0
D80-3.5	Diagonal	3.5	7,800	84	89	11.5	8.3	8.6	5.0
D100-3.5	Diagonal	3.5	7,900	108	89	10.2	8.0	6.8	5.0
D120-3.5	Diagonal	3.5	8,200	116	89	11.0	7.5	6.7	5.0
P80-2.5	Parallel	2.5	8,300	83	89	5.0	4.3	3.9	4.0 ^f
P100-2.5	Parallel	2.5	7,500	108	89	6.4	5.8	4.1	4.0 ^f

^a For notation and definitions, see APPENDIX A: NOTATION.

^b Shear stress associated with maximum applied shear V_{max} .

For D-type beams, $v_{max} = V_{max}/(b_w h)$.

For P-type beams, $v_{max} = V_{max}/(b_w d)$.

^c For D-type beams, $v_{nm} = (2A_{vd} f_{ym} \sin \alpha)/(b_w h)$.

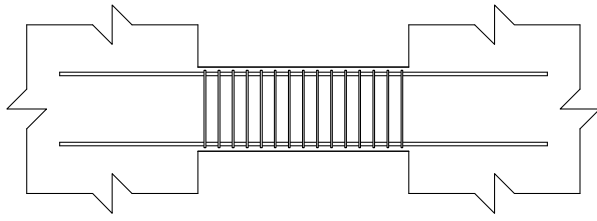
For P-type beams, $v_{nm} = (2M_{nm}/\ell_n)/(b_w d)$.

^d The average of the chord rotations in each loading direction where the envelope curve formed by connecting the maximum chord rotation of the first cycle of each loading step intersects with 80% of the maximum applied shear.

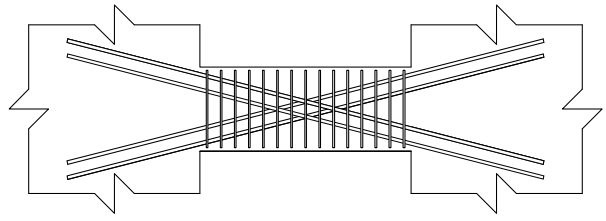
^e Chord rotation capacity from ASCE 41-17^[4] Table 10-19 corresponding to the maximum chord rotation associated with the residual strength defined by segment D-E in ASCE 41-17^[4] Figure 10-1(b). It is important to note that the measured chord rotation capacity (see footnote d) corresponds to a higher residual strength than those used in ASCE 41-17^[4], where the residual strength is defined as 80% of the strength at point B in Figure 10-1(b)^[4].

^f The reported ASCE 41-17^[4] chord rotation capacity is taken from Table 10-19^[4] and corresponds to a residual strength of 50% of the strength at point B in Figure 10-1(b)^[4]. In contrast, the measured chord rotation capacity (see footnote d) corresponds to the chord rotation associated with a post-peak strength of 80% of the maximum applied shear.

FIGURES



(a) P-type beam



(b) D-type beam

Figure 1 – Reinforcement layout types, parallel (P) and diagonal (D)

Scale 12"

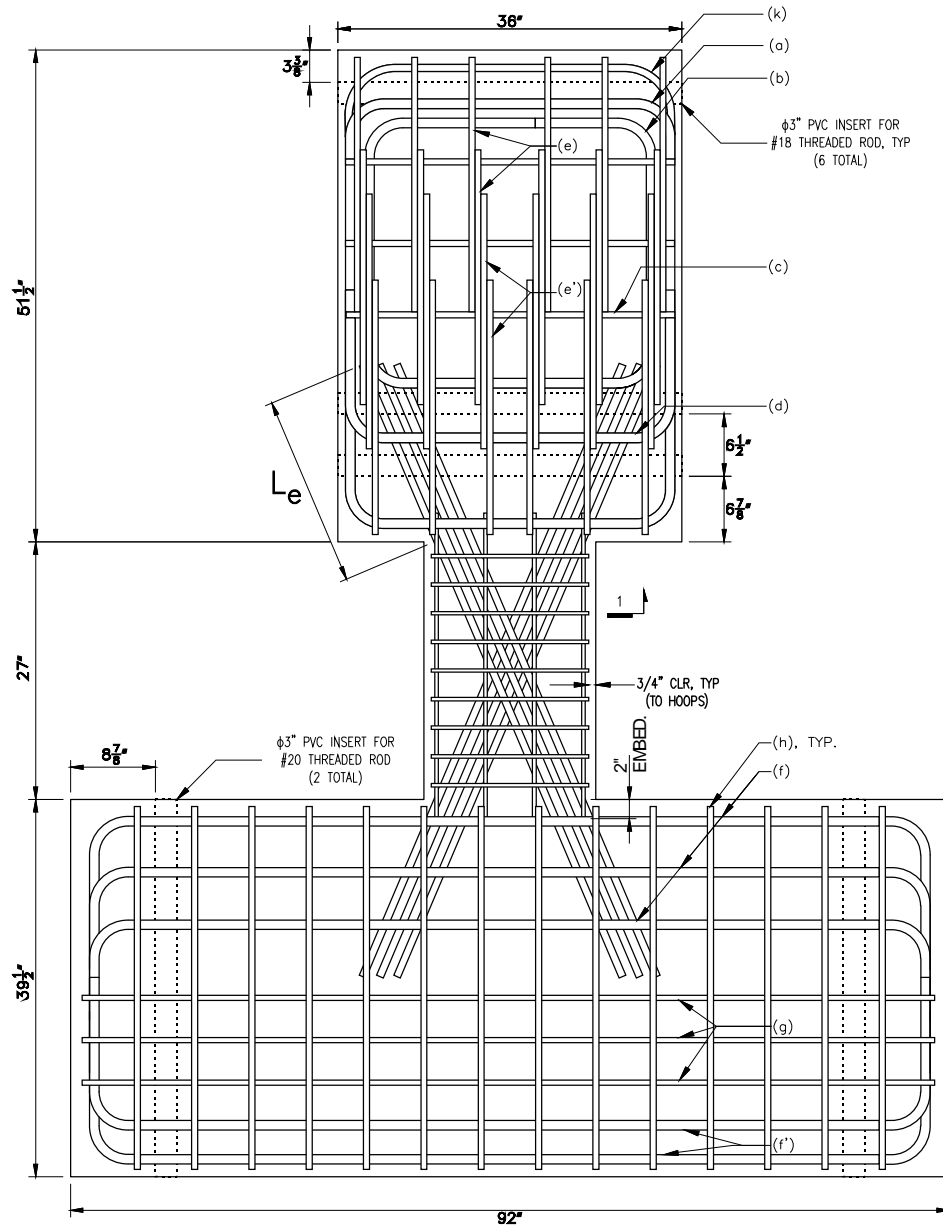


Figure 2 – Elevation view of D80-1.5 (1 in. = 25.4 mm)

Scale 12"

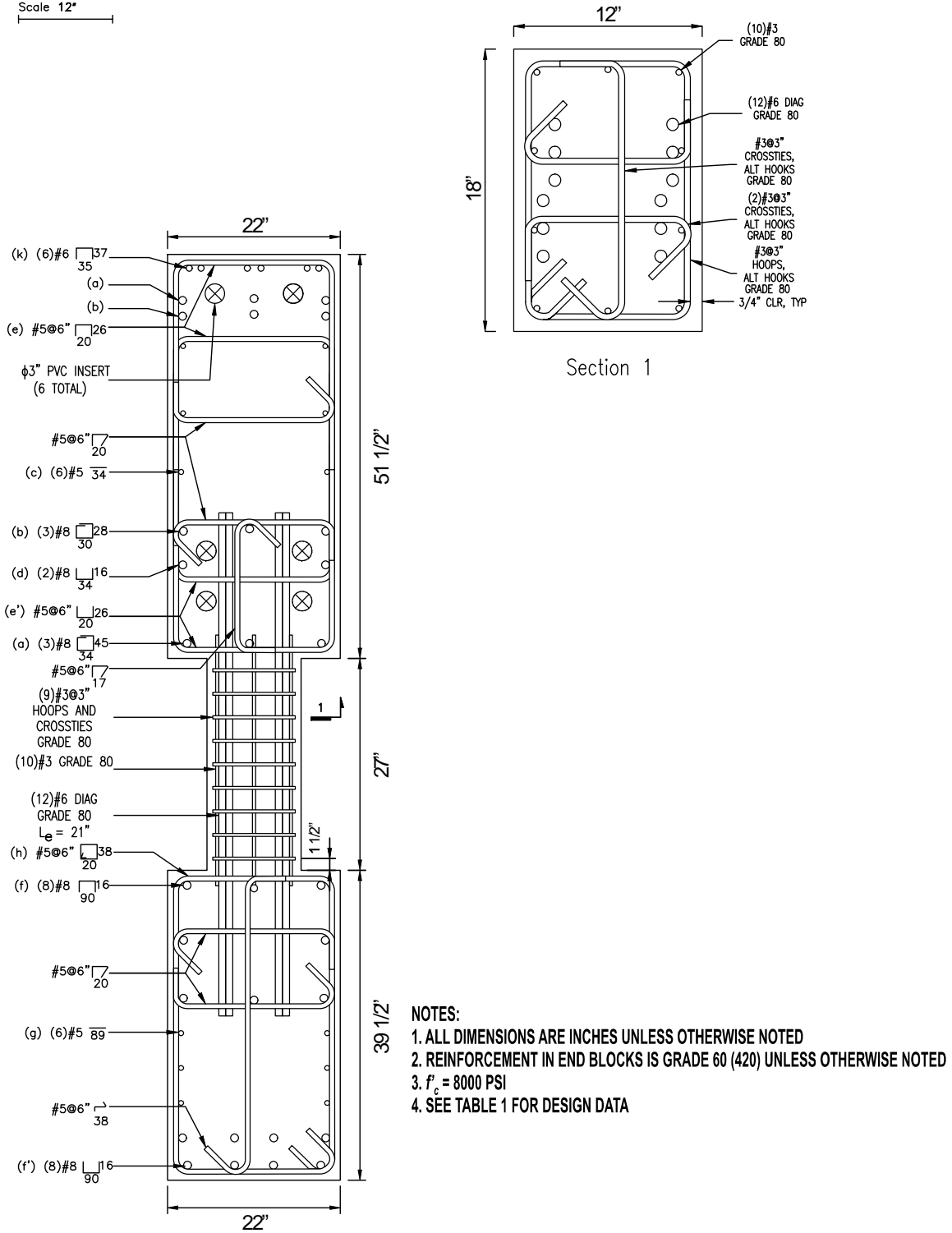


Figure 3 – Reinforcement details of D80-1.5 (1 in. = 25.4 mm, 1 ksi = 1,000 psi = 6.89 MPa)

Scale 1/2"

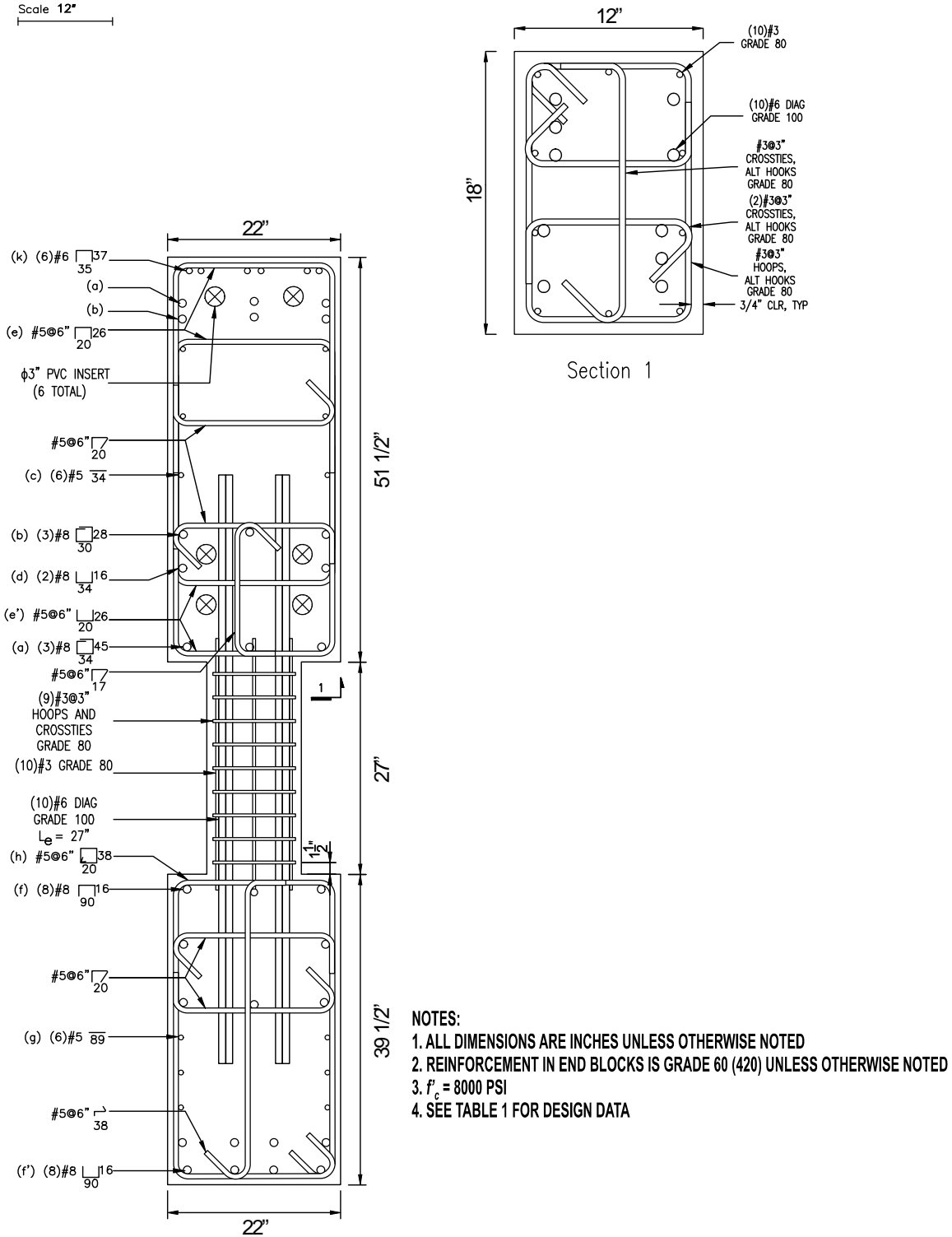


Figure 5 – Reinforcement details of D100-1.5 (1 in. = 25.4 mm, 1 ksi = 1,000 psi = 6.89 MPa)

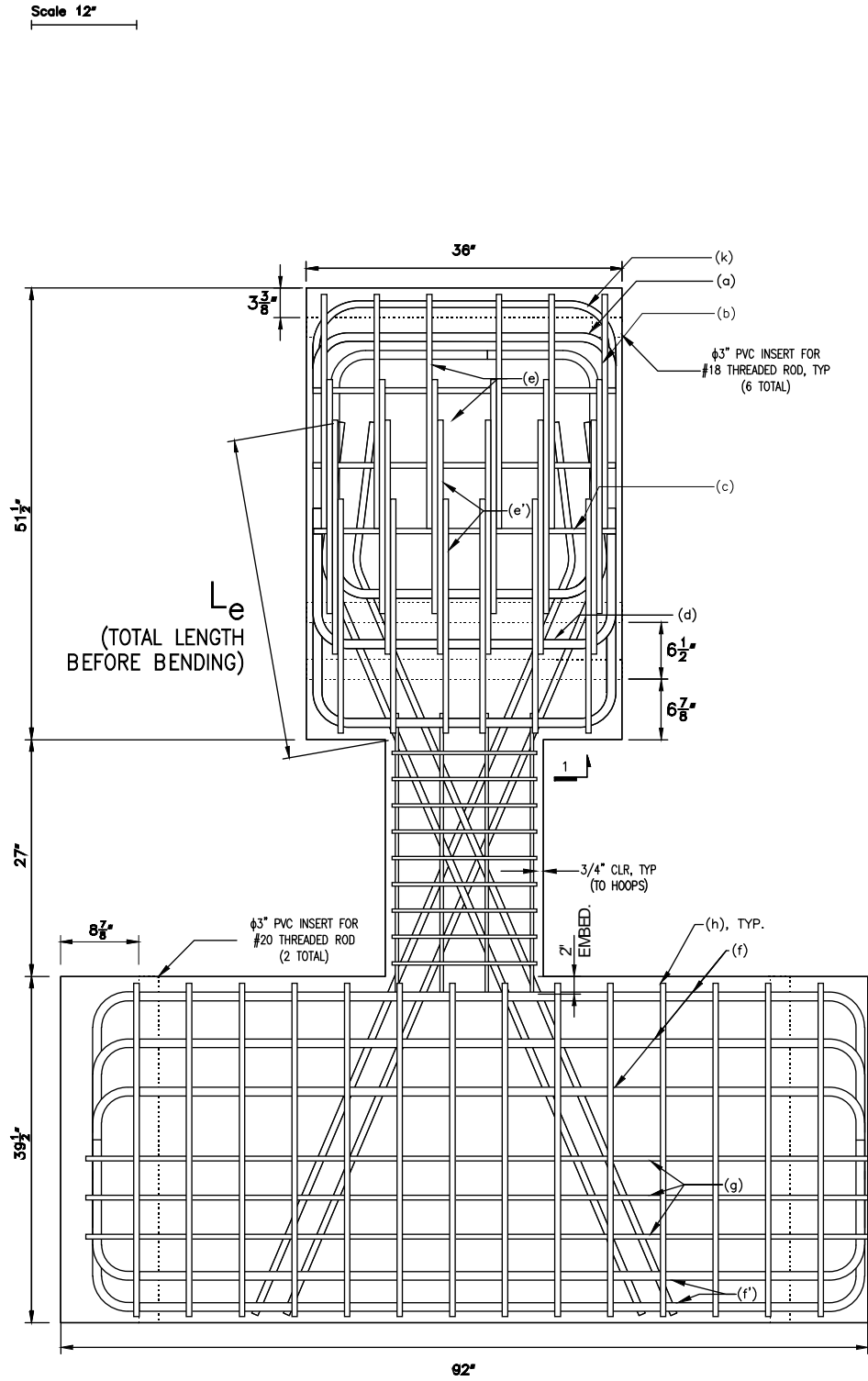


Figure 6 – Elevation view of D120-1.5 (1 in. = 25.4 mm)

Scale 1/2"

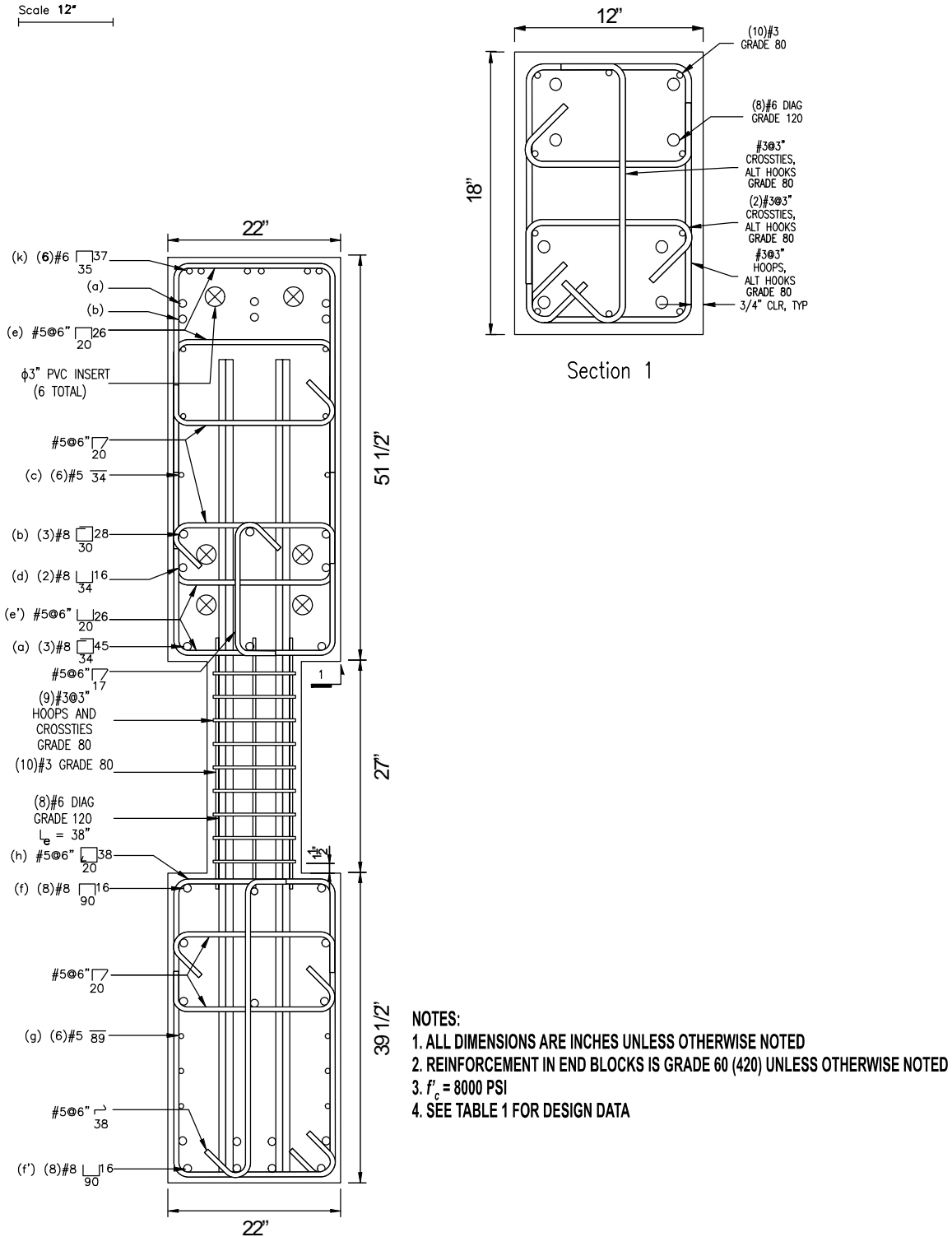


Figure 7 – Reinforcement details of D120-1.5 (1 in. = 25.4 mm, 1 ksi = 1,000 psi = 6.89 MPa)

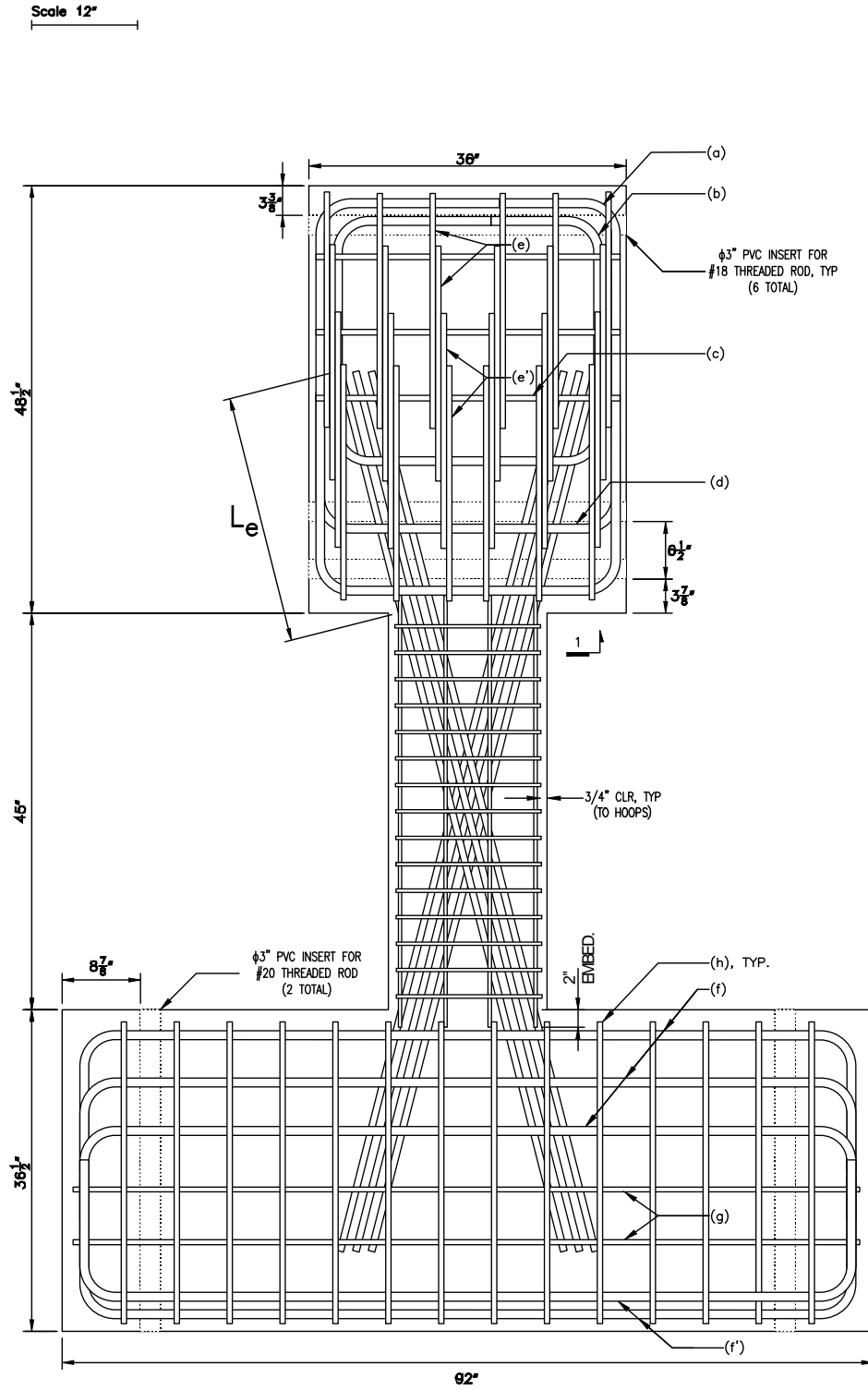


Figure 8 – Elevation view of D80-2.5 (1 in. = 25.4 mm)

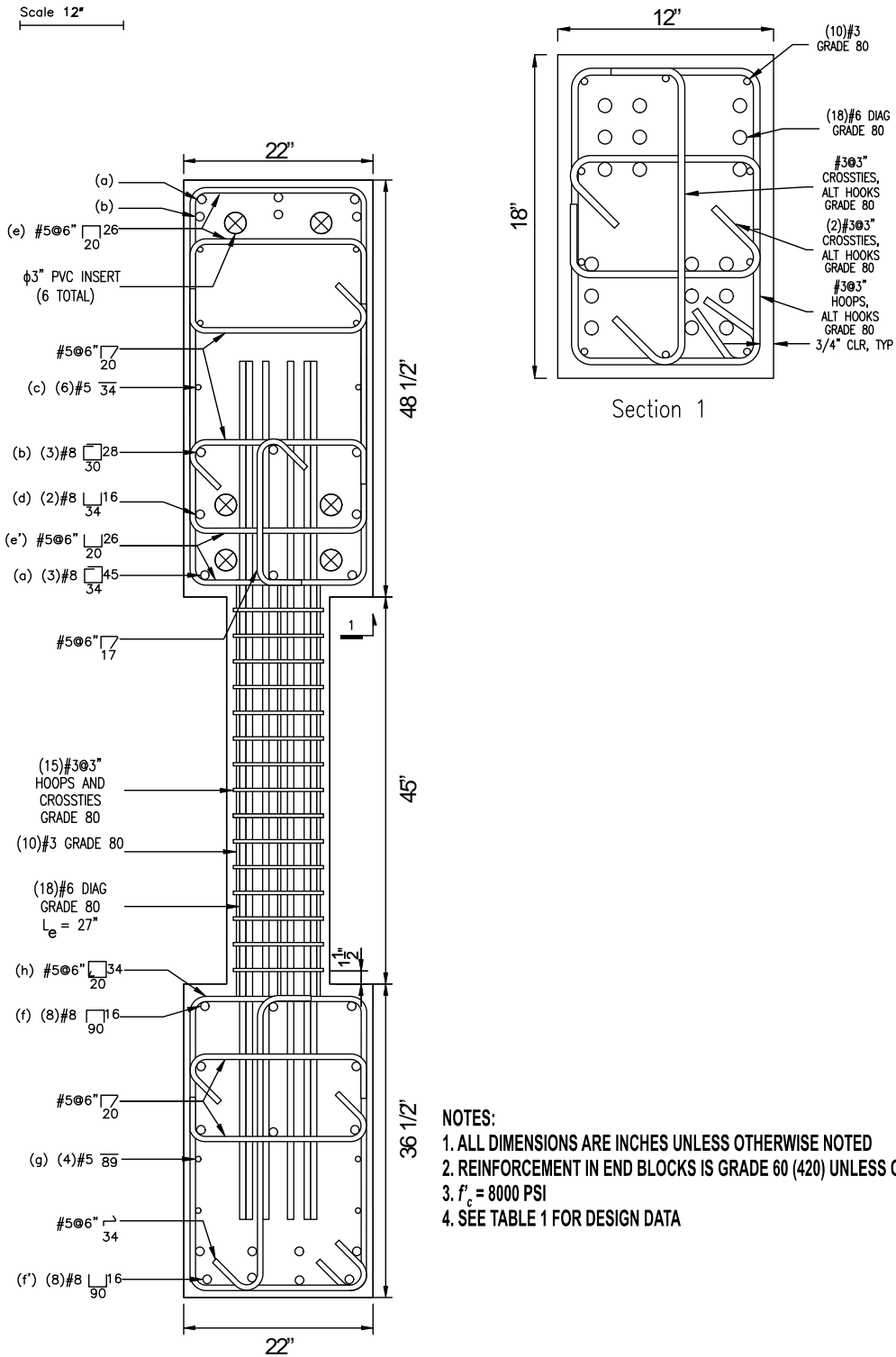


Figure 9 – Reinforcement details of D80-2.5 (1 in. = 25.4 mm, 1 ksi = 1,000 psi = 6.89 MPa)

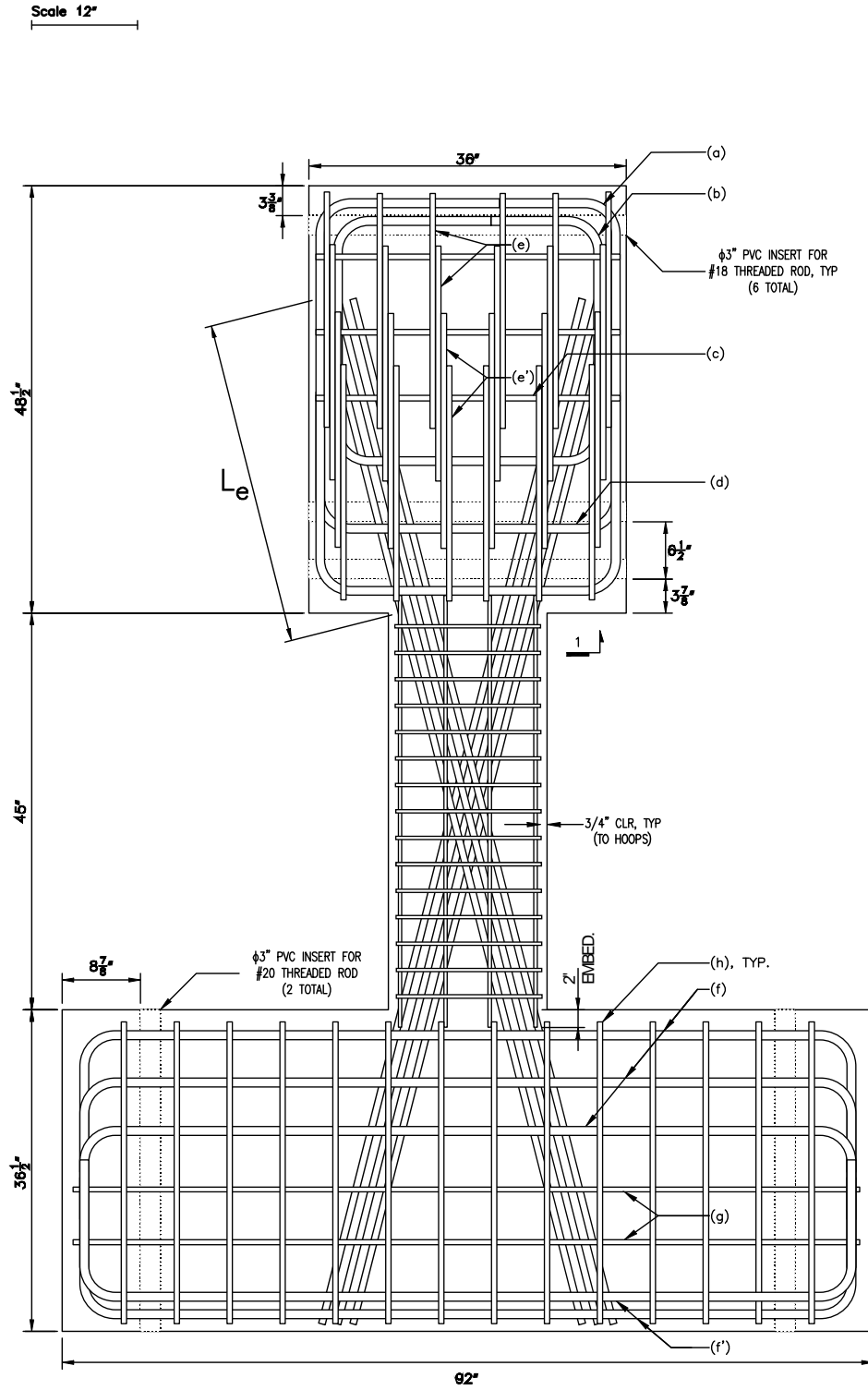
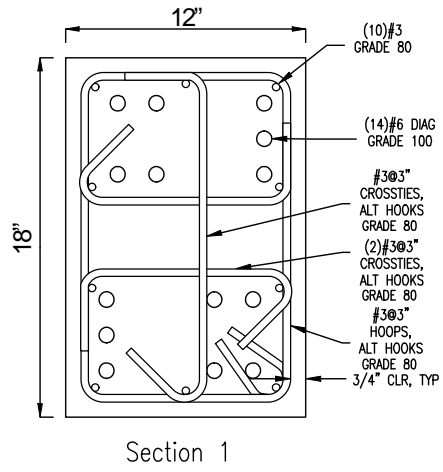
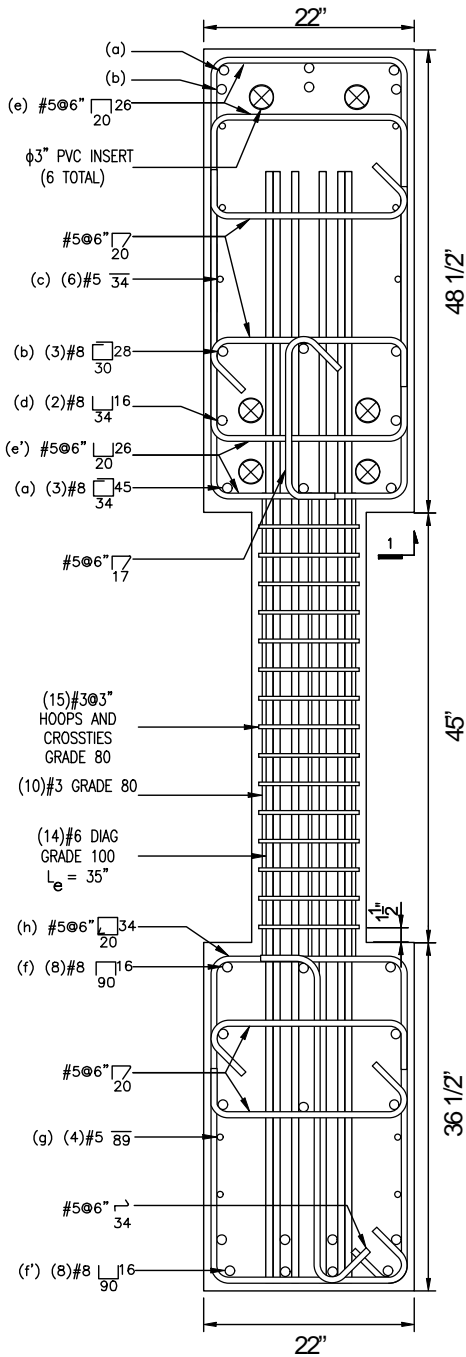


Figure 10 – Elevation view of D100-2.5 (1 in. = 25.4 mm)

Scale 12"



- NOTES:**
1. ALL DIMENSIONS ARE INCHES UNLESS OTHERWISE NOTED
 2. REINFORCEMENT IN END BLOCKS IS GRADE 60 (420) UNLESS OTHERWISE NOTED
 3. $f'_c = 8000$ PSI
 4. SEE TABLE 1 FOR DESIGN DATA

Figure 11 – Reinforcement details of D100-2.5 (1 in. = 25.4 mm, 1 ksi = 1,000 psi = 6.89 MPa)

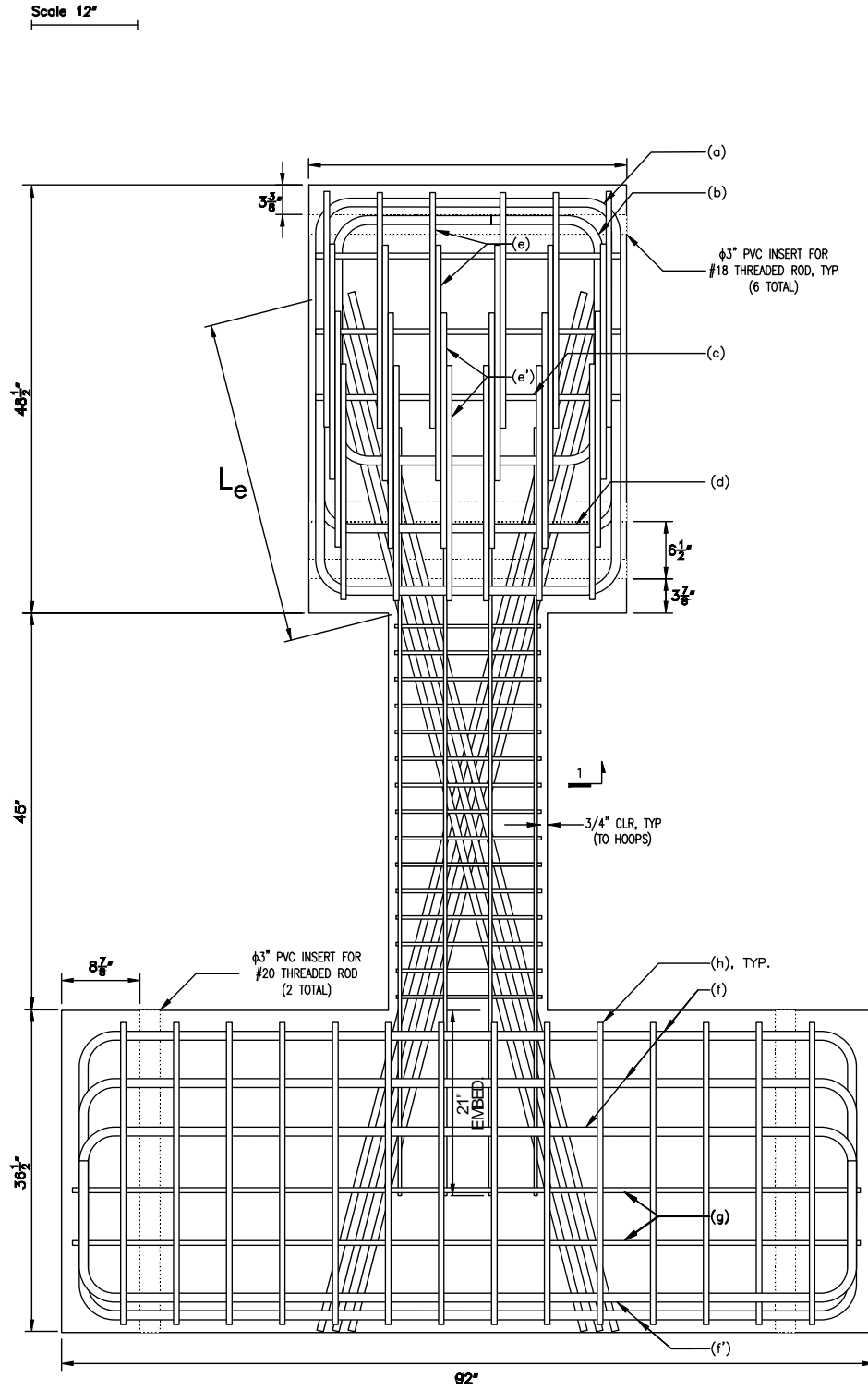


Figure 12 – Elevation view of D120-2.5 (1 in. = 25.4 mm)

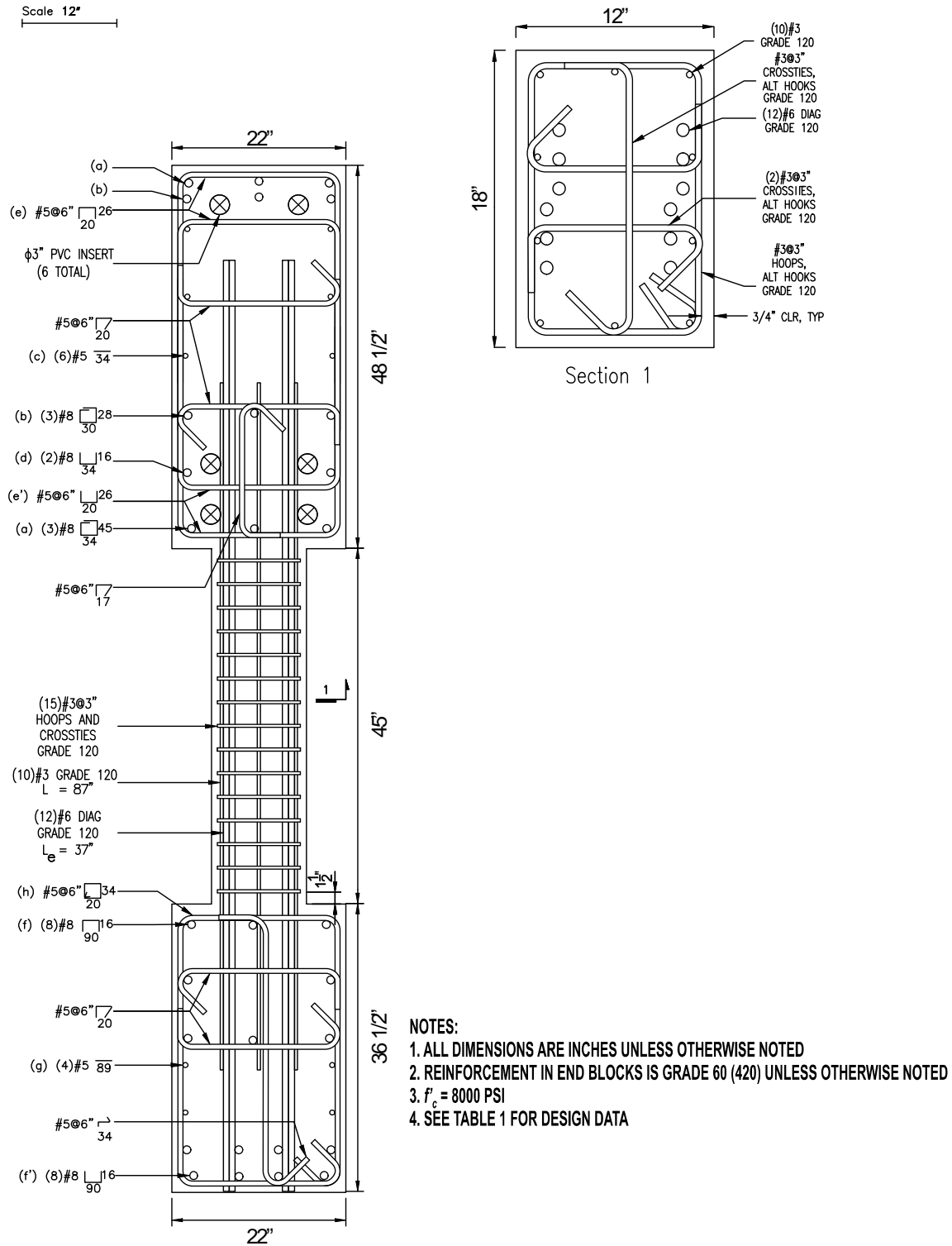


Figure 13 – Reinforcement details of D120-2.5 (1 in. = 25.4 mm, 1 ksi = 1,000 psi = 6.89 MPa)

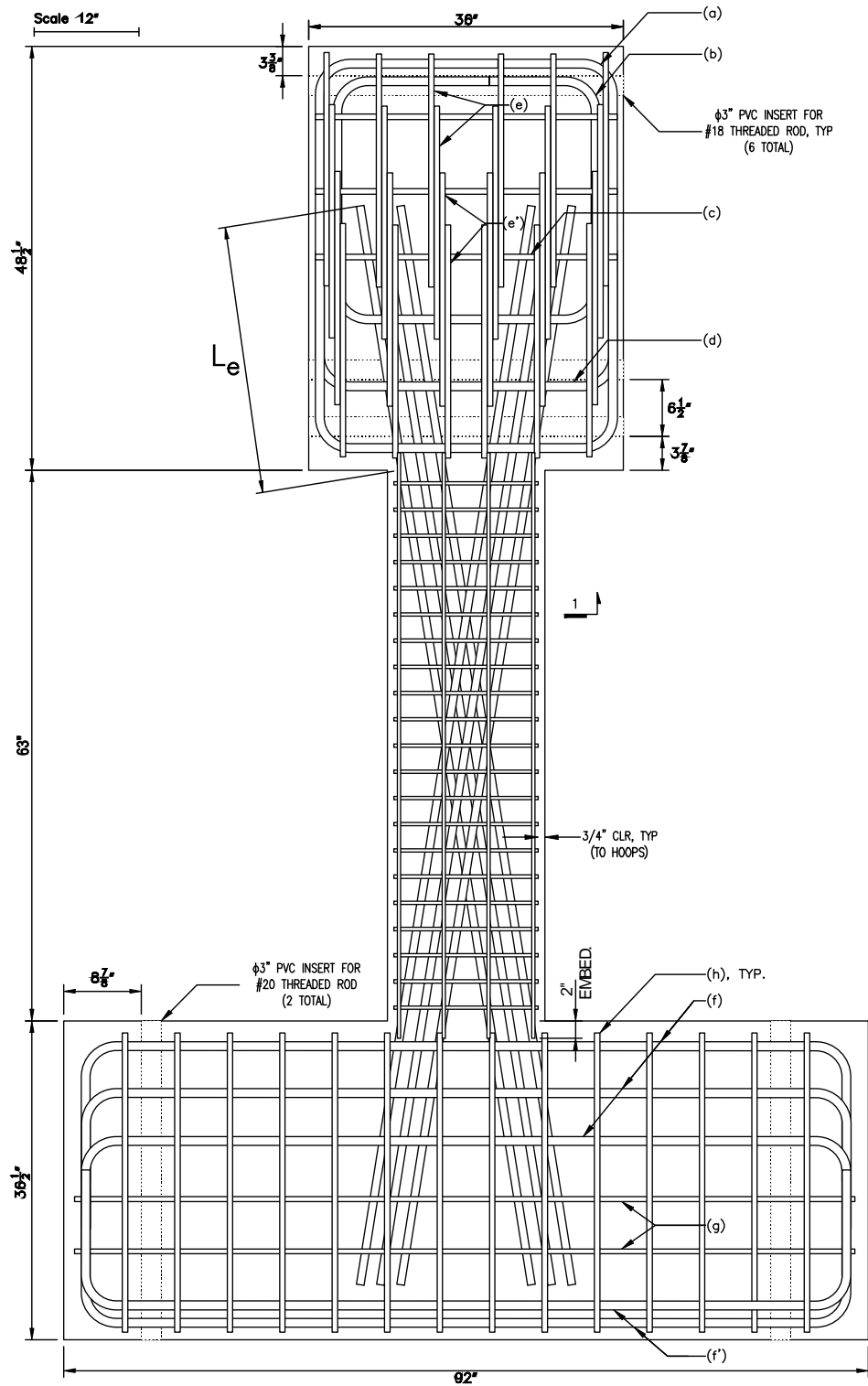


Figure 14 – Elevation view of D80-3.5 (1 in. = 25.4 mm)

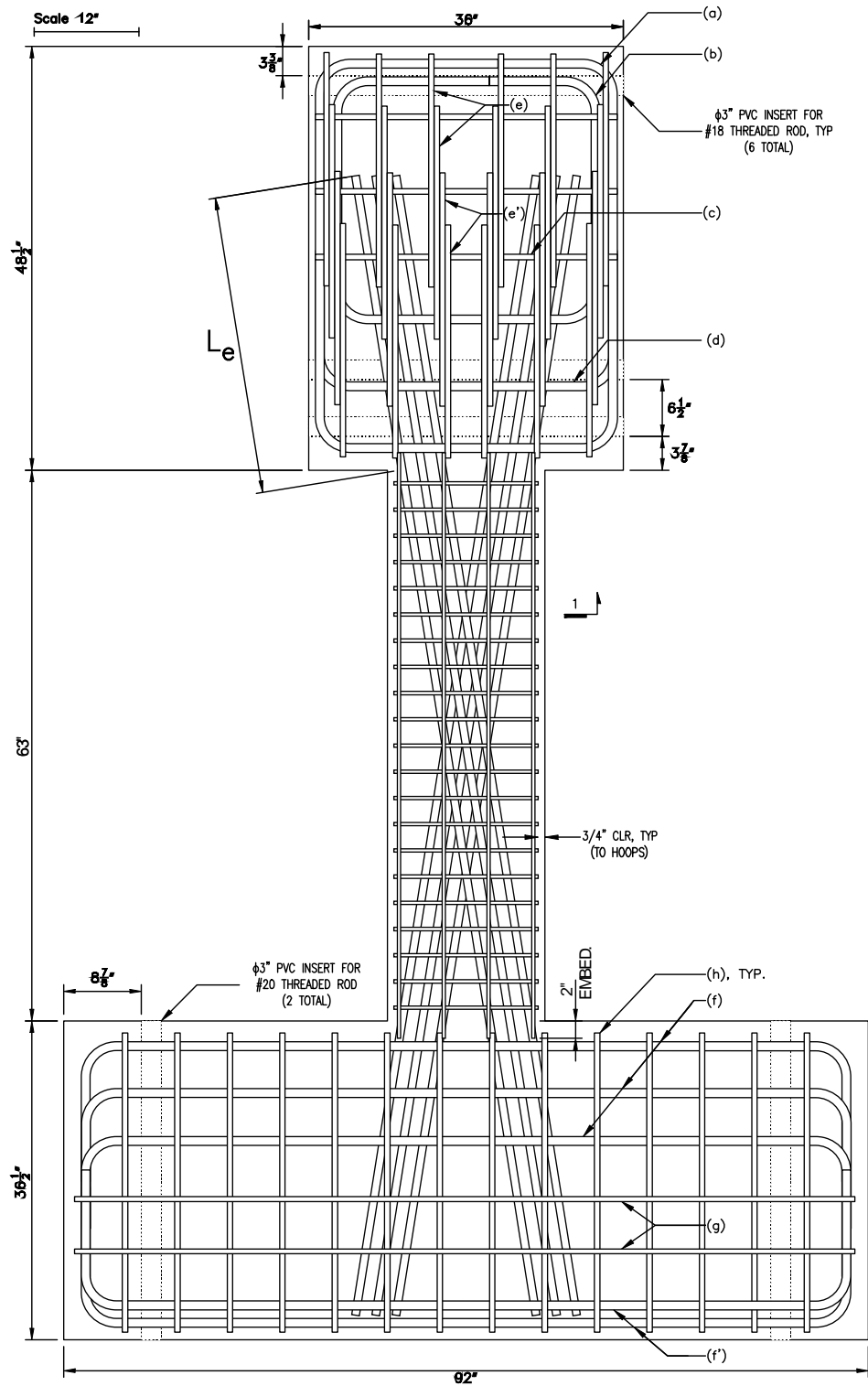


Figure 16 – Elevation view of D100-3.5 (1 in. = 25.4 mm)

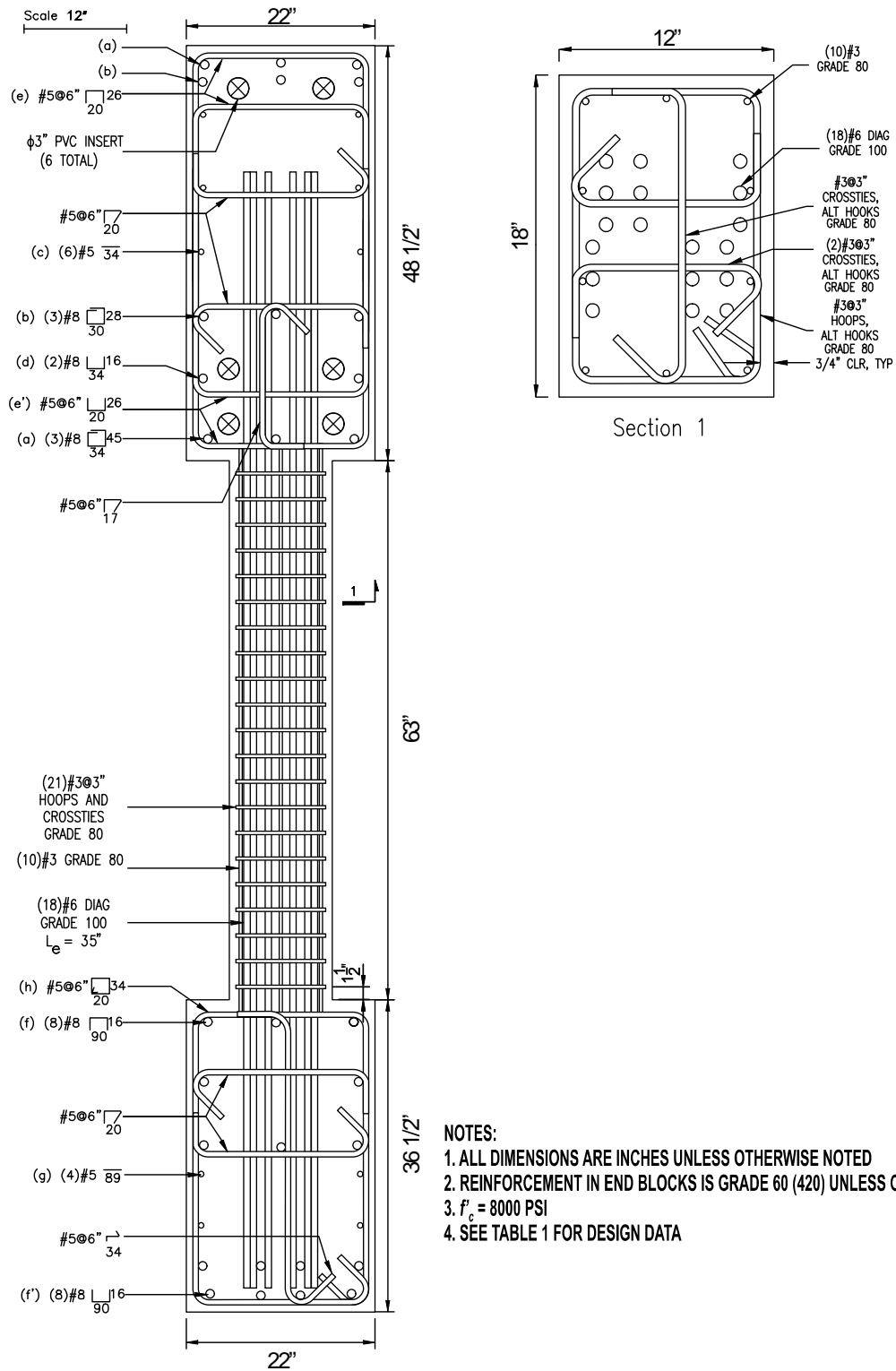


Figure 17 – Reinforcement details of D100-3.5 (1 in. = 25.4 mm, 1 ksi = 1,000 psi = 6.89 MPa)

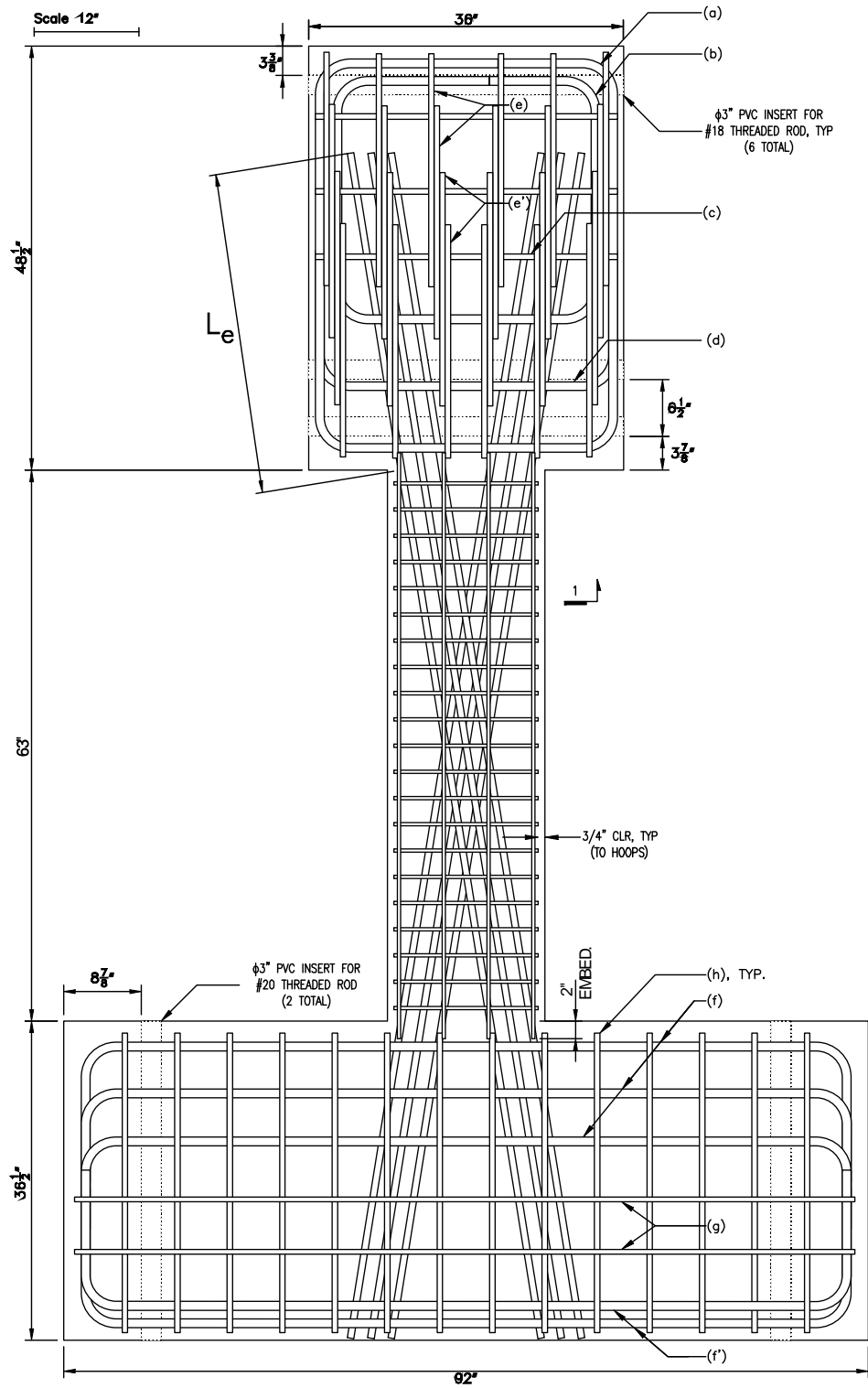


Figure 18 – Elevation view of D120-3.5 (1 in. = 25.4 mm)

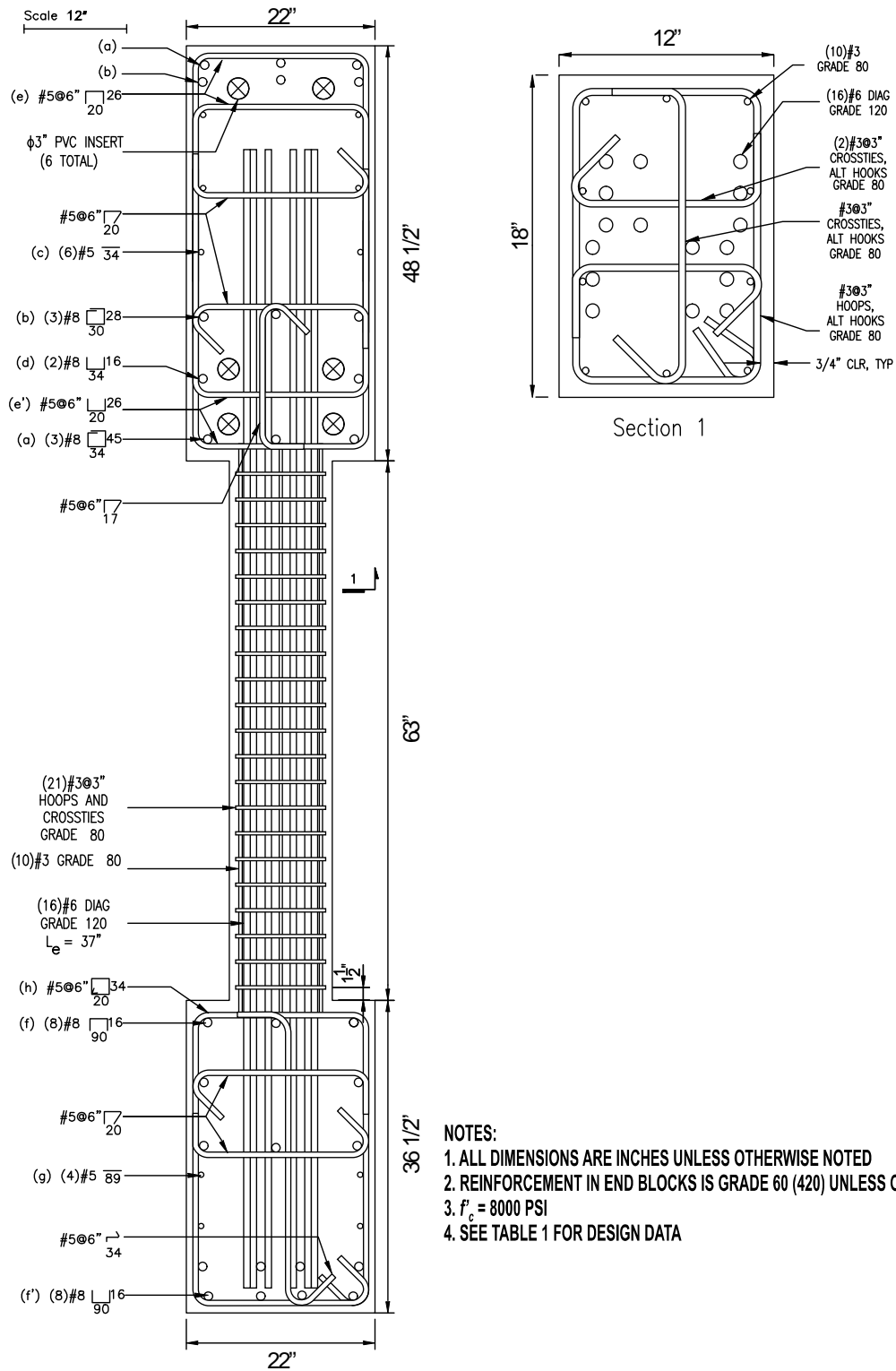


Figure 19 – Reinforcement details of D120-3.5 (1 in. = 25.4 mm, 1 ksi = 1,000 psi = 6.89 MPa)

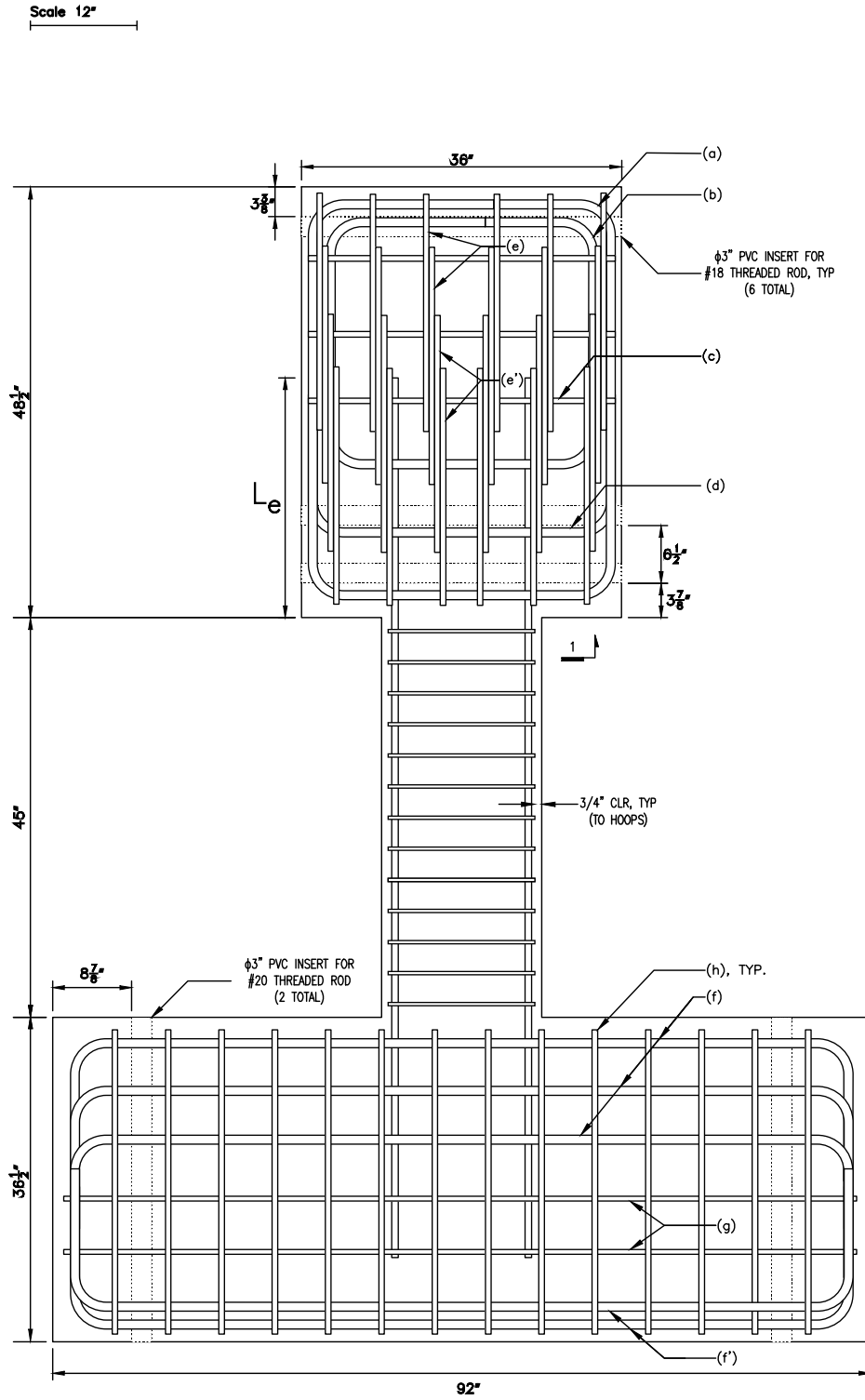


Figure 20 – Elevation view of P80-2.5 (1 in. = 25.4 mm)

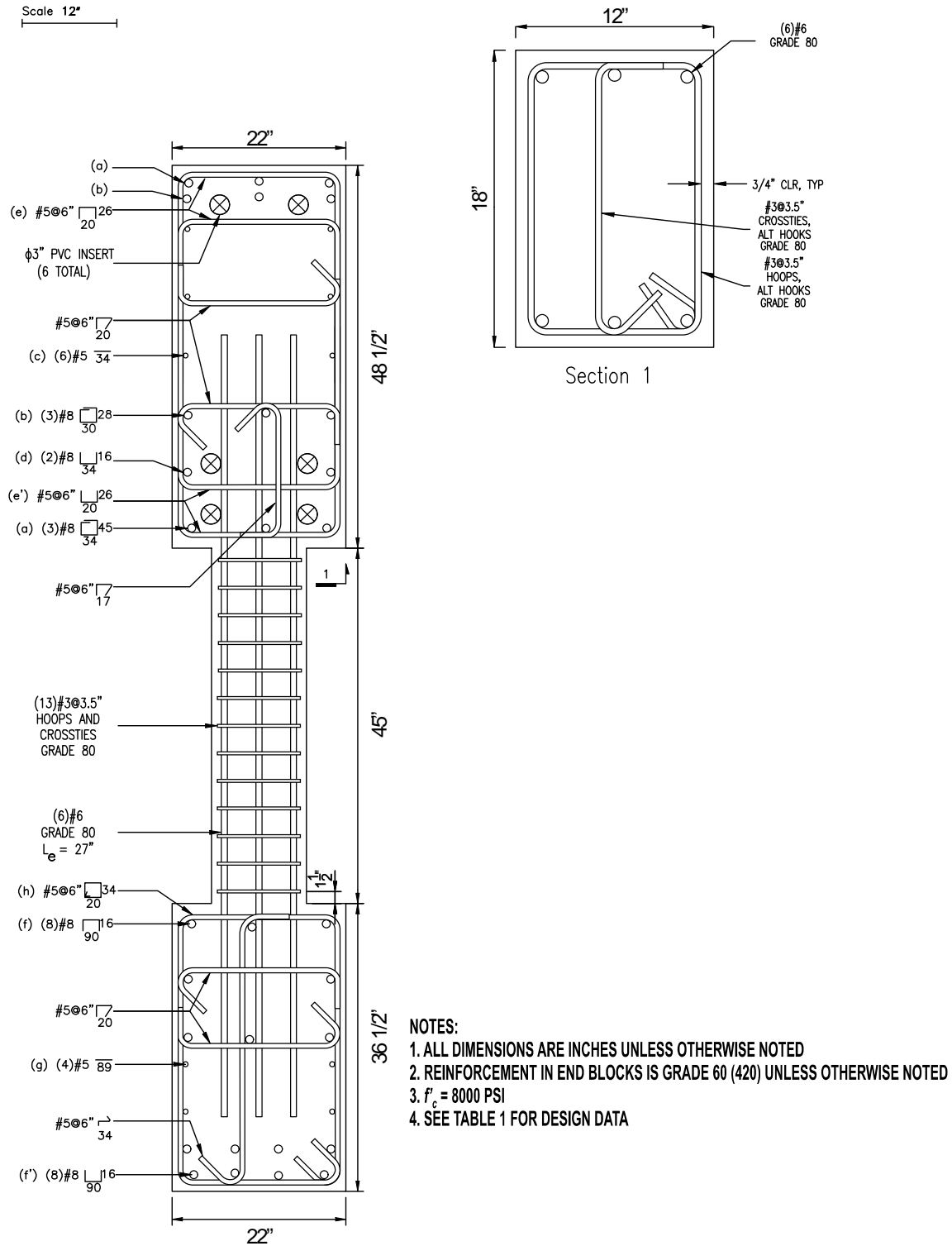


Figure 21 – Reinforcement details of P80-2.5 (1 in. = 25.4 mm, 1 ksi = 1,000 psi = 6.89 MPa)

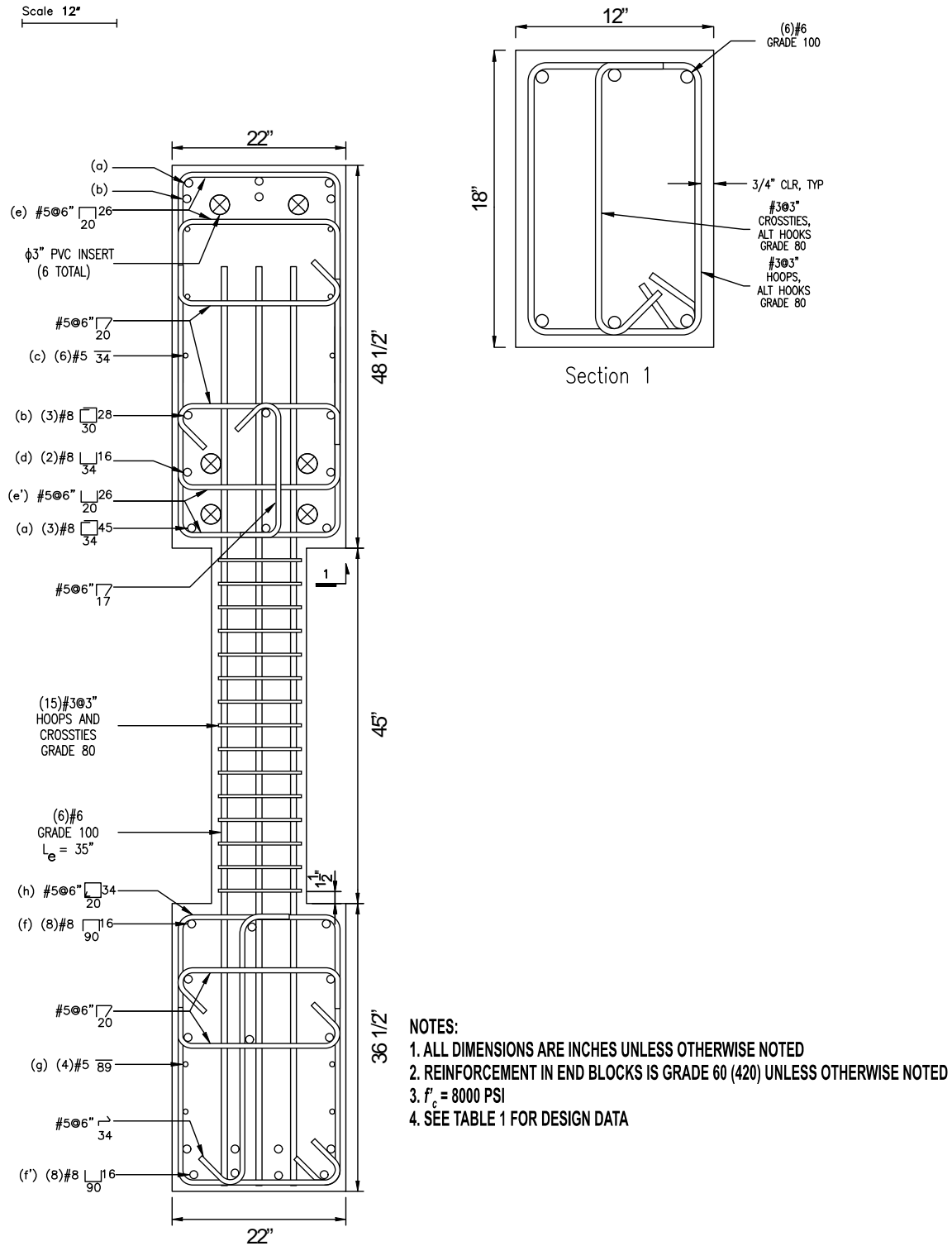


Figure 23 – Reinforcement details of P100-2.5 (1 in. = 25.4 mm, 1 ksi = 1,000 psi = 6.89 MPa)

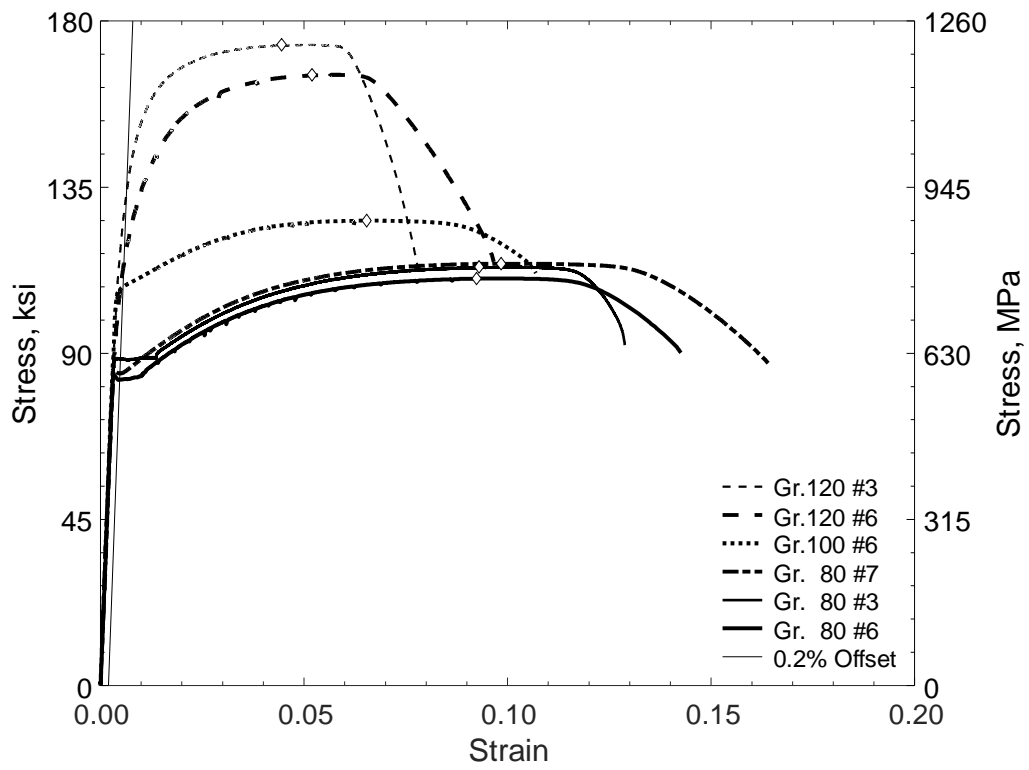


Figure 24 – Measured stress versus strain for reinforcement

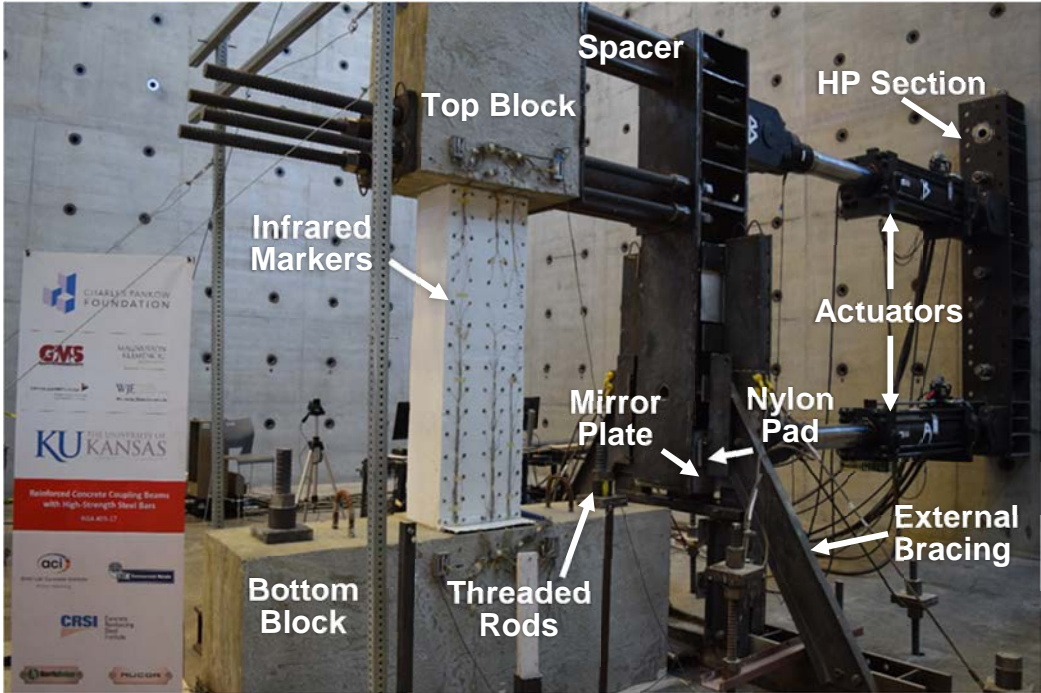


Figure 25 – Test setup, view from northeast

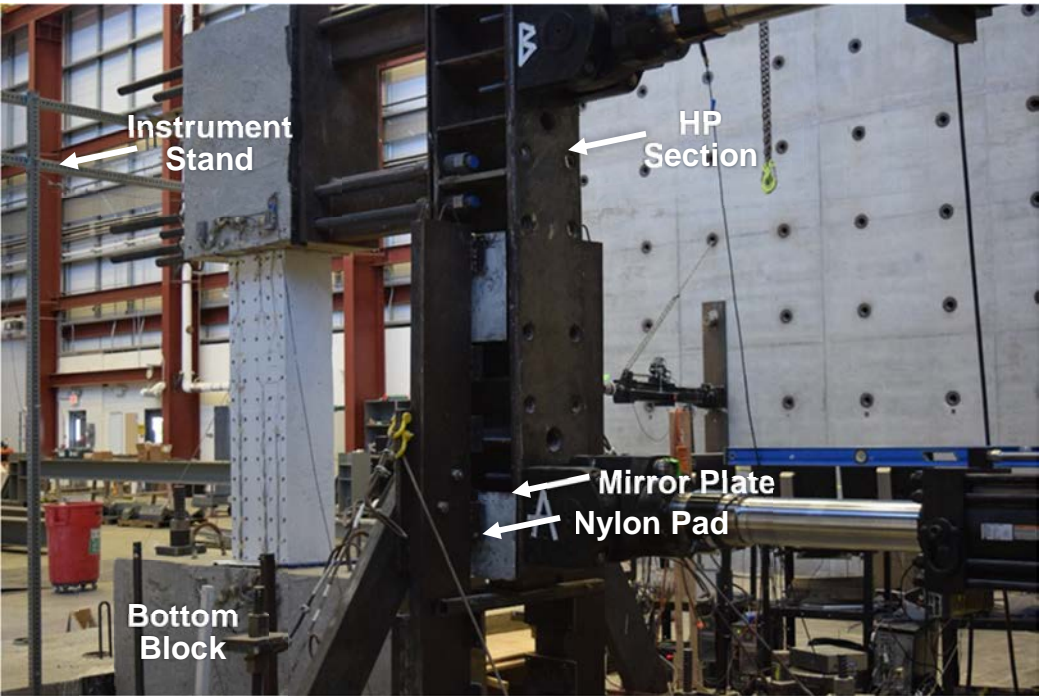


Figure 26 – Test setup, view from northwest

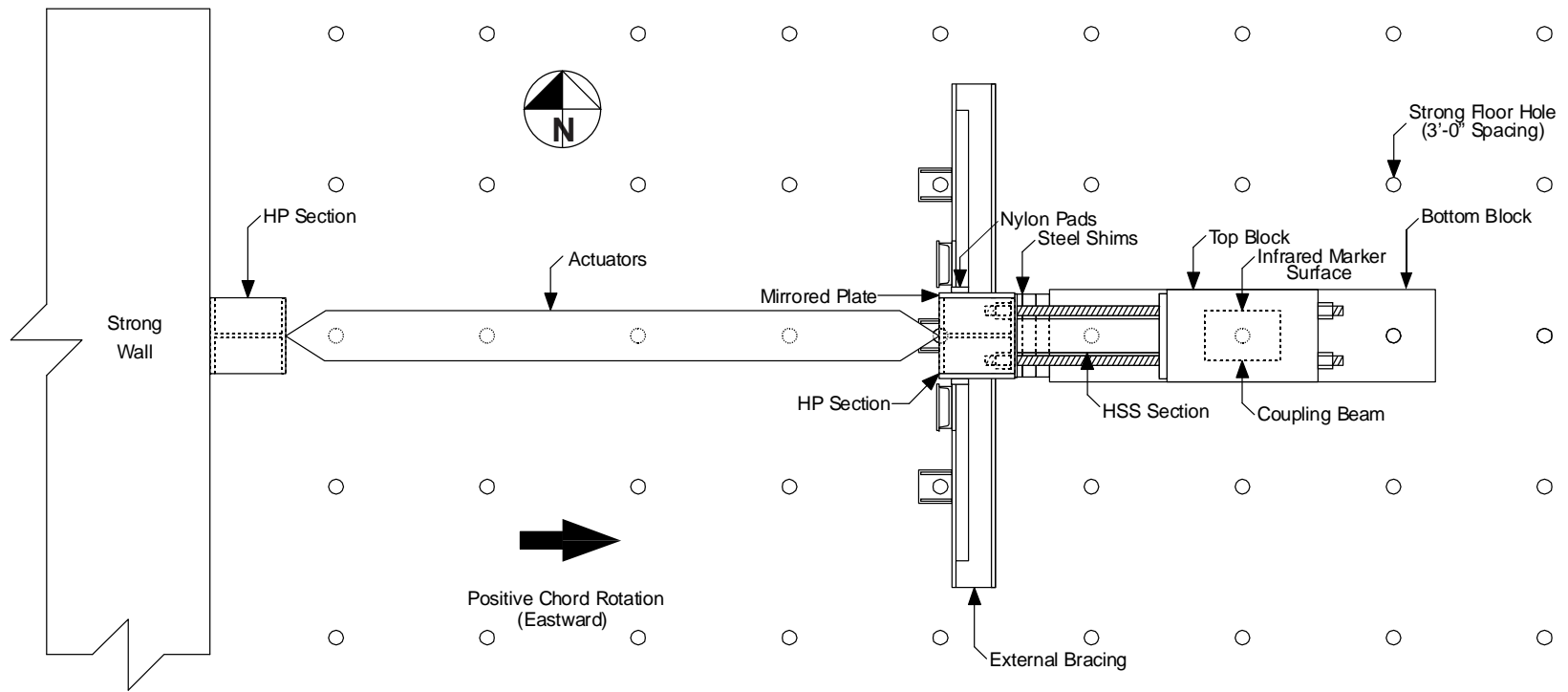


Figure 27 – Test setup, plan view

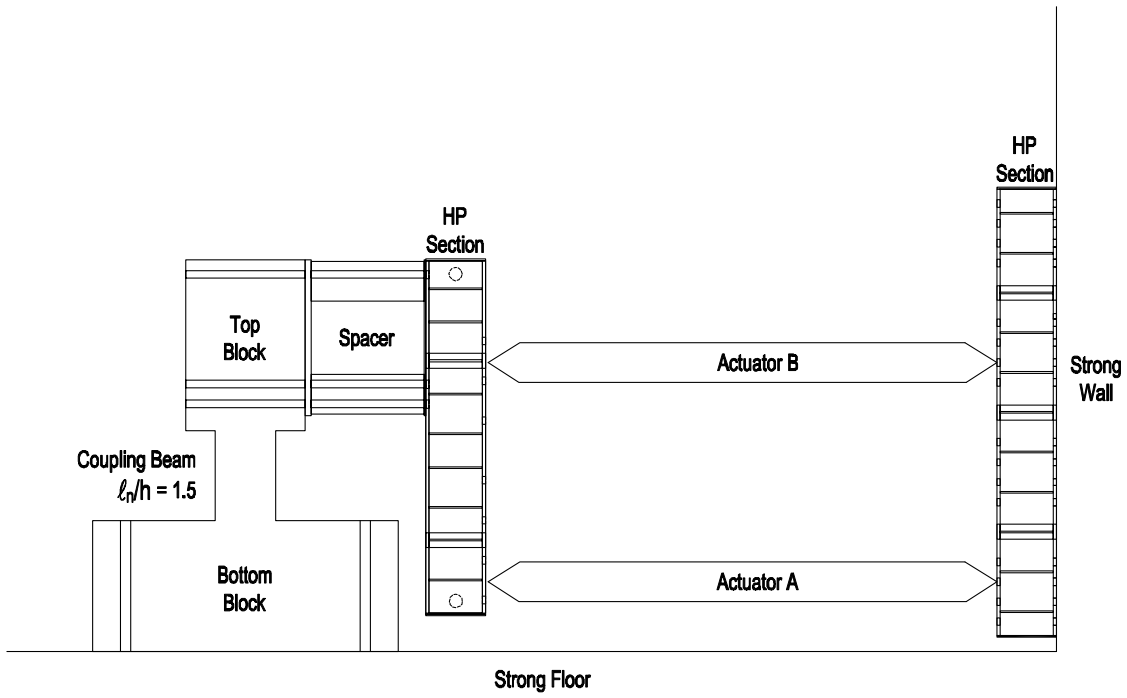


Figure 28 – Test setup for coupling beams with aspect ratio of 1.5^a

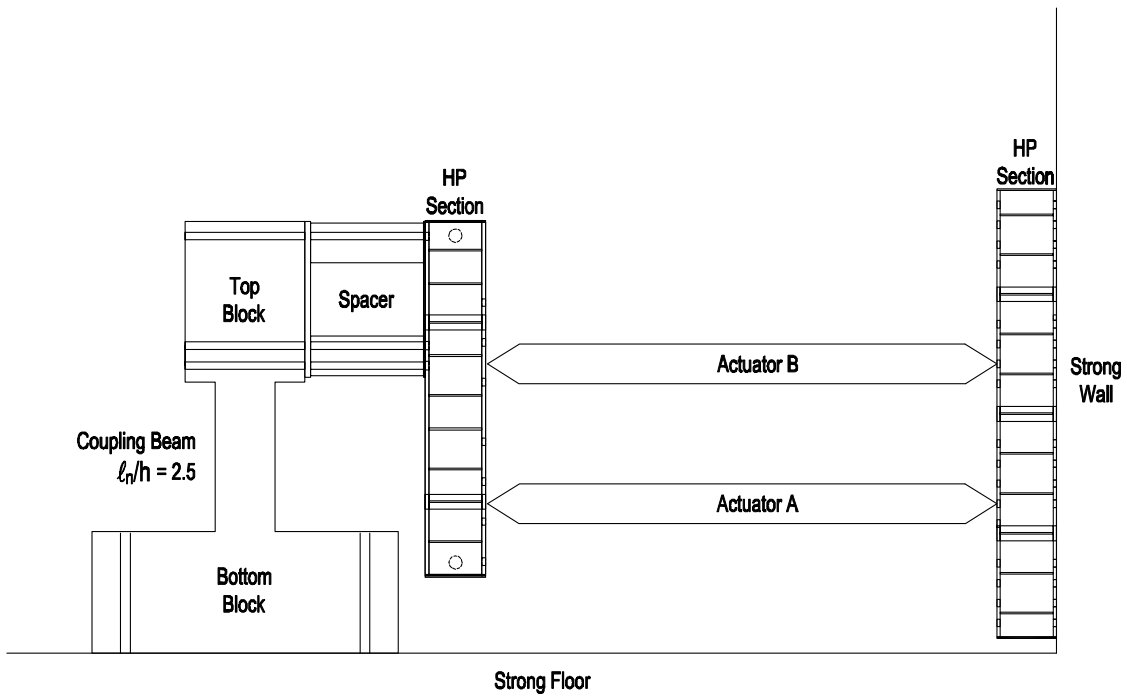


Figure 29 – Test setup for coupling beams with aspect ratio of 2.5^a

^a External bracing omitted for clarity. Actuator and coupling beam elevations in Table 5.

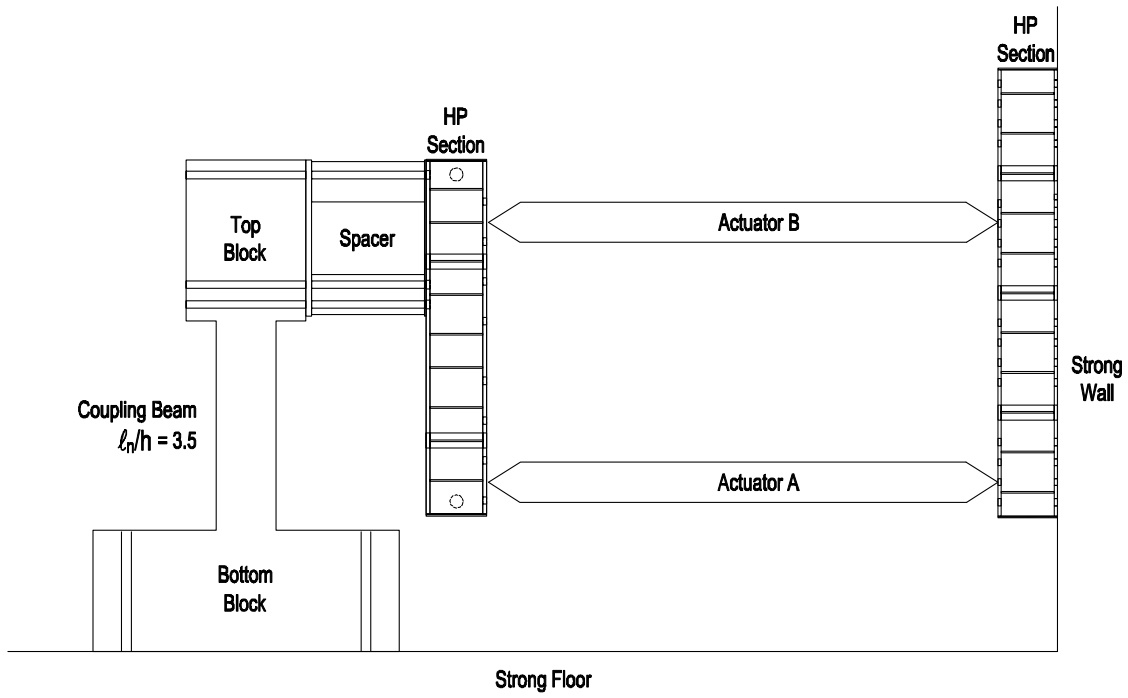


Figure 30 – Test setup for coupling beams with aspect ratio of 3.5^a

^a External bracing omitted for clarity. Actuator and coupling beam elevations in Table 5.

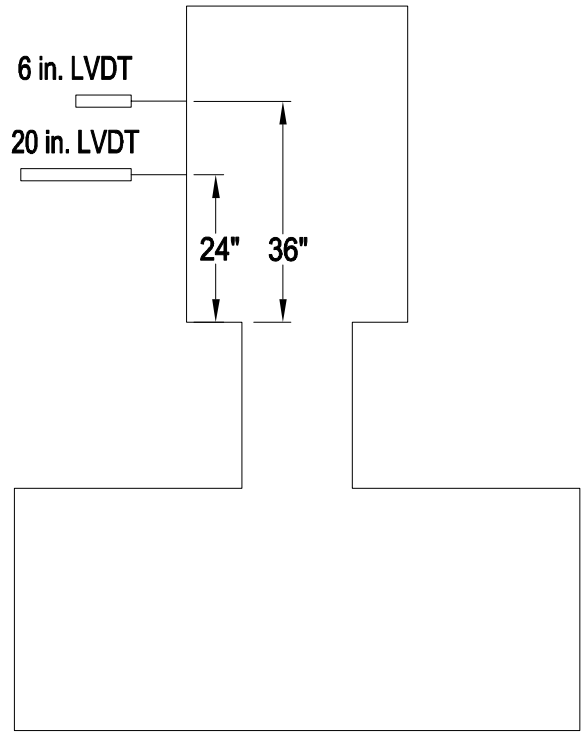


Figure 31 – LVDT locations (1 in. = 25.4 mm)

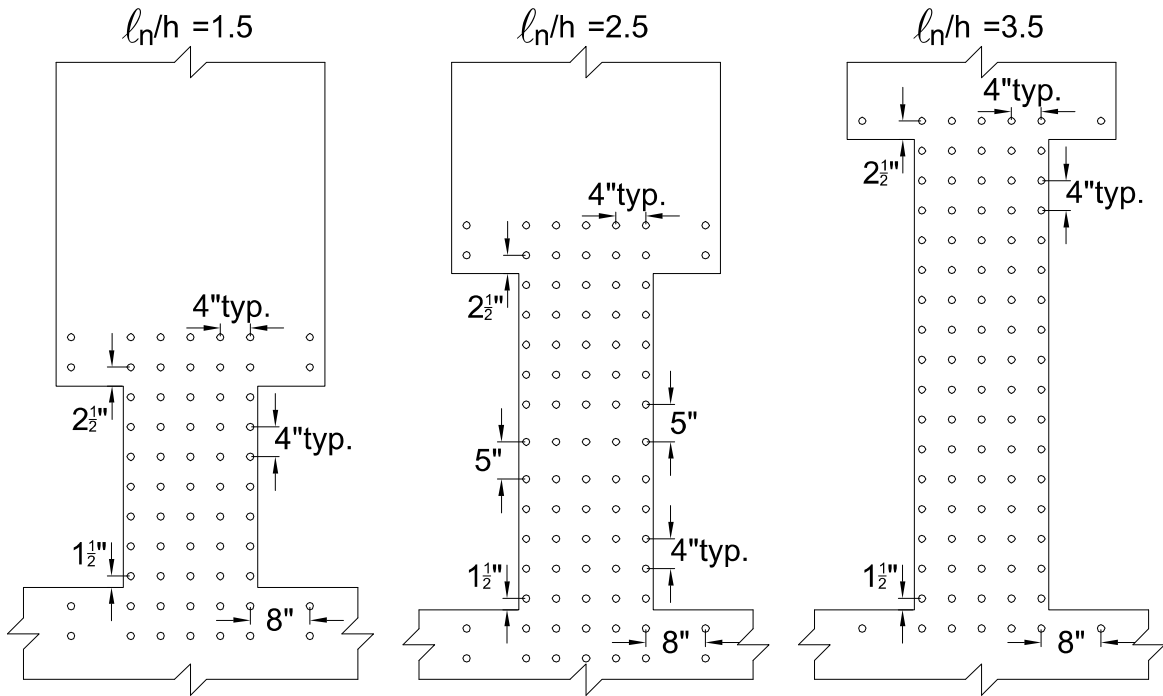


Figure 32 – Infrared marker positions (1 in. = 25.4 mm)

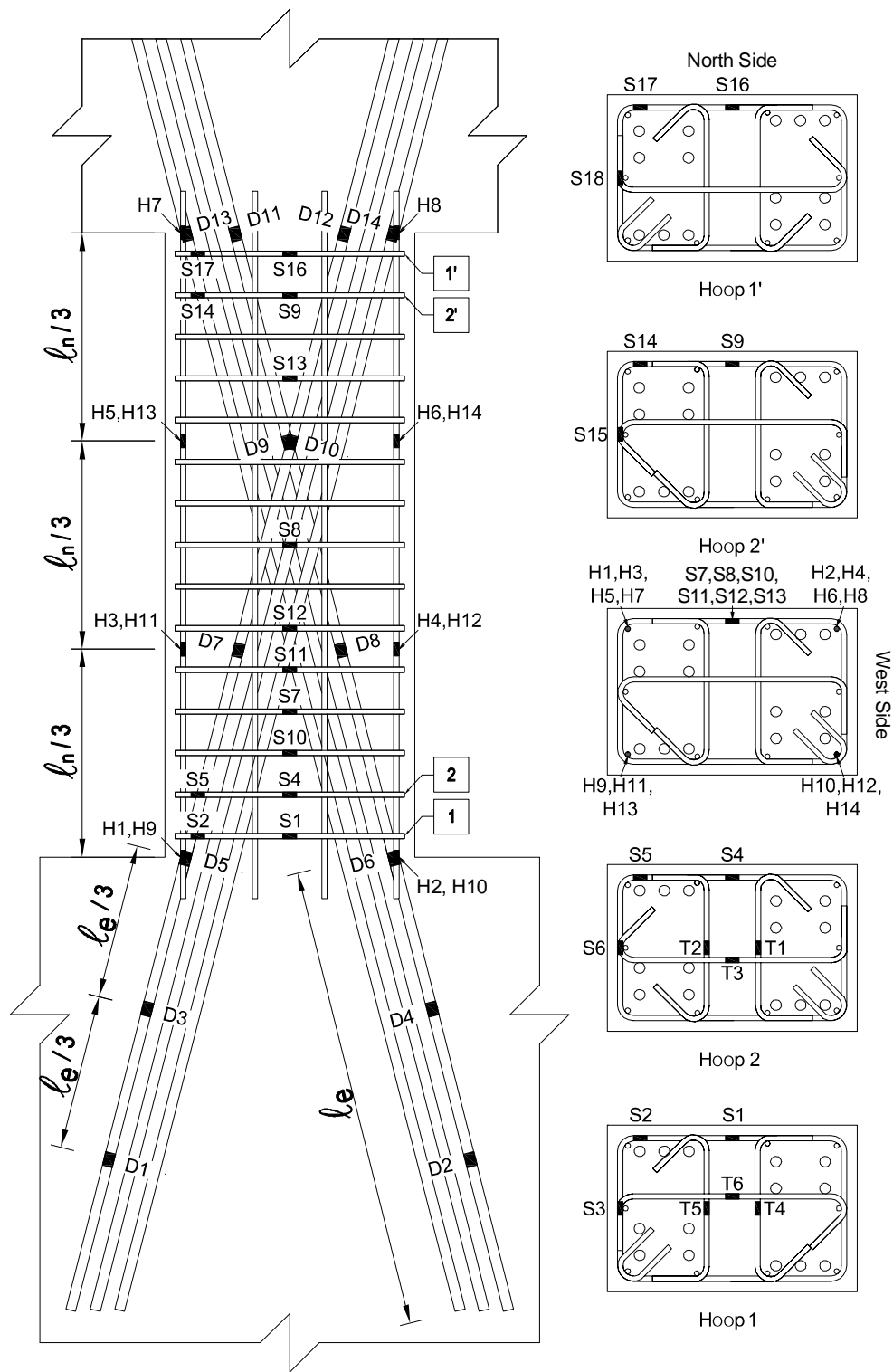


Figure 33 – Strain gauge layout (view from north), D-type specimens

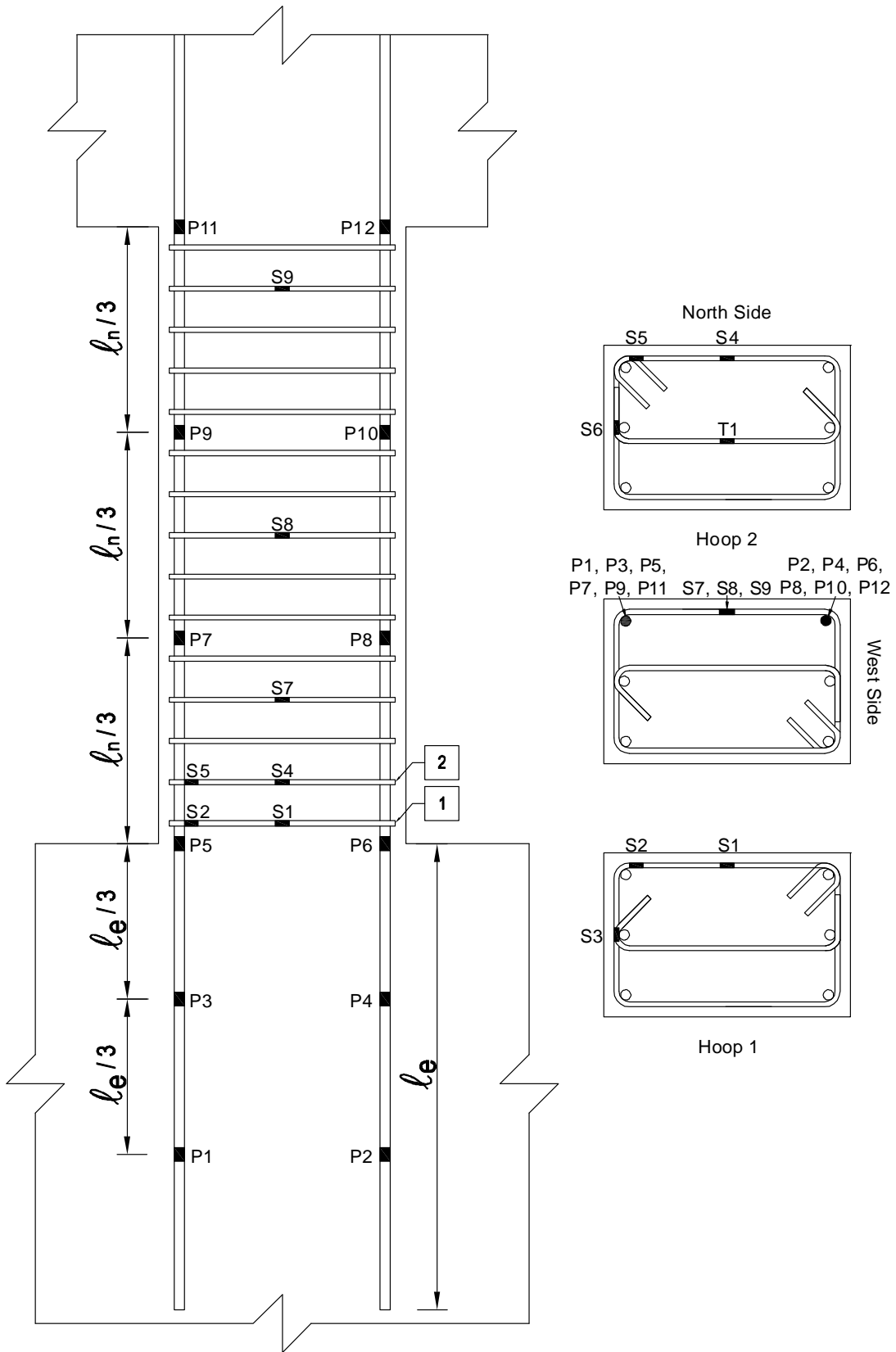


Figure 34 – Strain gauge layout (view from north), P-type specimens

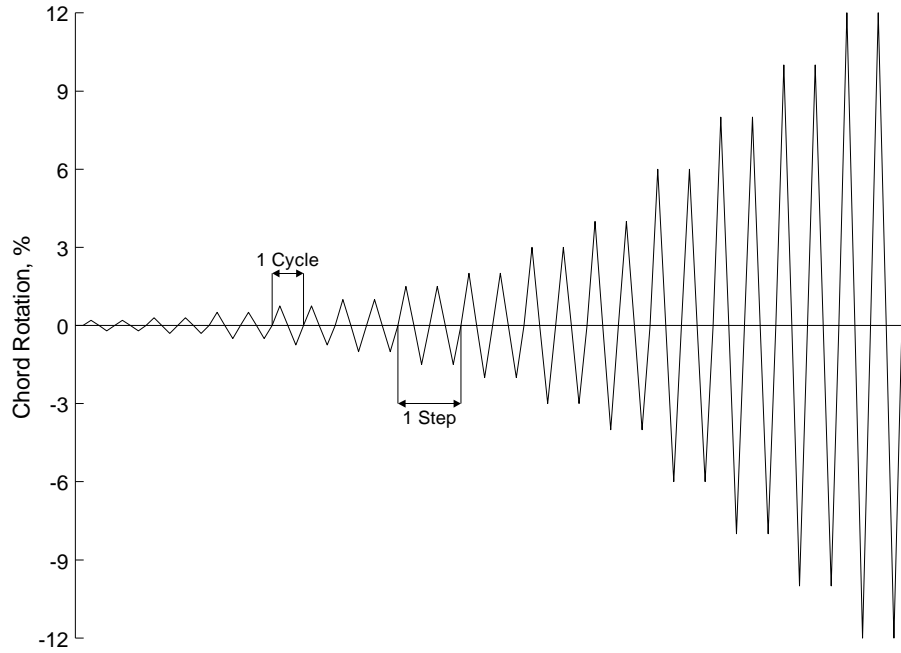


Figure 35 – Loading protocol^a

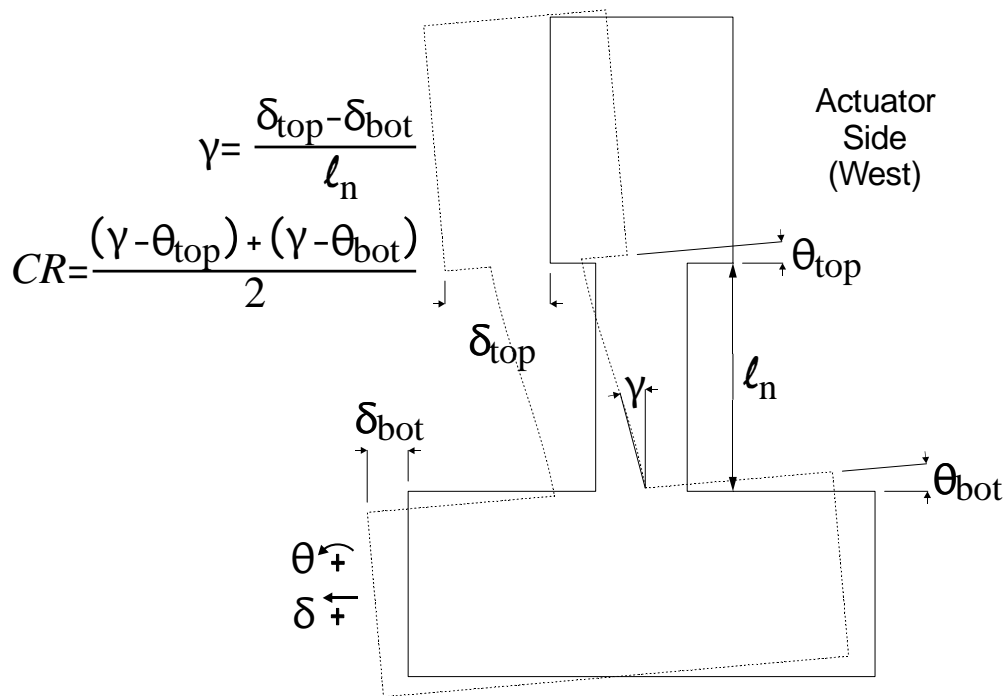


Figure 36 – General deformed shape of specimen, view from north^b

^a Values listed in Table 8.

^b Positive displacement corresponds to actuator extension toward laboratory east.

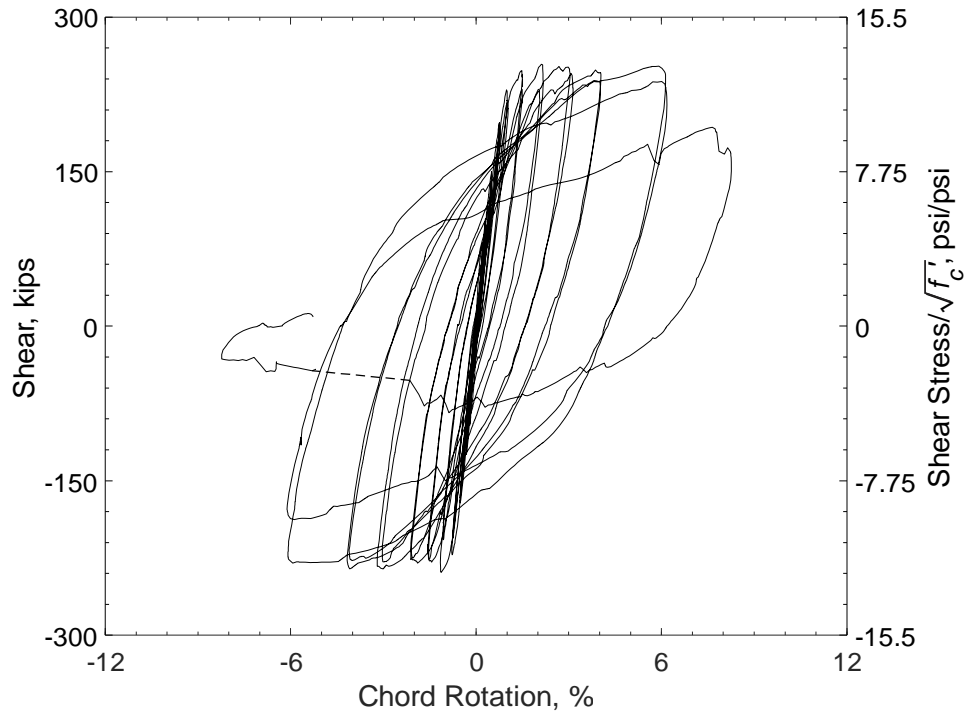


Figure 37 – Shear versus chord rotation for D80-1.5
 (1,000 psi = 6.89 MPa, 1 kip = 4.45 kN)

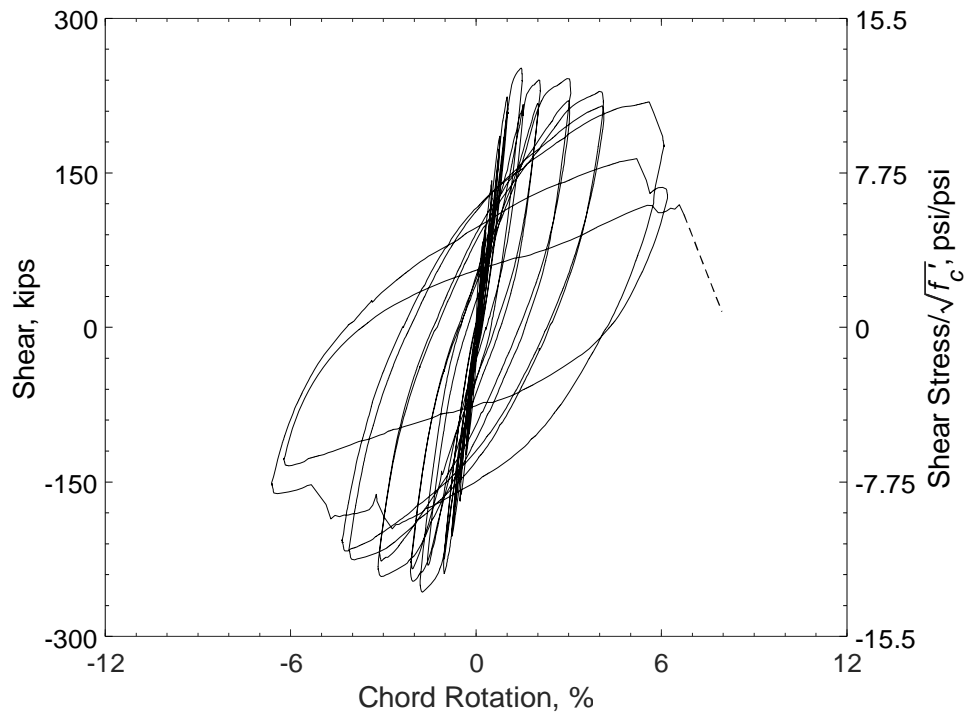


Figure 38 – Shear versus chord rotation for D100-1.5
 (1,000 psi = 6.89 MPa, 1 kip = 4.45 kN)

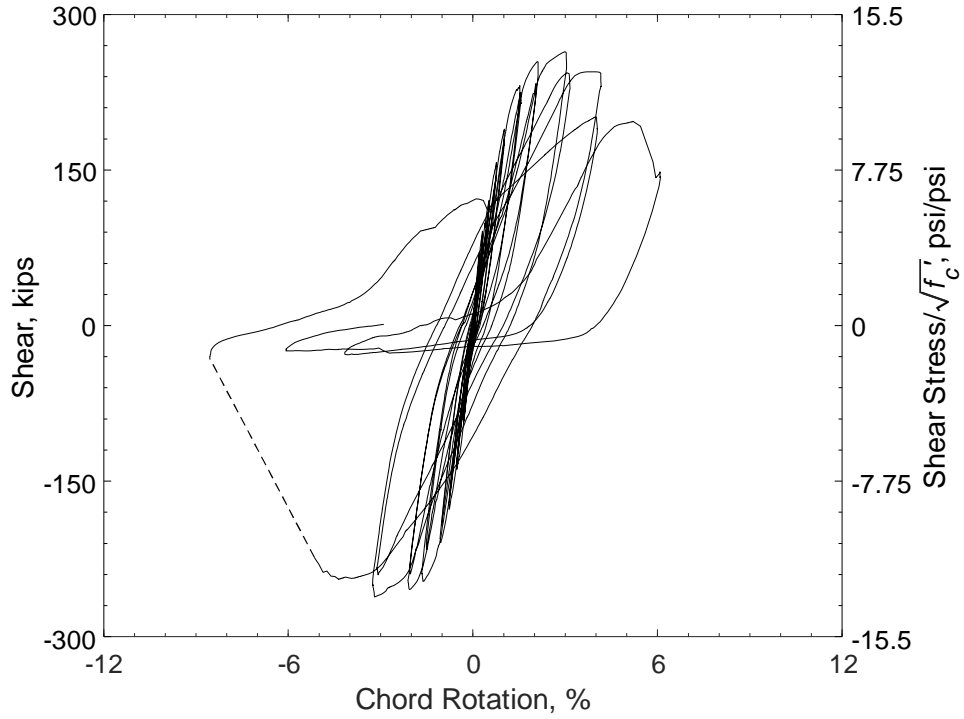


Figure 39 – Shear versus chord rotation for D120-1.5
(1,000 psi = 6.89 MPa, 1 kip = 4.45 kN)

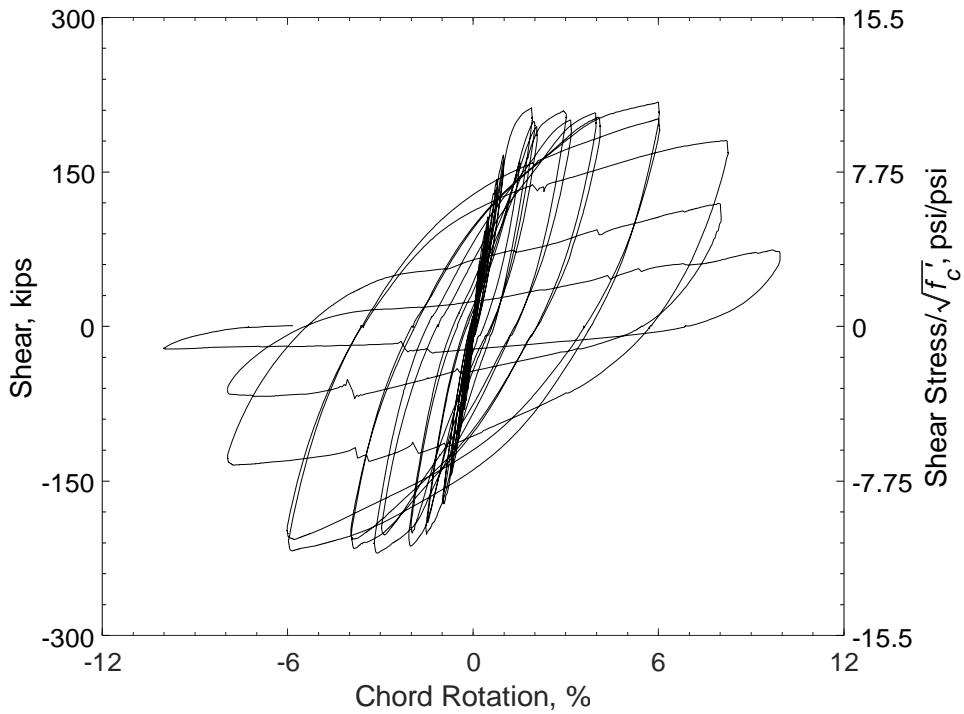


Figure 40 – Shear versus chord rotation for D80-2.5
(1,000 psi = 6.89 MPa, 1 kip = 4.45 kN)

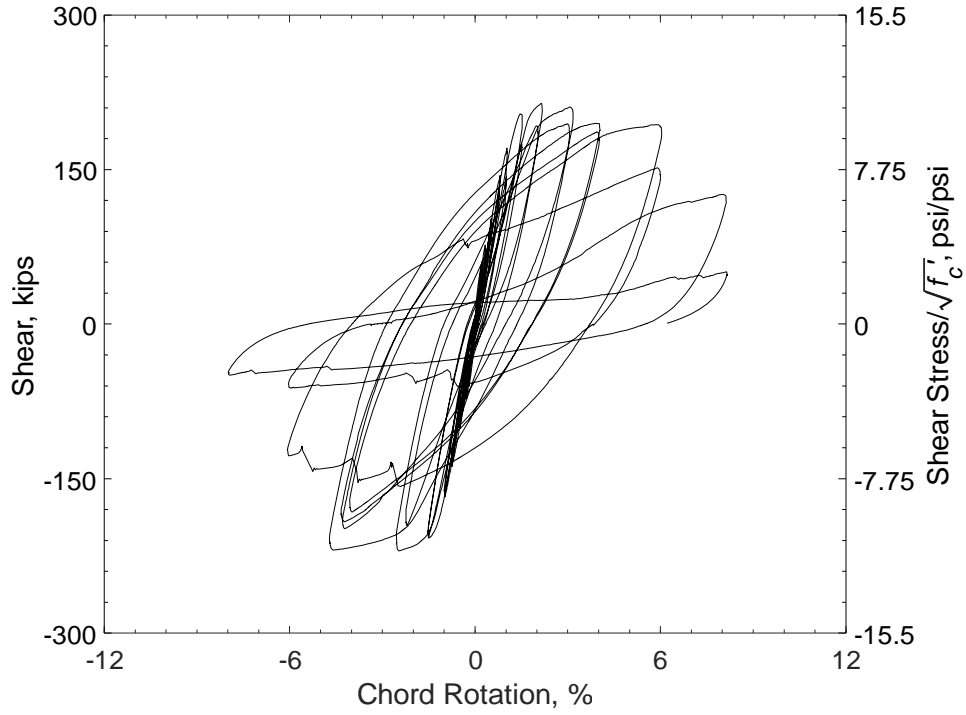


Figure 41 – Shear versus chord rotation for D100-2.5
(1,000 psi = 6.89 MPa, 1 kip = 4.45 kN)

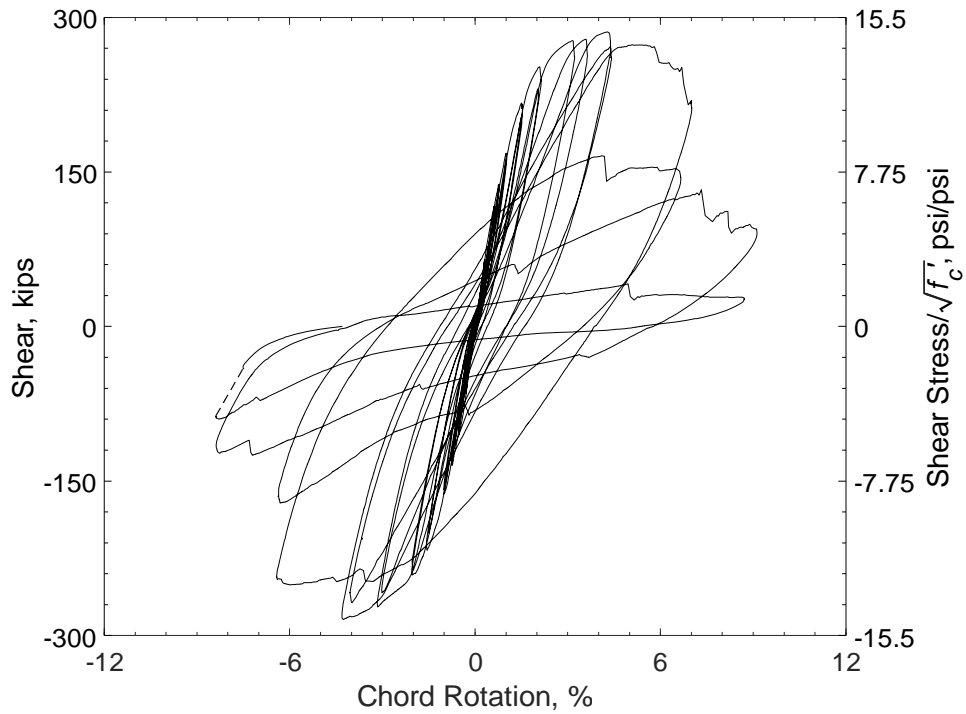


Figure 42 – Shear versus chord rotation for D120-2.5
(1,000 psi = 6.89 MPa, 1 kip = 4.45 kN)

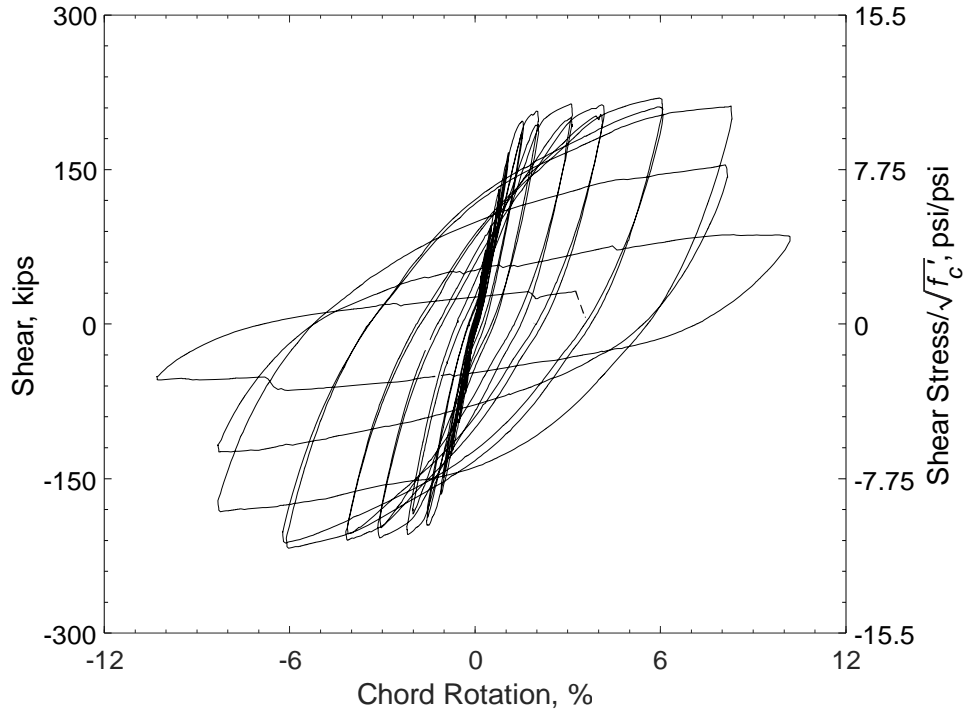


Figure 43 – Shear versus chord rotation for D80-3.5
(1,000 psi = 6.89 MPa, 1 kip = 4.45 kN)

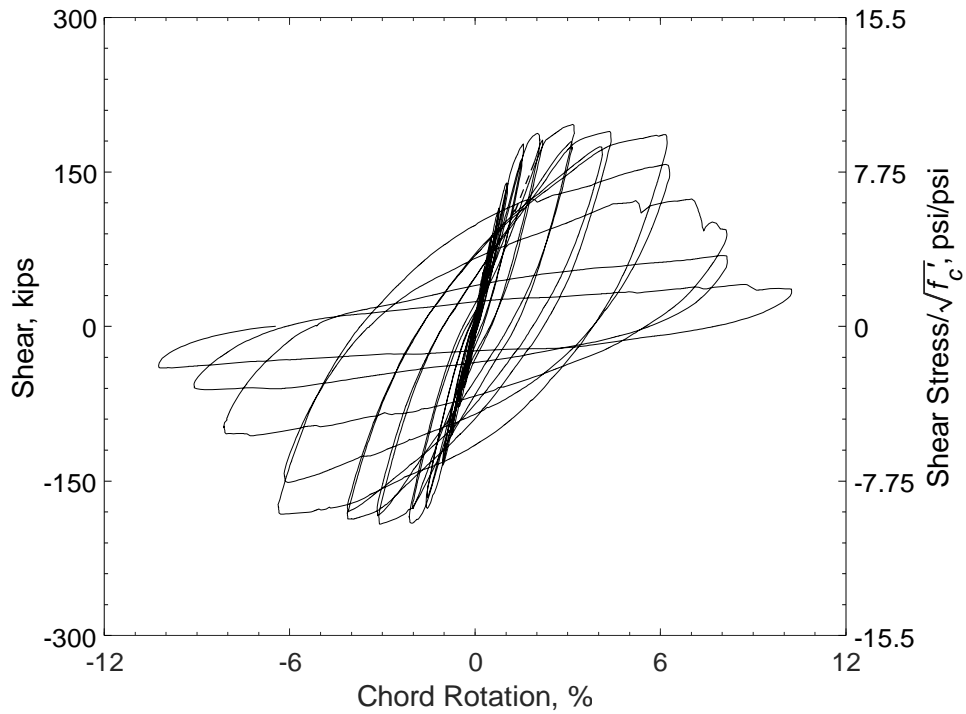


Figure 44 – Shear versus chord rotation for D100-3.5
(1,000 psi = 6.89 MPa, 1 kip = 4.45 kN)

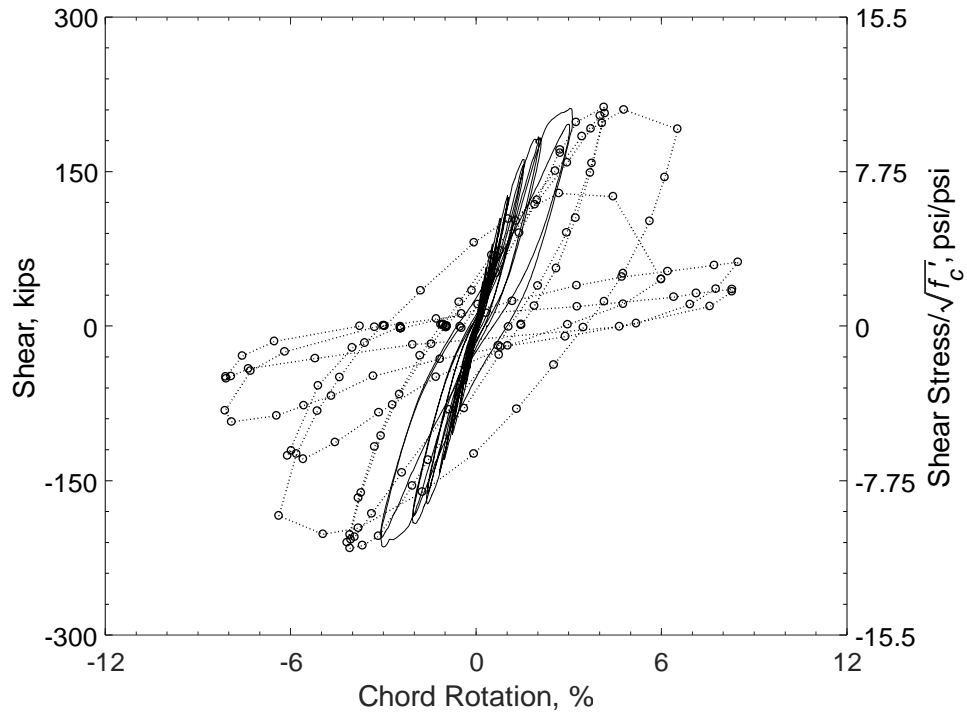


Figure 45 – Shear versus chord rotation for D120-3.5
 (1,000 psi = 6.89 MPa, 1 kip = 4.45 kN)

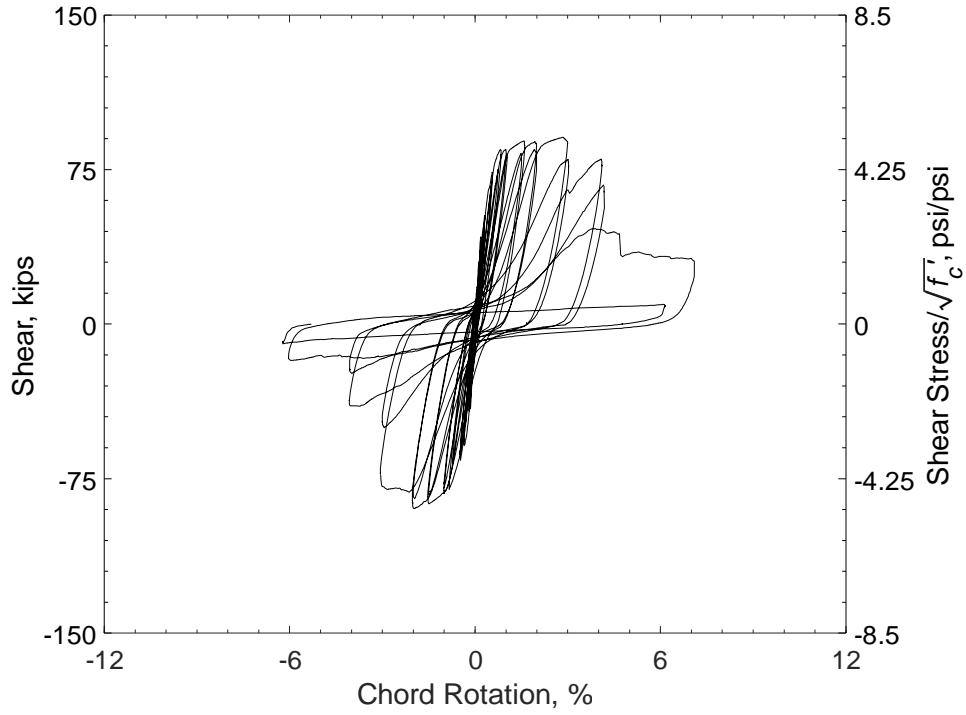


Figure 46 – Shear versus chord rotation for P80-2.5
 (1,000 psi = 6.89 MPa, 1 kip = 4.45 kN)

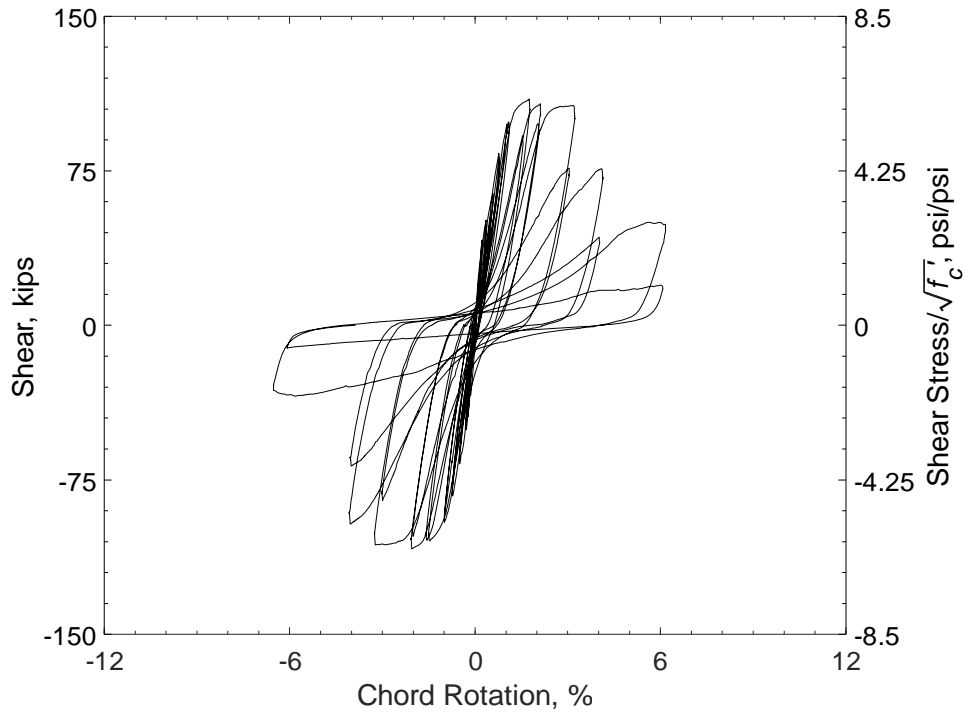


Figure 47 – Shear versus chord rotation for P100-2.5
 (1,000 psi = 6.89 MPa, 1 kip = 4.45 kN)

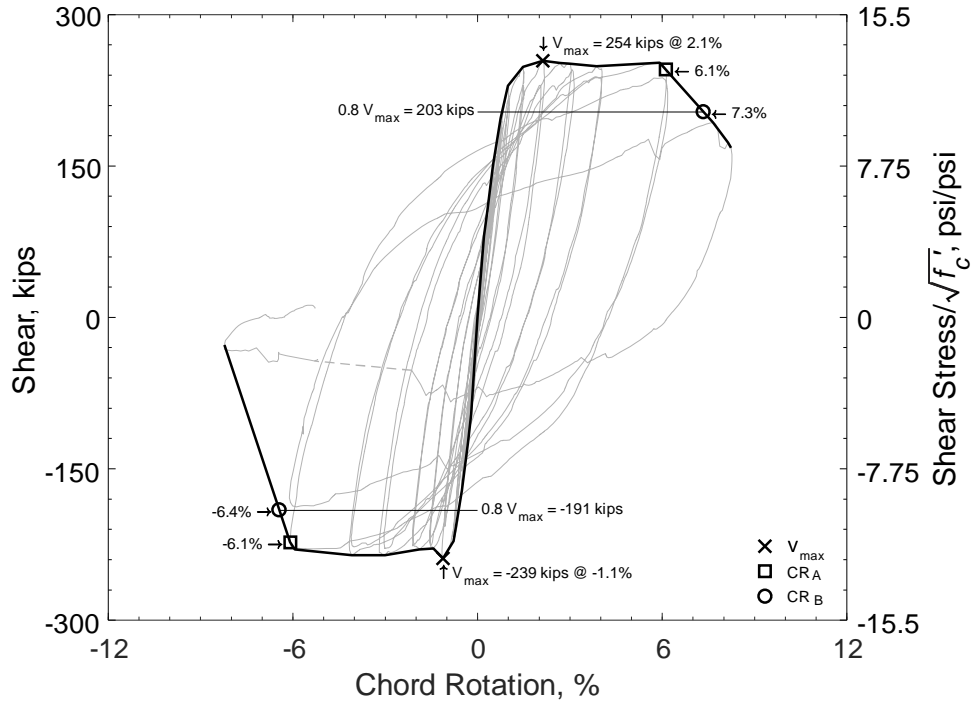


Figure 48 – Shear versus chord rotation envelope for D80-1.5
(1,000 psi = 6.89 MPa, 1 kip = 4.45 kN)

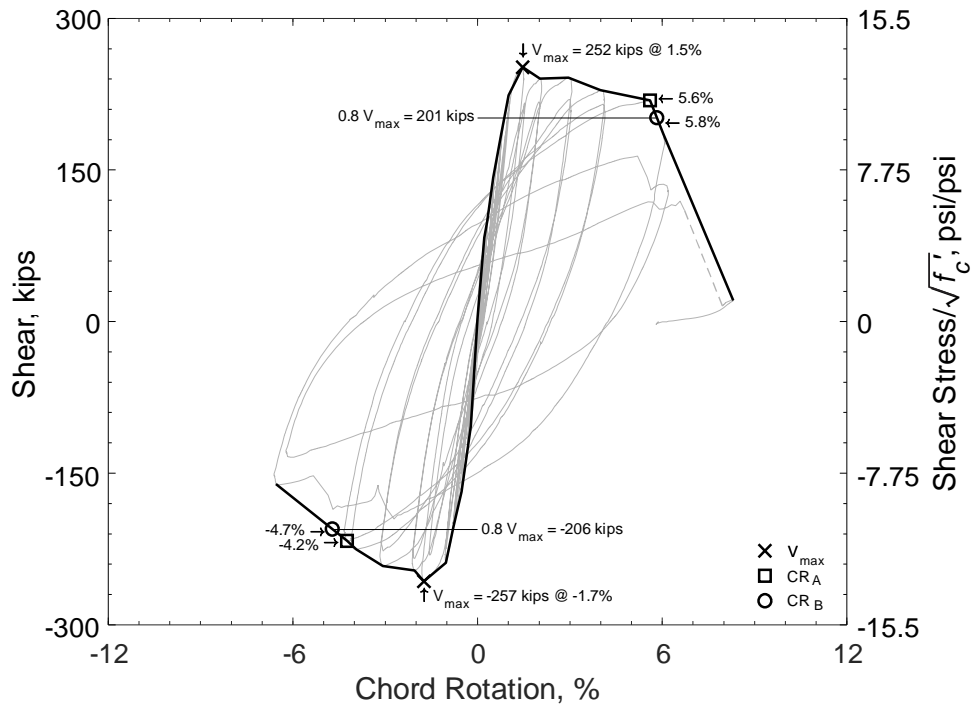


Figure 49 – Shear versus chord rotation envelope for D100-1.5
(1,000 psi = 6.89 MPa, 1 kip = 4.45 kN)

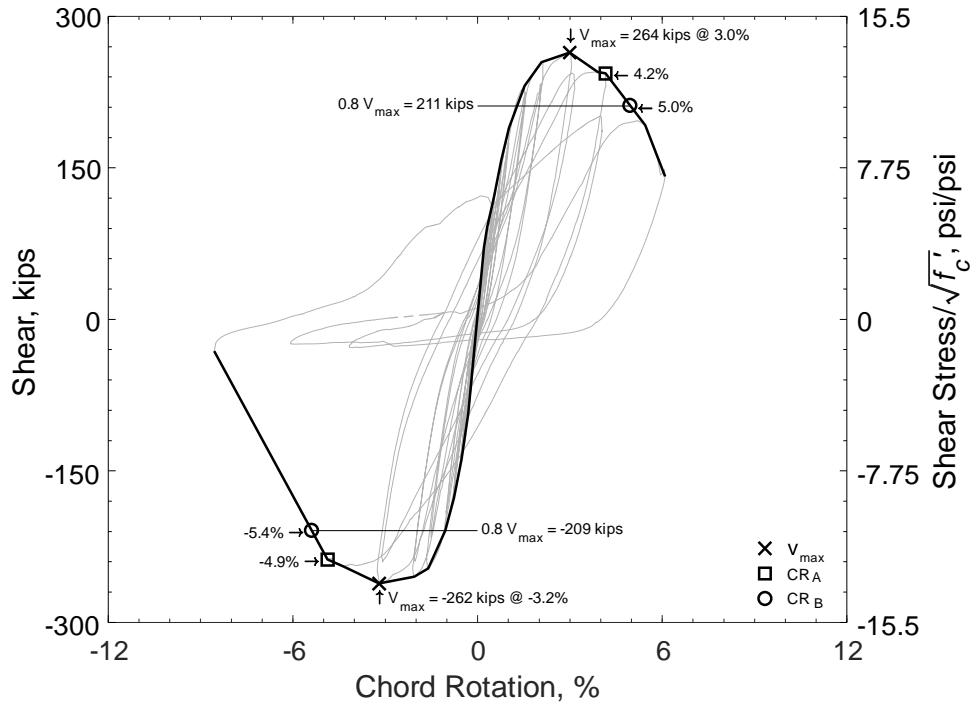


Figure 50 – Shear versus chord rotation envelope for D120-1.5
(1,000 psi = 6.89 MPa, 1 kip = 4.45 kN)

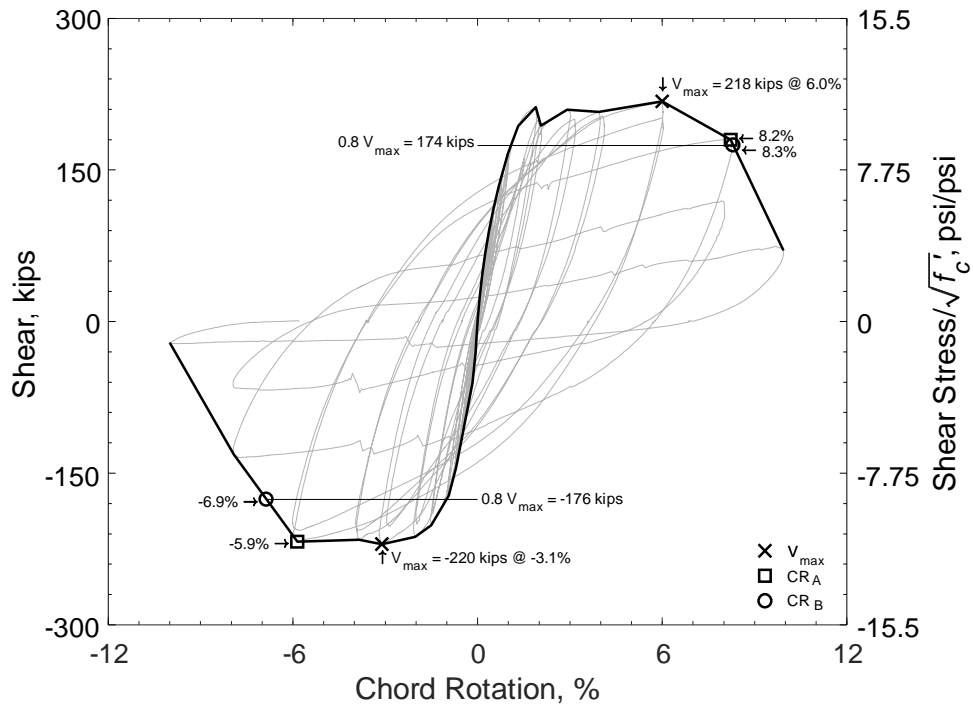


Figure 51 – Shear versus chord rotation envelope for D80-2.5
(1,000 psi = 6.89 MPa, 1 kip = 4.45 kN)

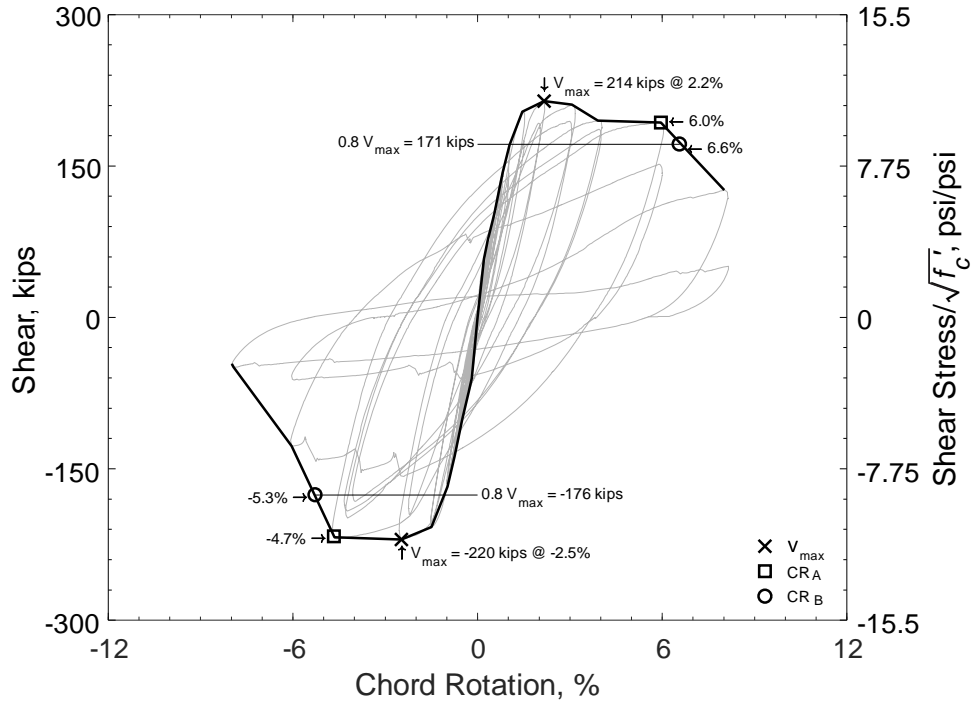


Figure 52 – Shear versus chord rotation envelope for D100-2.5
(1,000 psi = 6.89 MPa, 1 kip = 4.45 kN)

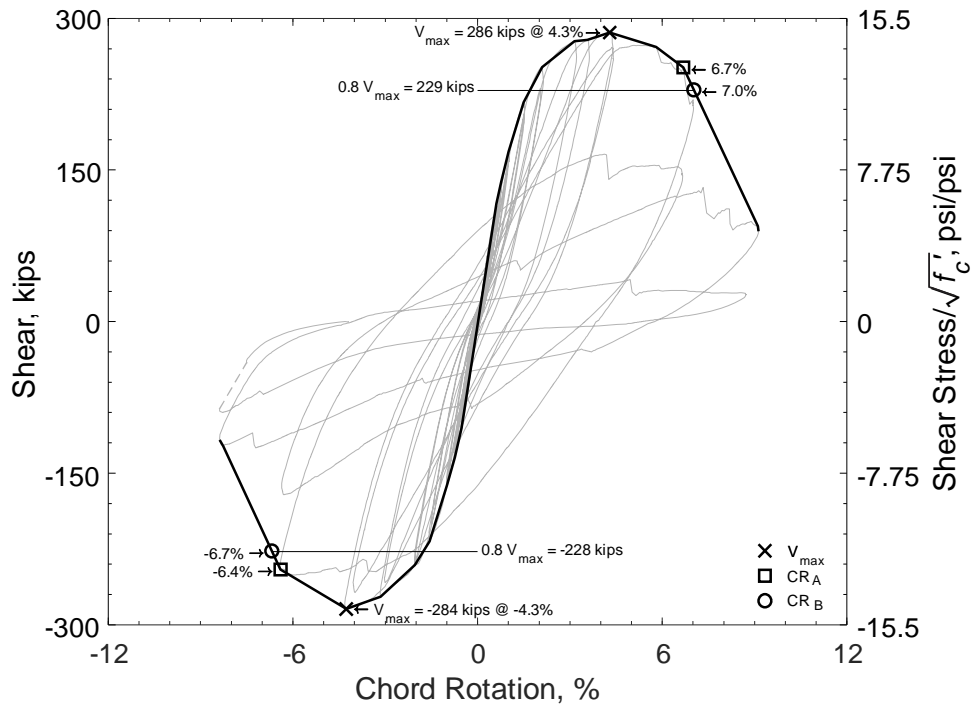


Figure 53 – Shear versus chord rotation envelope for D120-2.5
(1,000 psi = 6.89 MPa, 1 kip = 4.45 kN)

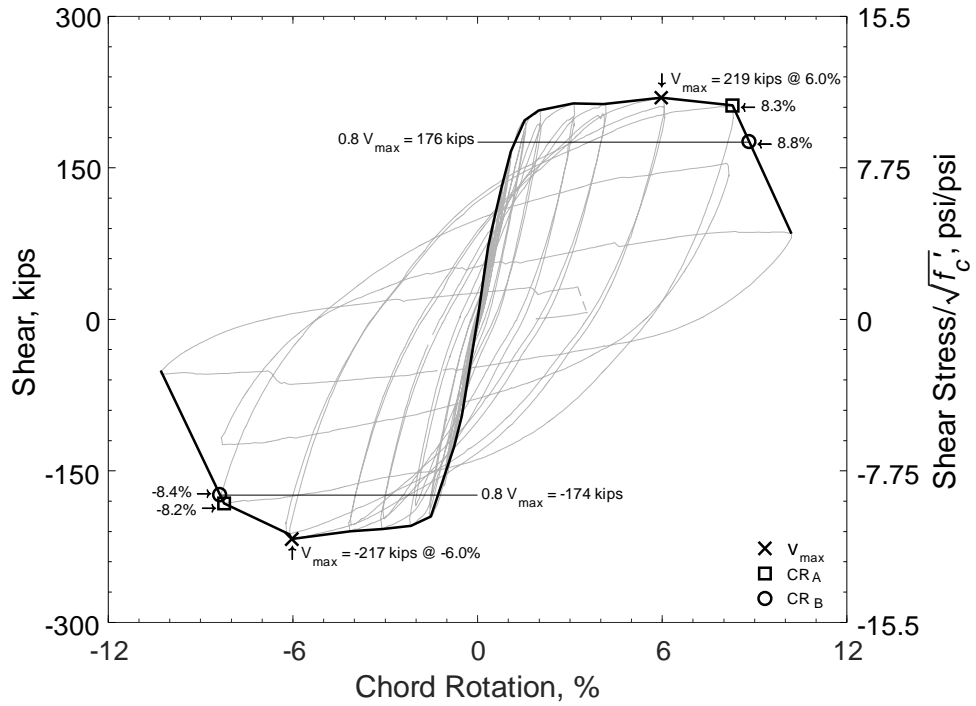


Figure 54 – Shear versus chord rotation envelope for D80-3.5
(1,000 psi = 6.89 MPa, 1 kip = 4.45 kN)

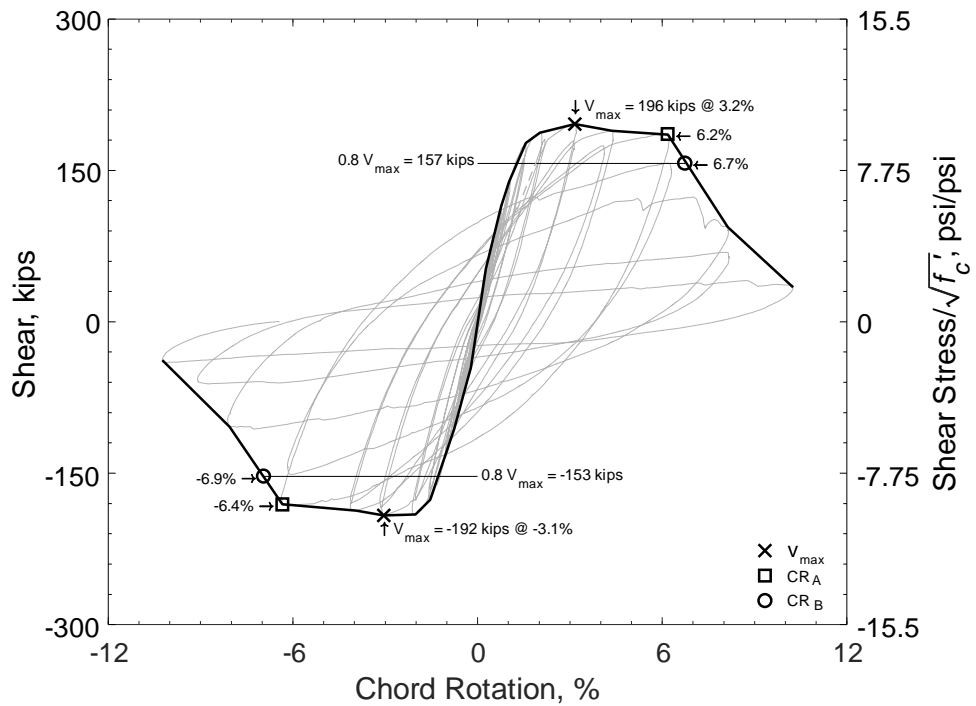


Figure 55 – Shear versus chord rotation envelope for D100-3.5
(1,000 psi = 6.89 MPa, 1 kip = 4.45 kN)

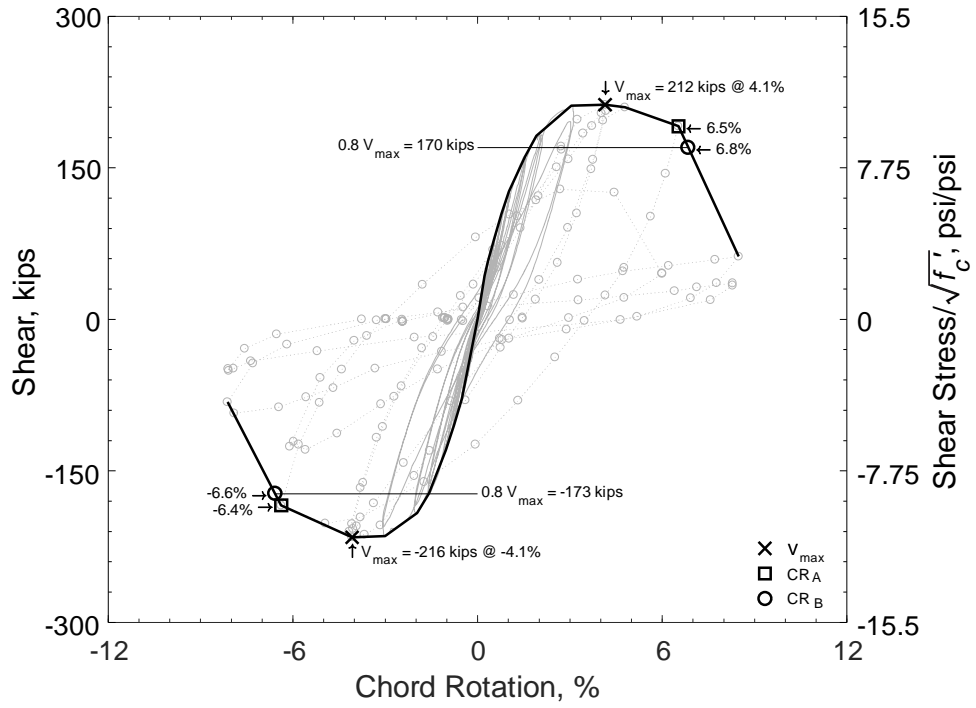


Figure 56 – Shear versus chord rotation envelope for D120-3.5
 (1,000 psi = 6.89 MPa, 1 kip = 4.45 kN)

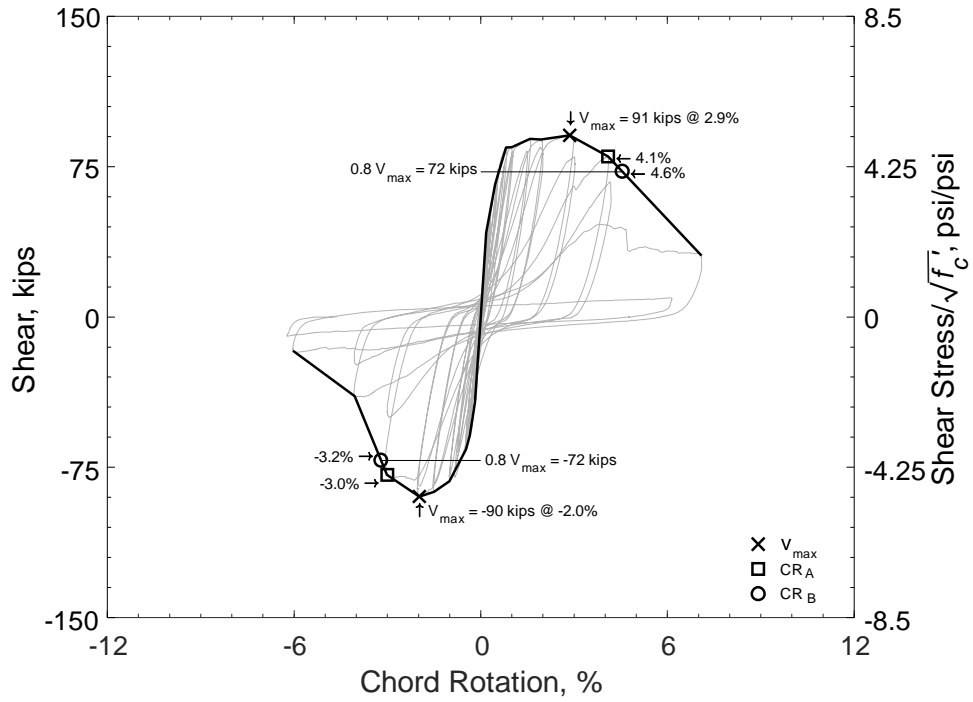


Figure 57 – Shear versus chord rotation envelope for P80-2.5
 (1,000 psi = 6.89 MPa, 1 kip = 4.45 kN)

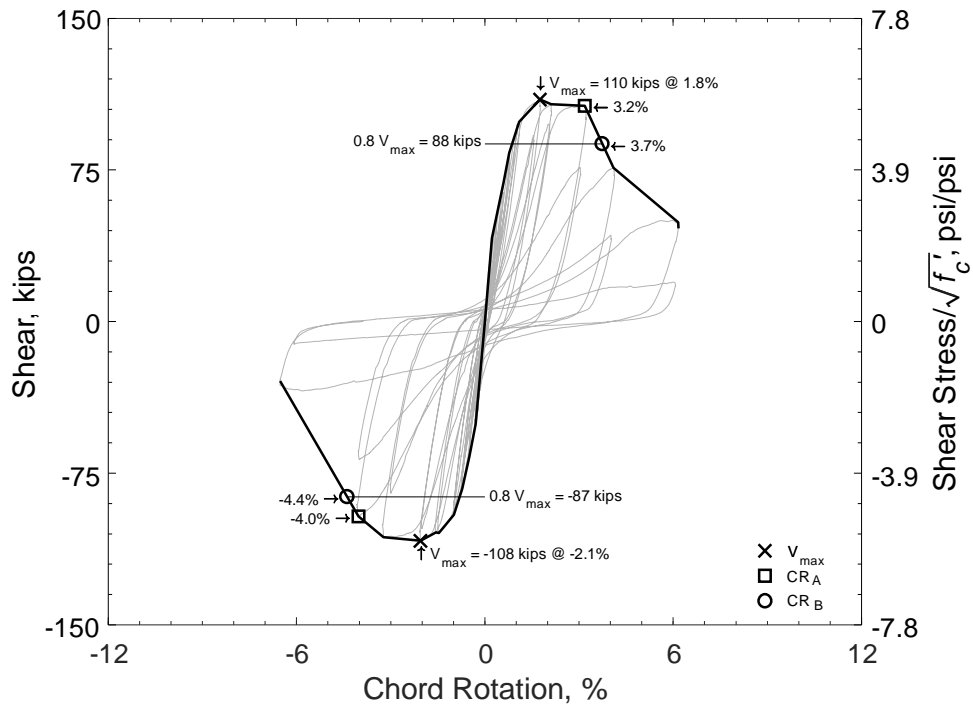


Figure 58 – Shear versus chord rotation envelope for P100-2.5
 (1,000 psi = 6.89 MPa, 1 kip = 4.45 kN)

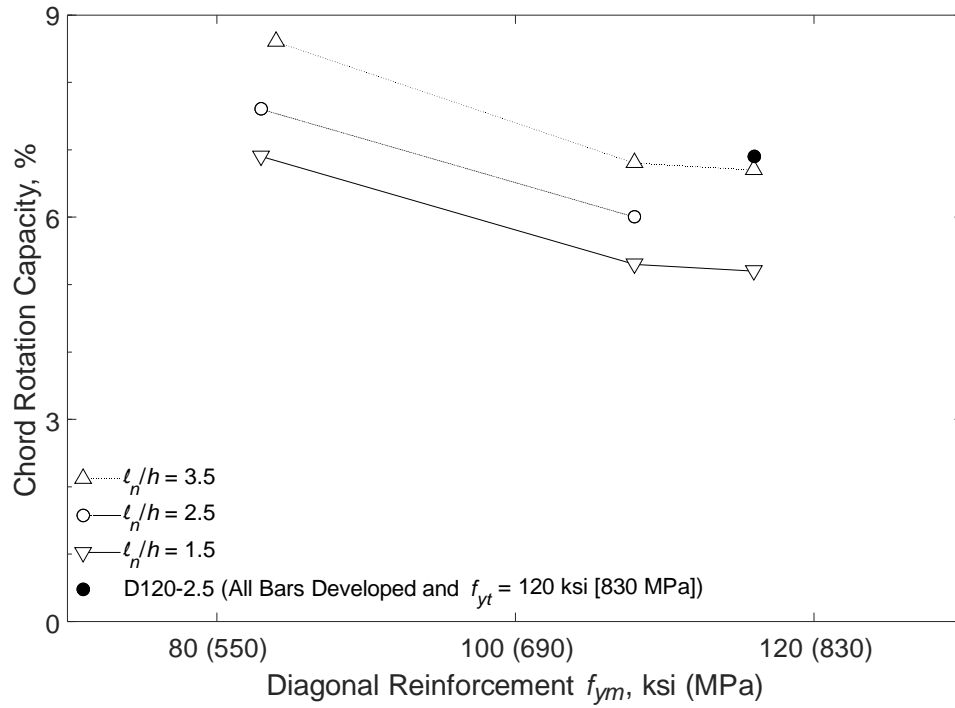


Figure 59 – Chord rotation capacity versus primary reinforcement grade for D-type coupling beams (1,000 psi = 6.89 MPa)

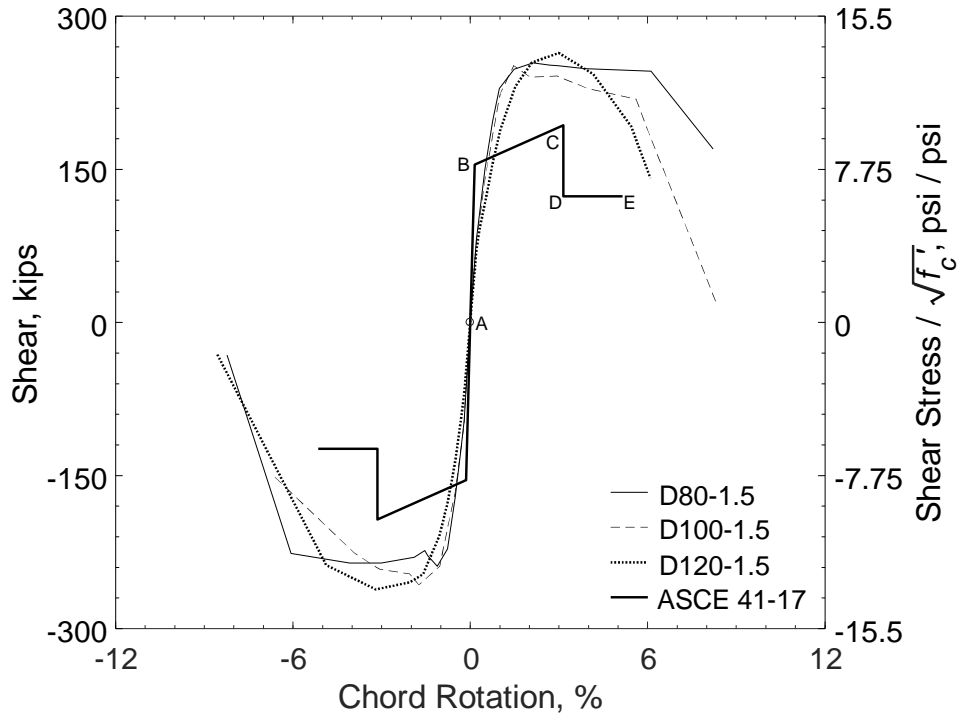


Figure 60 – Shear versus chord rotation envelopes for D80-1.5, D100-1.5, and D120-1.5 (1,000 psi = 6.89 MPa, 1 kip = 4.45 kN)

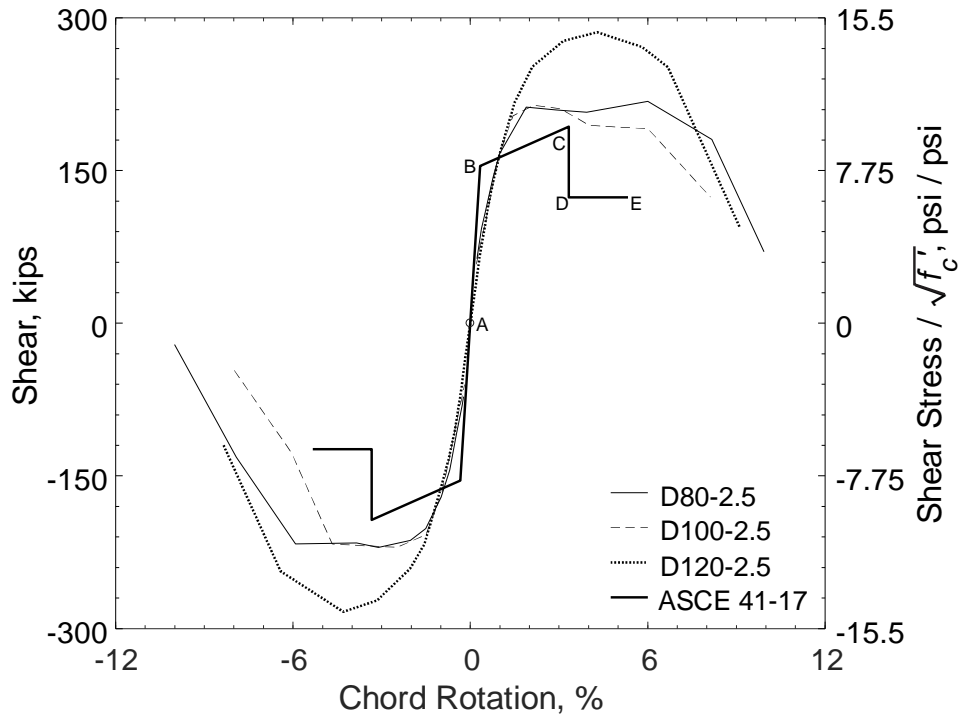


Figure 61 – Shear versus chord rotation envelopes for D80-2.5, D100-2.5, and D120-2.5 (1,000 psi = 6.89 MPa, 1 kip = 4.45 kN)

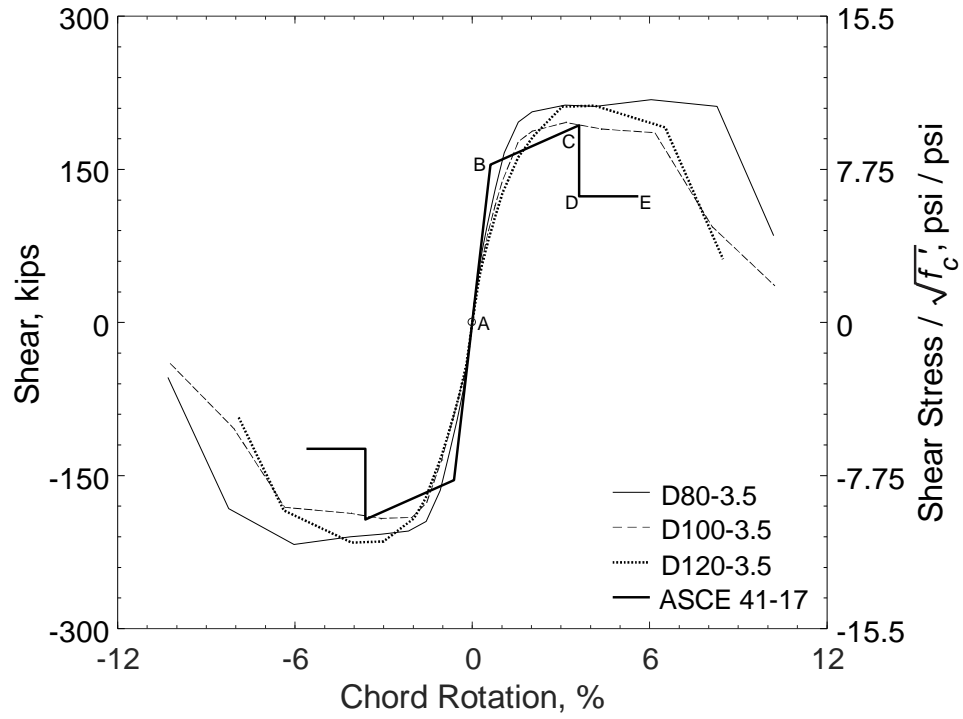


Figure 62 – Shear versus chord rotation envelopes for D80-3.5, D100-3.5, and D120-3.5
 (1,000 psi = 6.89 MPa, 1 kip = 4.45 kN)

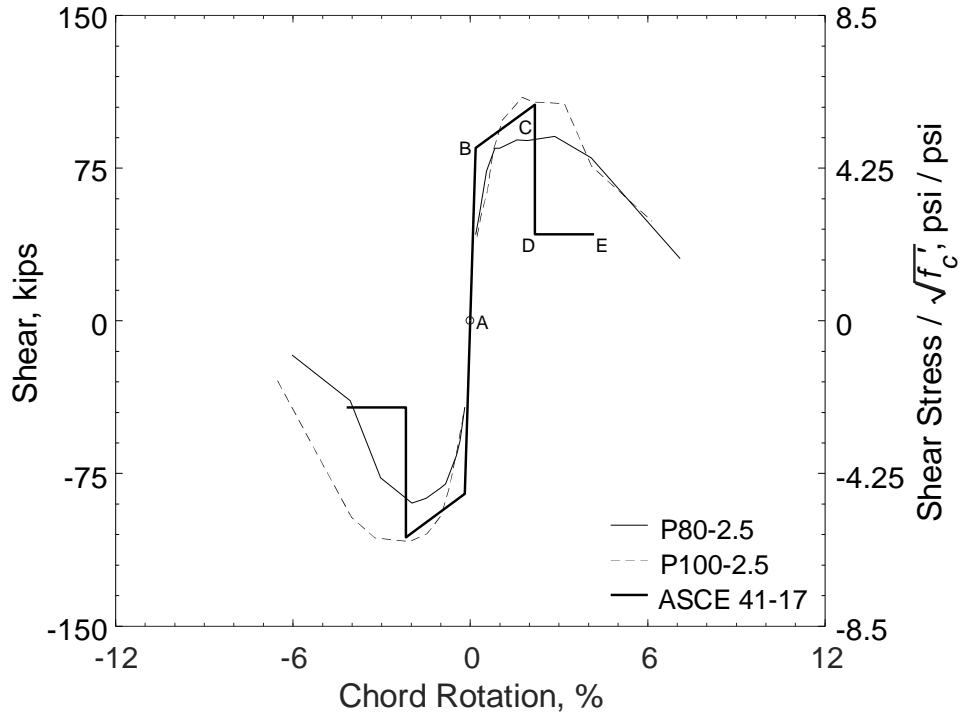


Figure 63 – Shear versus chord rotation envelopes for P80-2.5 and P100-2.5 (1,000 psi = 6.89 MPa, 1 kip = 4.45 kN)

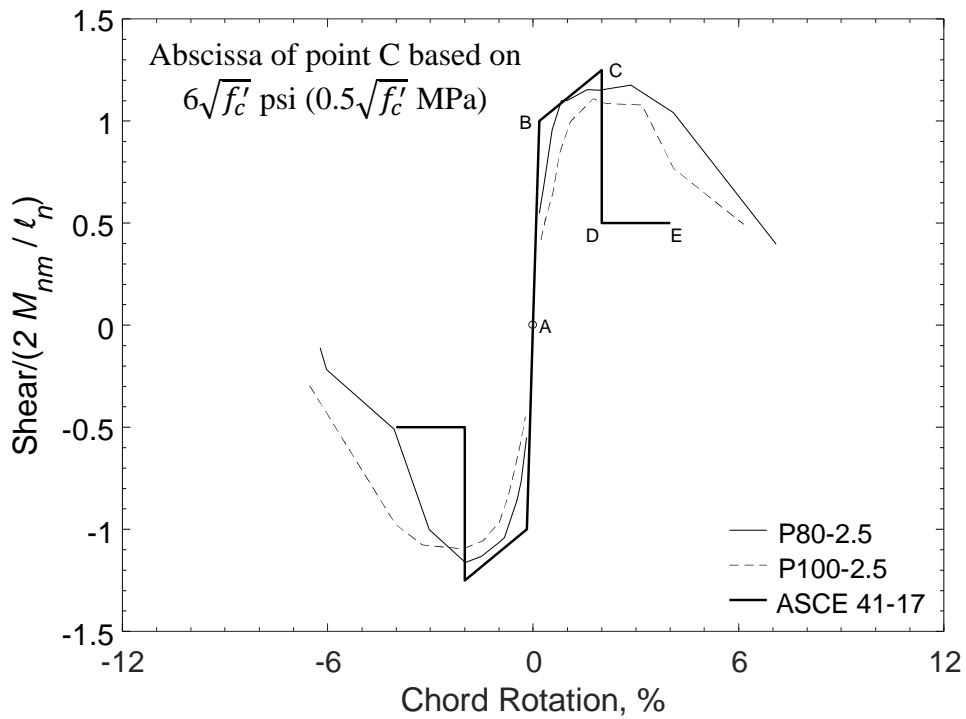


Figure 64 – Normalized shear versus chord rotation envelopes for P80-2.5 and P100-2.5 (1,000 psi = 6.89 MPa, 1 kip = 4.45 kN)

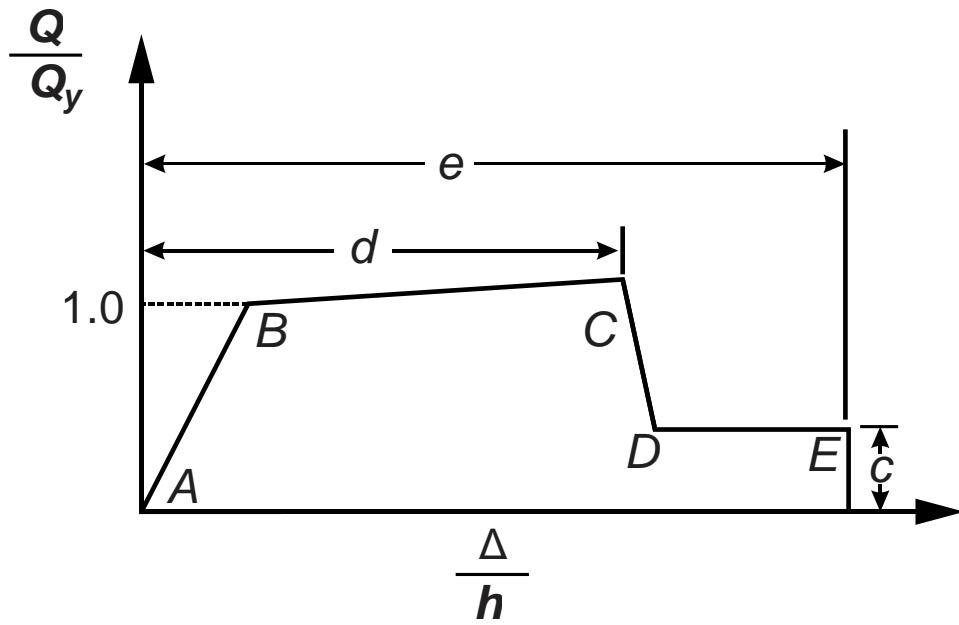
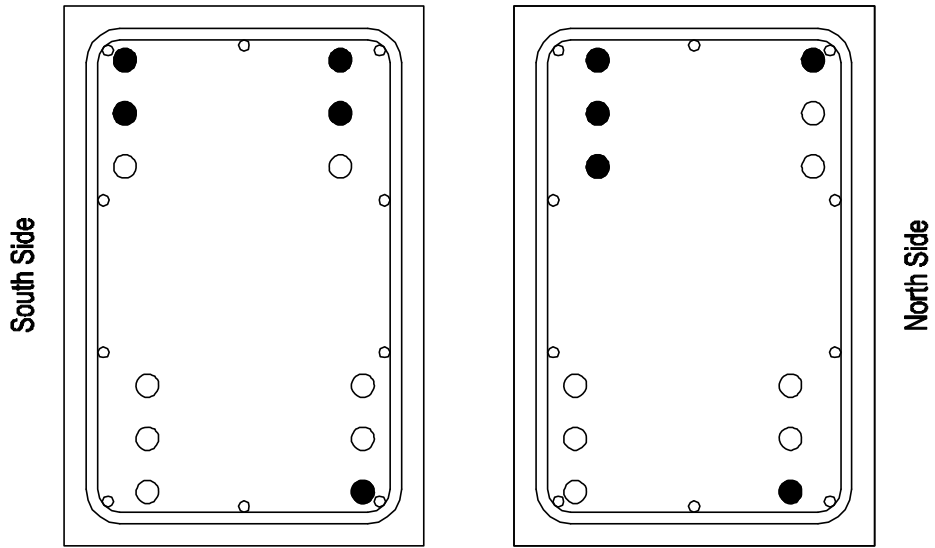


Figure 65 – Generalized force-deformation relationship for diagonally-reinforced concrete coupling beams (taken from ASCE 41-17 Figure 10-1(b)^[4])

West Side



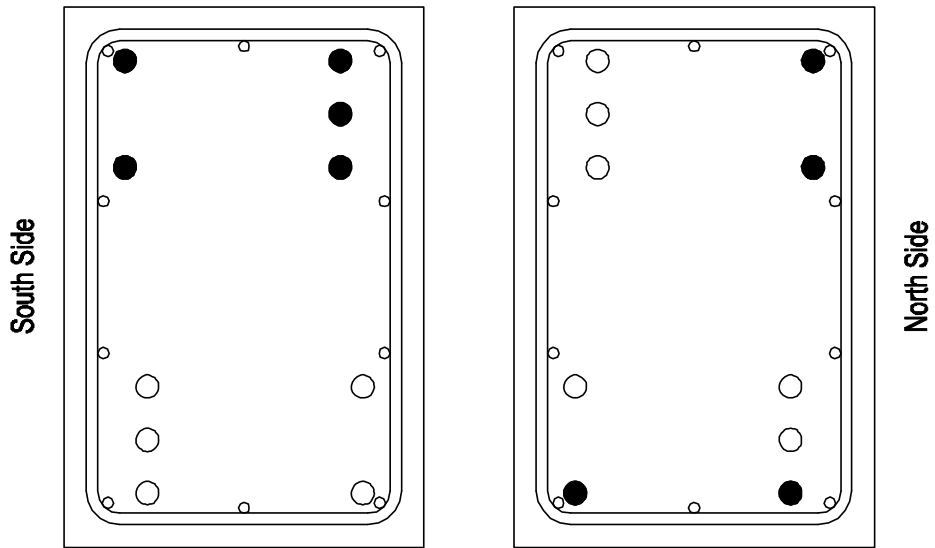
Section at Bottom

Section at Top

NOTES: Crossties and hooks not shown. Gray circle for bar necking and black circle for bar fracture.

Figure 66 – Reinforcing bar fracture locations, D80-1.5

West Side



Section at Bottom

Section at Top

NOTES: Crossties and hooks not shown. Gray circle for bar necking and black circle for bar fracture.

Figure 67 – Reinforcing bar fracture locations, D100-1.5

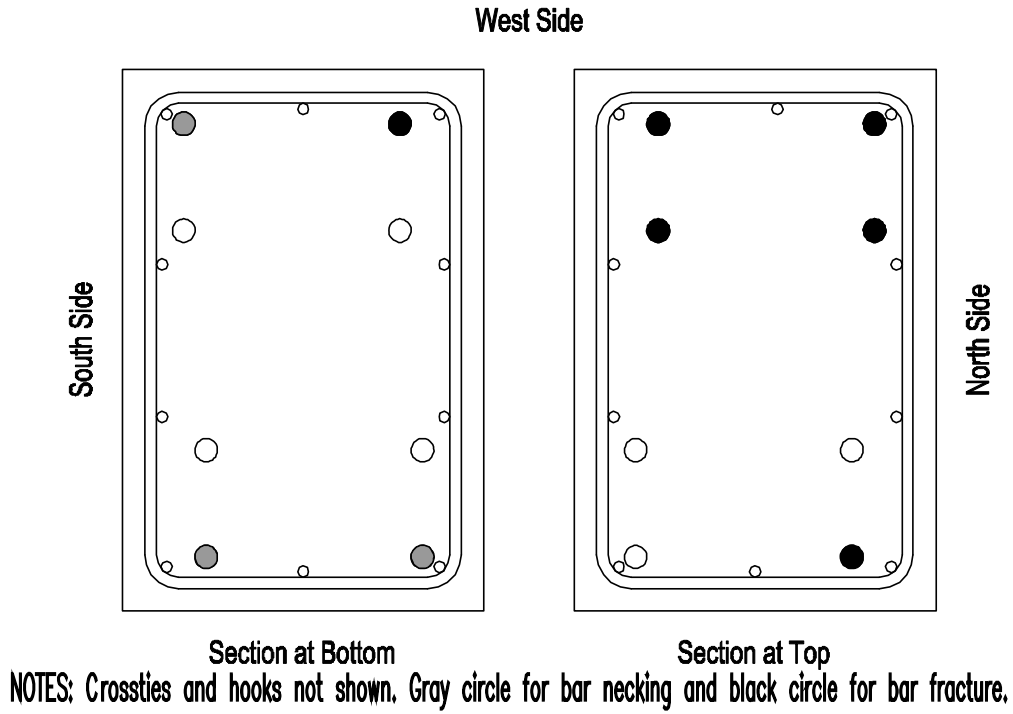


Figure 68 – Reinforcing bar fracture locations, D120-1.5

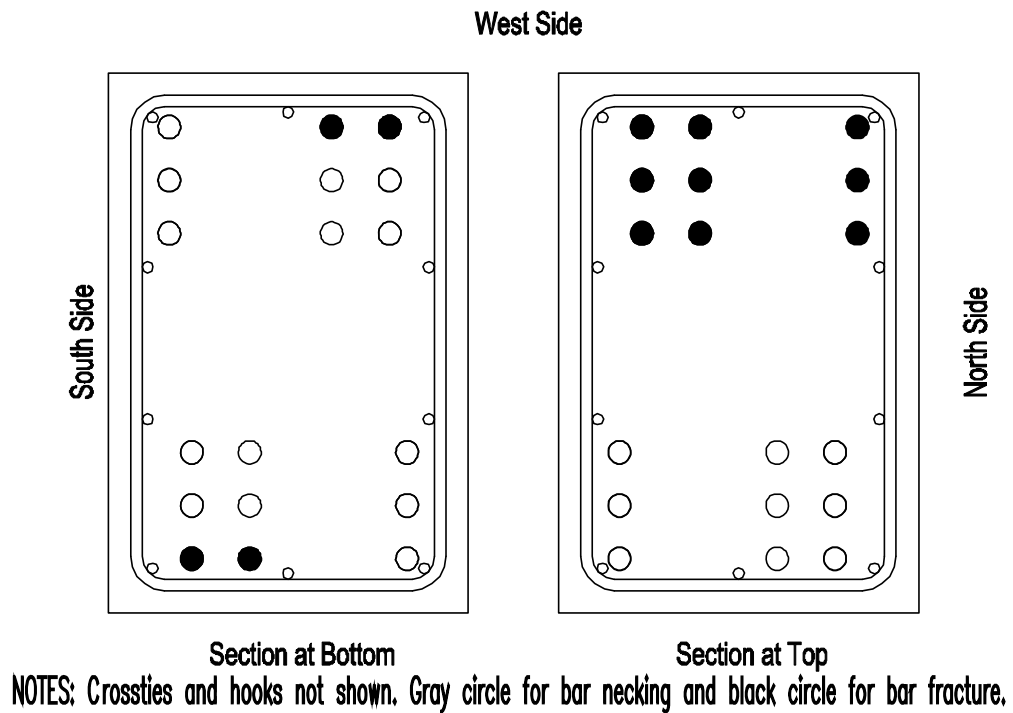


Figure 69 – Reinforcing bar fracture locations, D80-2.5

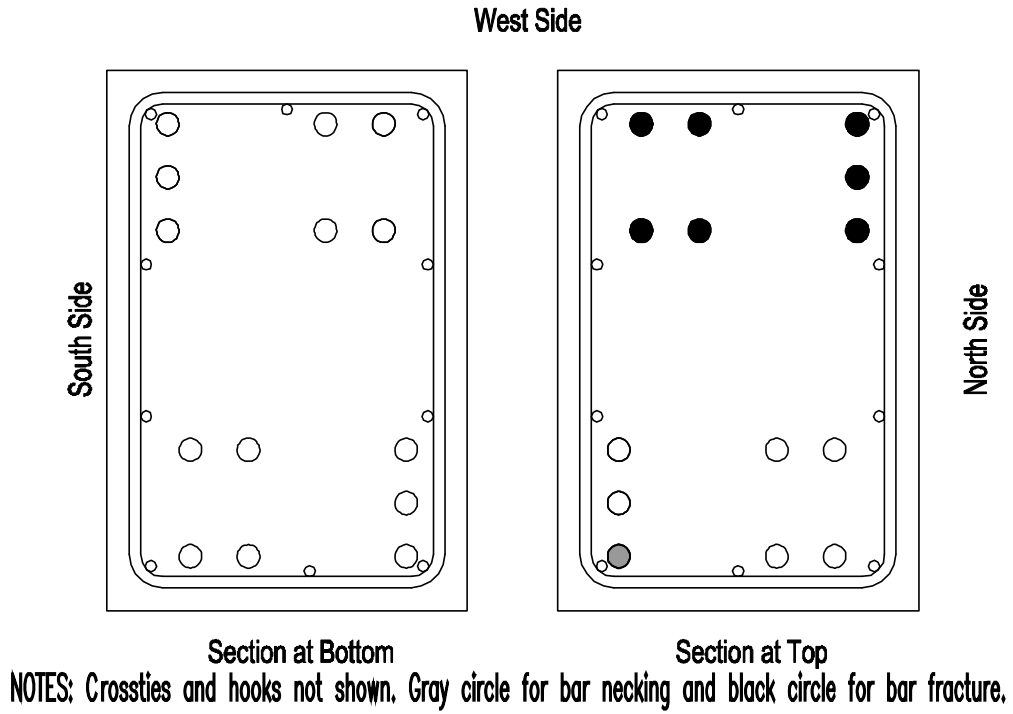


Figure 70 – Reinforcing bar fracture locations, D100-2.5

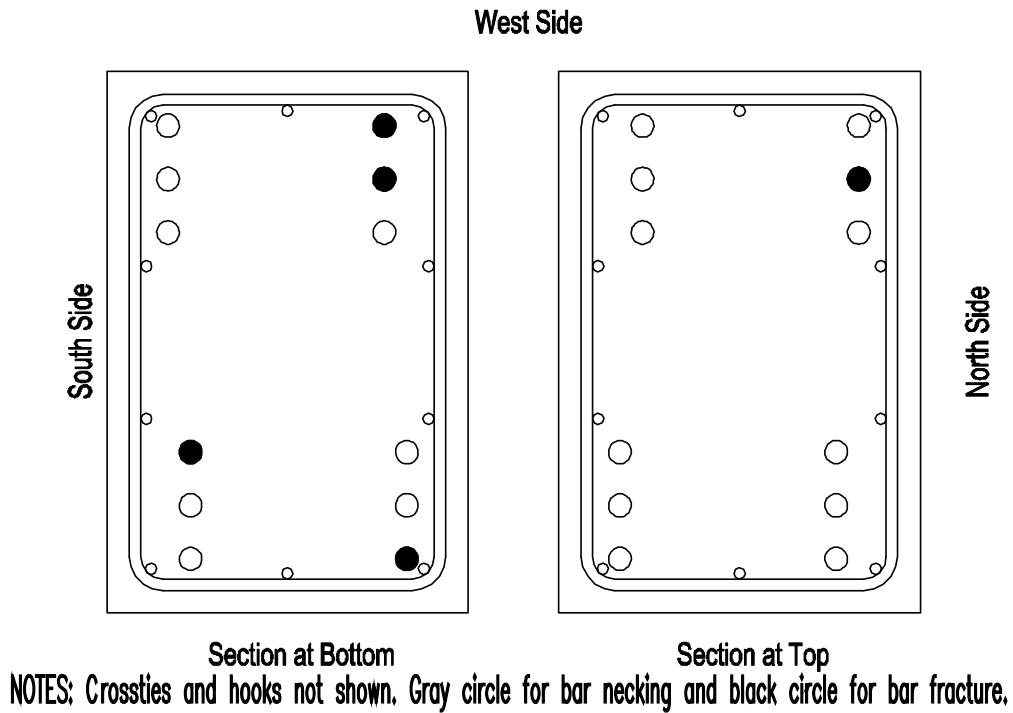


Figure 71 – Reinforcing bar fracture locations, D120-2.5

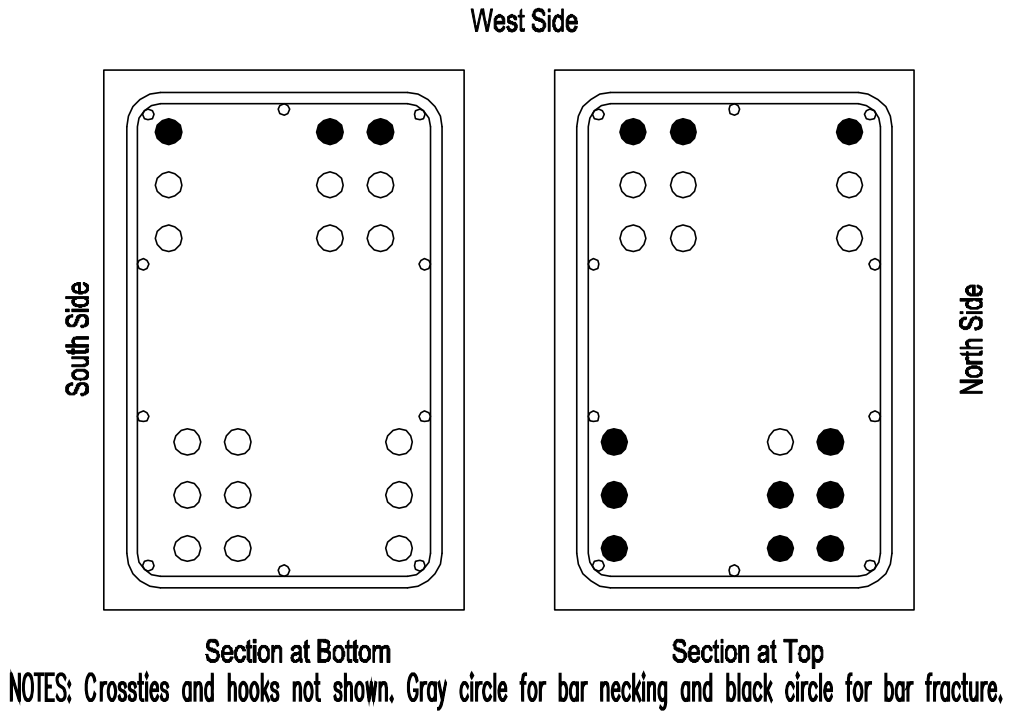


Figure 72 – Reinforcing bar fracture locations, D80-3.5

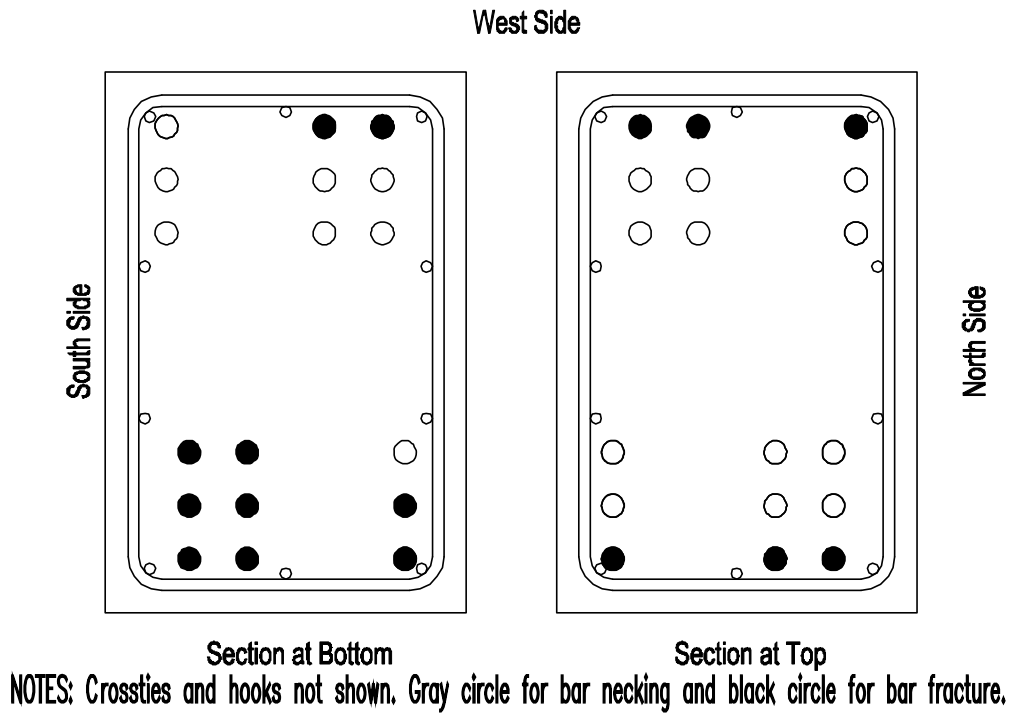
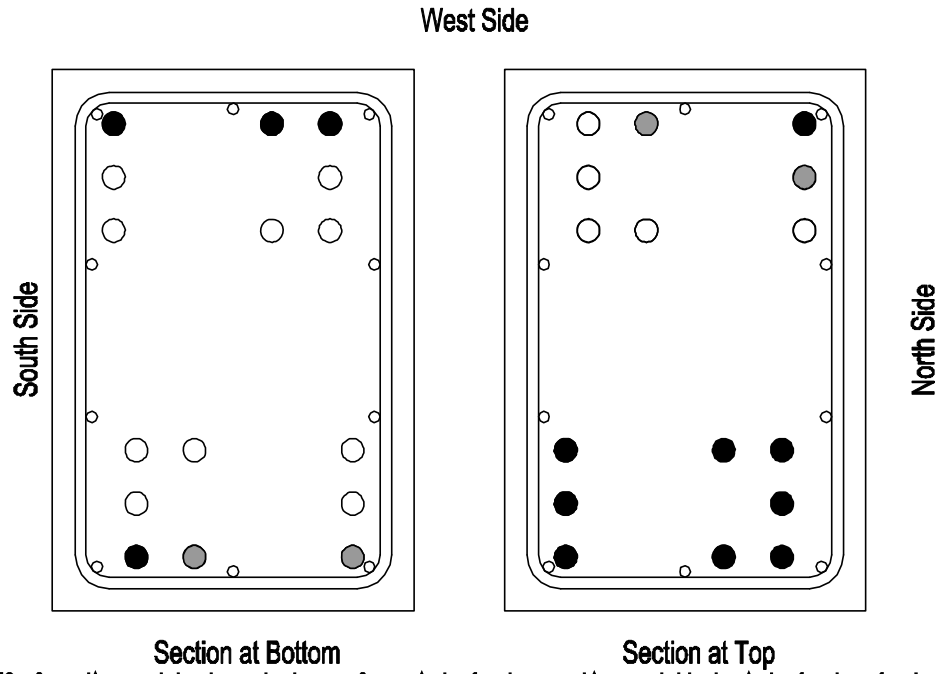


Figure 73 – Reinforcing bar fracture locations, D100-3.5



NOTES: Cross ties and hooks not shown. Gray circle for bar necking and black circle for bar fracture.

Figure 74 – Reinforcing bar fracture locations, D120-3.5

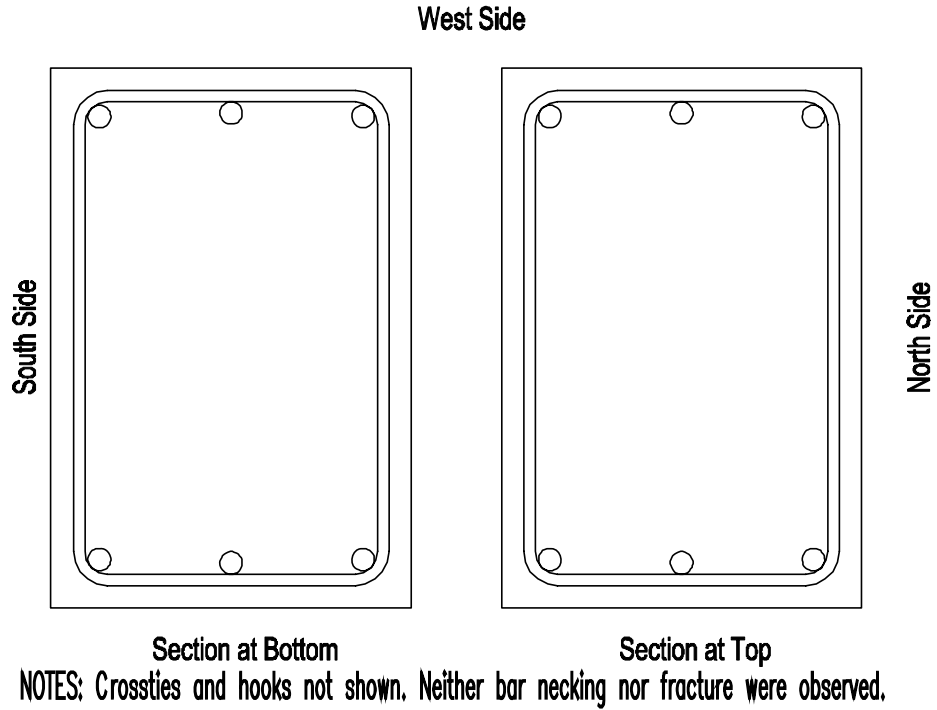


Figure 75 – Reinforcing bar fracture locations, P80-2.5

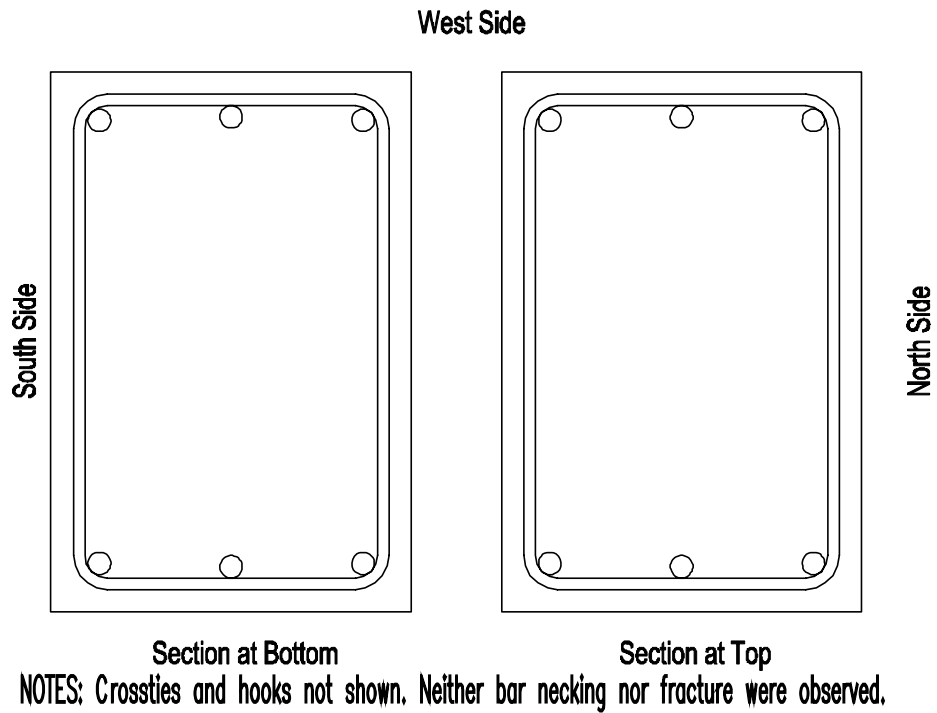


Figure 76 – Reinforcing bar fracture locations, P100-2.5

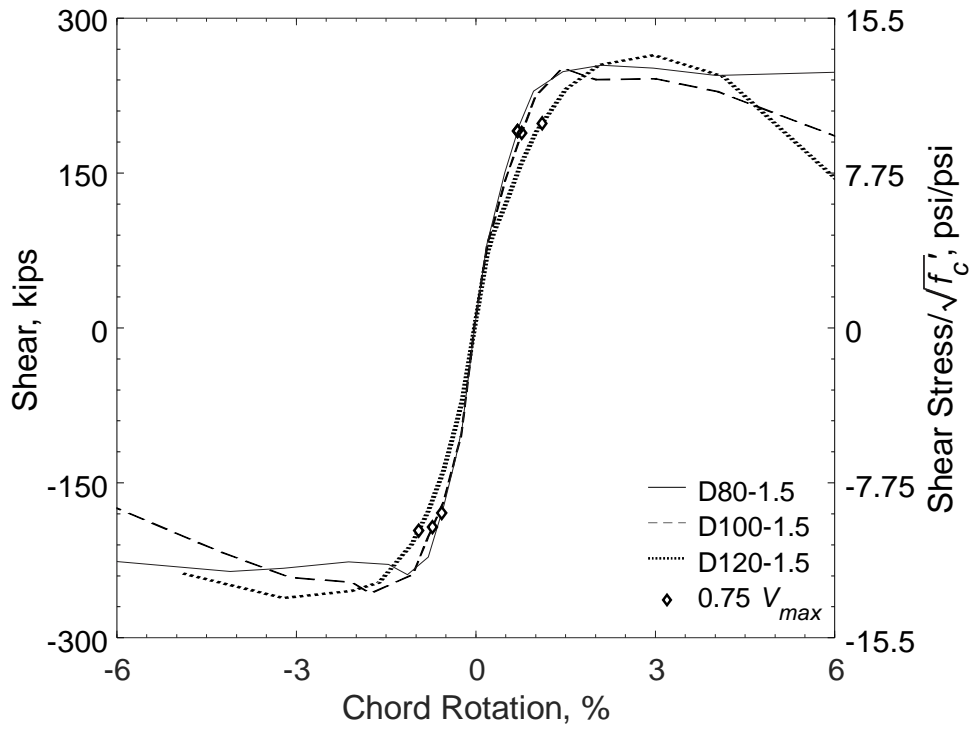


Figure 77 – Shear versus chord rotation envelopes for D80-1.5, D100-1.5, and D120-1.5

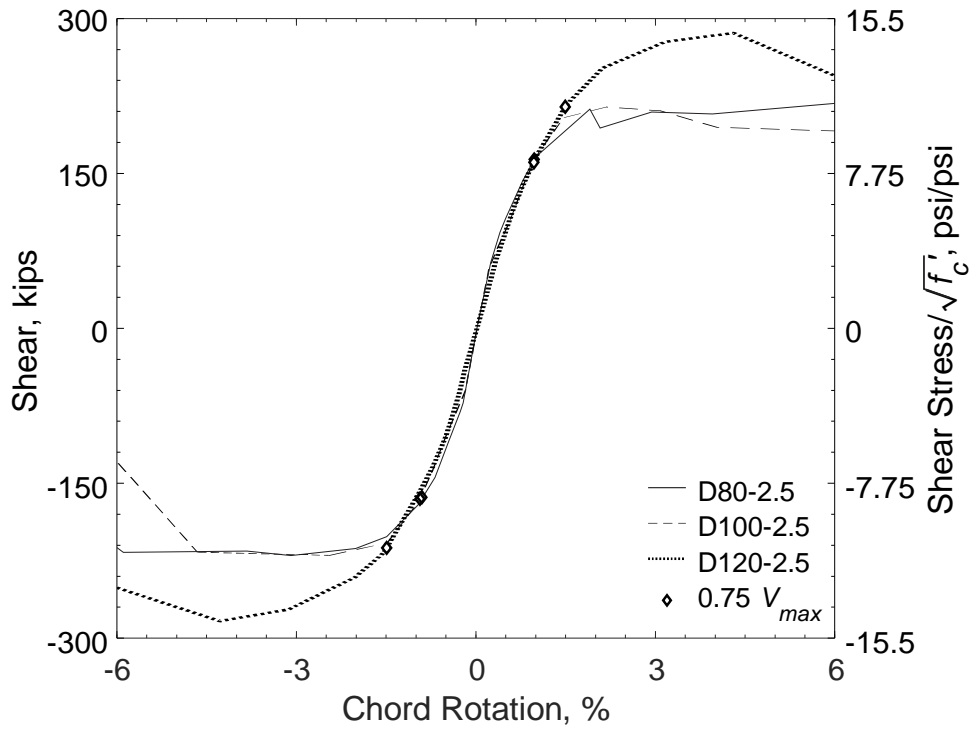


Figure 78 – Shear versus chord rotation envelopes for D80-2.5, D100-2.5, and D120-2.5

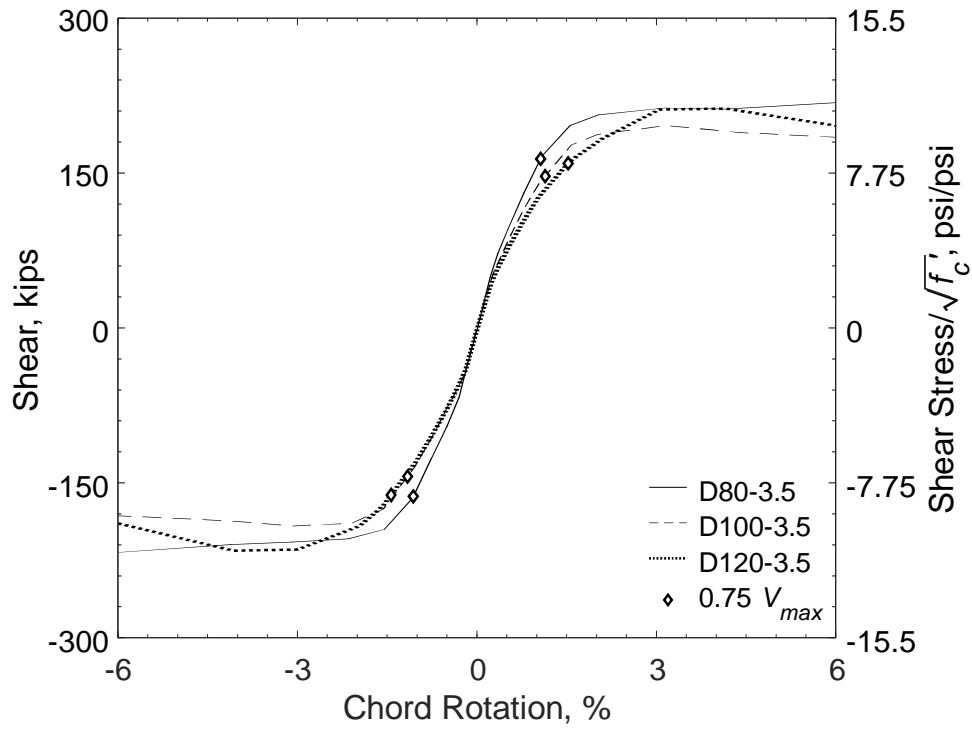


Figure 79 – Shear versus chord rotation envelopes for D80-3.5, D100-3.5, and D120-3.5

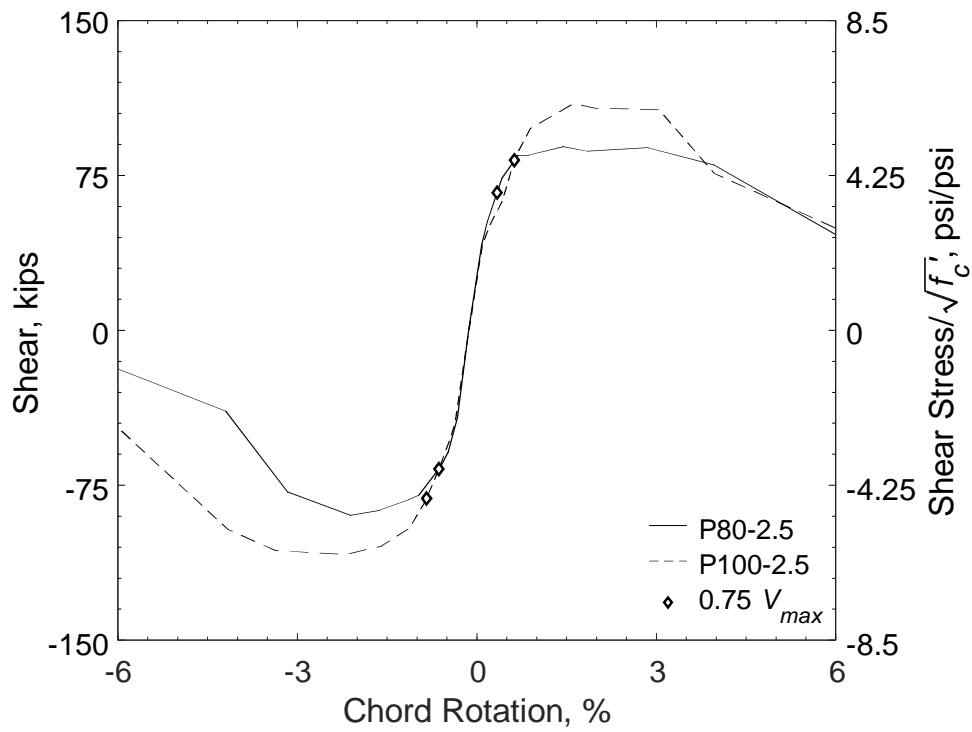


Figure 80 – Shear versus chord rotation envelopes for P80-2.5 and P100-2.5

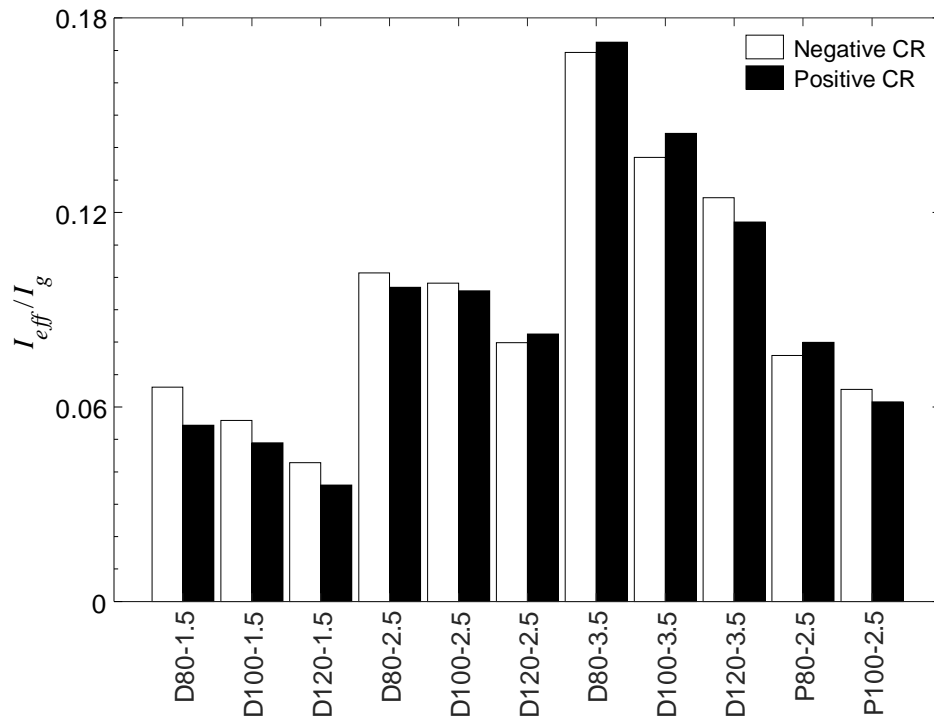


Figure 81 – Effective moment of inertia, I_{eff} , normalized by gross moment of inertia, I_g

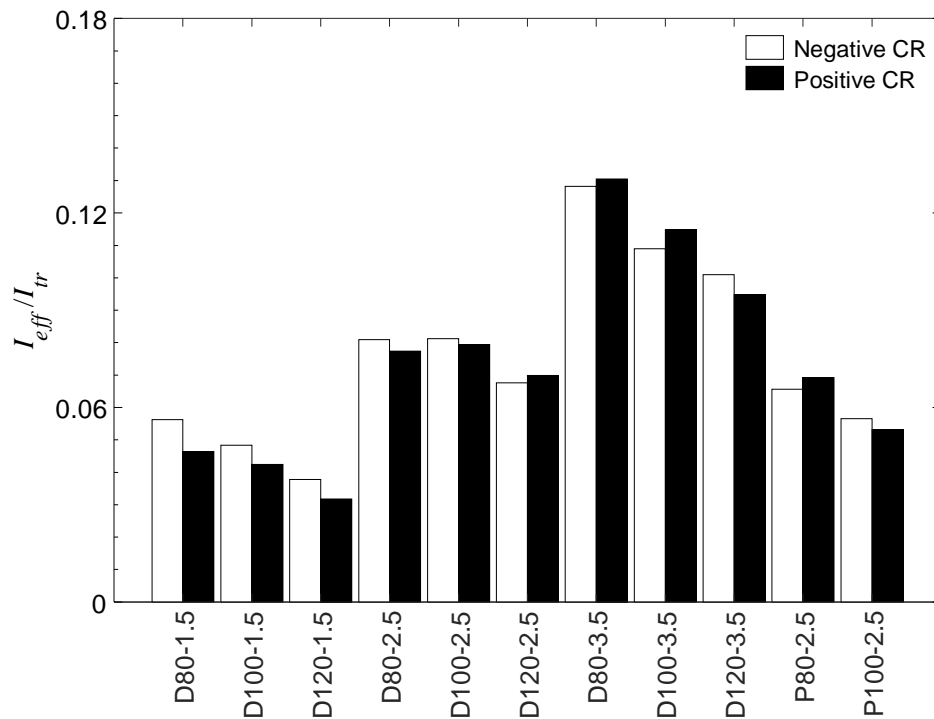


Figure 82 – Effective moment of inertia, I_{eff} , normalized by transformed uncracked moment of inertia, I_{tr}

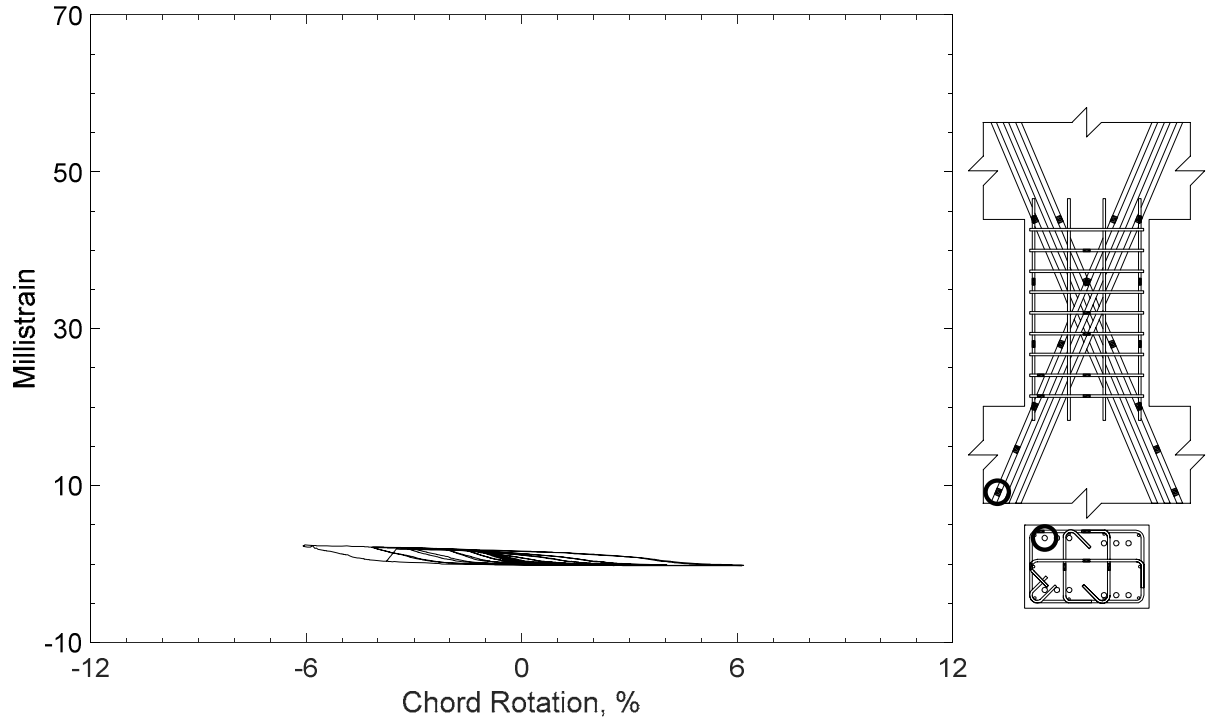


Figure 83 – Measured strain in diagonal bar of D80-1.5, strain gauge D1

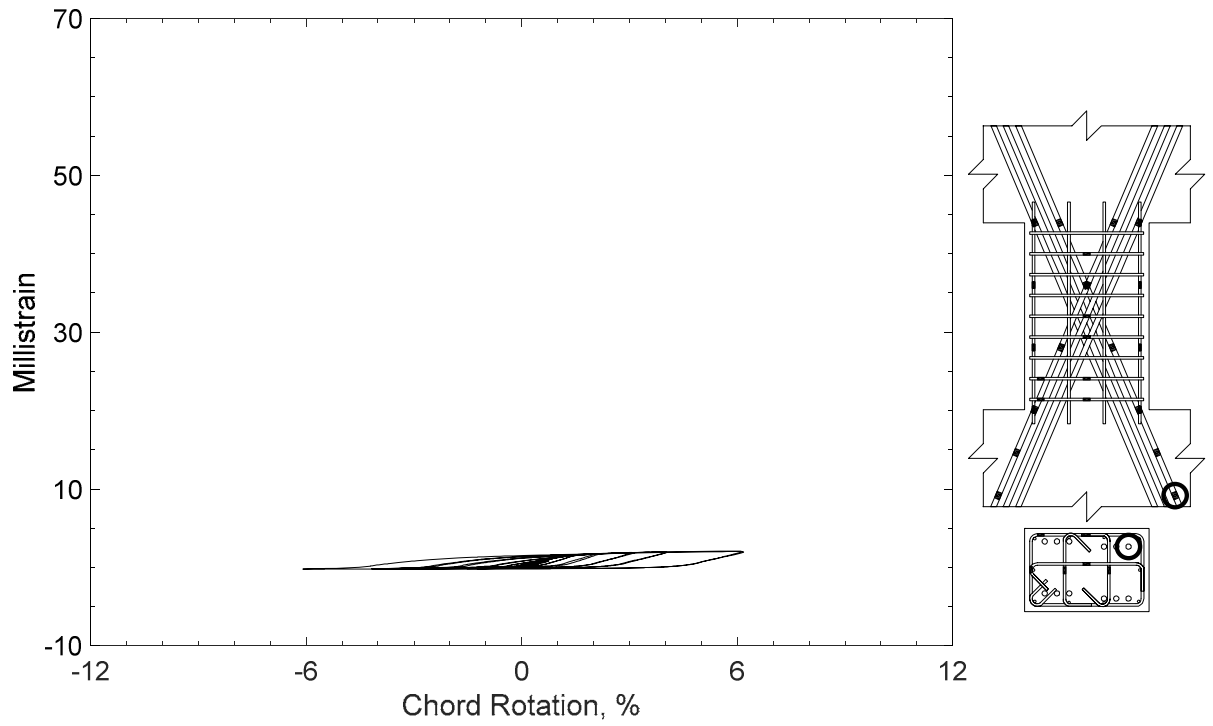


Figure 84 – Measured strain in diagonal bar of D80-1.5, strain gauge D2

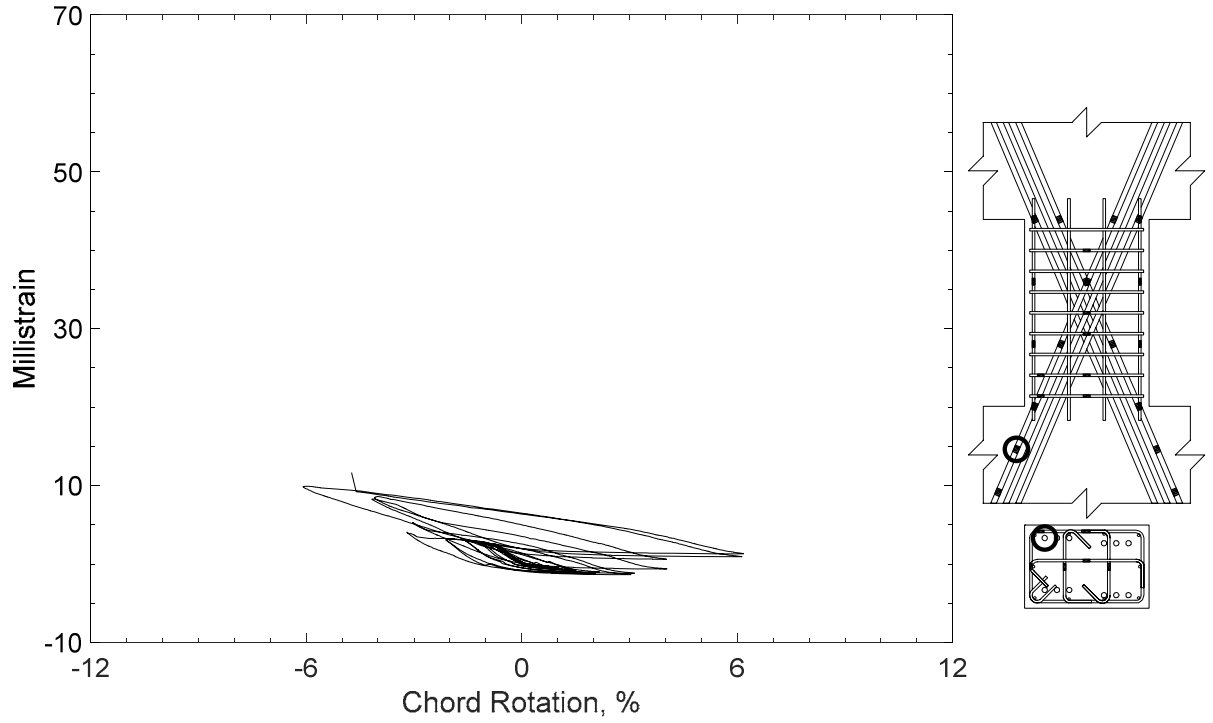


Figure 85 – Measured strain in diagonal bar of D80-1.5, strain gauge D3

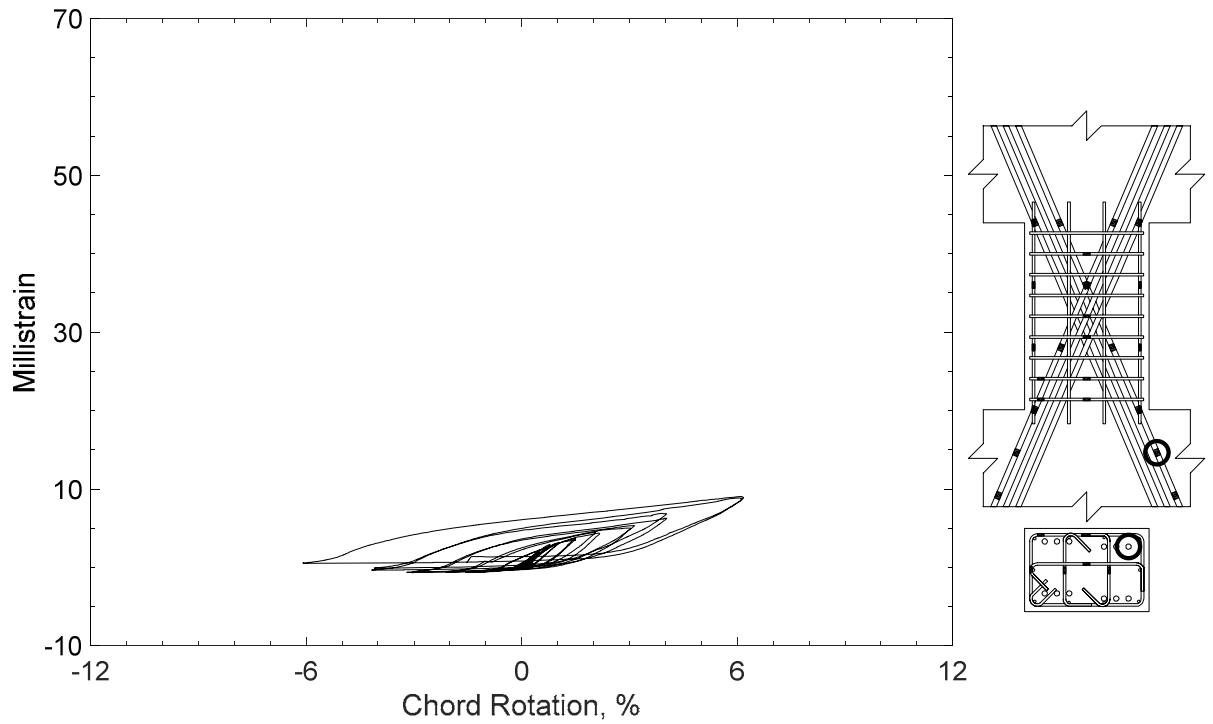


Figure 86 – Measured strain in diagonal bar of D80-1.5, strain gauge D4

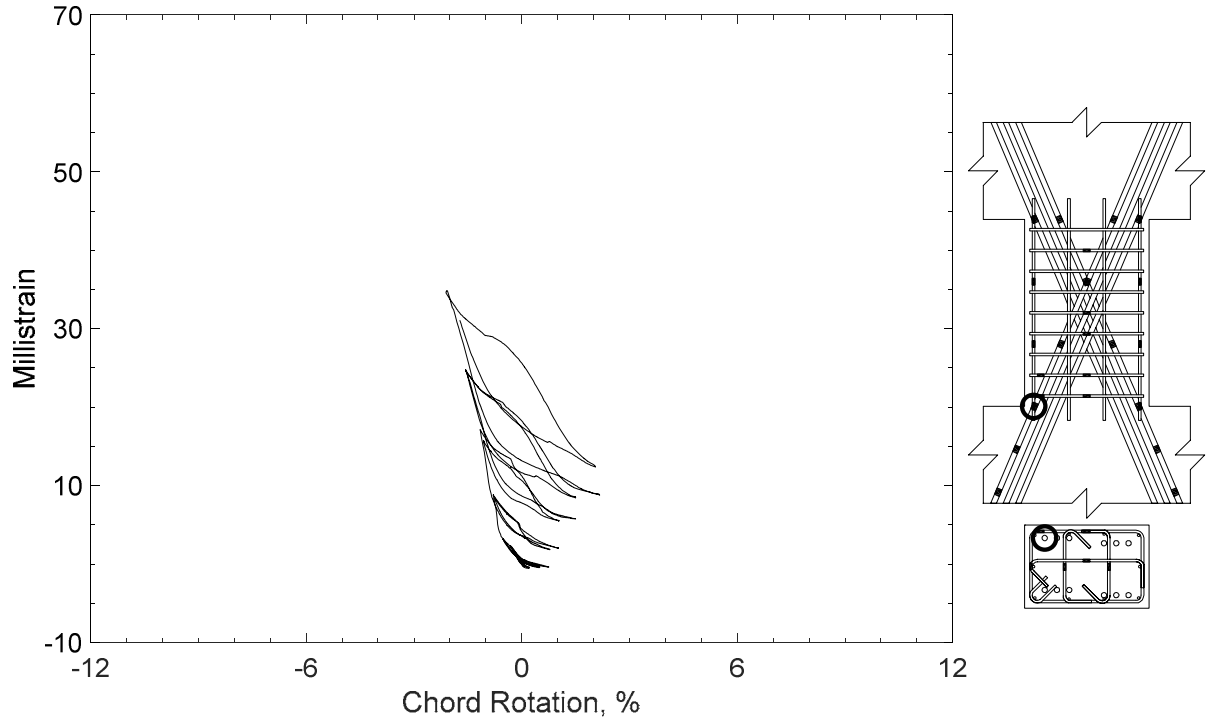


Figure 87 – Measured strain in diagonal bar of D80-1.5, strain gauge D5

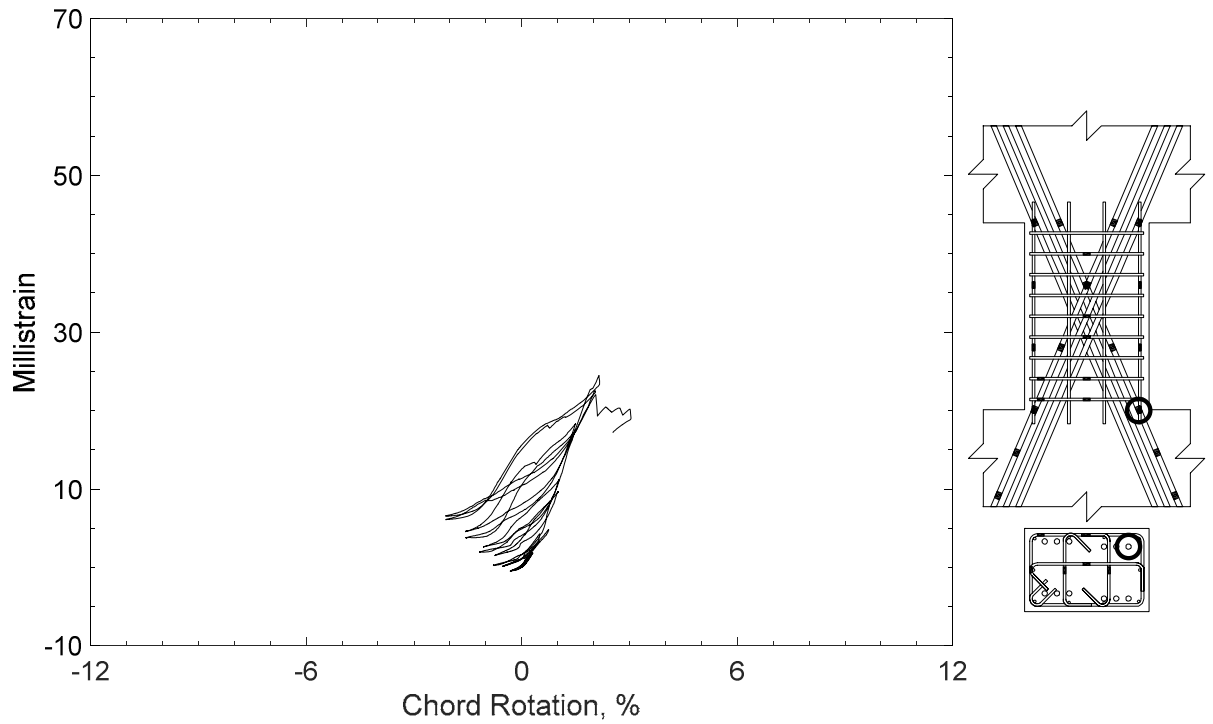


Figure 88 – Measured strain in diagonal bar of D80-1.5, strain gauge D6

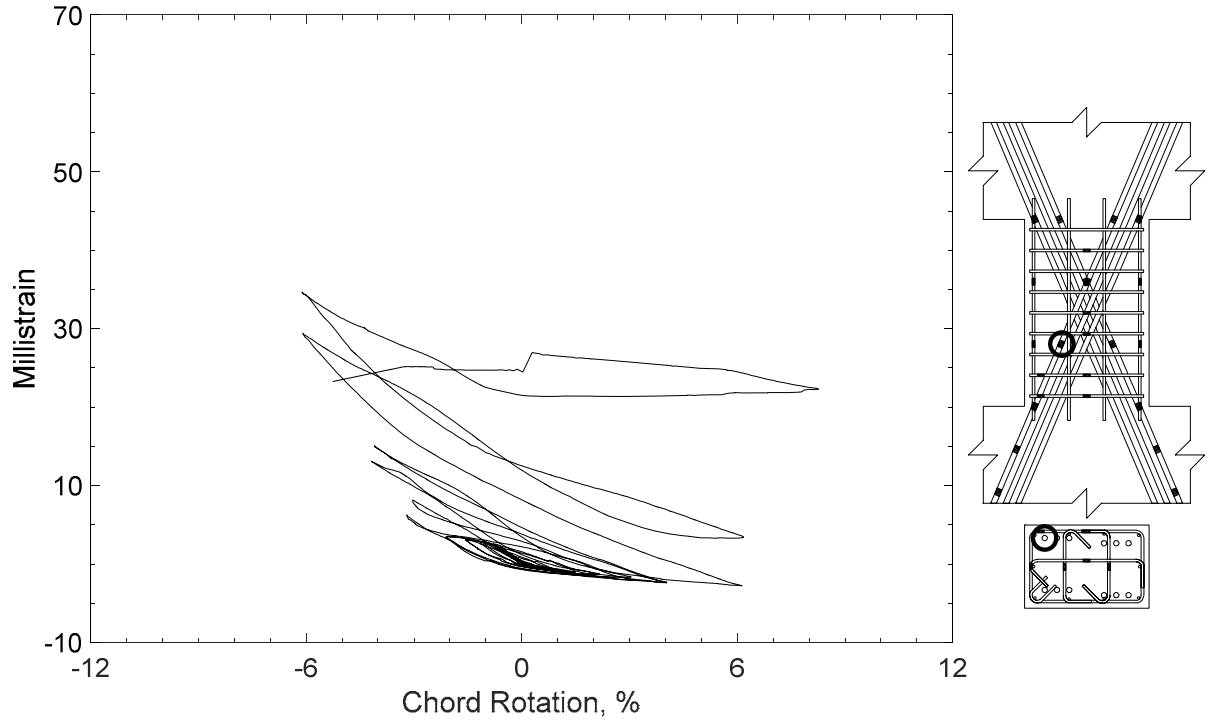


Figure 89 – Measured strain in diagonal bar of D80-1.5, strain gauge D7

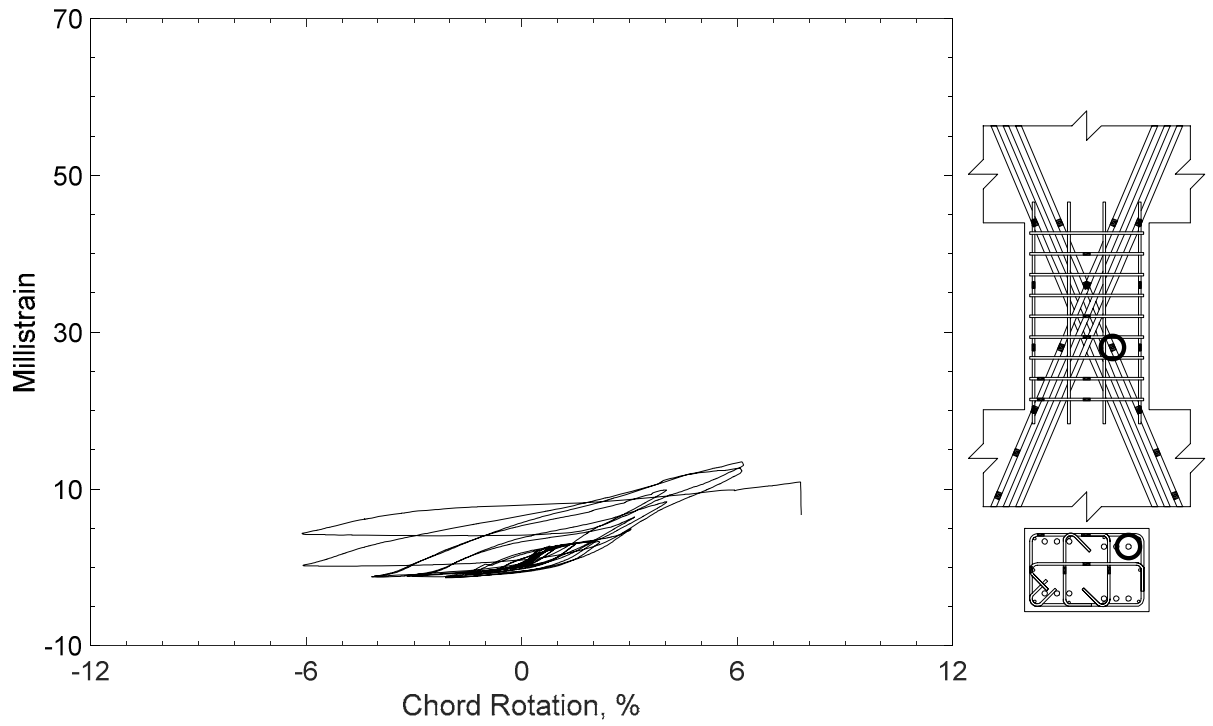


Figure 90 – Measured strain in diagonal bar of D80-1.5, strain gauge D8

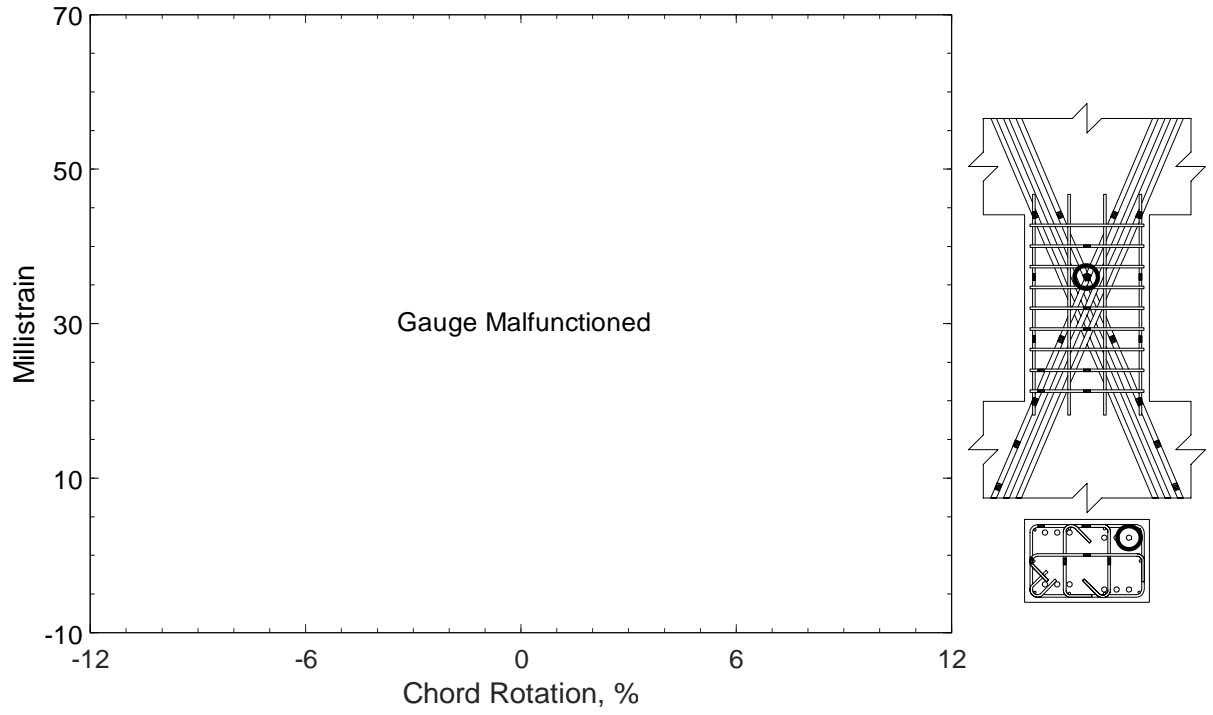


Figure 91 – Measured strain in diagonal bar of D80-1.5, strain gauge D9

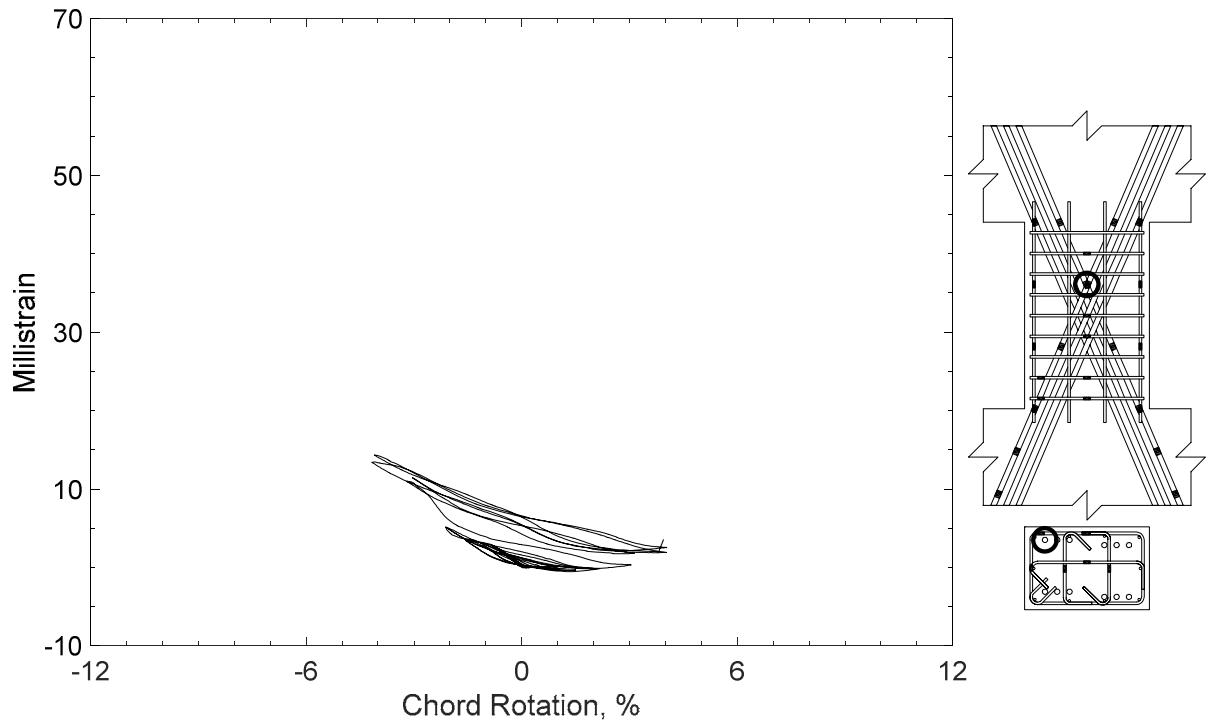


Figure 92 – Measured strain in diagonal bar of D80-1.5, strain gauge D10

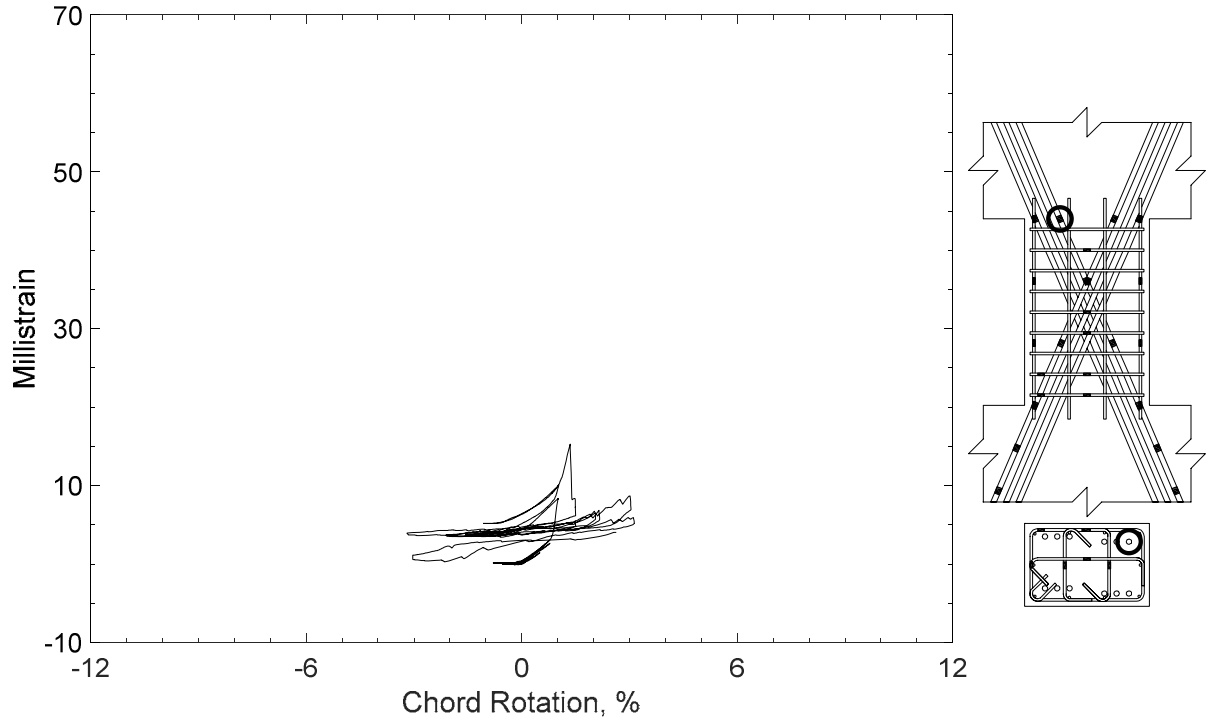


Figure 93 – Measured strain in diagonal bar of D80-1.5, strain gauge D11

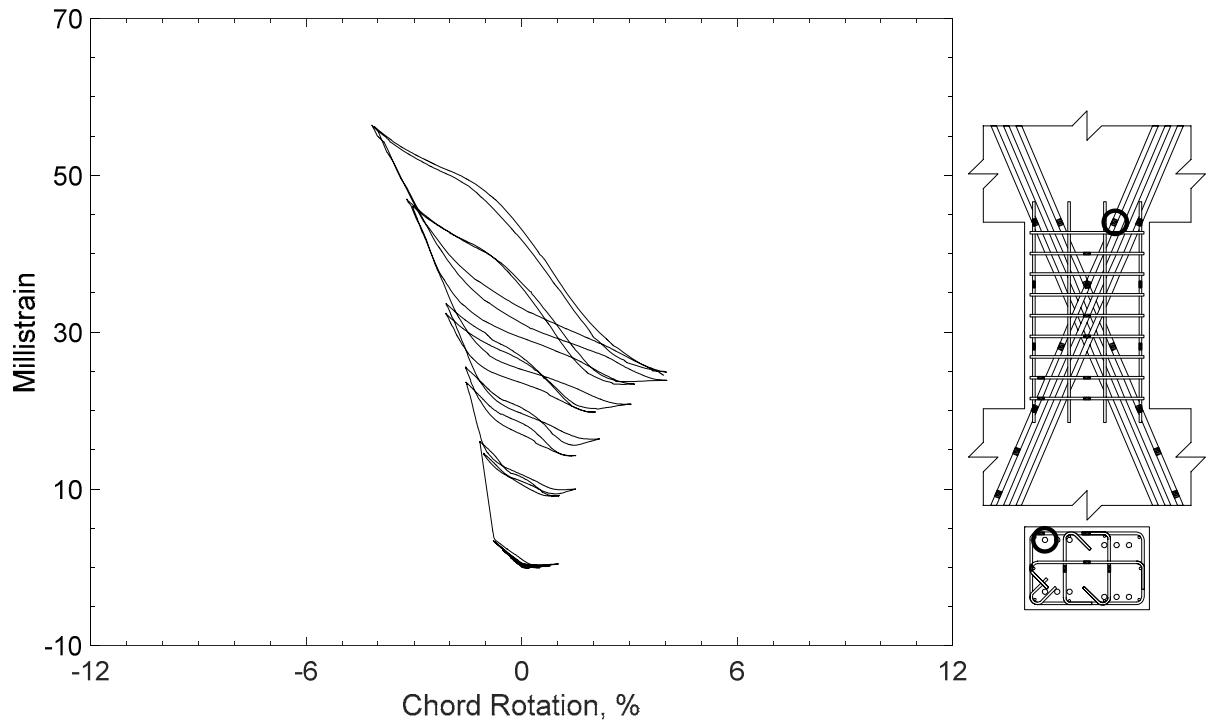


Figure 94 – Measured strain in diagonal bar of D80-1.5, strain gauge D12

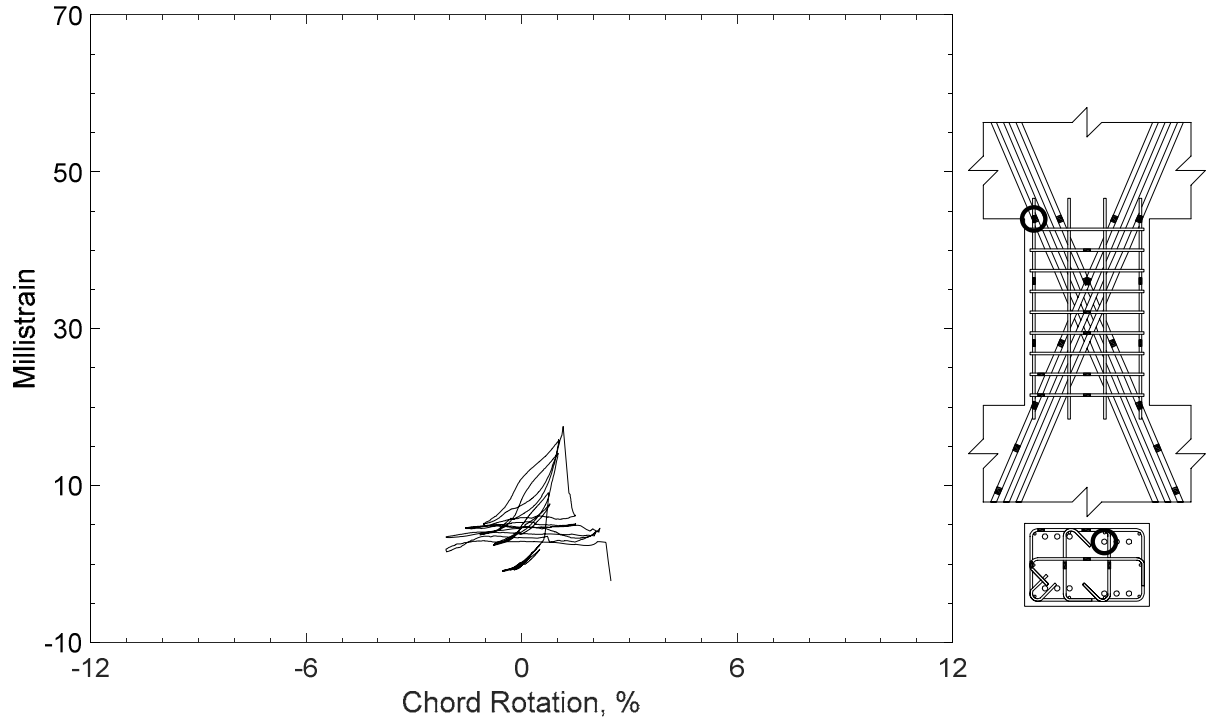


Figure 95 – Measured strain in diagonal bar of D80-1.5, strain gauge D13

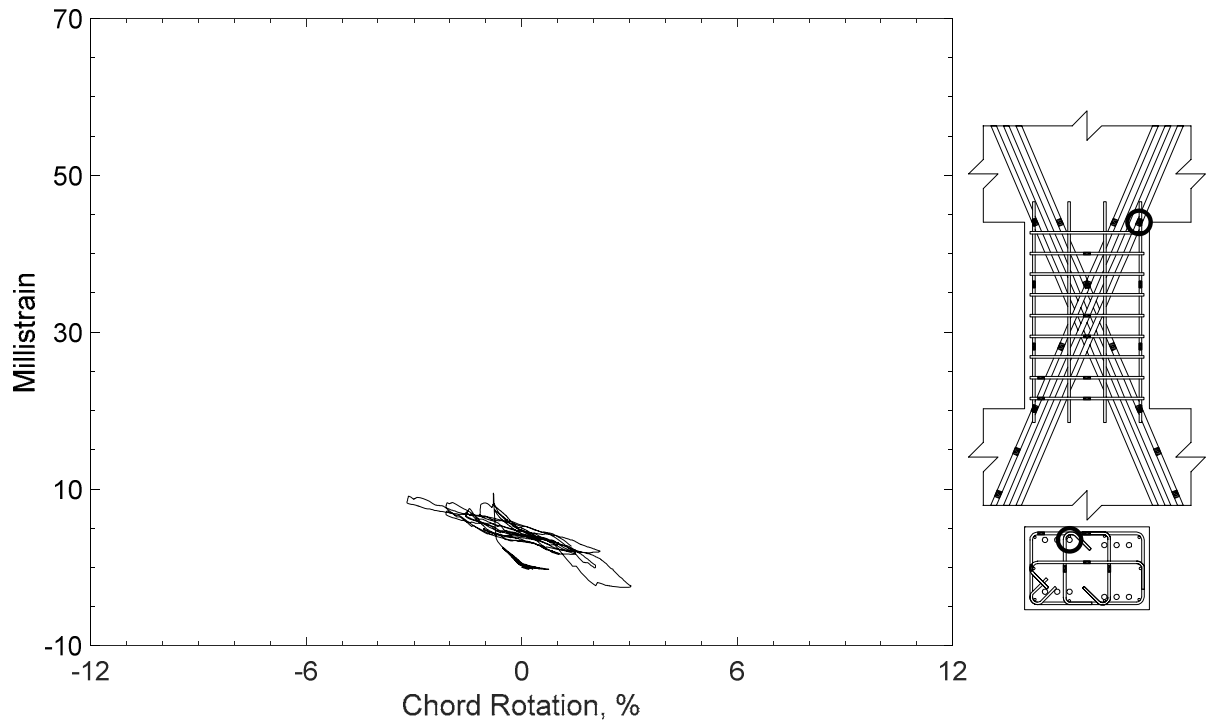


Figure 96 – Measured strain in diagonal bar of D80-1.5, strain gauge D14

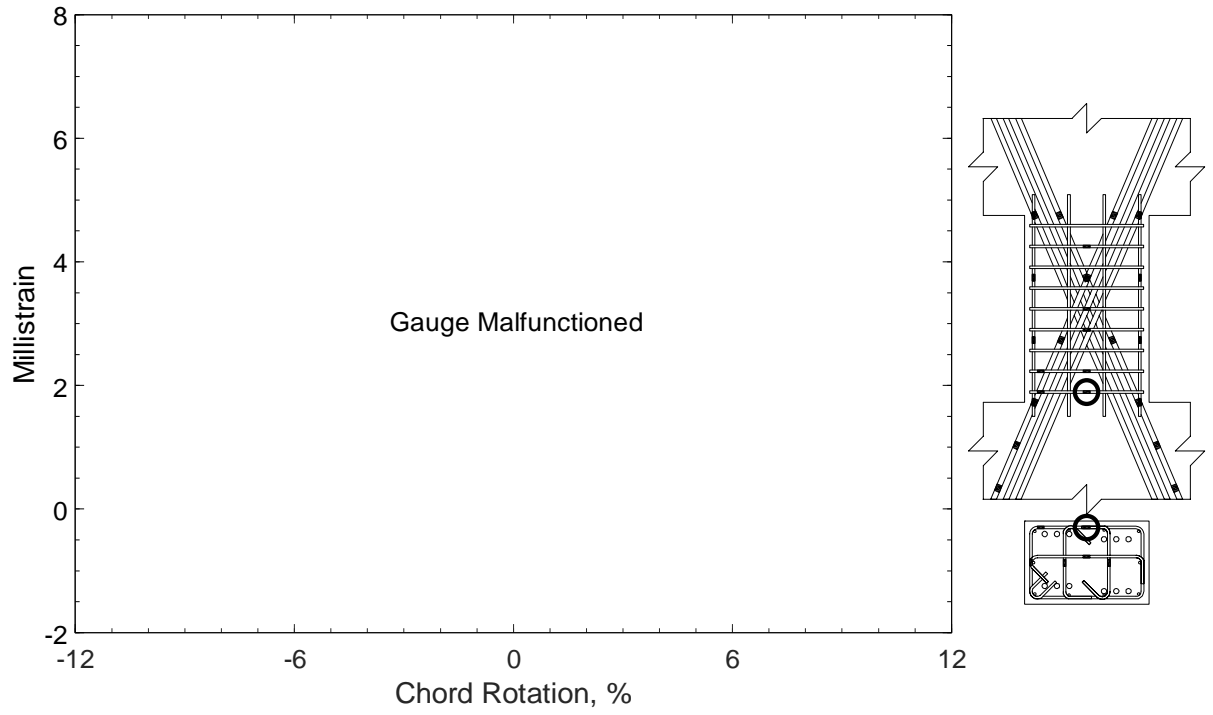


Figure 97 – Measured strain in closed stirrup of D80-1.5, strain gauge S1

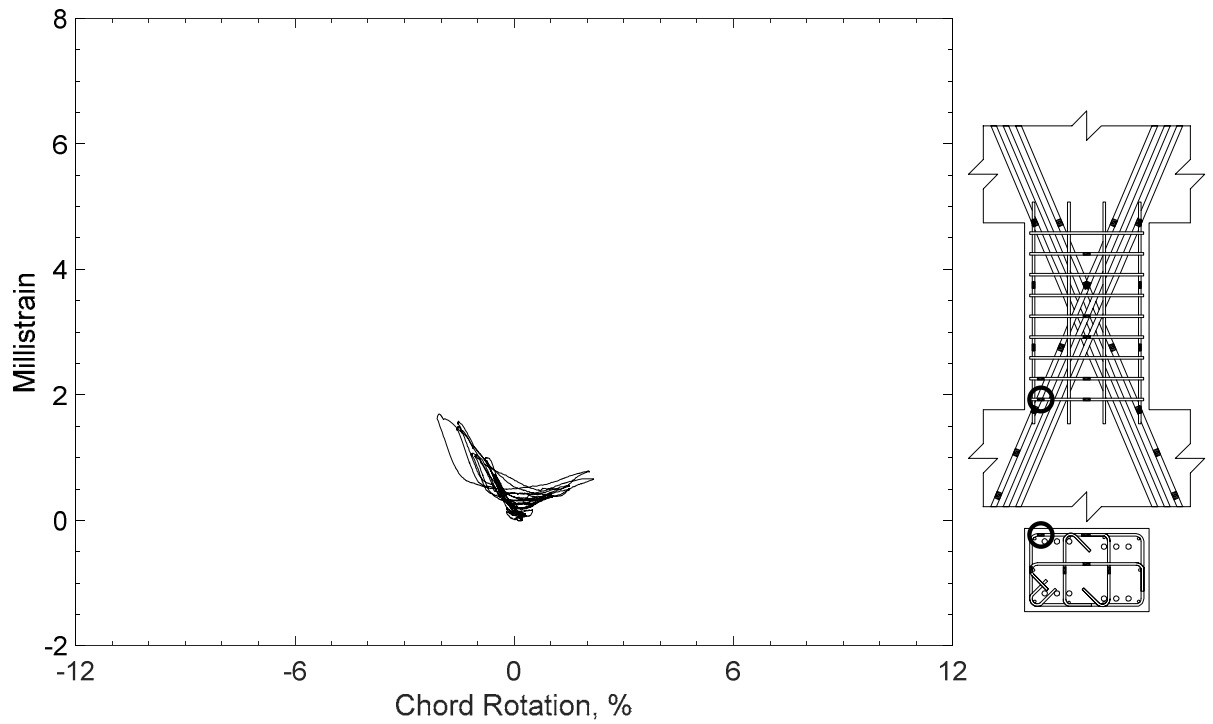


Figure 98 – Measured strain in closed stirrup of D80-1.5, strain gauge S2

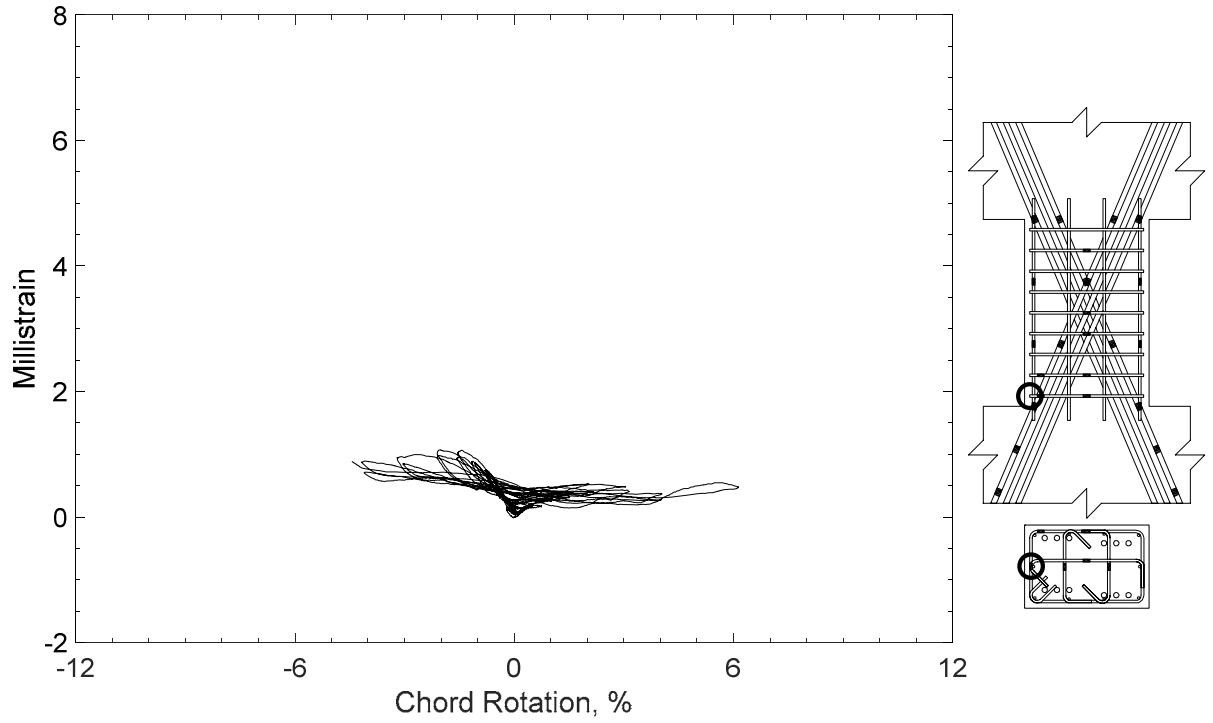


Figure 99 – Measured strain in closed stirrup of D80-1.5, strain gauge S3

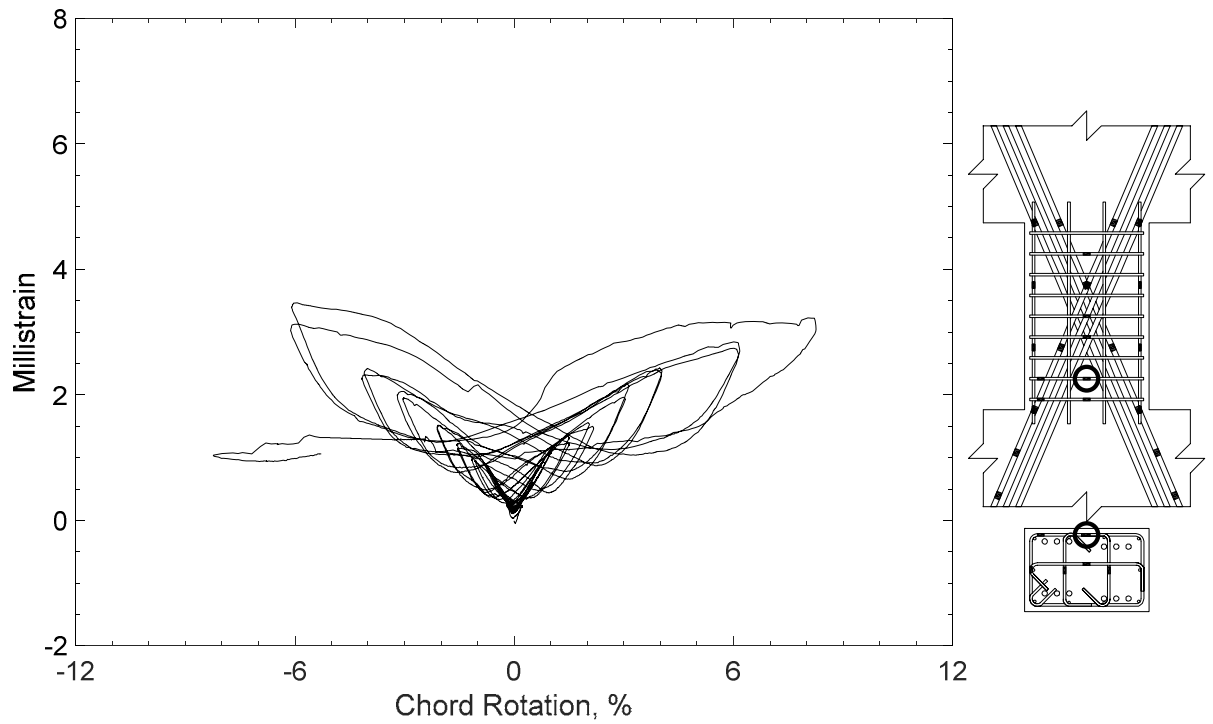


Figure 100 – Measured strain in closed stirrup of D80-1.5, strain gauge S4

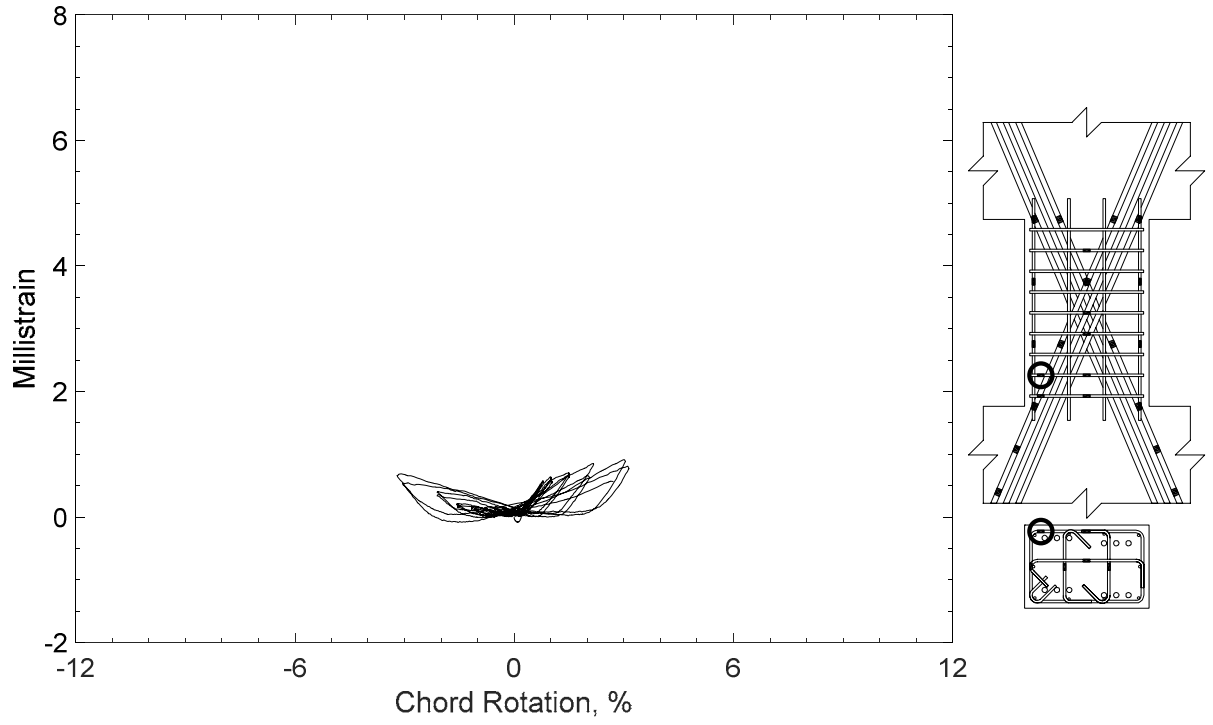


Figure 101 – Measured strain in closed stirrup of D80-1.5, strain gauge S5

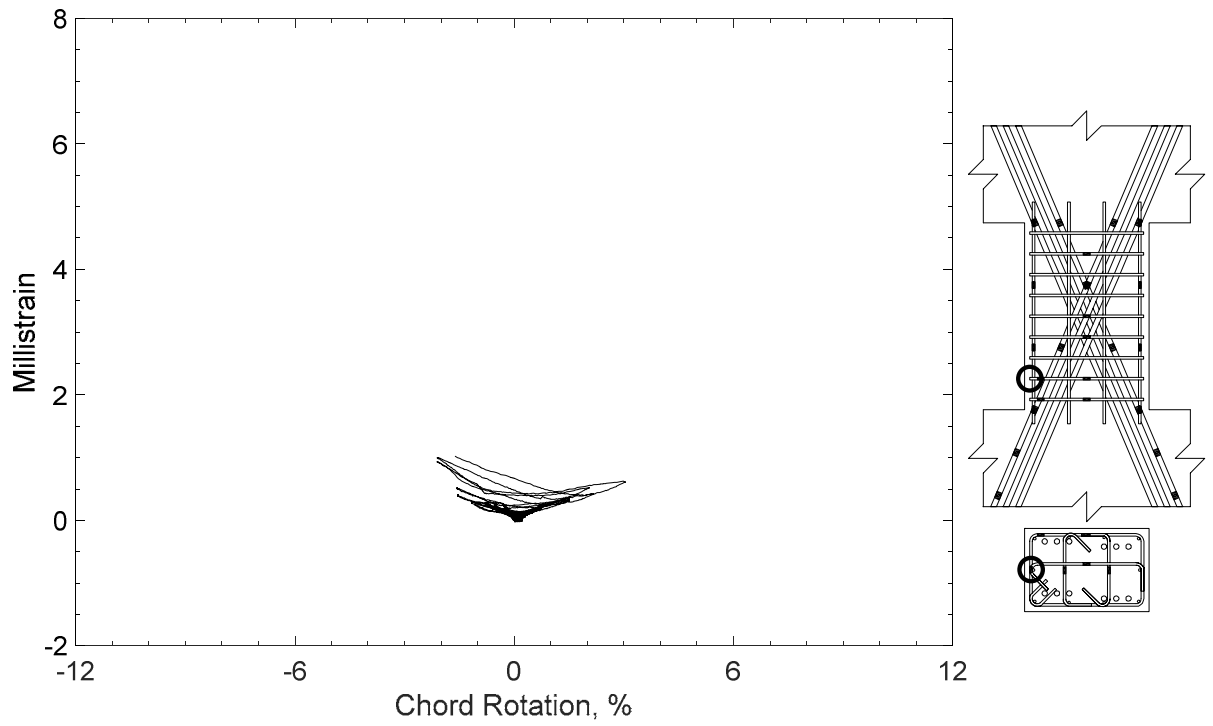


Figure 102 – Measured strain in closed stirrup of D80-1.5, strain gauge S6

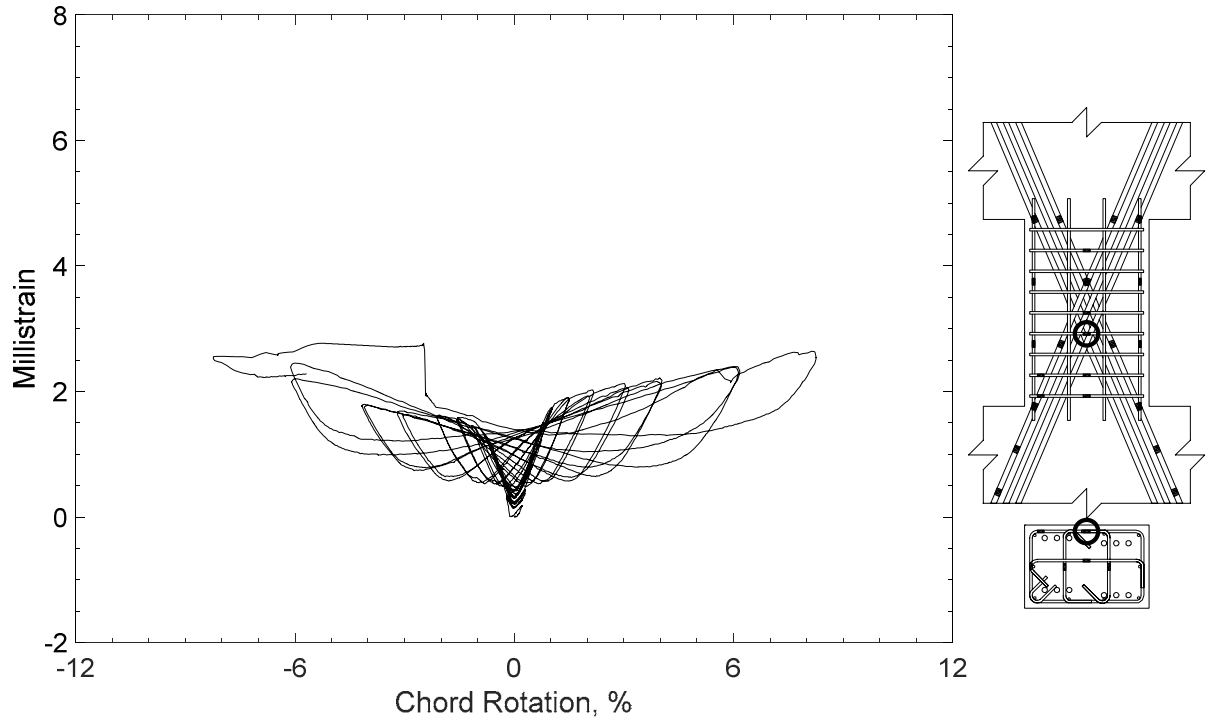


Figure 103 – Measured strain in closed stirrup of D80-1.5, strain gauge S7

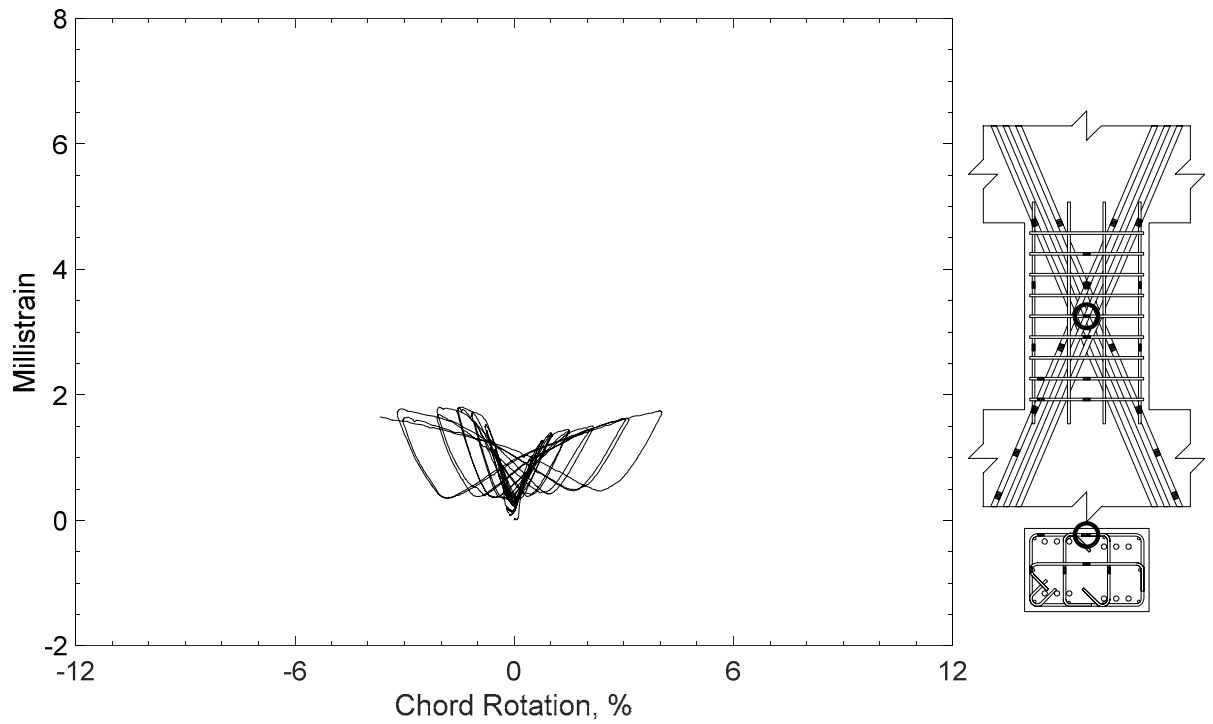


Figure 104 – Measured strain in closed stirrup of D80-1.5, strain gauge S8

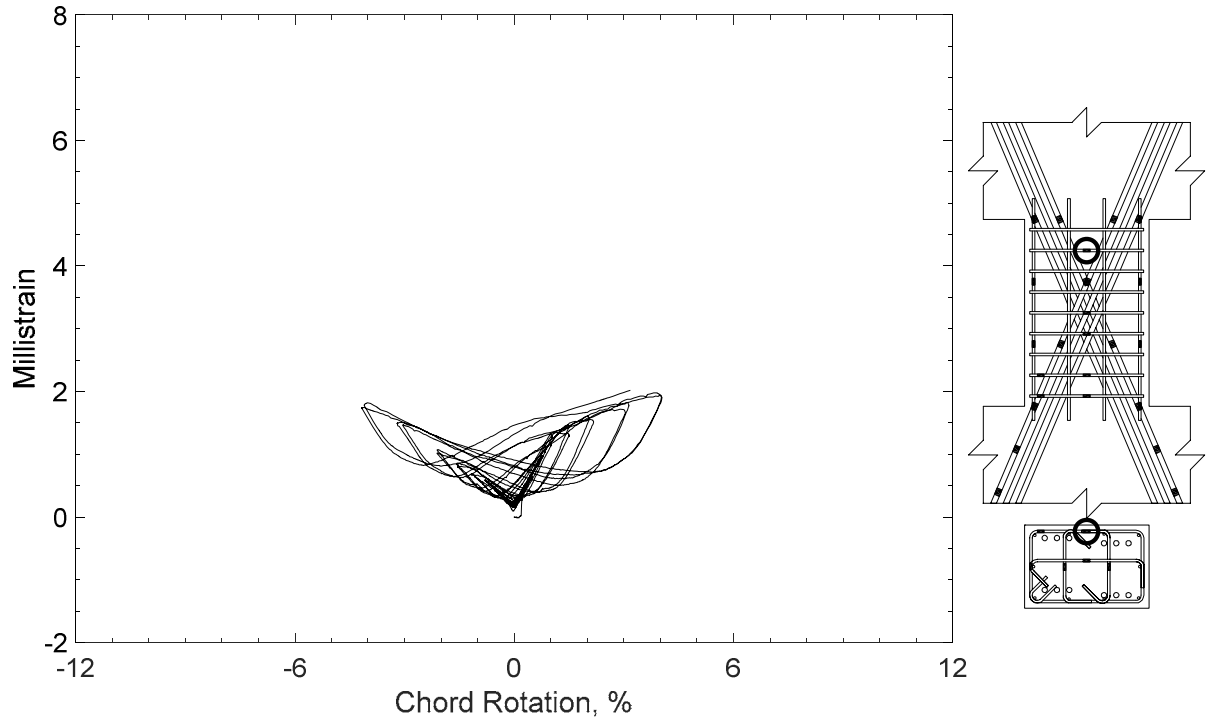


Figure 105 – Measured strain in closed stirrup of D80-1.5, strain gauge S9

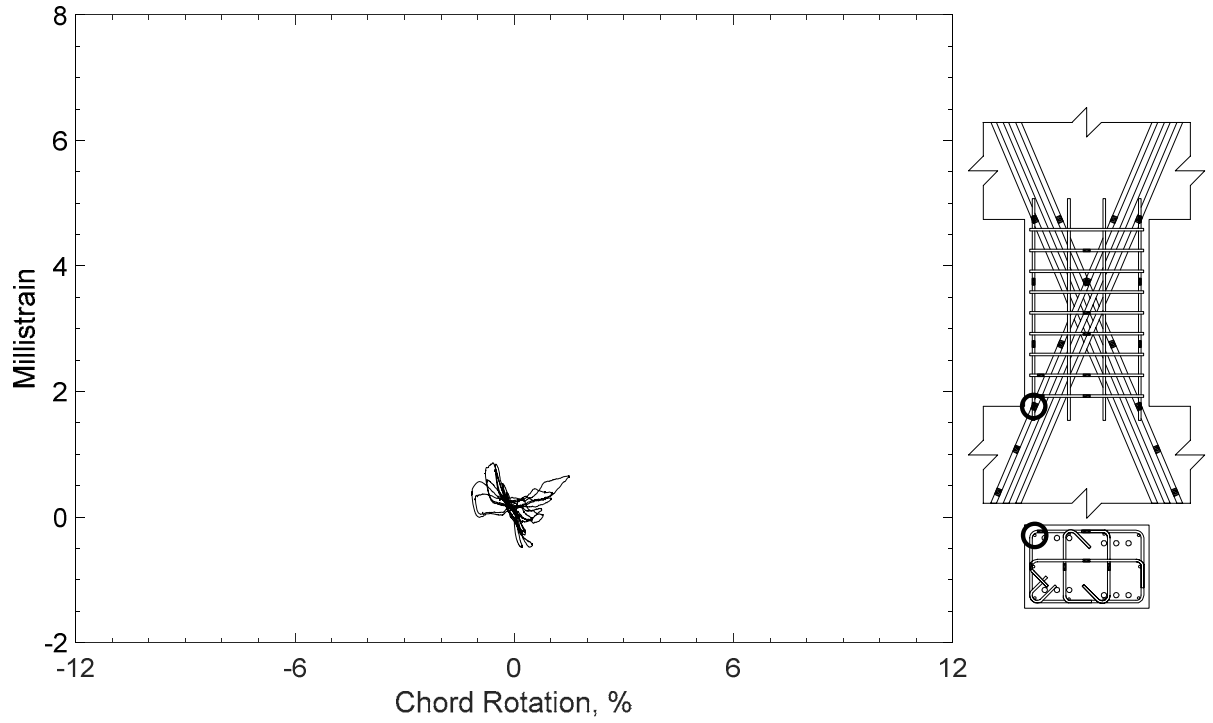


Figure 106 – Measured strain in parallel bar of D80-1.5, strain gauge H1

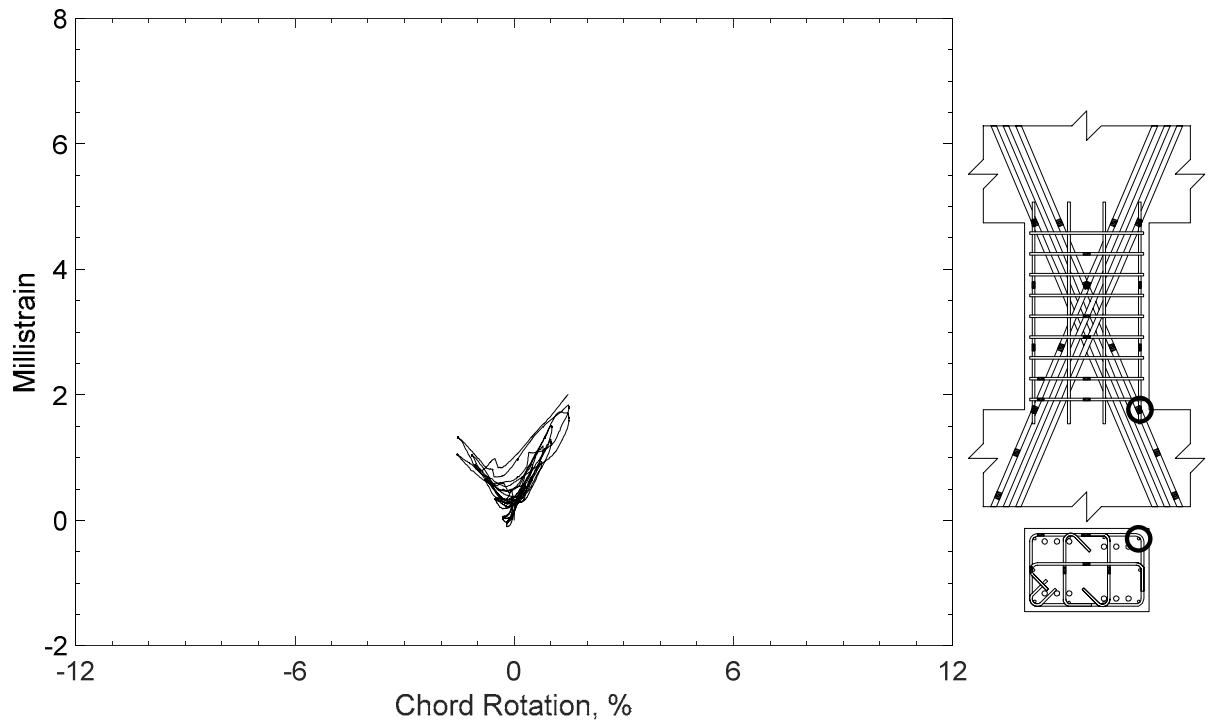


Figure 107 – Measured strain in parallel bar of D80-1.5, strain gauge H2

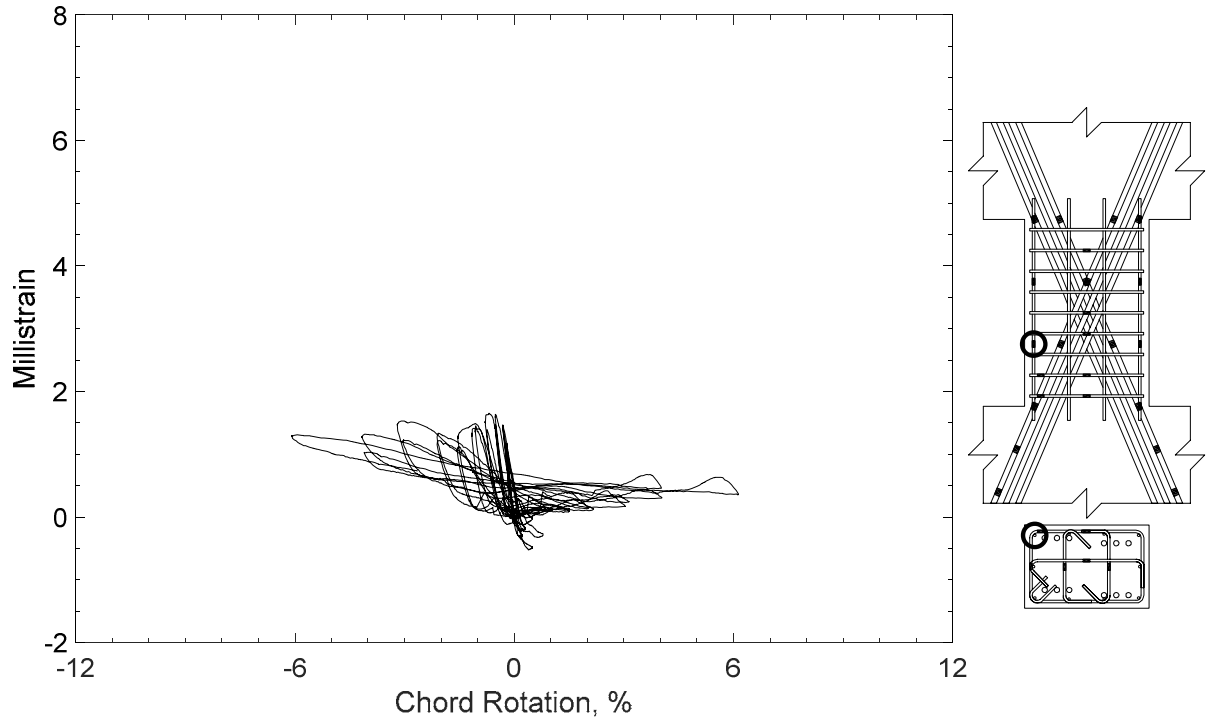


Figure 108 – Measured strain in parallel bar of D80-1.5, strain gauge H3

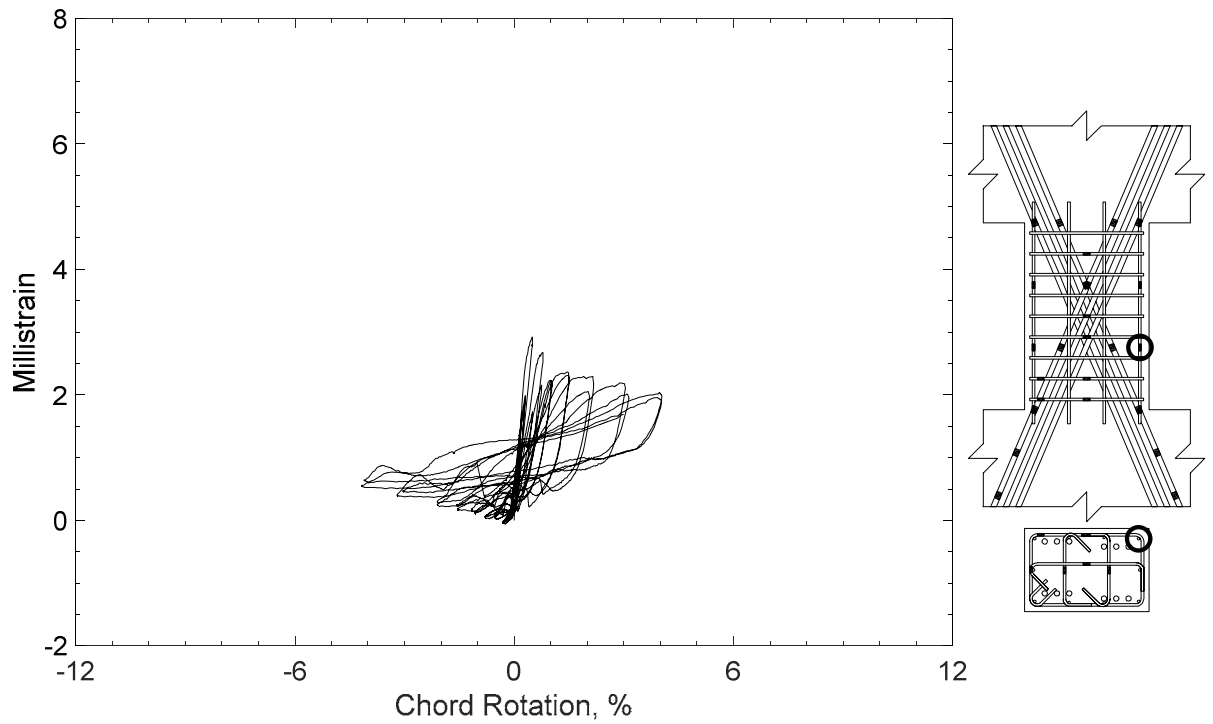


Figure 109 – Measured strain in parallel bar of D80-1.5, strain gauge H4

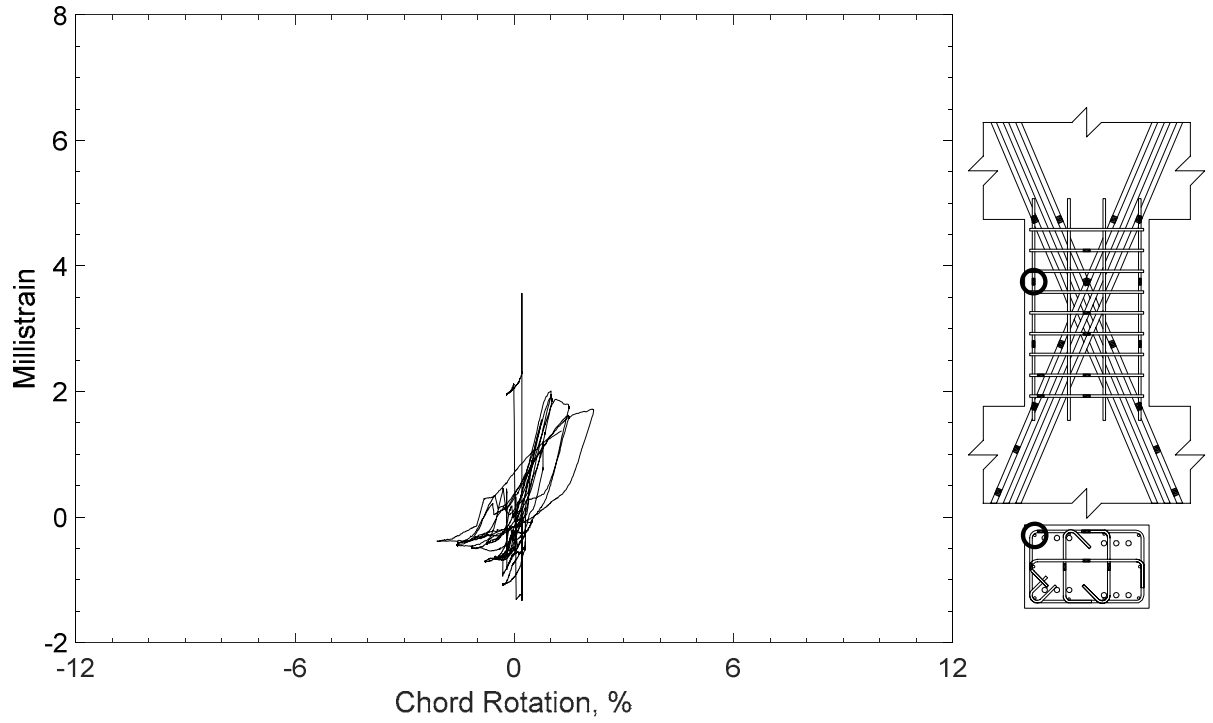


Figure 110 – Measured strain in parallel bar of D80-1.5, strain gauge H5

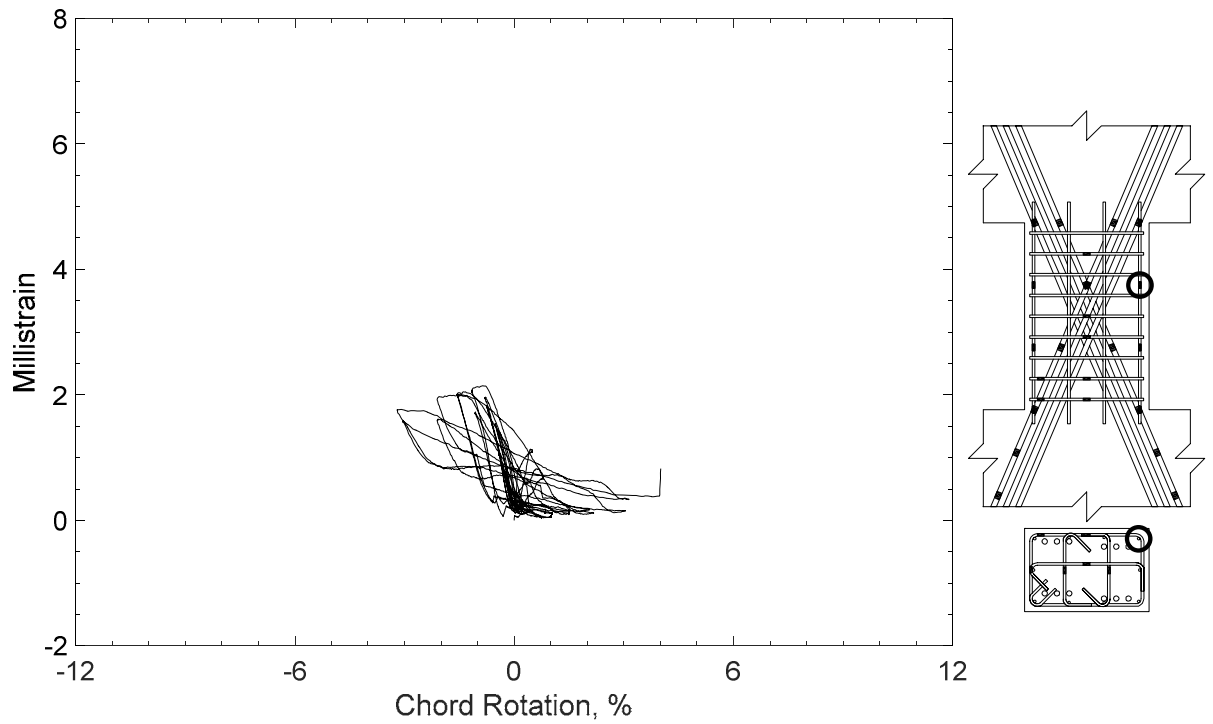


Figure 111 – Measured strain in parallel bar of D80-1.5, strain gauge H6

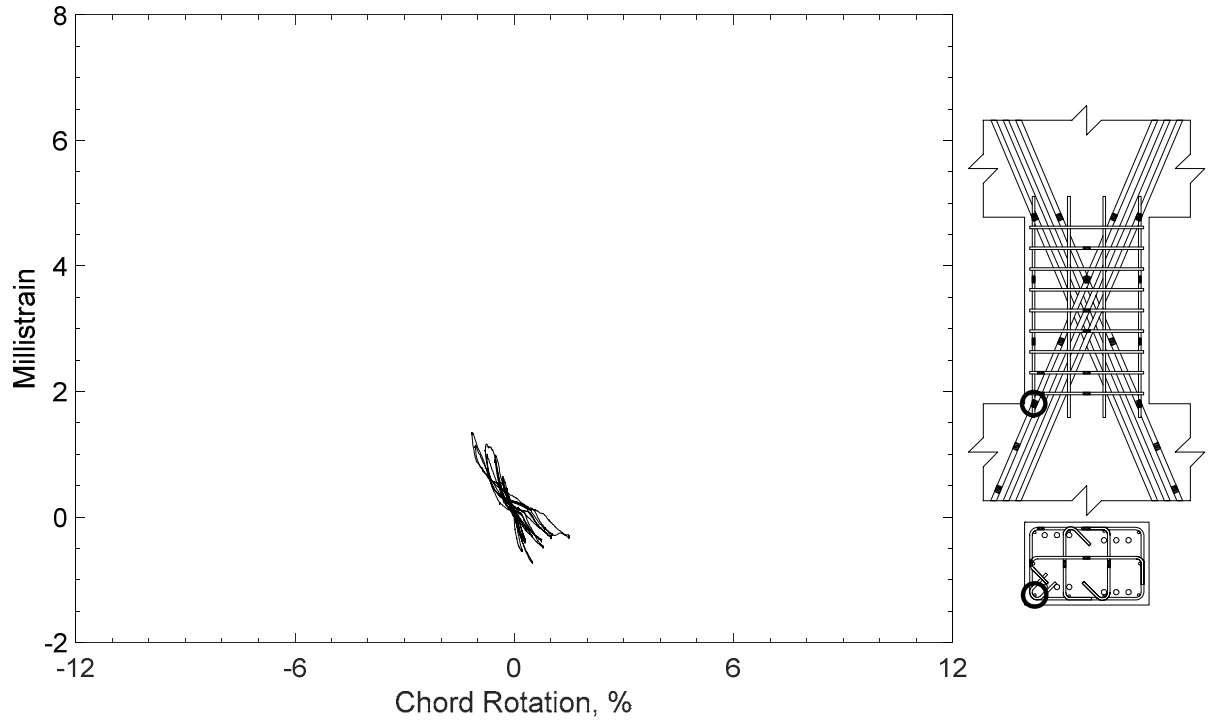


Figure 112 – Measured strain in parallel bar of D80-1.5, strain gauge H9

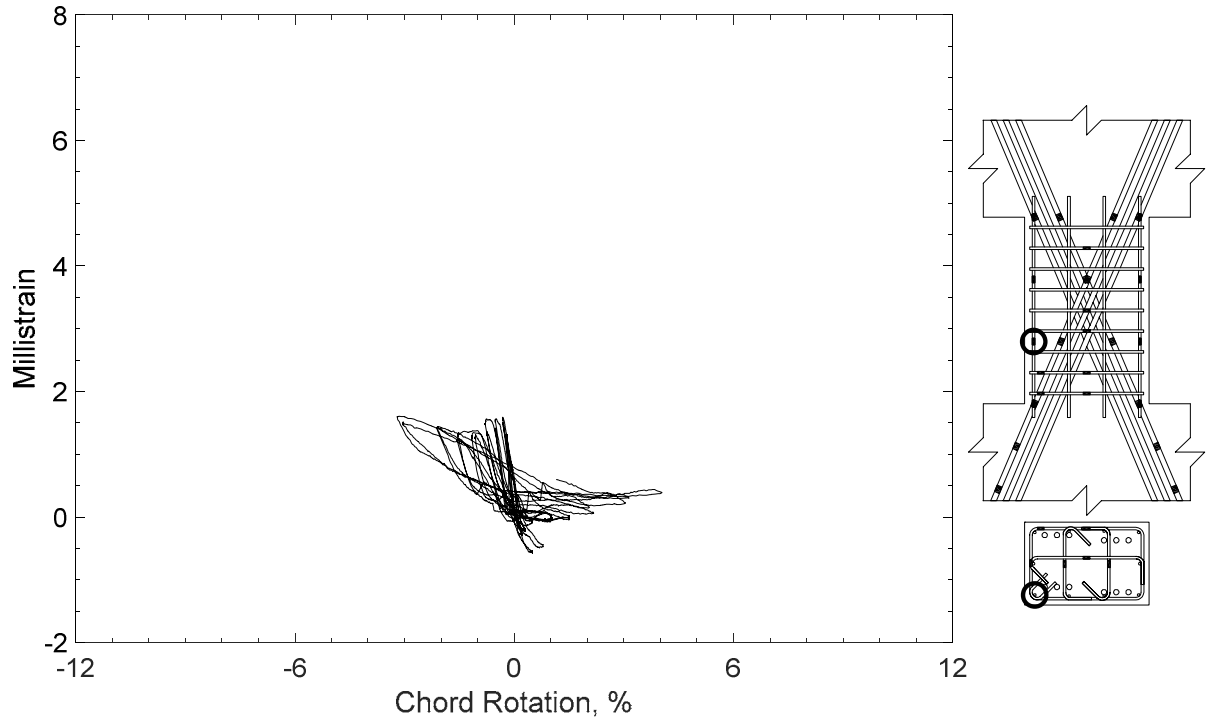


Figure 113 – Measured strain in parallel bar of D80-1.5, strain gauge H11

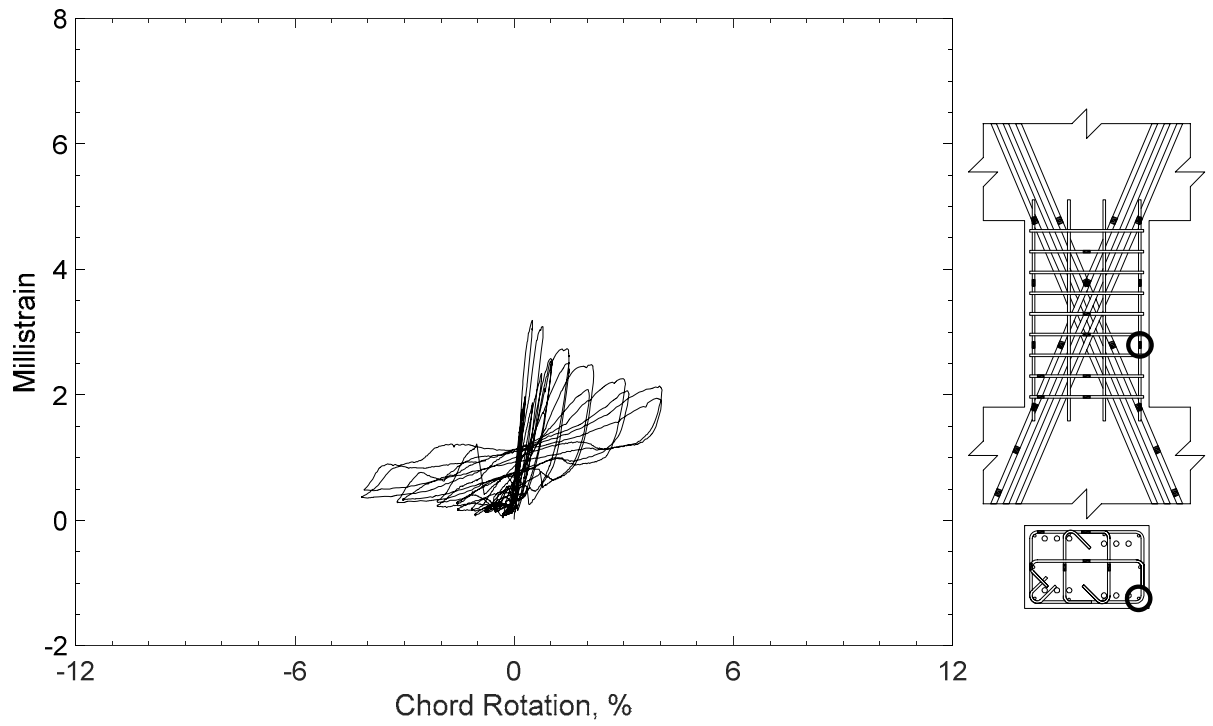


Figure 114 – Measured strain in parallel bar of D80-1.5, strain gauge H12

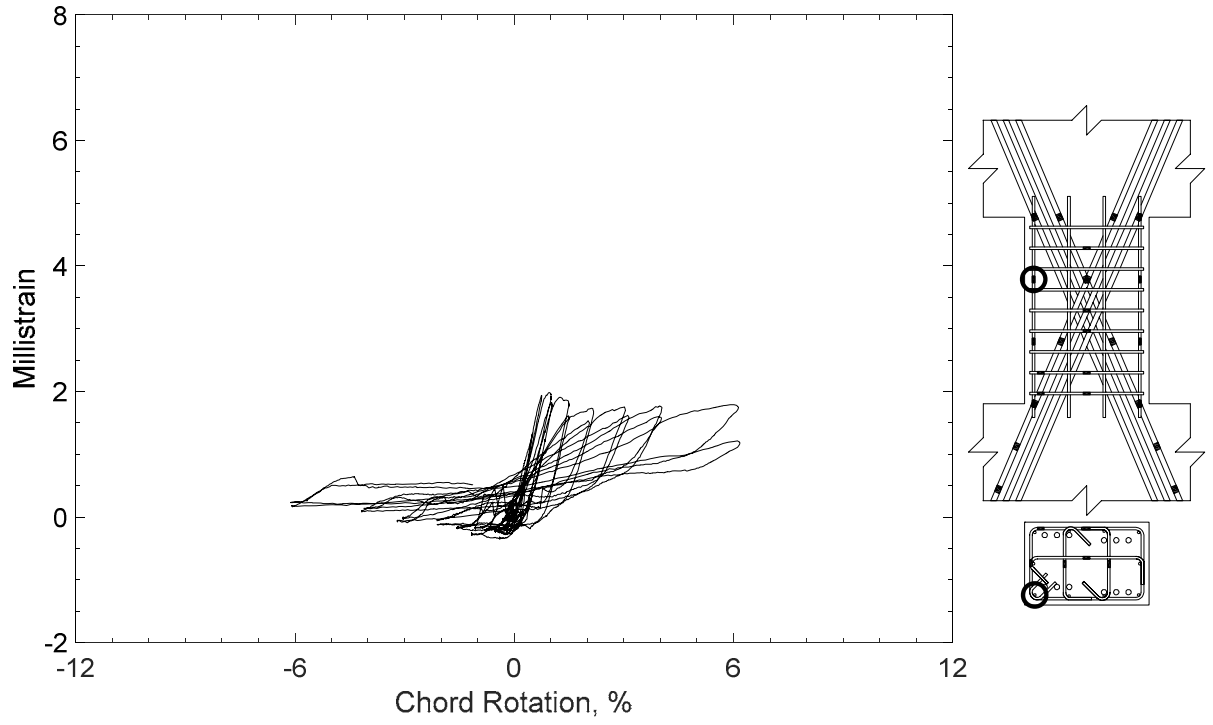


Figure 115 – Measured strain in parallel bar of D80-1.5, strain gauge H13

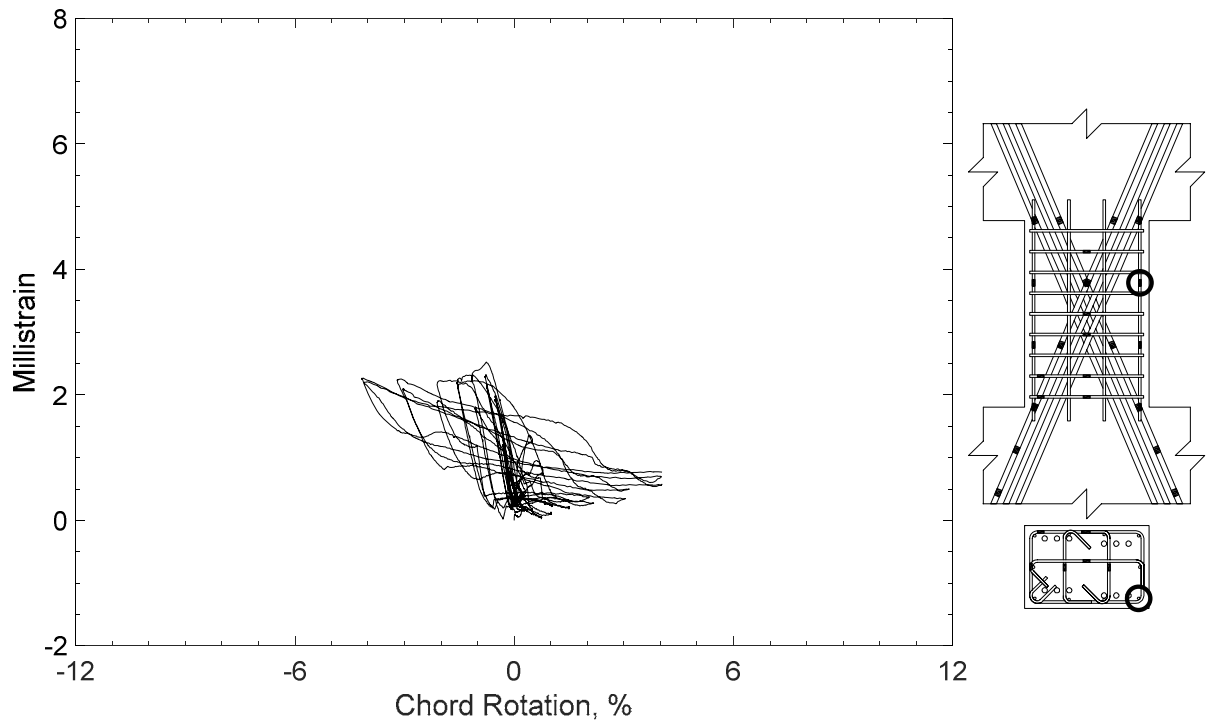


Figure 116 – Measured strain in parallel bar of D80-1.5, strain gauge H14

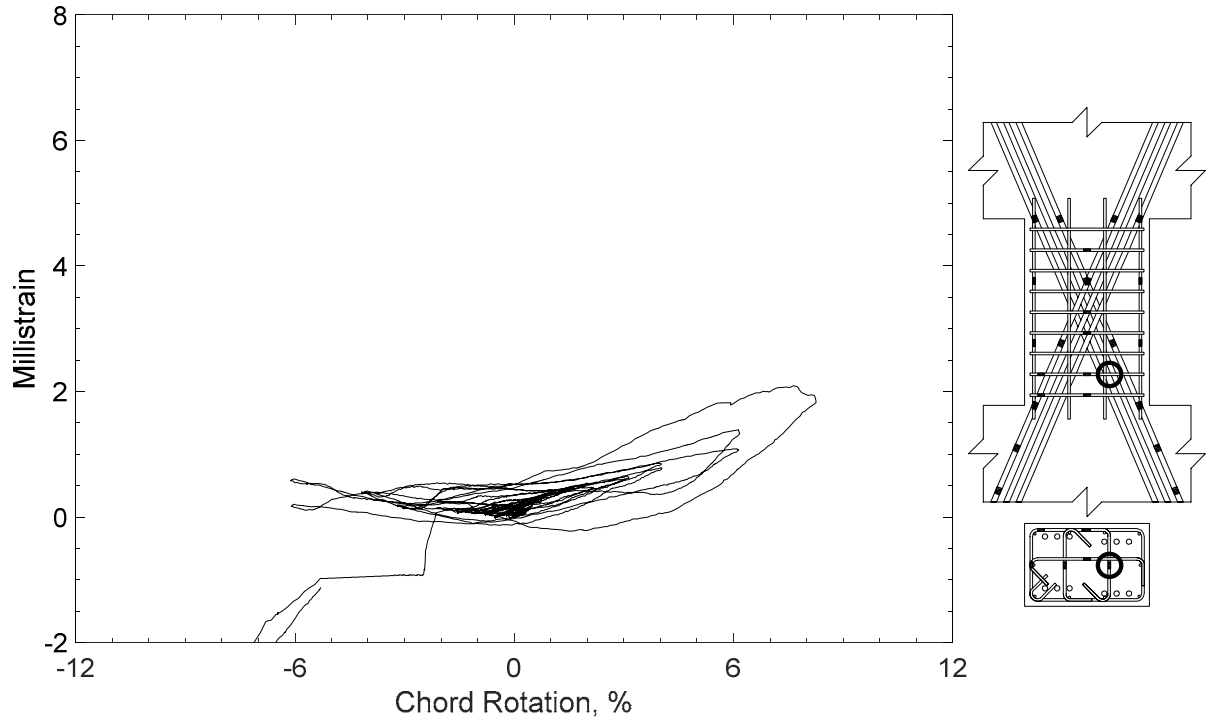


Figure 117 – Measured strain in crosstie of D80-1.5, strain gauge T1

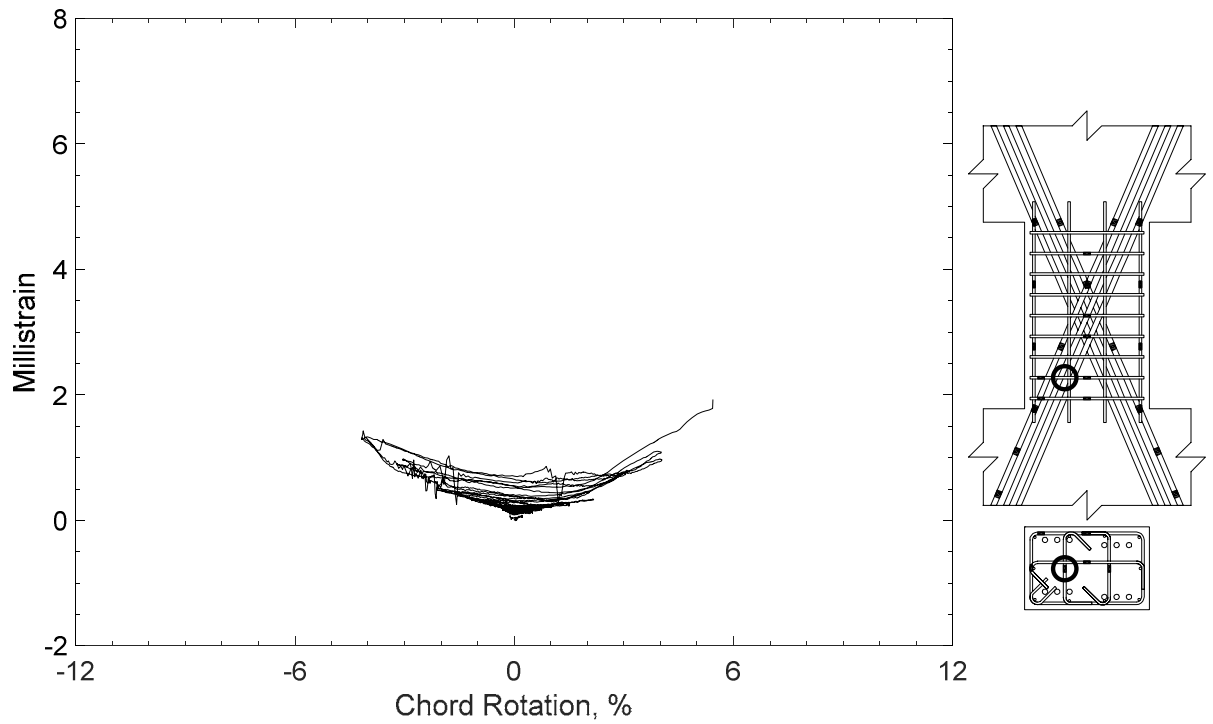


Figure 118 – Measured strain in crosstie of D80-1.5, strain gauge T2

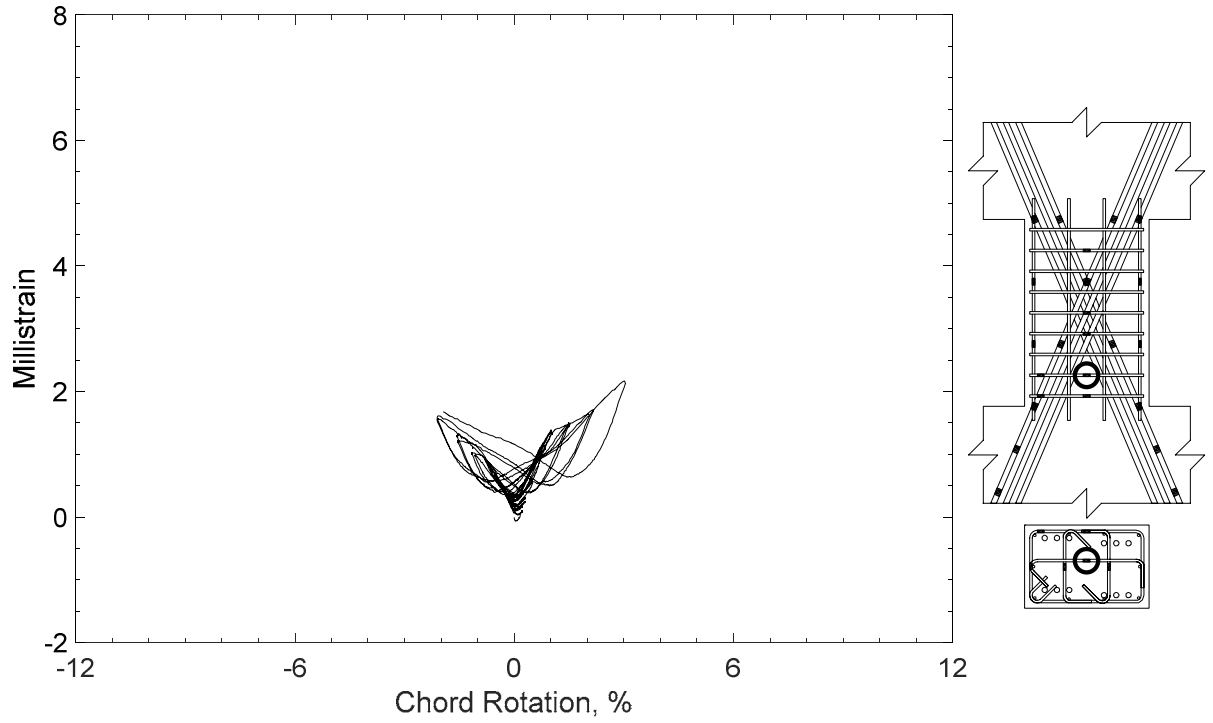


Figure 119 – Measured strain in crosstie of D80-1.5, strain gauge T3

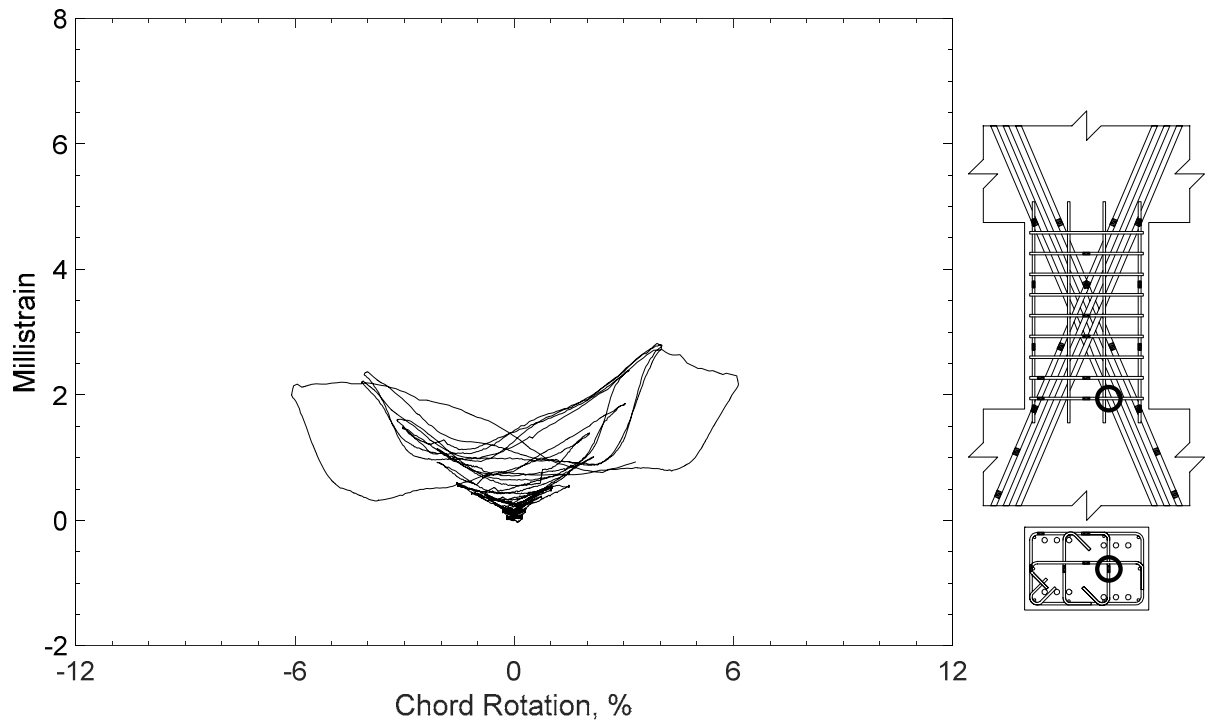


Figure 120 – Measured strain in crosstie of D80-1.5, strain gauge T4

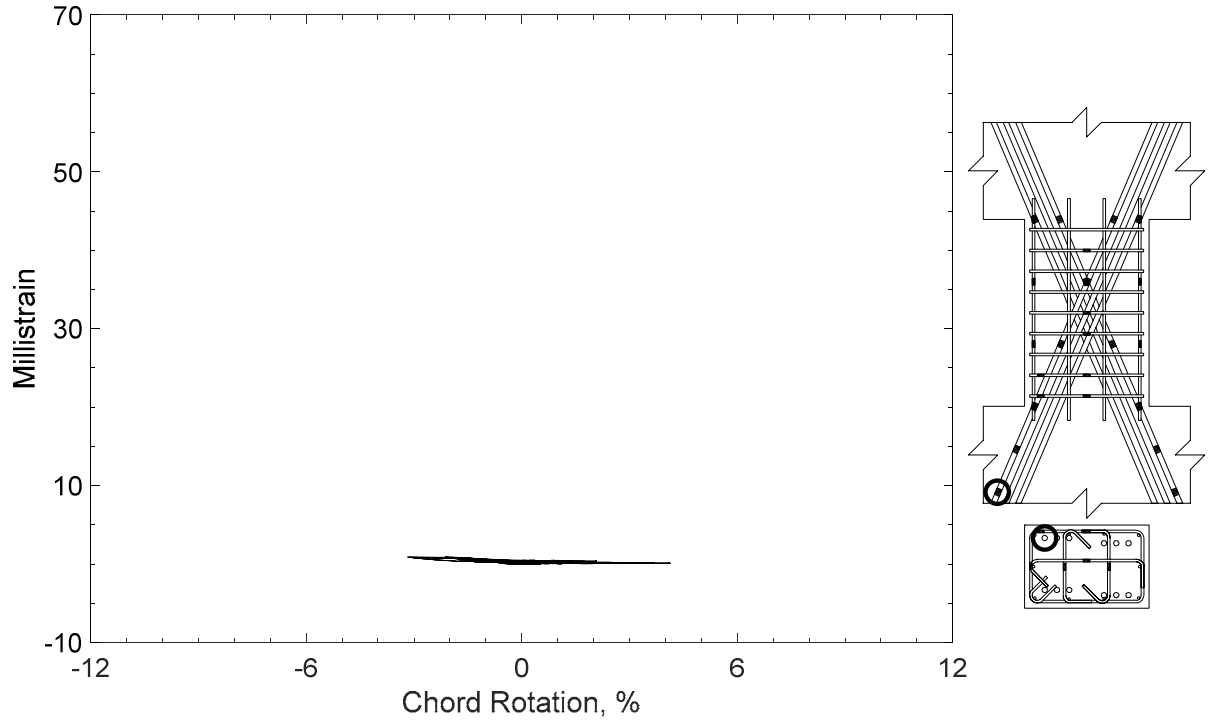


Figure 121 – Measured strain in diagonal bar of D100-1.5, strain gauge D1

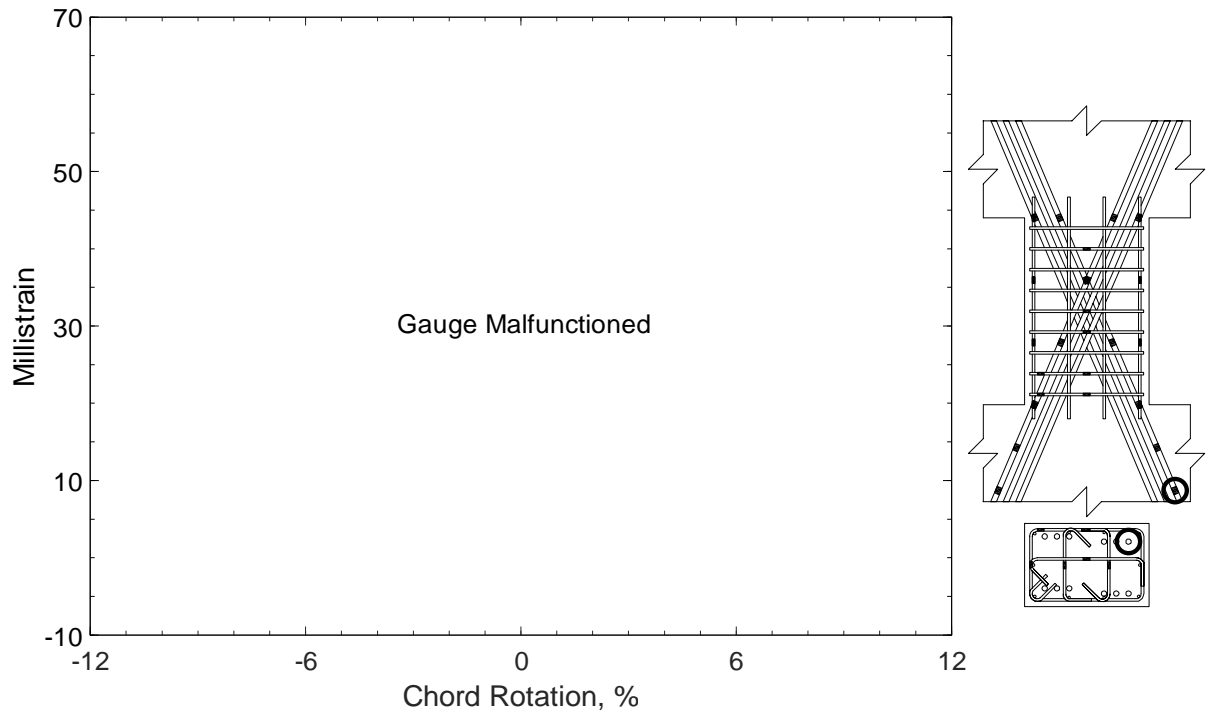


Figure 122 – Measured strain in diagonal bar of D100-1.5, strain gauge D2

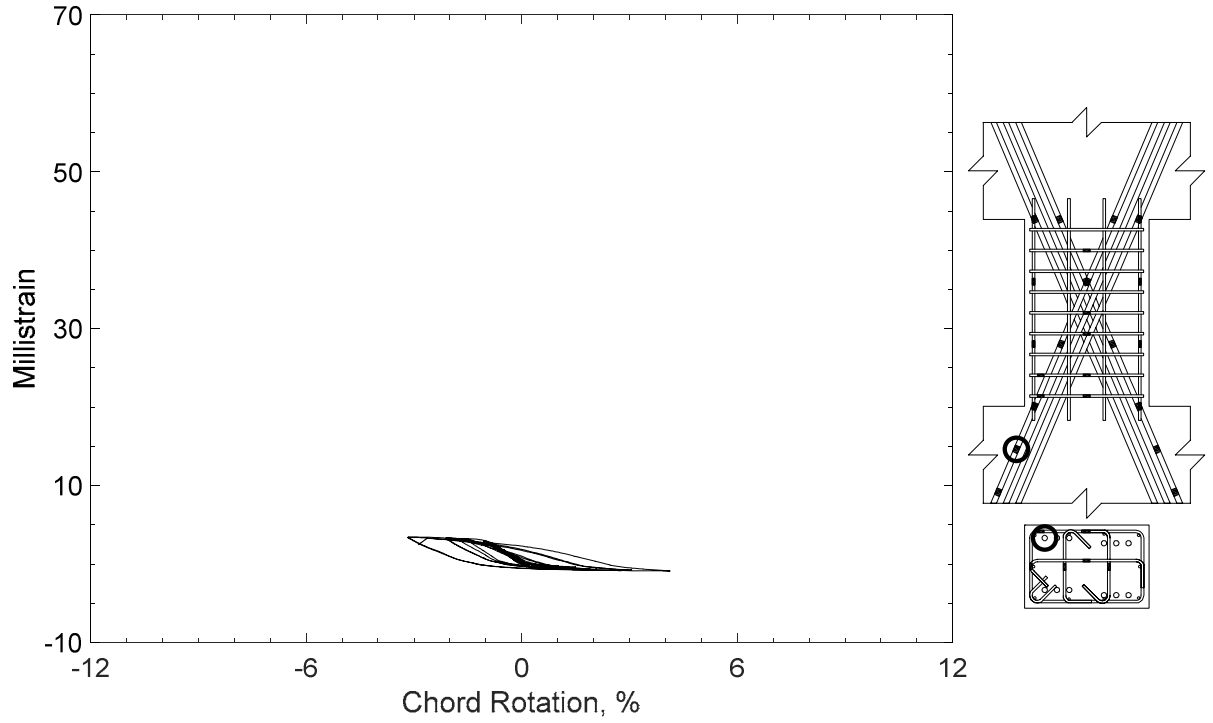


Figure 123 – Measured strain in diagonal bar of D100-1.5, strain gauge D3

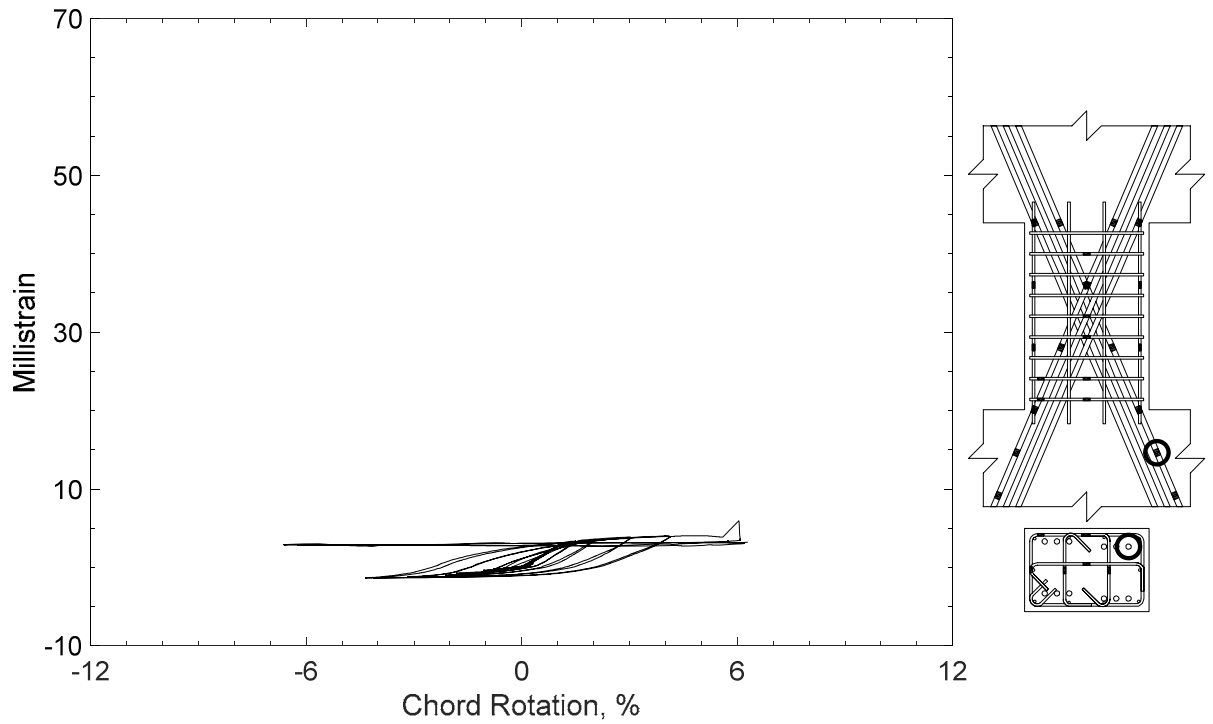


Figure 124 – Measured strain in diagonal bar of D100-1.5, strain gauge D4

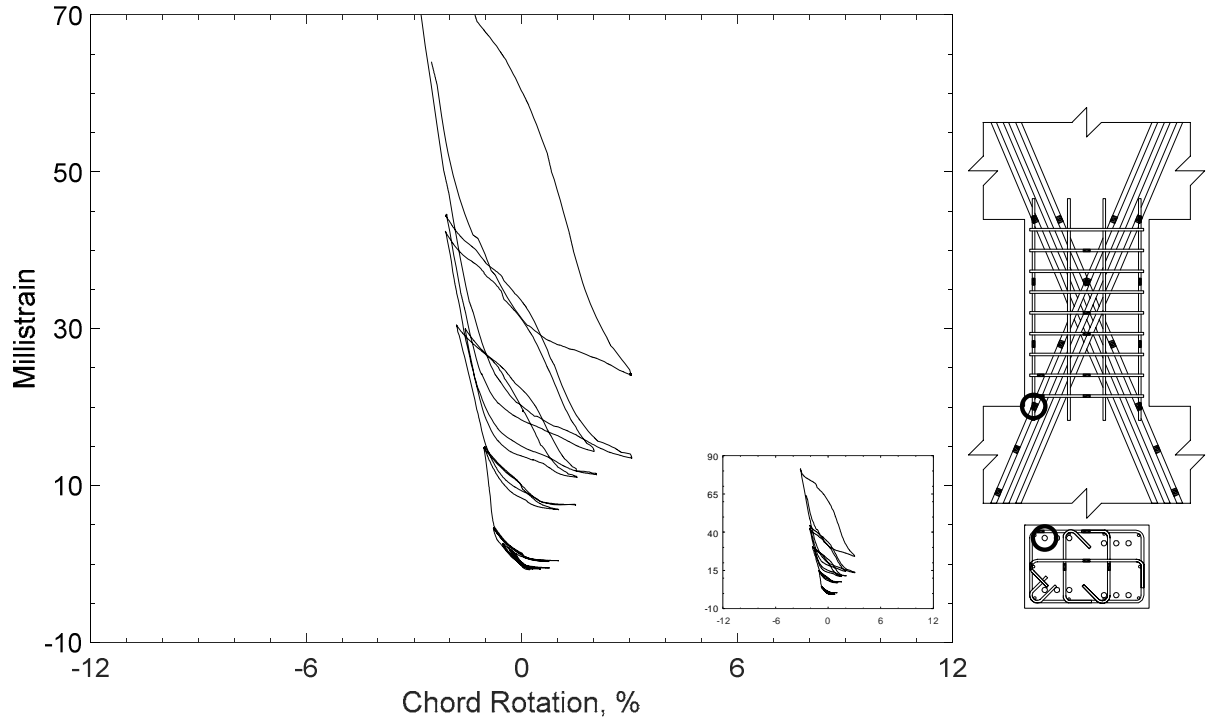


Figure 125 – Measured strain in diagonal bar of D100-1.5, strain gauge D5

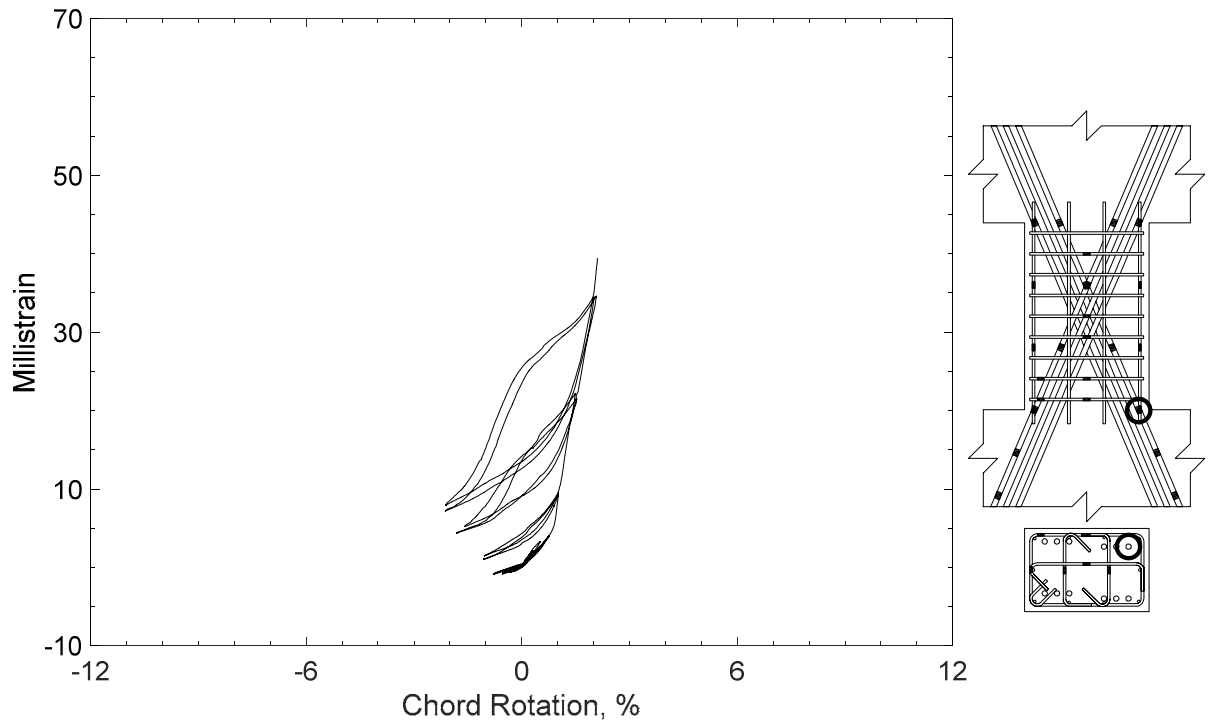


Figure 126 – Measured strain in diagonal bar of D100-1.5, strain gauge D6

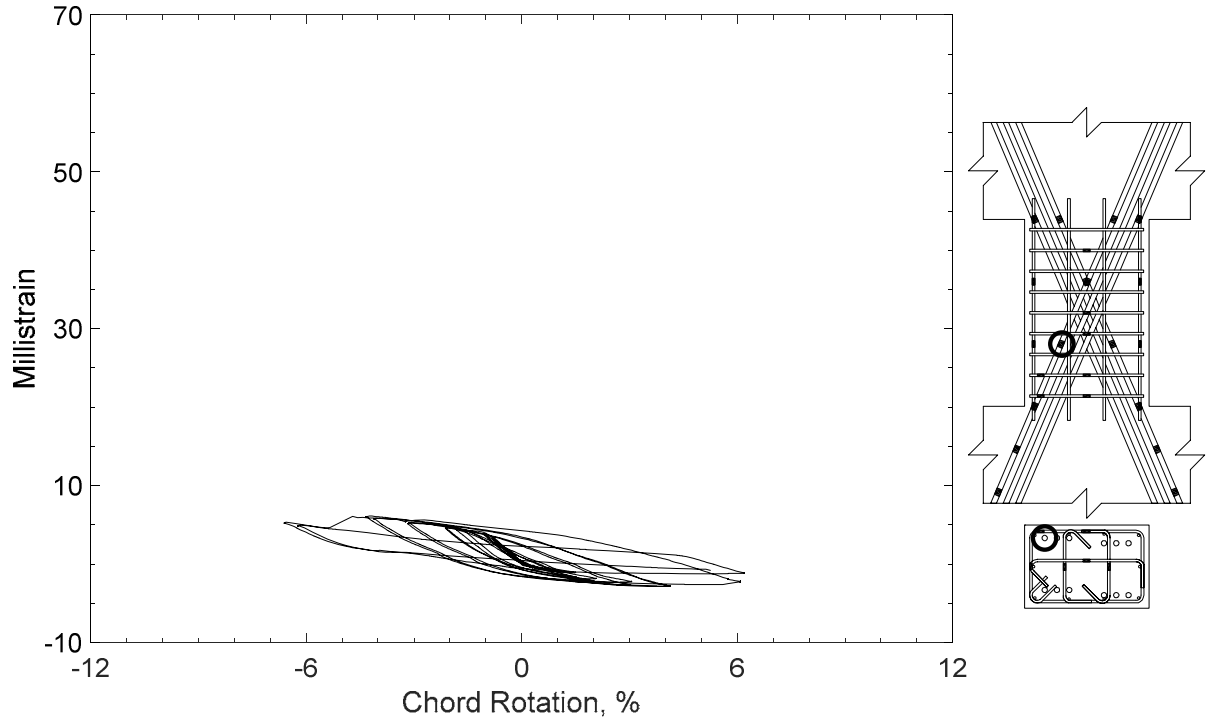


Figure 127 – Measured strain in diagonal bar of D100-1.5, strain gauge D7

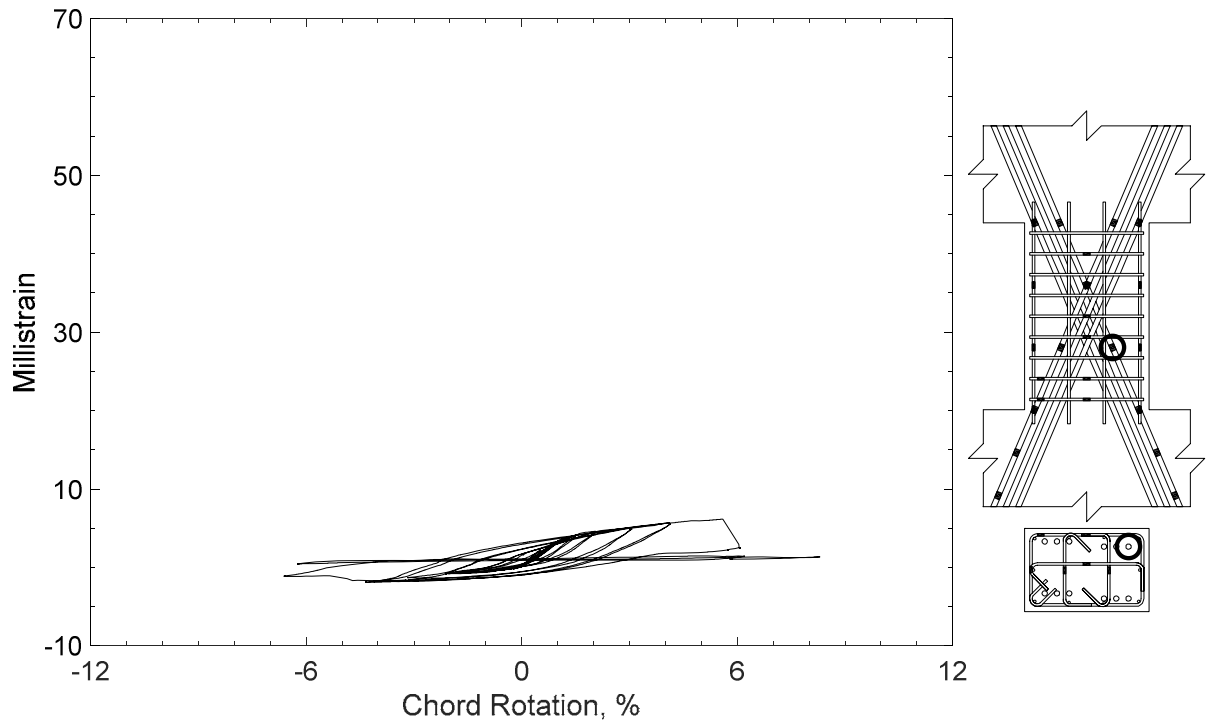


Figure 128 – Measured strain in diagonal bar of D100-1.5, strain gauge D8

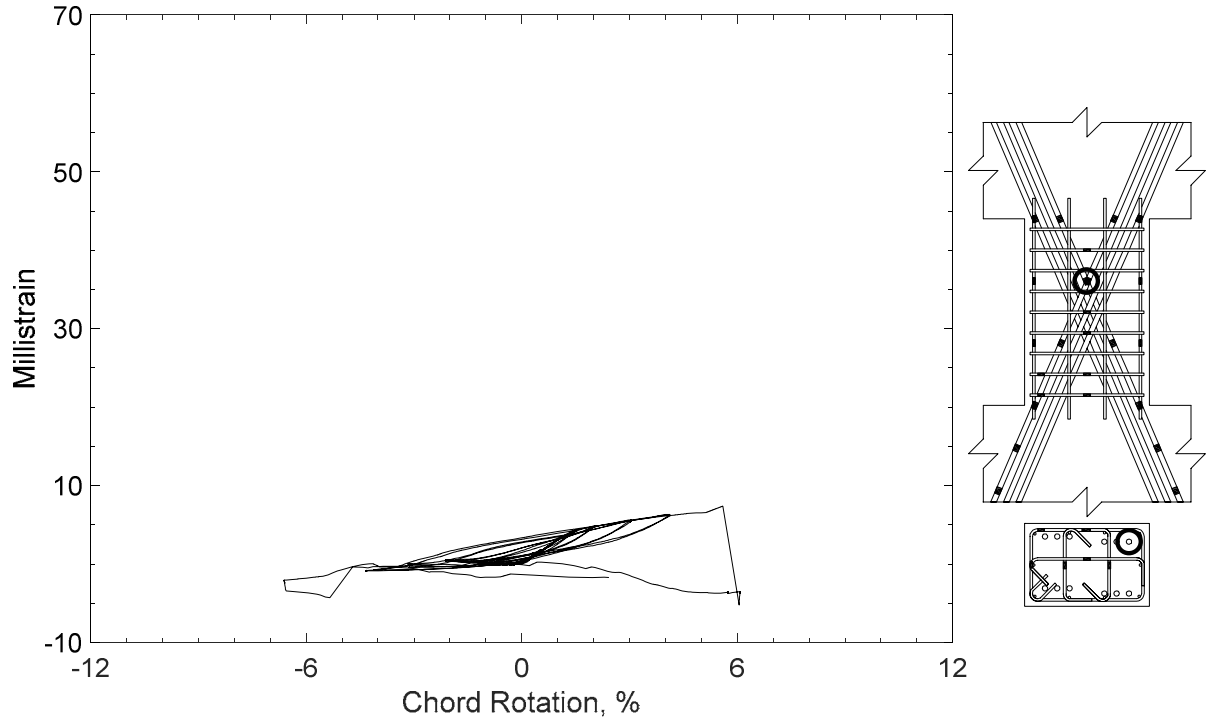


Figure 129 – Measured strain in diagonal bar of D100-1.5, strain gauge D9

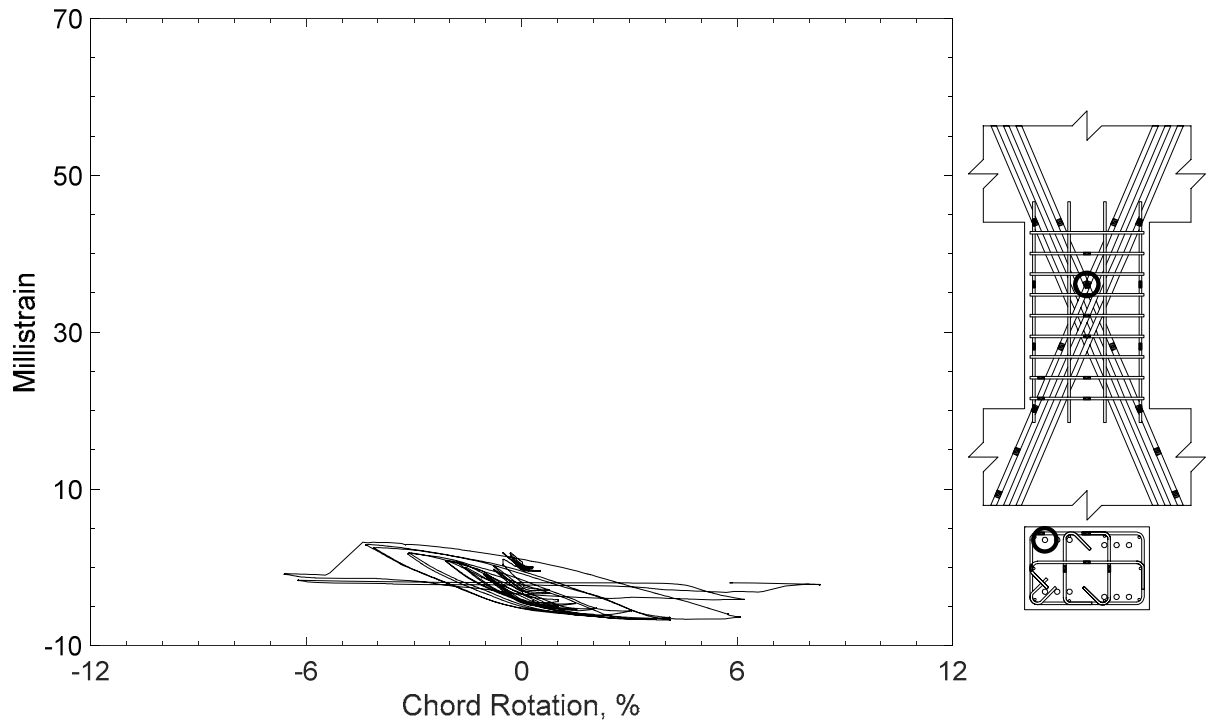


Figure 130 – Measured strain in diagonal bar of D100-1.5, strain gauge D10

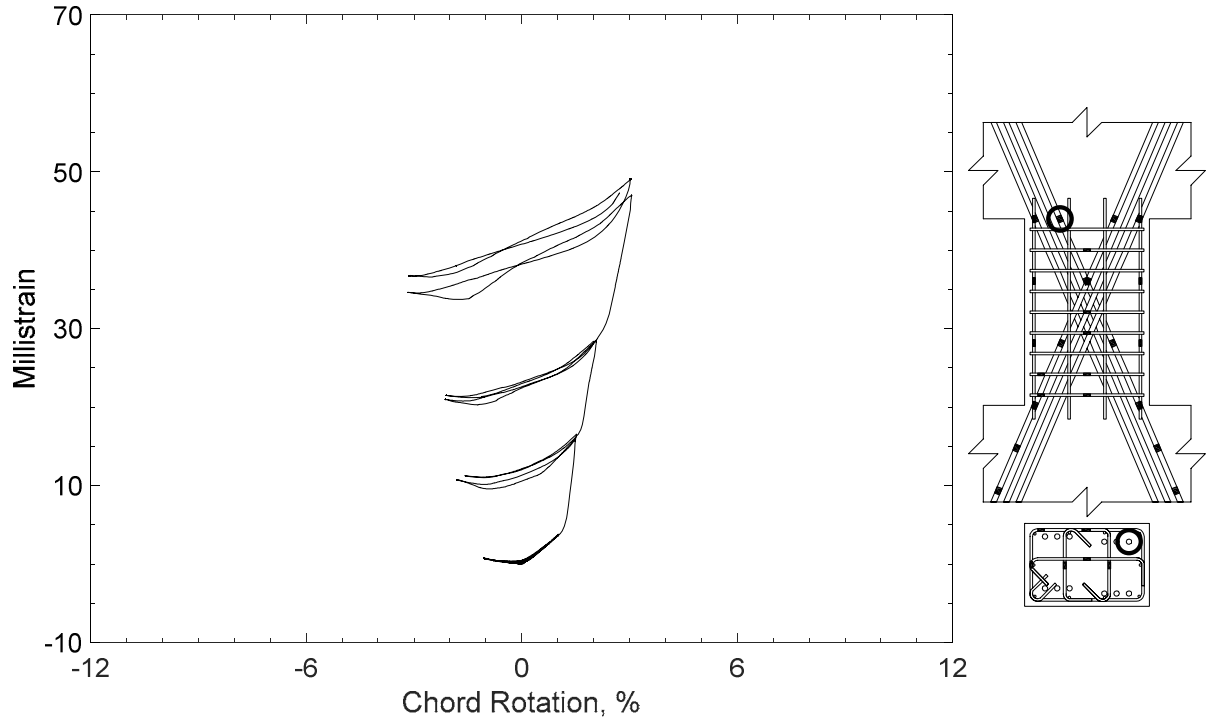


Figure 131 – Measured strain in diagonal bar of D100-1.5, strain gauge D11

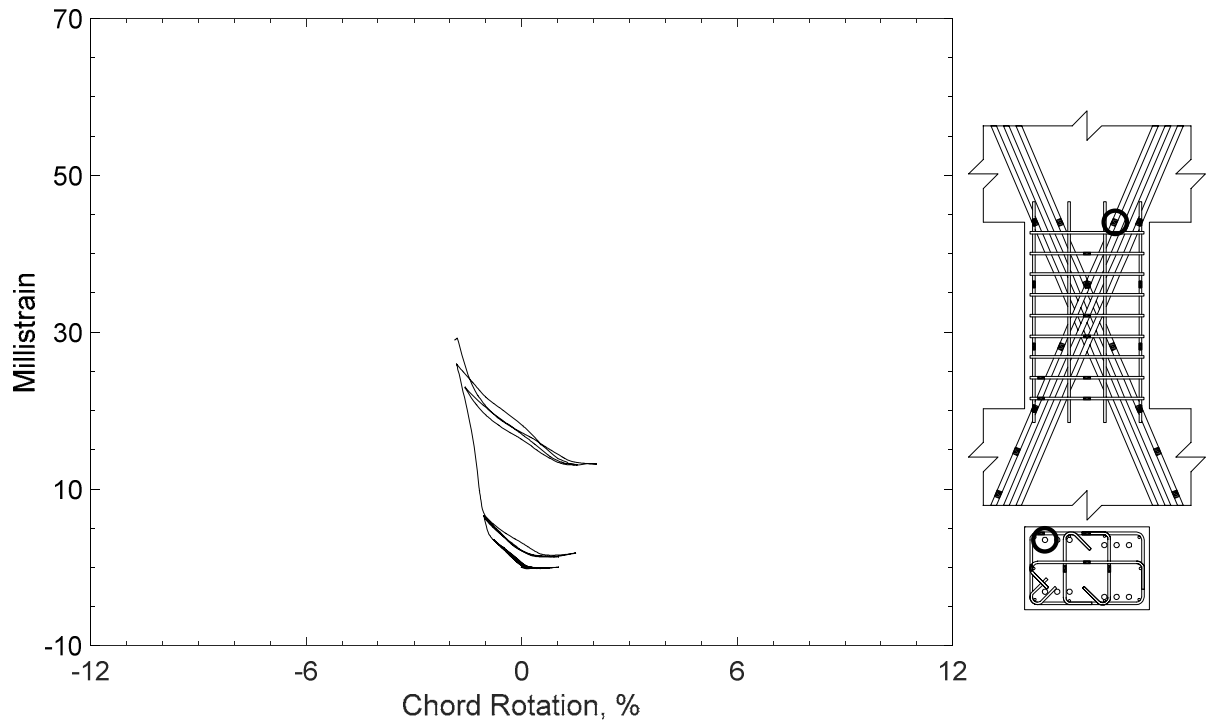


Figure 132 – Measured strain in diagonal bar of D100-1.5, strain gauge D12

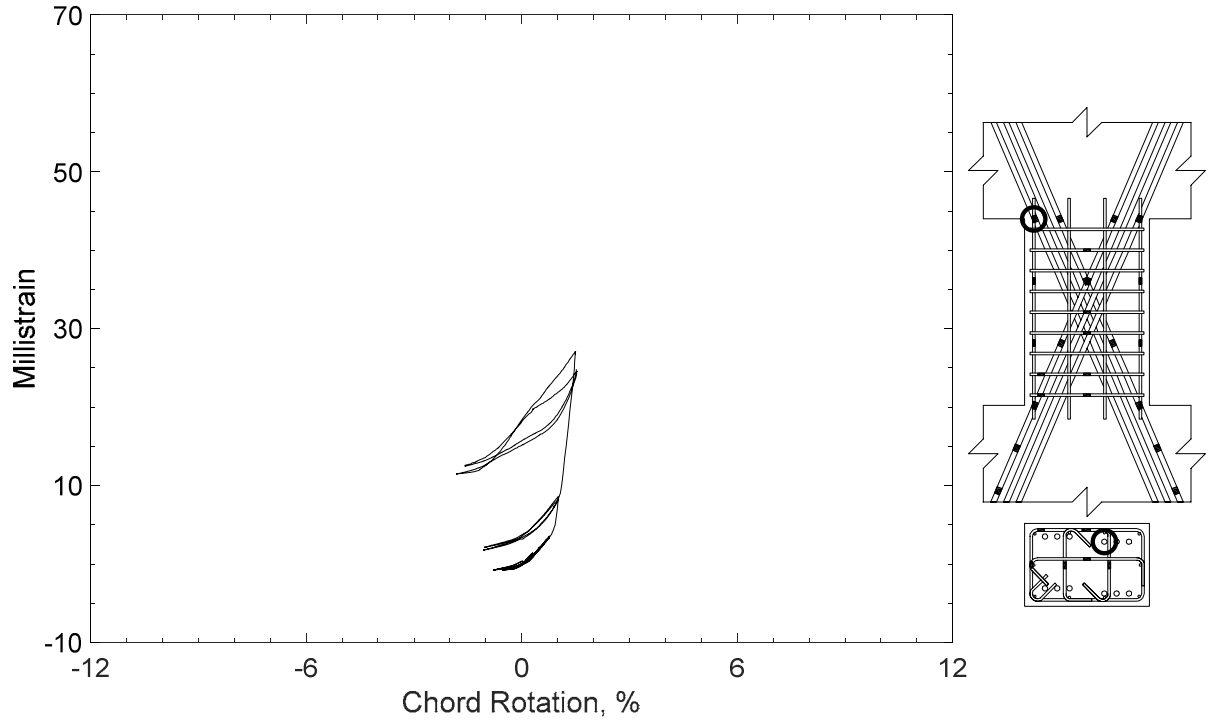


Figure 133 – Measured strain in diagonal bar of D100-1.5, strain gauge D13

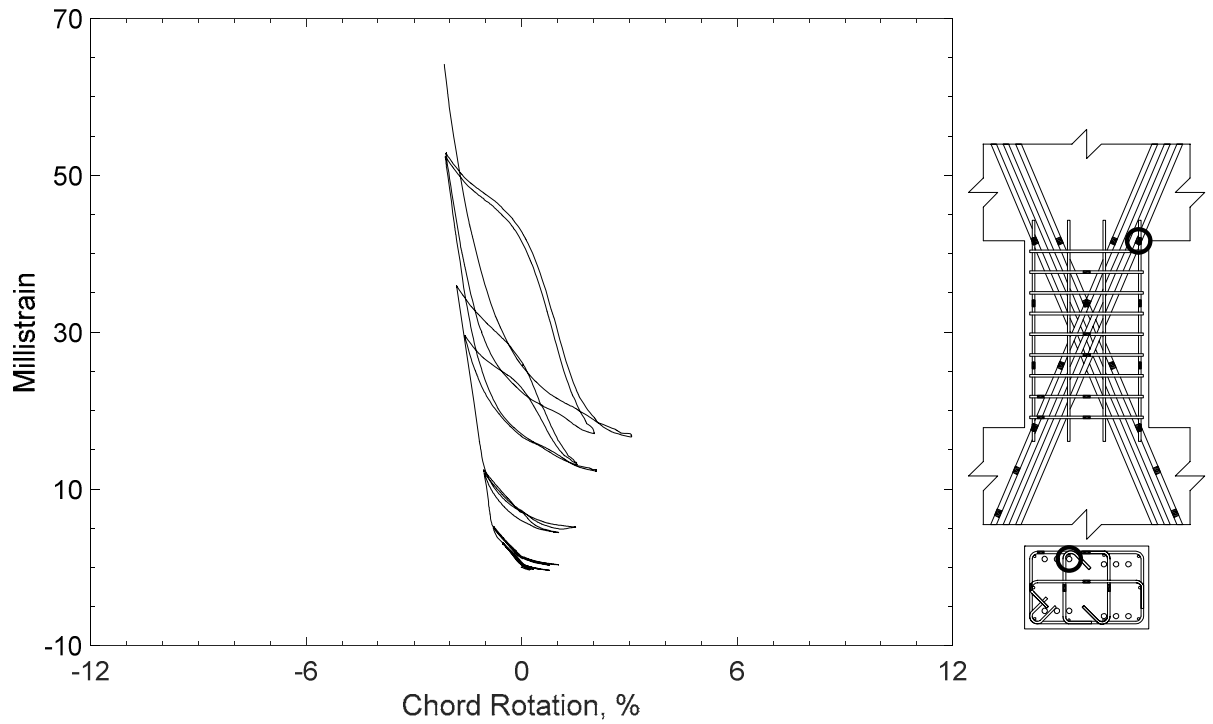


Figure 134 – Measured strain in diagonal bar of D100-1.5, strain gauge D14

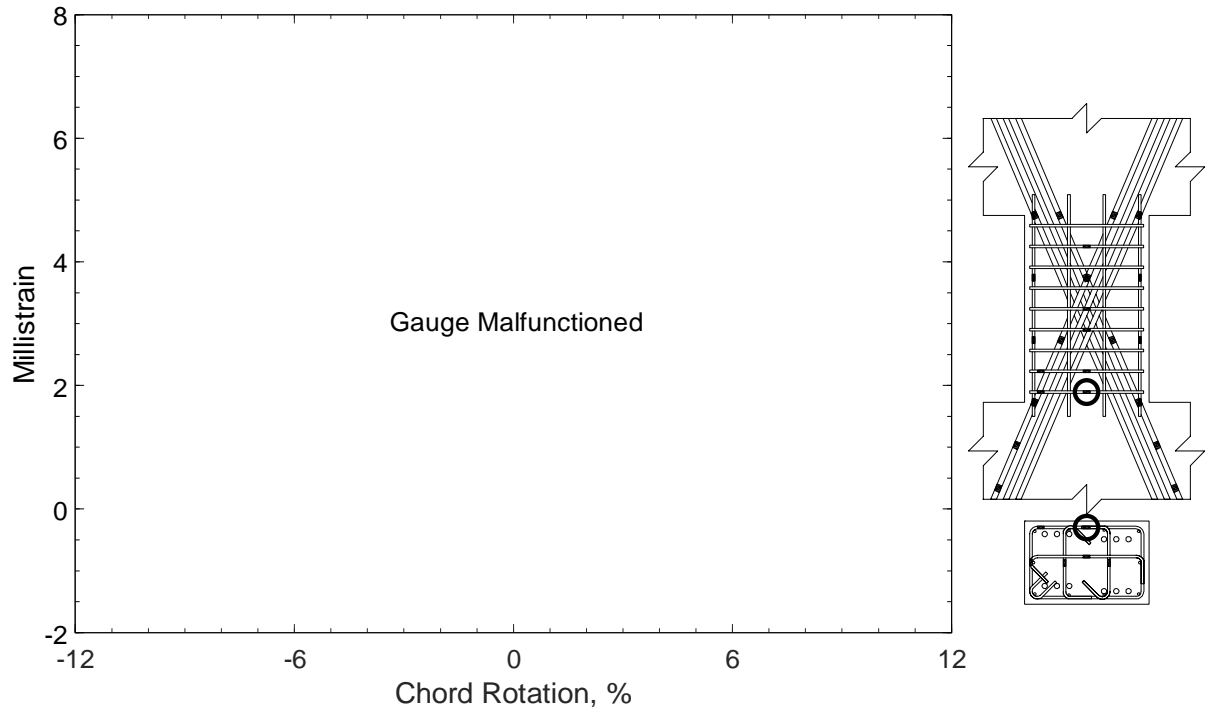


Figure 135 – Measured strain in closed stirrup of D100-1.5, strain gauge S1

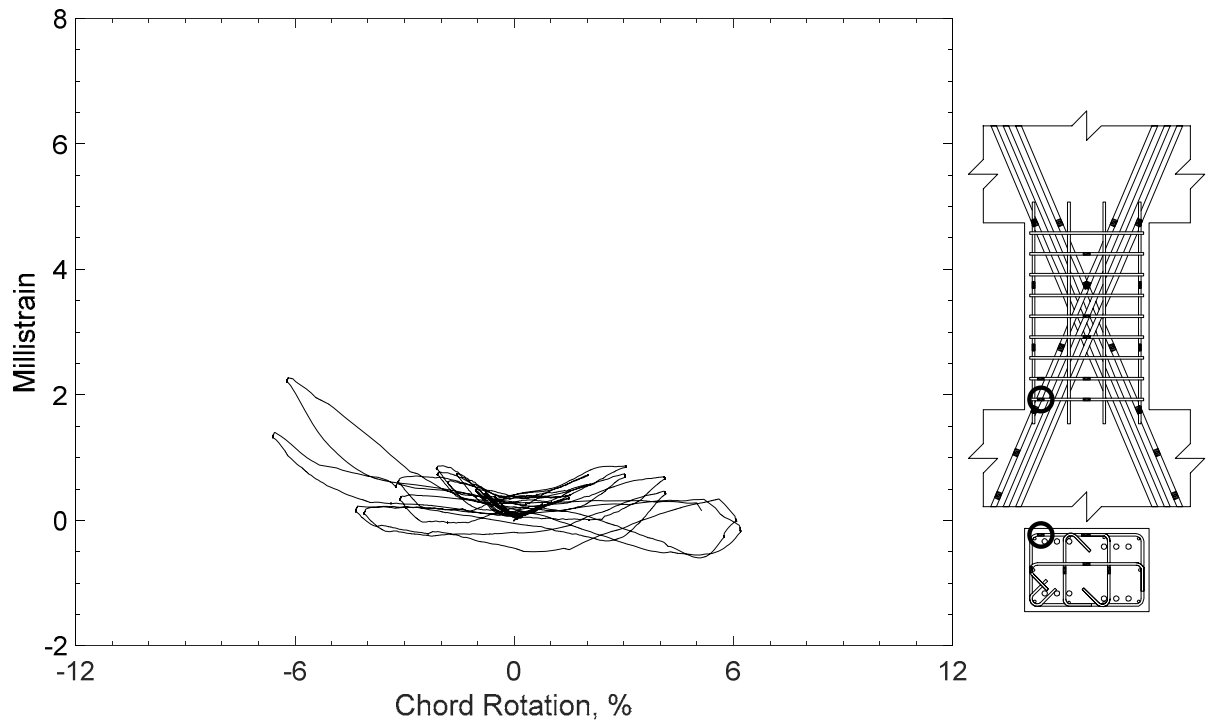


Figure 136 – Measured strain in closed stirrup of D100-1.5, strain gauge S2

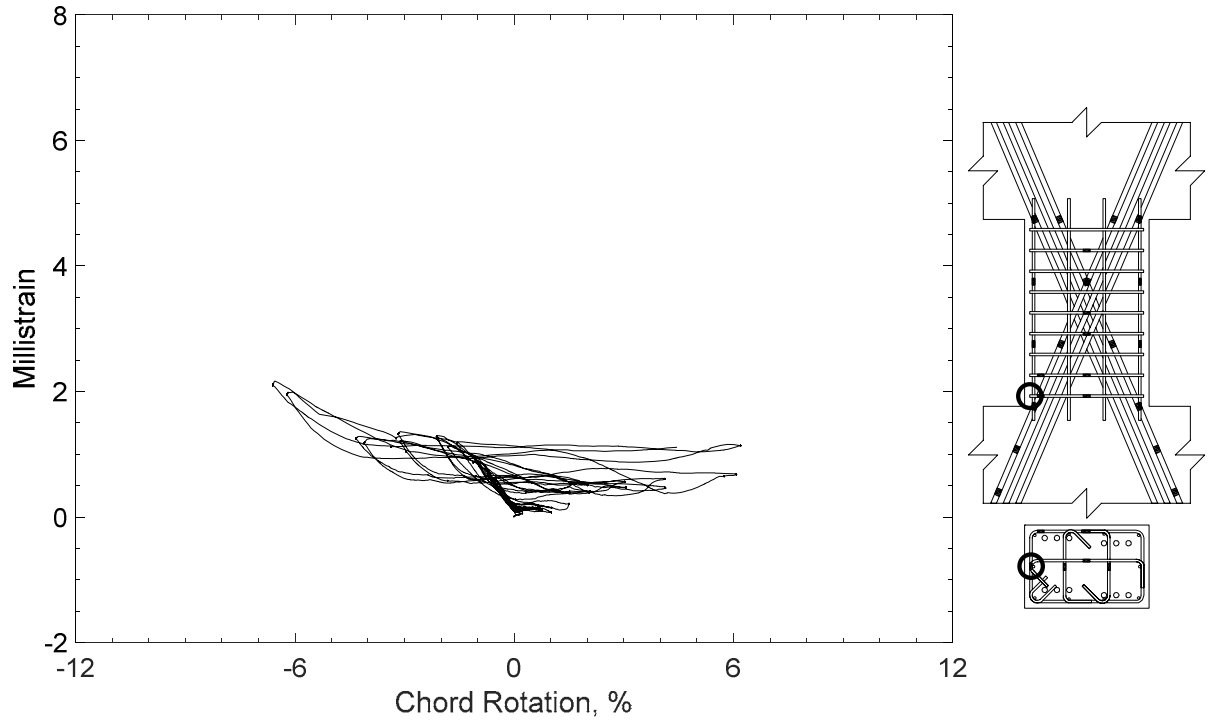


Figure 137 – Measured strain in closed stirrup of D100-1.5, strain gauge S3

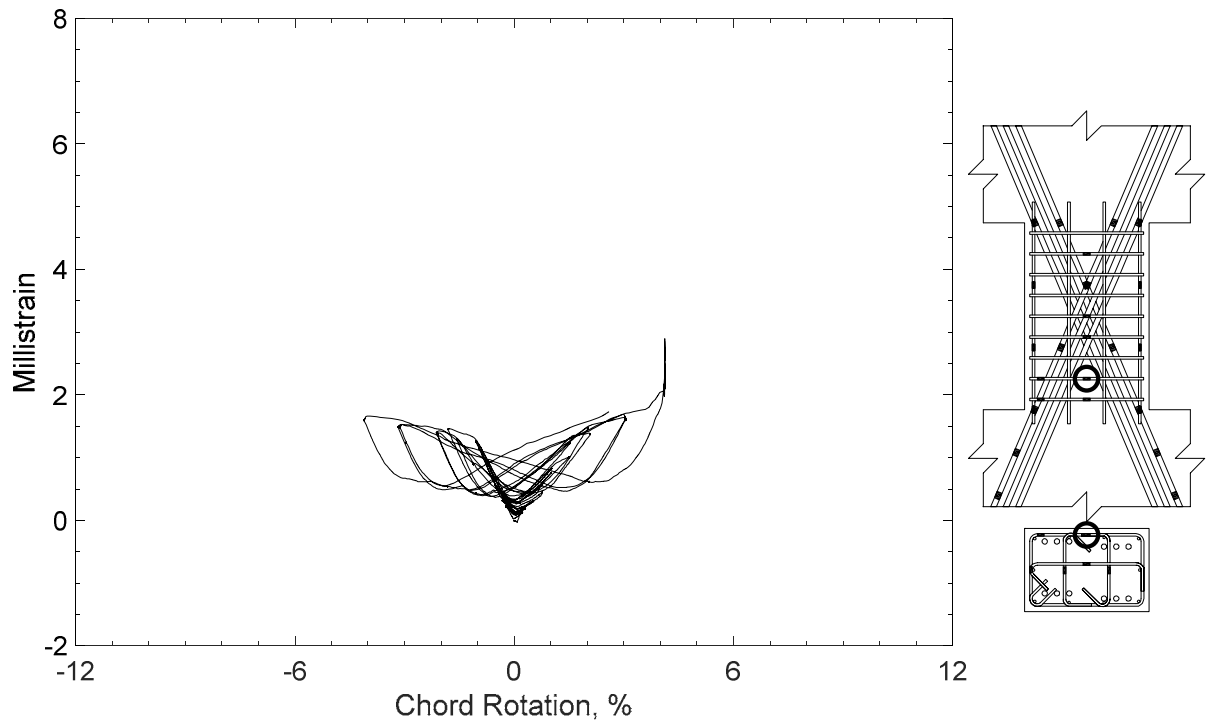


Figure 138 – Measured strain in closed stirrup of D100-1.5, strain gauge S4

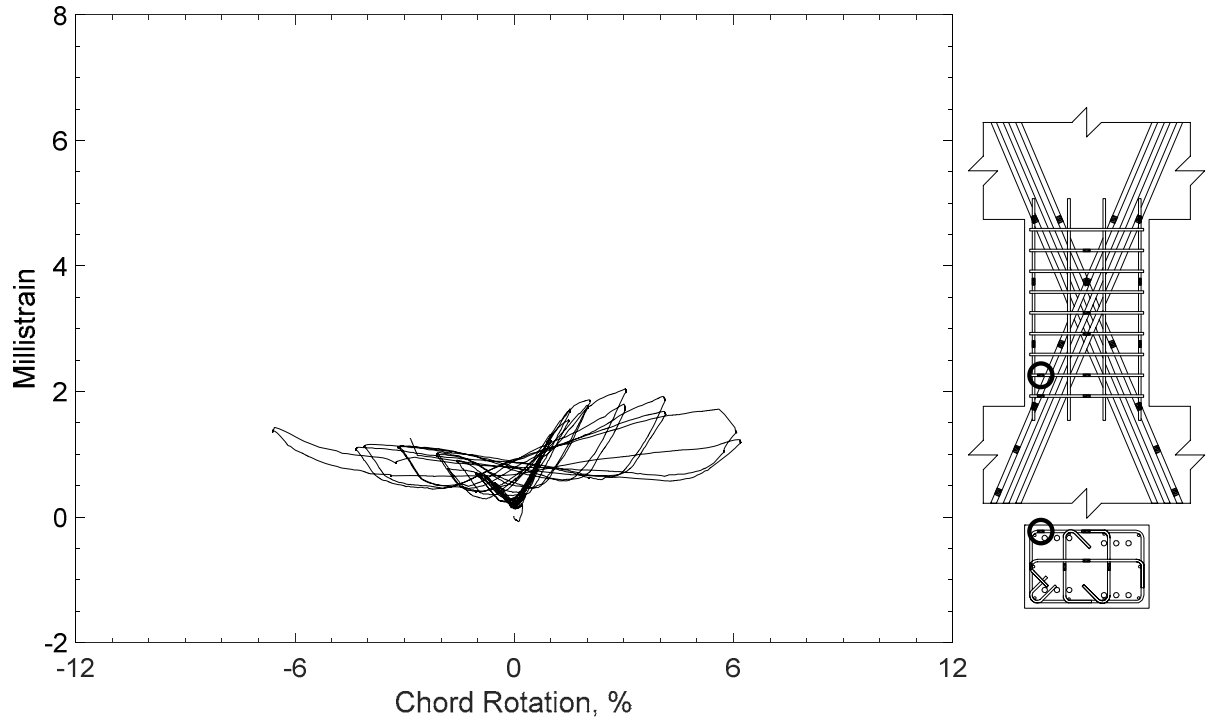


Figure 139 – Measured strain in closed stirrup of D100-1.5, strain gauge S5

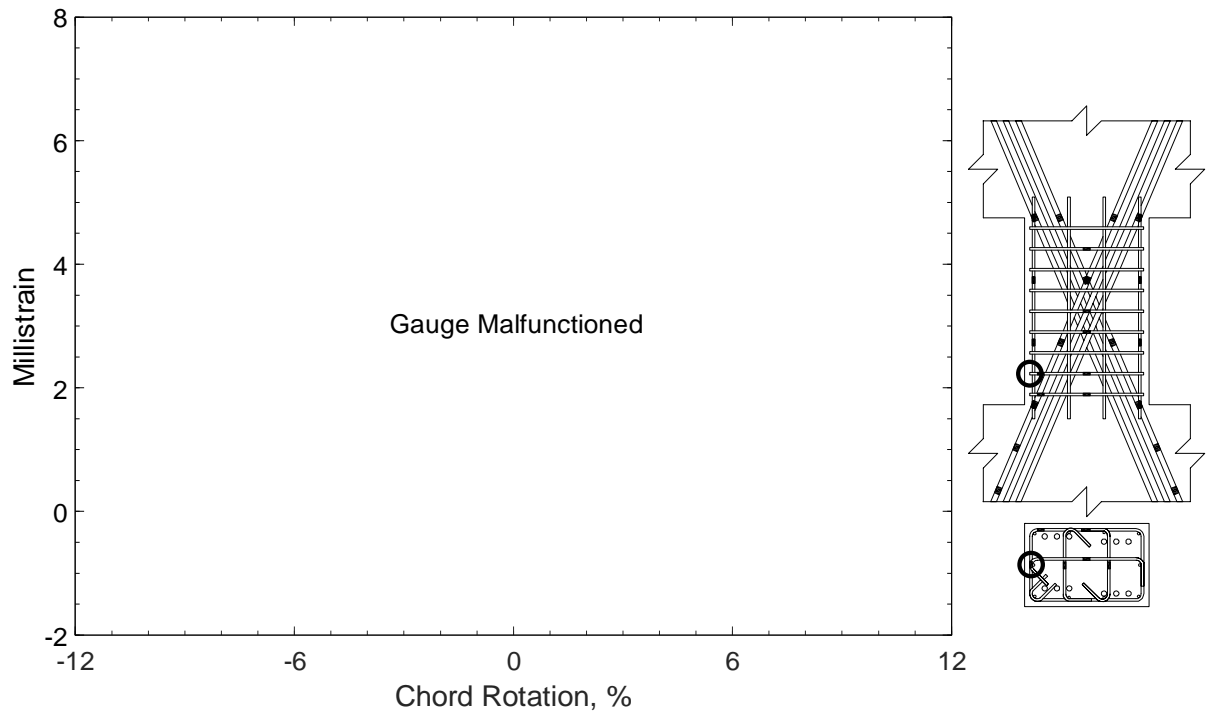


Figure 140 – Measured strain in closed stirrup of D100-1.5, strain gauge S6

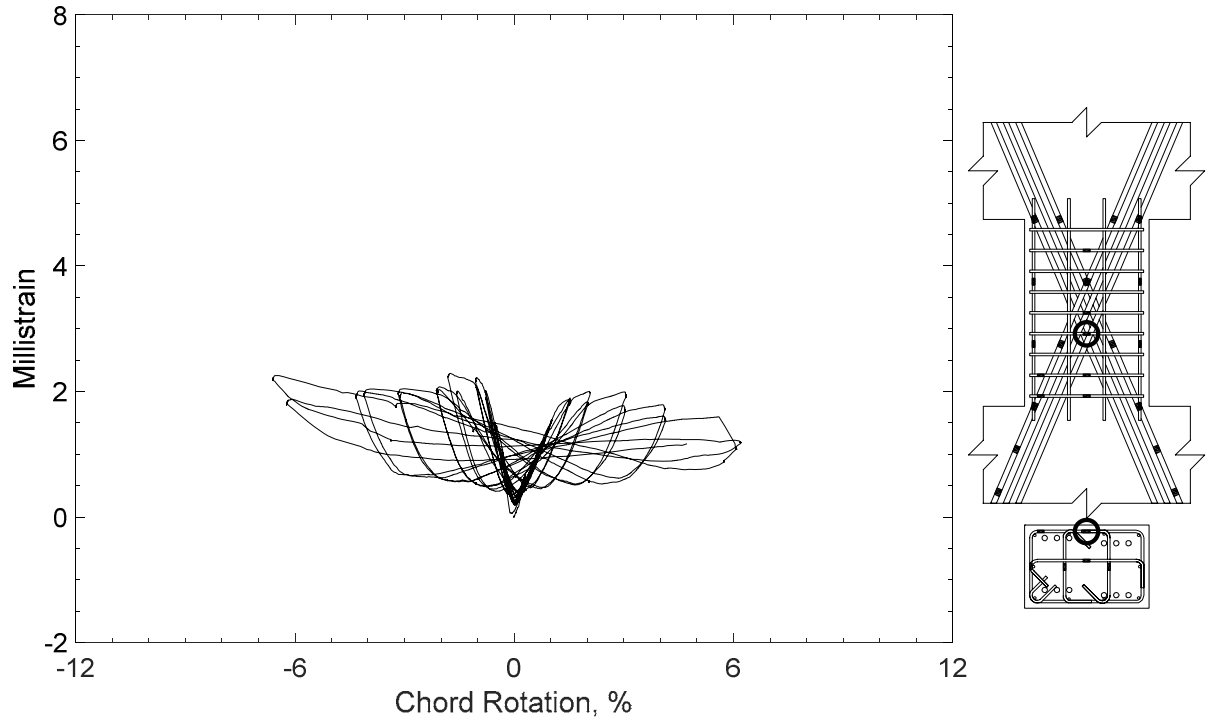


Figure 141 – Measured strain in closed stirrup of D100-1.5, strain gauge S7

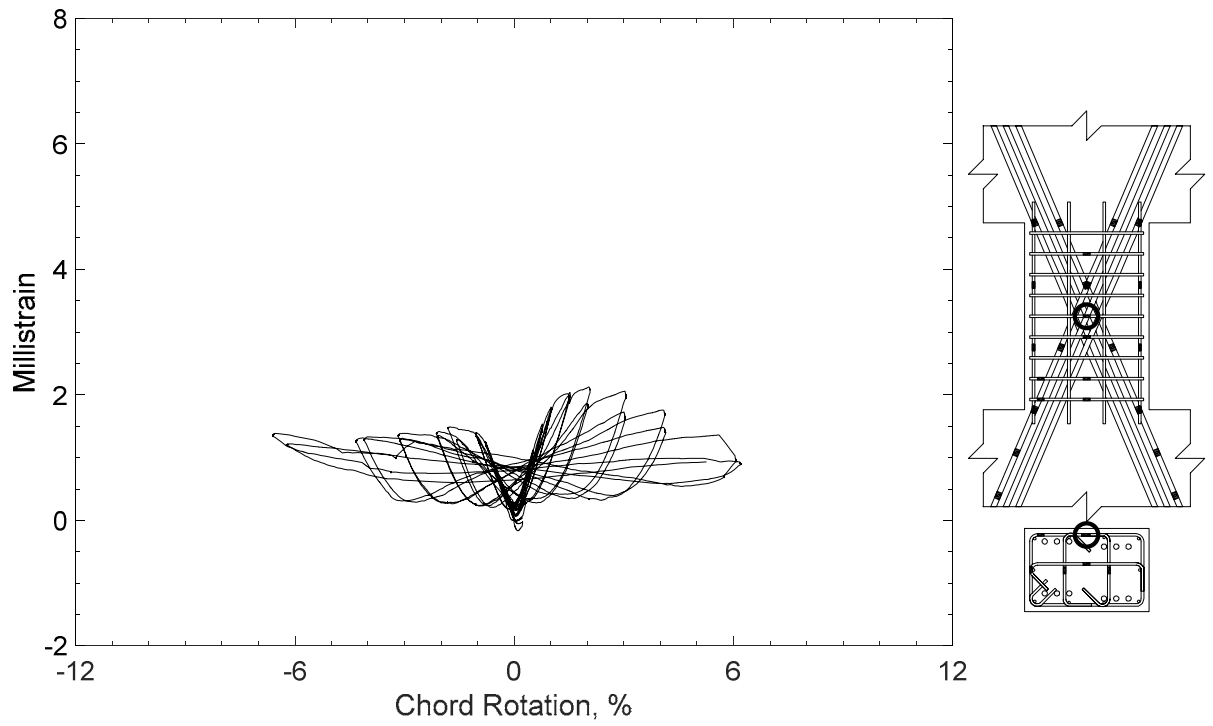


Figure 142 – Measured strain in closed stirrup of D100-1.5, strain gauge S8

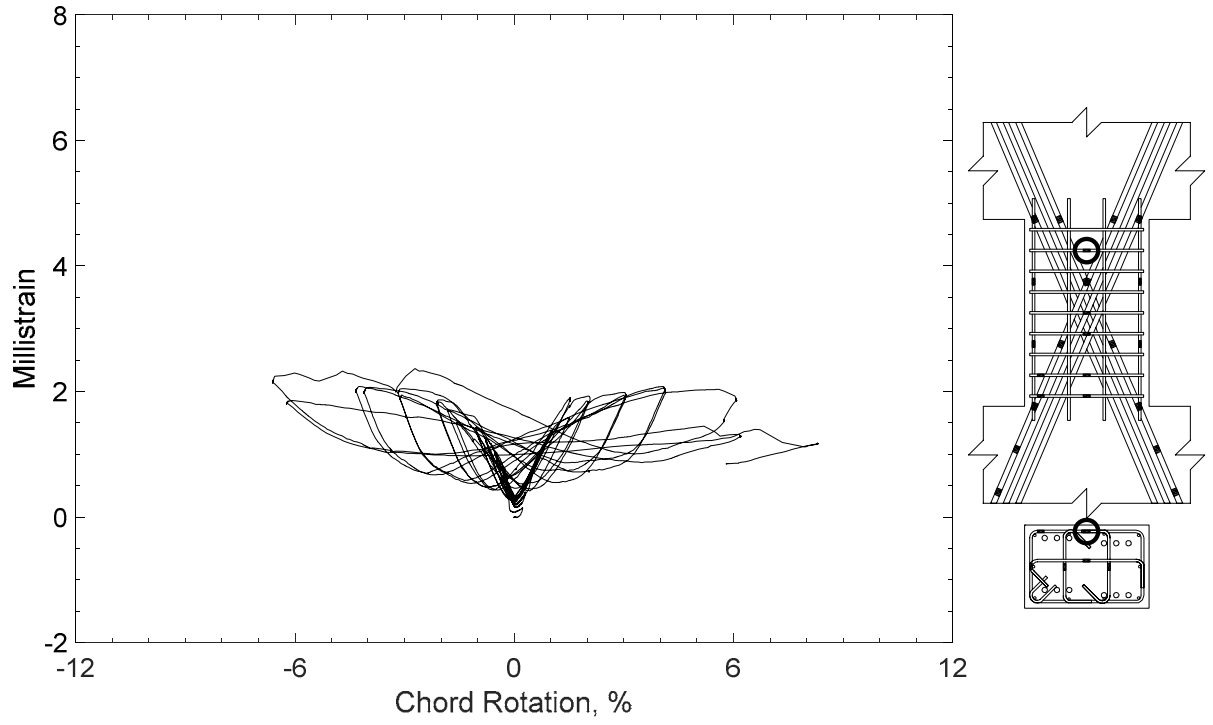


Figure 143 – Measured strain in closed stirrup of D100-1.5, strain gauge S9

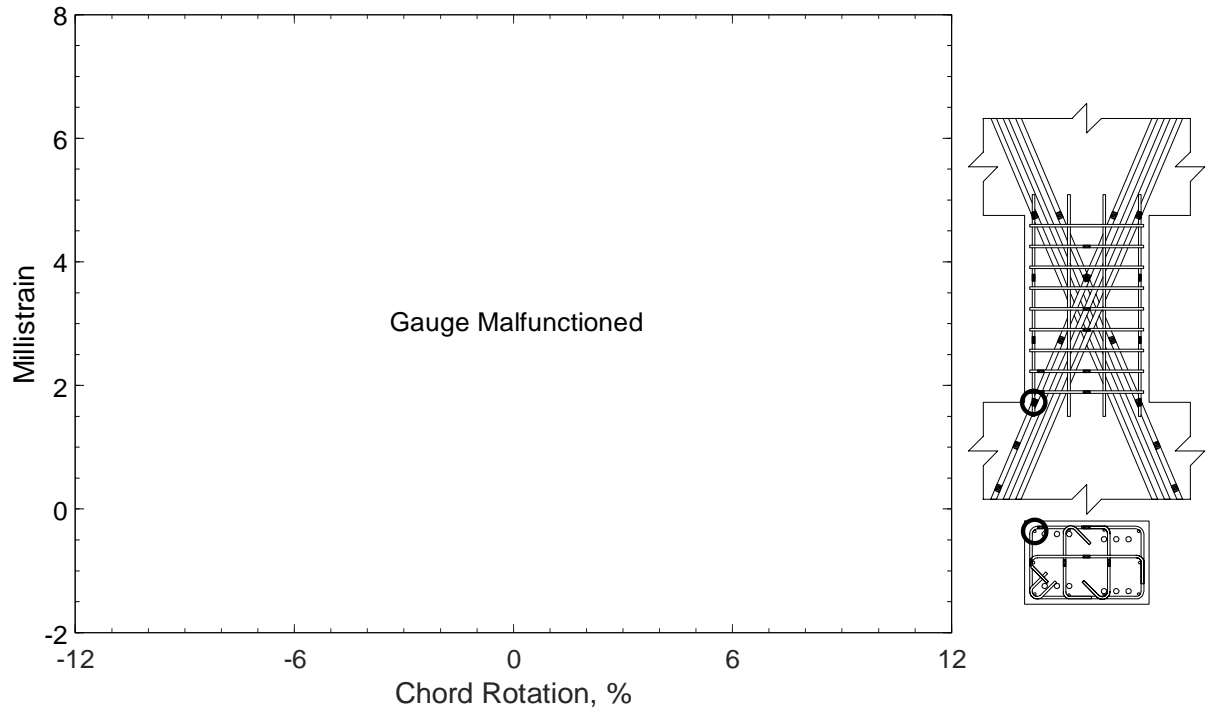


Figure 144 – Measured strain in parallel bar of D100-1.5, strain gauge H1

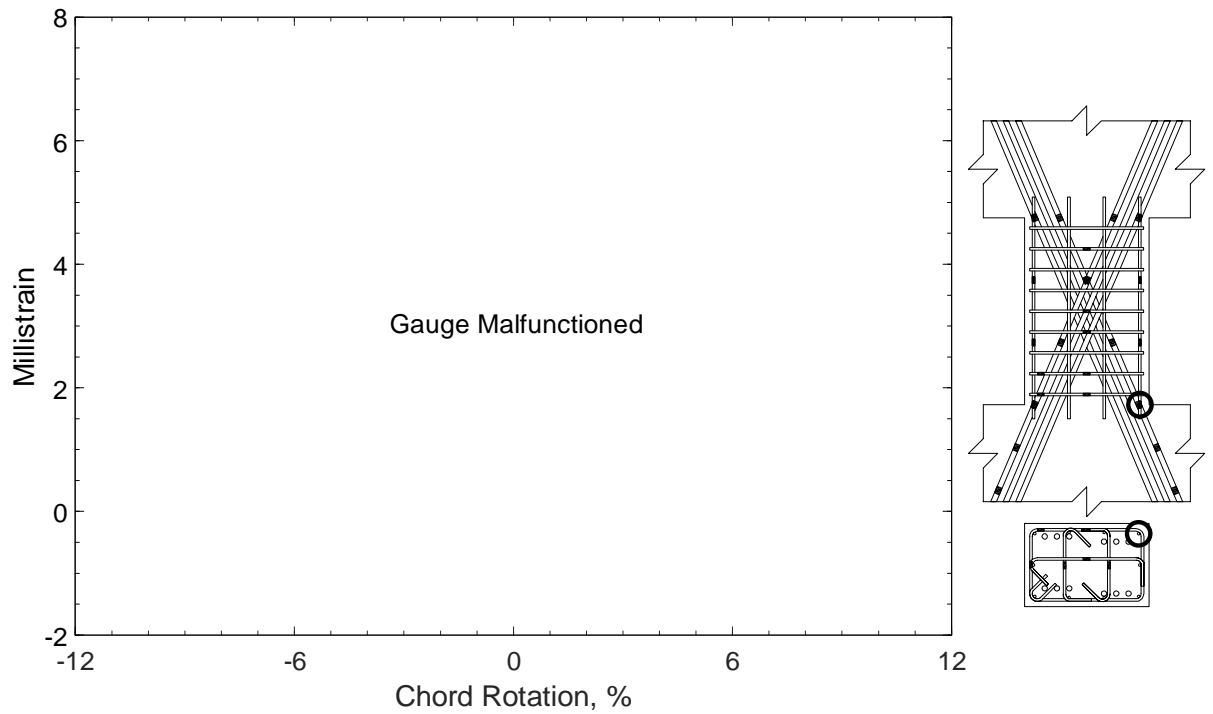


Figure 145 – Measured strain in parallel bar of D100-1.5, strain gauge H2

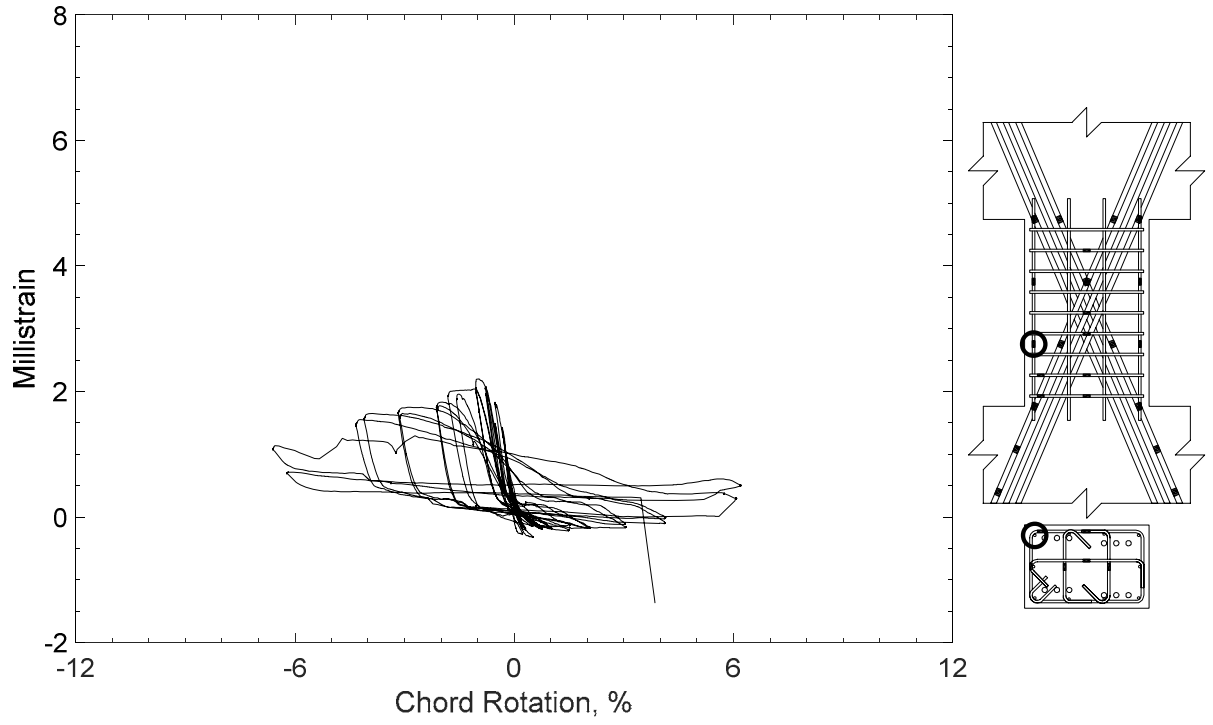


Figure 146 – Measured strain in parallel bar of D100-1.5, strain gauge H3

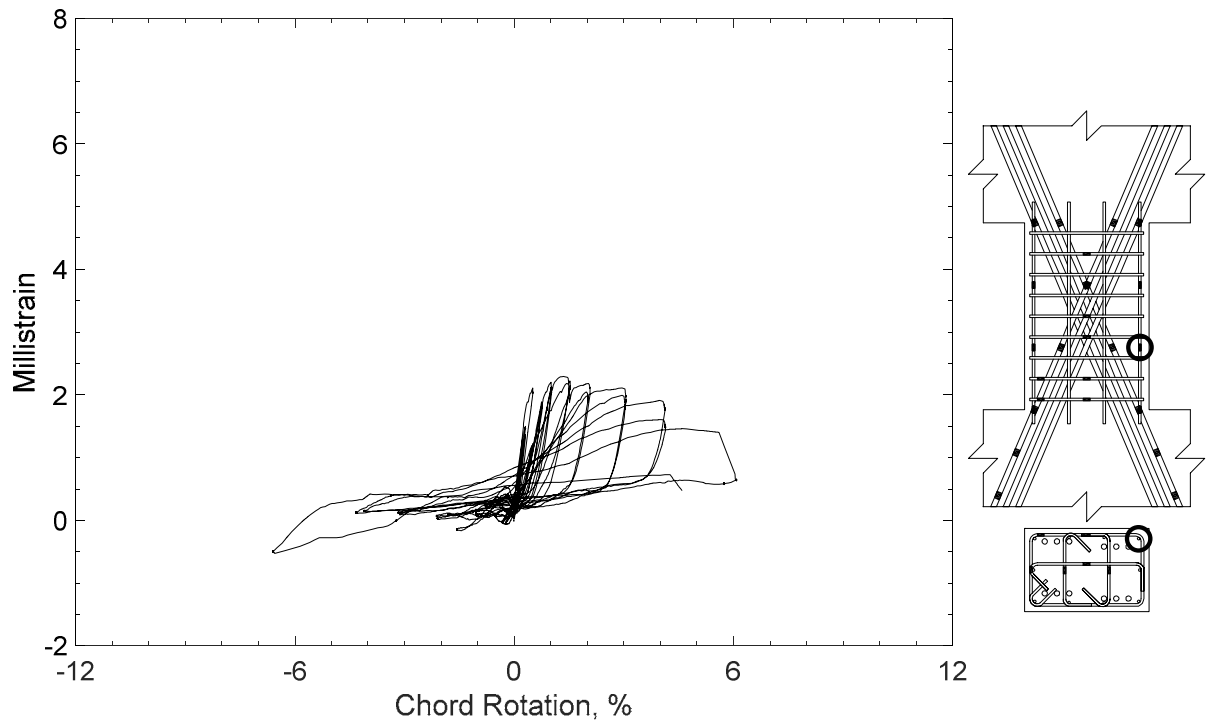


Figure 147 – Measured strain in parallel bar of D100-1.5, strain gauge H4

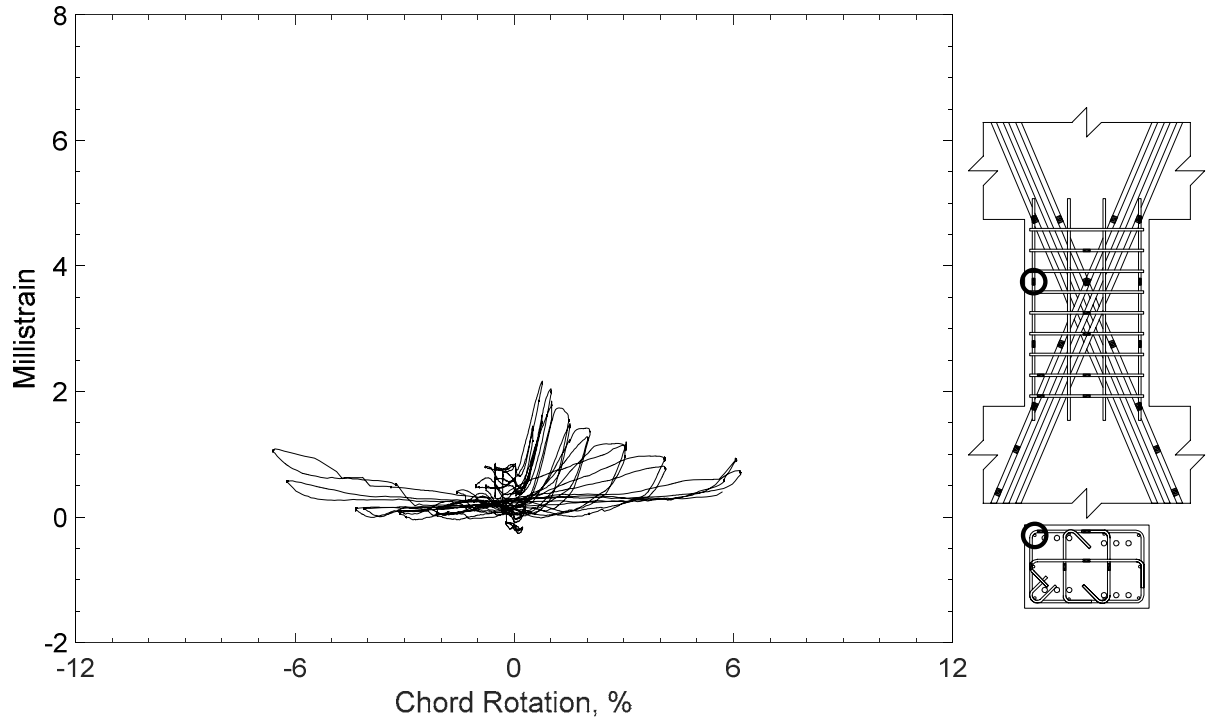


Figure 148 – Measured strain in parallel bar of D100-1.5, strain gauge H5

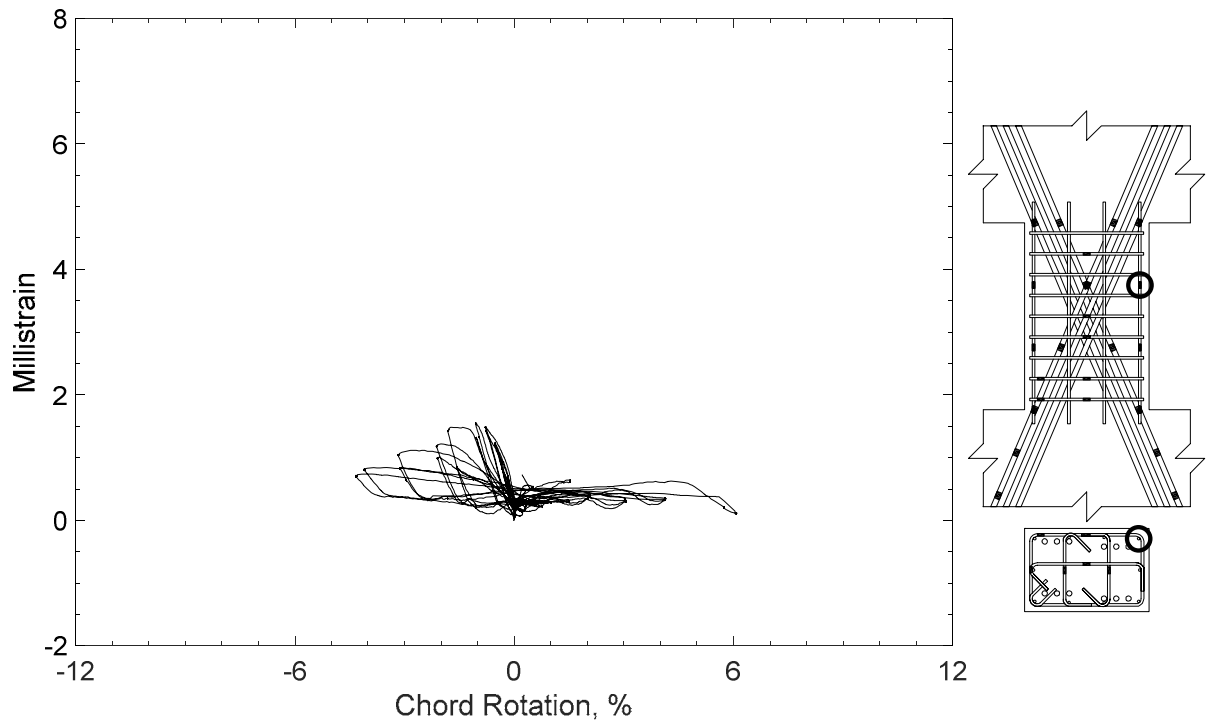


Figure 149 – Measured strain in parallel bar of D100-1.5, strain gauge H6

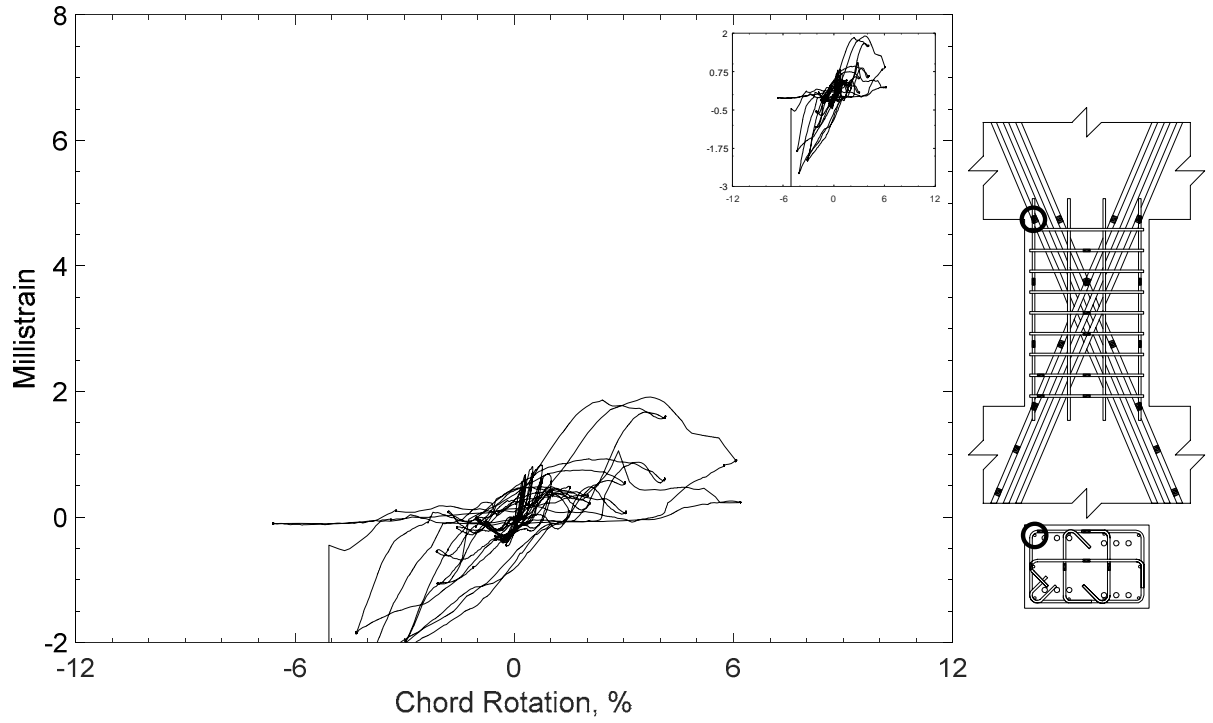


Figure 150 – Measured strain in parallel bar of D100-1.5, strain gauge H7

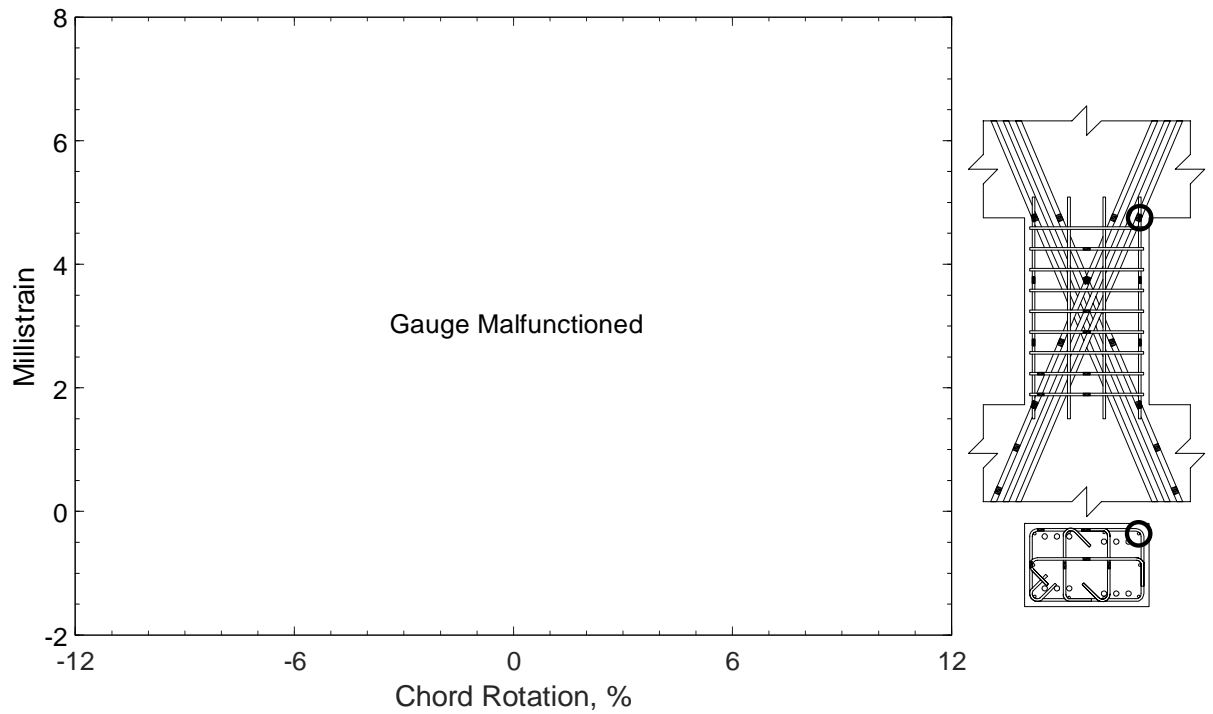


Figure 151 – Measured strain in parallel bar of D100-1.5, strain gauge H8

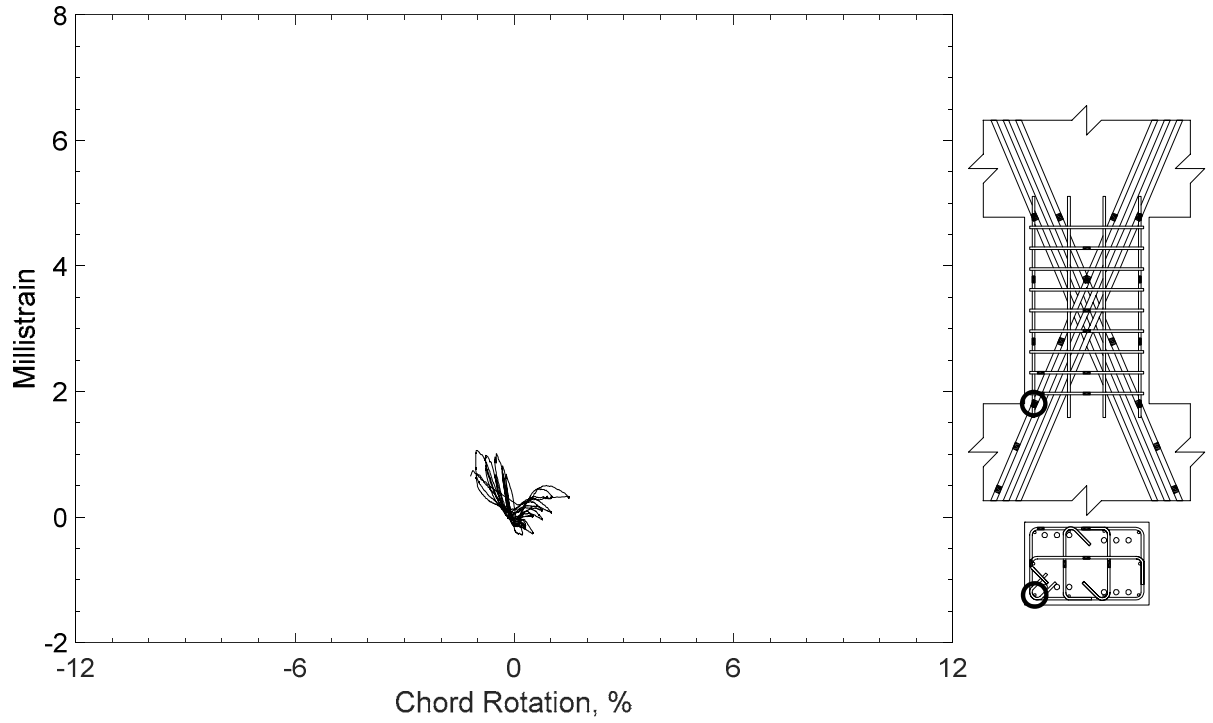


Figure 152 – Measured strain in parallel bar of D100-1.5, strain gauge H9

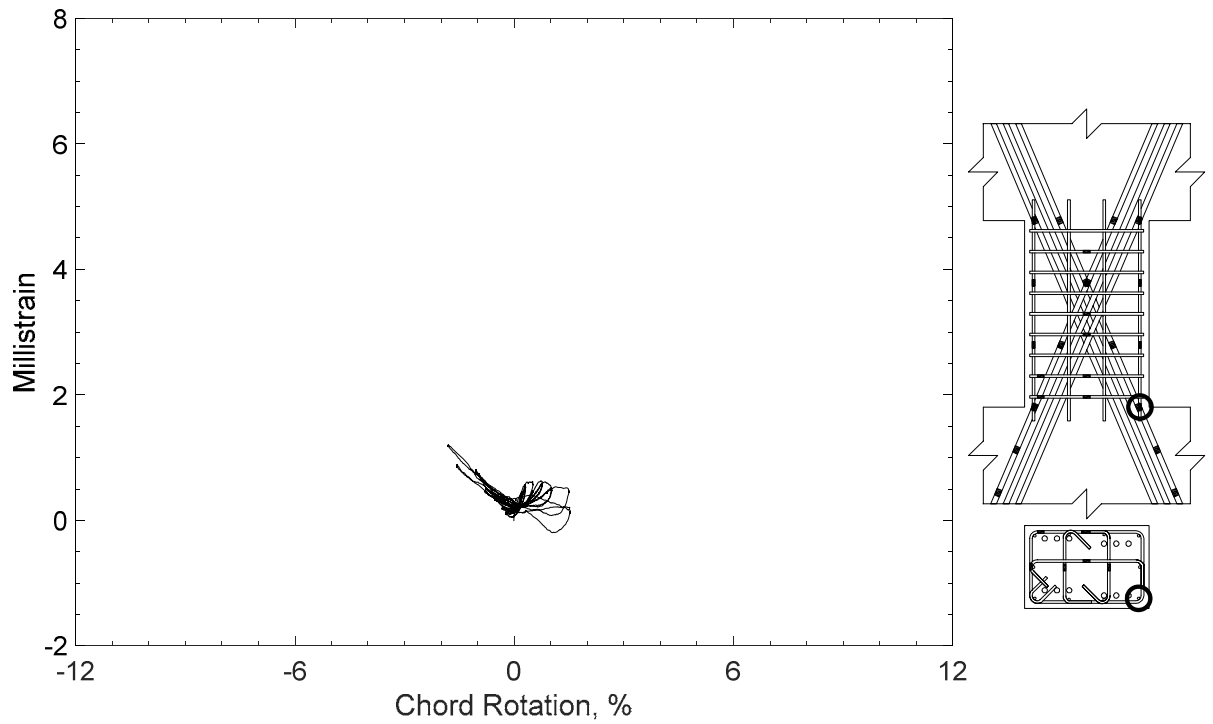


Figure 153 – Measured strain in parallel bar of D100-1.5, strain gauge H10

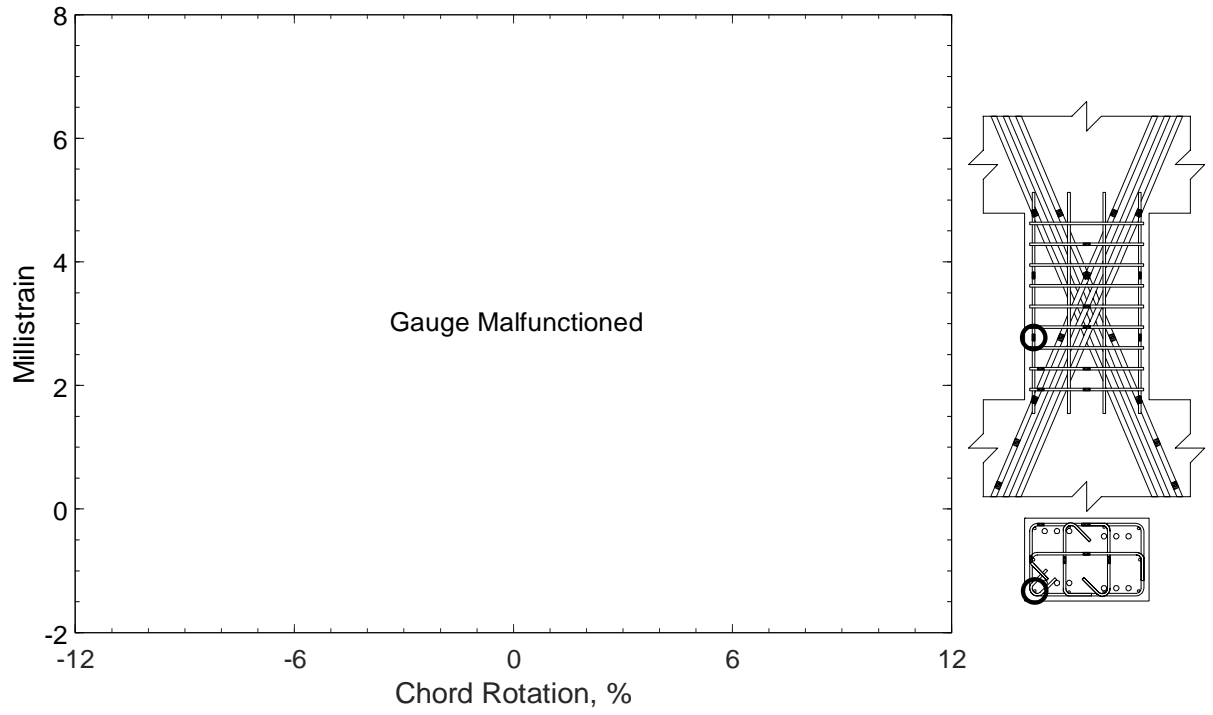


Figure 154 – Measured strain in parallel bar of D100-1.5, strain gauge H11

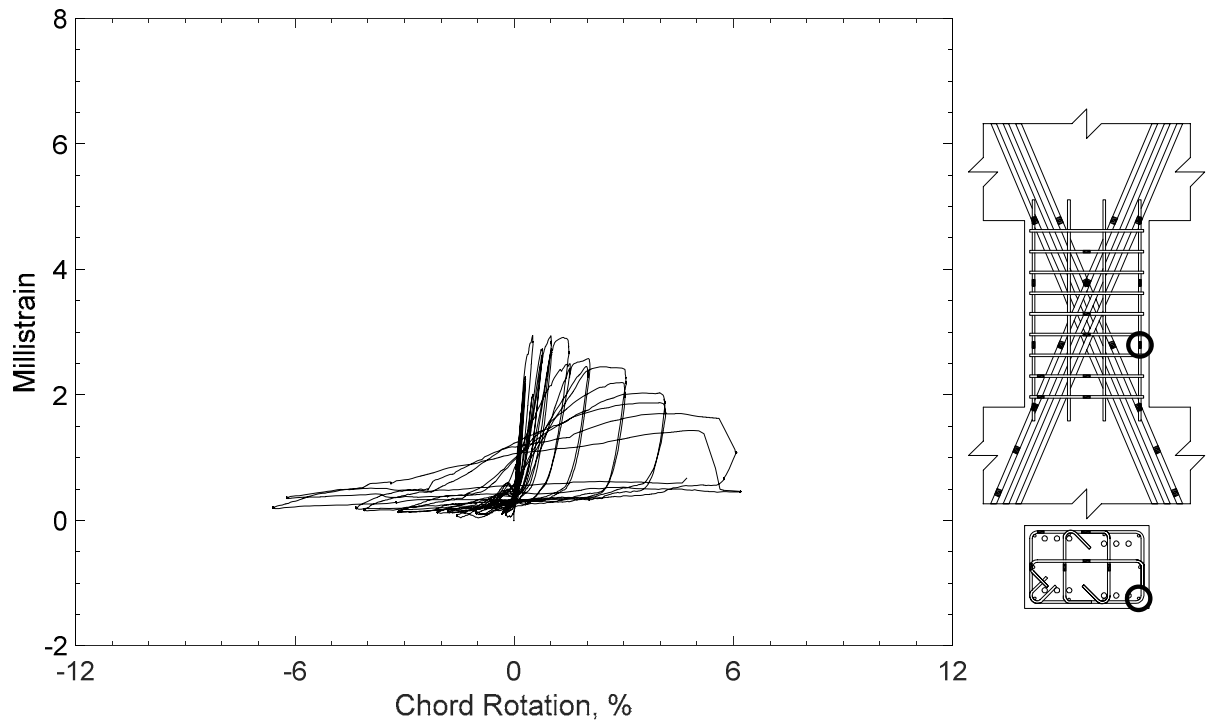


Figure 155 – Measured strain in parallel bar of D100-1.5, strain gauge H12

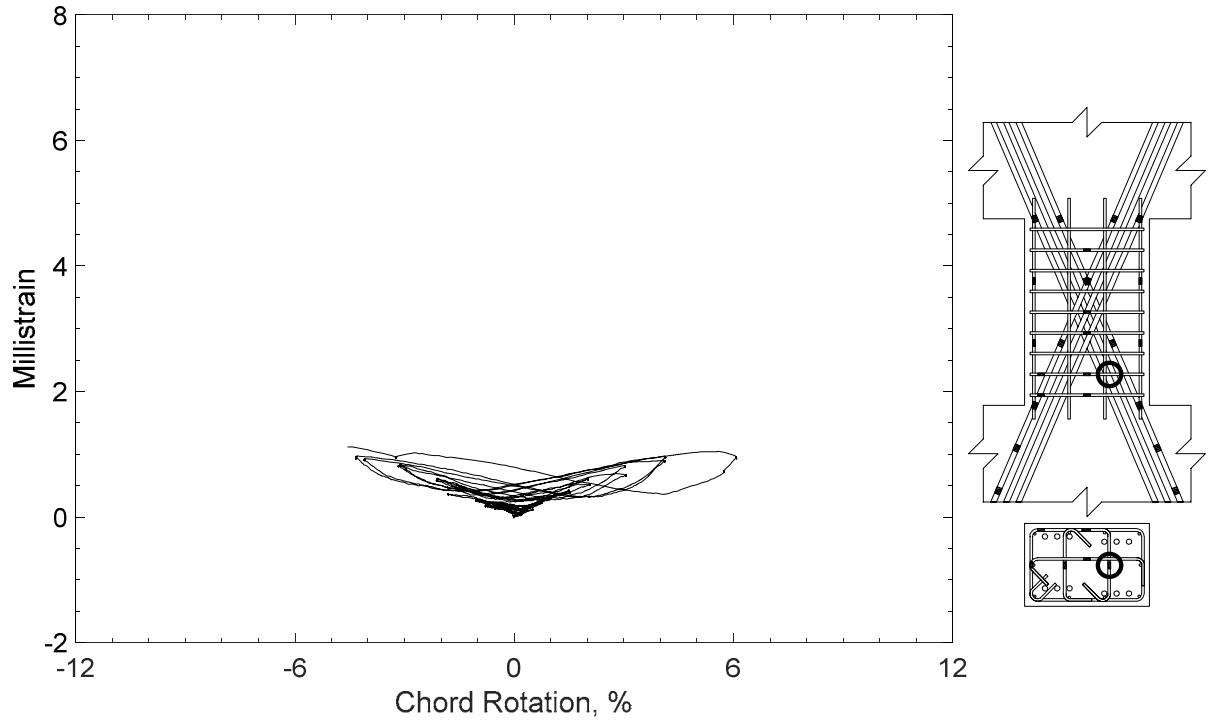


Figure 156 – Measured strain in cross-tie of D100-1.5, strain gauge T1

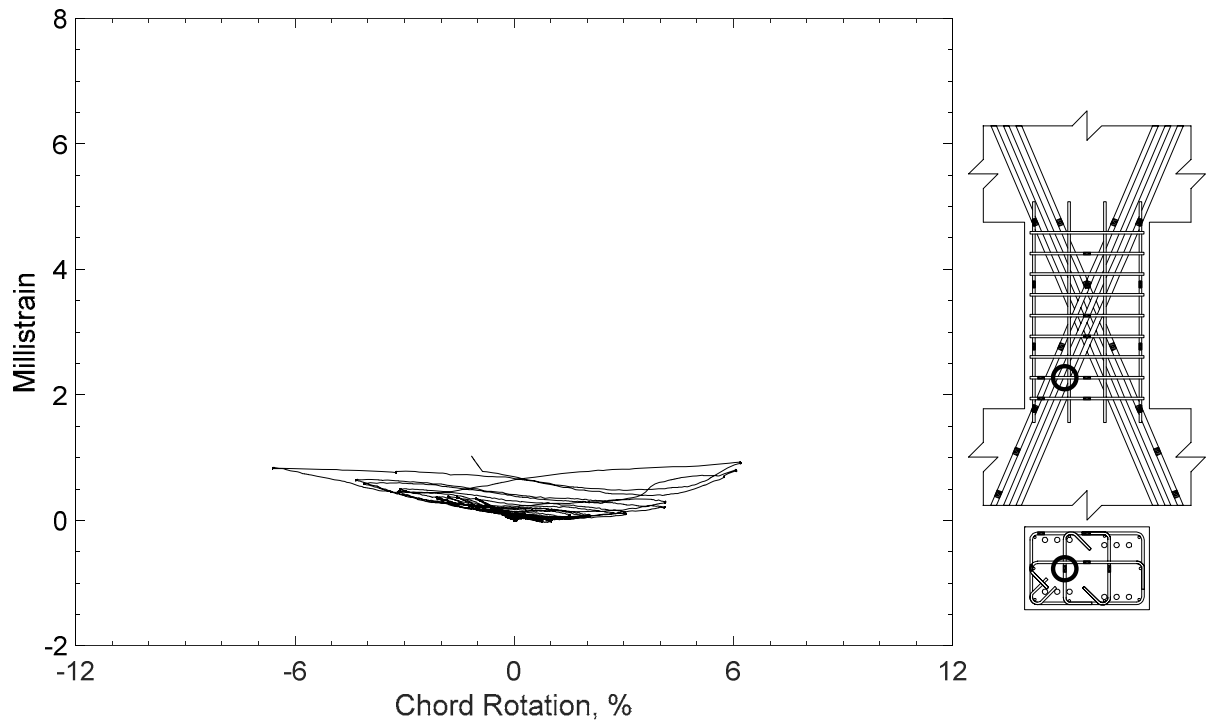


Figure 157 – Measured strain in cross-tie of D100-1.5, strain gauge T2

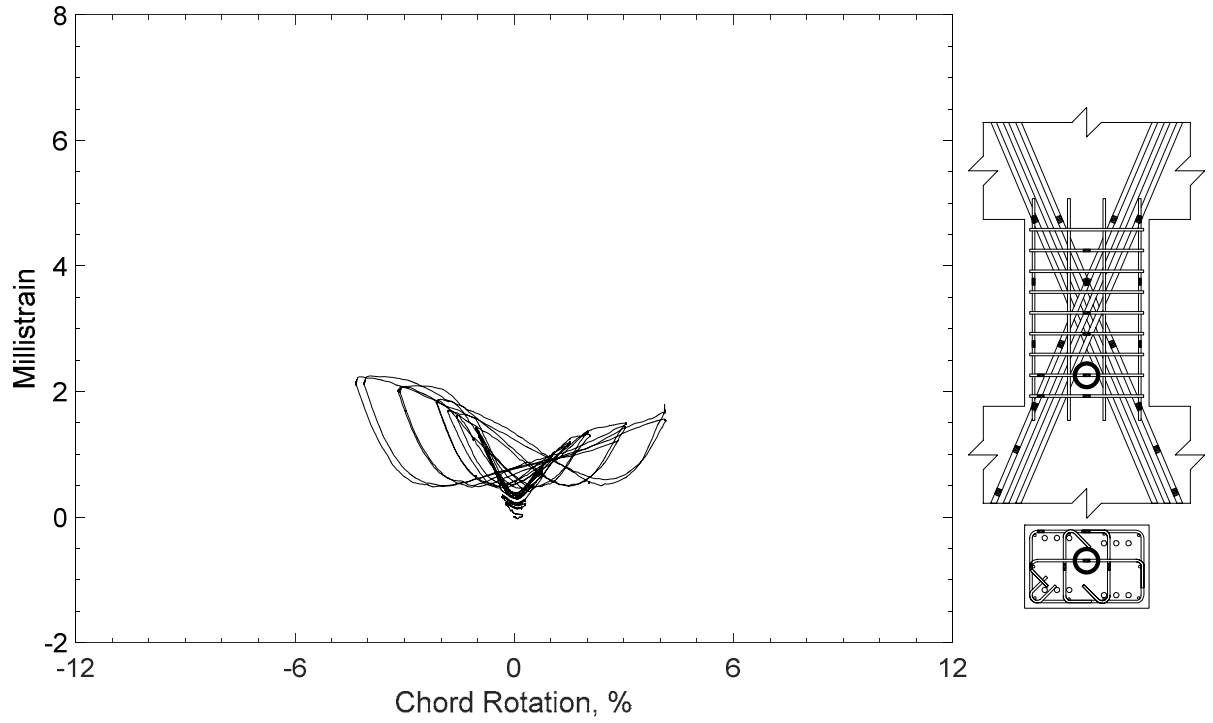


Figure 158 – Measured strain in crosstie of D100-1.5, strain gauge T3

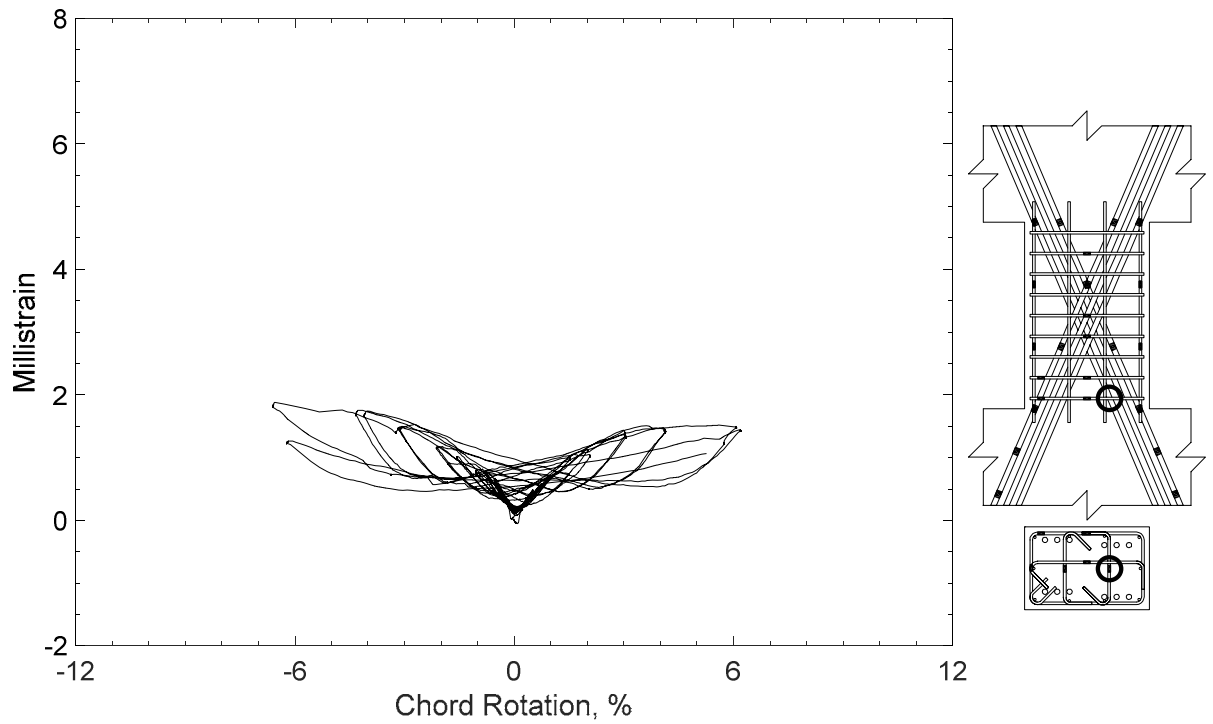


Figure 159 – Measured strain in crosstie of D100-1.5, strain gauge T4

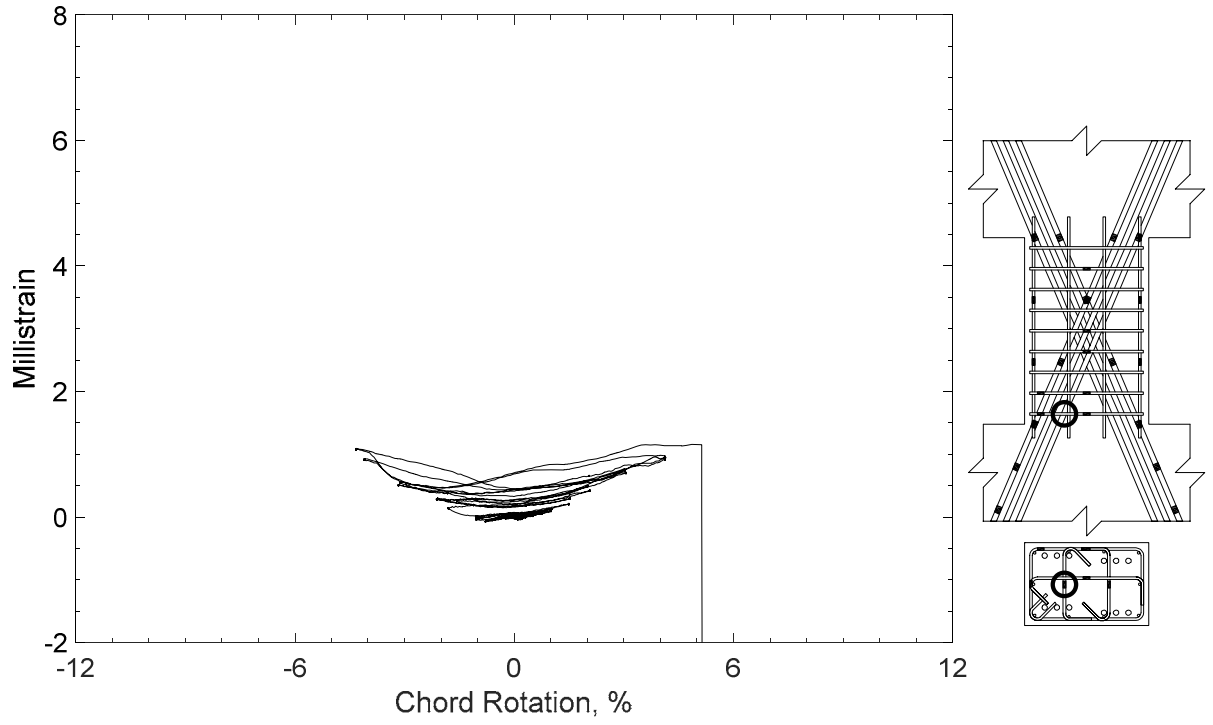


Figure 160 – Measured strain in crosstie of D100-1.5, strain gauge T5

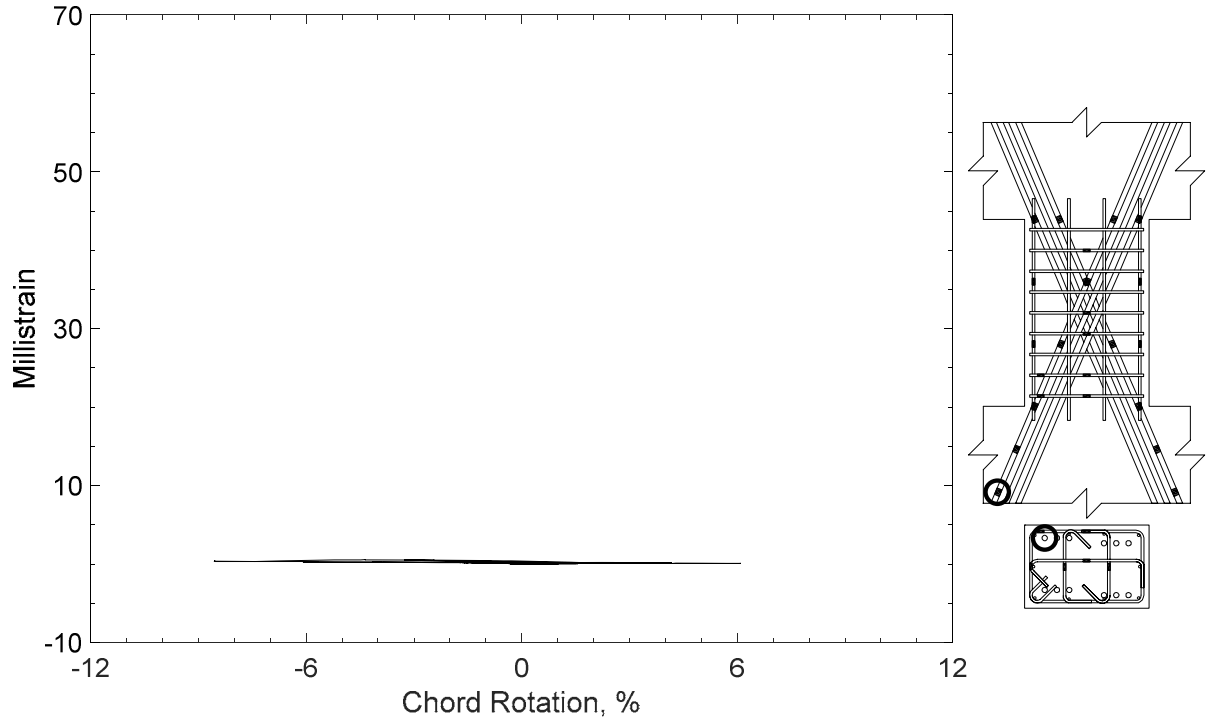


Figure 161 – Measured strain in diagonal bar of D120-1.5, strain gauge D1

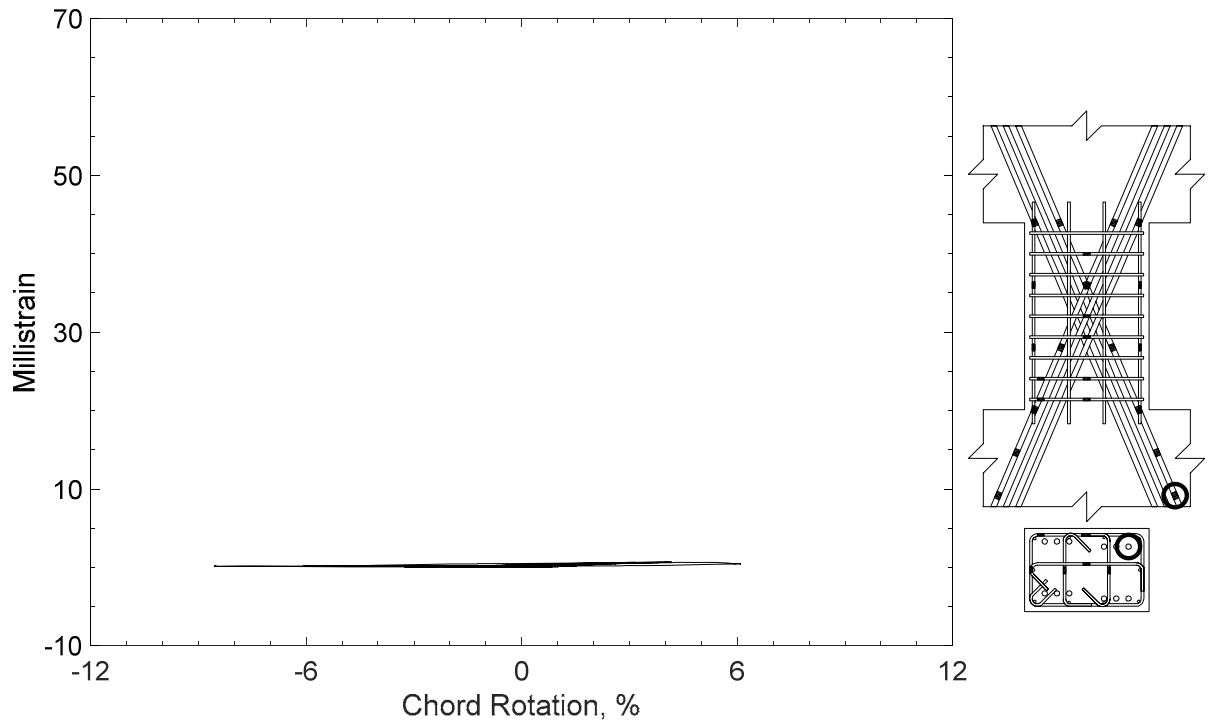


Figure 162 – Measured strain in diagonal bar of D120-1.5, strain gauge D2

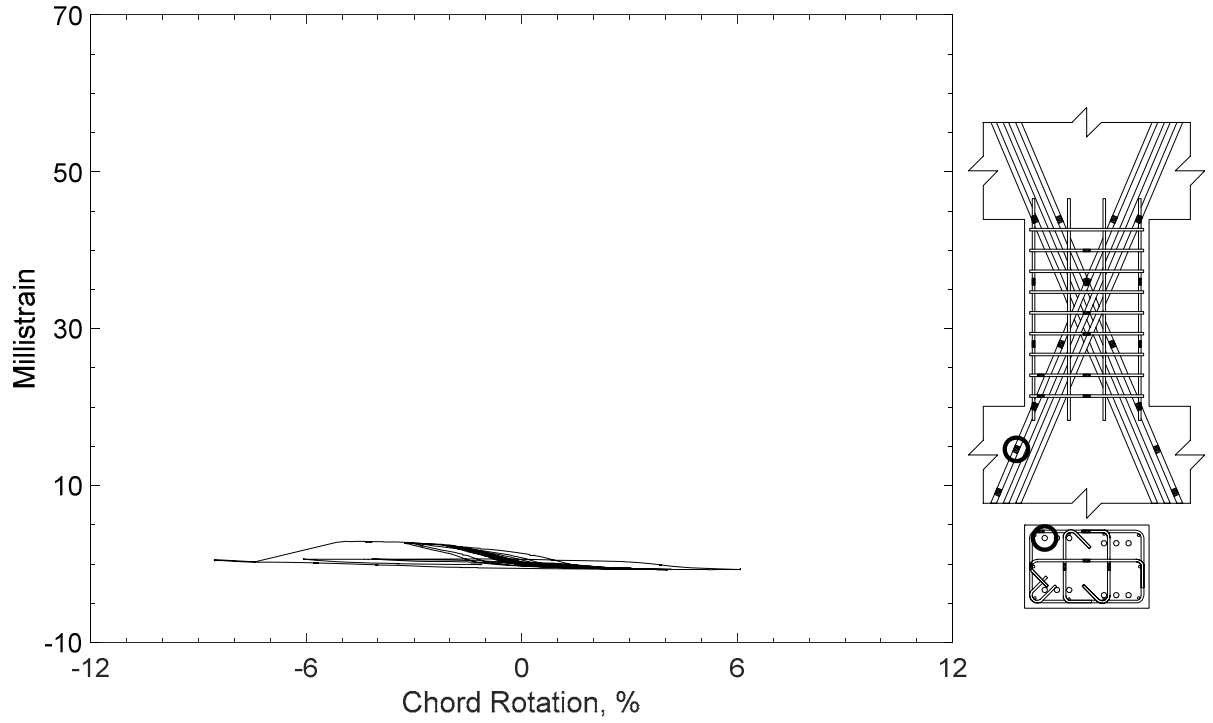


Figure 163 – Measured strain in diagonal bar of D120-1.5, strain gauge D3

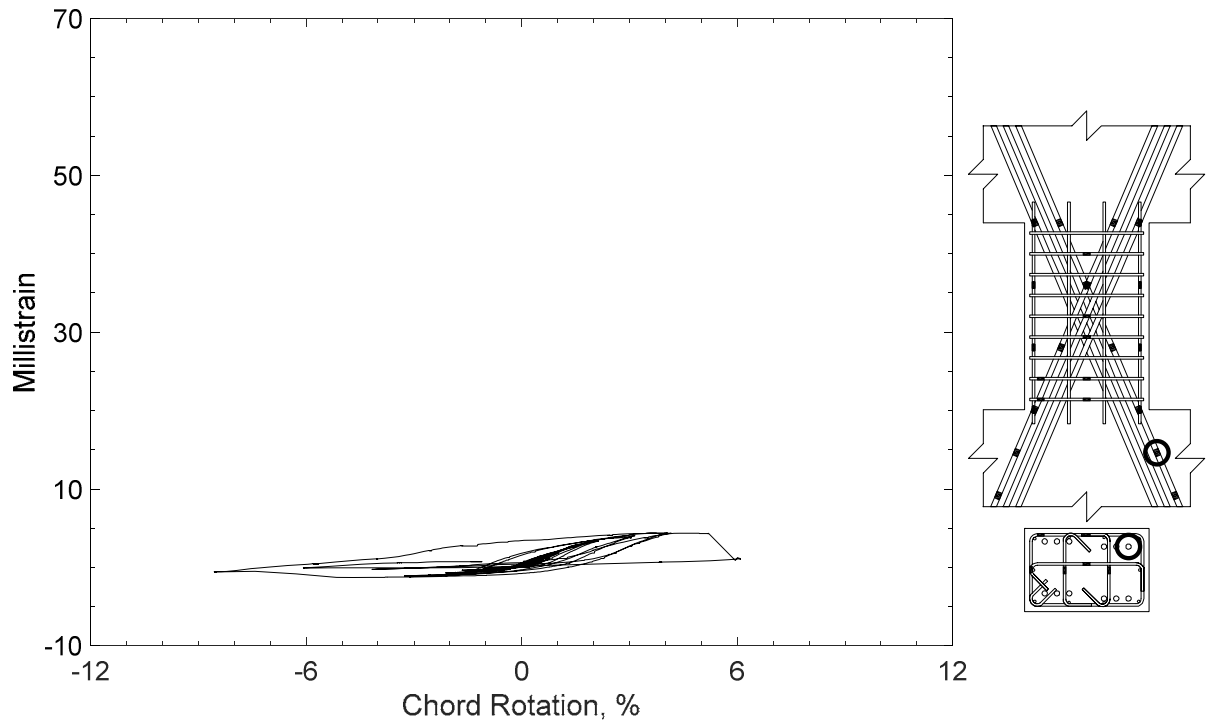


Figure 164 – Measured strain in diagonal bar of D120-1.5, strain gauge D4

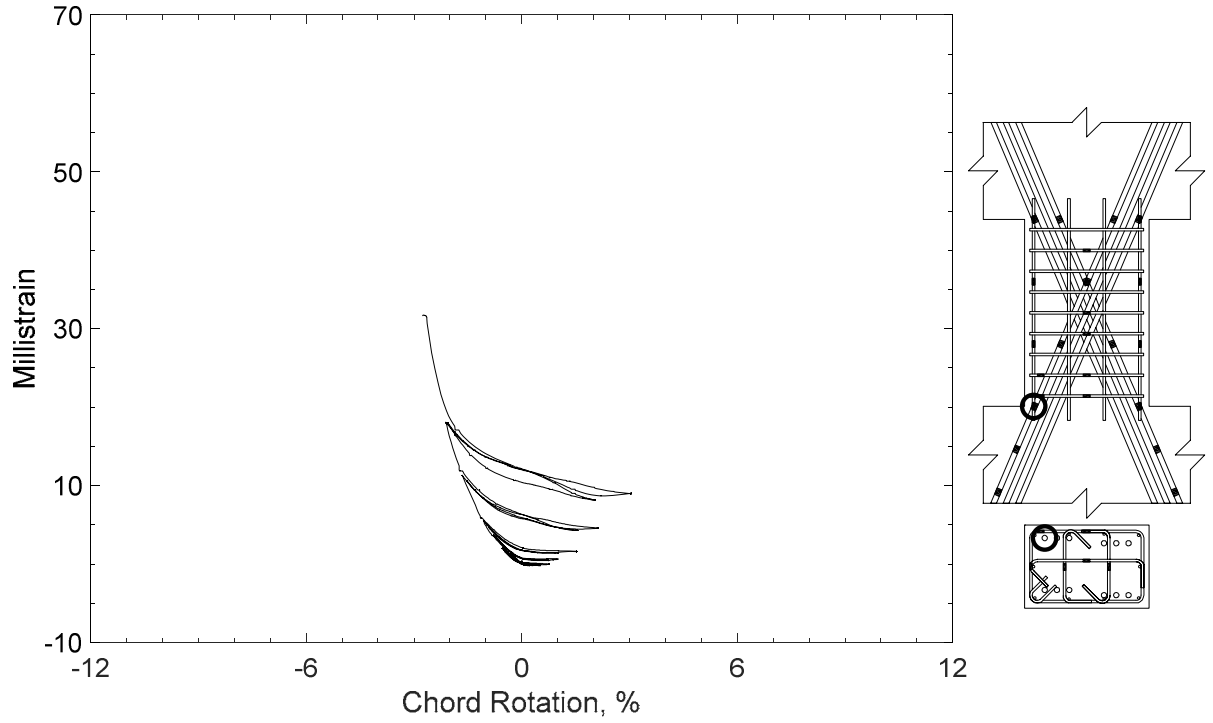


Figure 165 – Measured strain in diagonal bar of D120-1.5, strain gauge D5

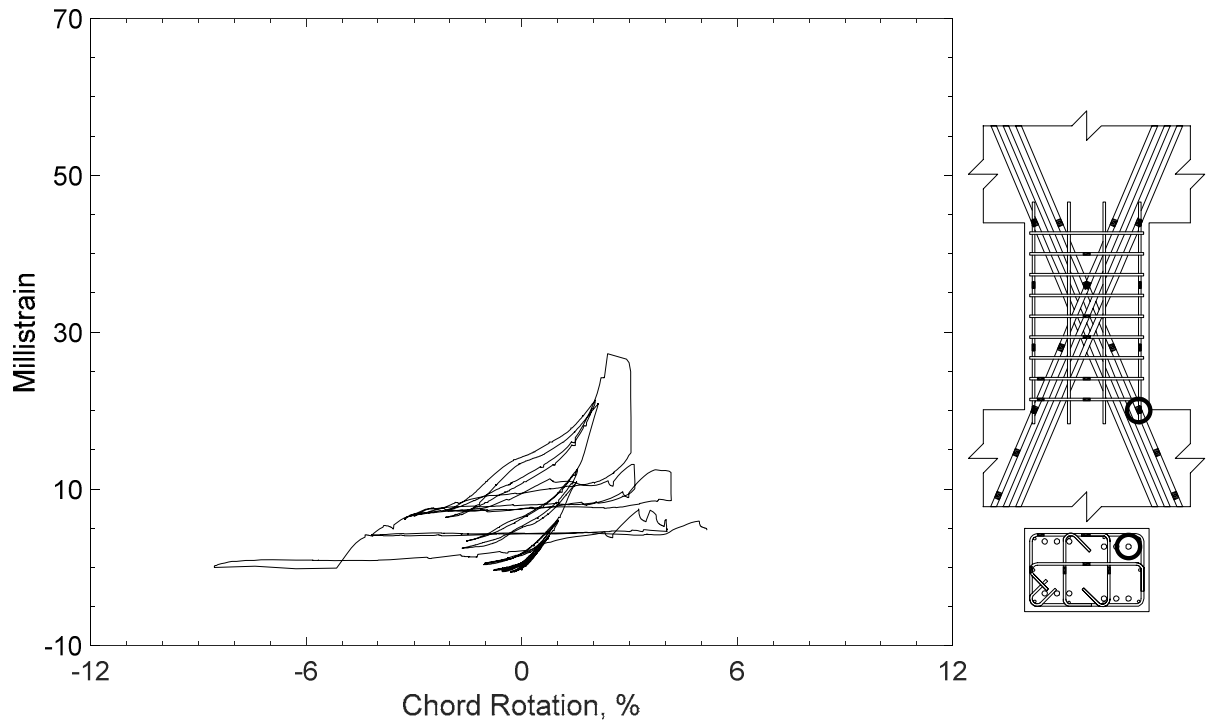


Figure 166 – Measured strain in diagonal bar of D120-1.5, strain gauge D6

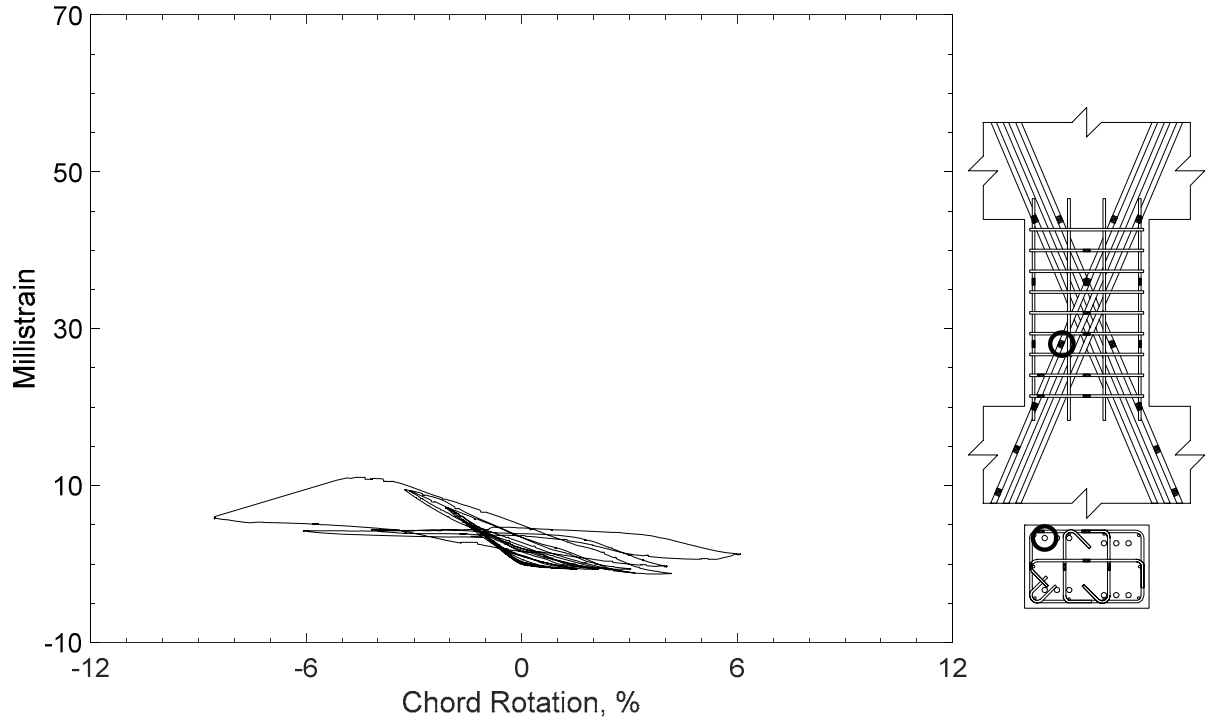


Figure 167 – Measured strain in diagonal bar of D120-1.5, strain gauge D7

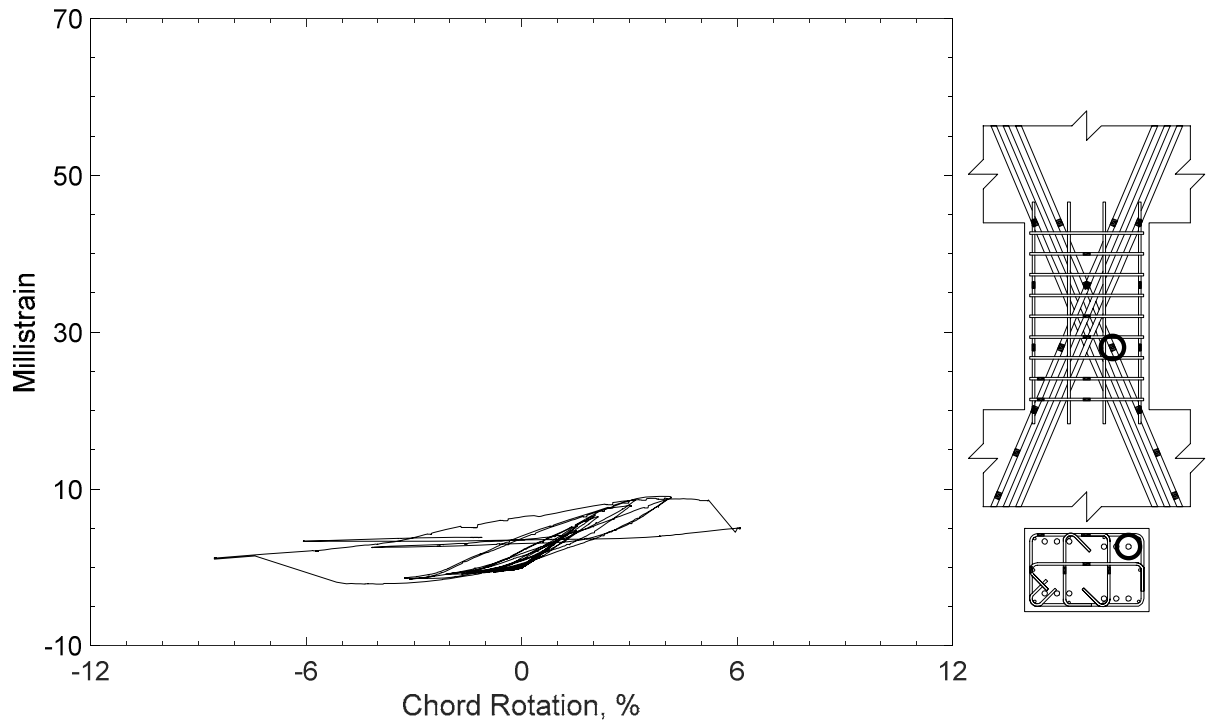


Figure 168 – Measured strain in diagonal bar of D120-1.5, strain gauge D8

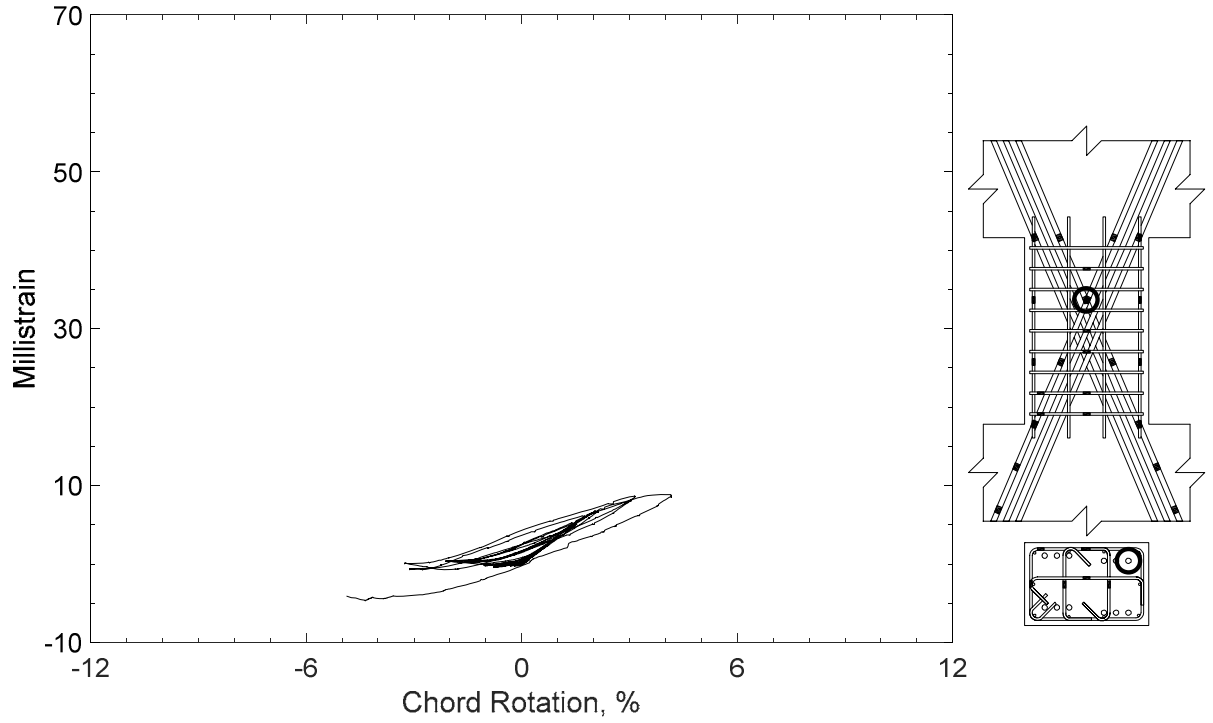


Figure 169 – Measured strain in diagonal bar of D120-1.5, strain gauge D9

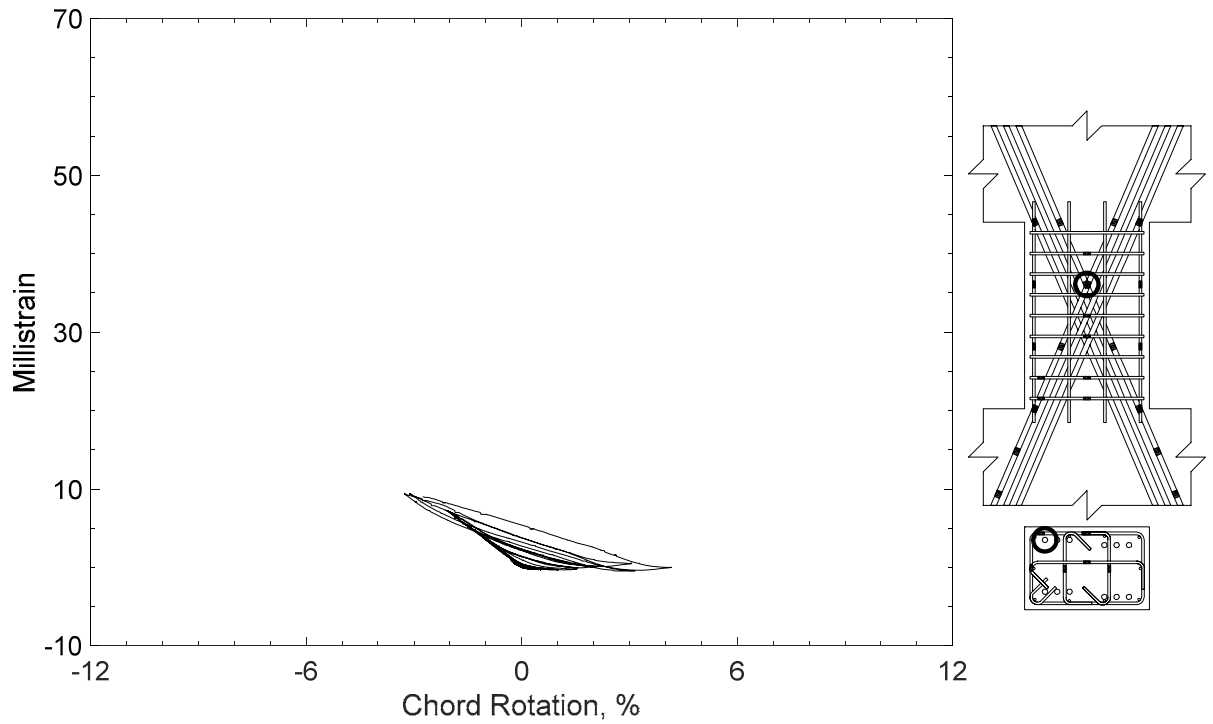


Figure 170 – Measured strain in diagonal bar of D120-1.5, strain gauge D10

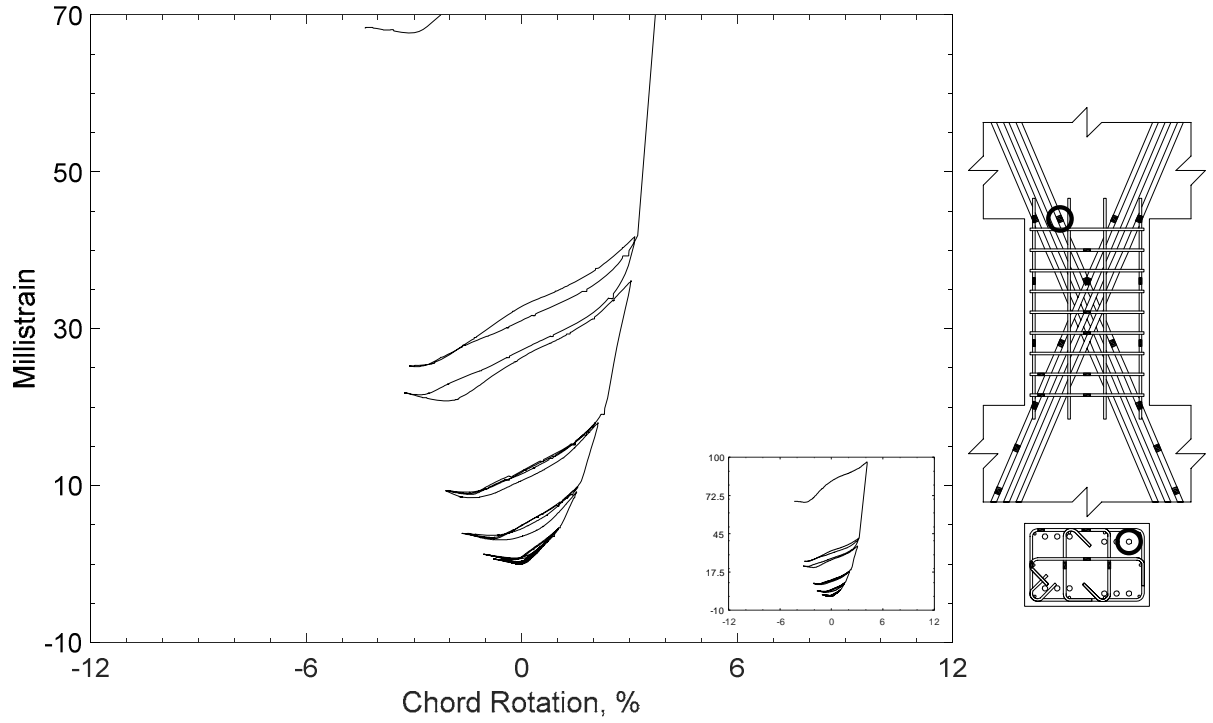


Figure 171 – Measured strain in diagonal bar of D120-1.5, strain gauge D11

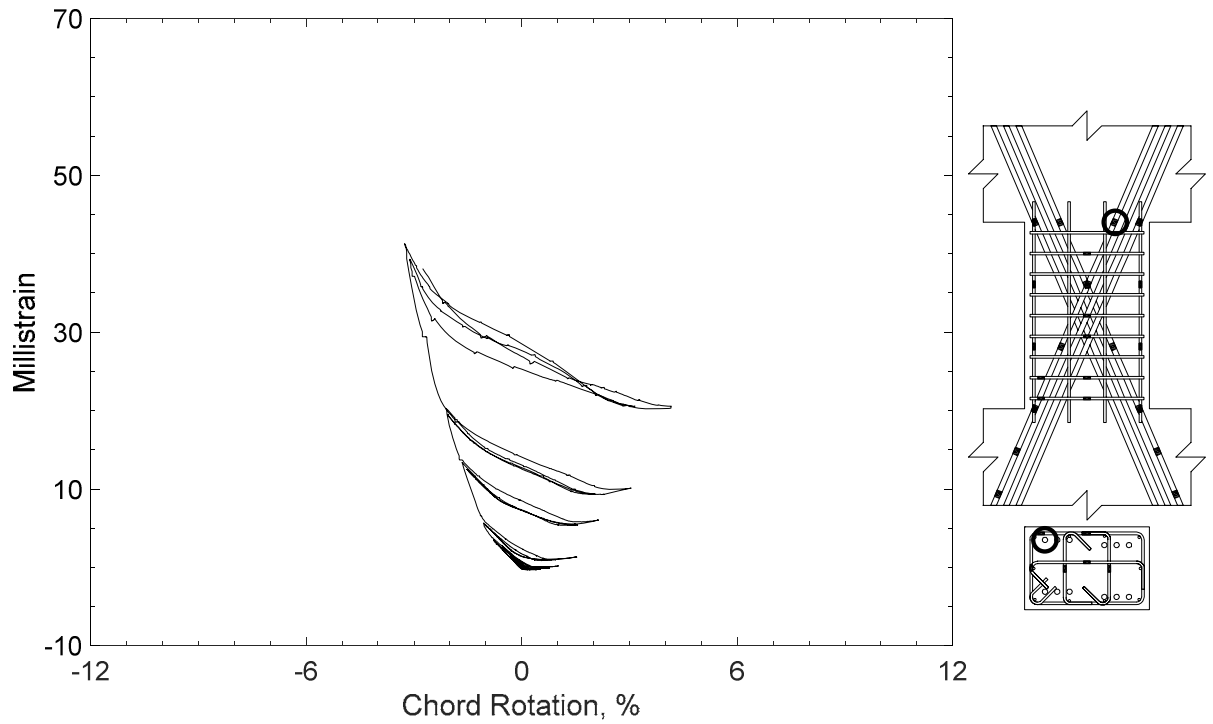


Figure 172 – Measured strain in diagonal bar of D120-1.5, strain gauge D12

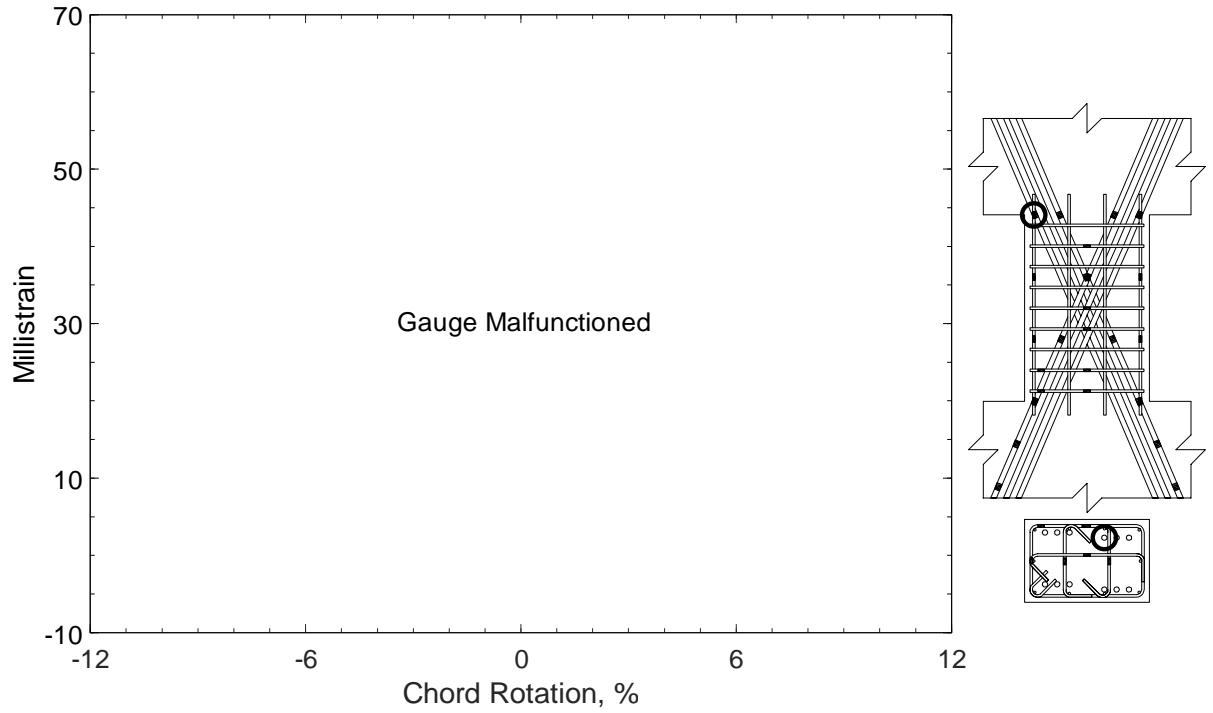


Figure 173 – Measured strain in diagonal bar of D120-1.5, strain gauge D13

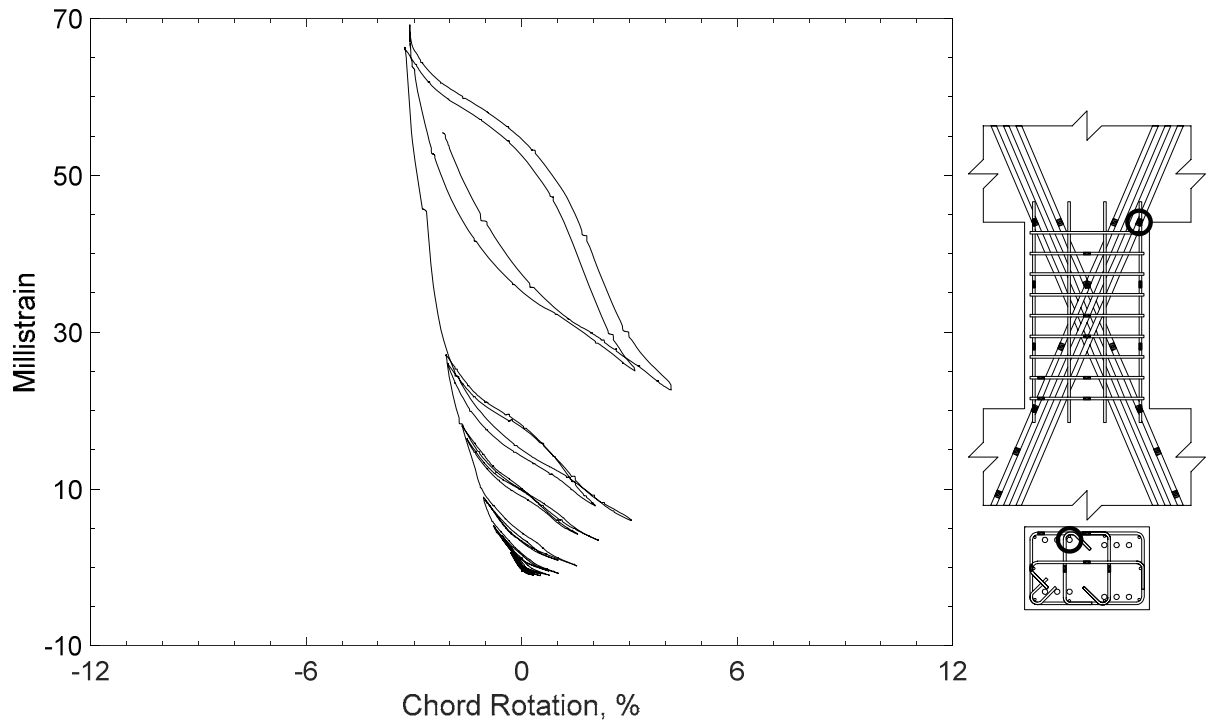


Figure 174 – Measured strain in diagonal bar of D120-1.5, strain gauge D14

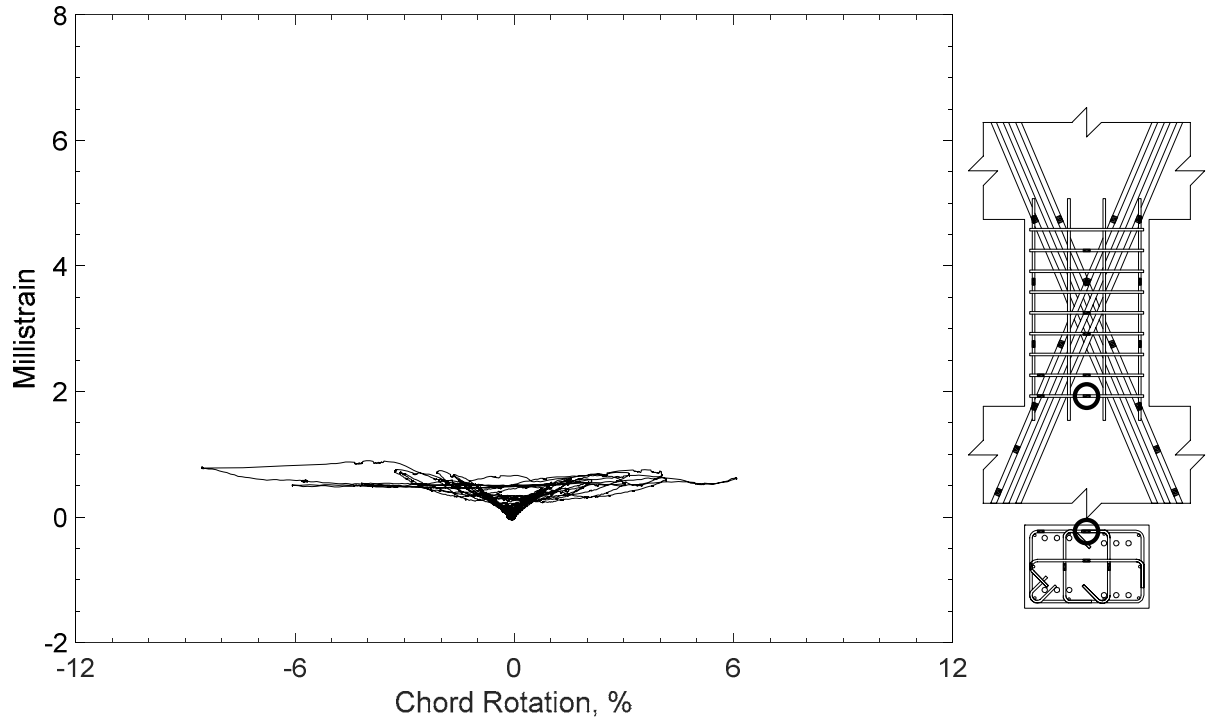


Figure 175 – Measured strain in closed stirrup of D120-1.5, strain gauge S1

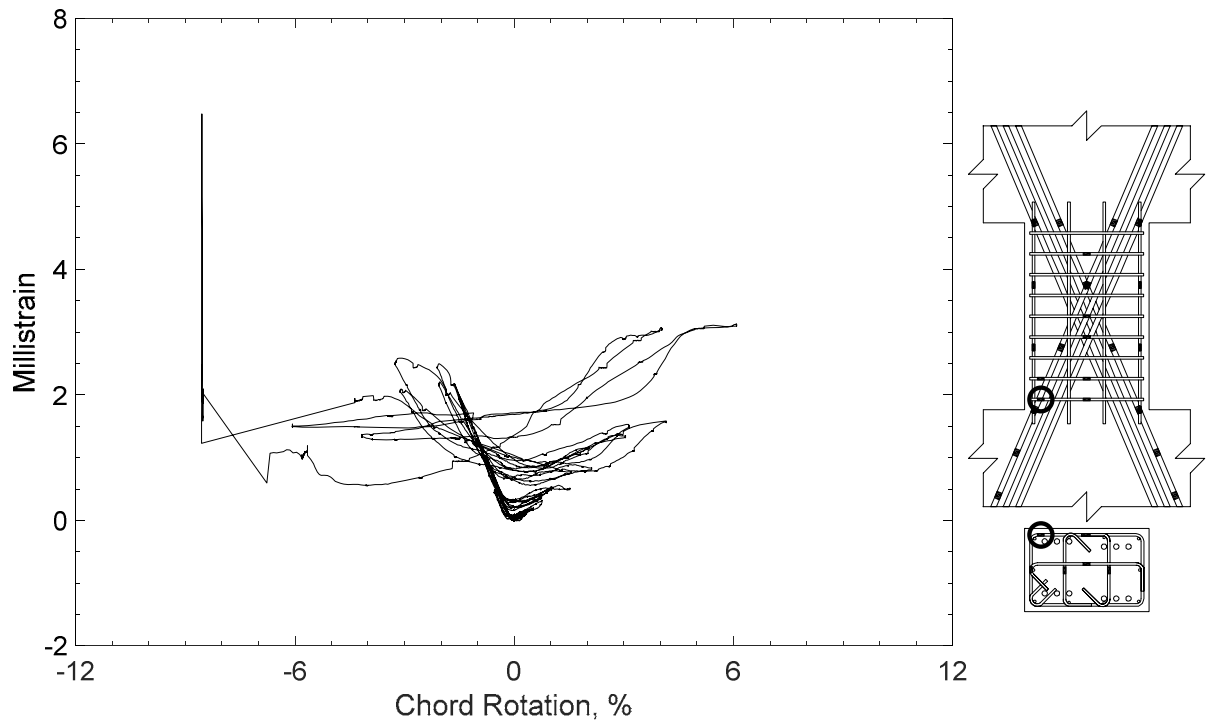


Figure 176 – Measured strain in closed stirrup of D120-1.5, strain gauge S2

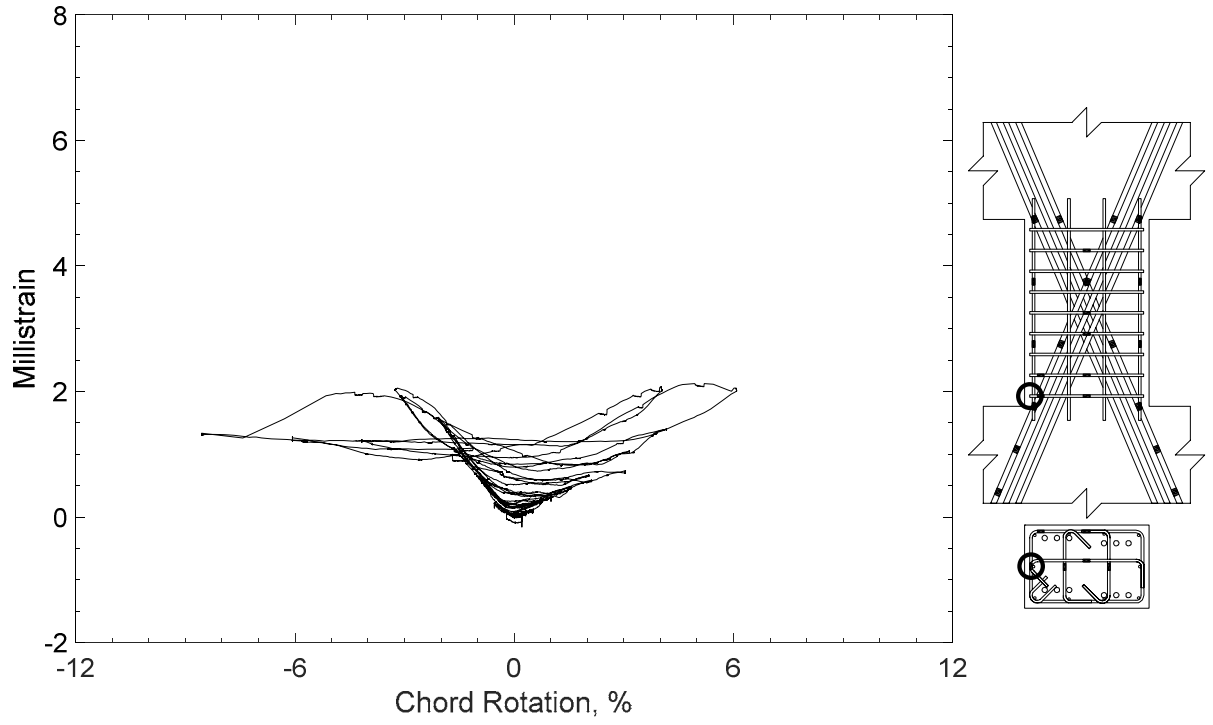


Figure 177 – Measured strain in closed stirrup of D120-1.5, strain gauge S3

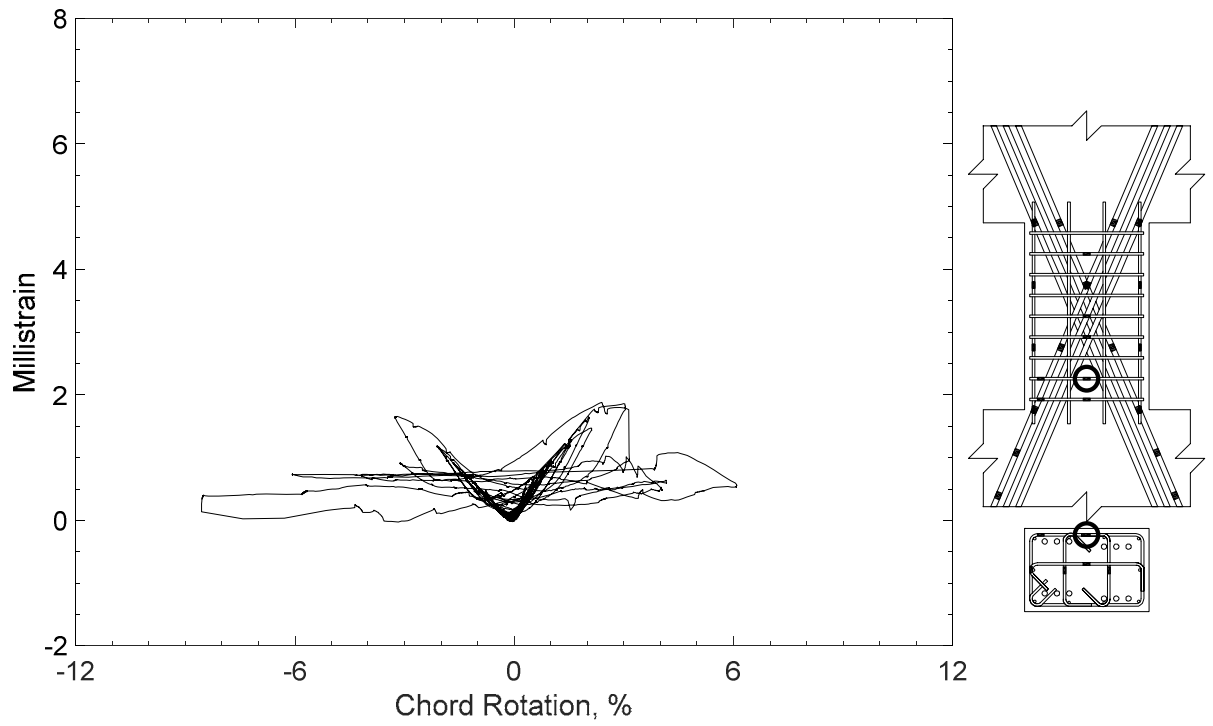


Figure 178 – Measured strain in closed stirrup of D120-1.5, strain gauge S4

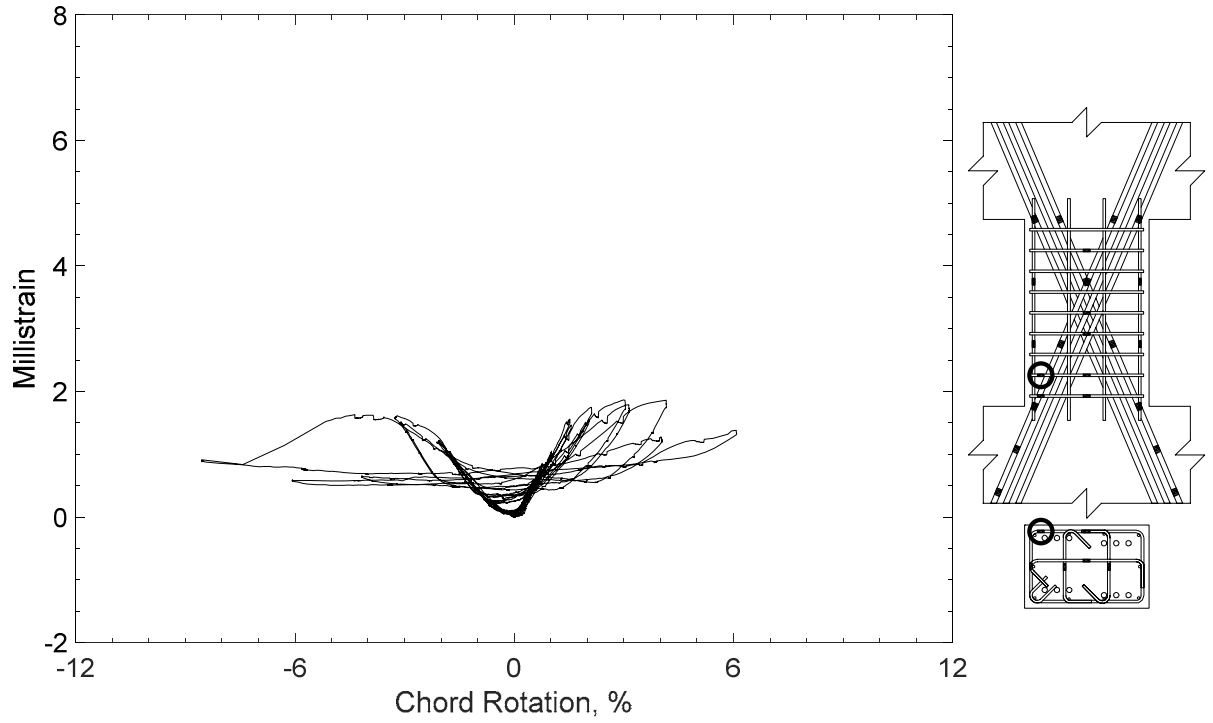


Figure 179 – Measured strain in closed stirrup of D120-1.5, strain gauge S5

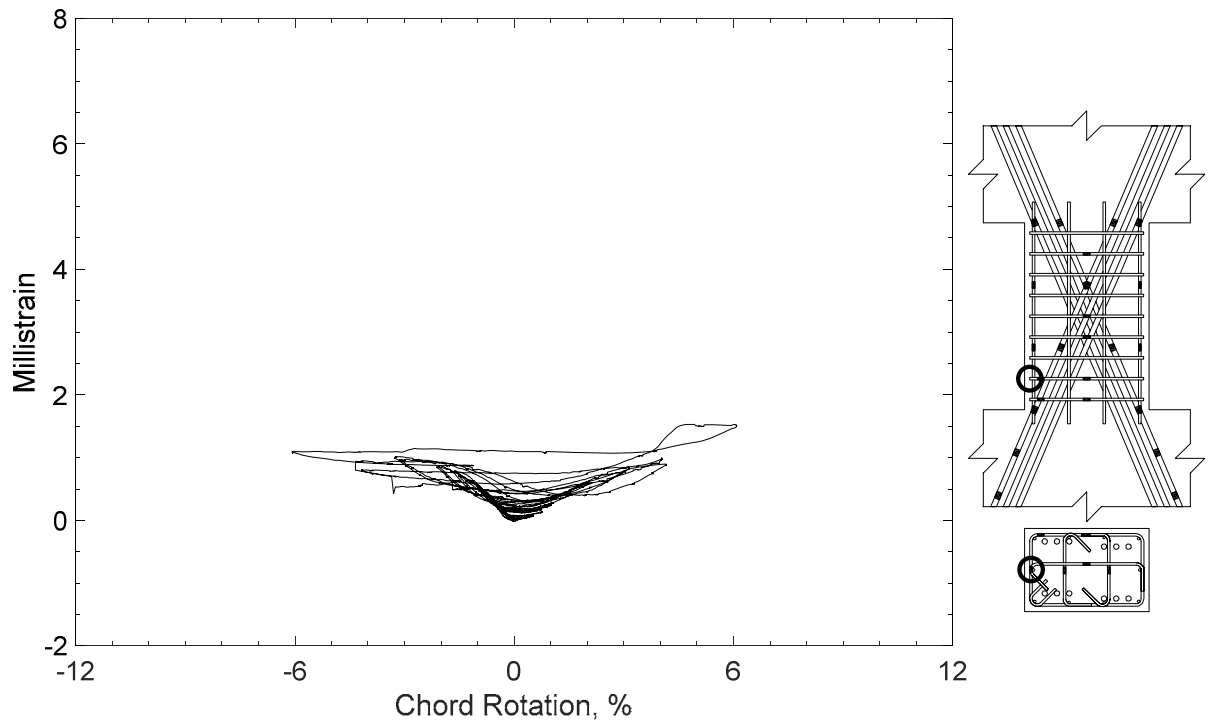


Figure 180 – Measured strain in closed stirrup of D120-1.5, strain gauge S6

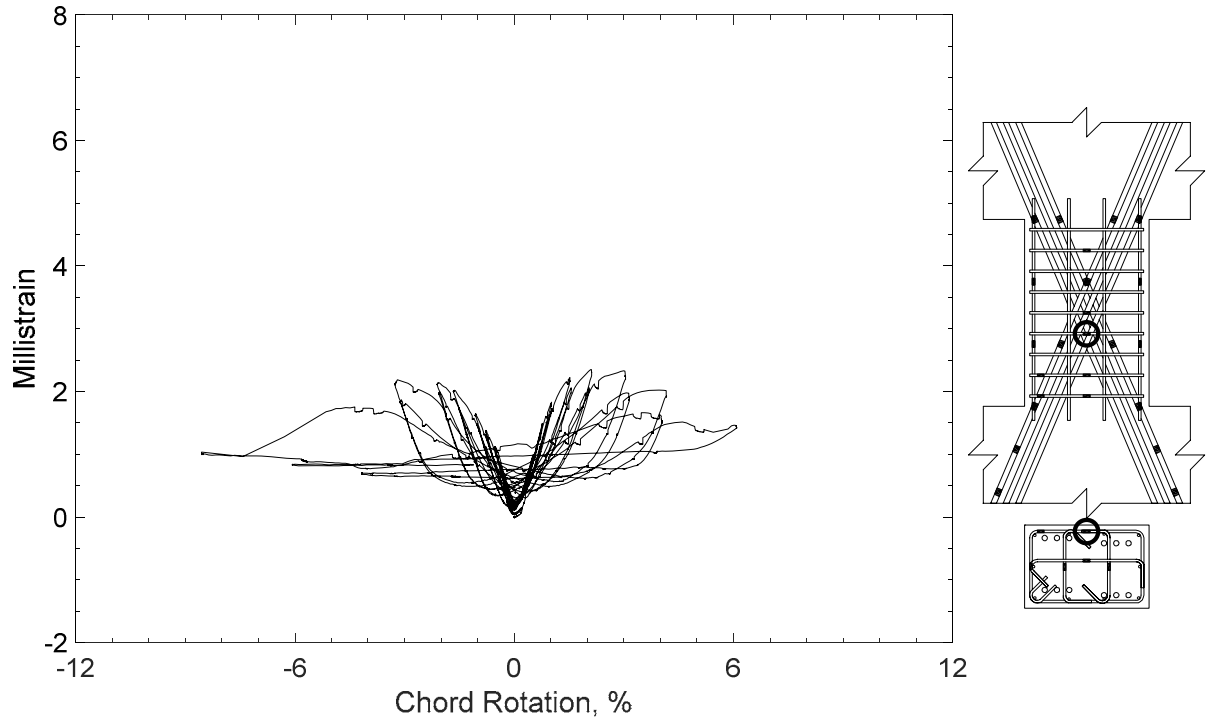


Figure 181 – Measured strain in closed stirrup of D120-1.5, strain gauge S7

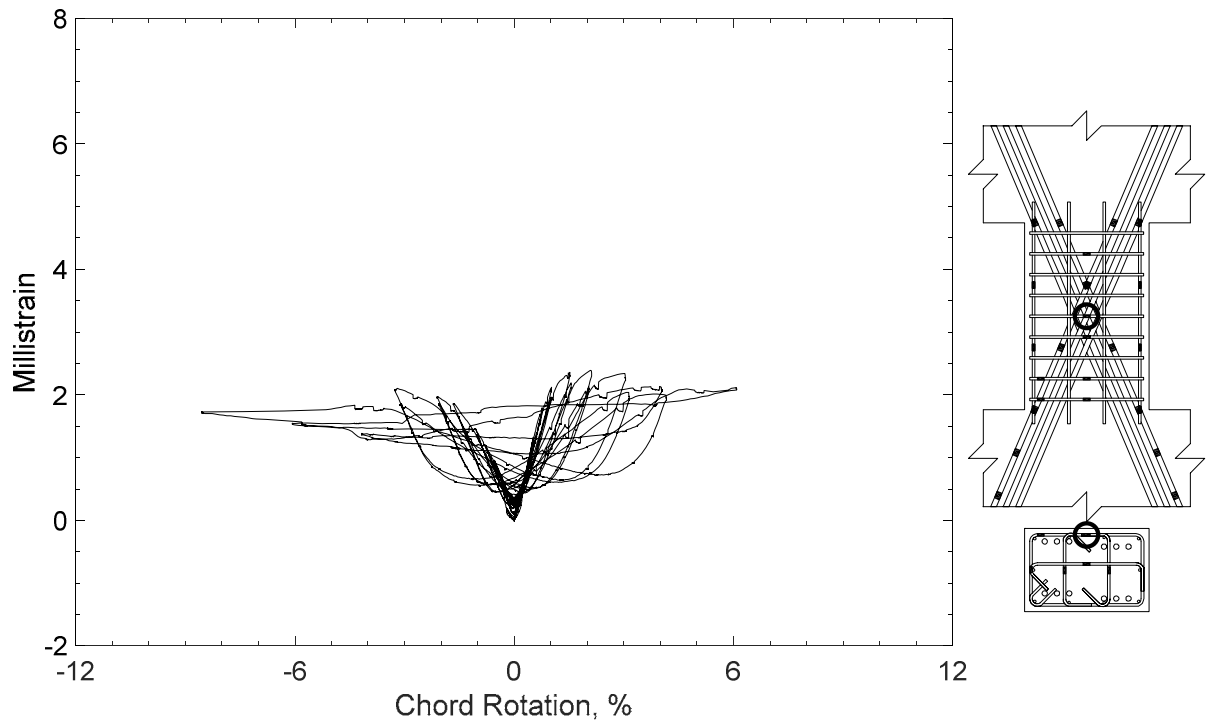


Figure 182 – Measured strain in closed stirrup of D120-1.5, strain gauge S8

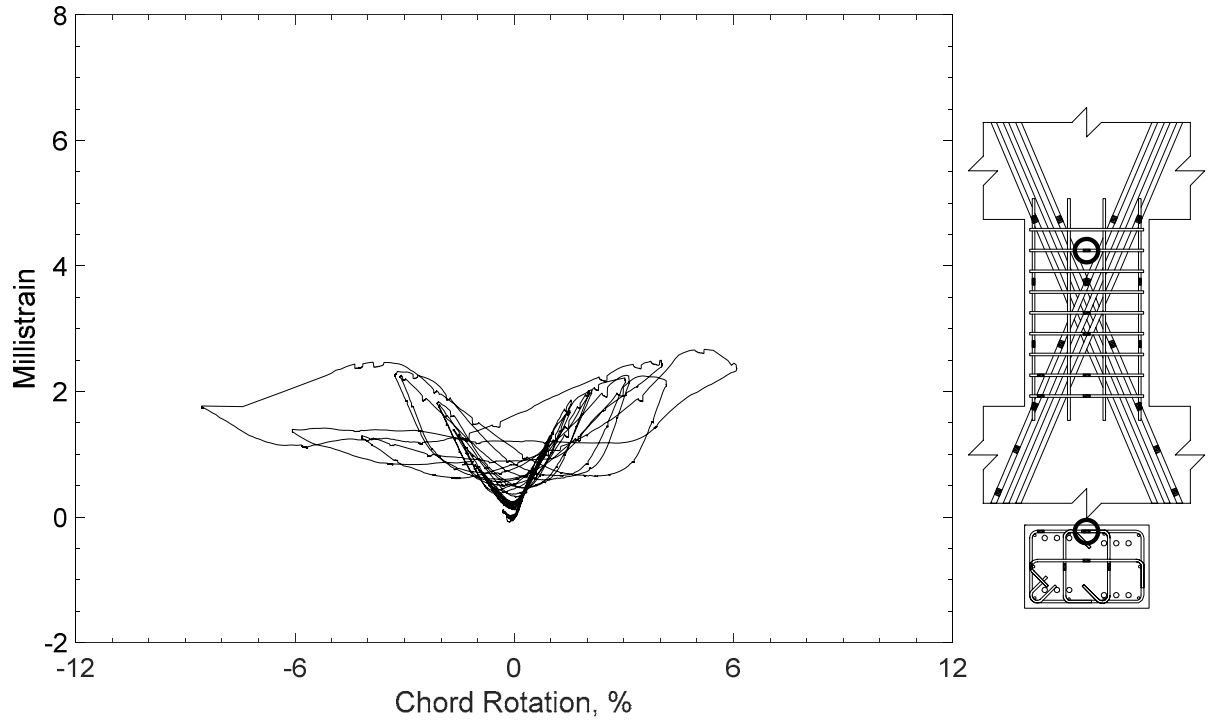


Figure 183 – Measured strain in closed stirrup of D120-1.5, strain gauge S9

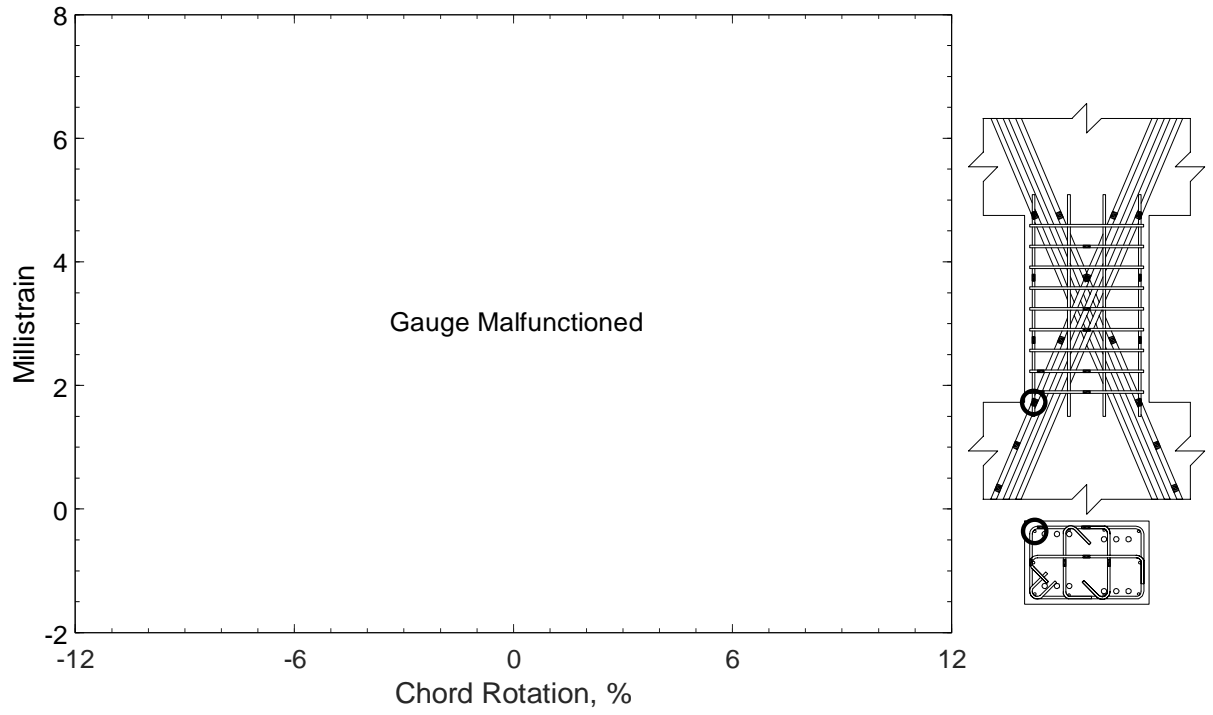


Figure 184 – Measured strain in parallel bar of D120-1.5, strain gauge H1

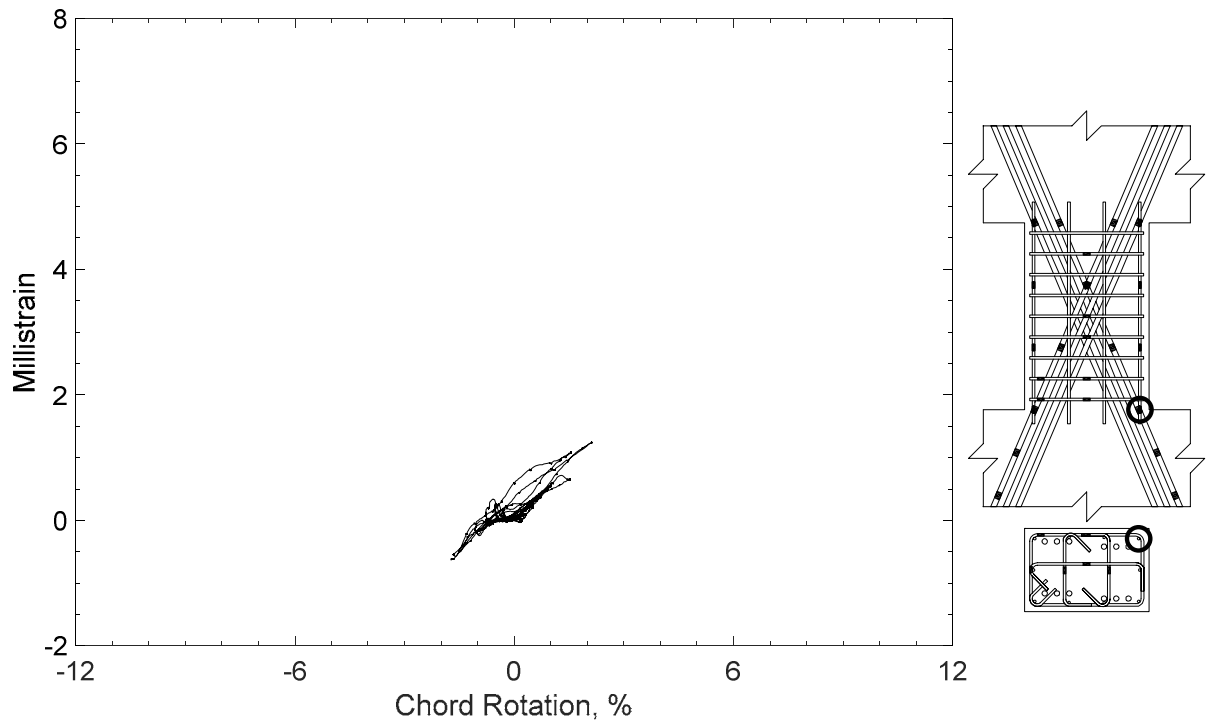


Figure 185 – Measured strain in parallel bar of D120-1.5, strain gauge H2

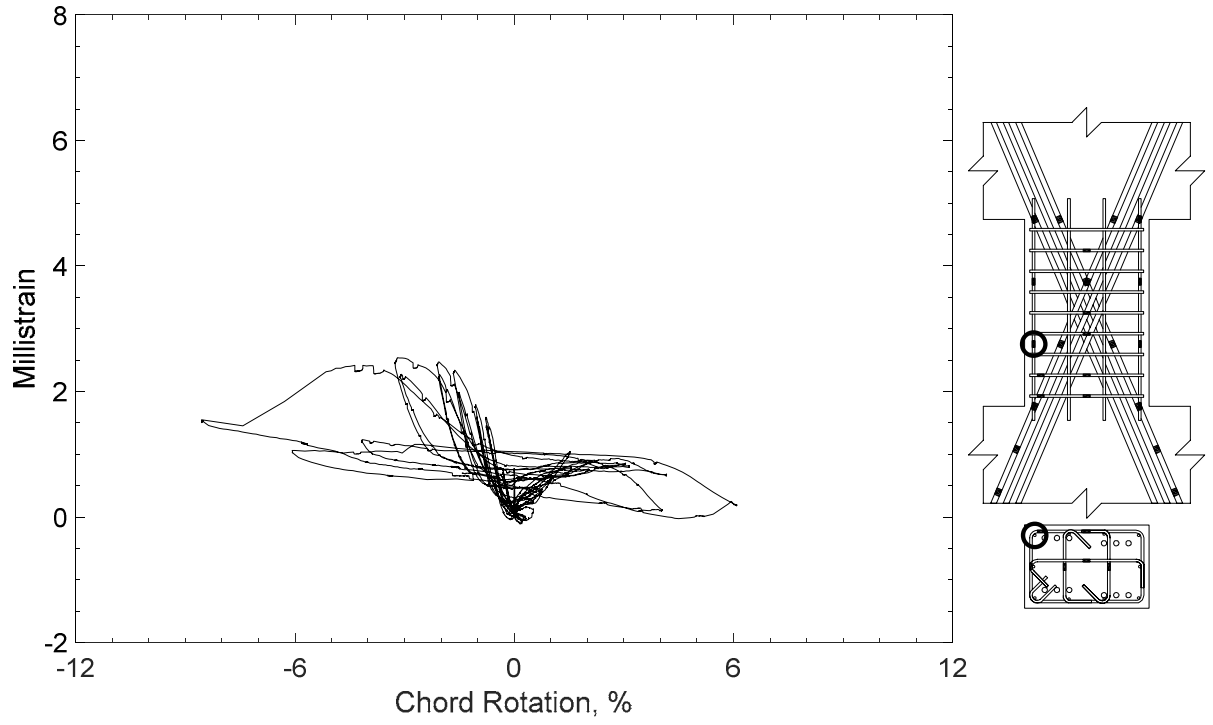


Figure 186 – Measured strain in parallel bar of D120-1.5, strain gauge H3

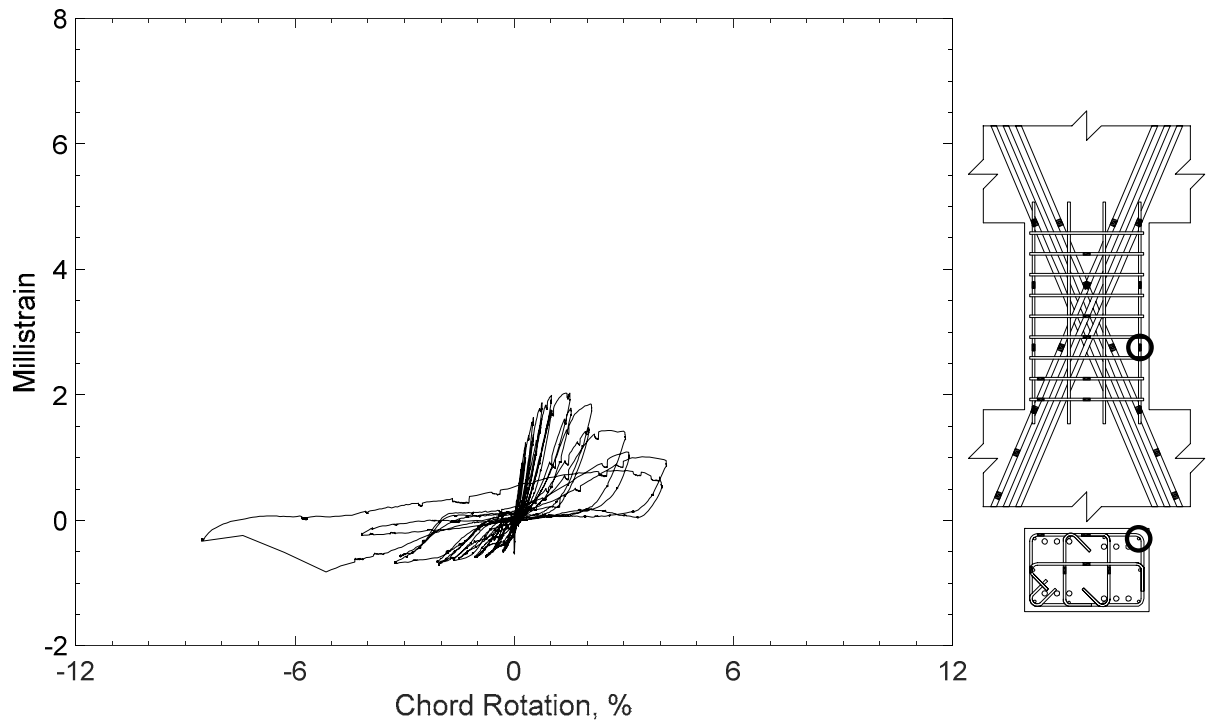


Figure 187 – Measured strain in parallel bar of D120-1.5, strain gauge H4

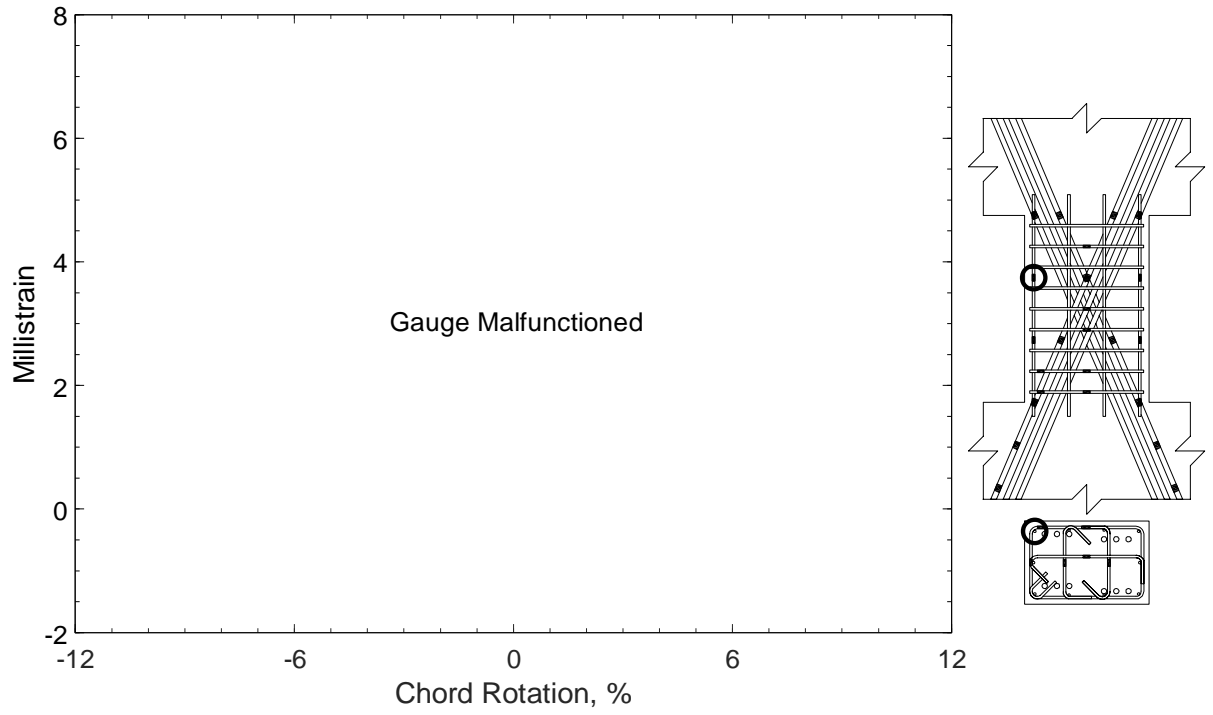


Figure 188 – Measured strain in parallel bar of D120-1.5, strain gauge H5

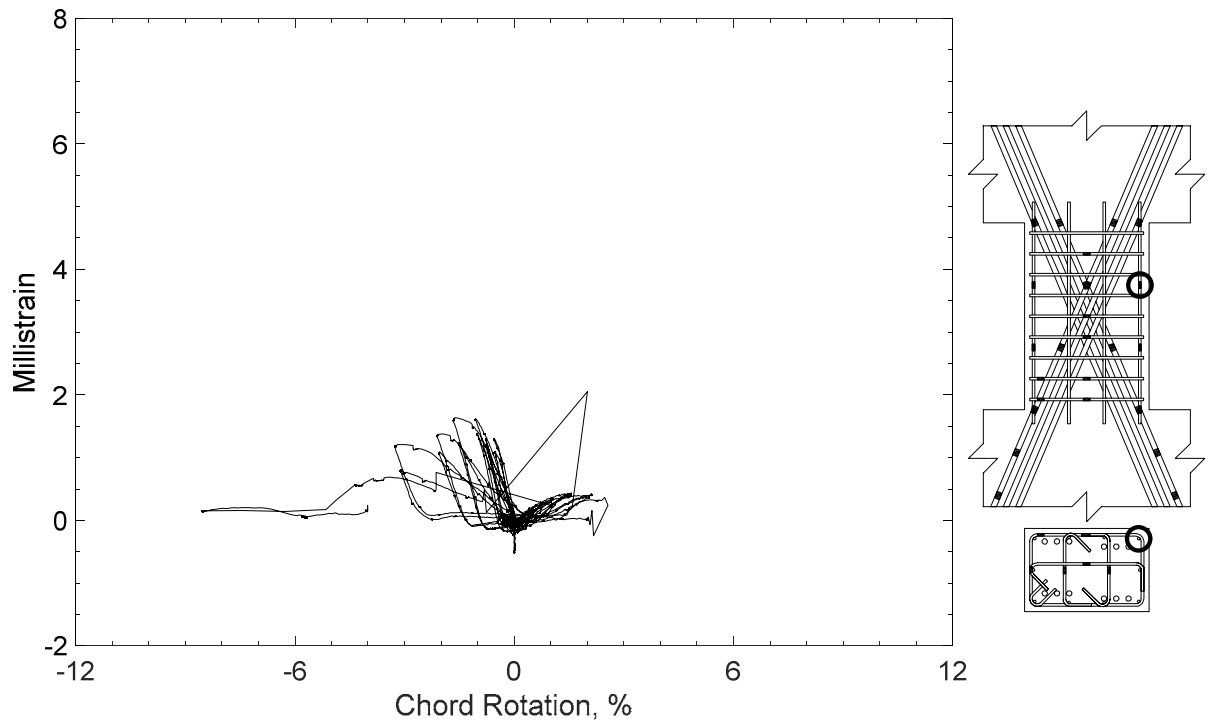


Figure 189 – Measured strain in parallel bar of D120-1.5, strain gauge H6

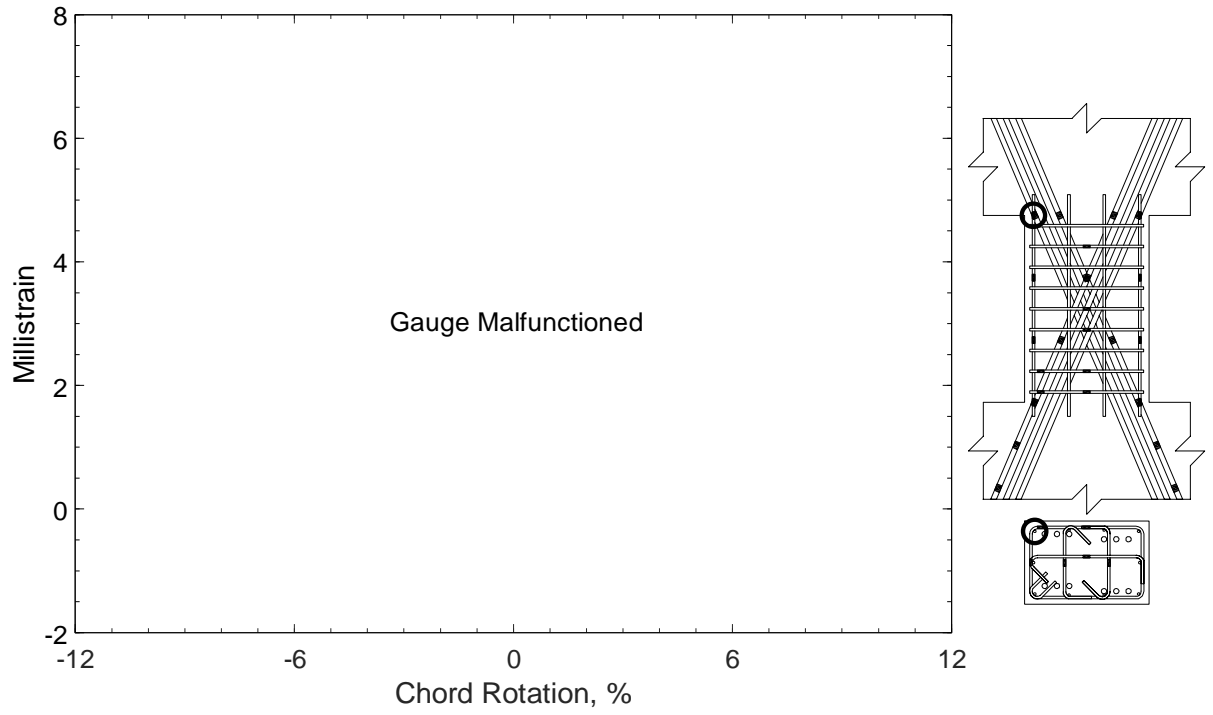


Figure 190 – Measured strain in parallel bar of D120-1.5, strain gauge H7

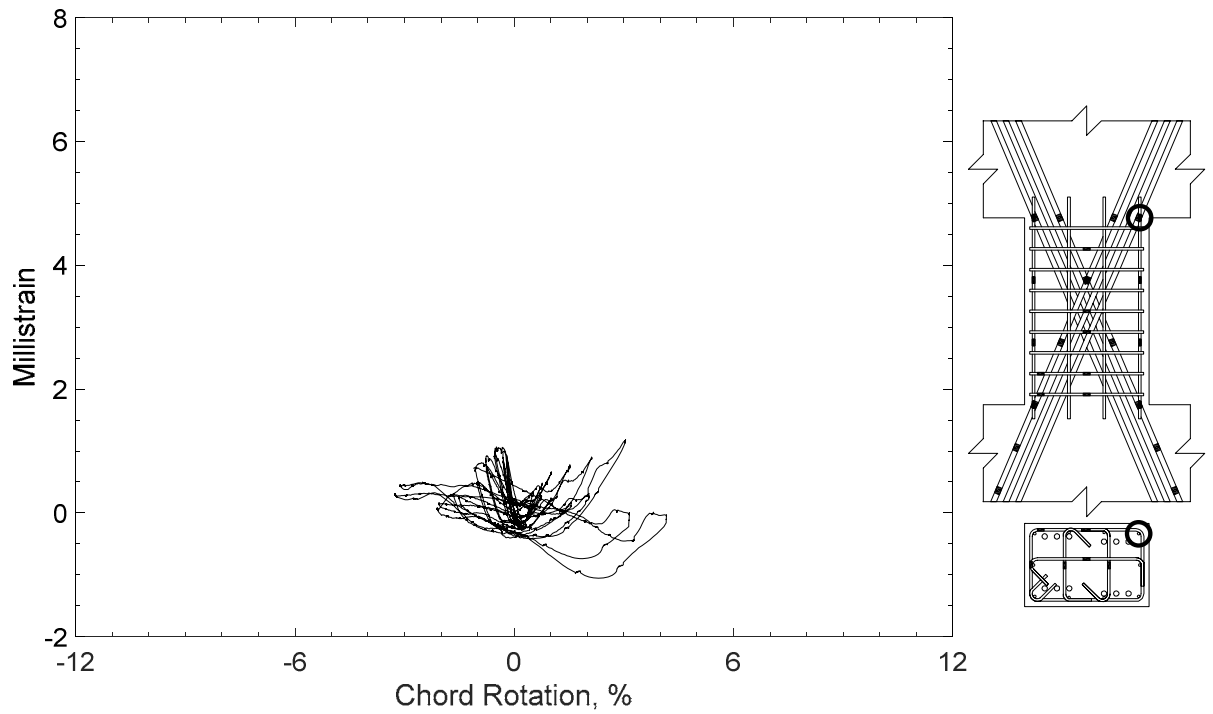


Figure 191 – Measured strain in parallel bar of D120-1.5, strain gauge H8

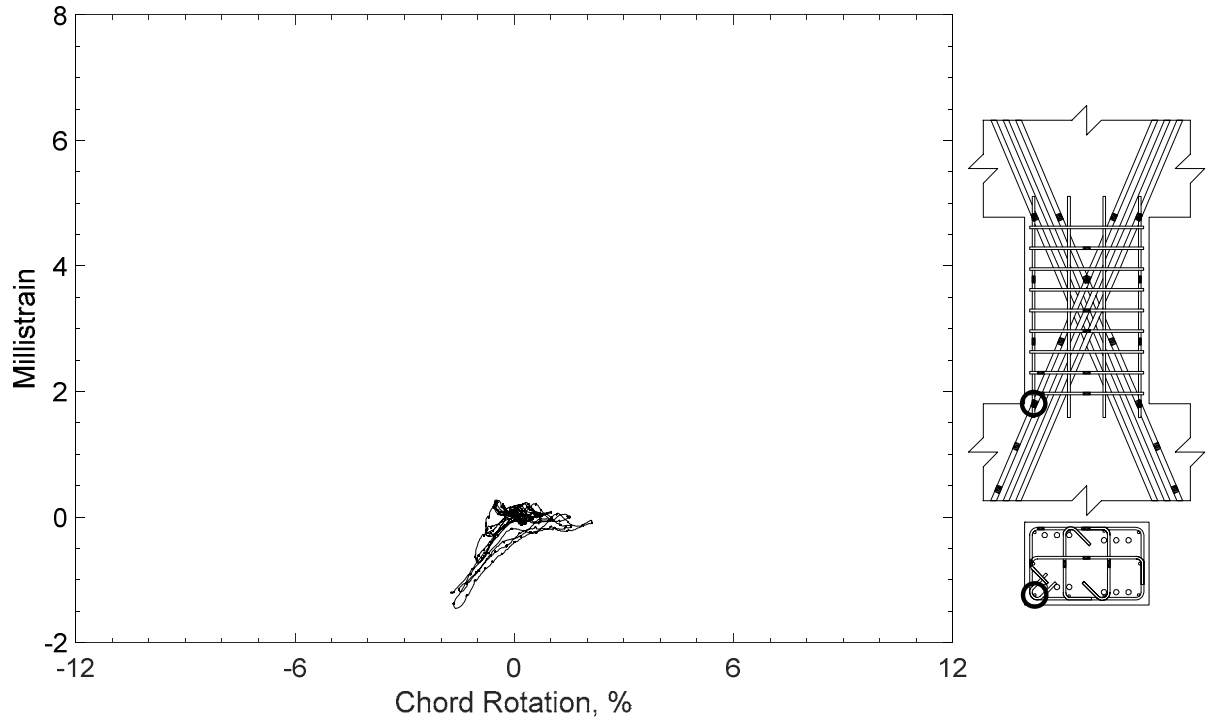


Figure 192 – Measured strain in parallel bar of D120-1.5, strain gauge H9

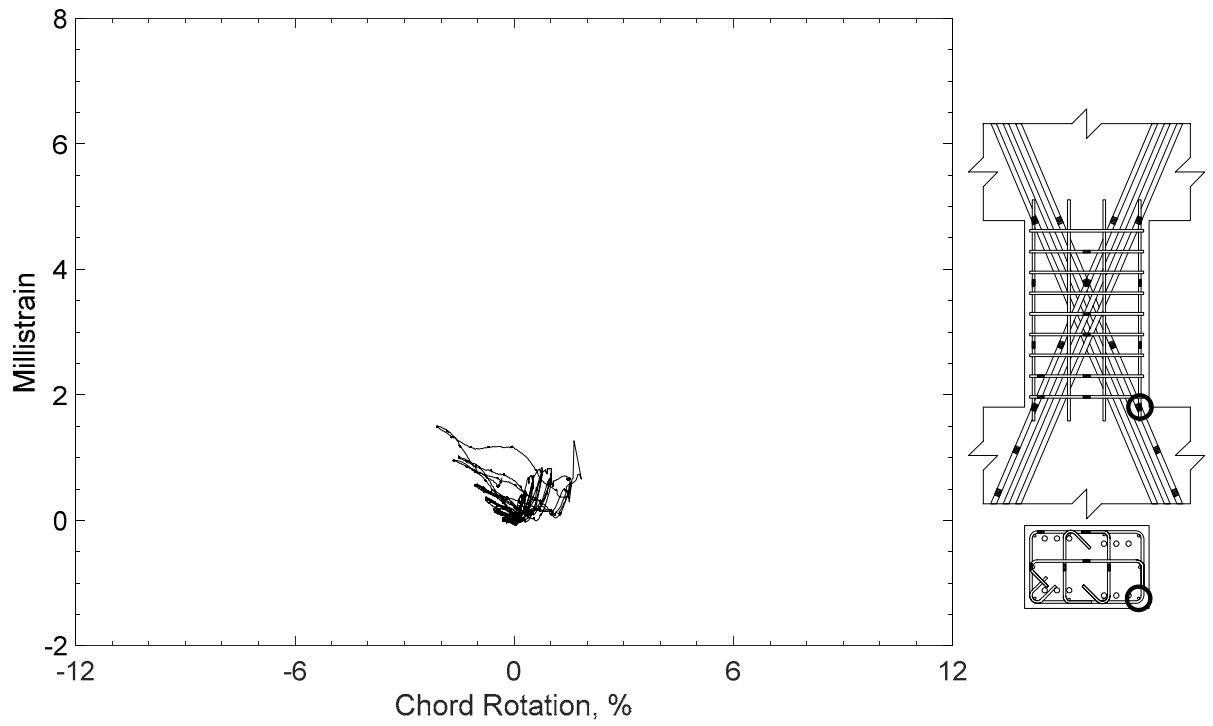


Figure 193 – Measured strain in parallel bar of D120-1.5, strain gauge H10

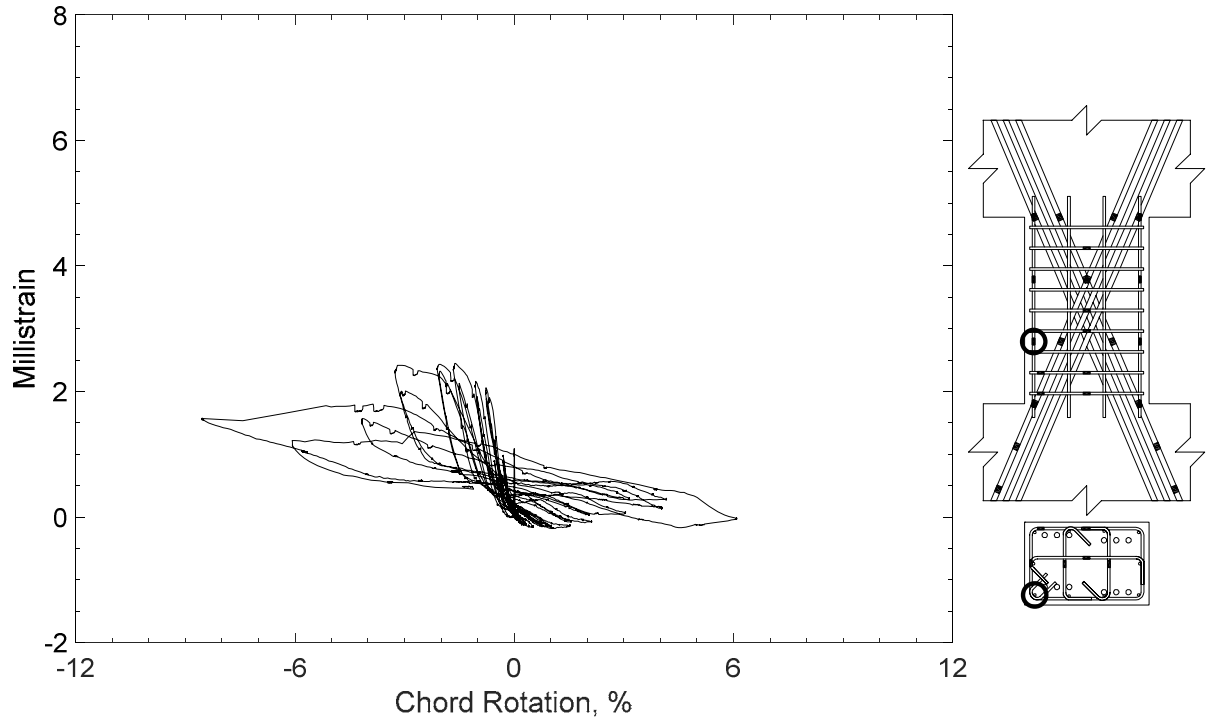


Figure 194 – Measured strain in parallel bar of D120-1.5, strain gauge H11

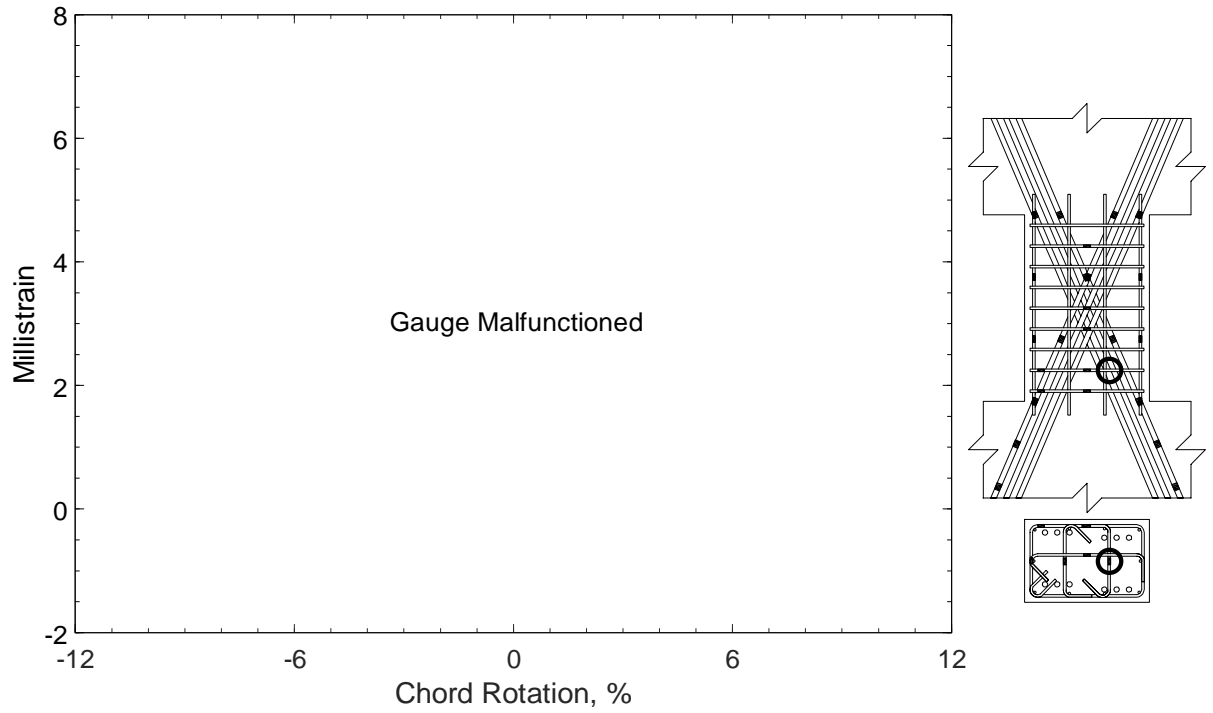


Figure 195 – Measured strain in cross-tie of D120-1.5, strain gauge T1

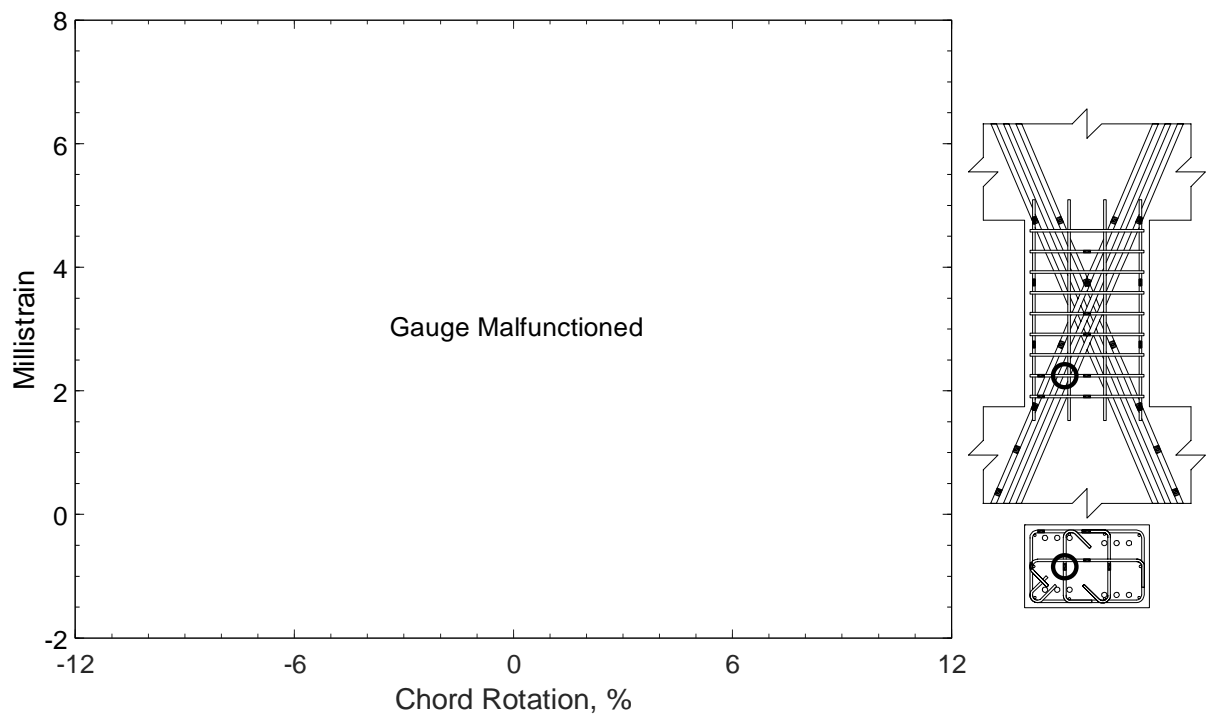


Figure 196 – Measured strain in cross-tie of D120-1.5, strain gauge T2

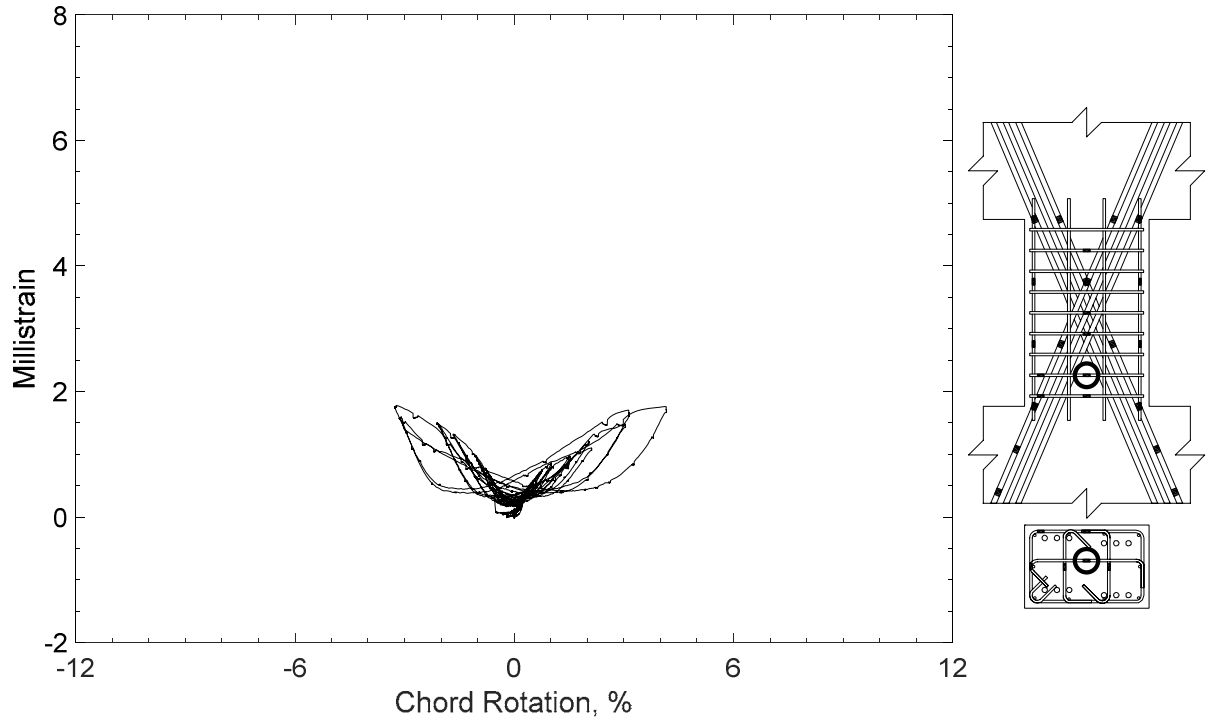


Figure 197 – Measured strain in crosstie of D120-1.5, strain gauge T3

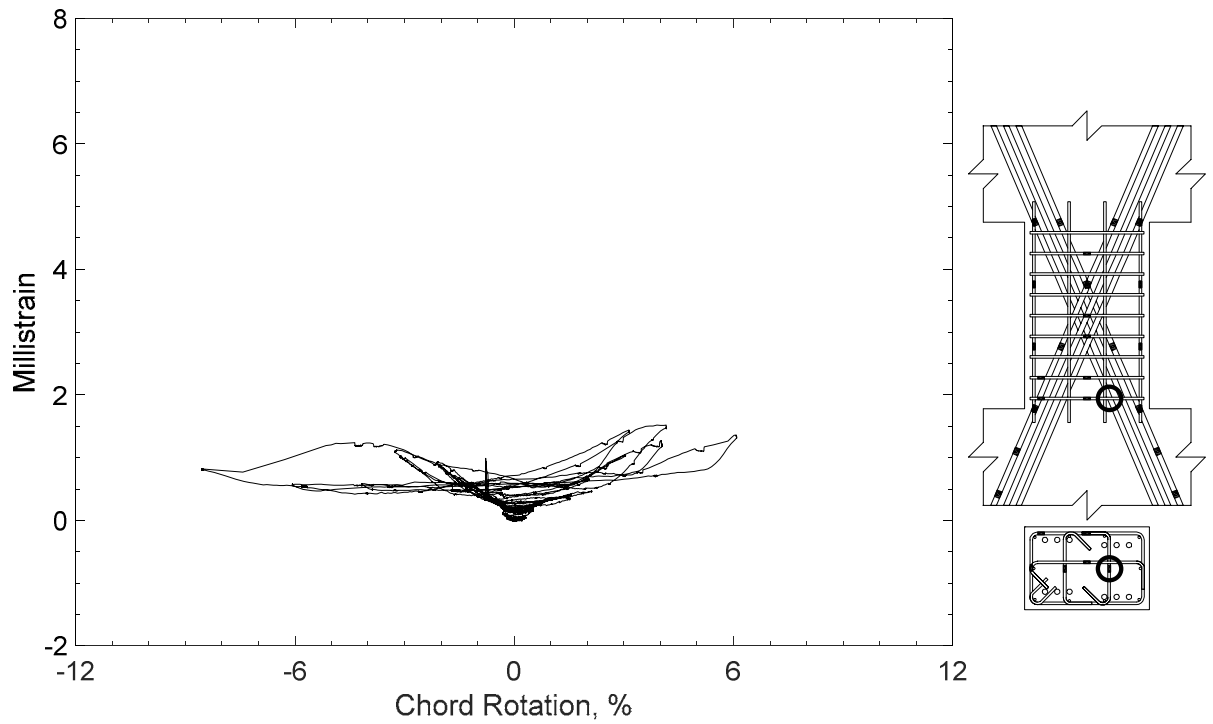


Figure 198 – Measured strain in crosstie of D120-1.5, strain gauge T4

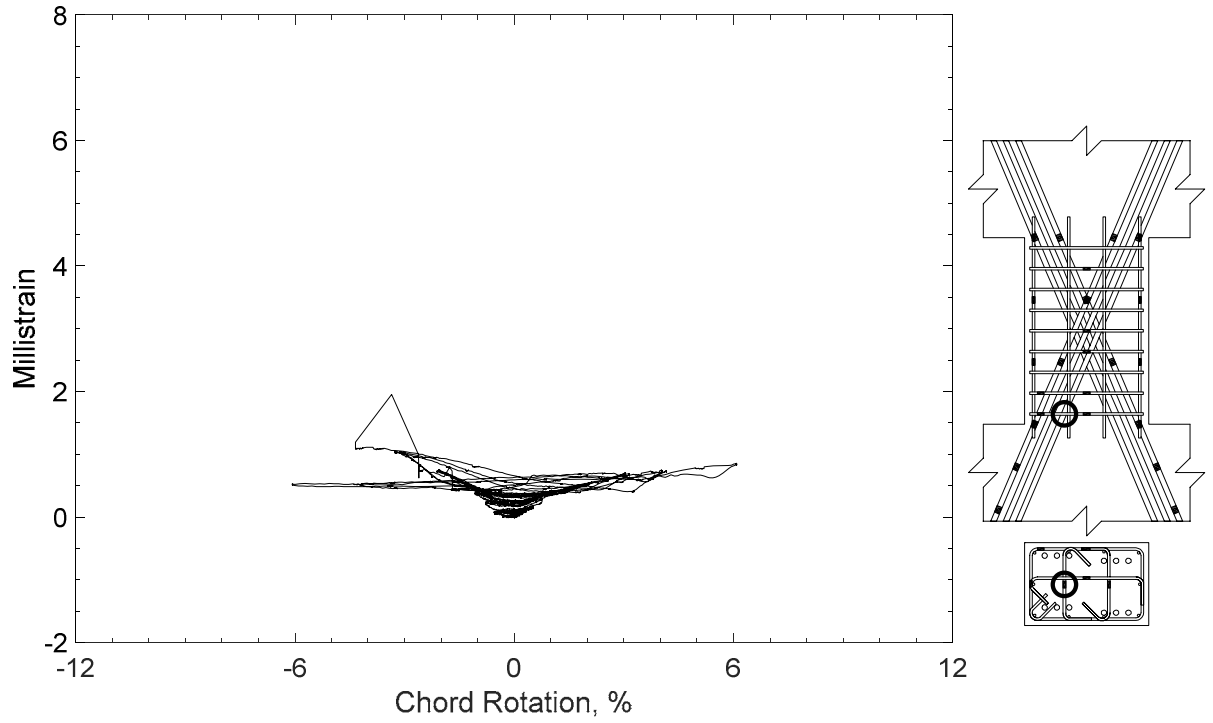


Figure 199 – Measured strain in crosstie of D120-1.5, strain gauge T5

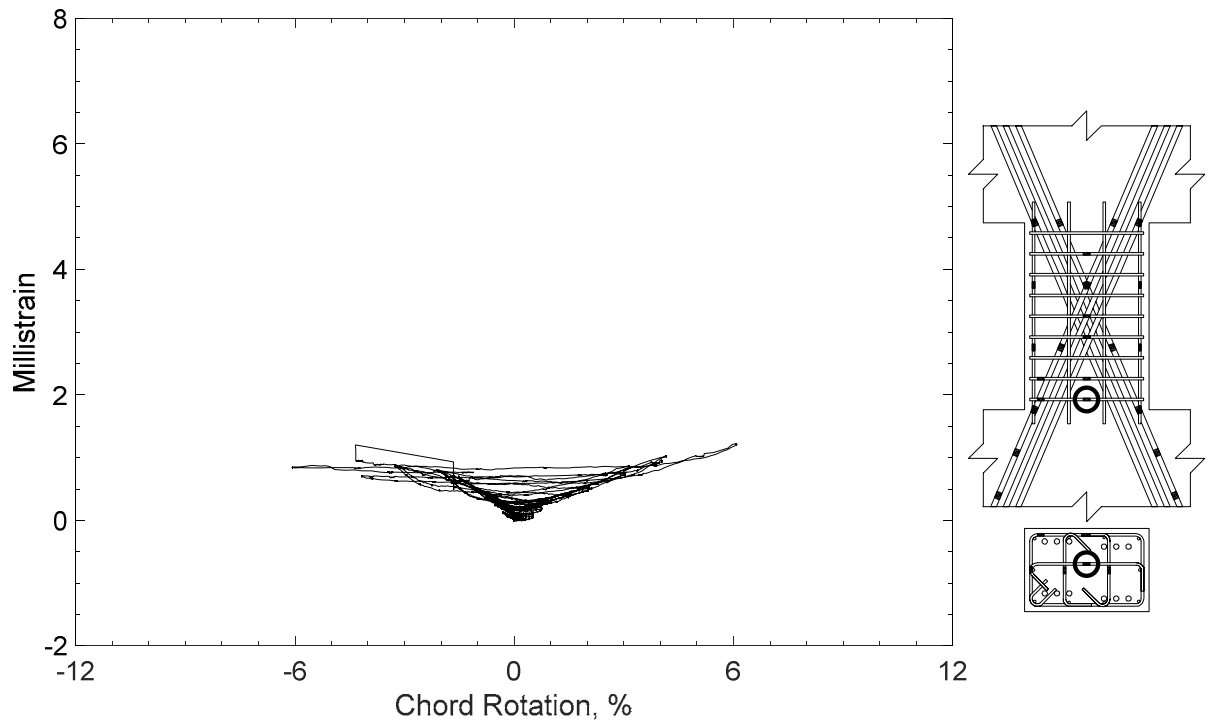


Figure 200 – Measured strain in crosstie of D120-1.5, strain gauge T6

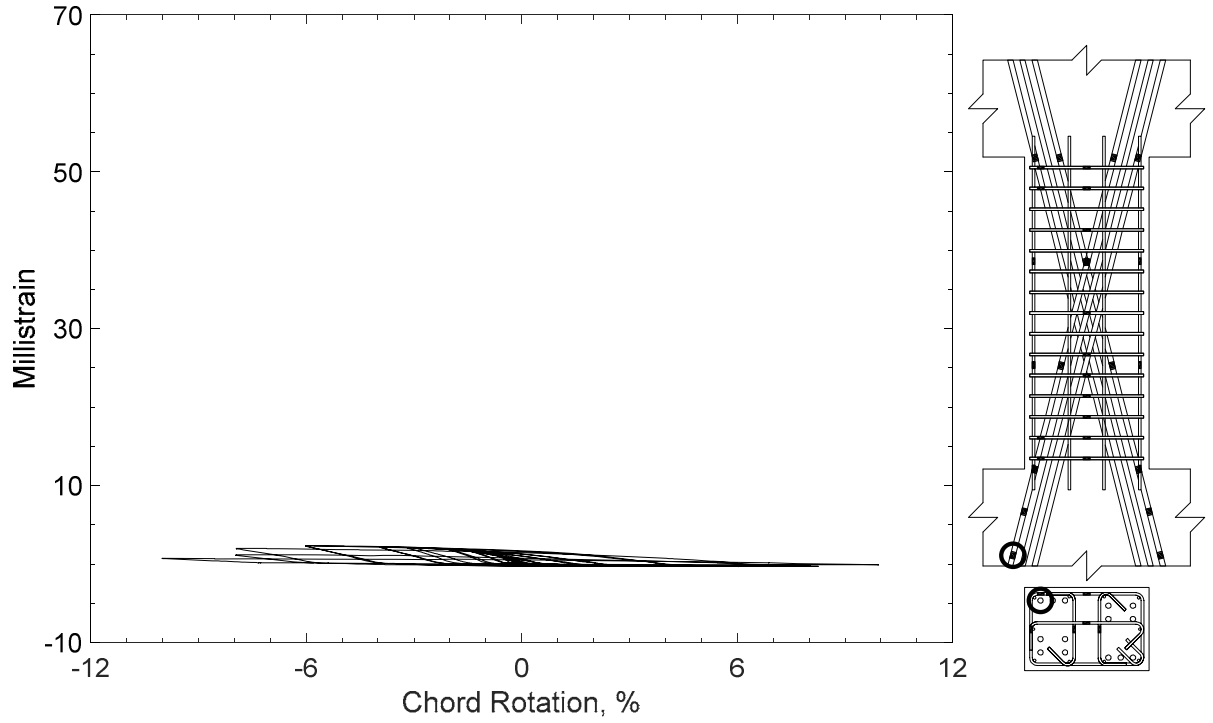


Figure 201 – Measured strain in diagonal bar of D80-2.5, strain gauge D1

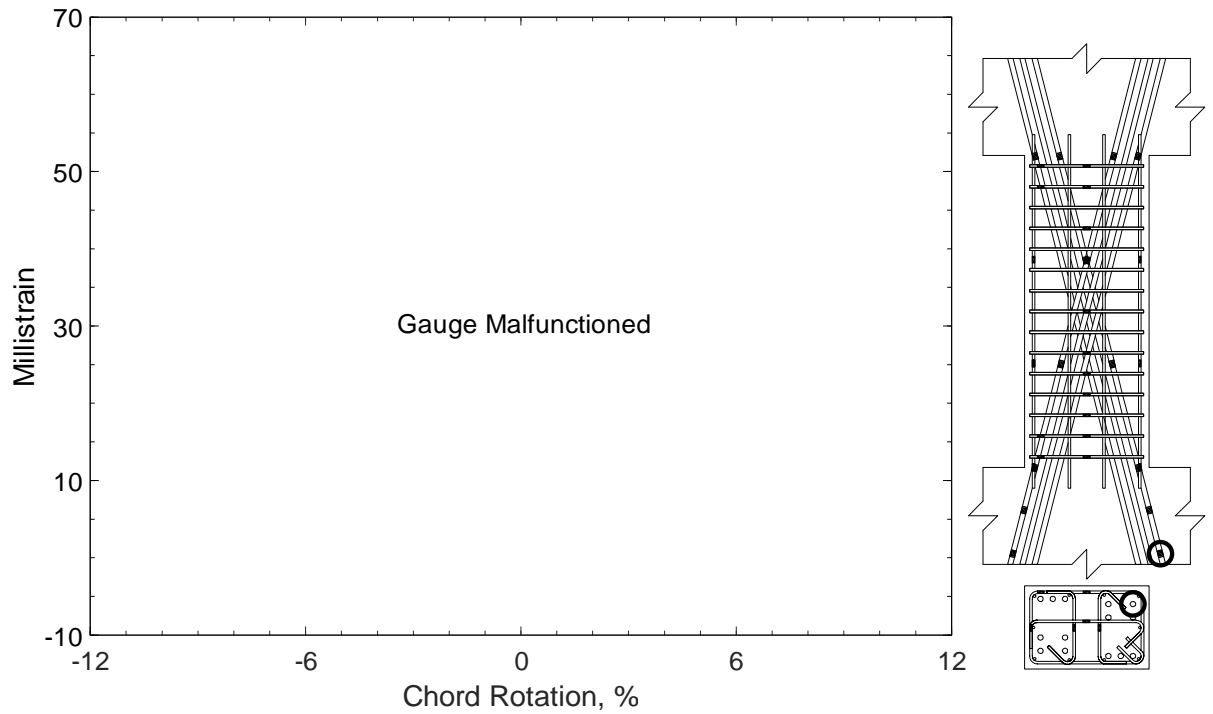


Figure 202 – Measured strain in diagonal bar of D80-2.5, strain gauge D2

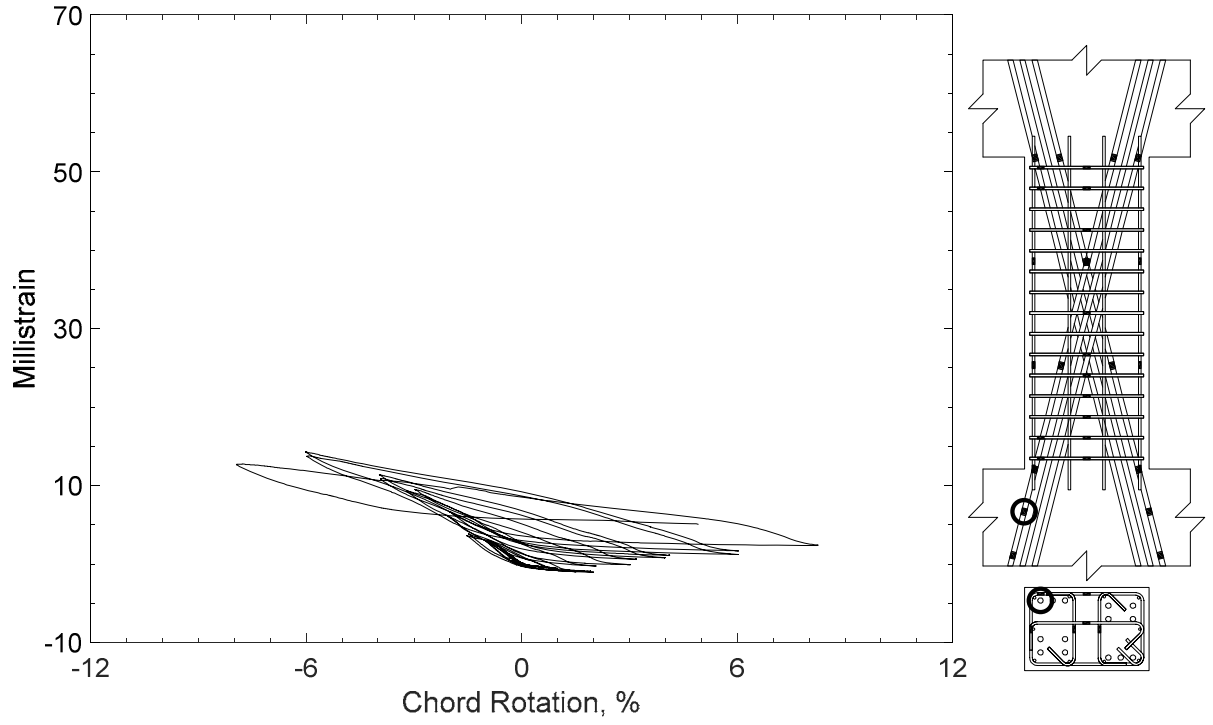


Figure 203 – Measured strain in diagonal bar of D80-2.5, strain gauge D3

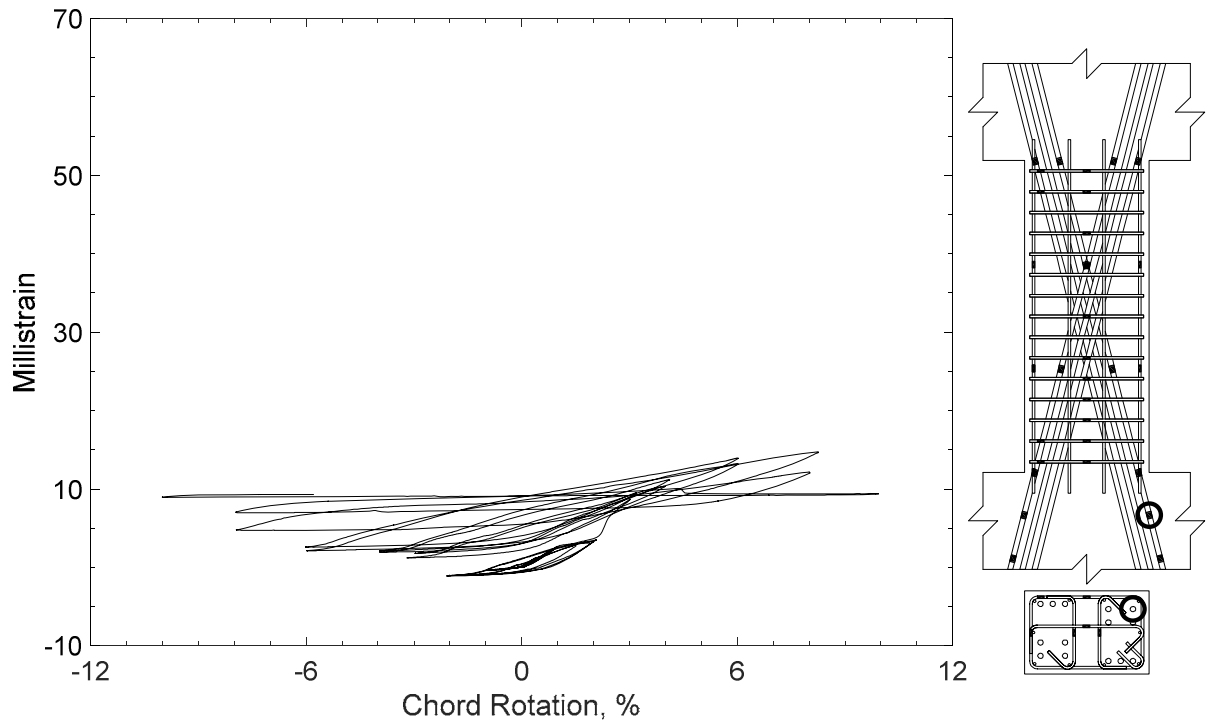


Figure 204 – Measured strain in diagonal bar of D80-2.5, strain gauge D4

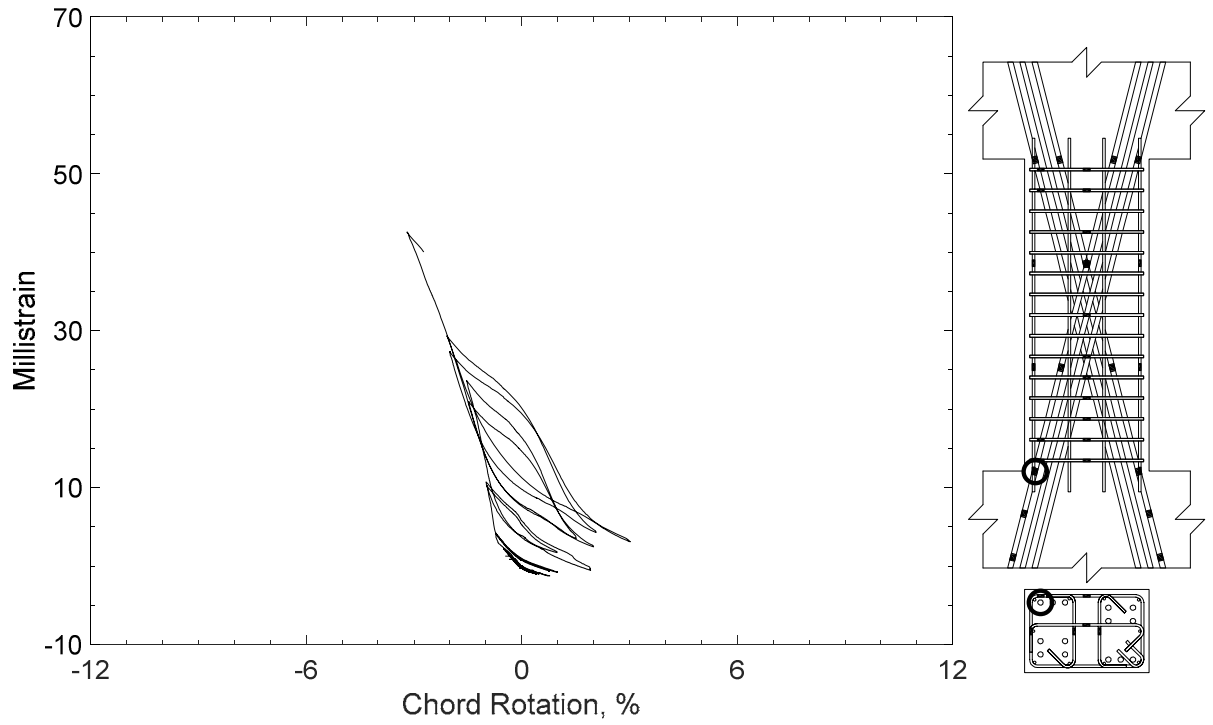


Figure 205 – Measured strain in diagonal bar of D80-2.5, strain gauge D5

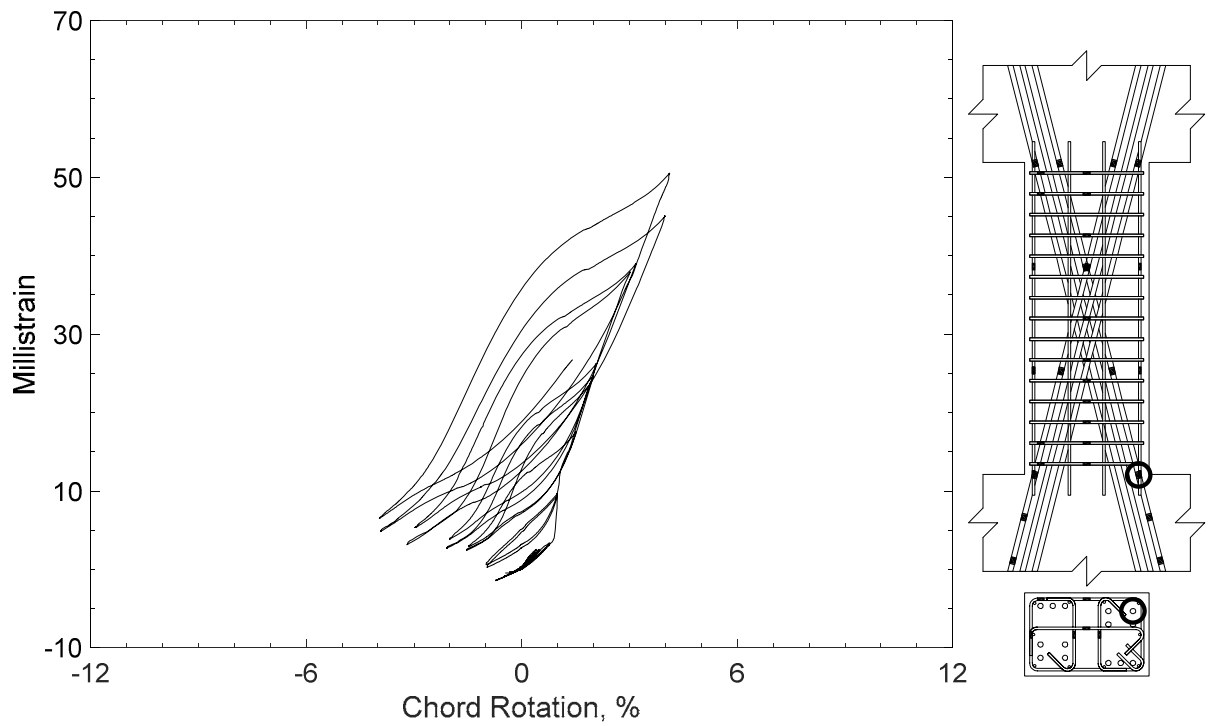


Figure 206 – Measured strain in diagonal bar of D80-2.5, strain gauge D6

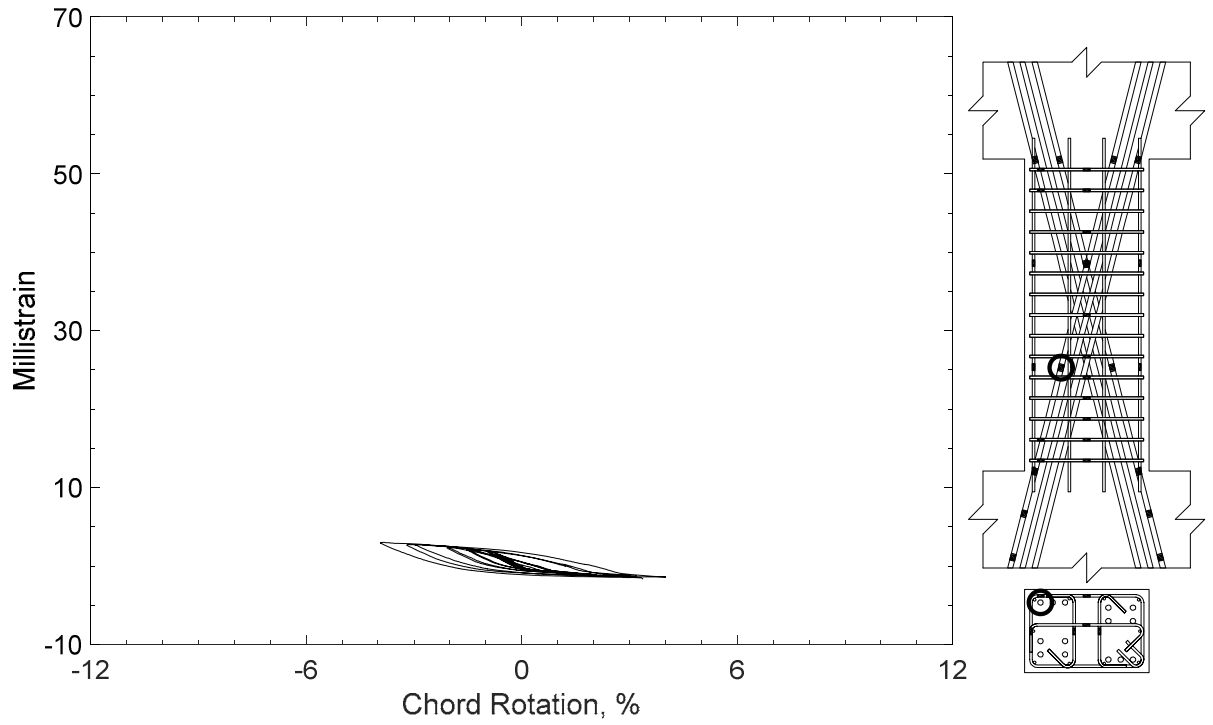


Figure 207 – Measured strain in diagonal bar of D80-2.5, strain gauge D7

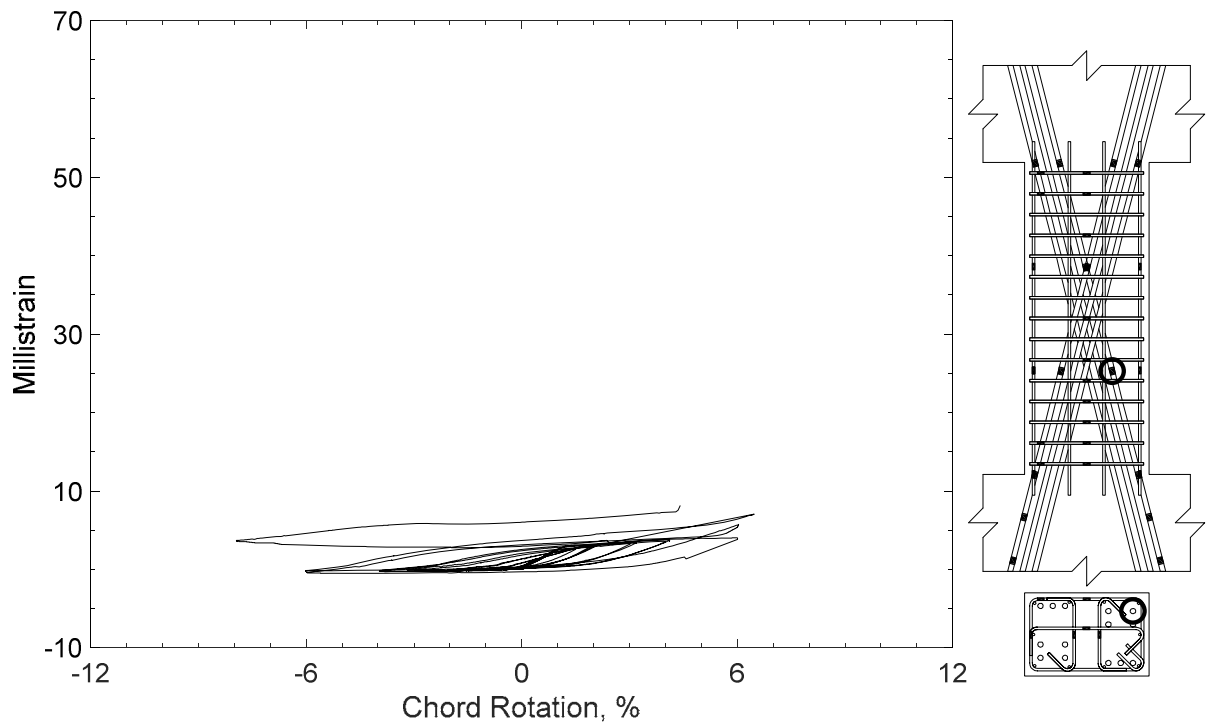


Figure 208 – Measured strain in diagonal bar of D80-2.5, strain gauge D8

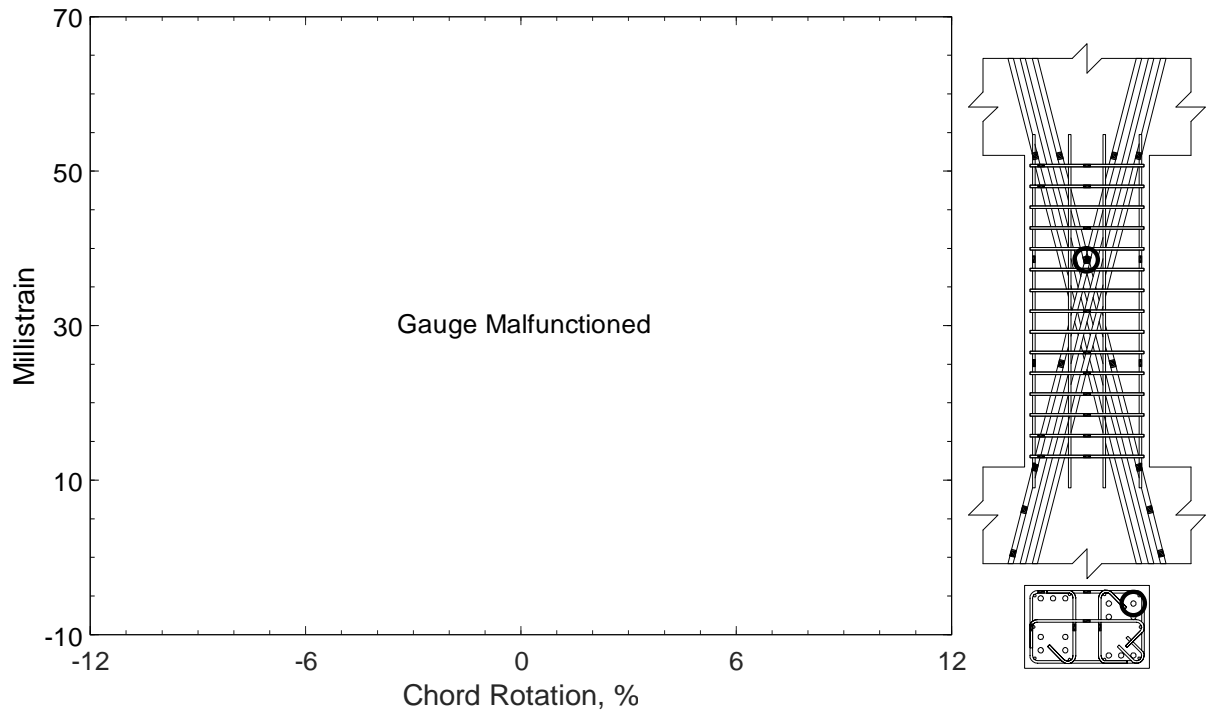


Figure 209 – Measured strain in diagonal bar of D80-2.5, strain gauge D9

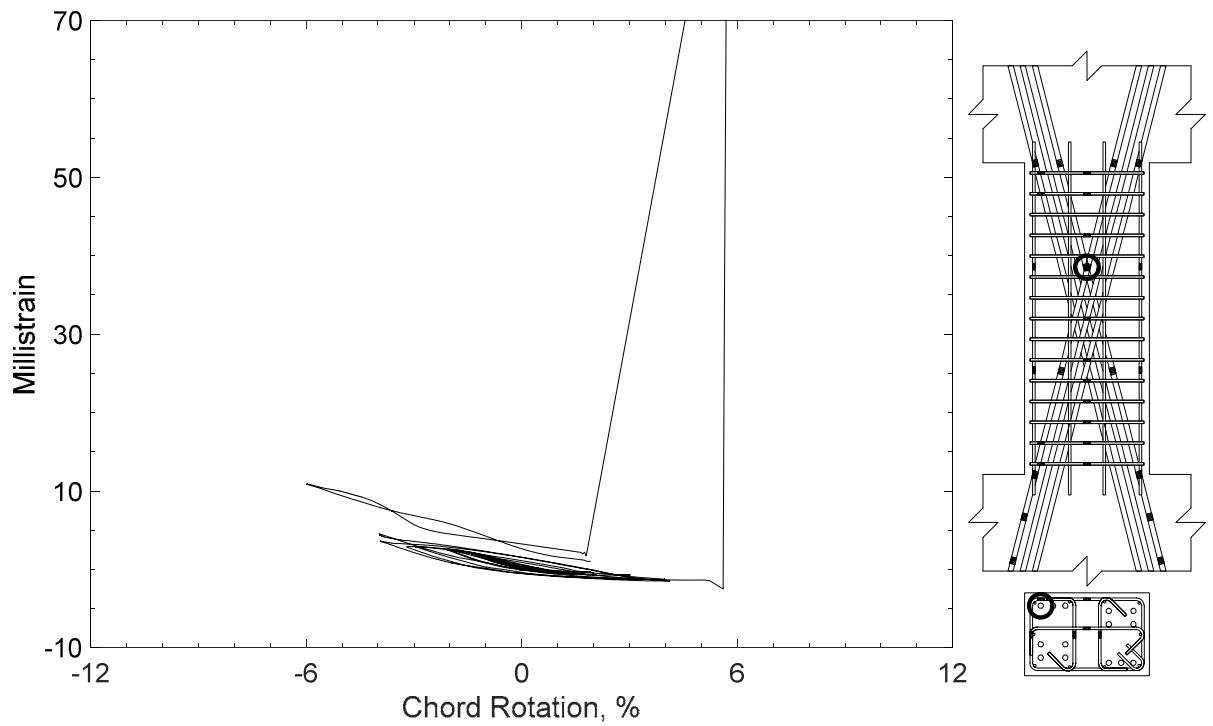


Figure 210 – Measured strain in diagonal bar of D80-2.5, strain gauge D10

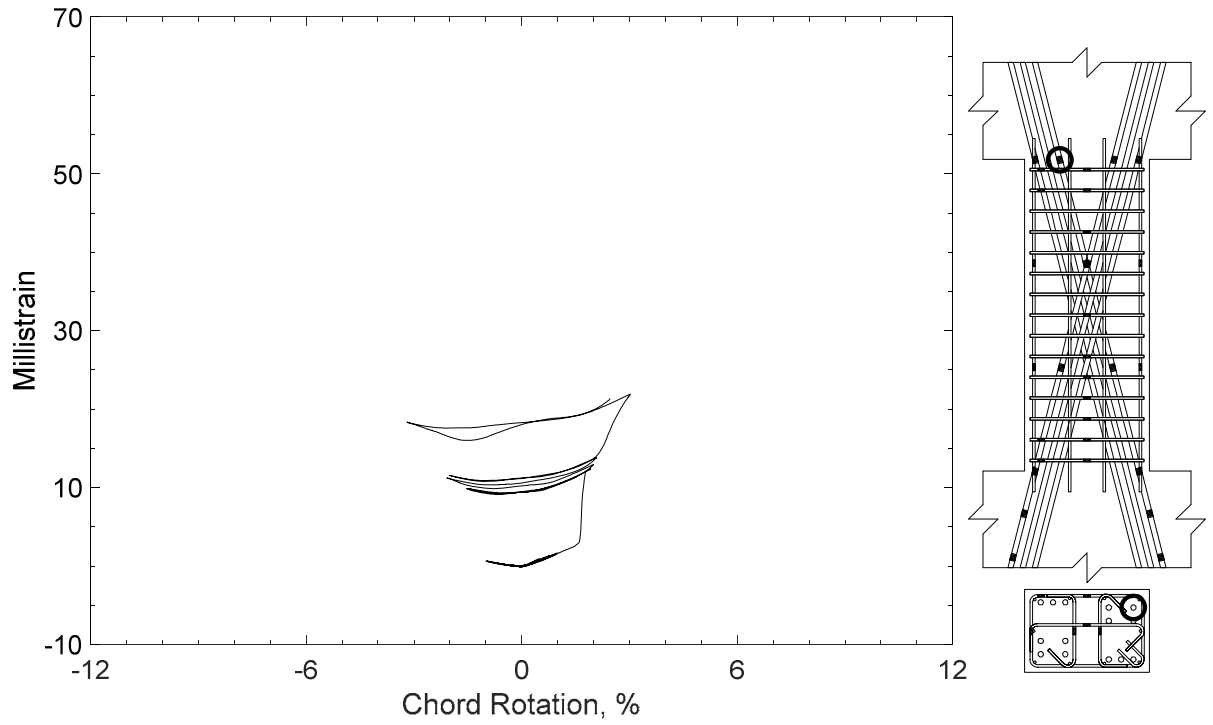


Figure 211 – Measured strain in diagonal bar of D80-2.5, strain gauge D11

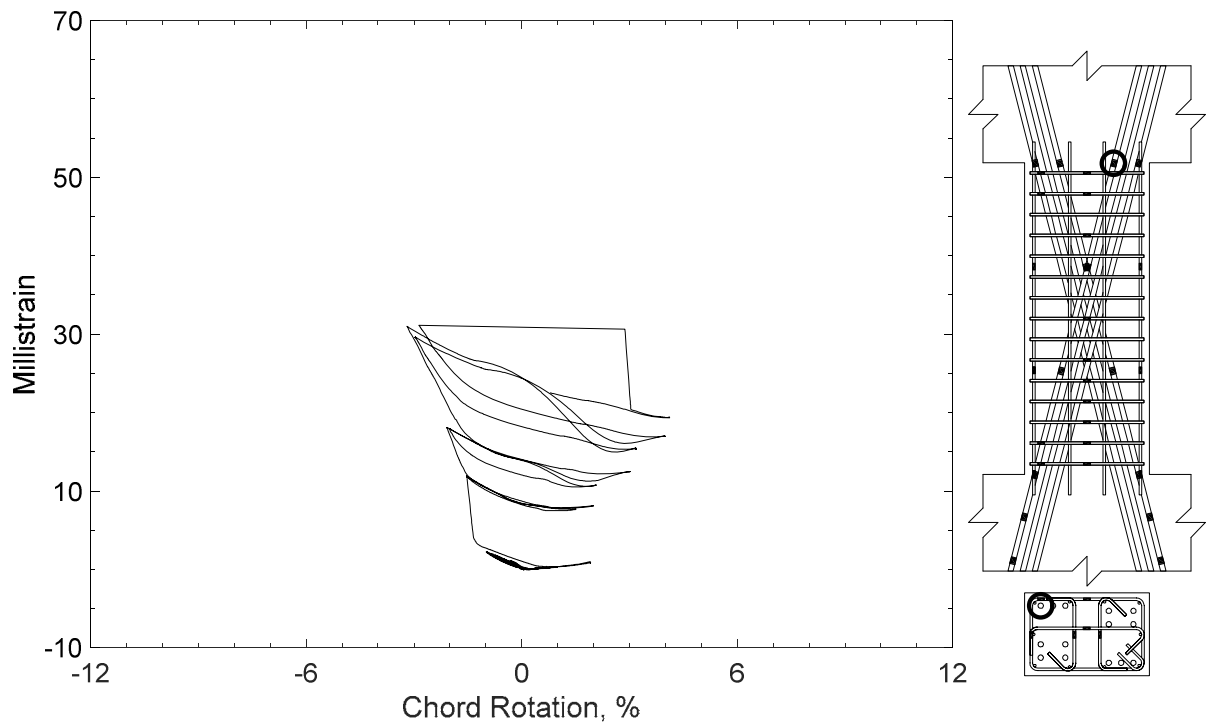


Figure 212 – Measured strain in diagonal bar of D80-2.5, strain gauge D12

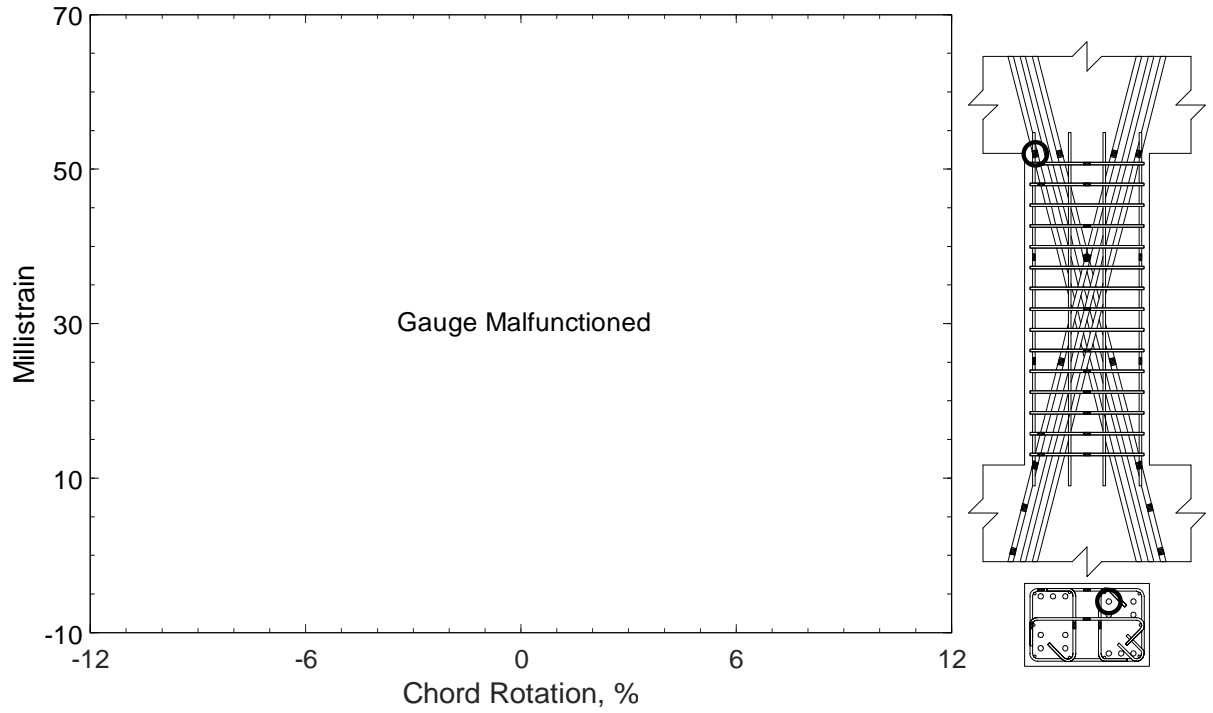


Figure 213 – Measured strain in diagonal bar of D80-2.5, strain gauge D13

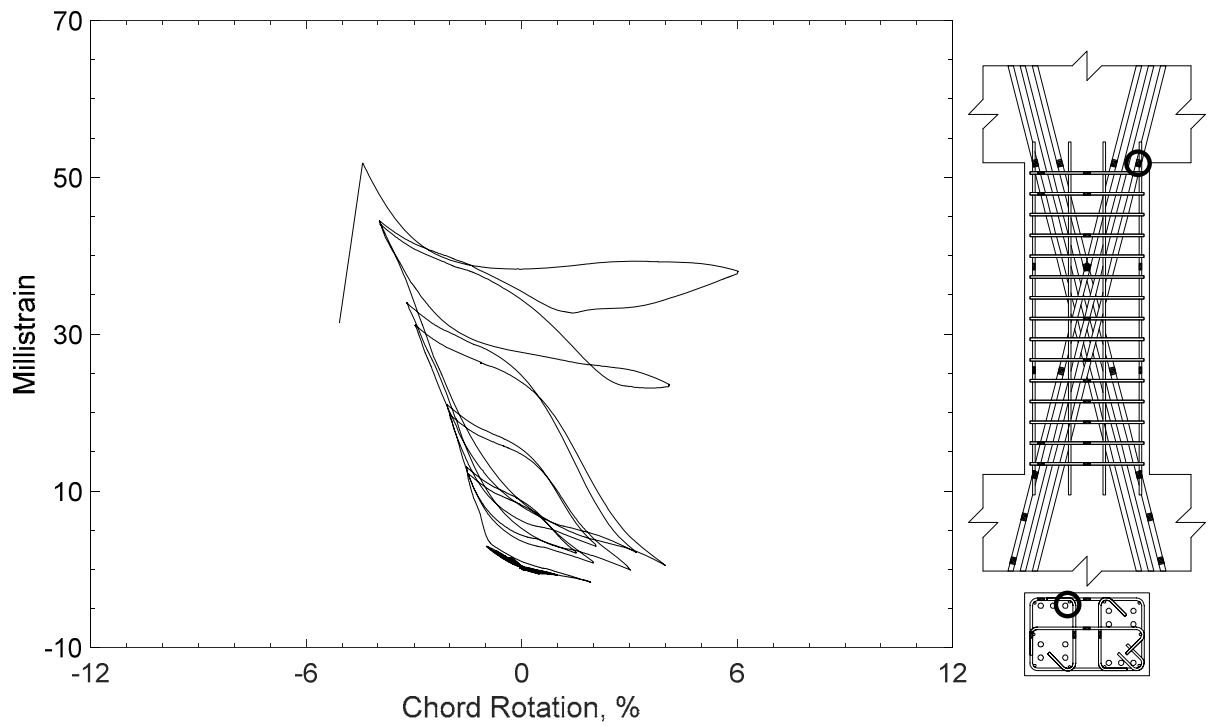


Figure 214 – Measured strain in diagonal bar of D80-2.5, strain gauge D14

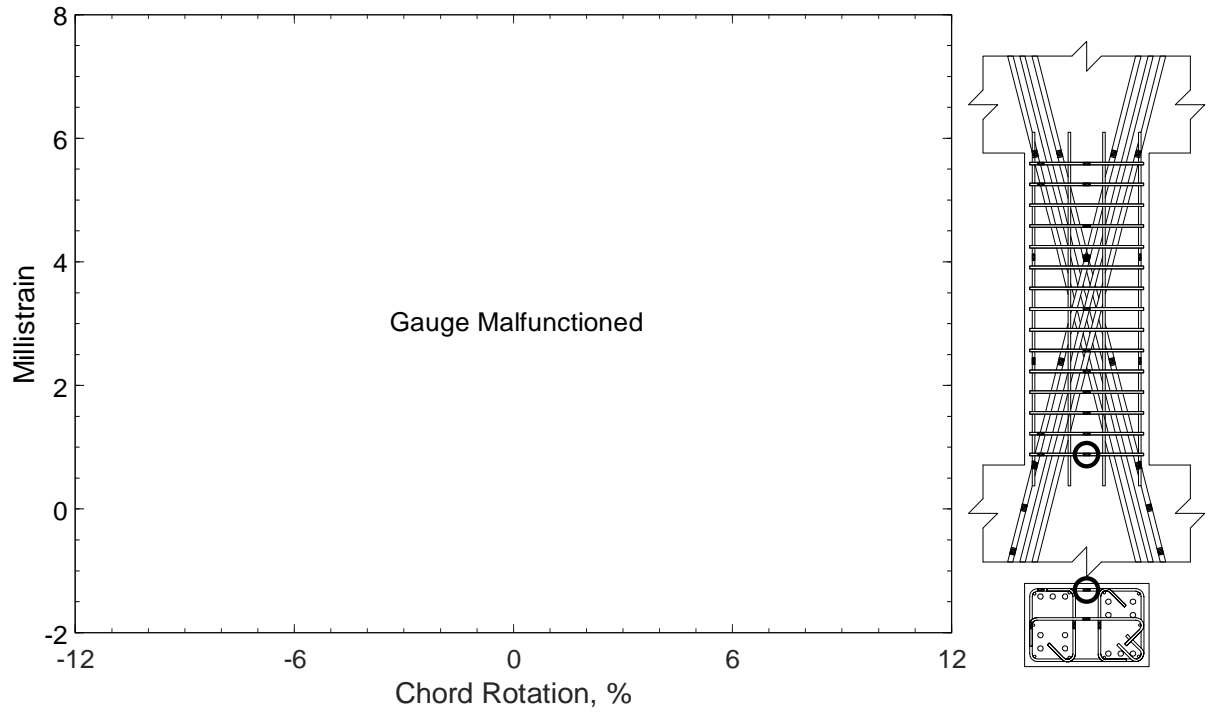


Figure 215 – Measured strain in closed stirrup of D80-2.5, strain gauge S1

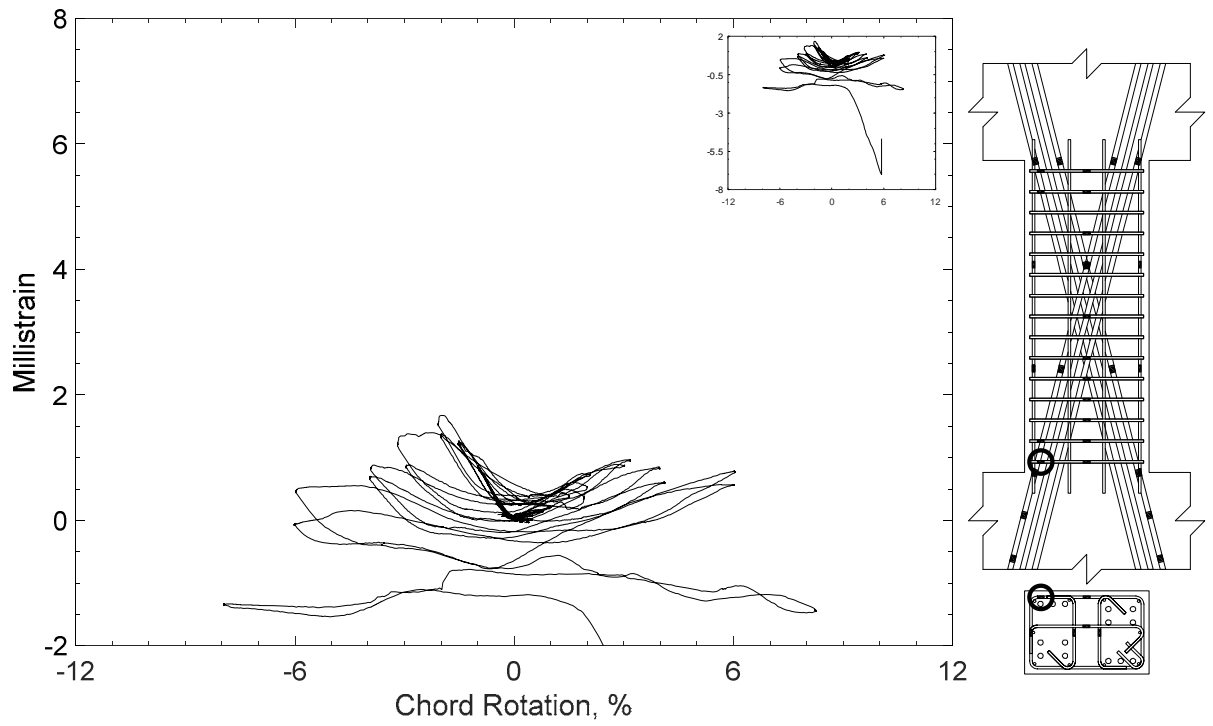


Figure 216 – Measured strain in closed stirrup of D80-2.5, strain gauge S2

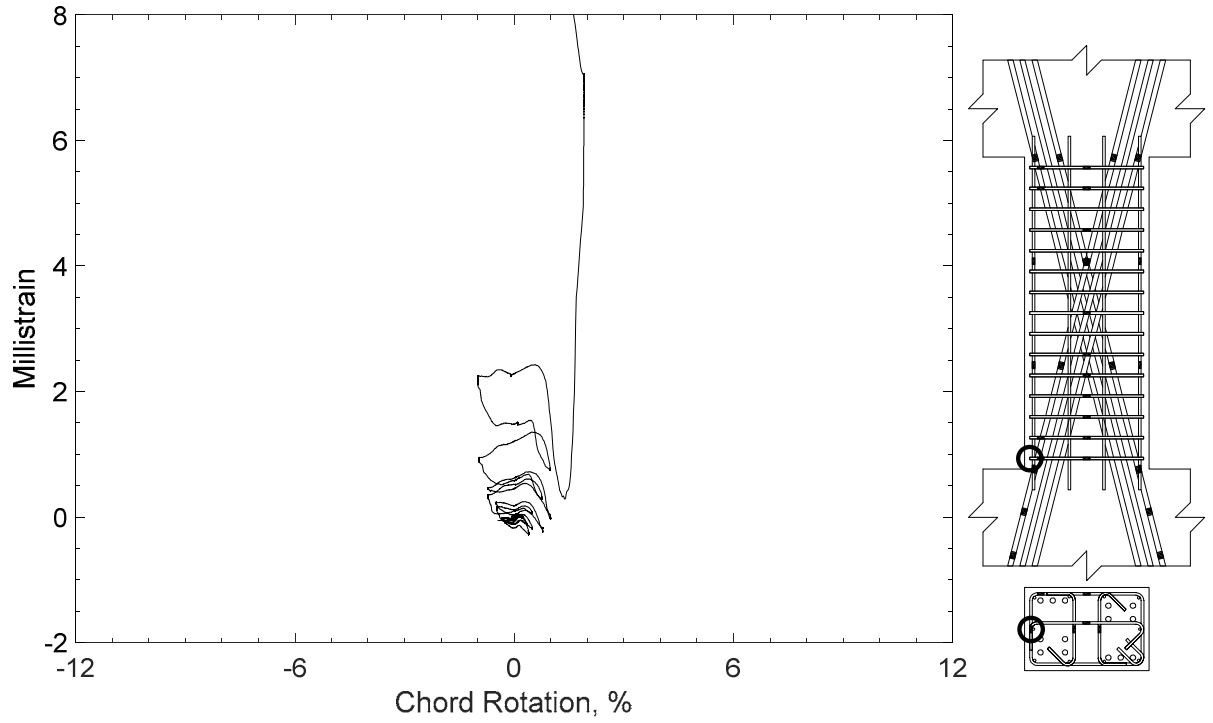


Figure 217 – Measured strain in closed stirrup of D80-2.5, strain gauge S3

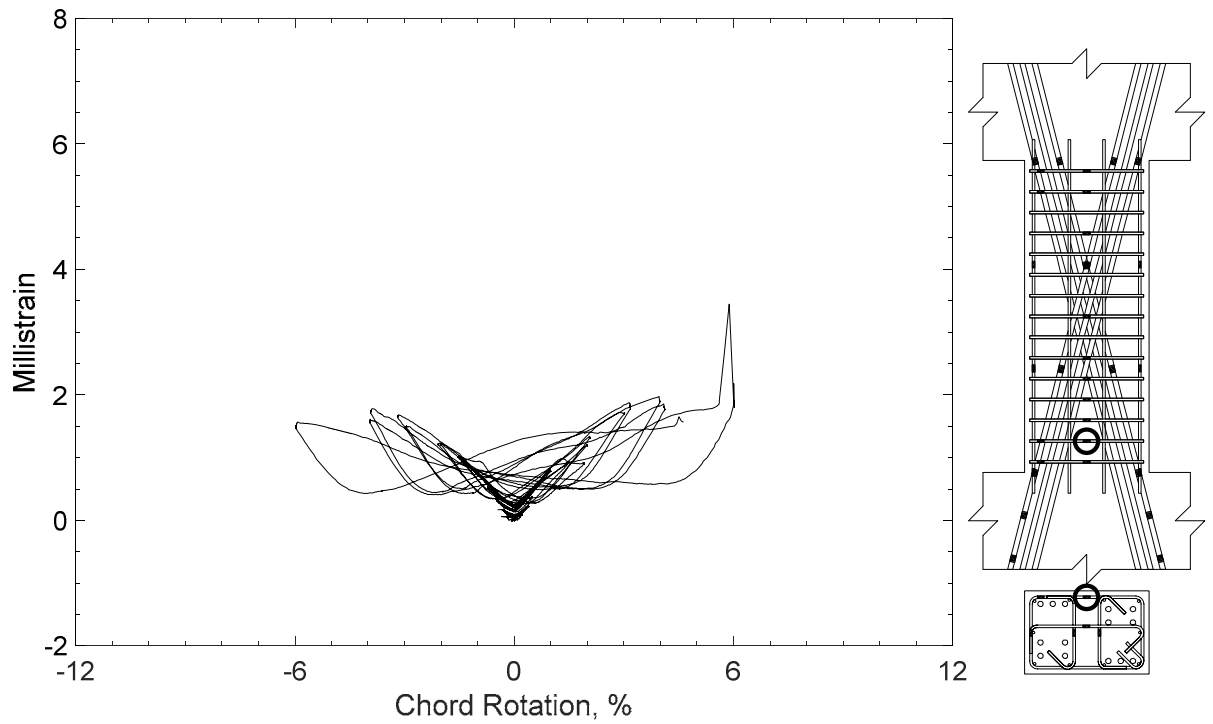


Figure 218 – Measured strain in closed stirrup of D80-2.5, strain gauge S4

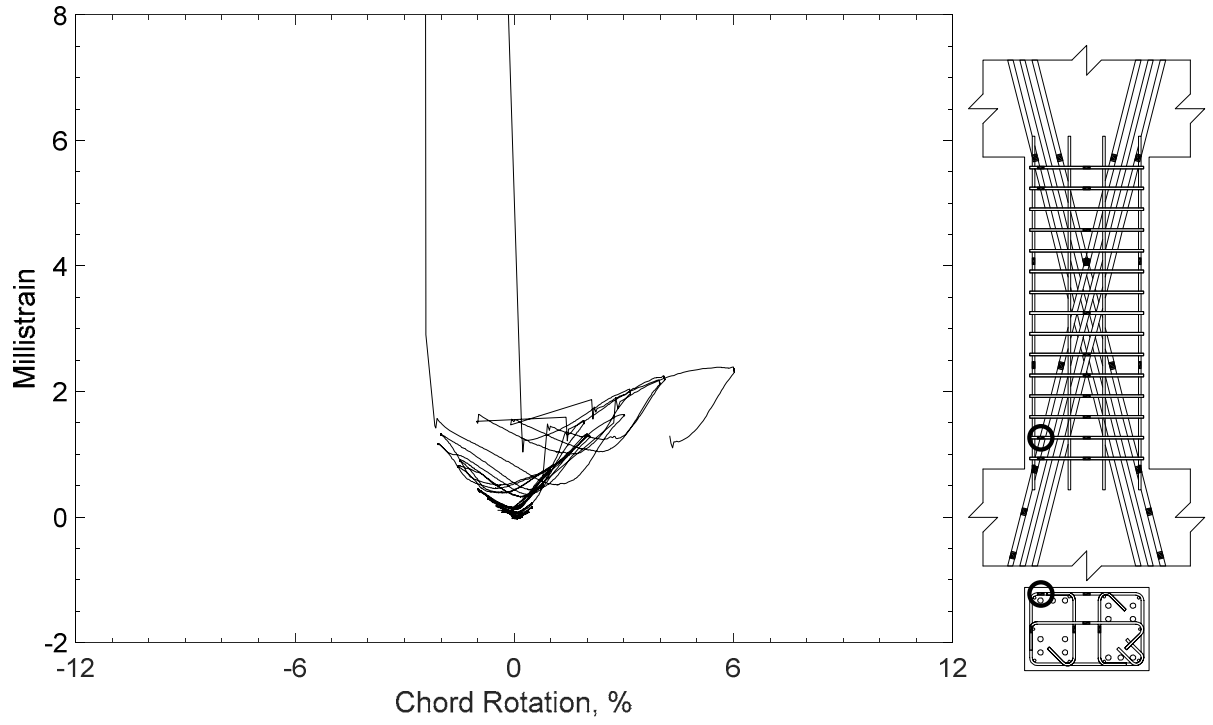


Figure 219 – Measured strain in closed stirrup of D80-2.5, strain gauge S5

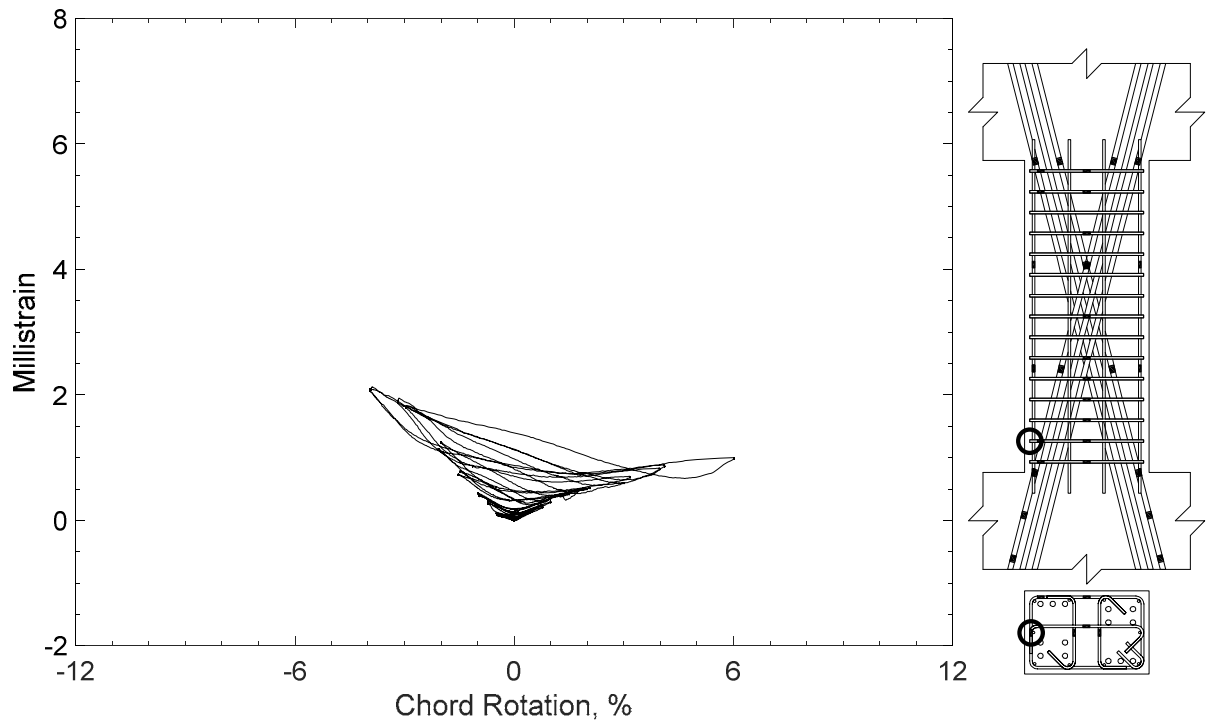


Figure 220 – Measured strain in closed stirrup of D80-2.5, strain gauge S6

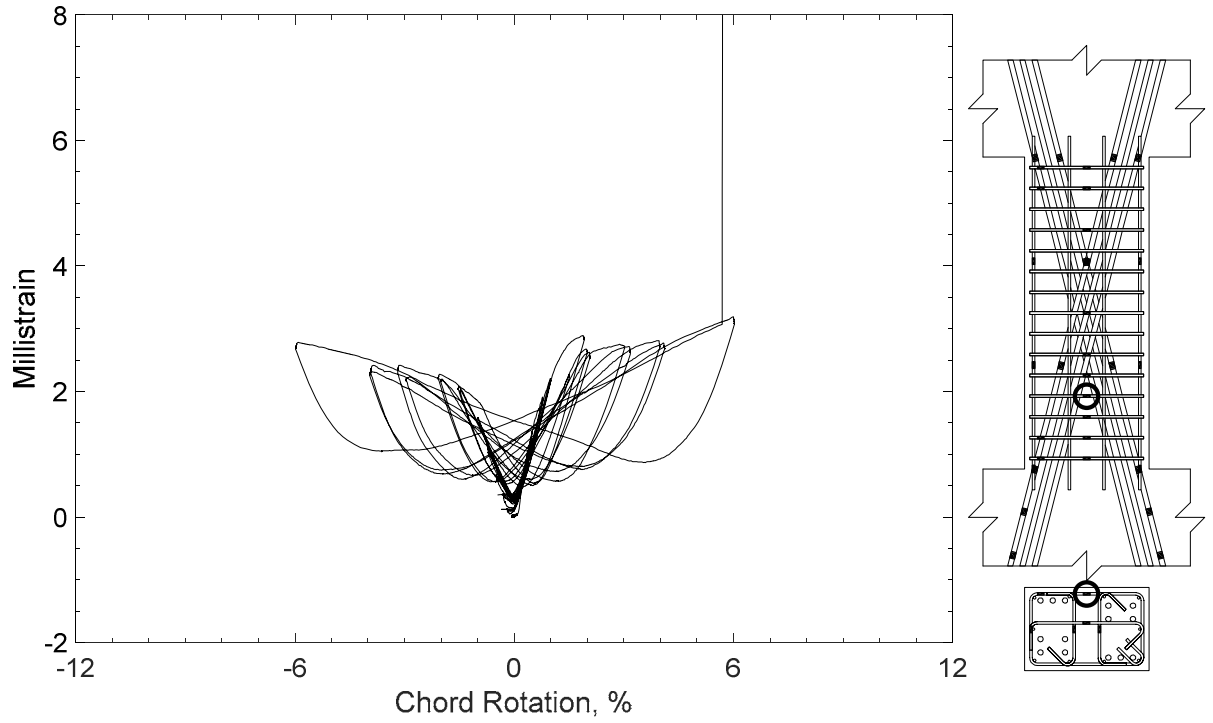


Figure 221 – Measured strain in closed stirrup of D80-2.5, strain gauge S7

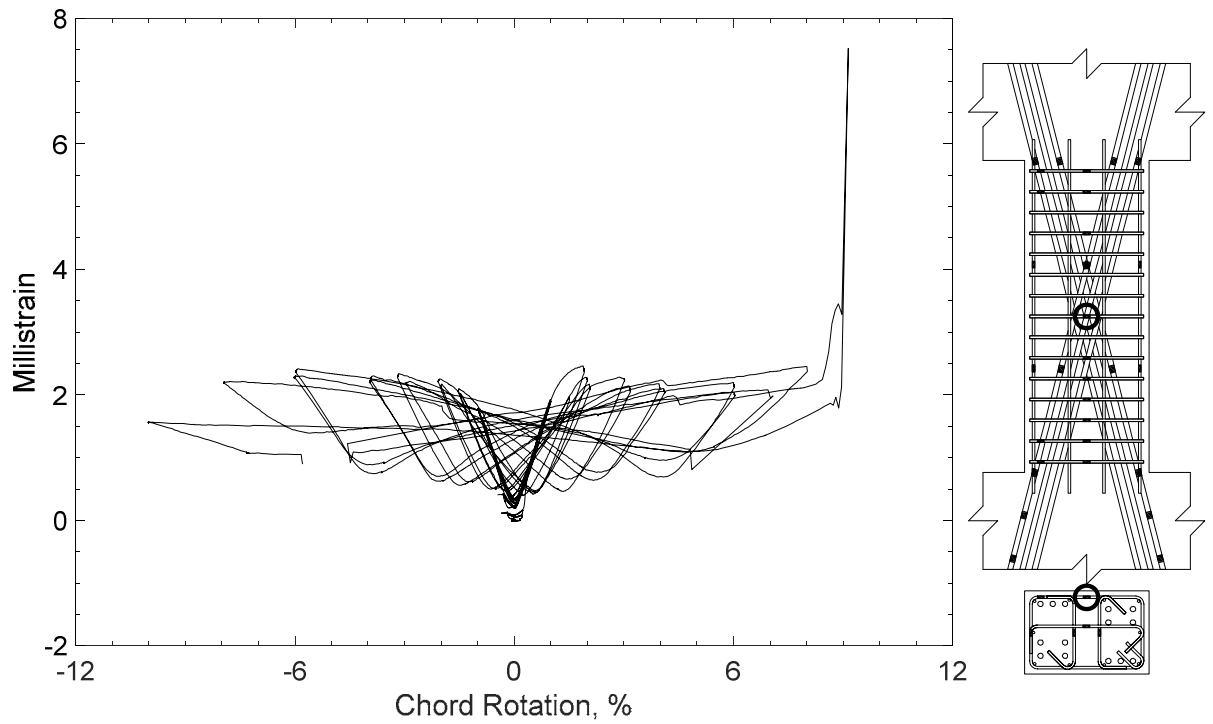


Figure 222 – Measured strain in closed stirrup of D80-2.5, strain gauge S8

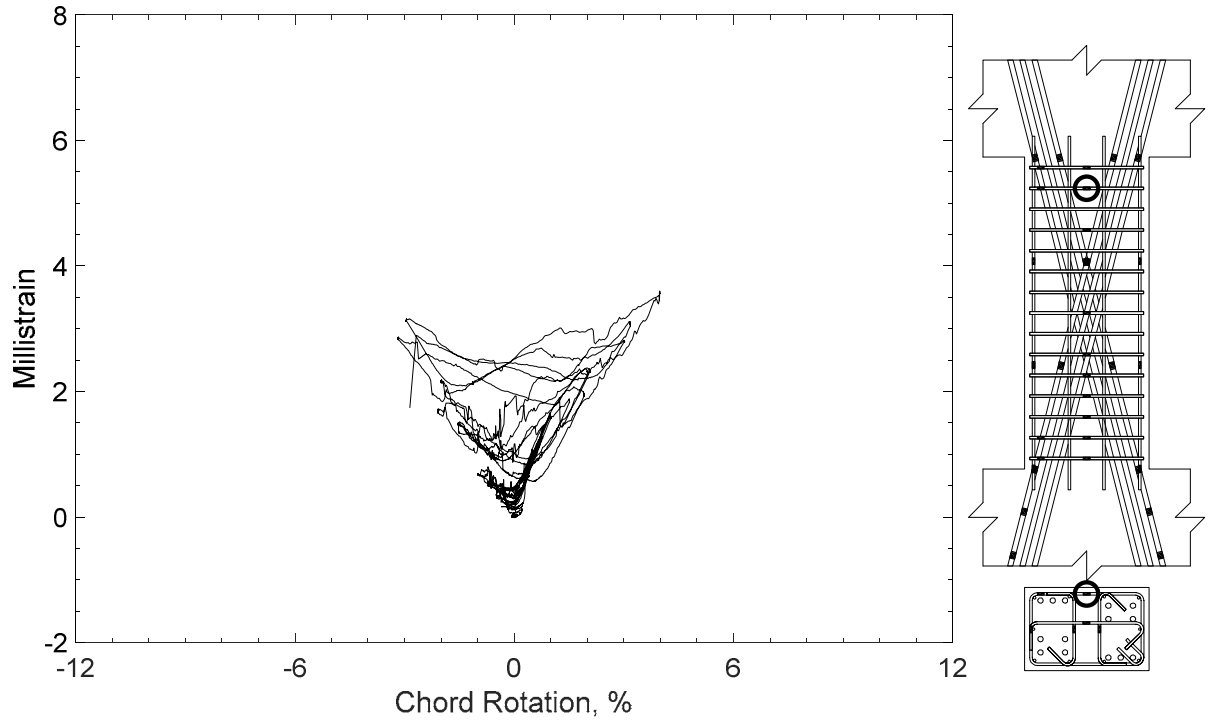


Figure 223 – Measured strain in closed stirrup of D80-2.5, strain gauge S9

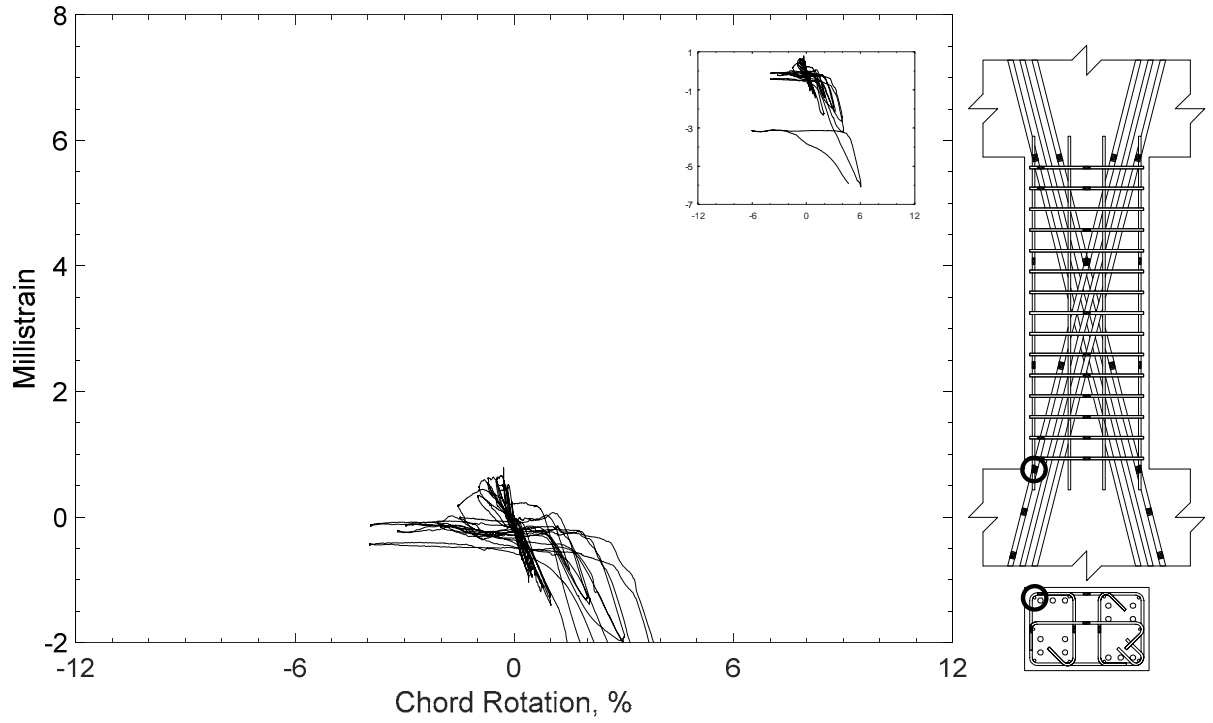


Figure 224 – Measured strain in parallel bar of D80-2.5, strain gauge H1

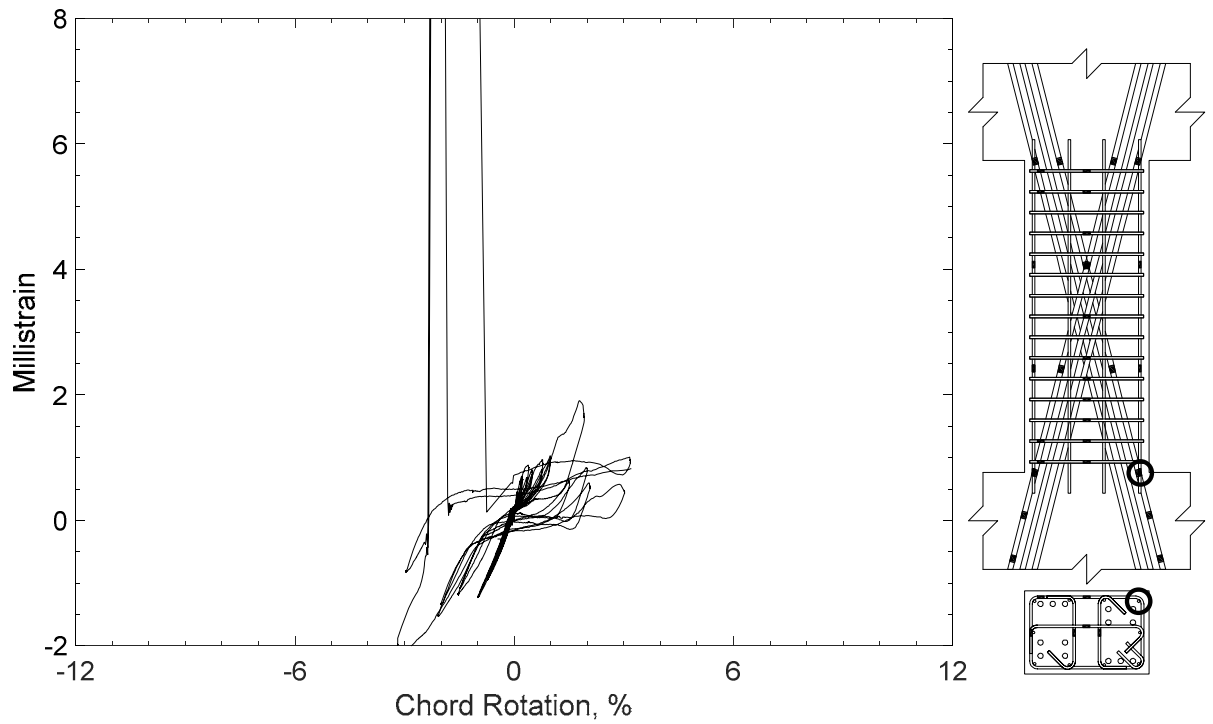


Figure 225 – Measured strain in parallel bar of D80-2.5, strain gauge H2

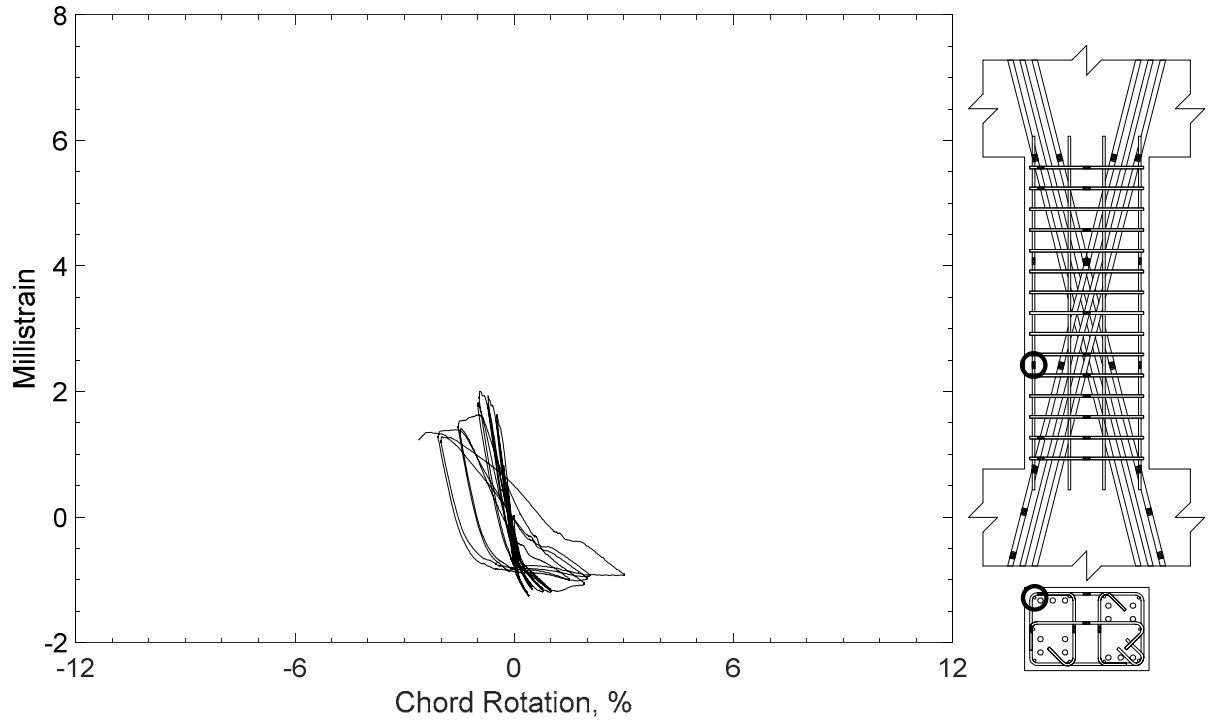


Figure 226 – Measured strain in parallel bar of D80-2.5, strain gauge H3

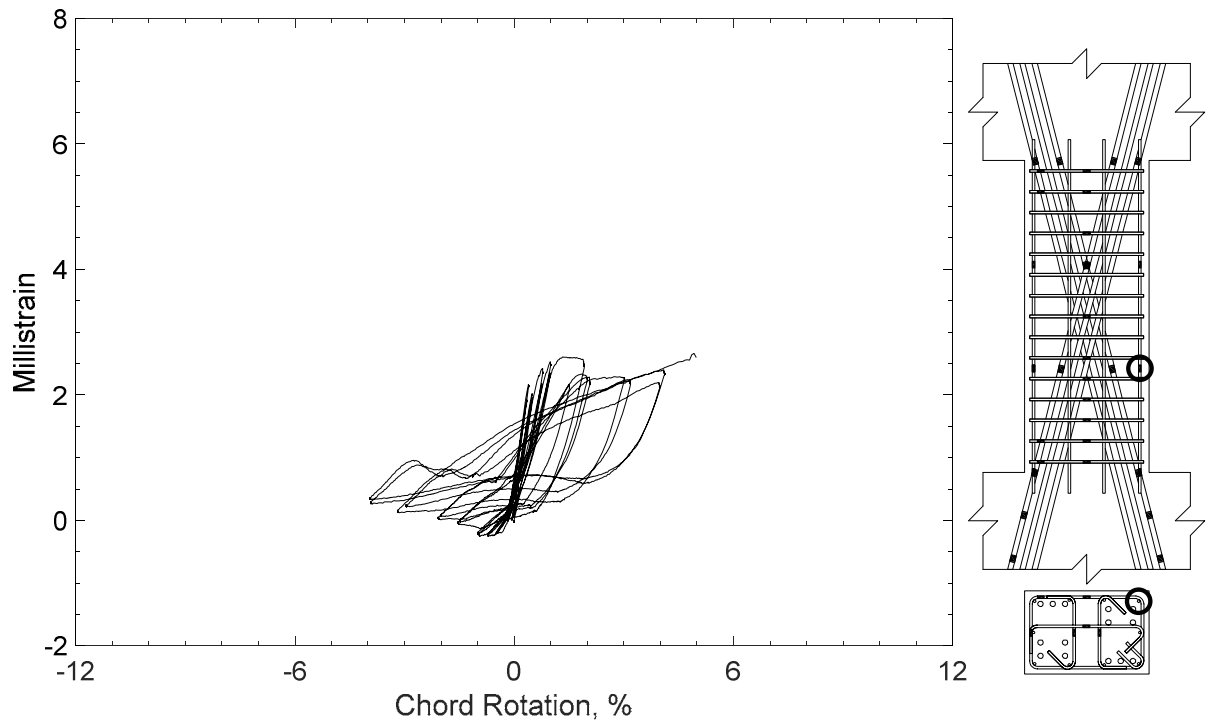


Figure 227 – Measured strain in parallel bar of D80-2.5, strain gauge H4

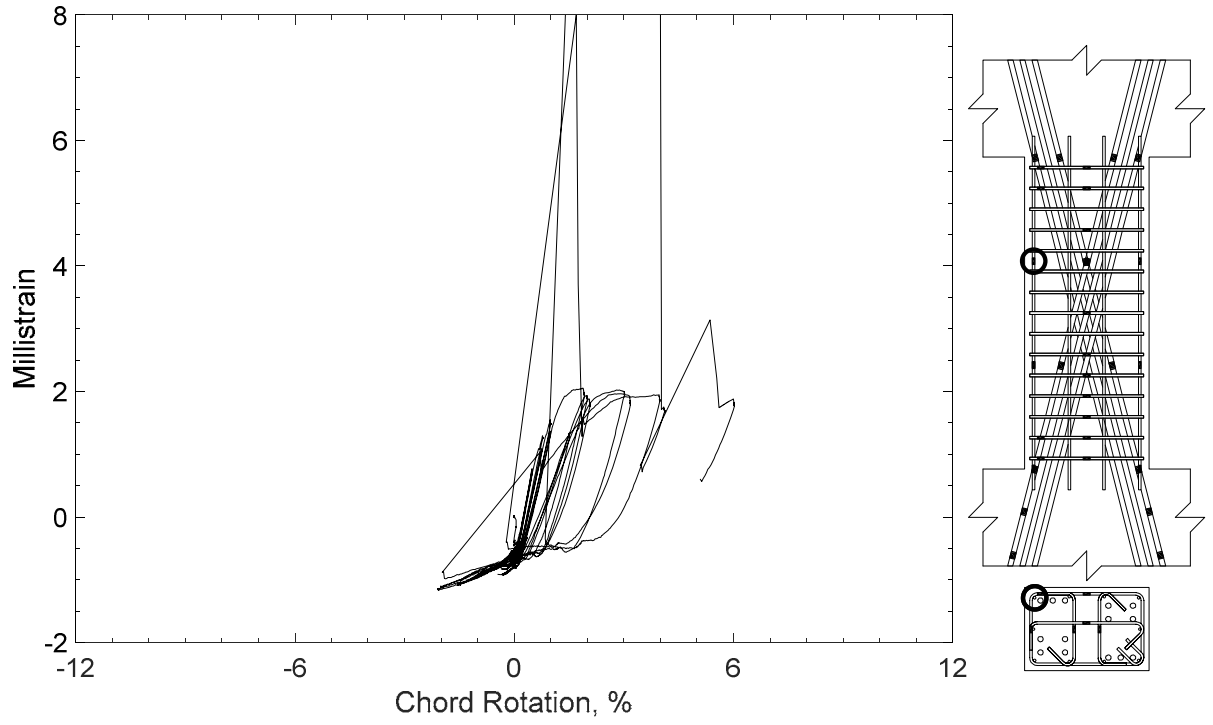


Figure 228 – Measured strain in parallel bar of D80-2.5, strain gauge H5

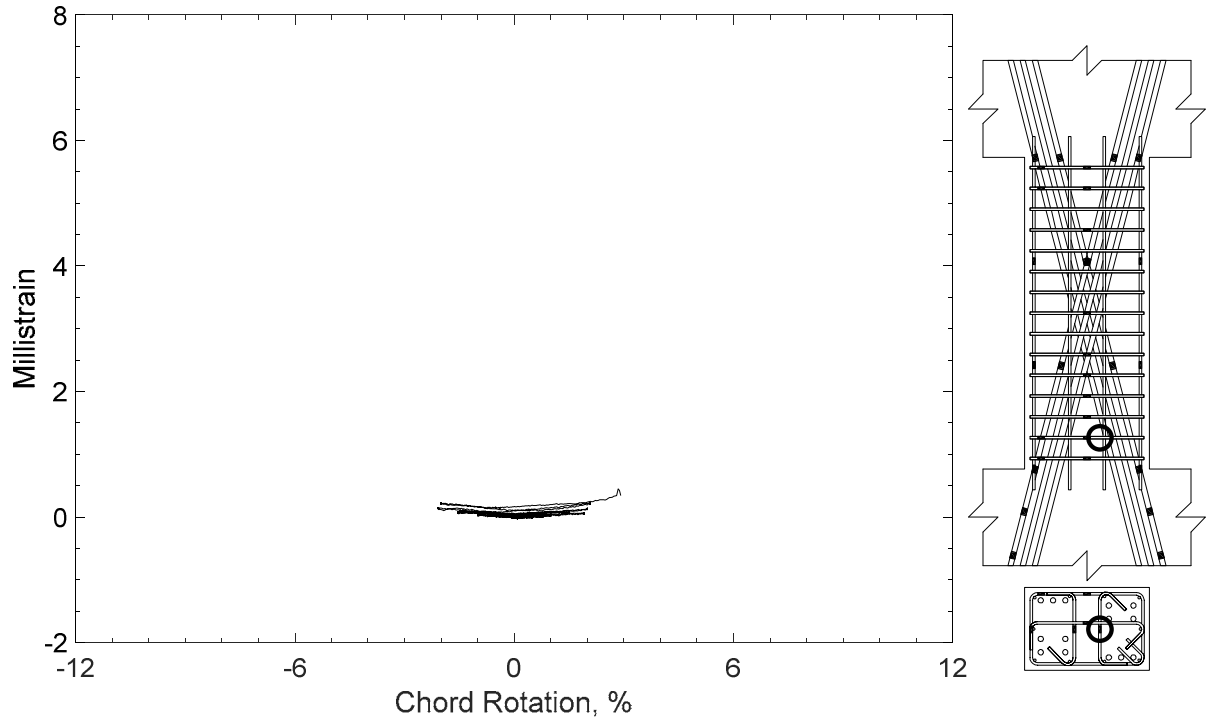


Figure 229 – Measured strain in crosstie of D80-2.5, strain gauge T1

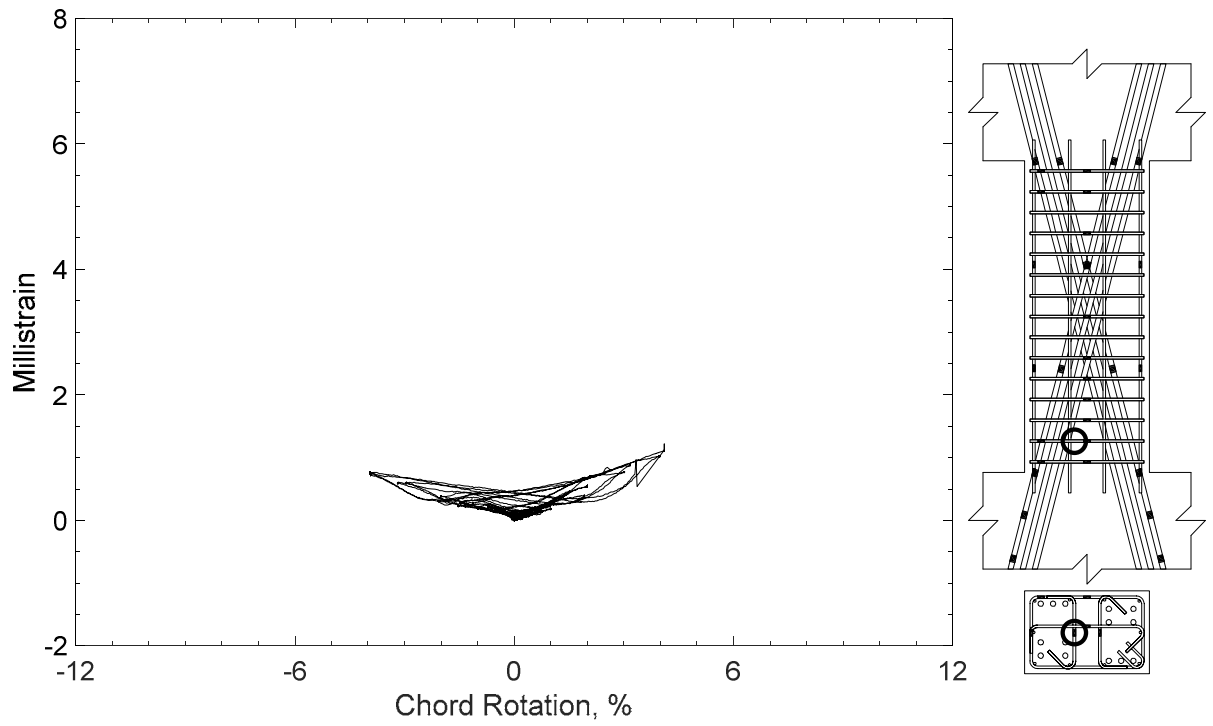


Figure 230 – Measured strain in crosstie of D80-2.5, strain gauge T2

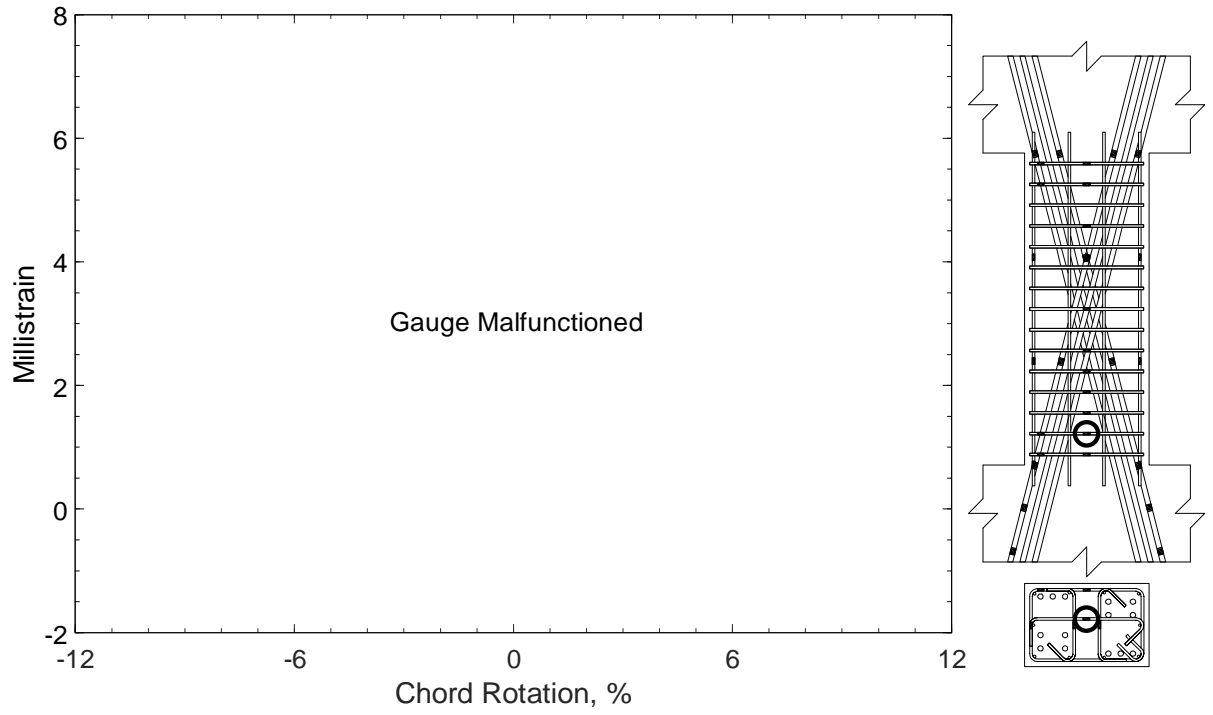


Figure 231 – Measured strain in crosstie of D80-2.5, strain gauge T3

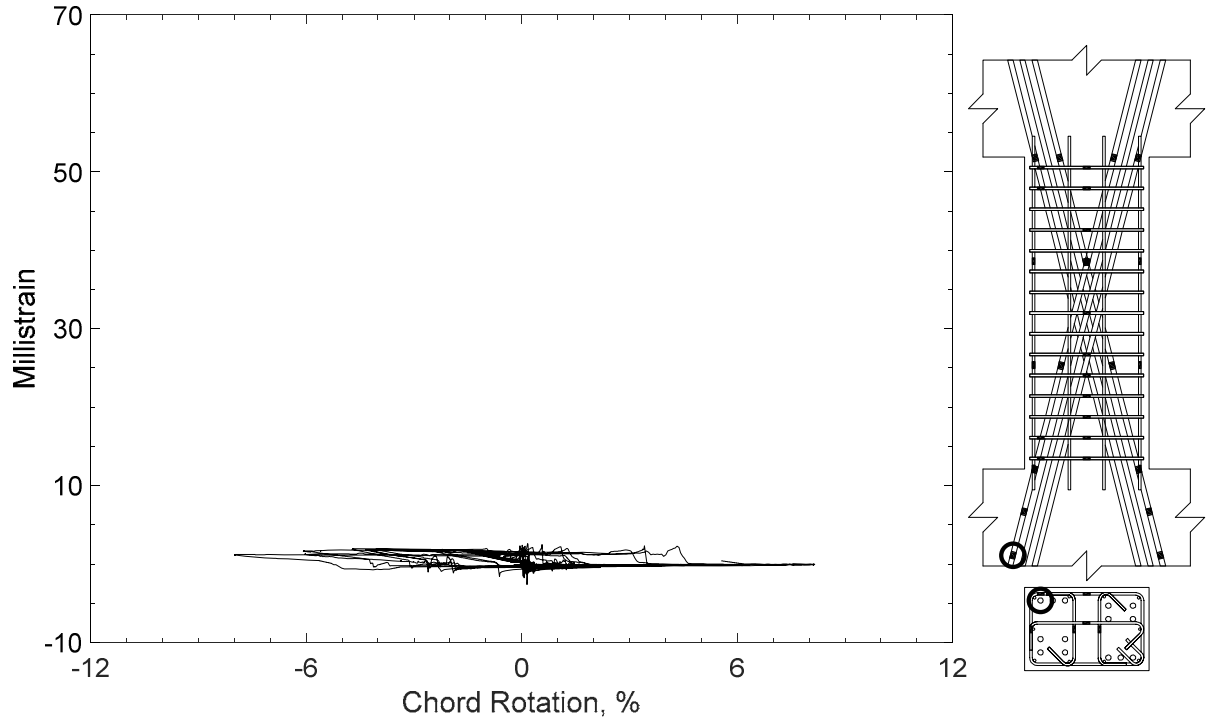


Figure 232 – Measured strain in diagonal bar of D100-2.5, strain gauge D1

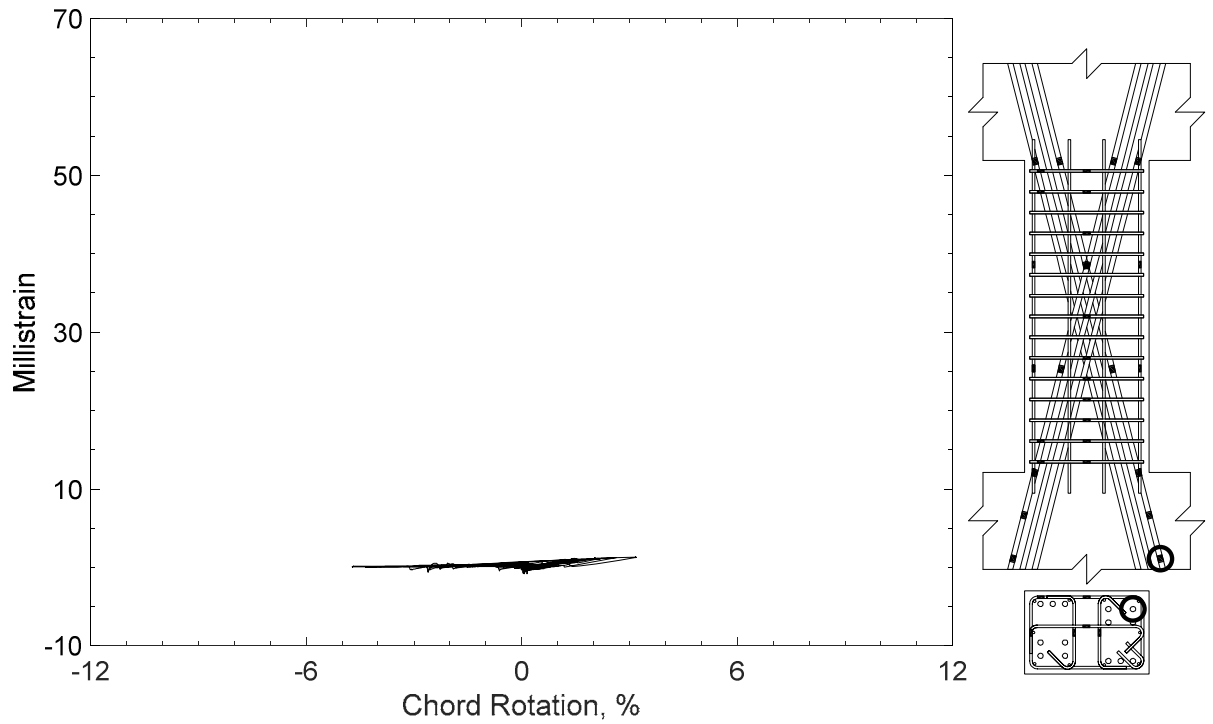


Figure 233 – Measured strain in diagonal bar of D100-2.5, strain gauge D2

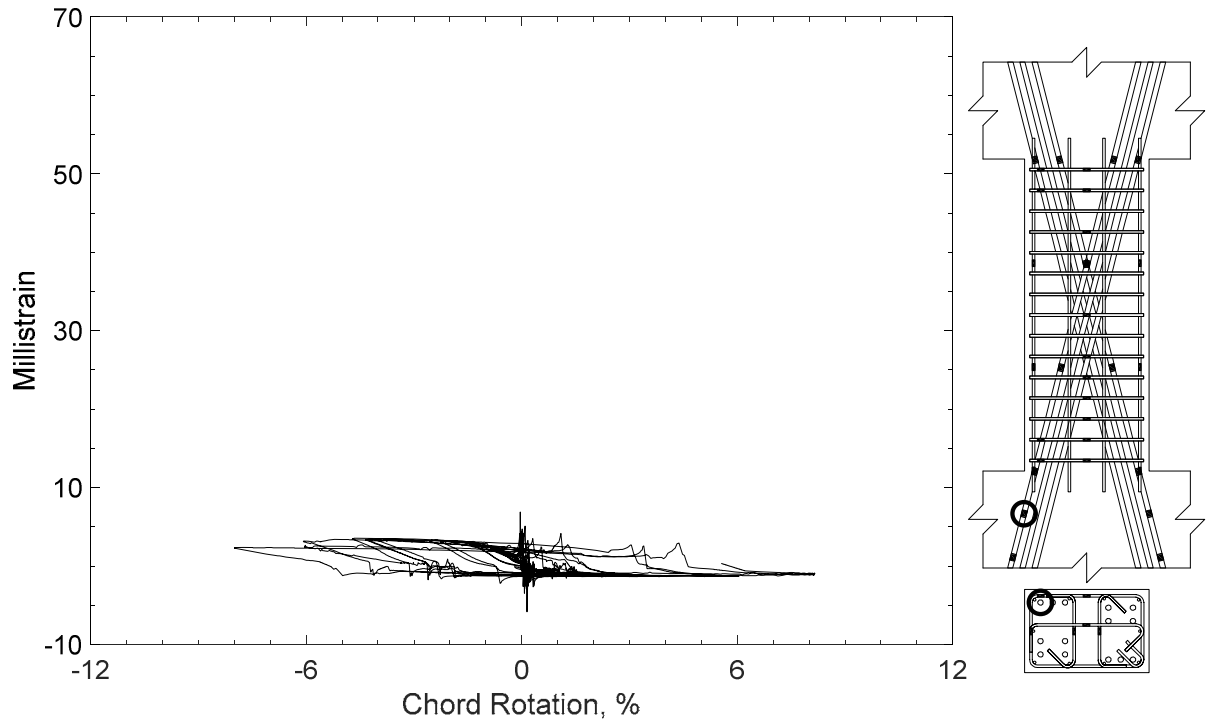


Figure 234 – Measured strain in diagonal bar of D100-2.5, strain gauge D3

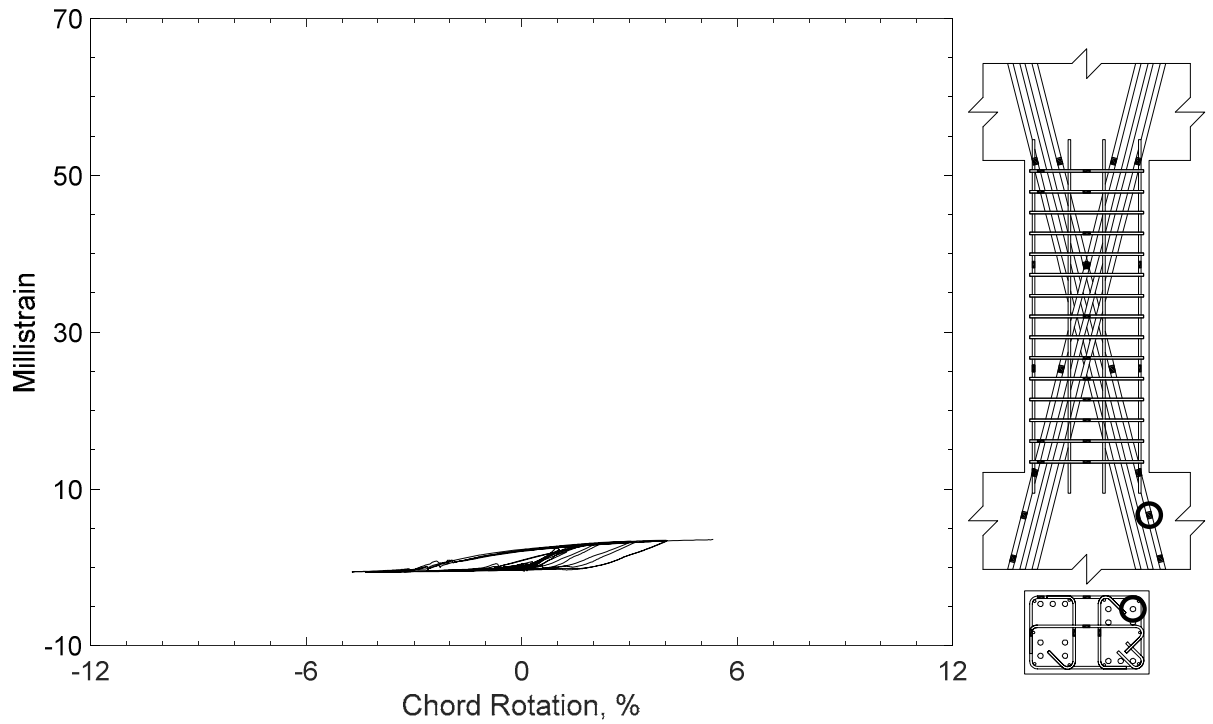


Figure 235 – Measured strain in diagonal bar of D100-2.5, strain gauge D4

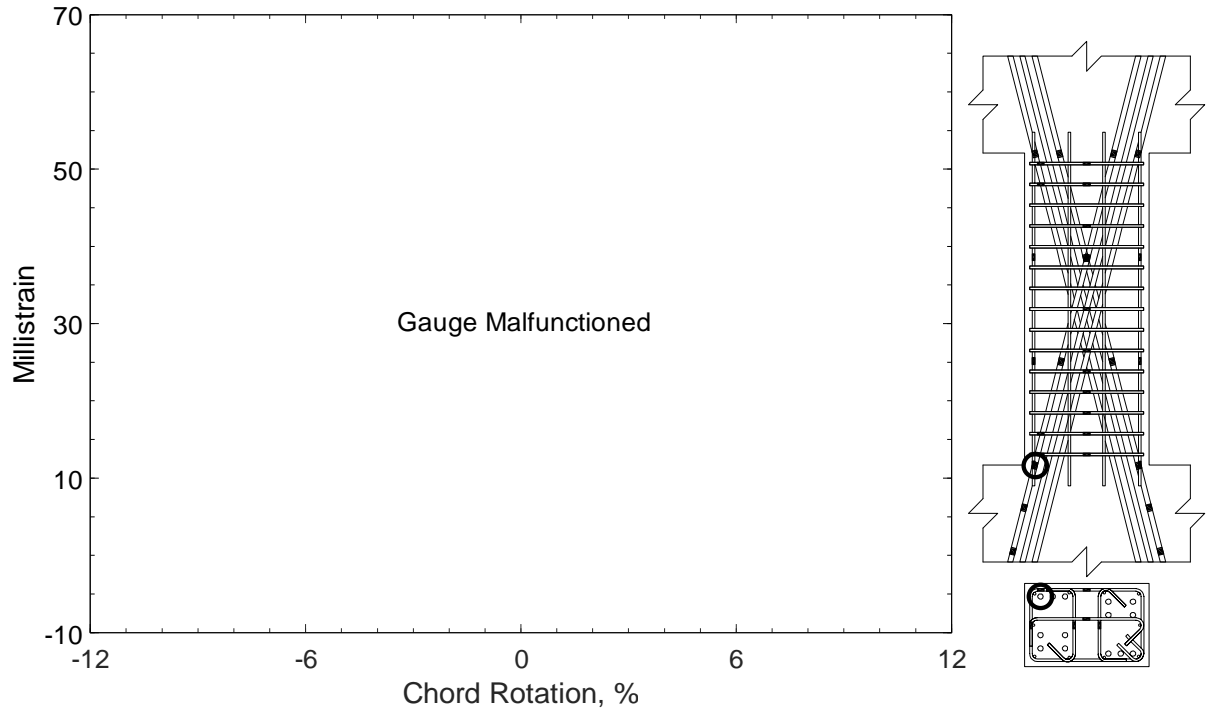


Figure 236 – Measured strain in diagonal bar of D100-2.5, strain gauge D5

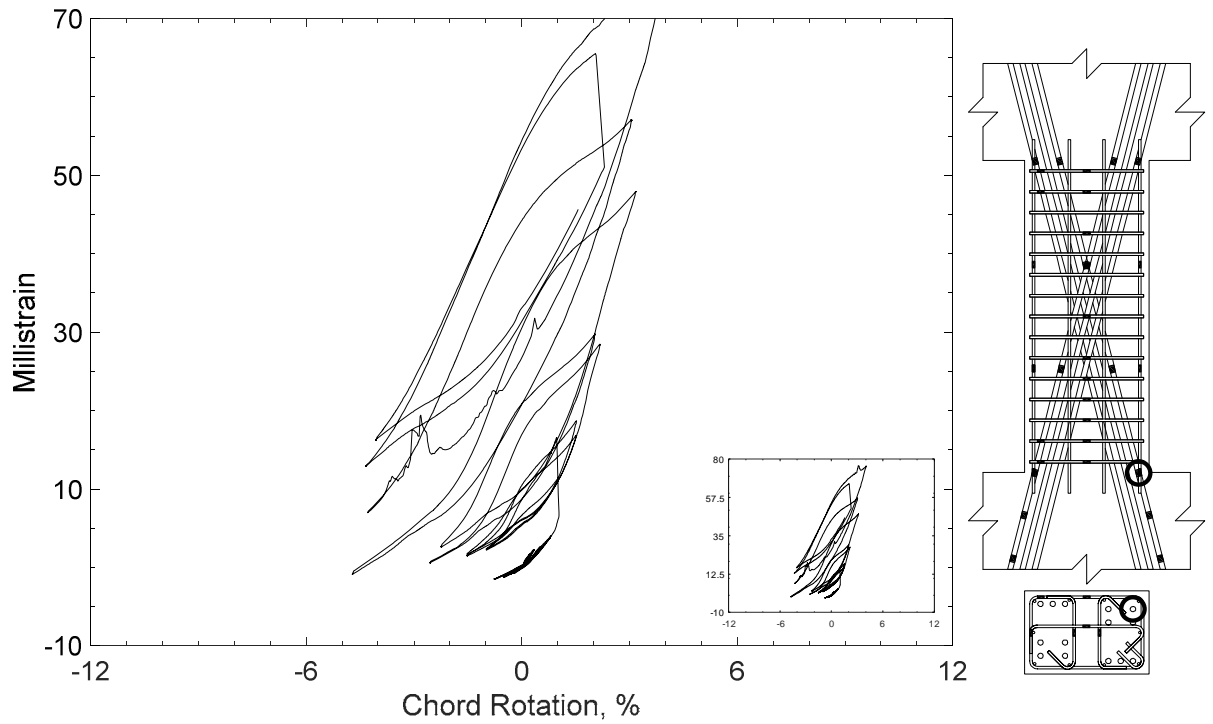


Figure 237 – Measured strain in diagonal bar of D100-2.5, strain gauge D6

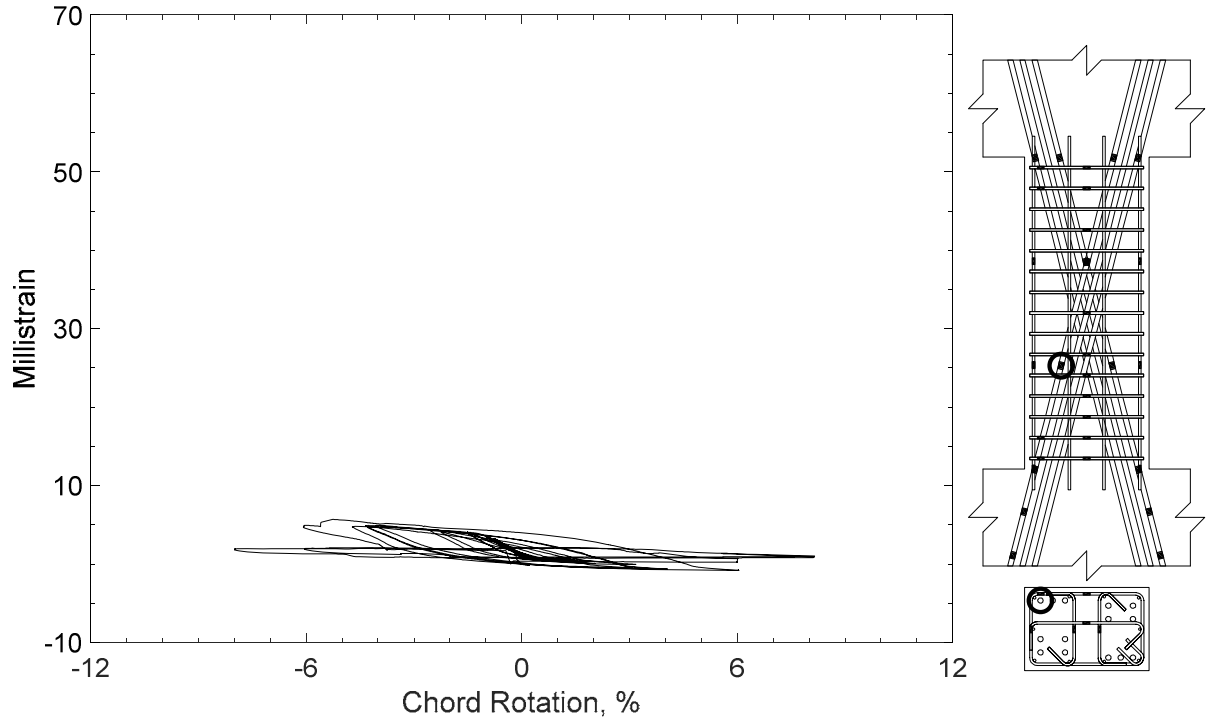


Figure 238 – Measured strain in diagonal bar of D100-2.5, strain gauge D7

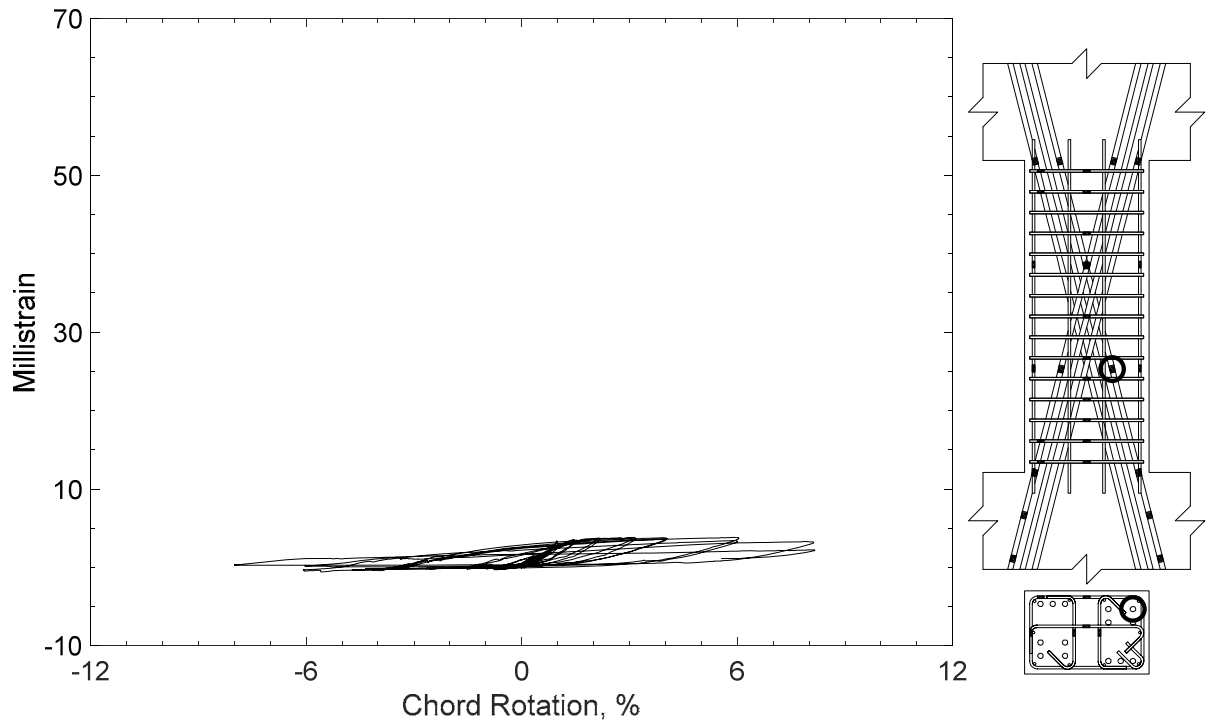


Figure 239 – Measured strain in diagonal bar of D100-2.5, strain gauge D8

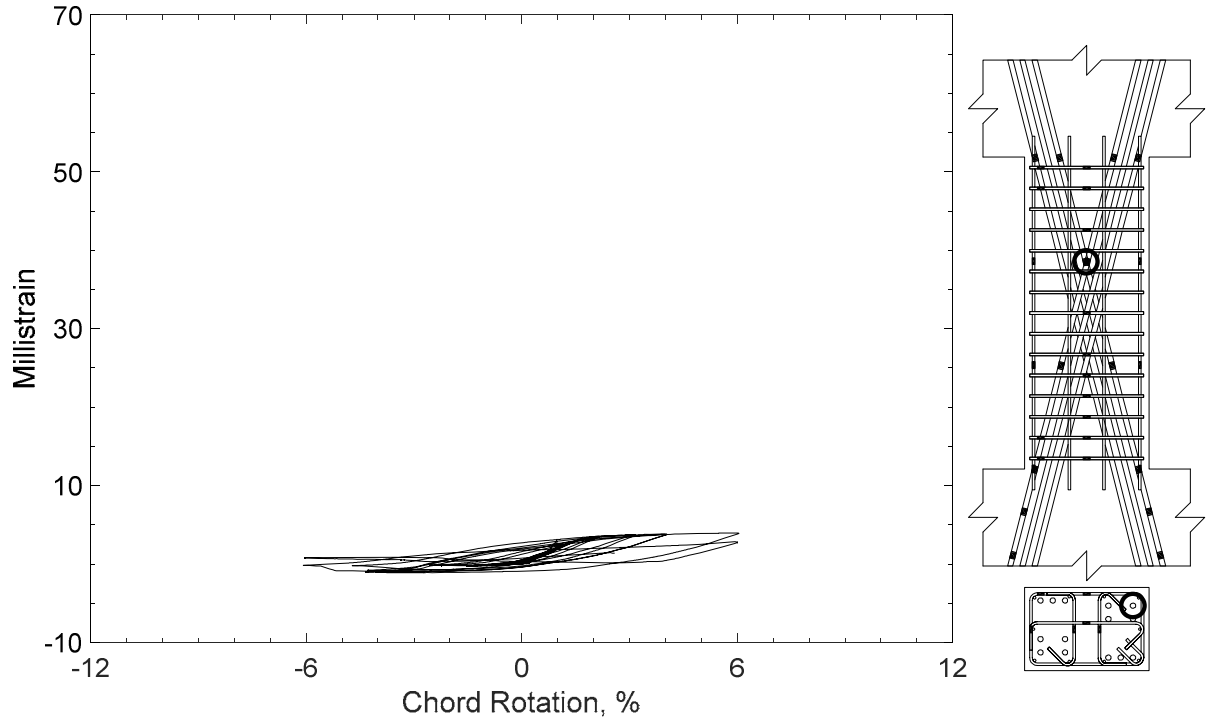


Figure 240 – Measured strain in diagonal bar of D100-2.5, strain gauge D9

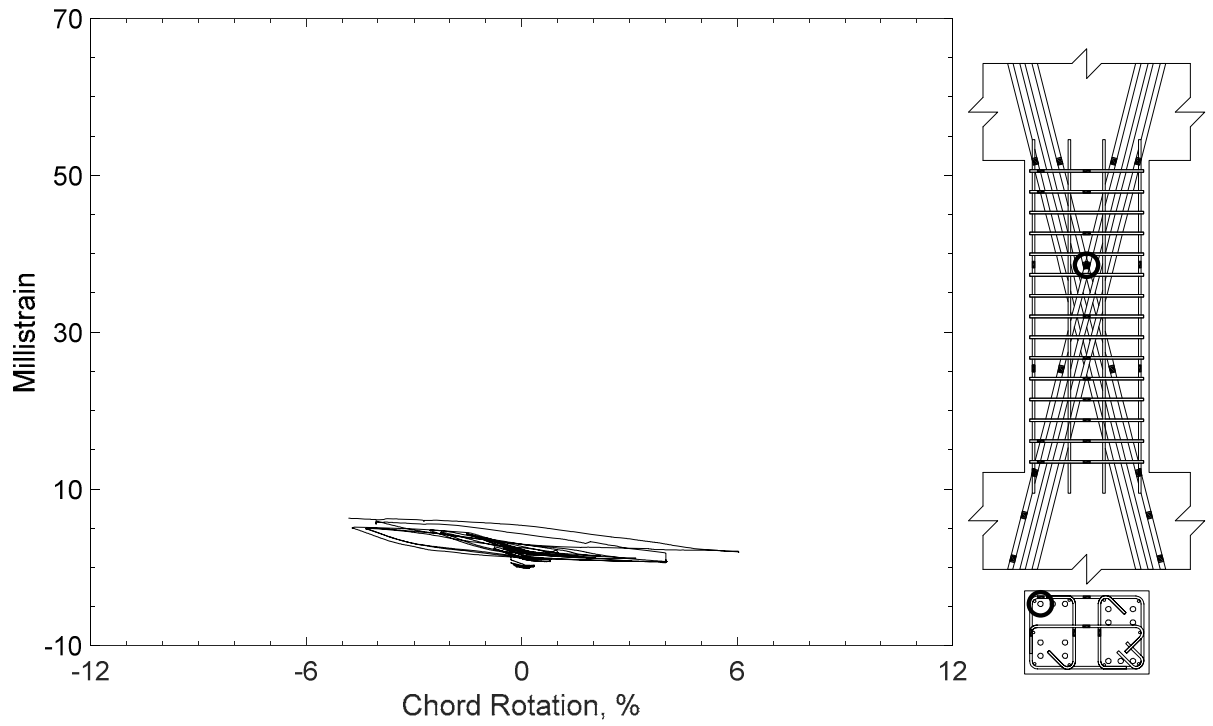


Figure 241 – Measured strain in diagonal bar of D100-2.5, strain gauge D10

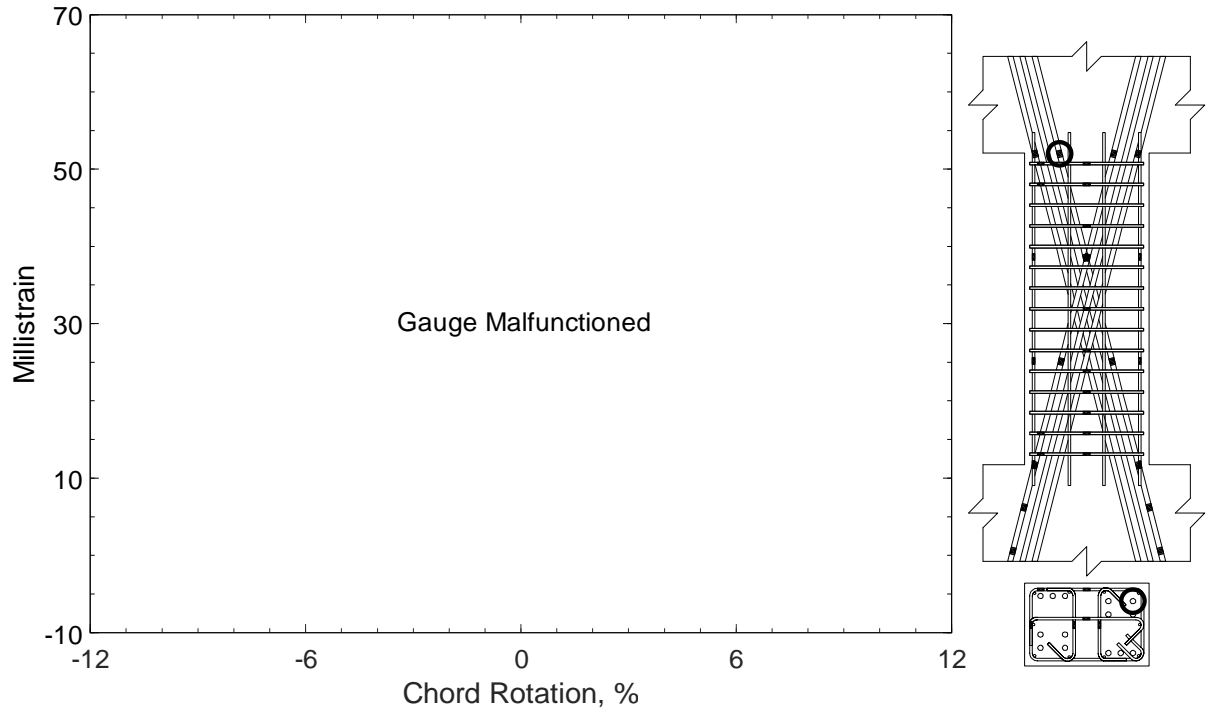


Figure 242 – Measured strain in diagonal bar of D100-2.5, strain gauge D11

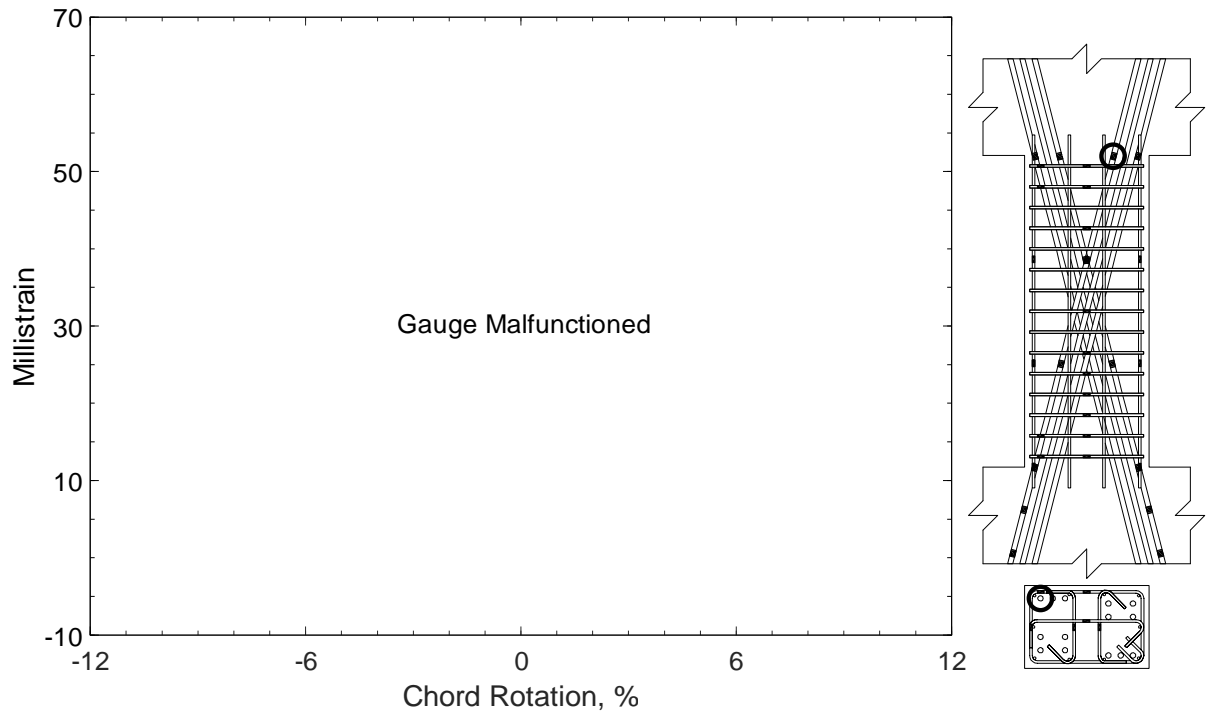


Figure 243 – Measured strain in diagonal bar of D100-2.5, strain gauge D12

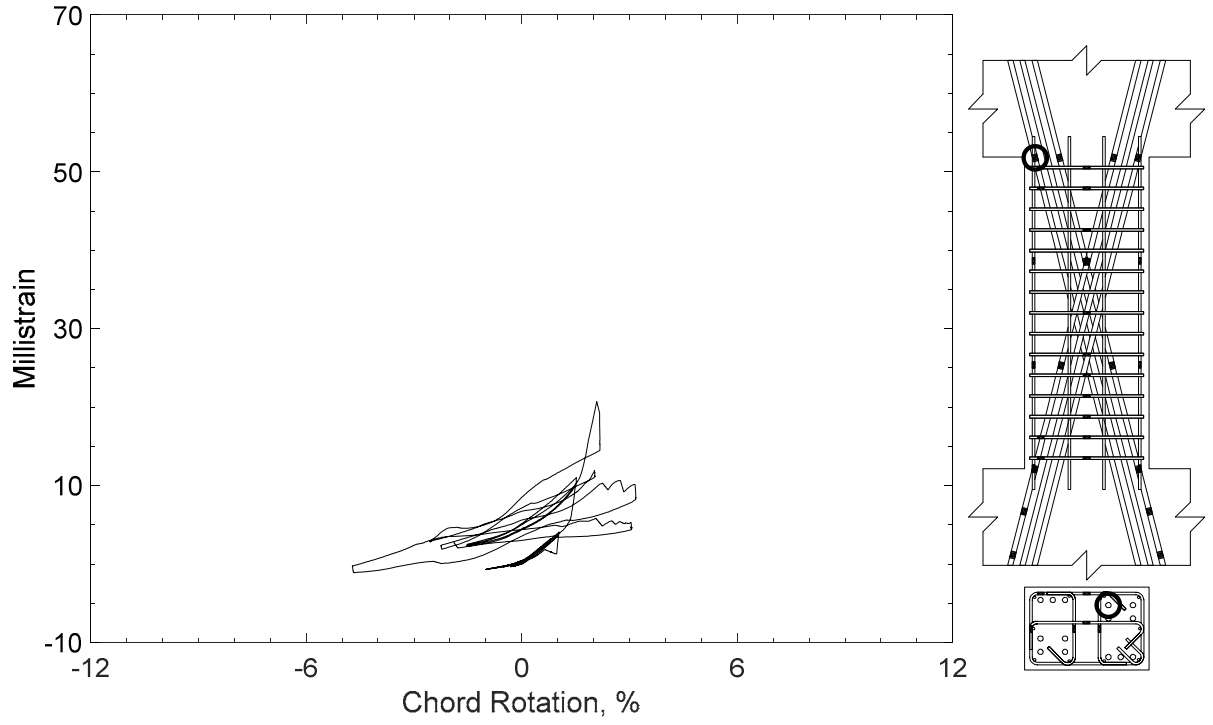


Figure 244 – Measured strain in diagonal bar of D100-2.5, strain gauge D13

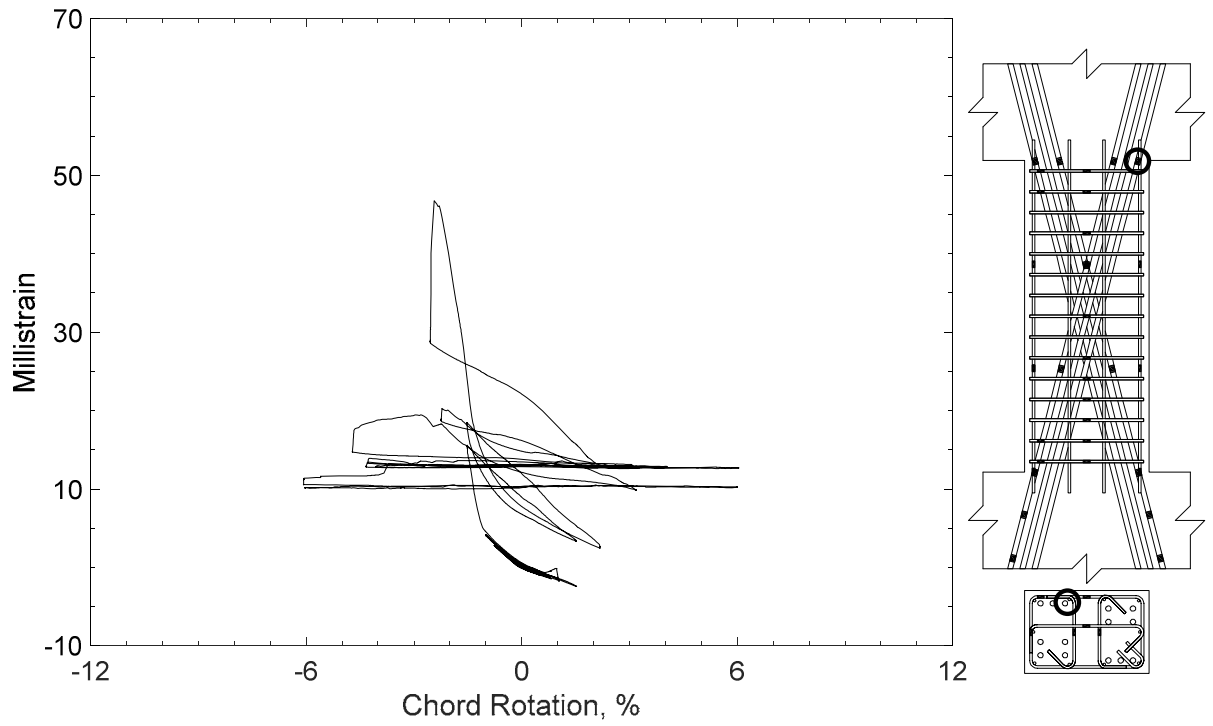


Figure 245 – Measured strain in diagonal bar of D100-2.5, strain gauge D14

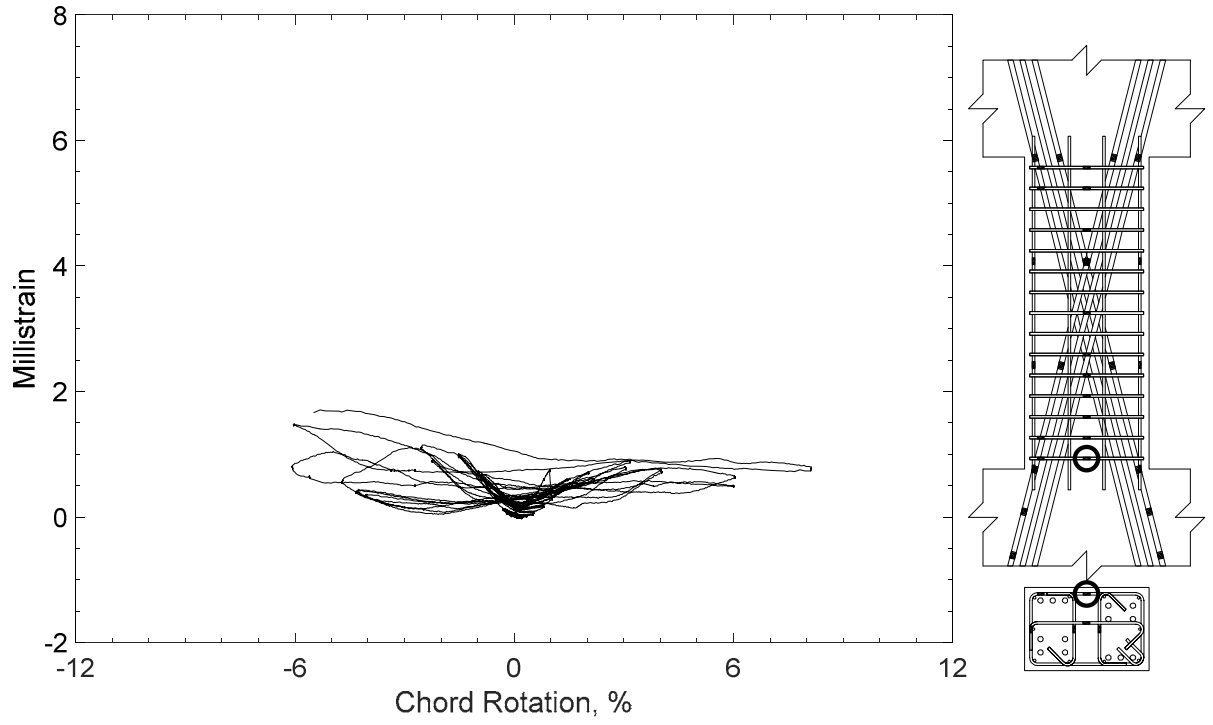


Figure 246 – Measured strain in closed stirrup of D100-2.5, strain gauge S1

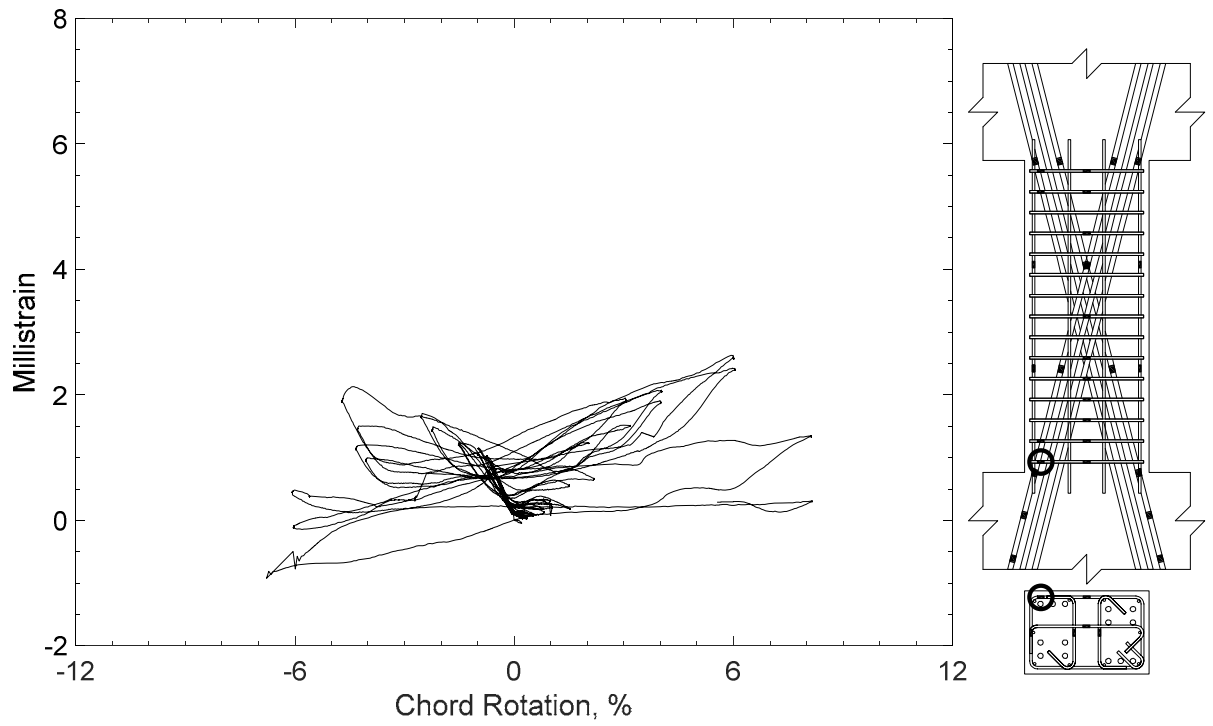


Figure 247 – Measured strain in closed stirrup of D100-2.5, strain gauge S2

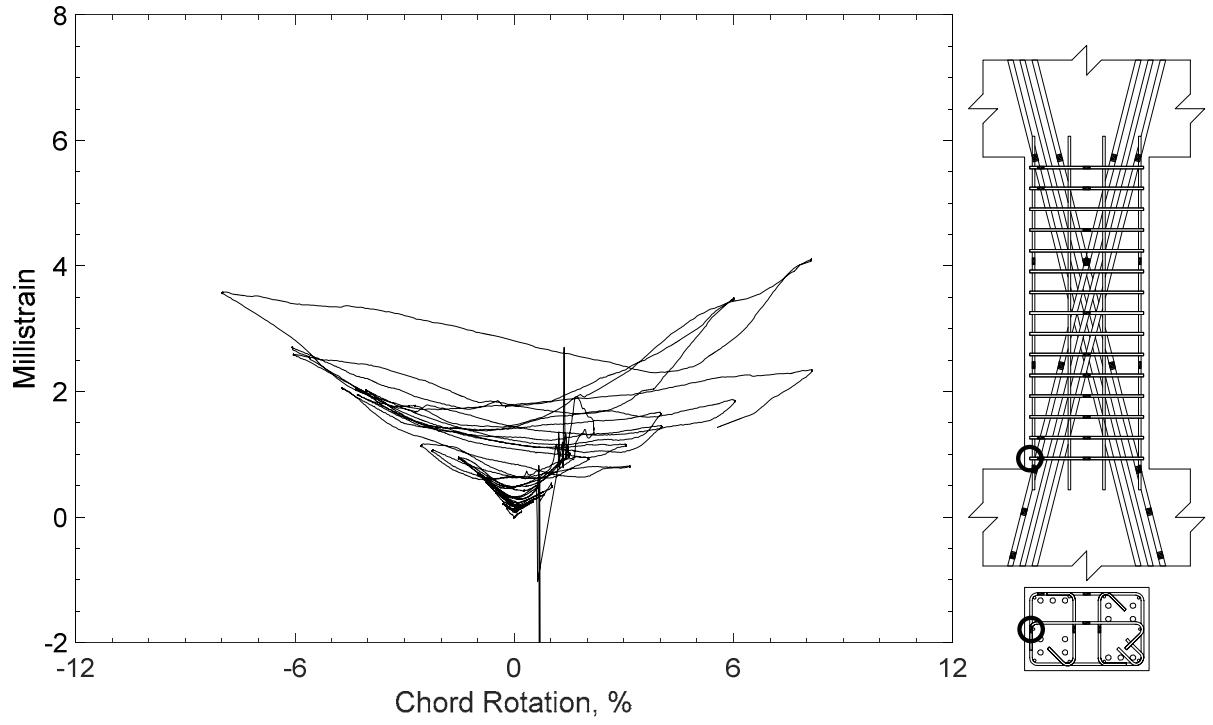


Figure 248 – Measured strain in closed stirrup of D100-2.5, strain gauge S3

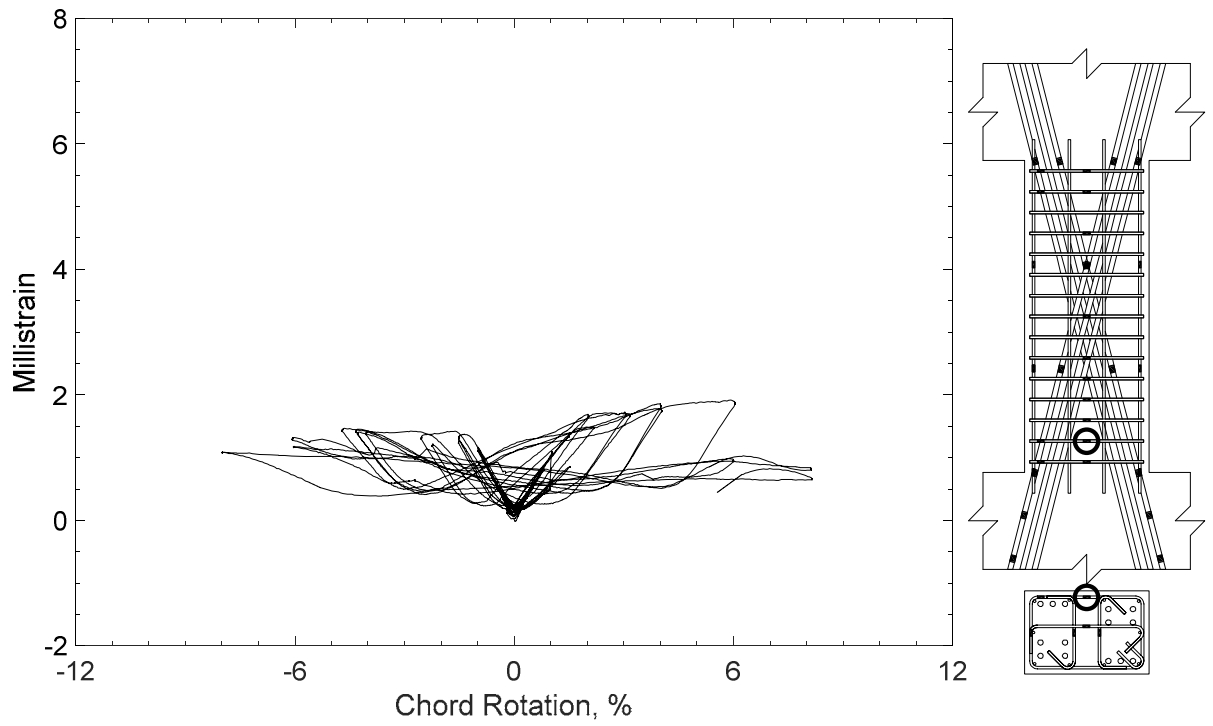


Figure 249 – Measured strain in closed stirrup of D100-2.5, strain gauge S4

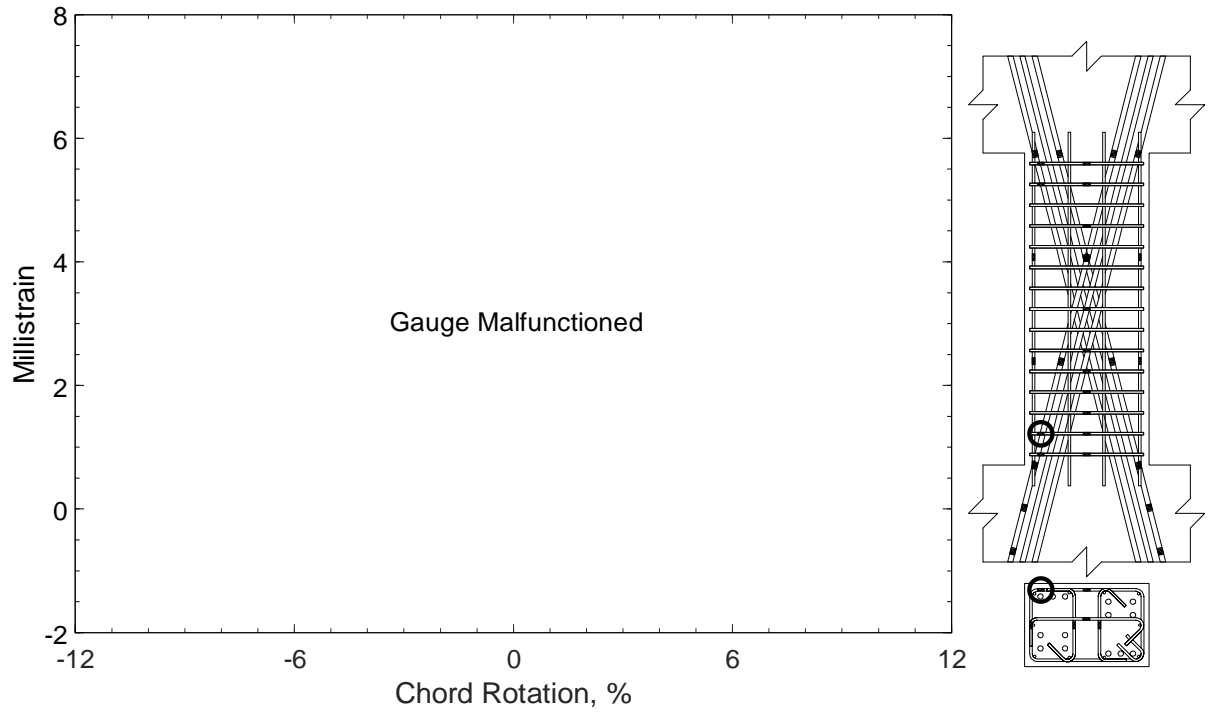


Figure 250 – Measured strain in closed stirrup of D100-2.5, strain gauge S5

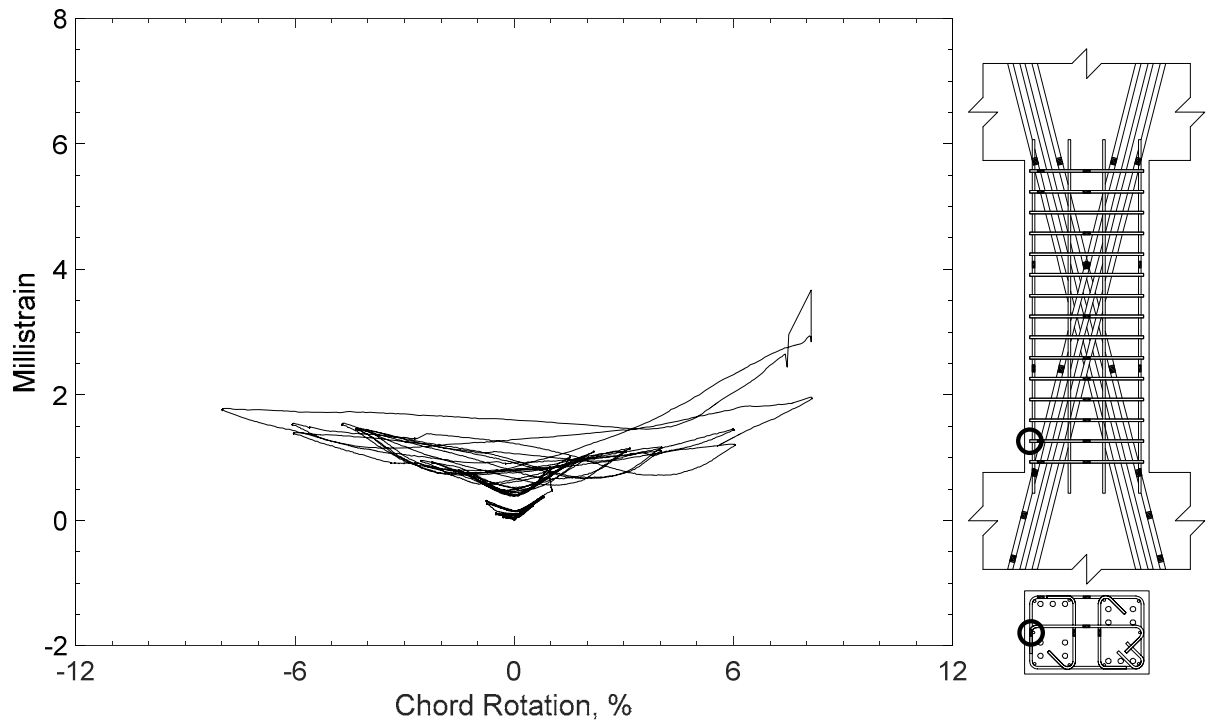


Figure 251 – Measured strain in closed stirrup of D100-2.5, strain gauge S6

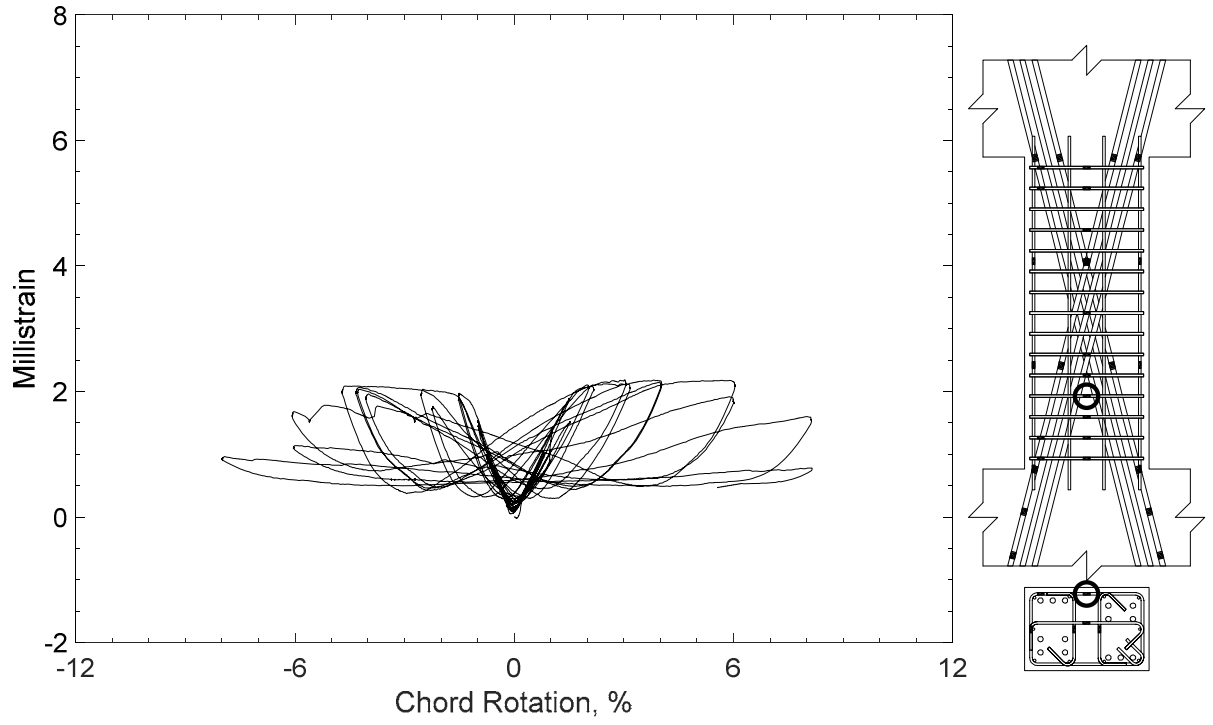


Figure 252 – Measured strain in closed stirrup of D100-2.5, strain gauge S7

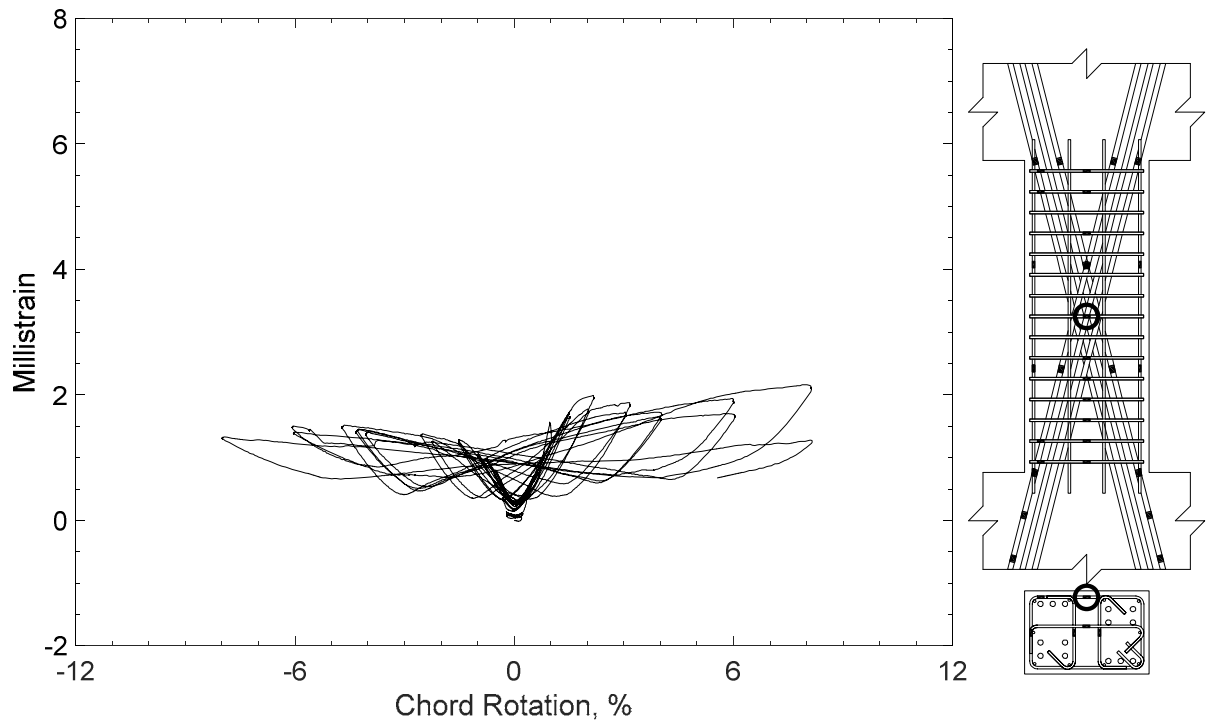


Figure 253 – Measured strain in closed stirrup of D100-2.5, strain gauge S8

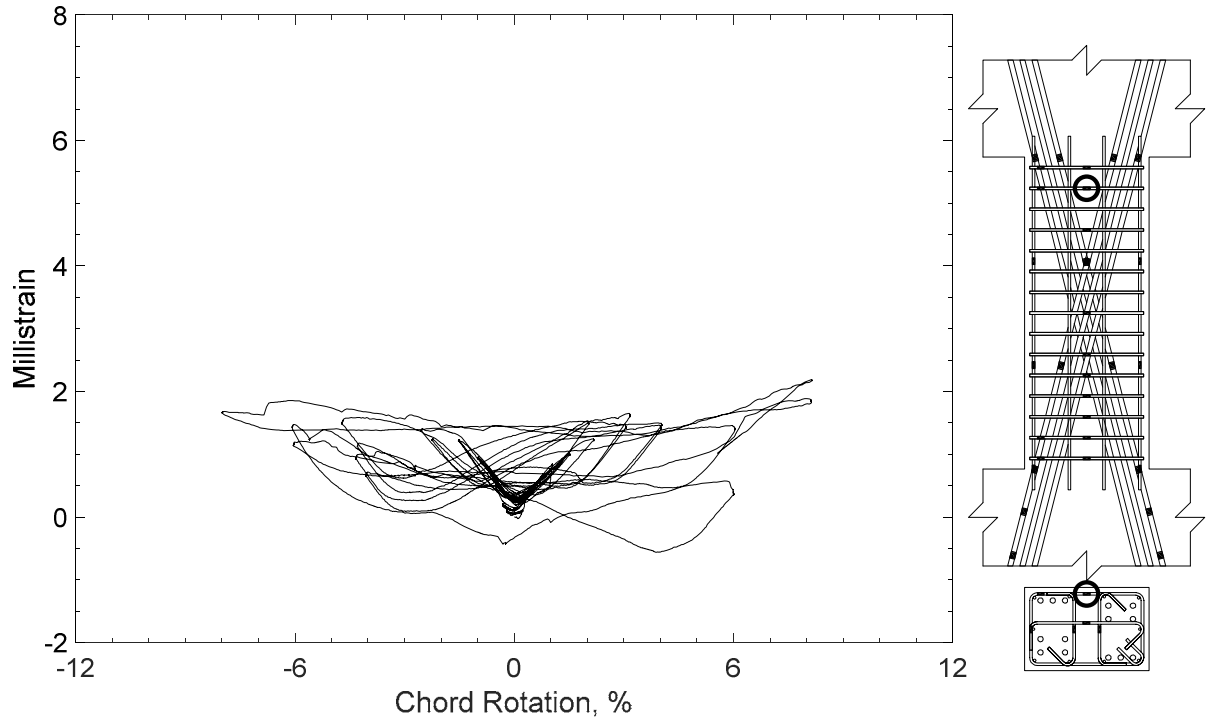


Figure 254 – Measured strain in closed stirrup of D100-2.5, strain gauge S9

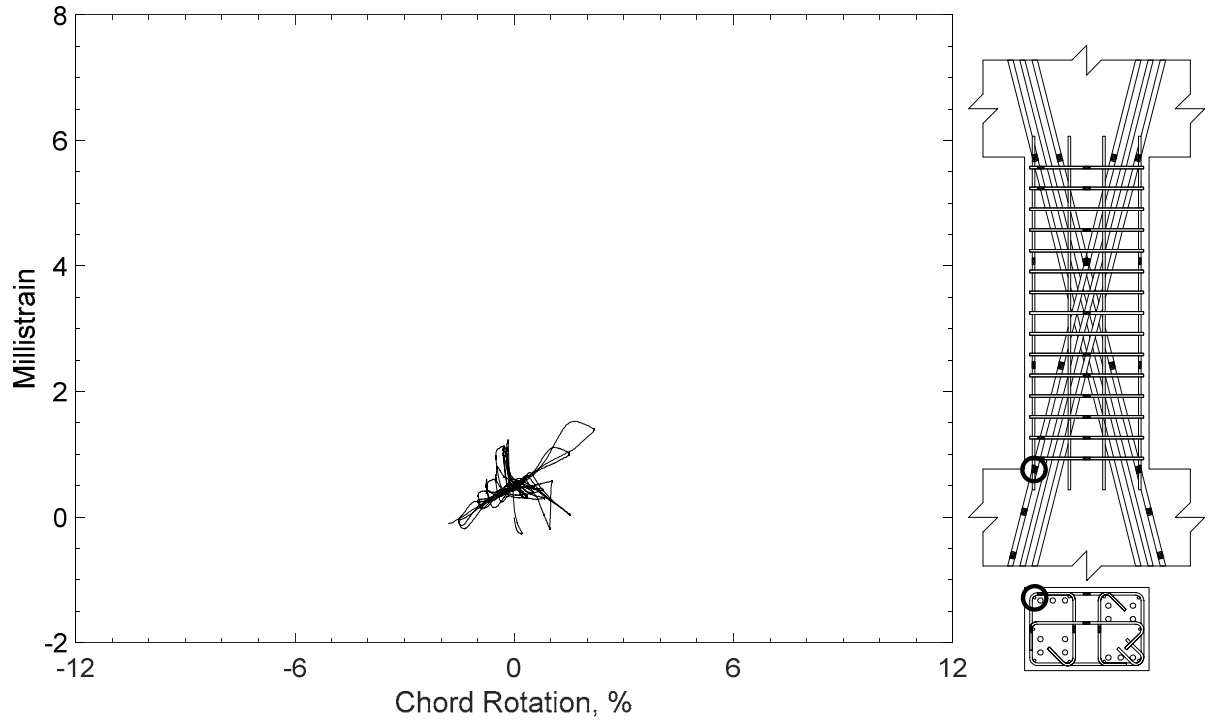


Figure 255 – Measured strain in parallel bar of D100-2.5, strain gauge H1

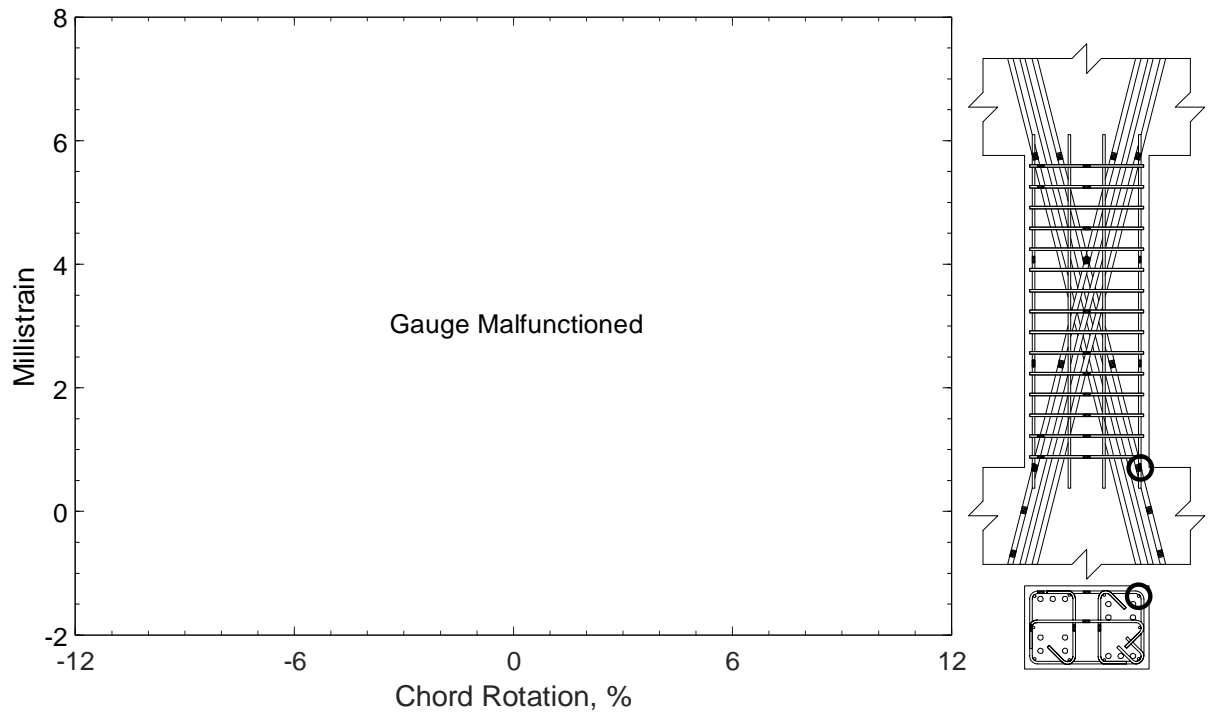


Figure 256 – Measured strain in parallel bar of D100-2.5, strain gauge H2

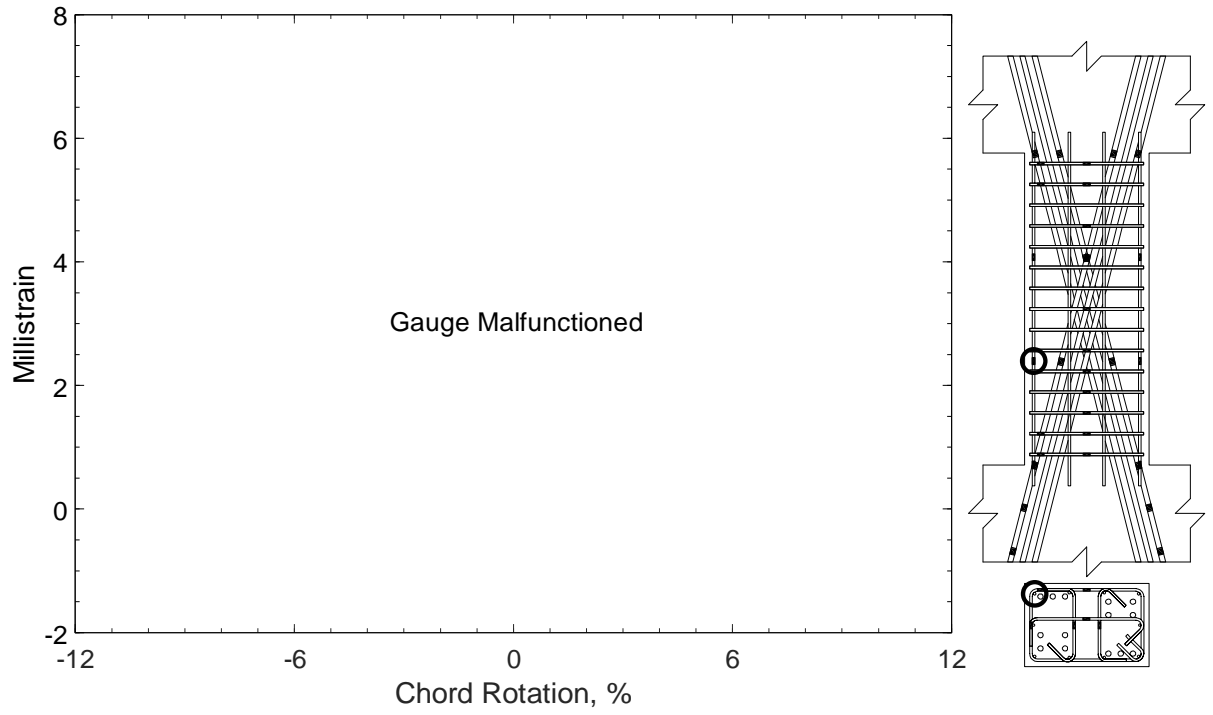


Figure 257 – Measured strain in parallel bar of D100-2.5, strain gauge H3

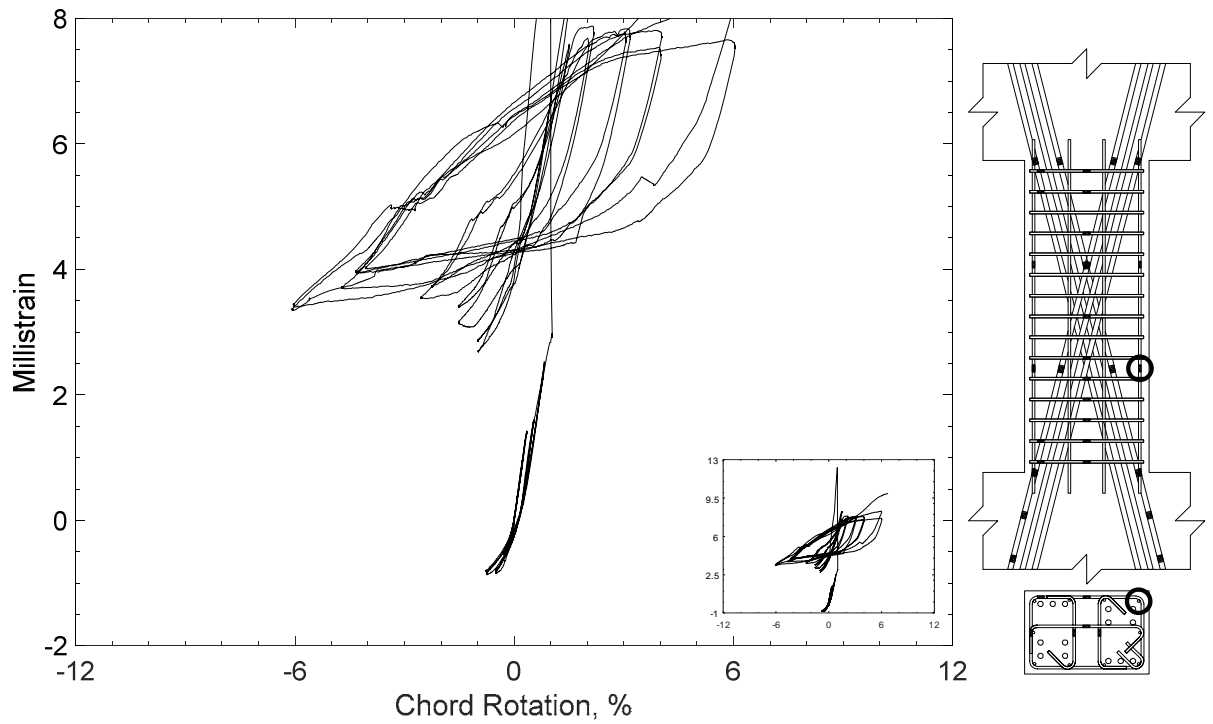


Figure 258 – Measured strain in parallel bar of D100-2.5, strain gauge H4

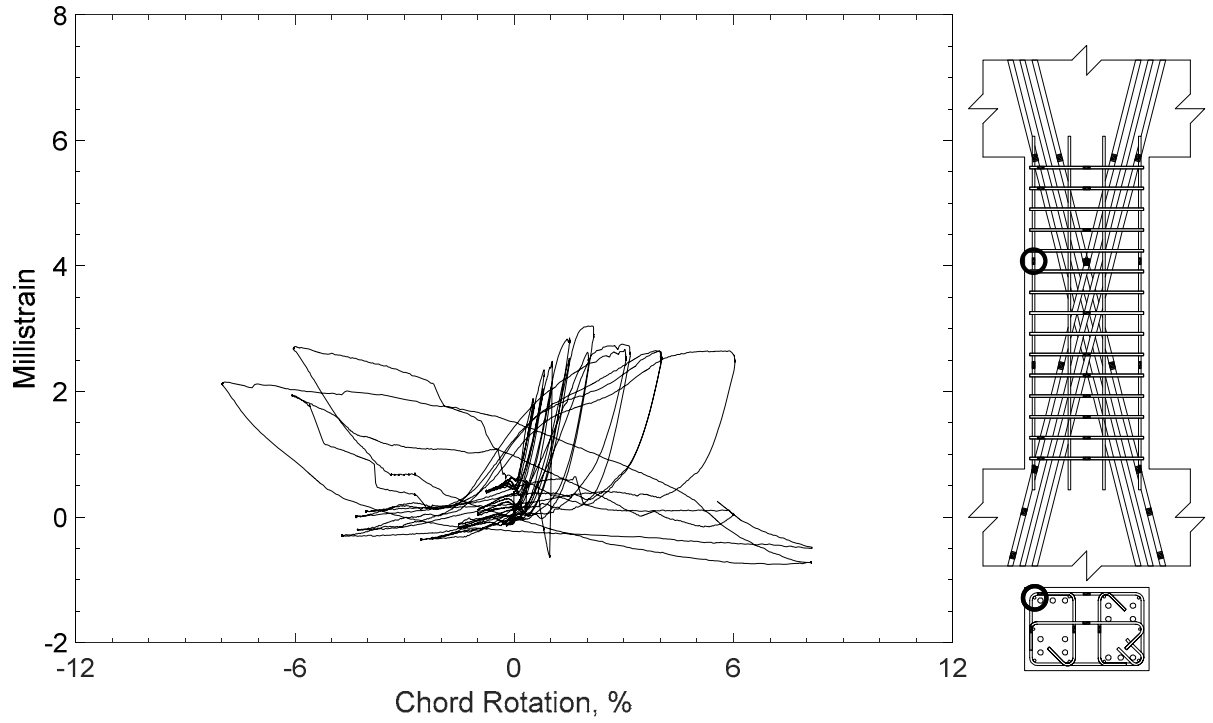


Figure 259 – Measured strain in parallel bar of D100-2.5, strain gauge H5

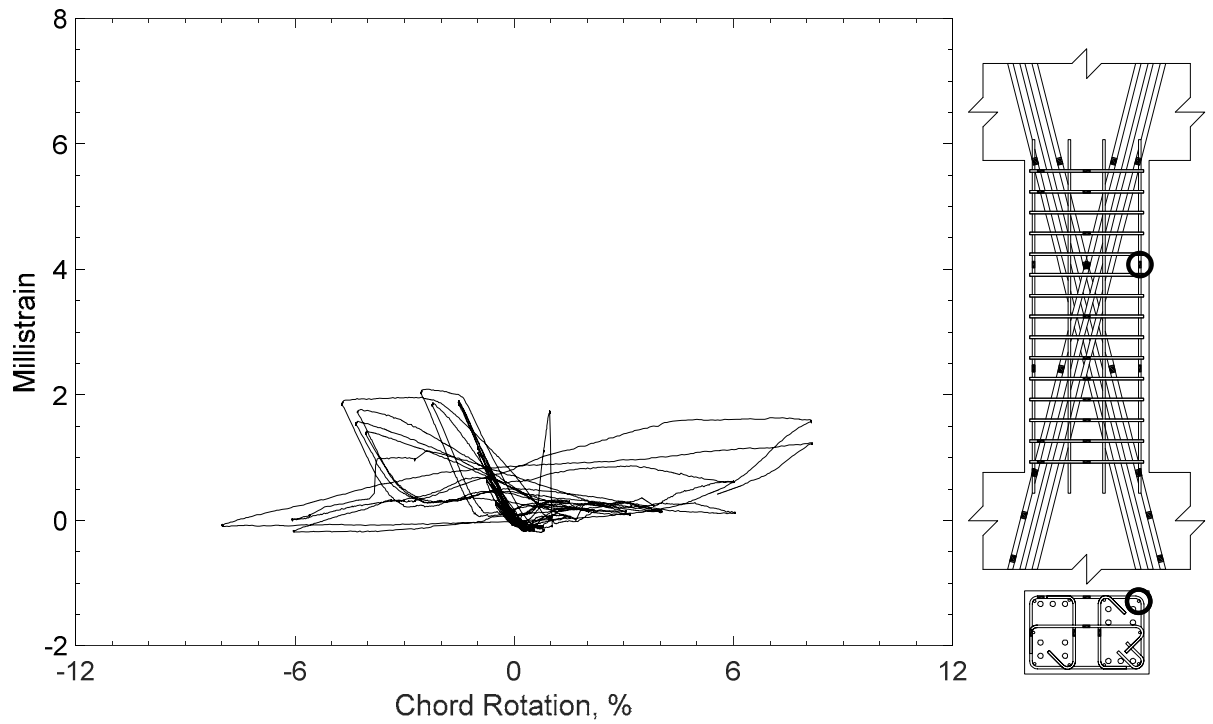


Figure 260 – Measured strain in parallel bar of D100-2.5, strain gauge H6

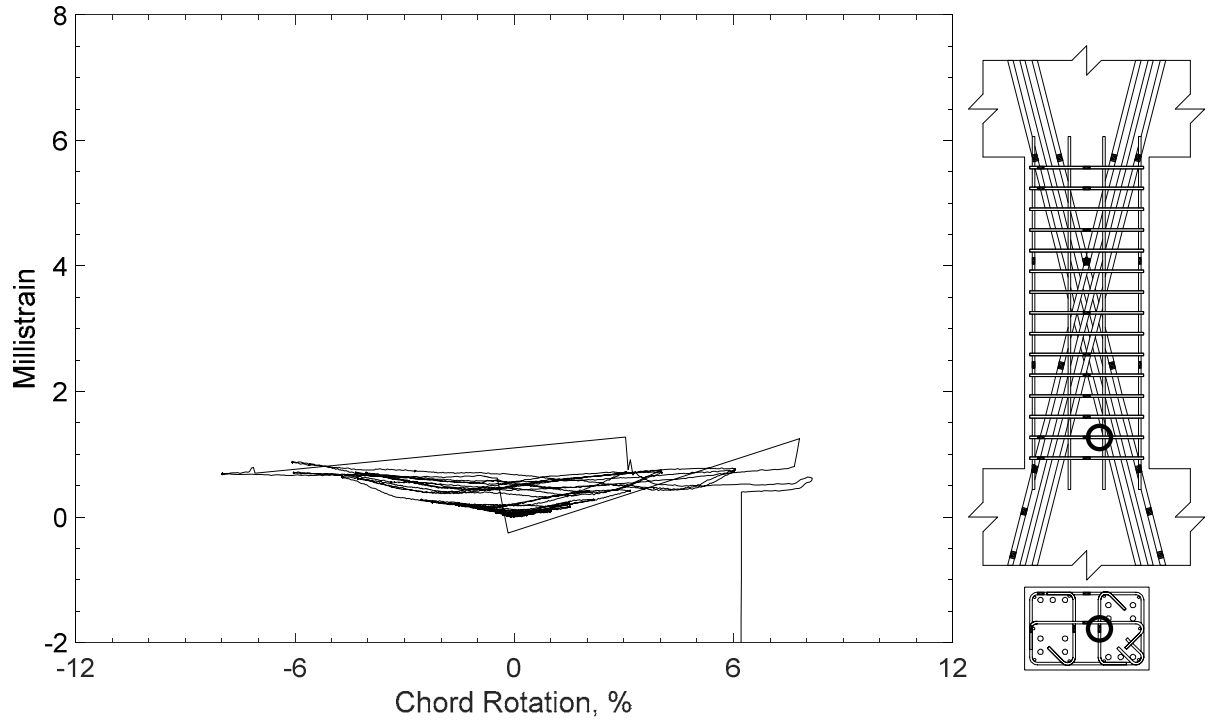


Figure 261 – Measured strain in cross-tie of D100-2.5, strain gauge T1

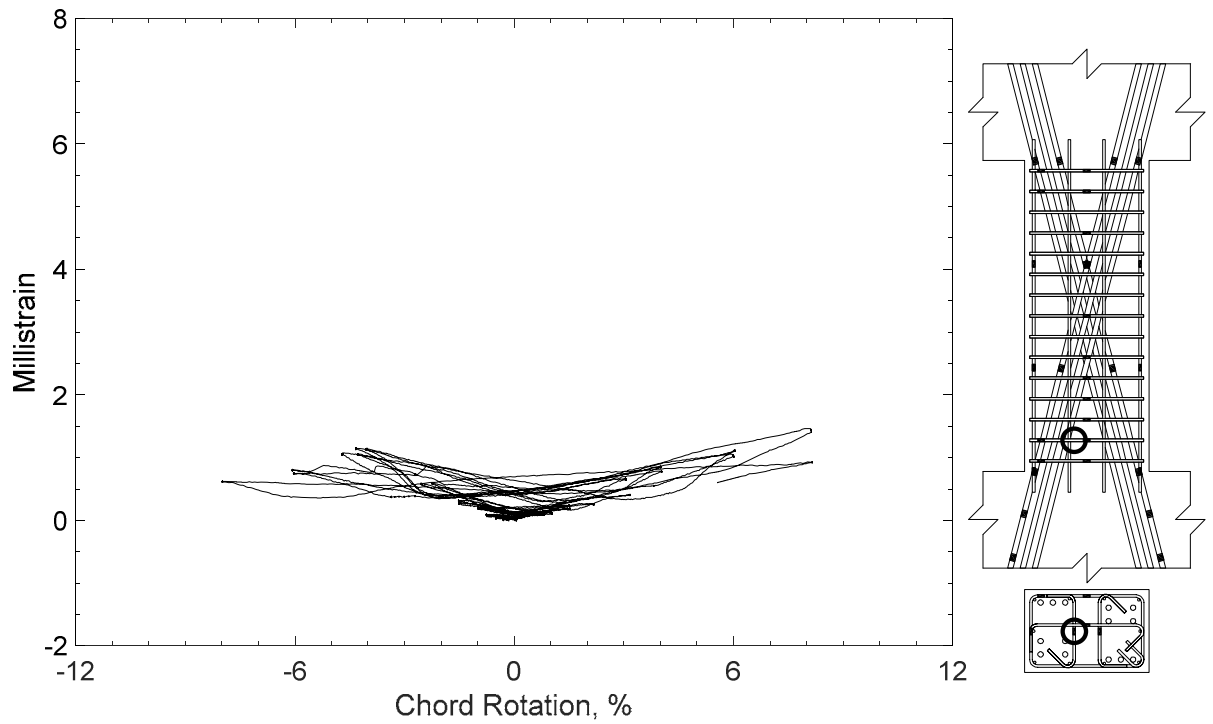


Figure 262 – Measured strain in cross-tie of D100-2.5, strain gauge T2

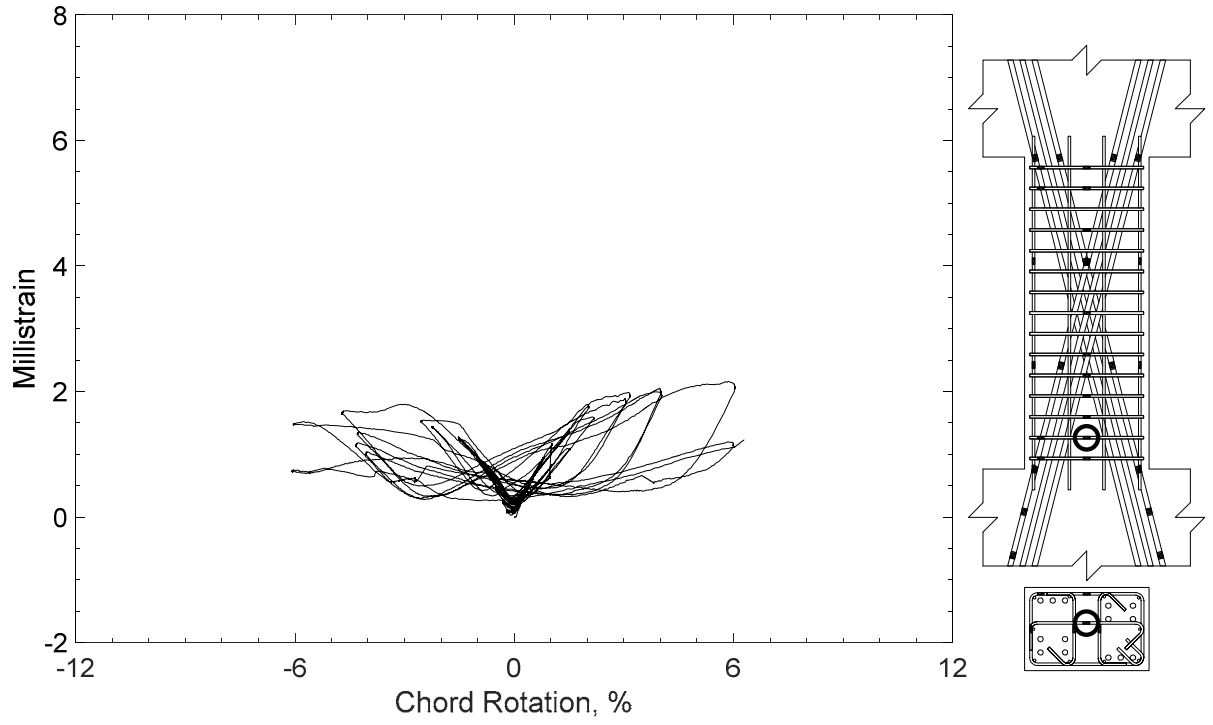


Figure 263 – Measured strain in cross-tie of D100-2.5, strain gauge T3

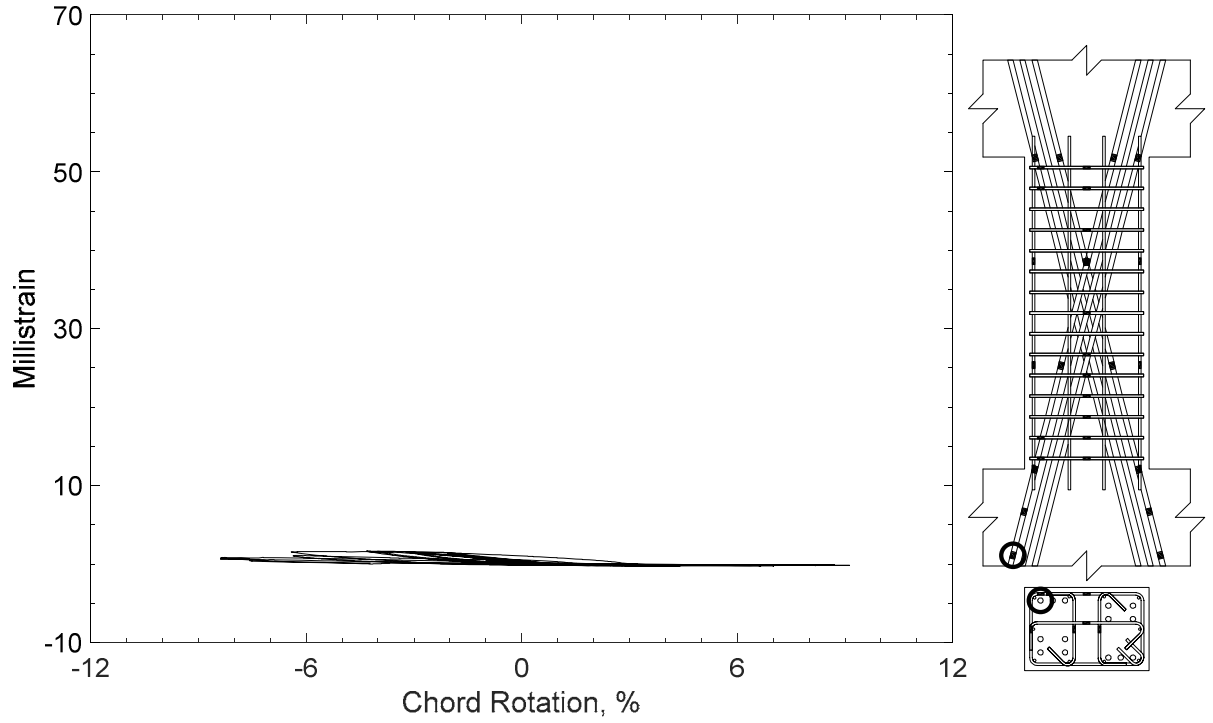


Figure 264 – Measured strain in diagonal bar of D120-2.5, strain gauge D1

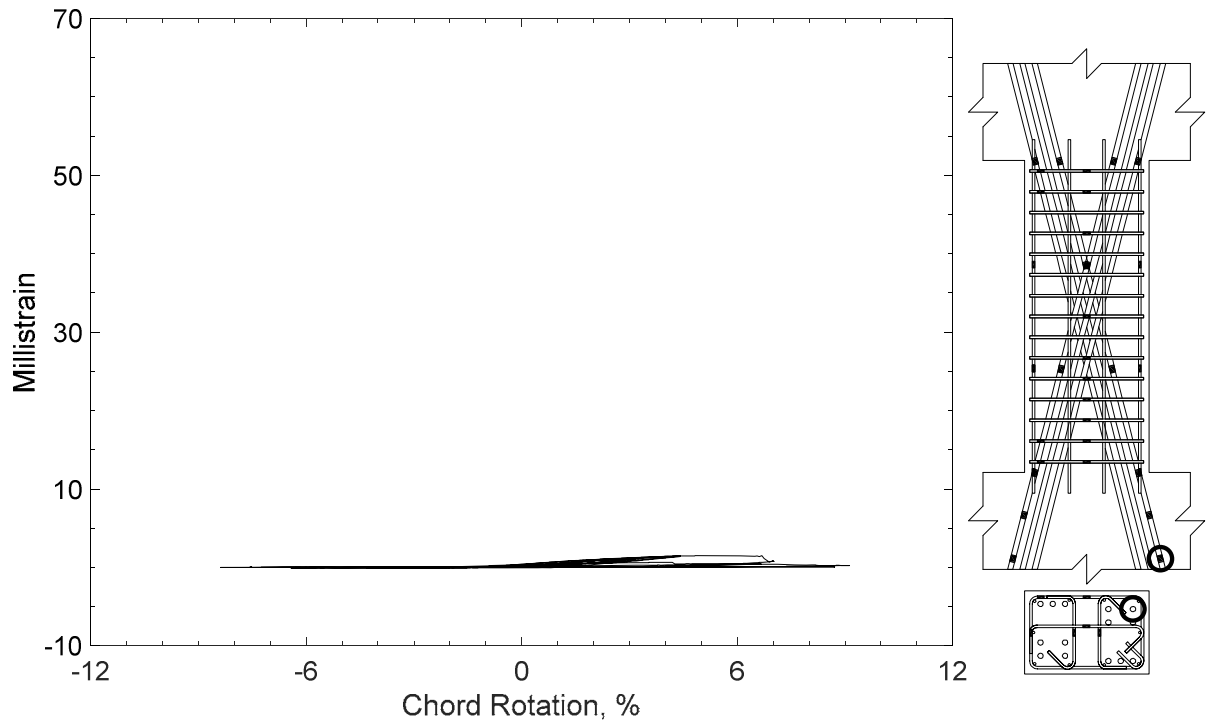


Figure 265 – Measured strain in diagonal bar of D120-2.5, strain gauge D2

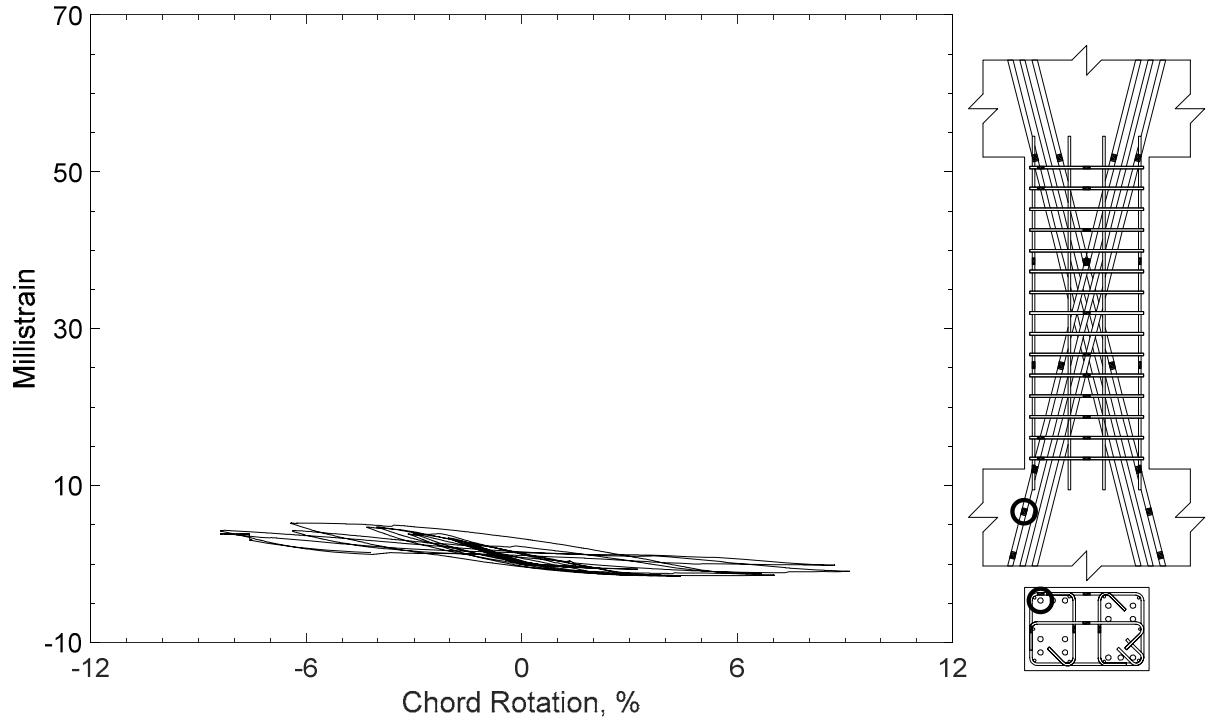


Figure 266 – Measured strain in diagonal bar of D120-2.5, strain gauge D3

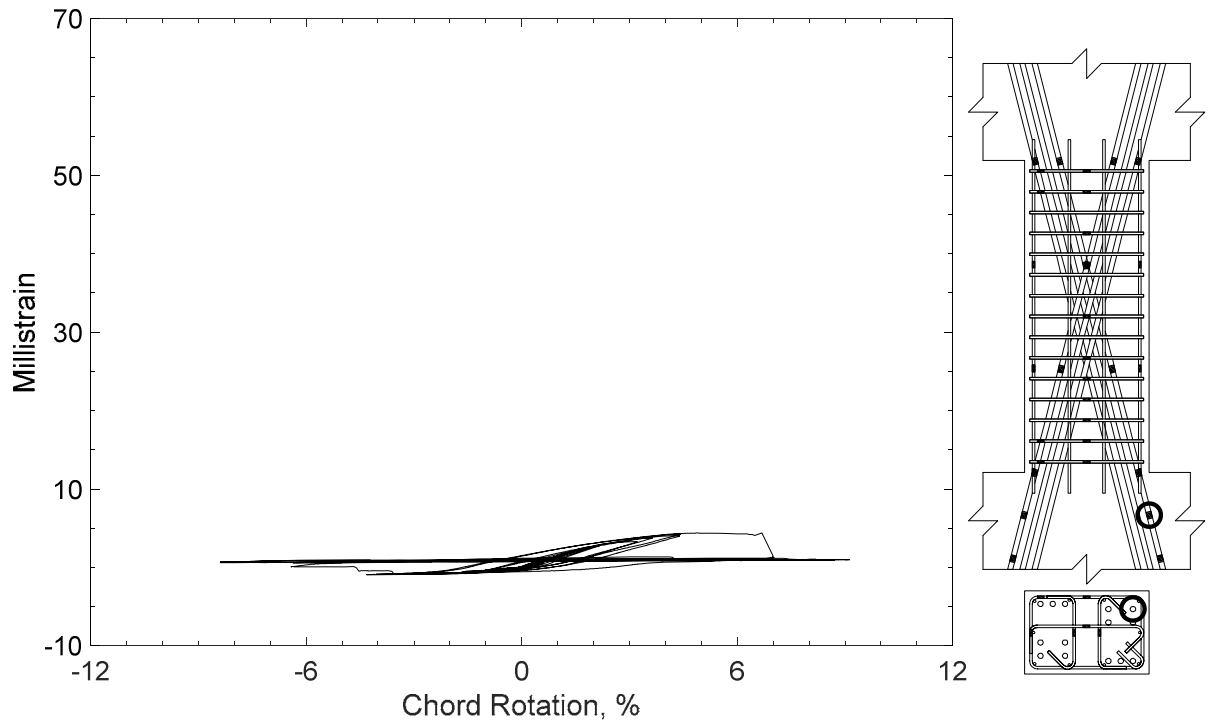


Figure 267 – Measured strain in diagonal bar of D120-2.5, strain gauge D4

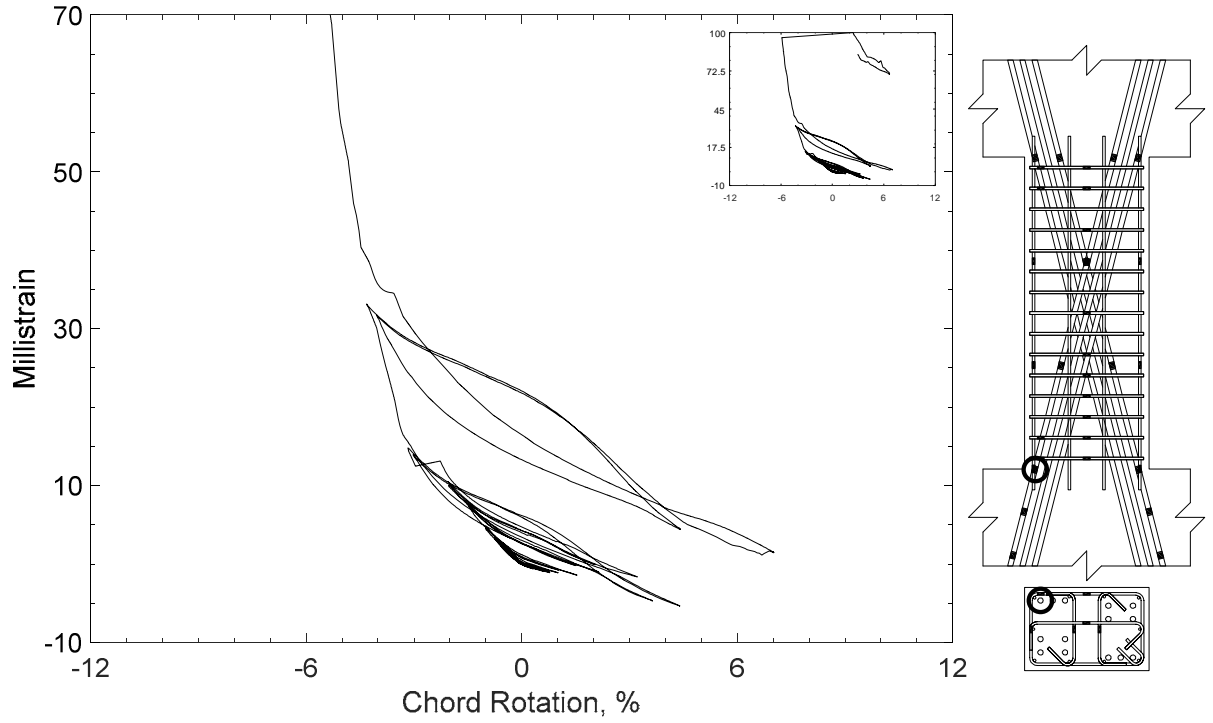


Figure 268 – Measured strain in diagonal bar of D120-2.5, strain gauge D5

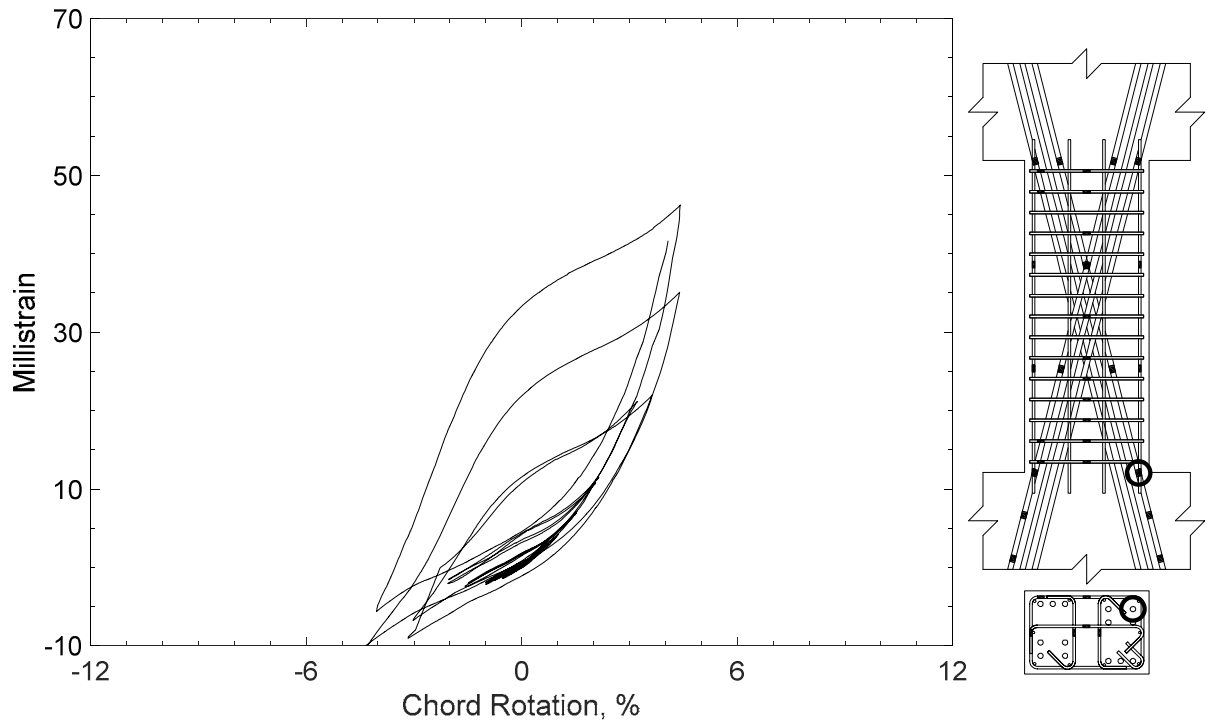


Figure 269 – Measured strain in diagonal bar of D120-2.5, strain gauge D6

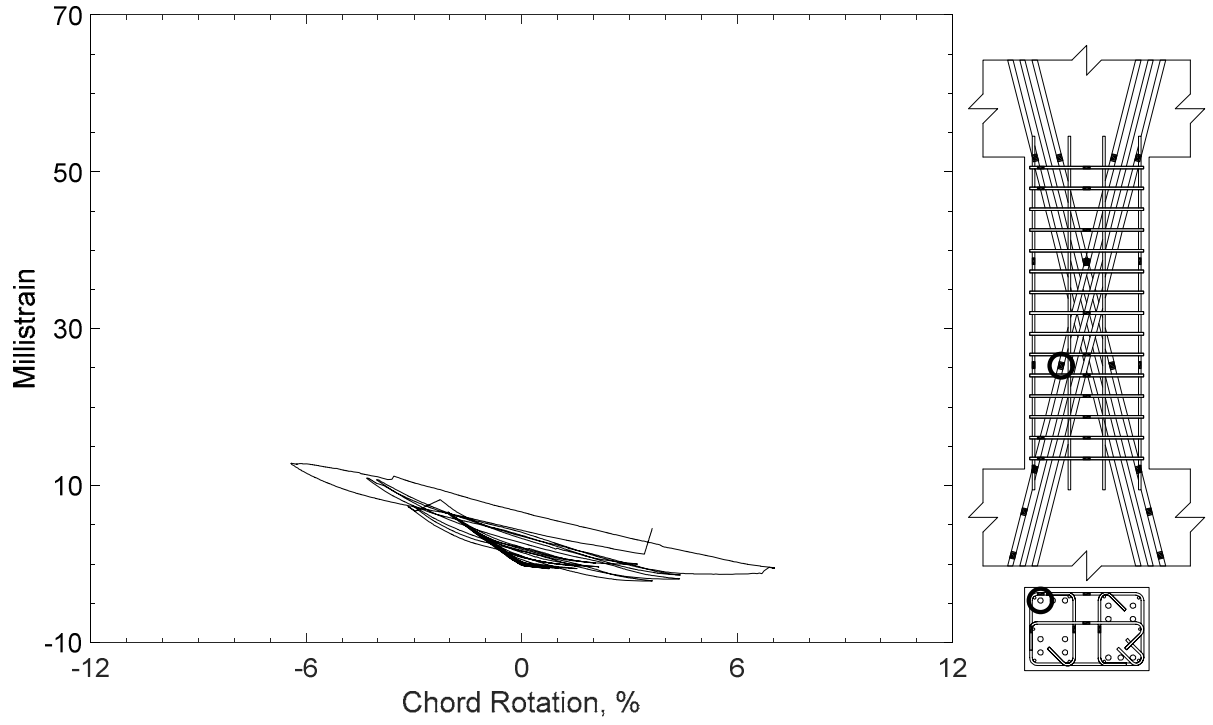


Figure 270 – Measured strain in diagonal bar of D120-2.5, strain gauge D7

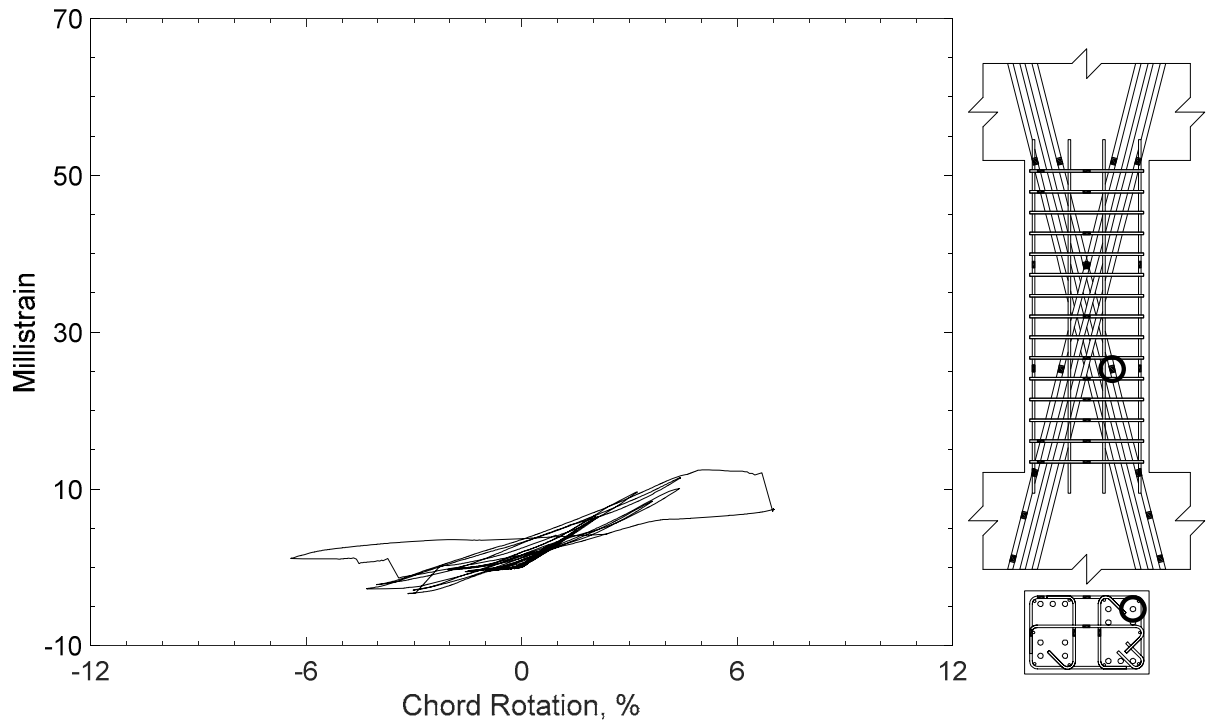


Figure 271 – Measured strain in diagonal bar of D120-2.5, strain gauge D8

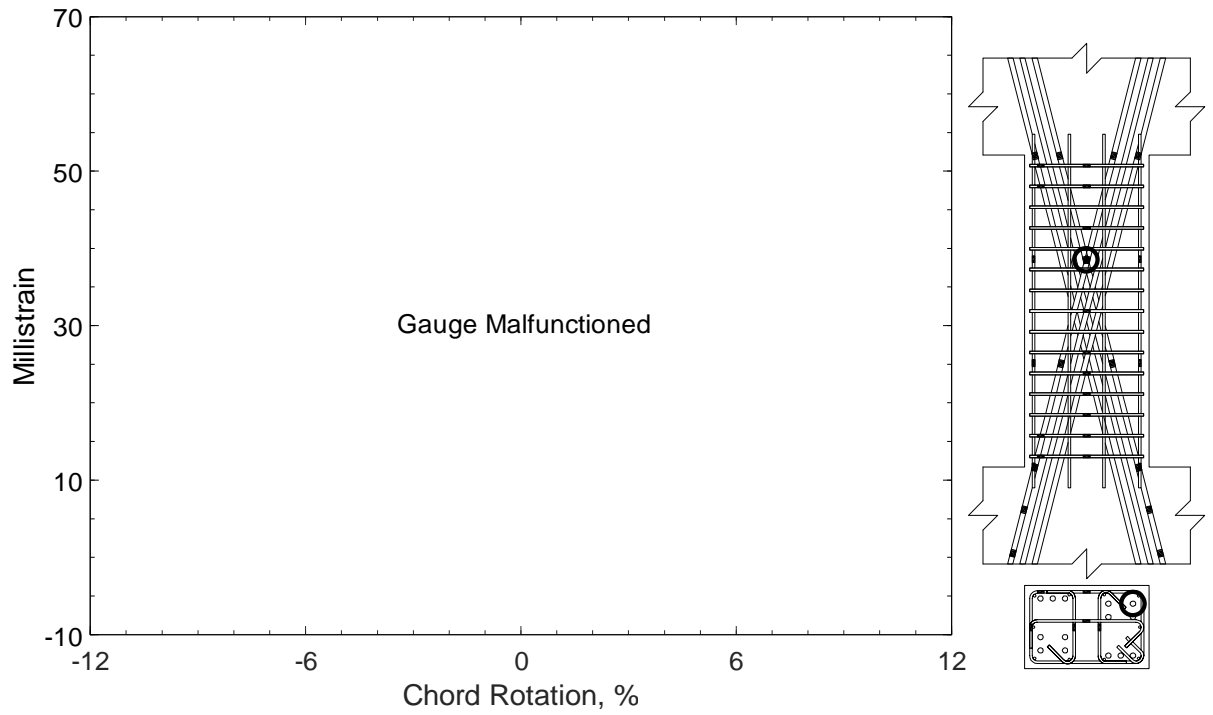


Figure 272 – Measured strain in diagonal bar of D120-2.5, strain gauge D9

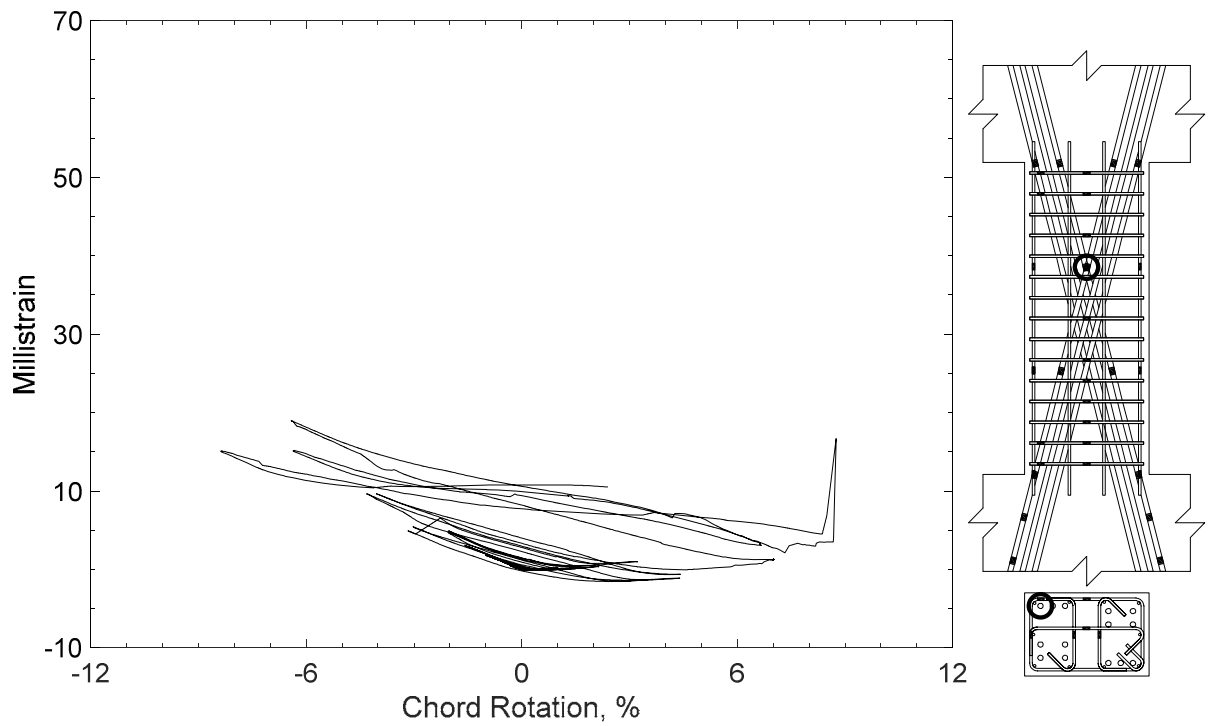


Figure 273 – Measured strain in diagonal bar of D120-2.5, strain gauge D10

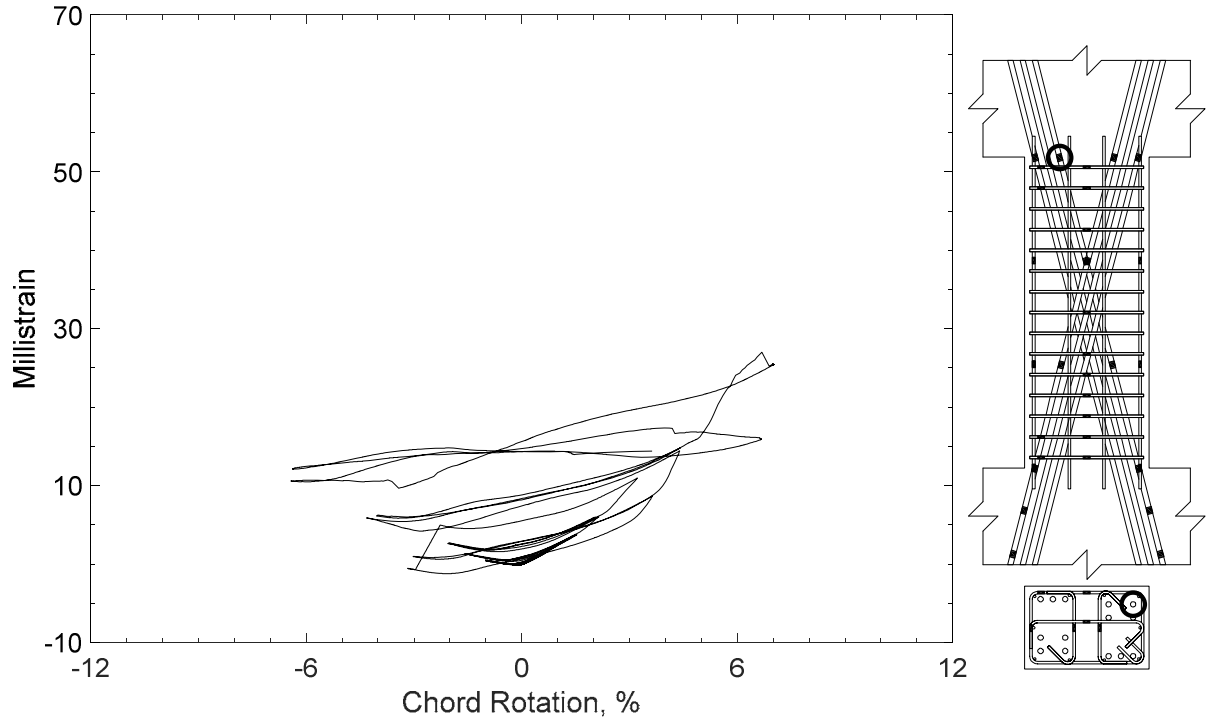


Figure 274 – Measured strain in diagonal bar of D120-2.5, strain gauge D11

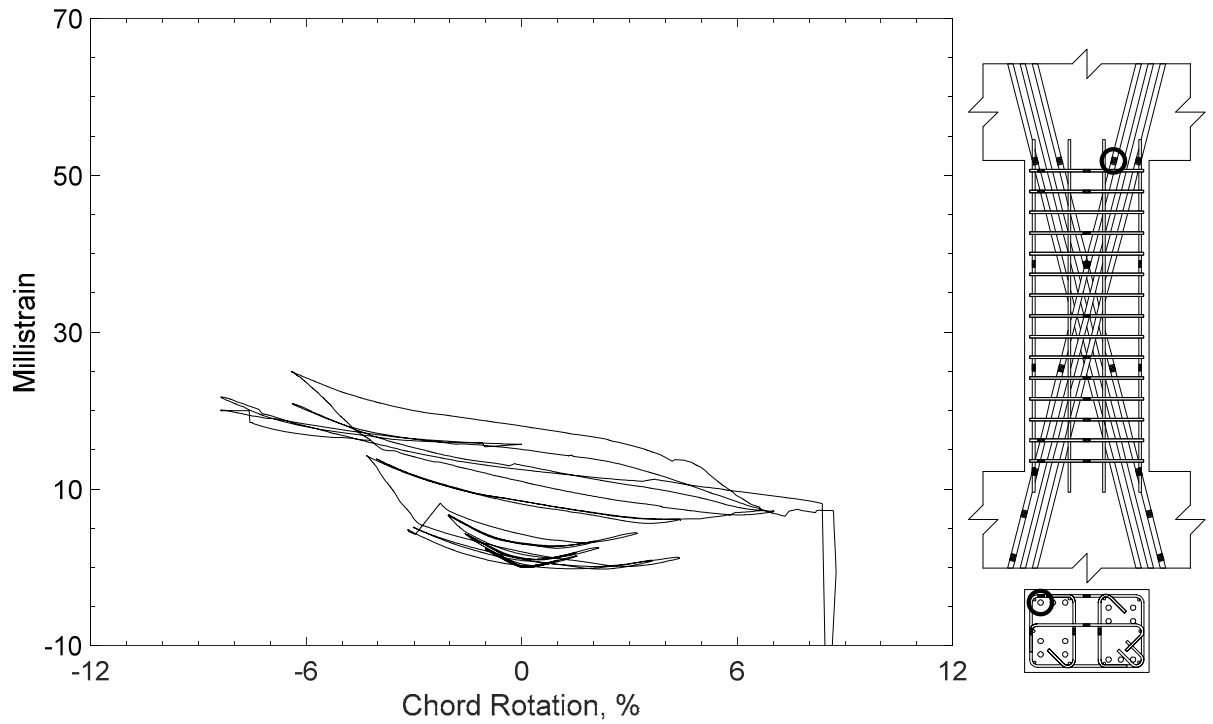


Figure 275 – Measured strain in diagonal bar of D120-2.5, strain gauge D12

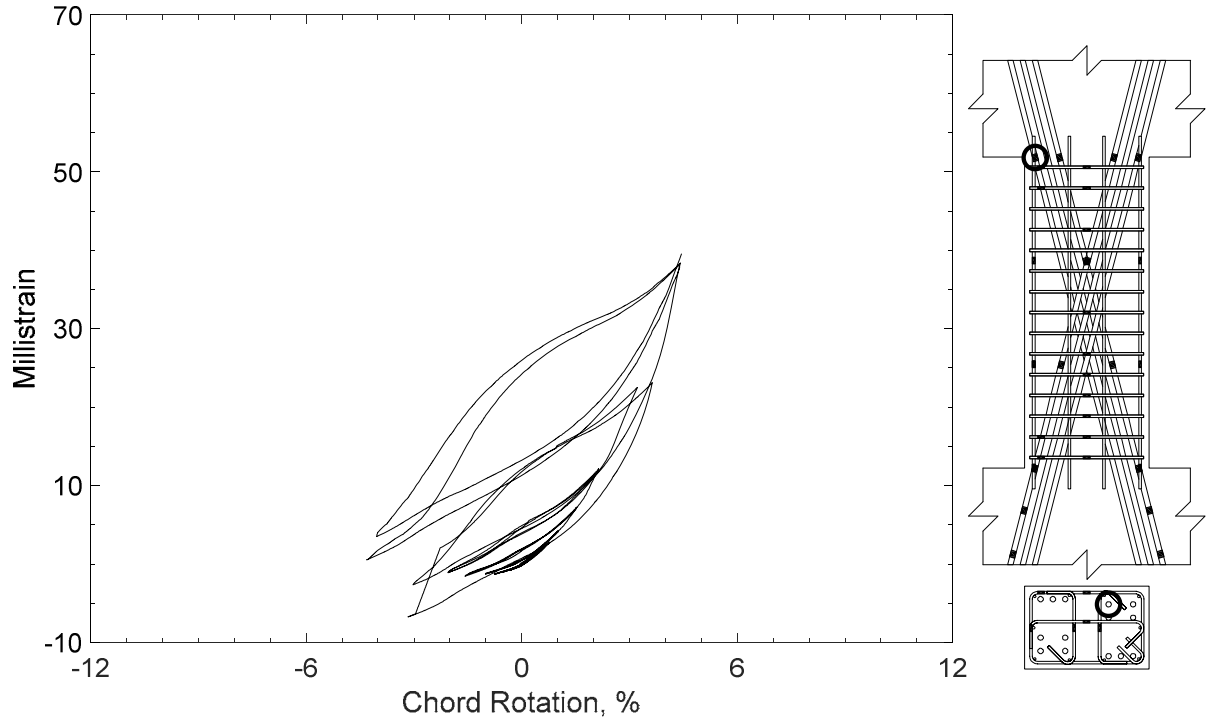


Figure 276 – Measured strain in diagonal bar of D120-2.5, strain gauge D13

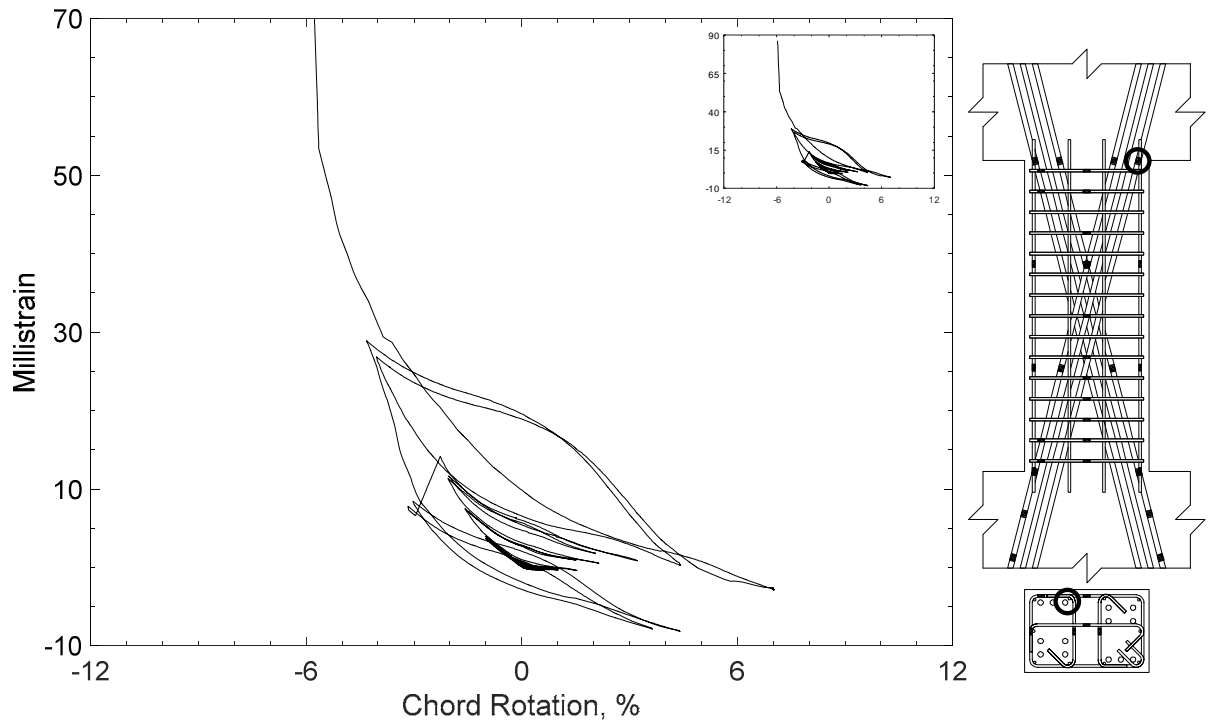


Figure 277 – Measured strain in diagonal bar of D120-2.5, strain gauge D14

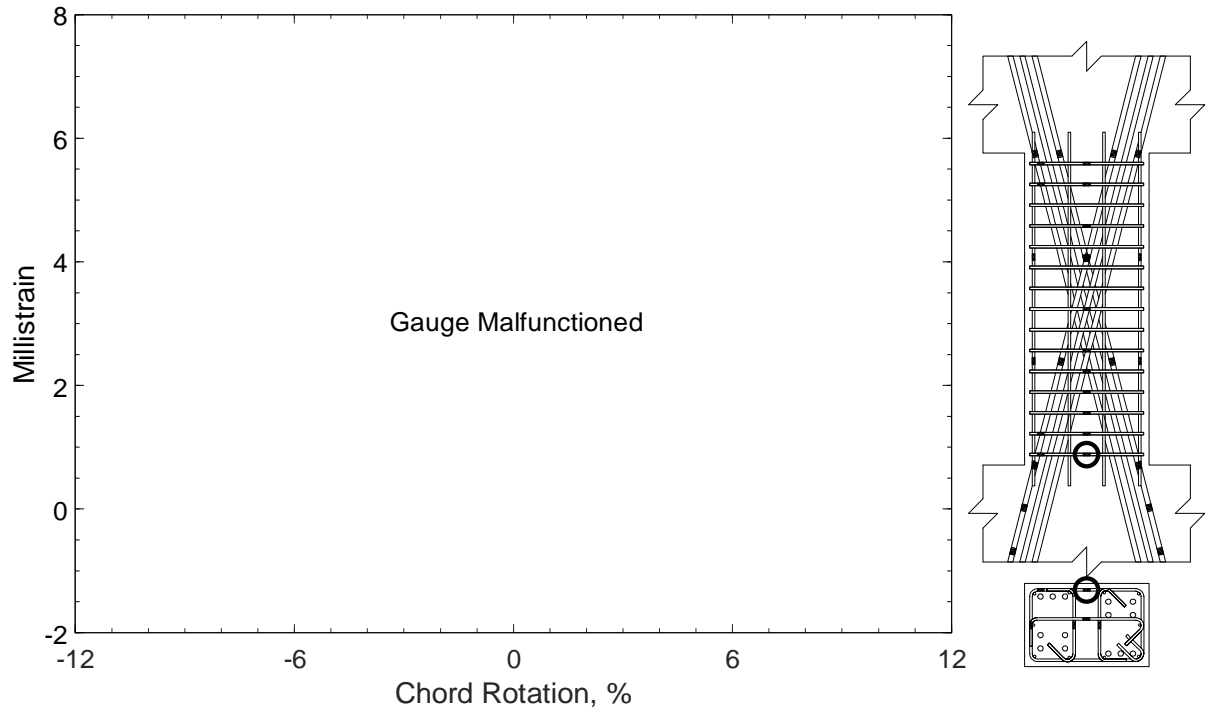


Figure 278 – Measured strain in closed stirrup of D120-2.5, strain gauge S1

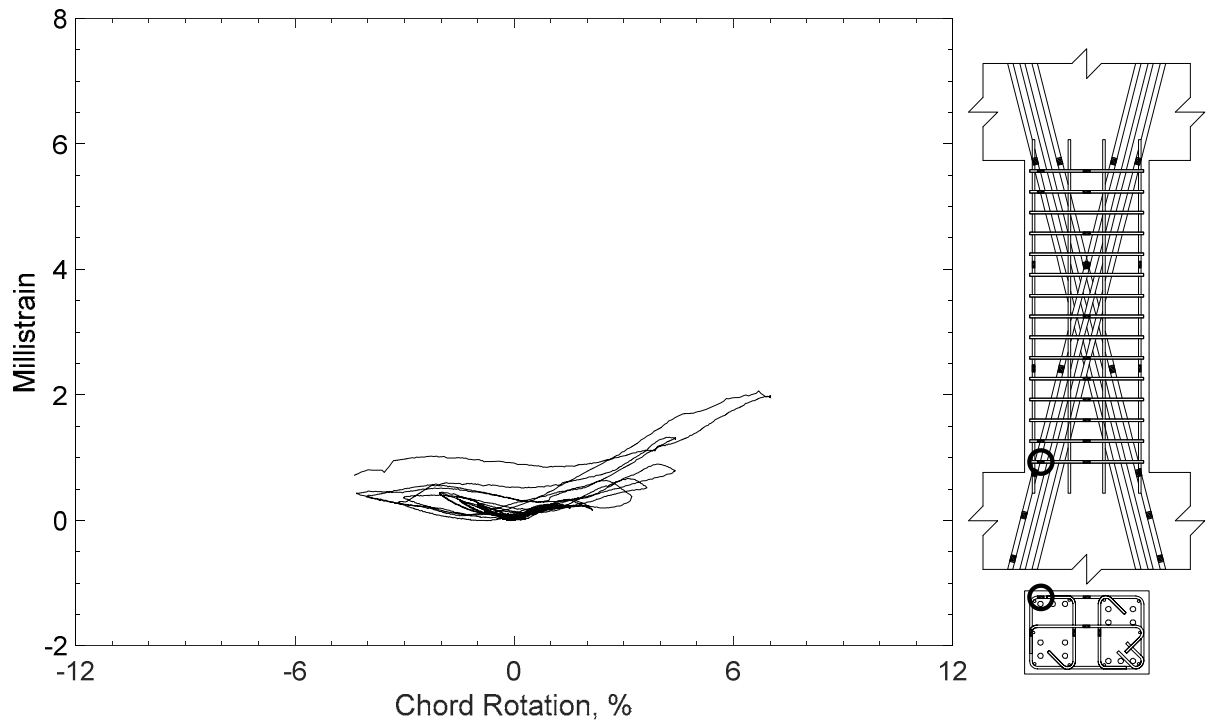


Figure 279 – Measured strain in closed stirrup of D120-2.5, strain gauge S2

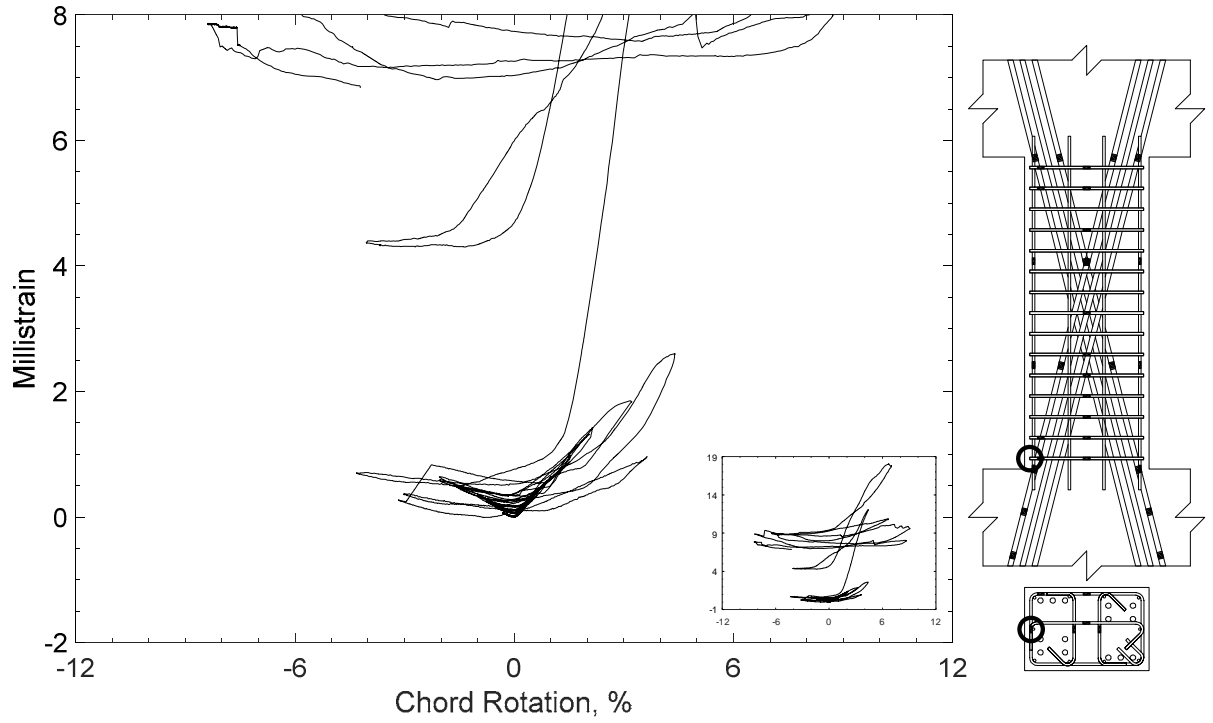


Figure 280 – Measured strain in closed stirrup of D120-2.5, strain gauge S3

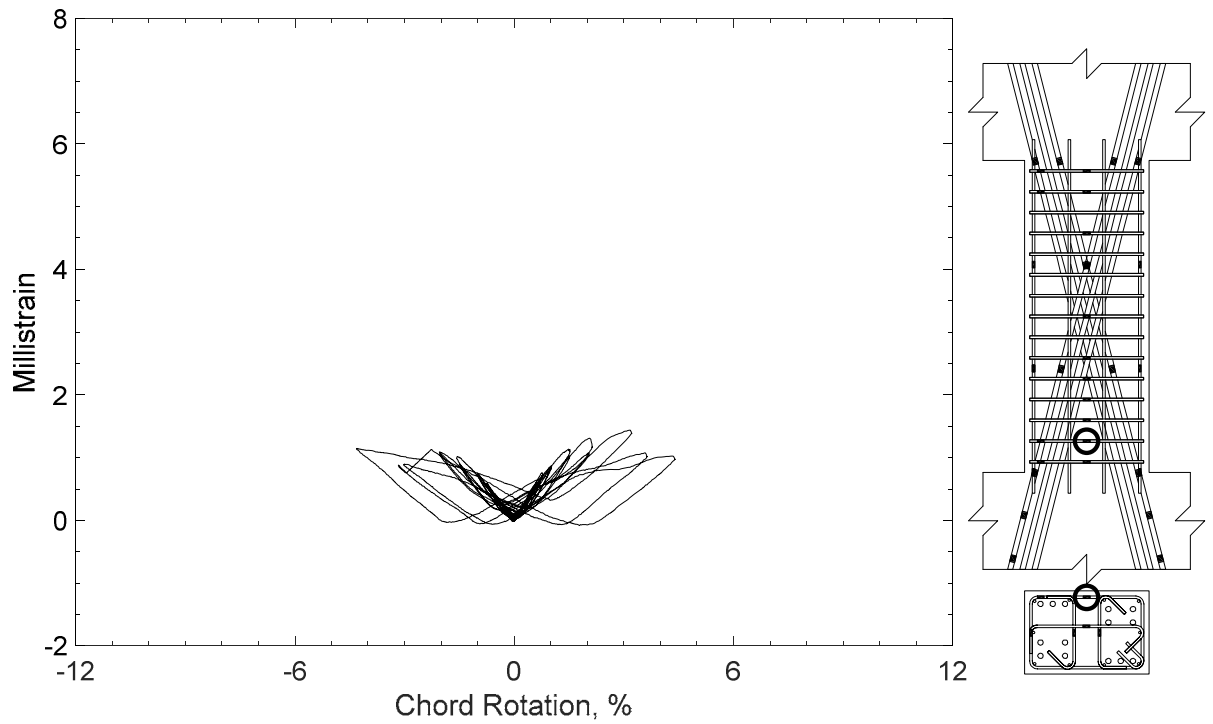


Figure 281 – Measured strain in closed stirrup of D120-2.5, strain gauge S4

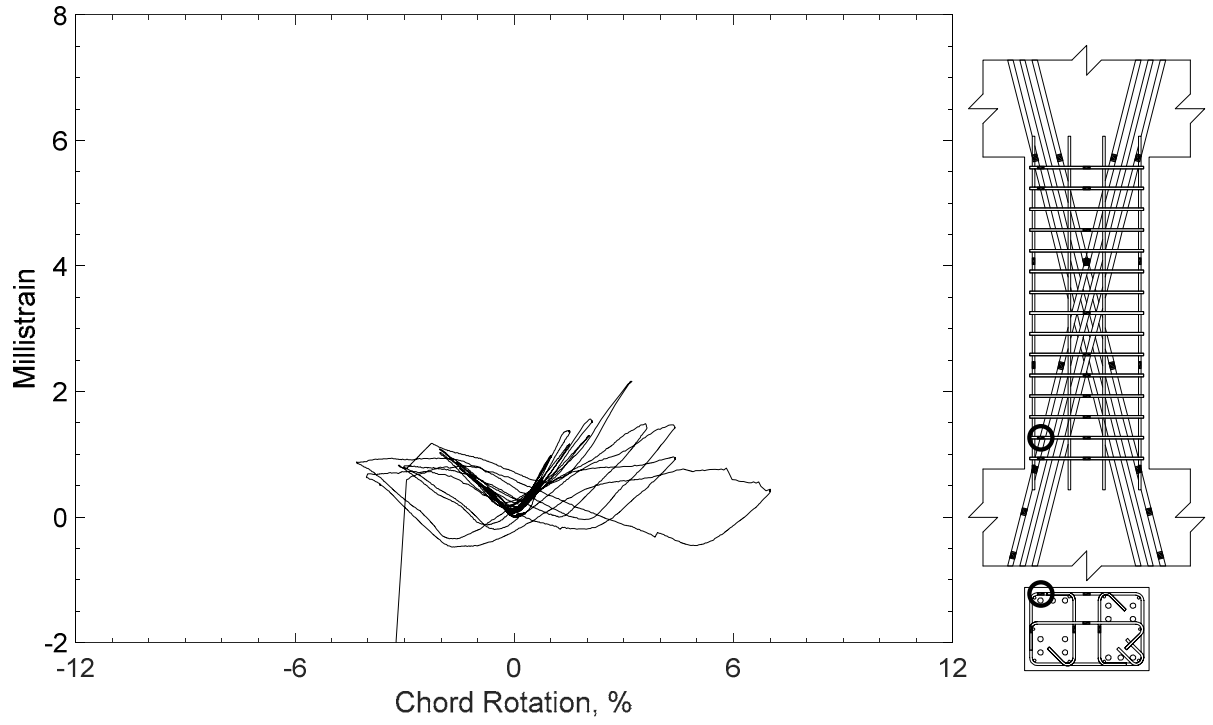


Figure 282 – Measured strain in closed stirrup of D120-2.5, strain gauge S5

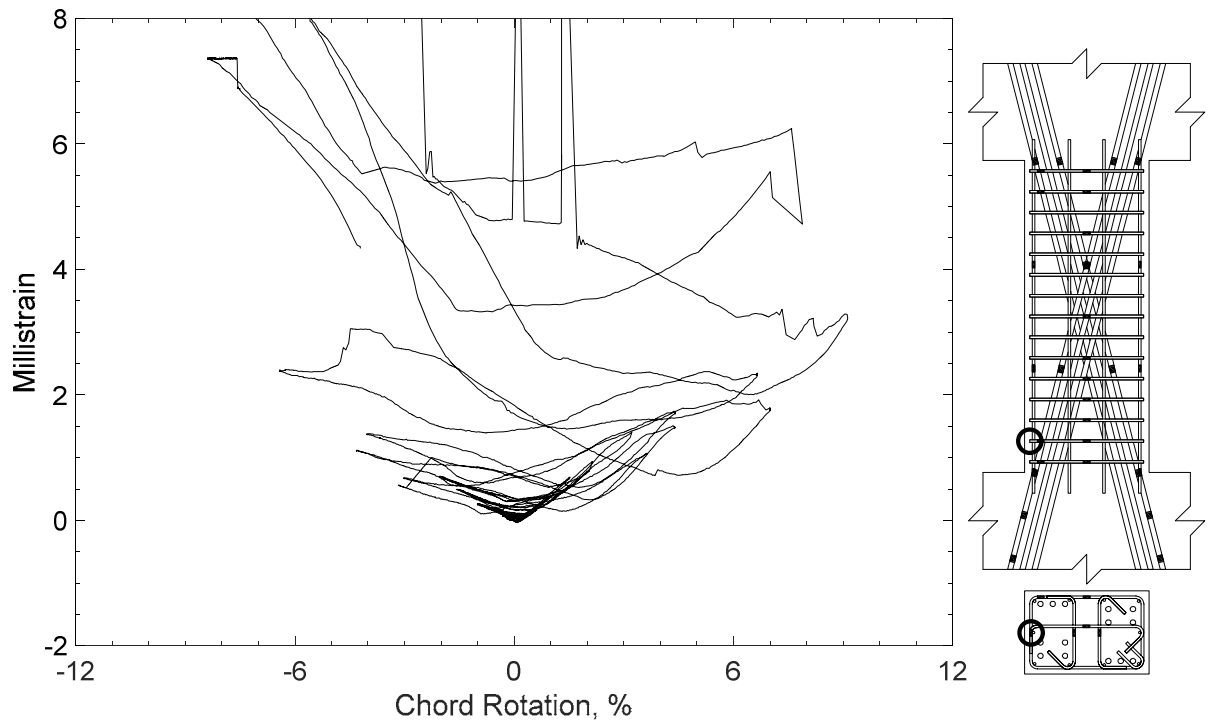


Figure 283 – Measured strain in closed stirrup of D120-2.5, strain gauge S6

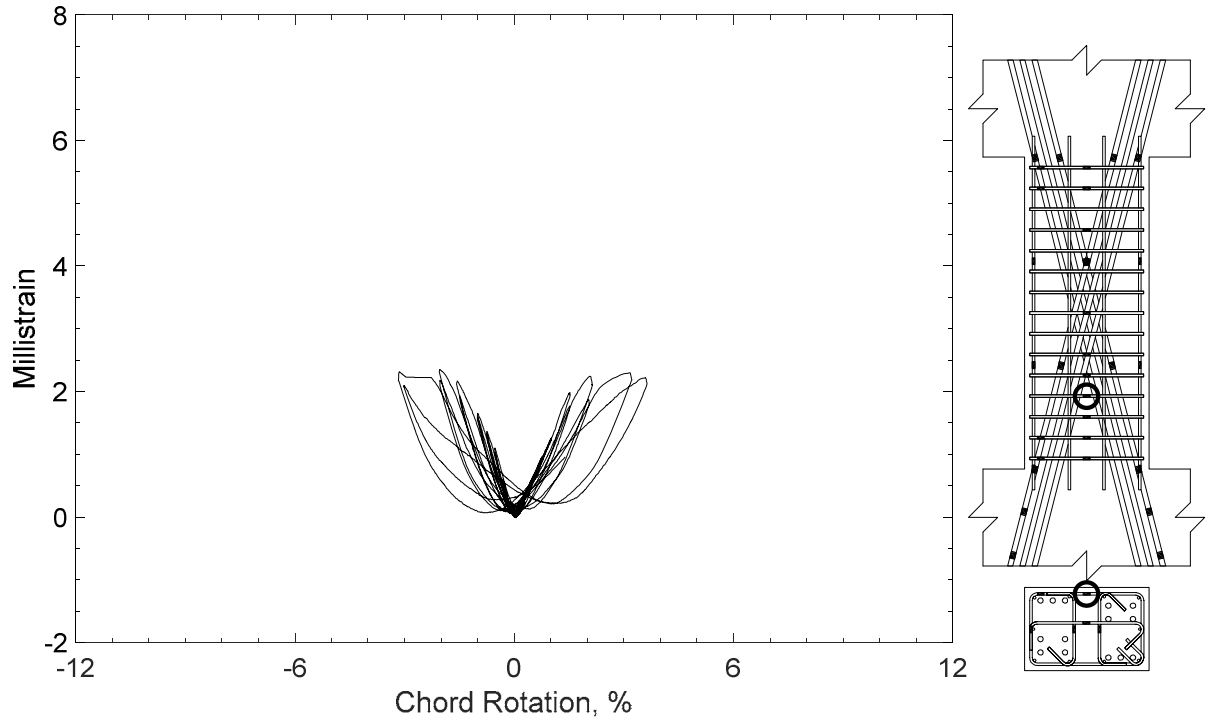


Figure 284 – Measured strain in closed stirrup of D120-2.5, strain gauge S7

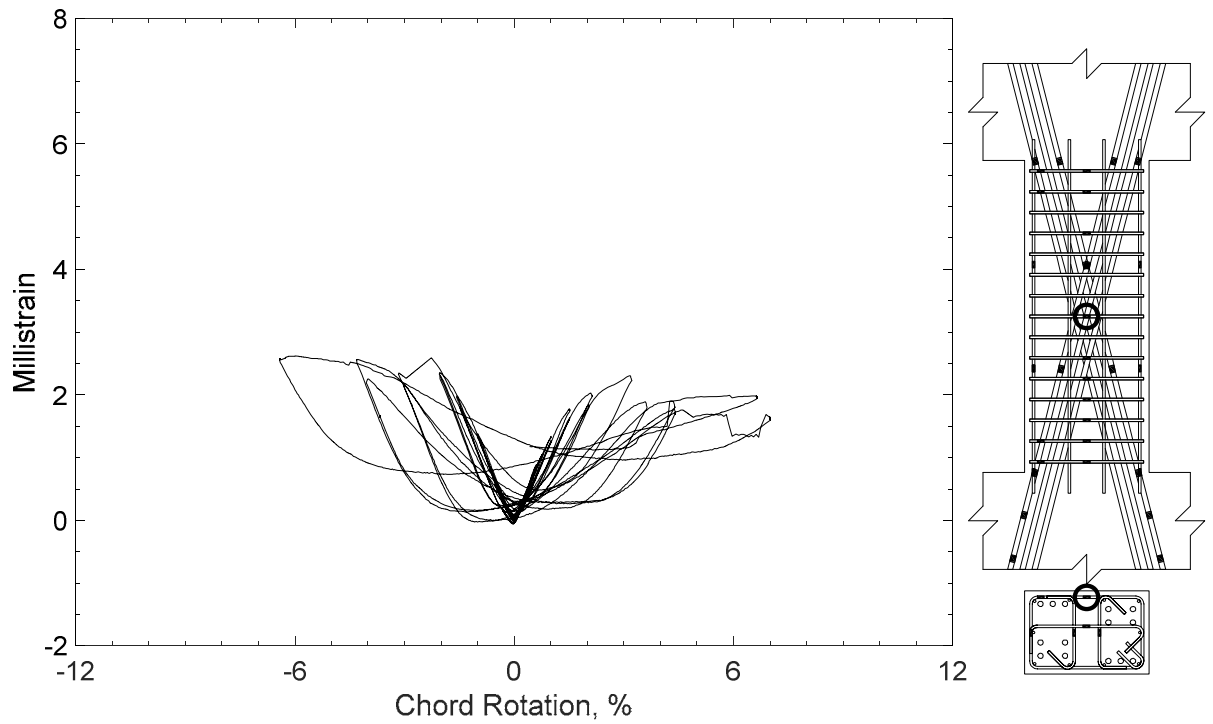


Figure 285 – Measured strain in closed stirrup of D120-2.5, strain gauge S8

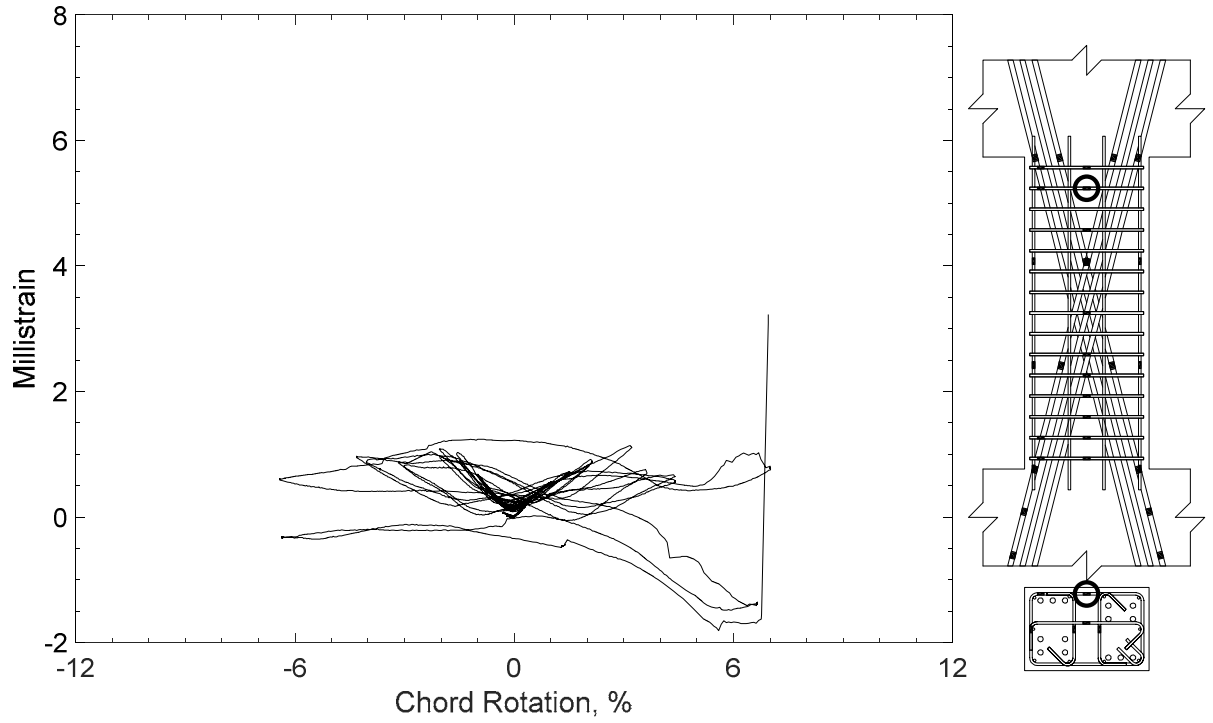


Figure 286 – Measured strain in closed stirrup of D120-2.5, strain gauge S9

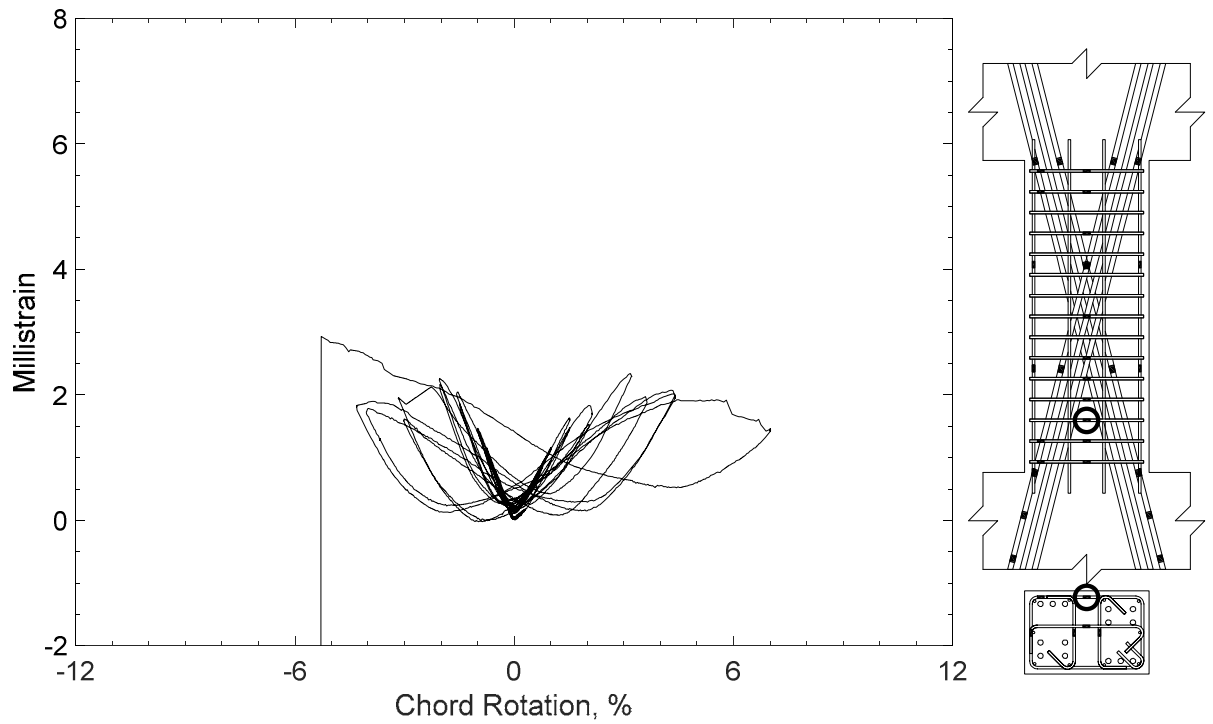


Figure 287 – Measured strain in closed stirrup of D120-2.5, strain gauge S10

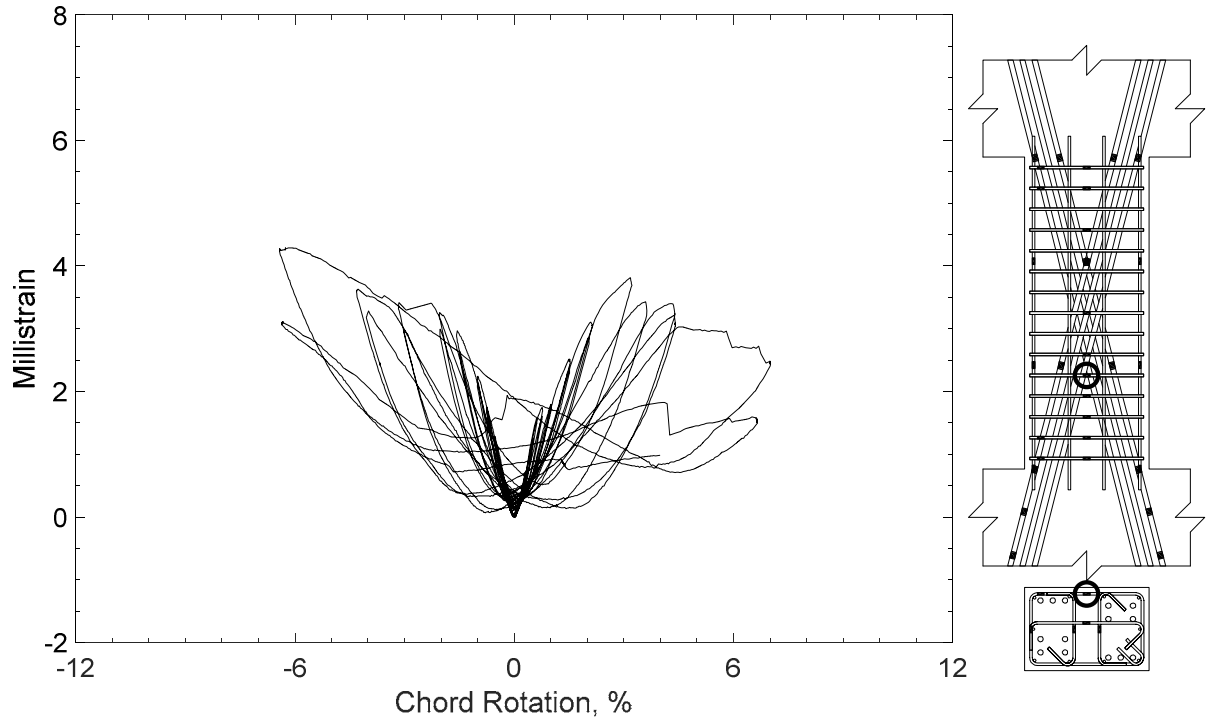


Figure 288 – Measured strain in closed stirrup of D120-2.5, strain gauge S11

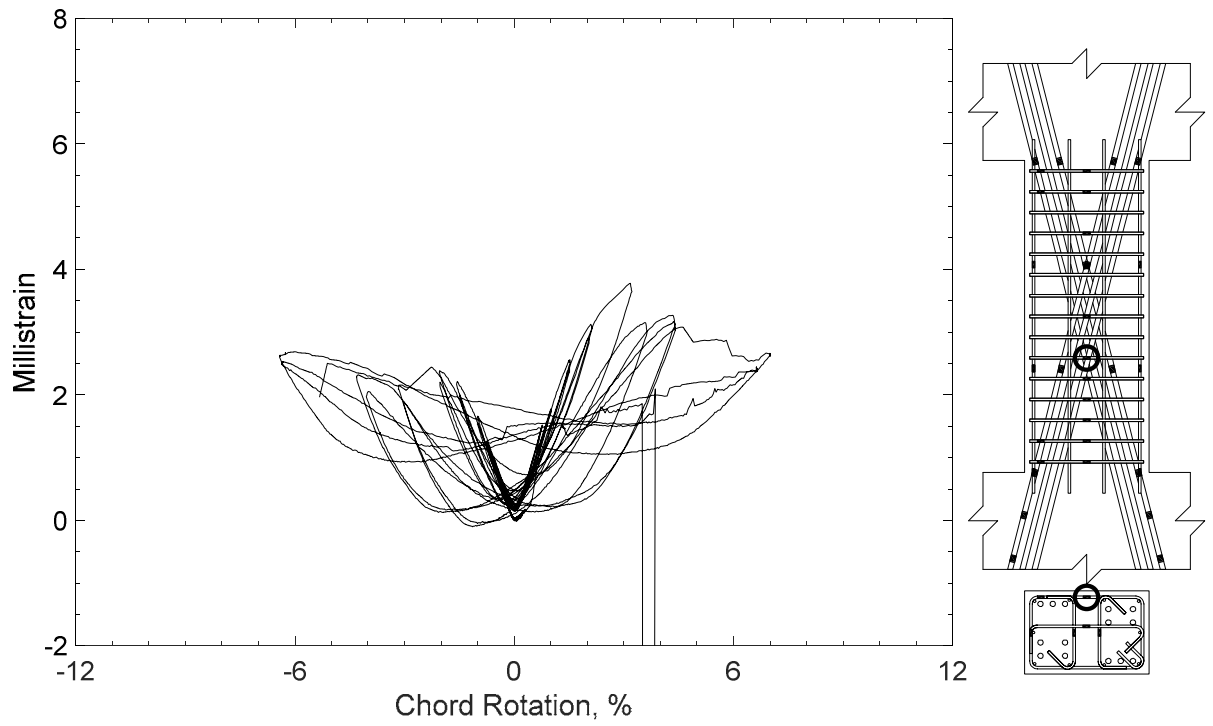


Figure 289 – Measured strain in closed stirrup of D120-2.5, strain gauge S12

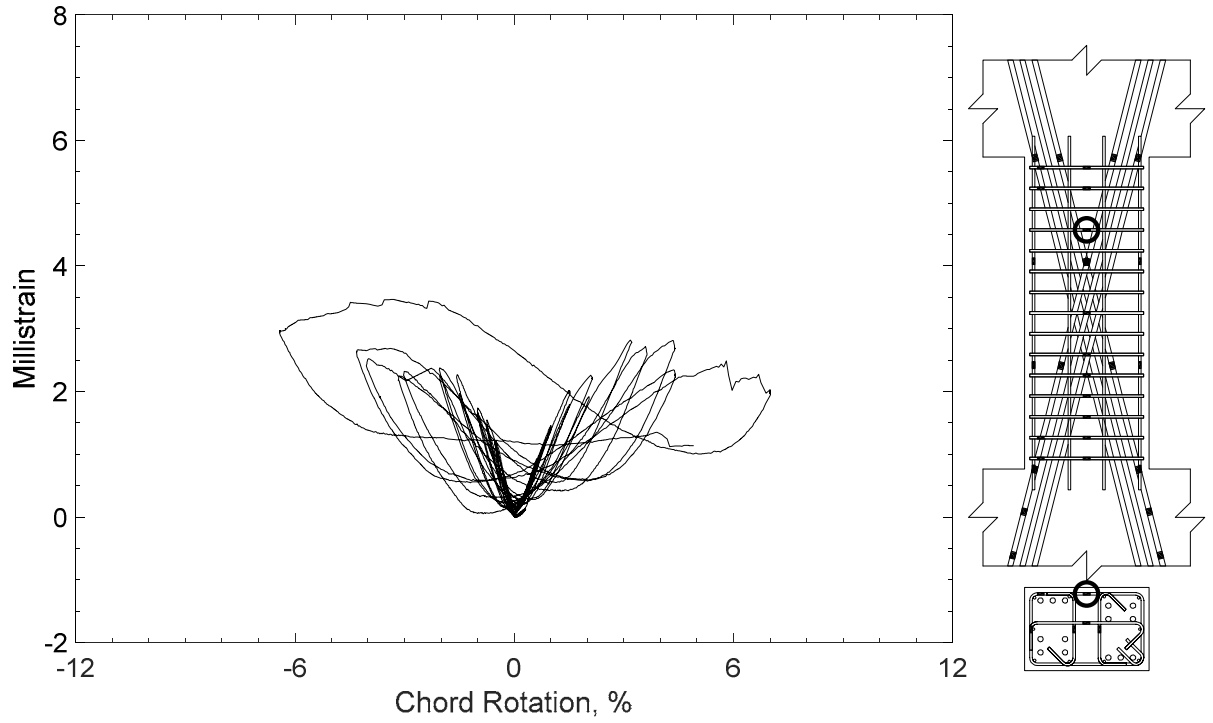


Figure 290 – Measured strain in closed stirrup of D120-2.5, strain gauge S13

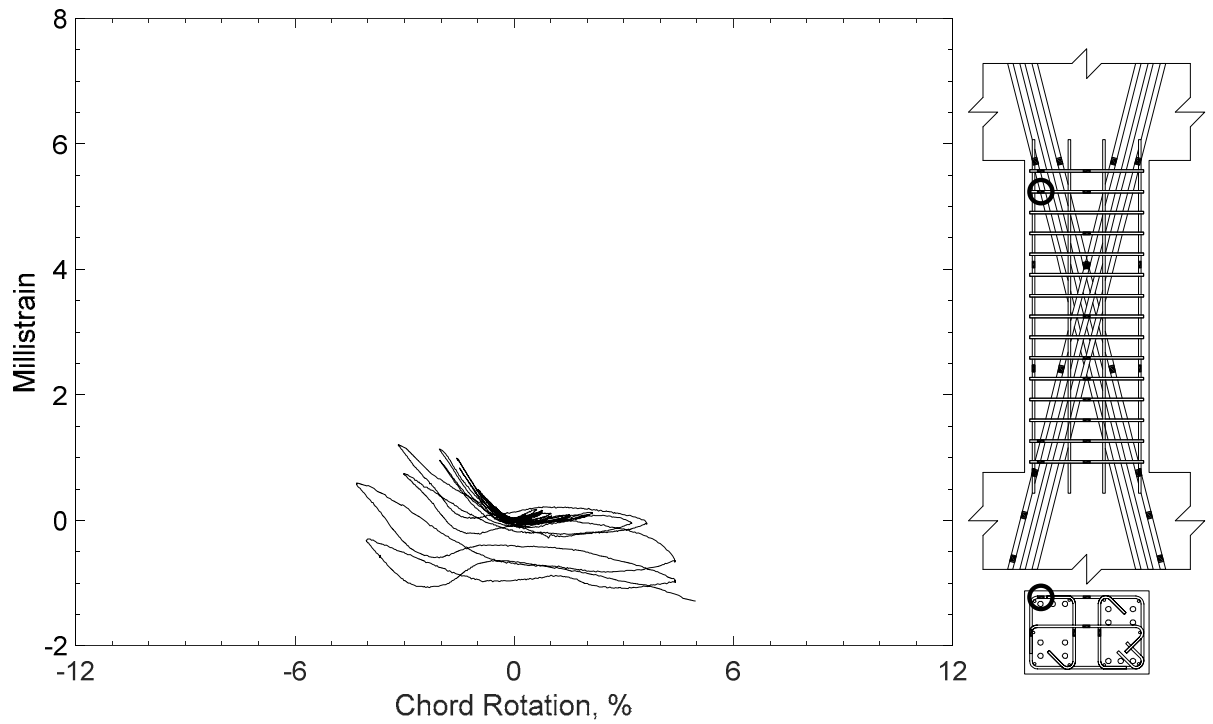


Figure 291 – Measured strain in closed stirrup of D120-2.5, strain gauge S14

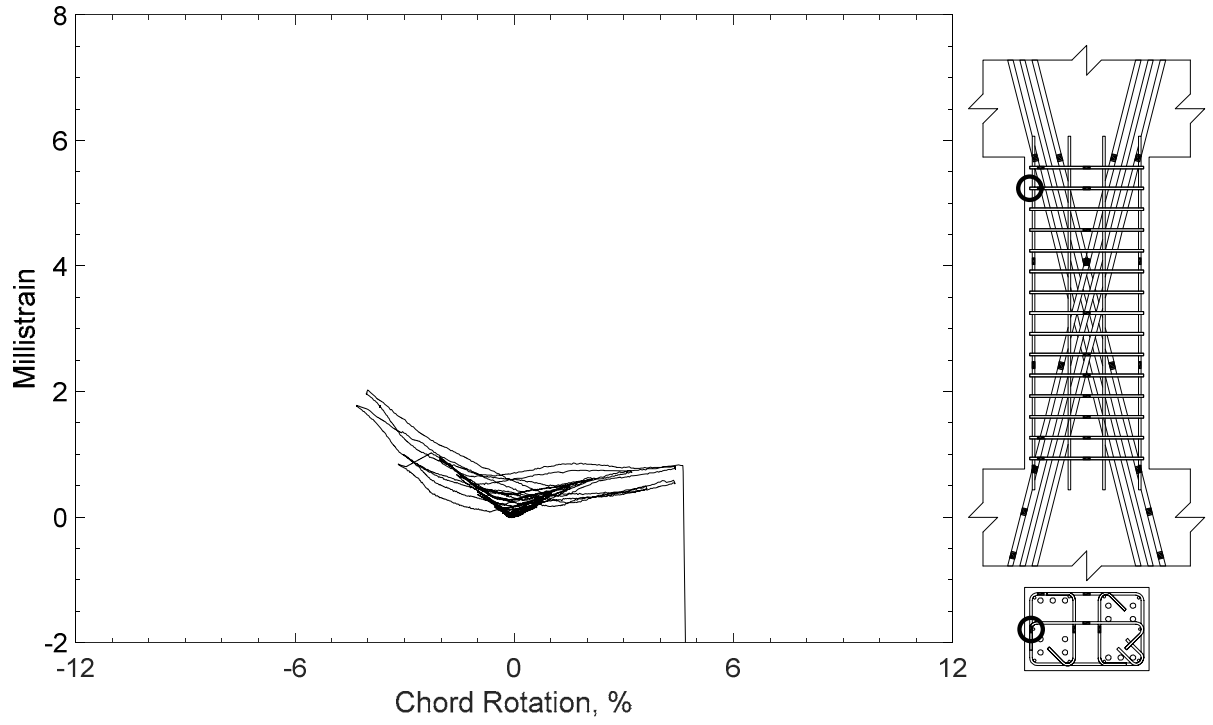


Figure 292 – Measured strain in closed stirrup of D120-2.5, strain gauge S15

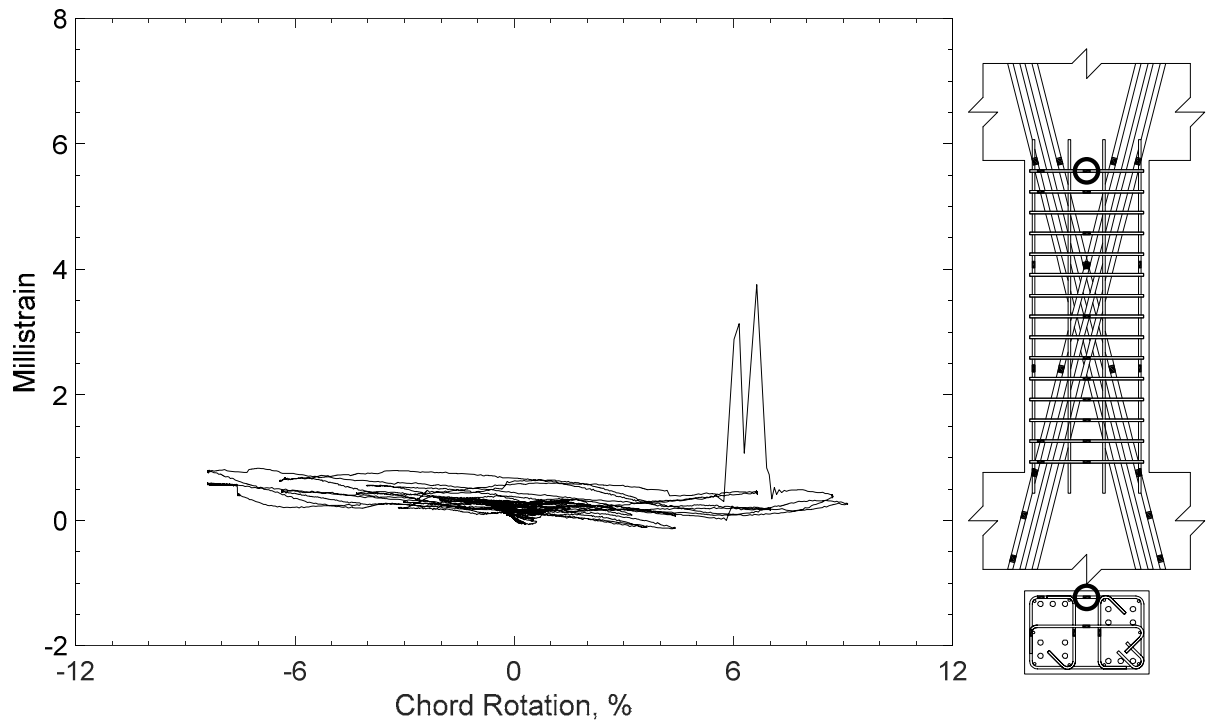


Figure 293 – Measured strain in closed stirrup of D120-2.5, strain gauge S16

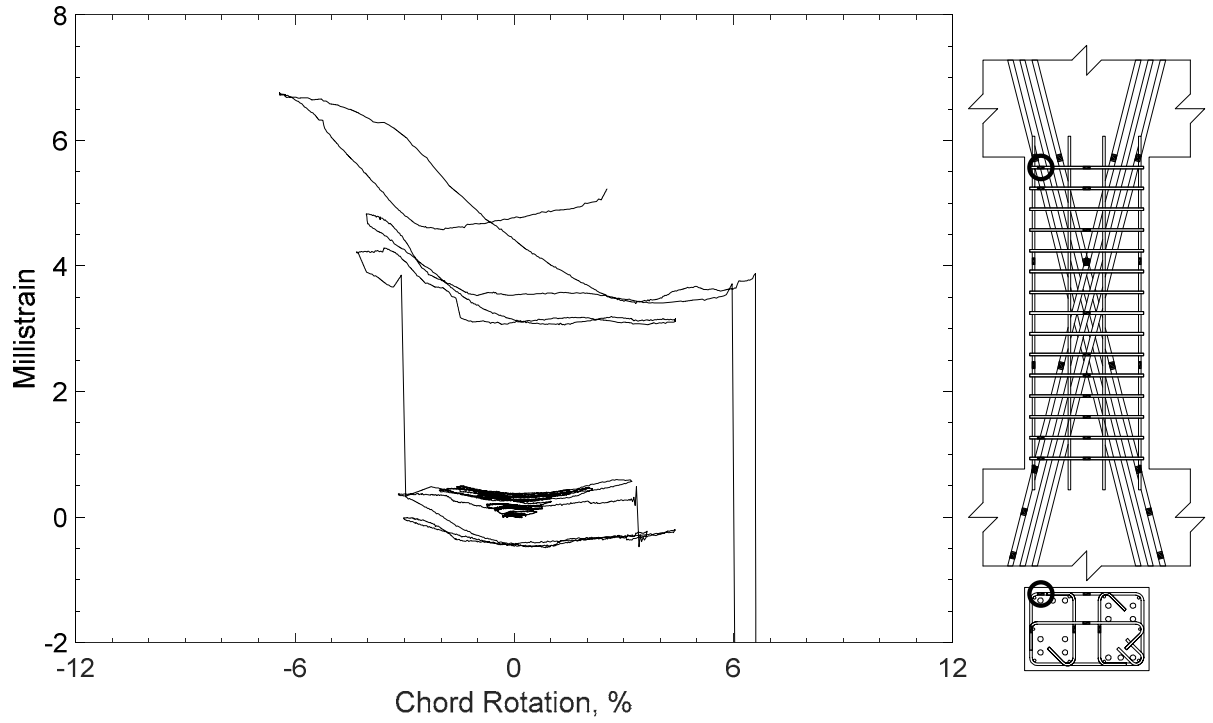


Figure 294 – Measured strain in closed stirrup of D120-2.5, strain gauge S17

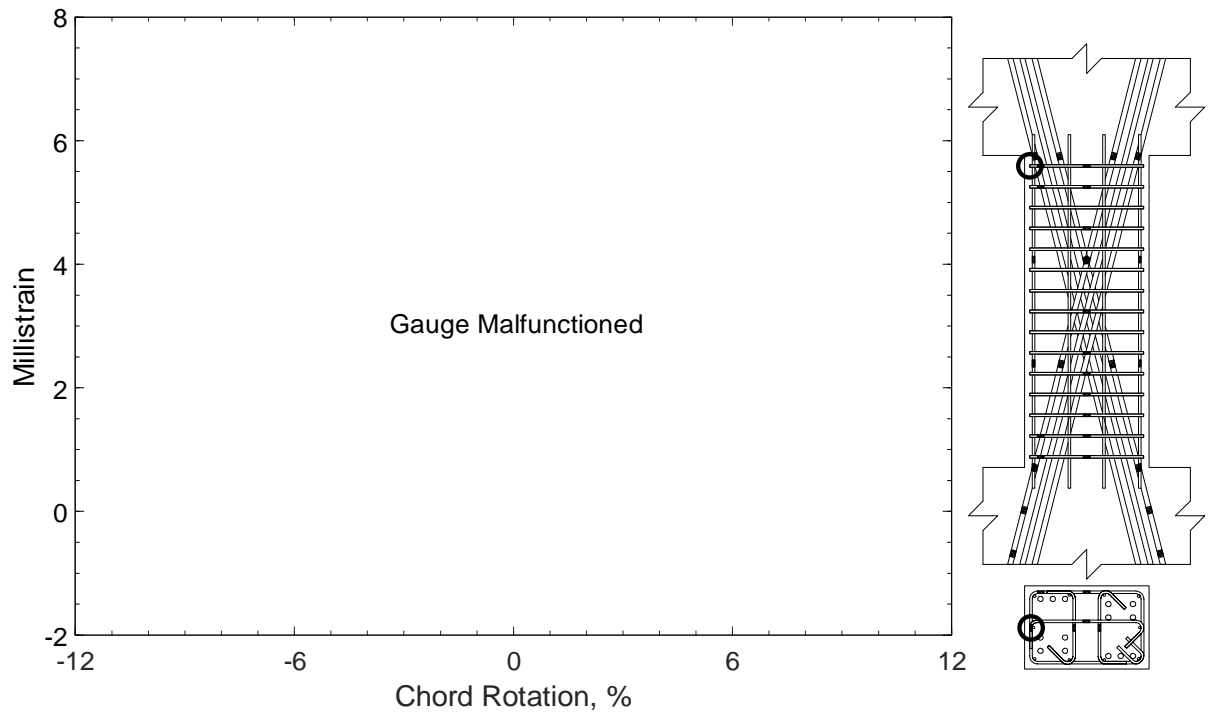


Figure 295 – Measured strain in closed stirrup of D120-2.5, strain gauge S18

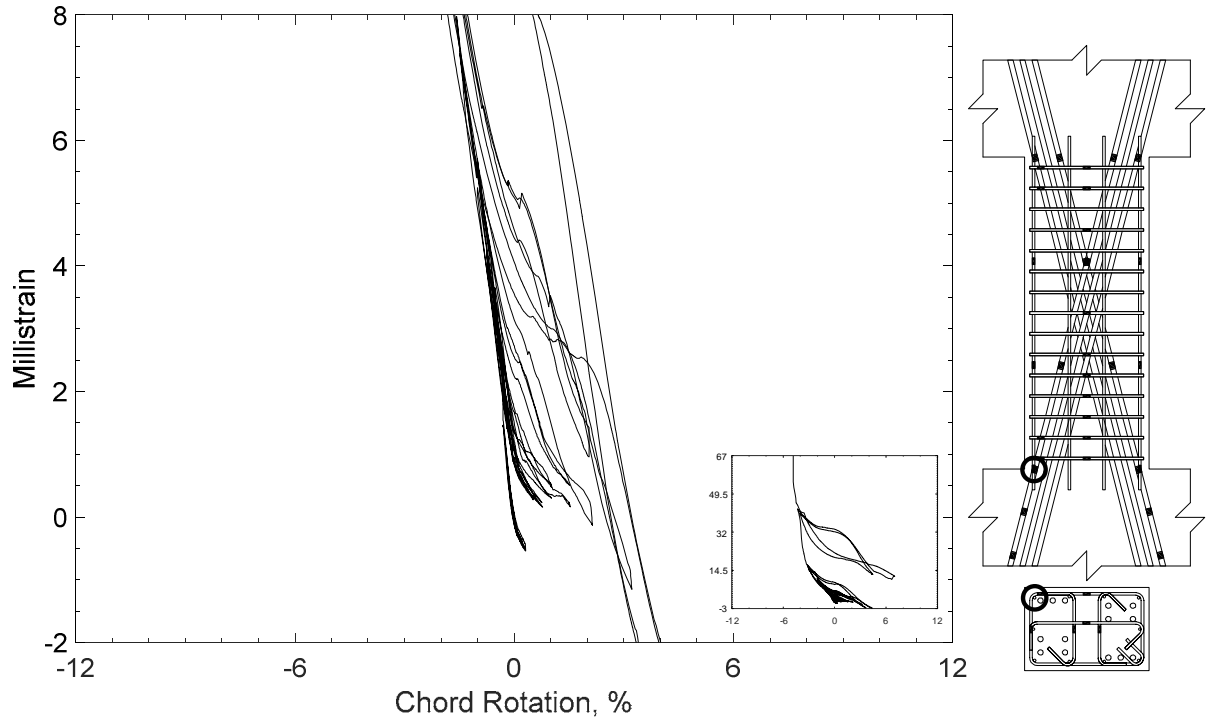


Figure 296 – Measured strain in parallel bar of D120-2.5, strain gauge H1

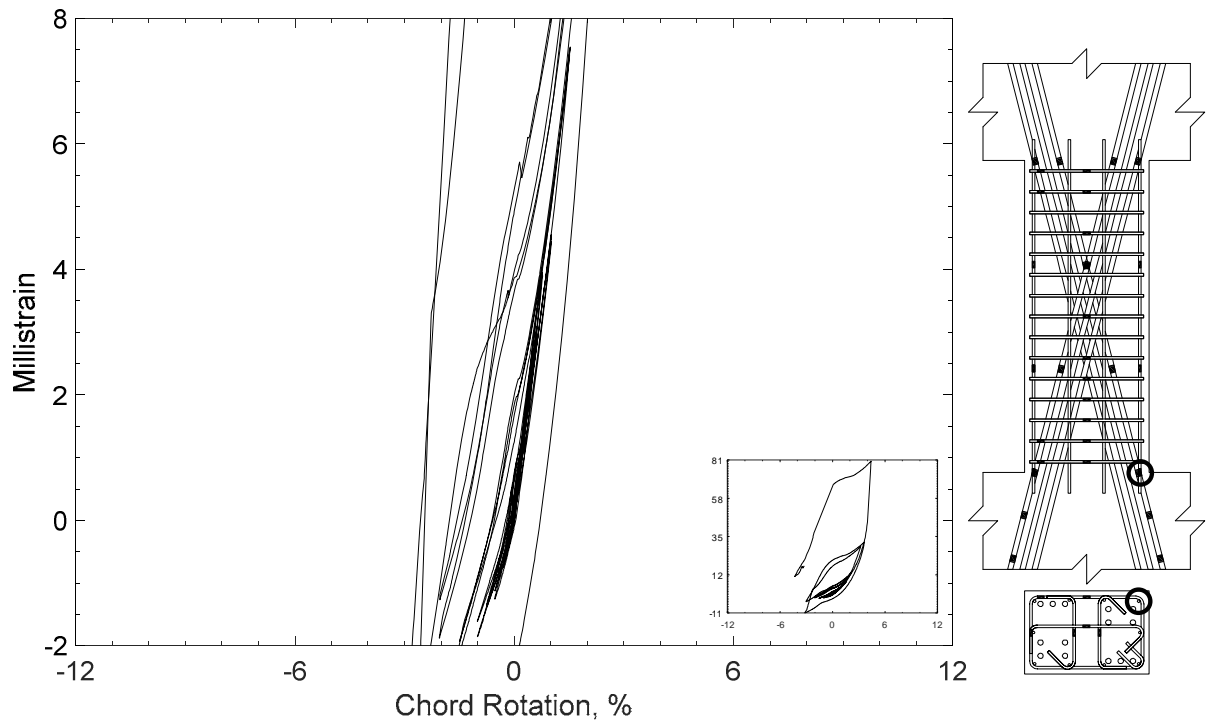


Figure 297 – Measured strain in parallel bar of D120-2.5, strain gauge H2

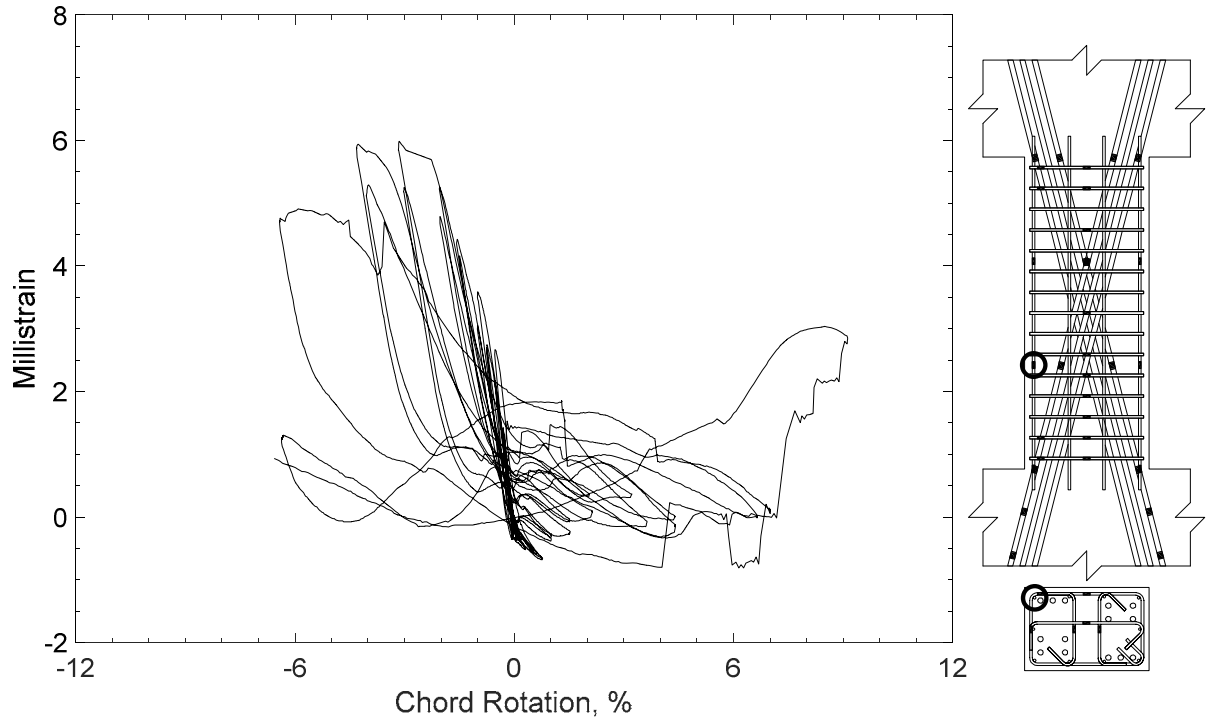


Figure 298 – Measured strain in parallel bar of D120-2.5, strain gauge H3

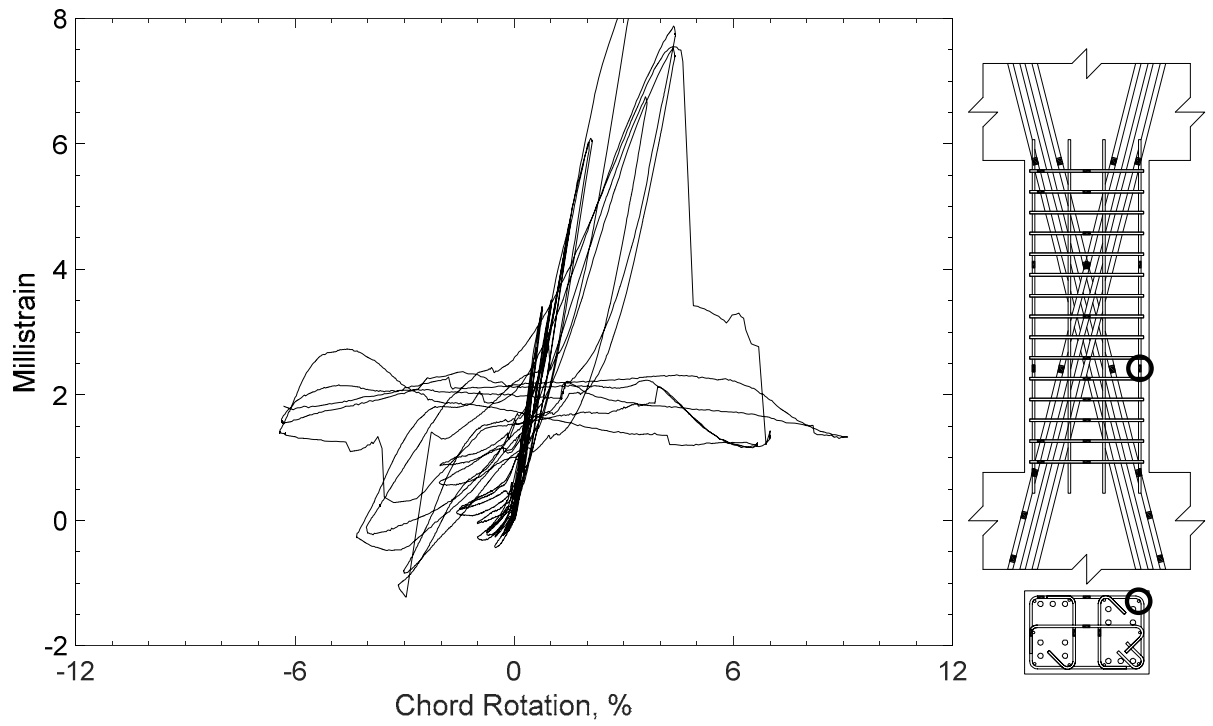


Figure 299 – Measured strain in parallel bar of D120-2.5, strain gauge H4

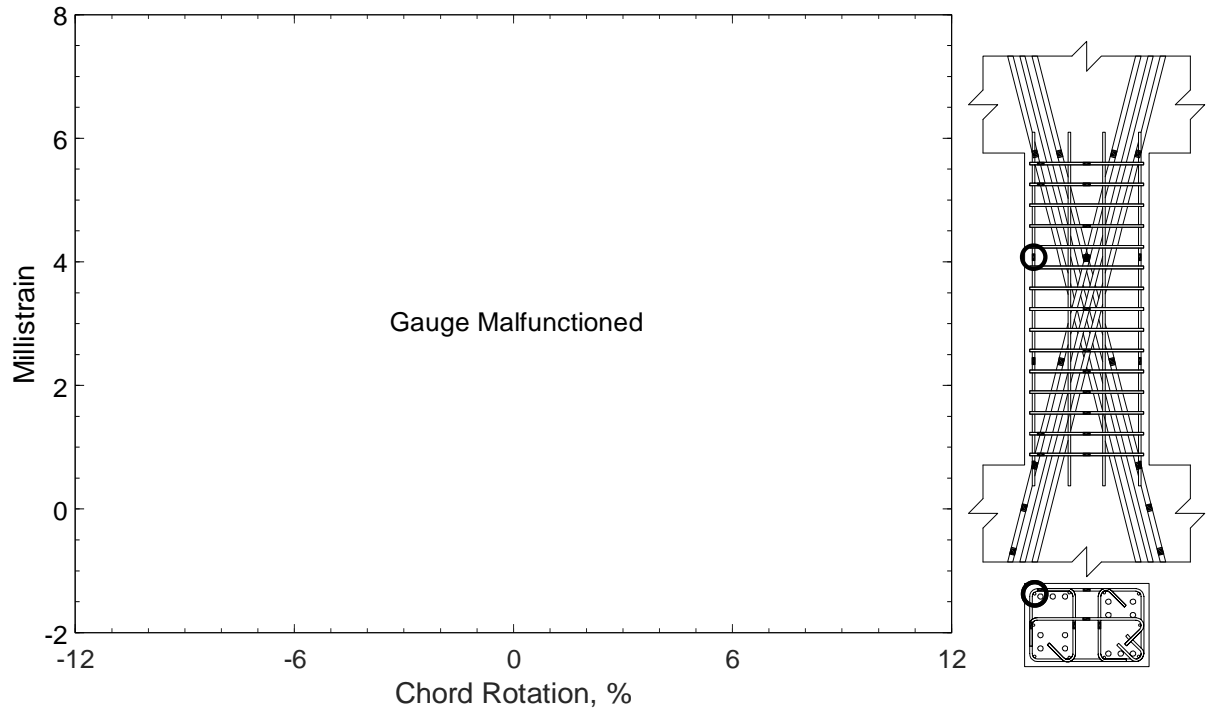


Figure 300 – Measured strain in parallel bar of D120-2.5, strain gauge H5

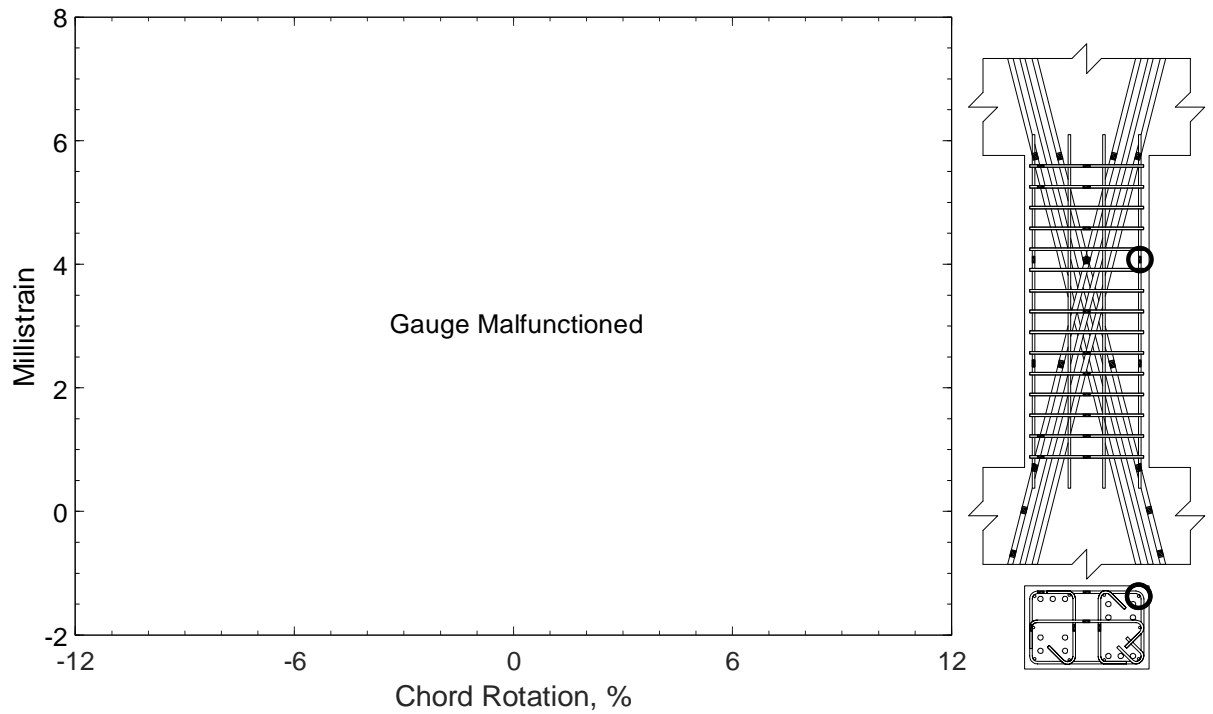


Figure 301 – Measured strain in parallel bar of D120-2.5, strain gauge H6

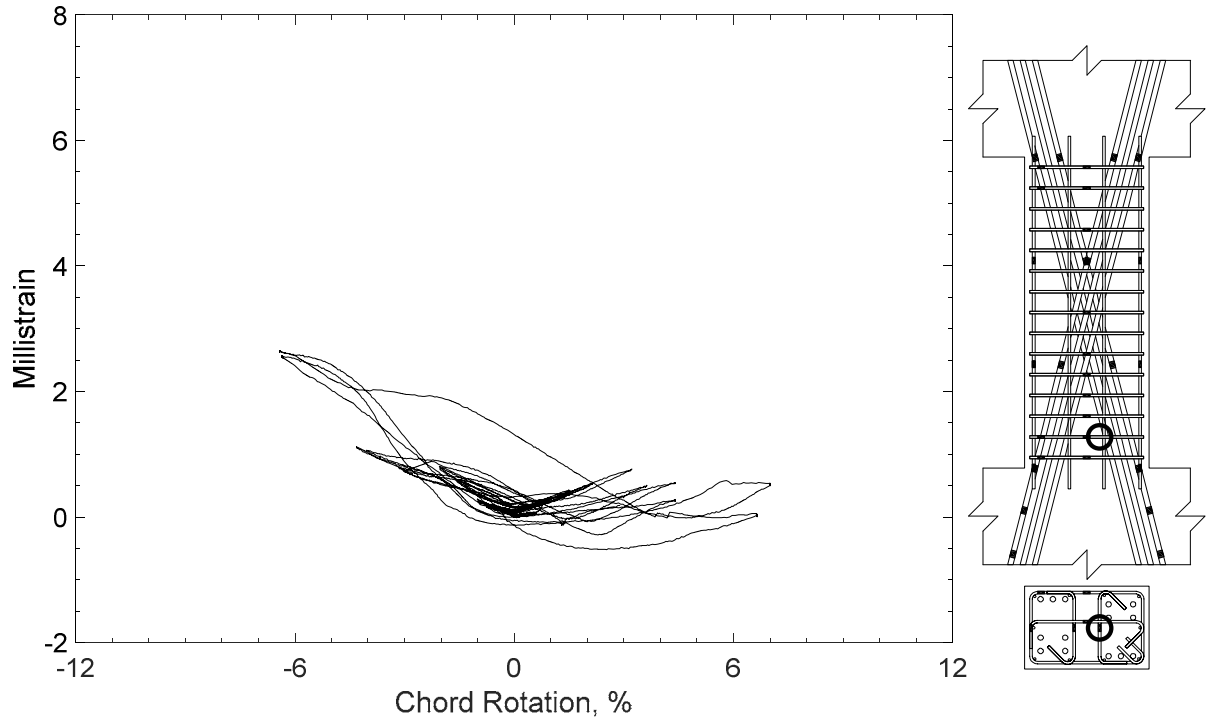


Figure 302 – Measured strain in crosstie of D120-2.5, strain gauge T1

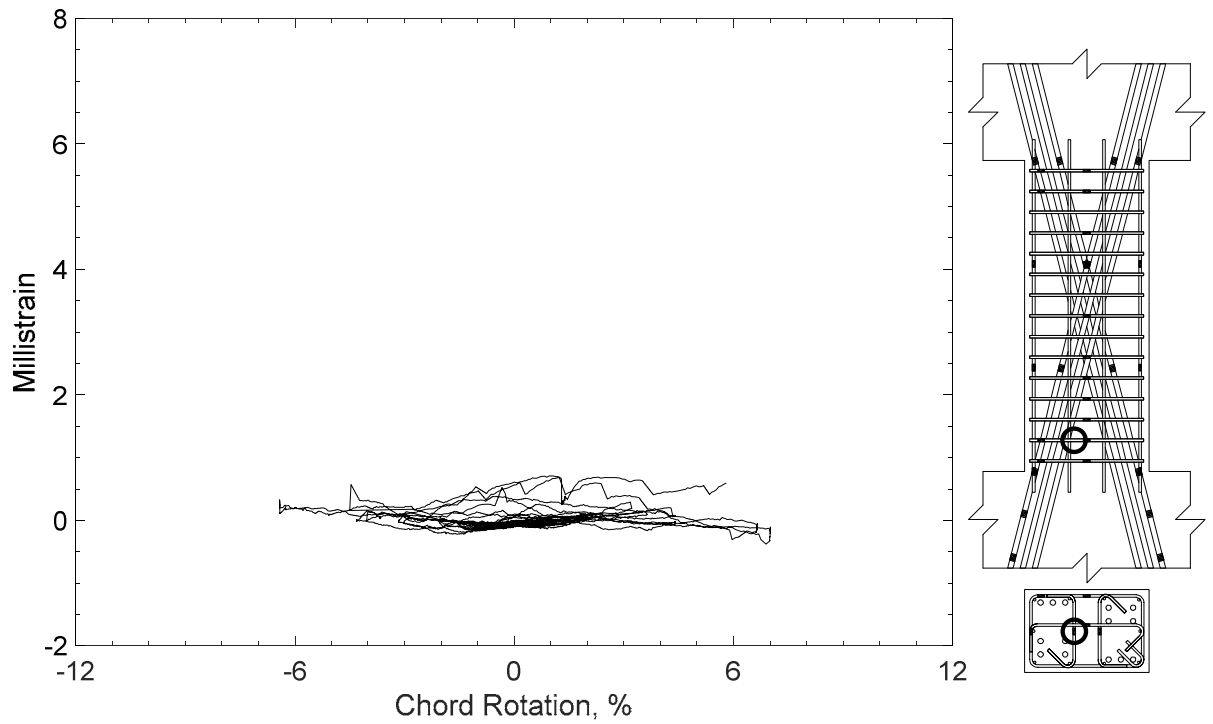


Figure 303 – Measured strain in crosstie of D120-2.5, strain gauge T2

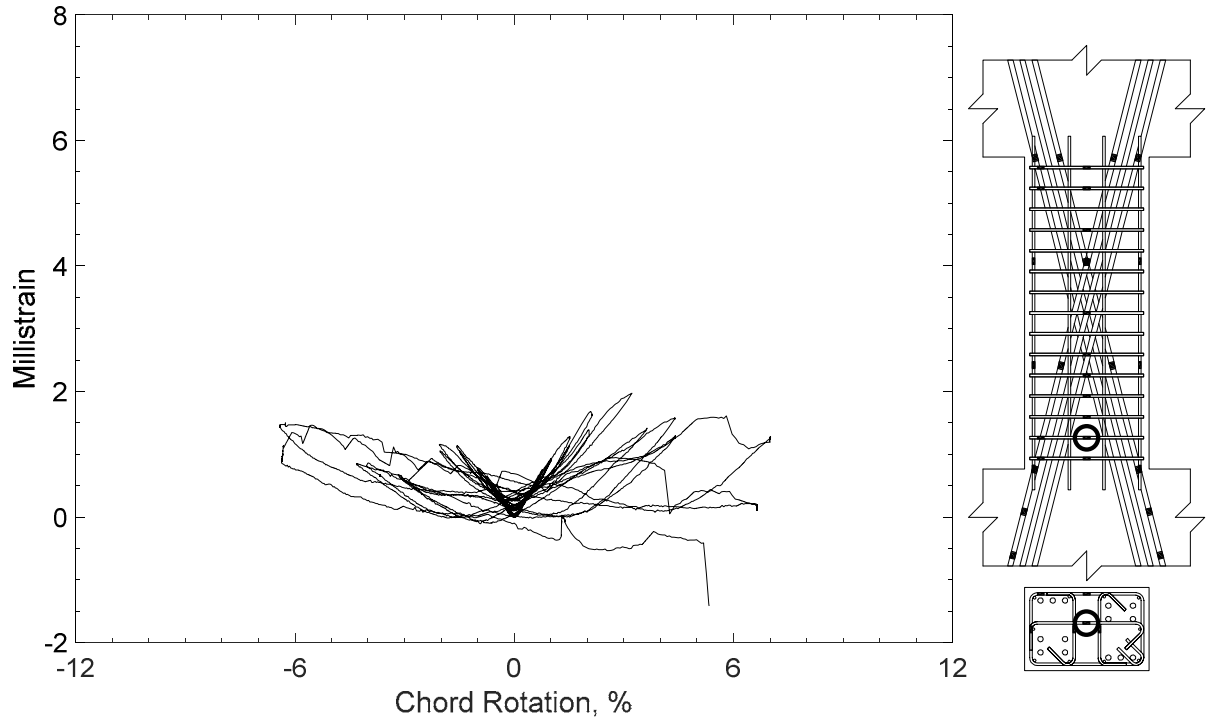


Figure 304 – Measured strain in crossie of D120-2.5, strain gauge T3

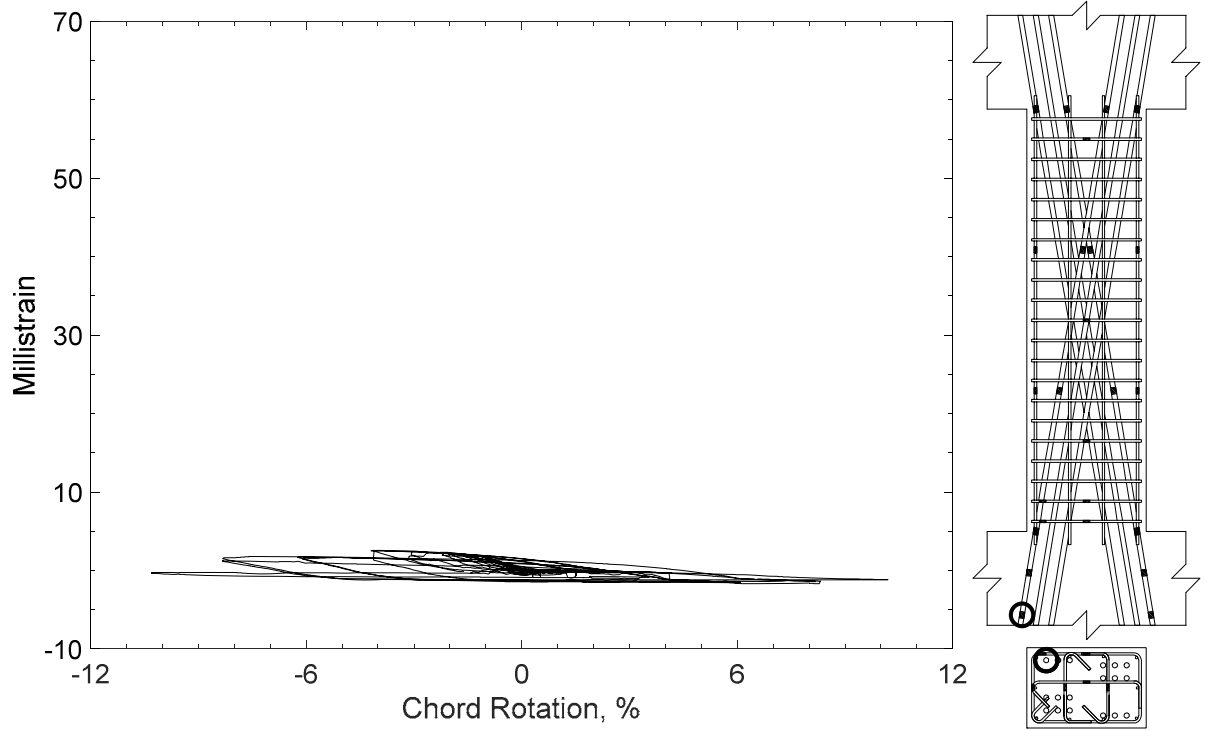


Figure 305 – Measured strain in diagonal bar of D80-3.5, strain gauge D1

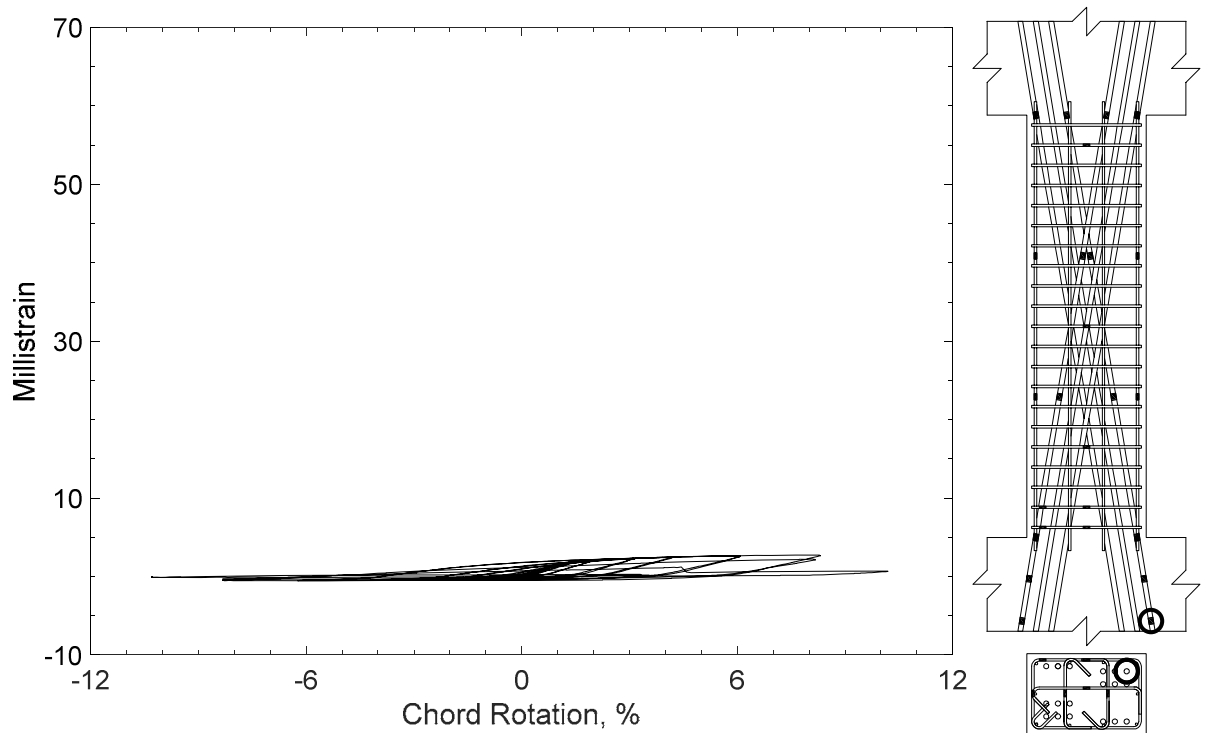


Figure 306 – Measured strain in diagonal bar of D80-3.5, strain gauge D2

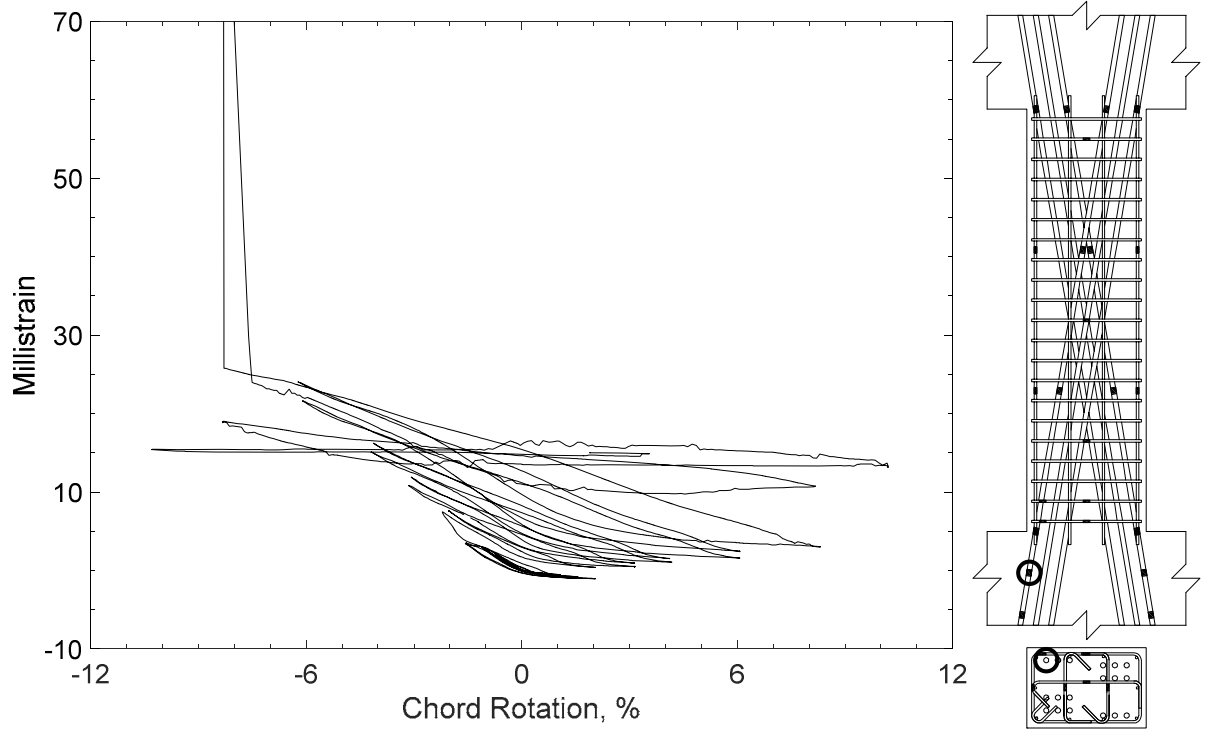


Figure 307 – Measured strain in diagonal bar of D80-3.5, strain gauge D3

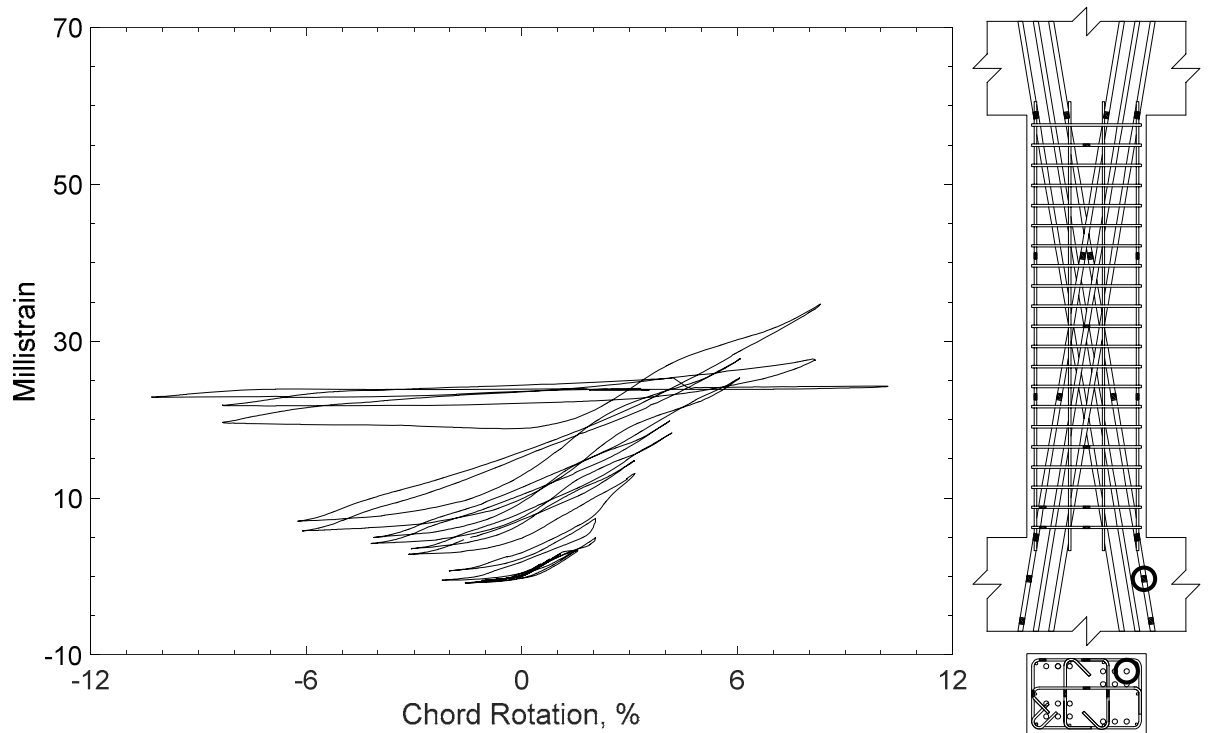


Figure 308 – Measured strain in diagonal bar of D80-3.5, strain gauge D4

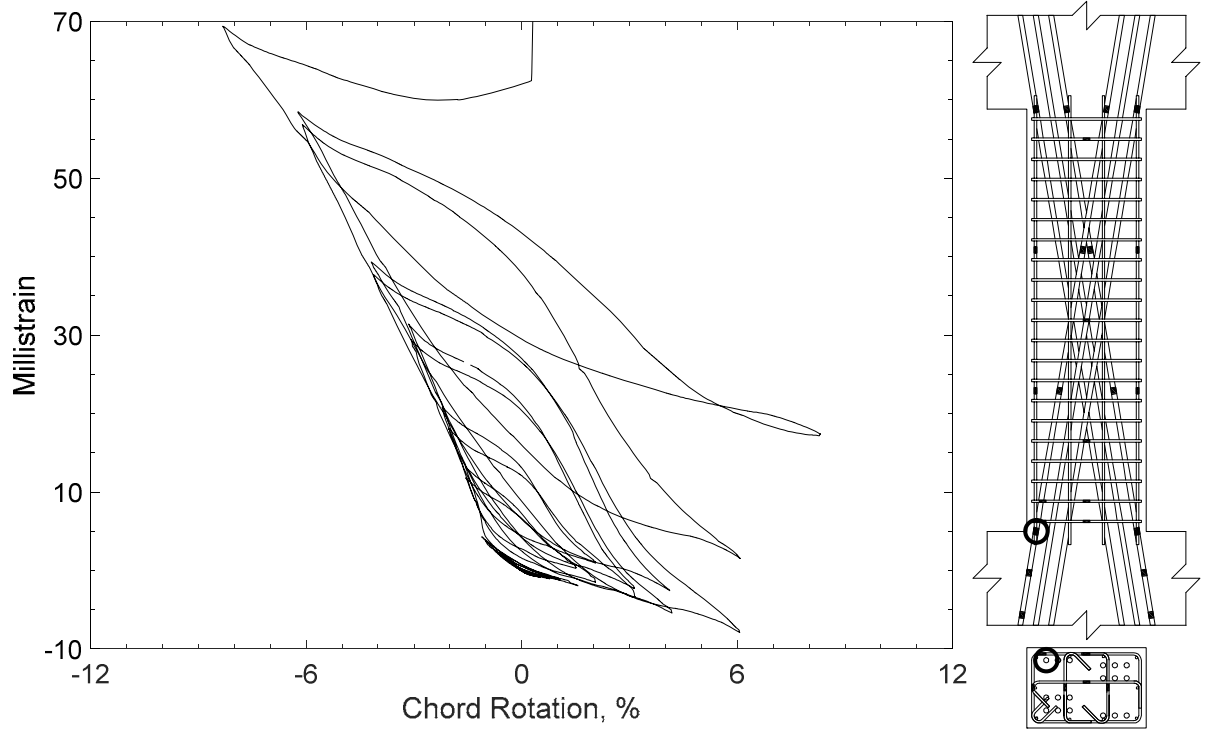


Figure 309 – Measured strain in diagonal bar of D80-3.5, strain gauge D5

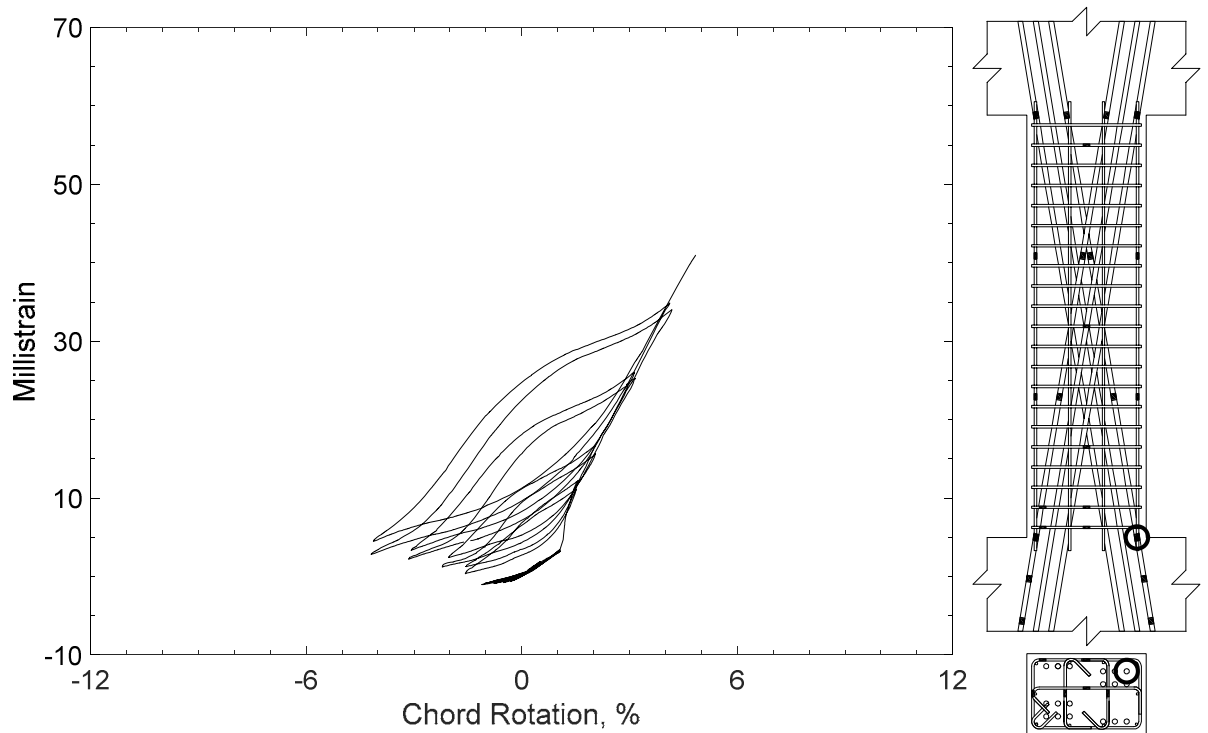


Figure 310 – Measured strain in diagonal bar of D80-3.5, strain gauge D6

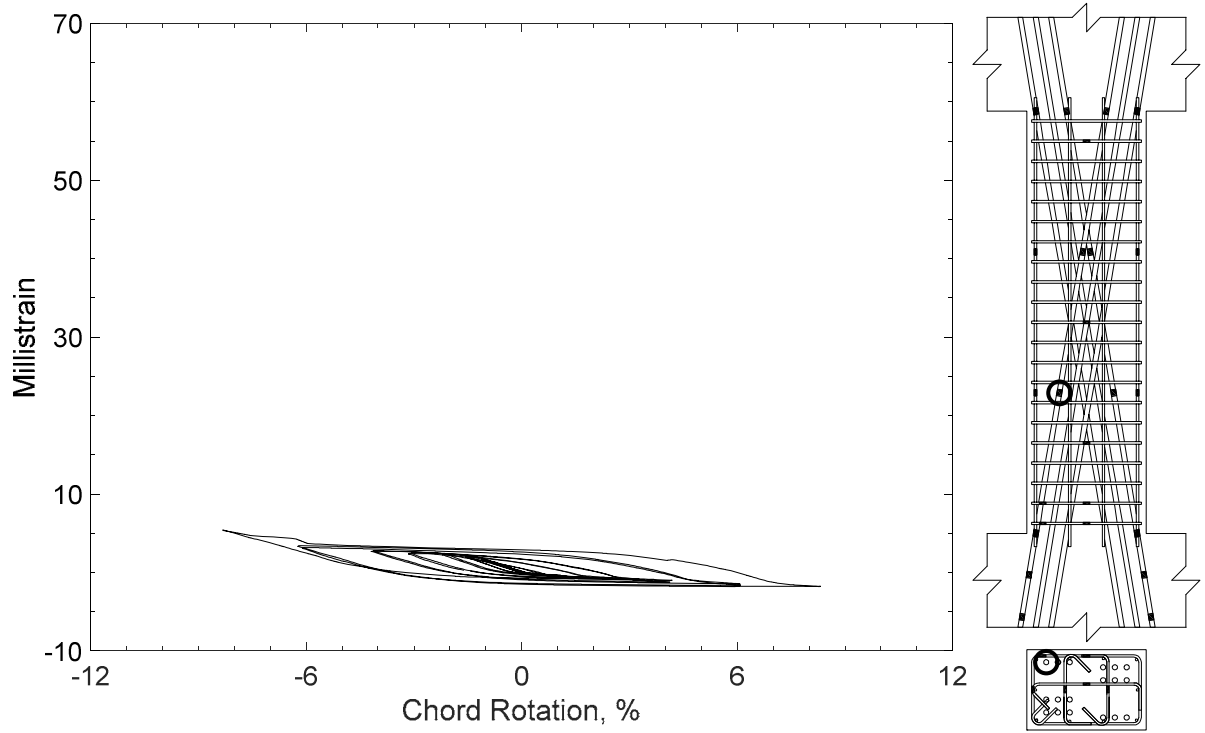


Figure 311 – Measured strain in diagonal bar of D80-3.5, strain gauge D7

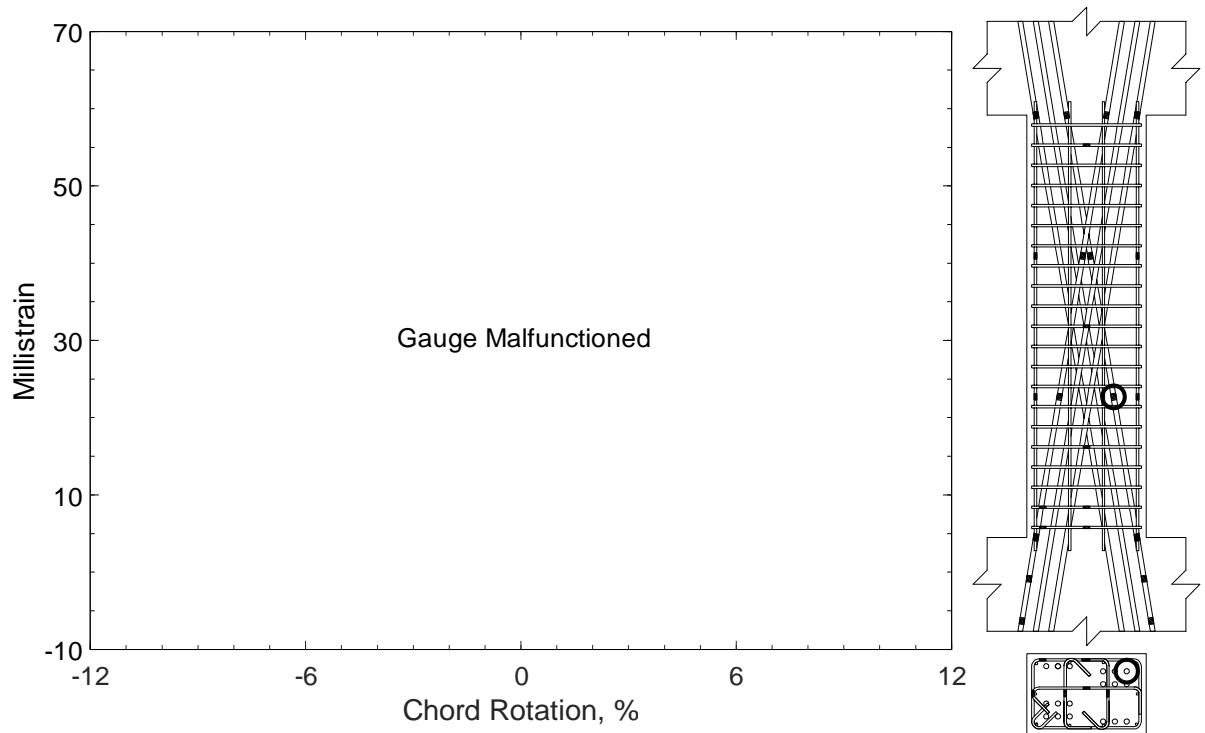


Figure 312 – Measured strain in diagonal bar of D80-3.5, strain gauge D8

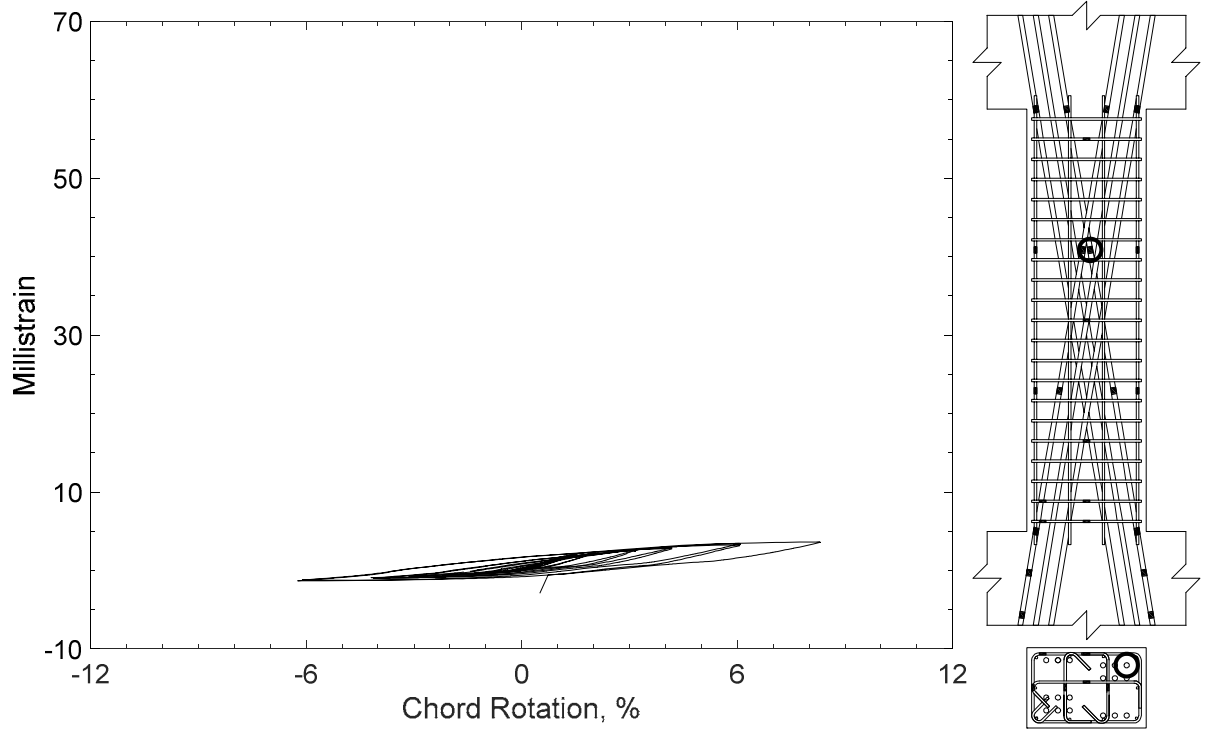


Figure 313 – Measured strain in diagonal bar of D80-3.5, strain gauge D9

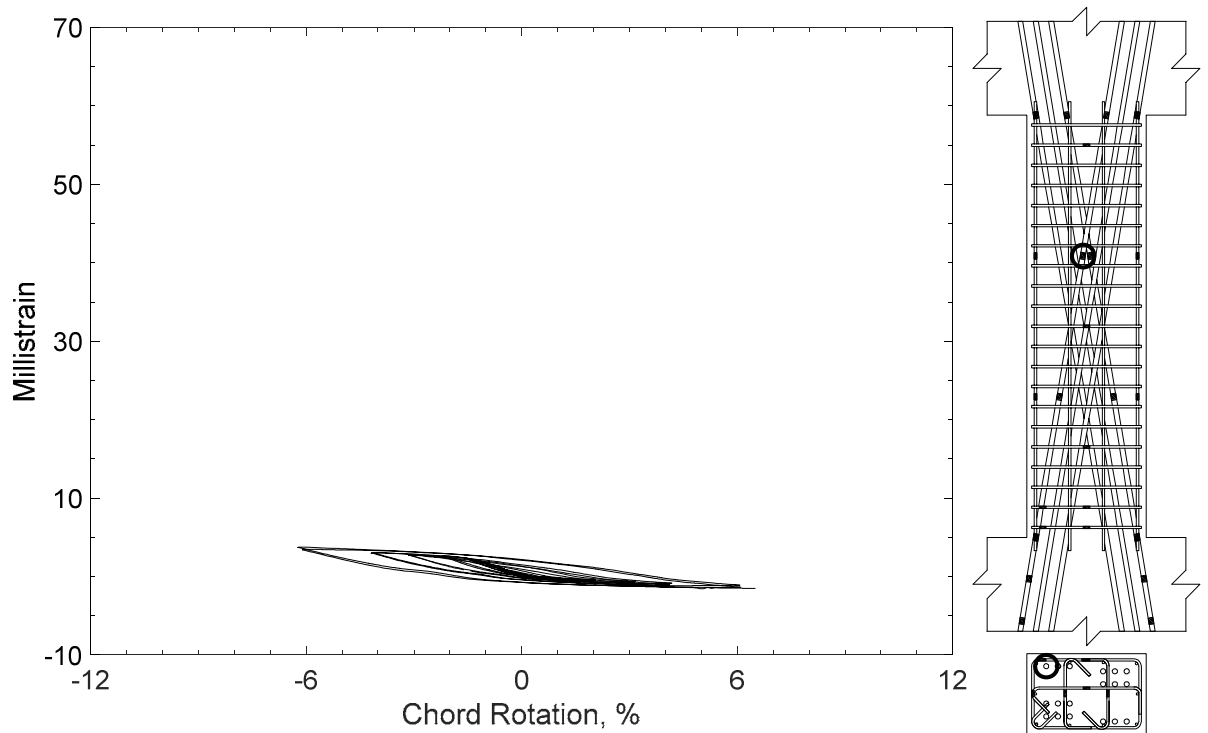


Figure 314 – Measured strain in diagonal bar of D80-3.5, strain gauge D10

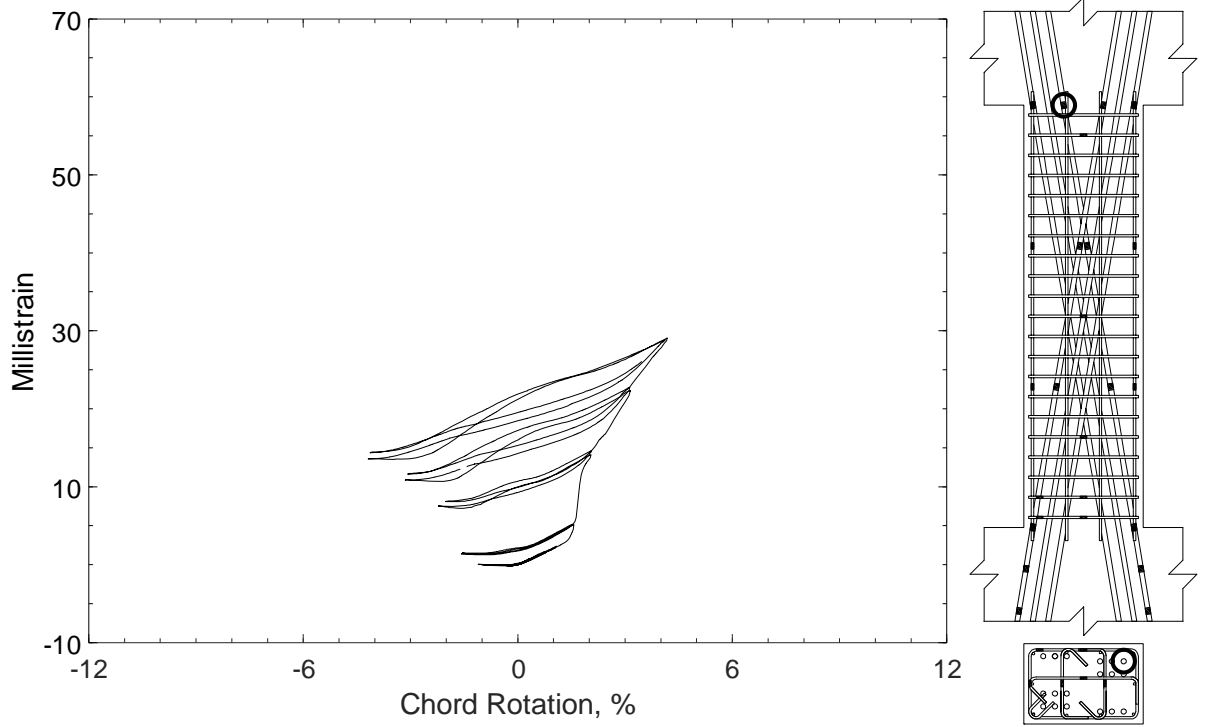


Figure 315 – Measured strain in diagonal bar of D80-3.5, strain gauge D11

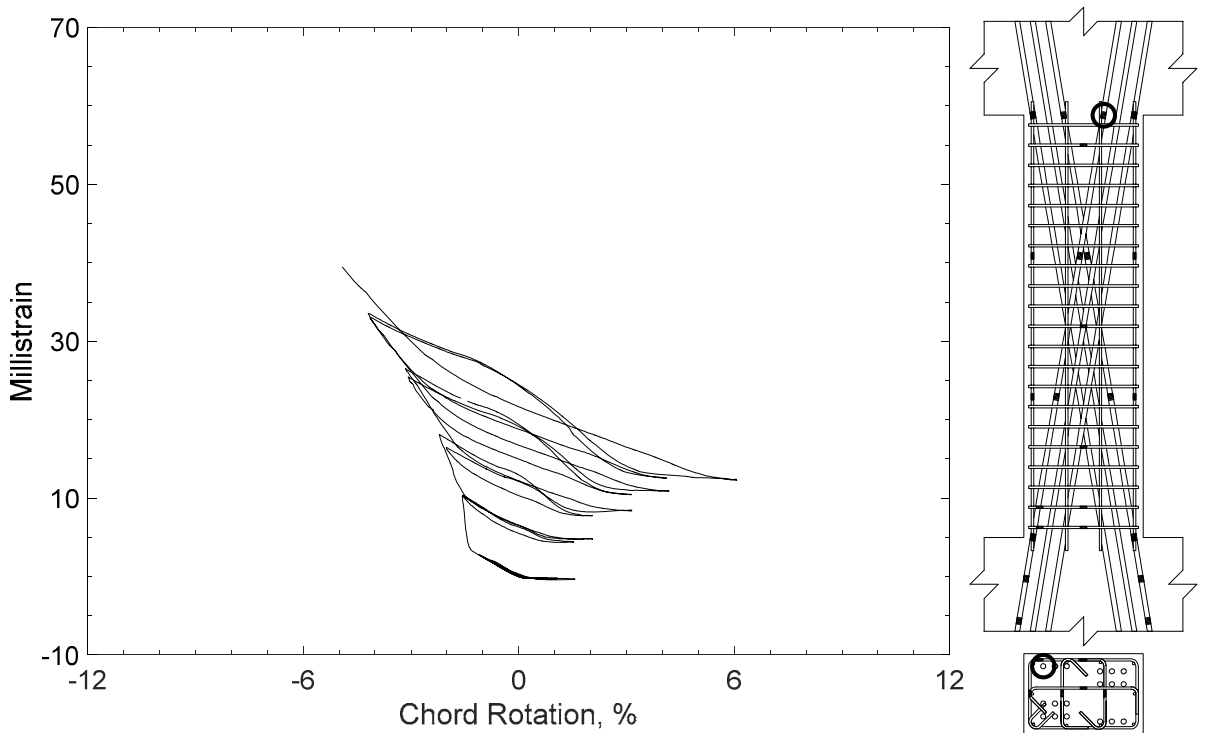


Figure 316 – Measured strain in diagonal bar of D80-3.5, strain gauge D12

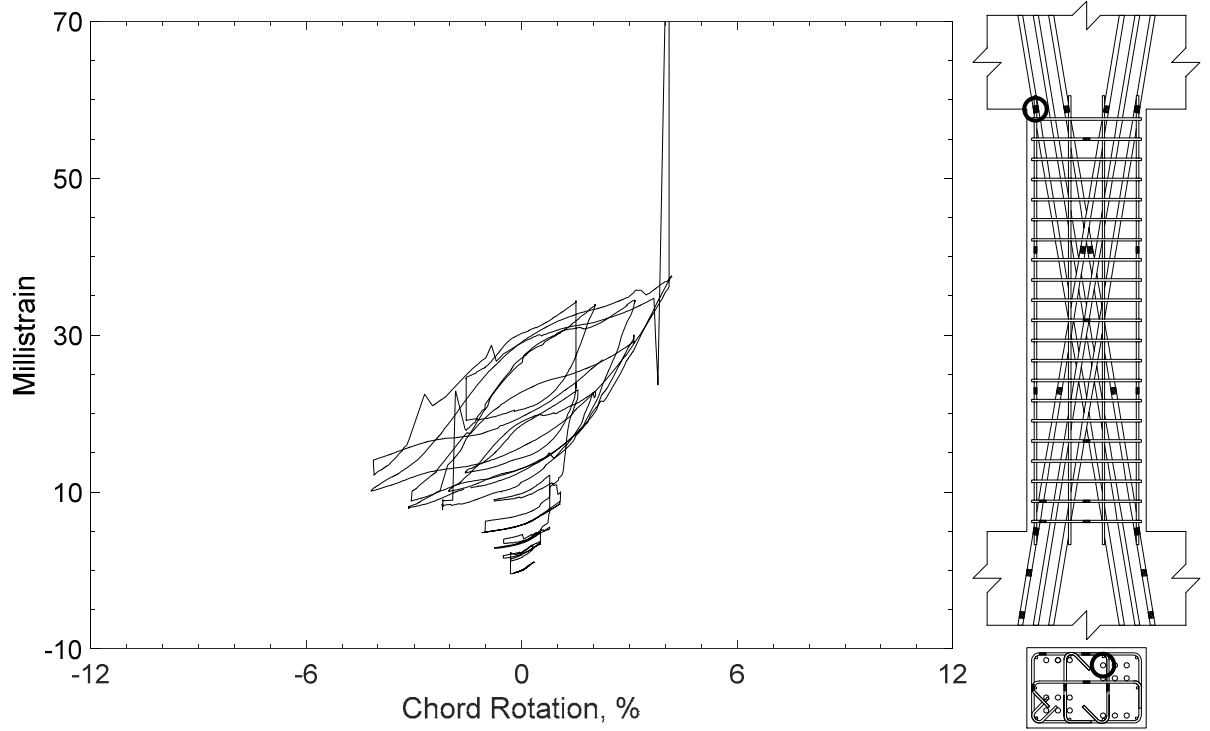


Figure 317 – Measured strain in diagonal bar of D80-3.5, strain gauge D13

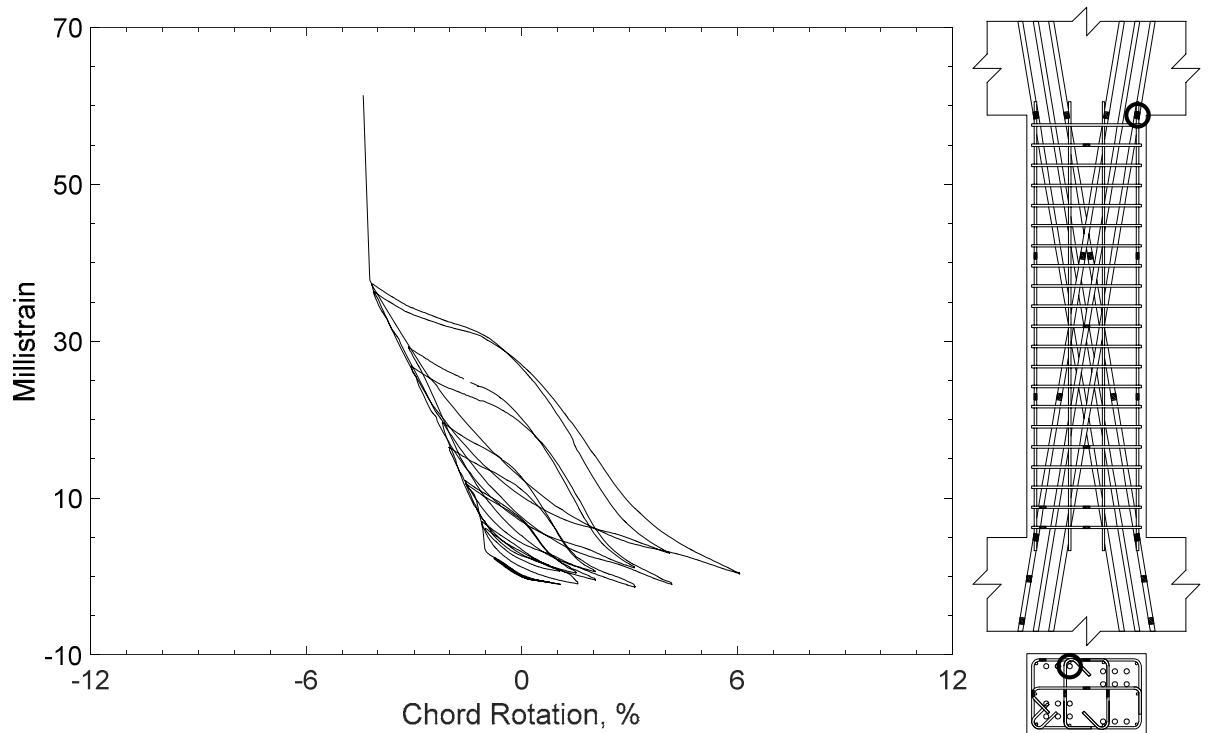


Figure 318 – Measured strain in diagonal bar of D80-3.5, strain gauge D14

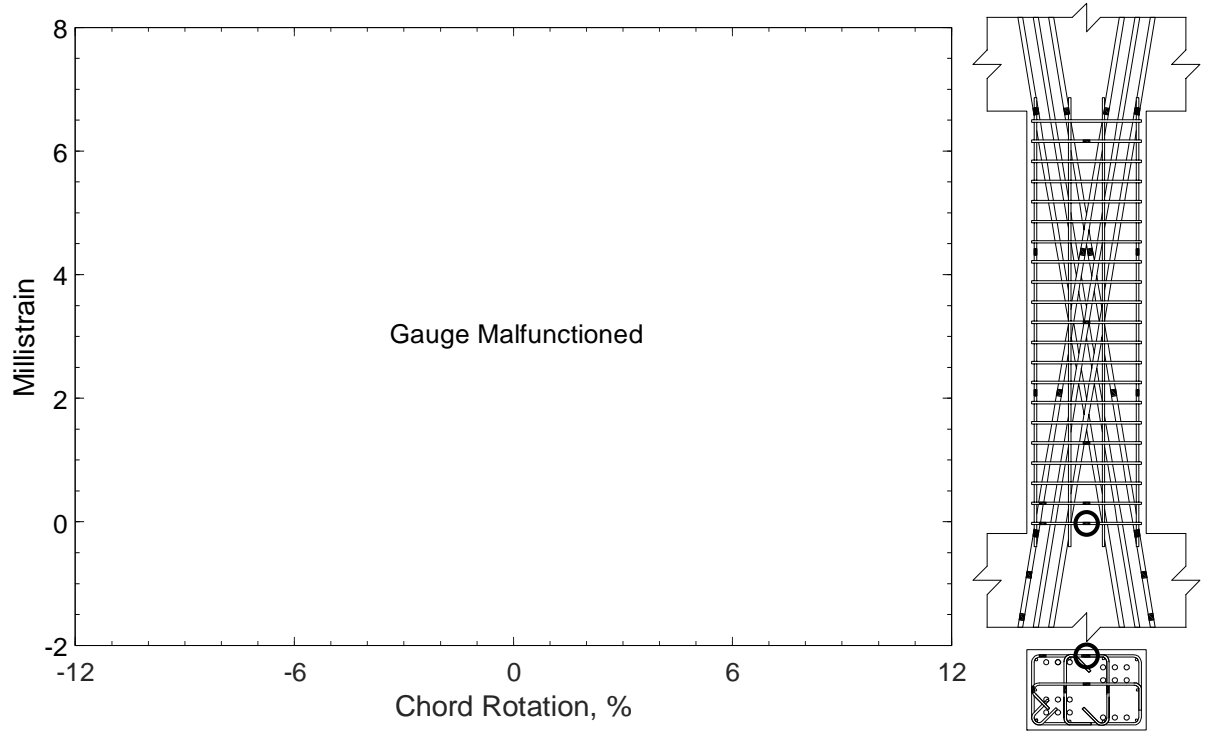


Figure 319 – Measured strain in closed stirrup of D80-3.5, strain gauge S1

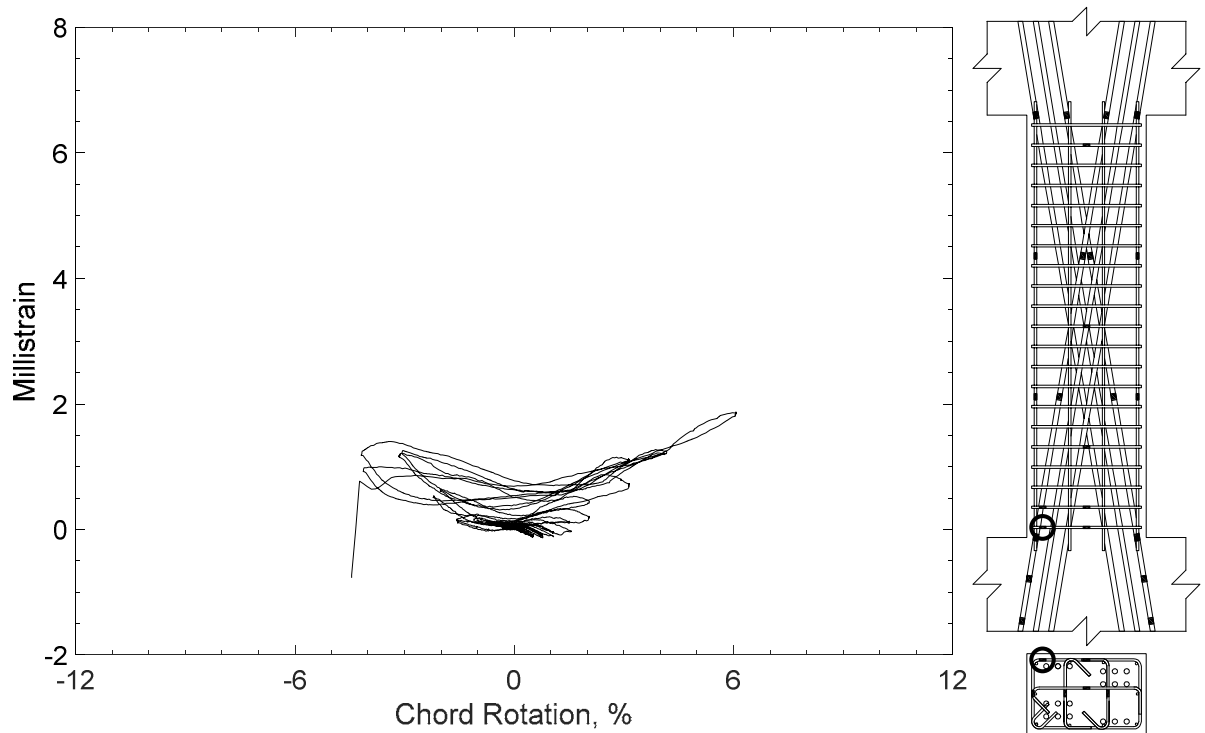


Figure 320 – Measured strain in closed stirrup of D80-3.5, strain gauge S2

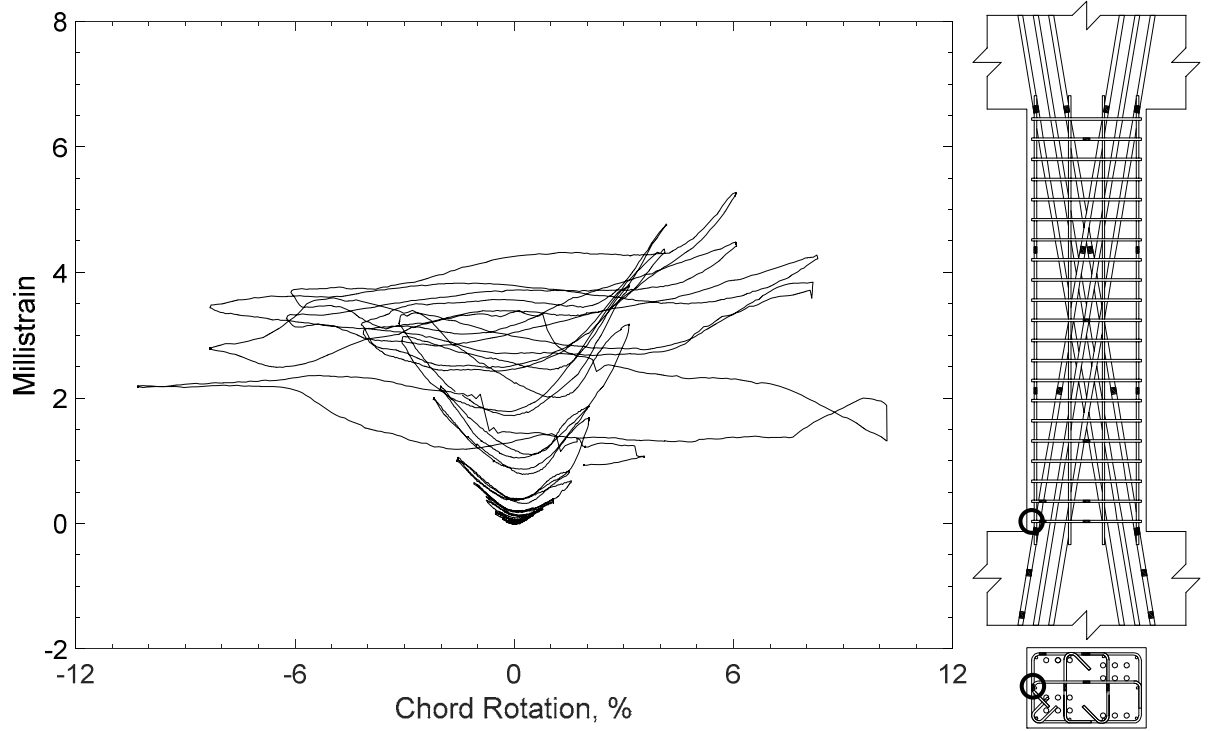


Figure 321 – Measured strain in closed stirrup of D80-3.5, strain gauge S3

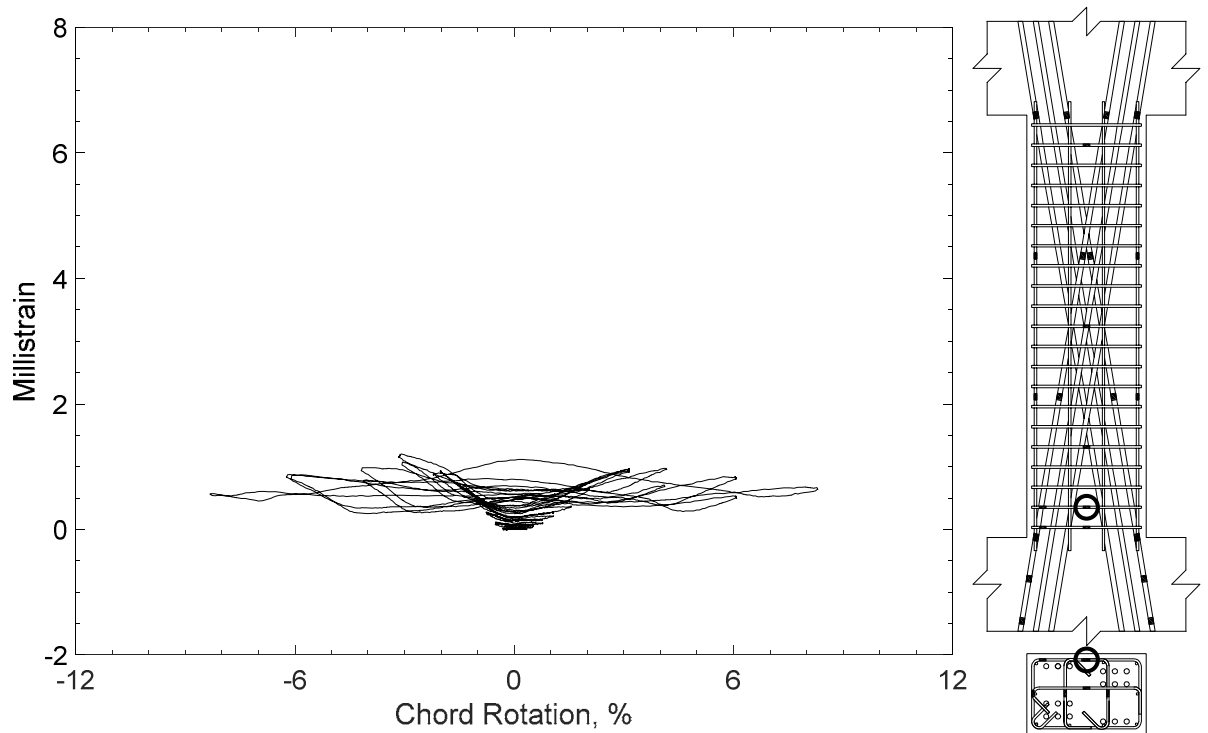


Figure 322 – Measured strain in closed stirrup of D80-3.5, strain gauge S4

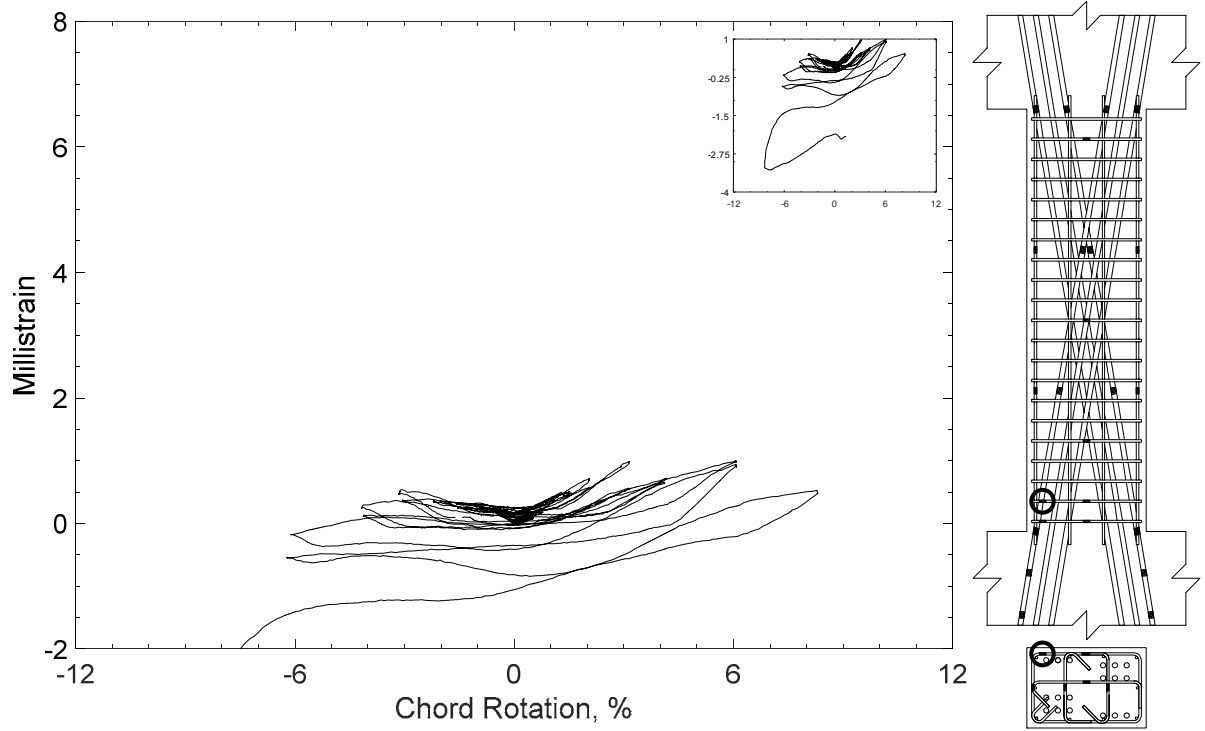


Figure 323 – Measured strain in closed stirrup of D80-3.5, strain gauge S5

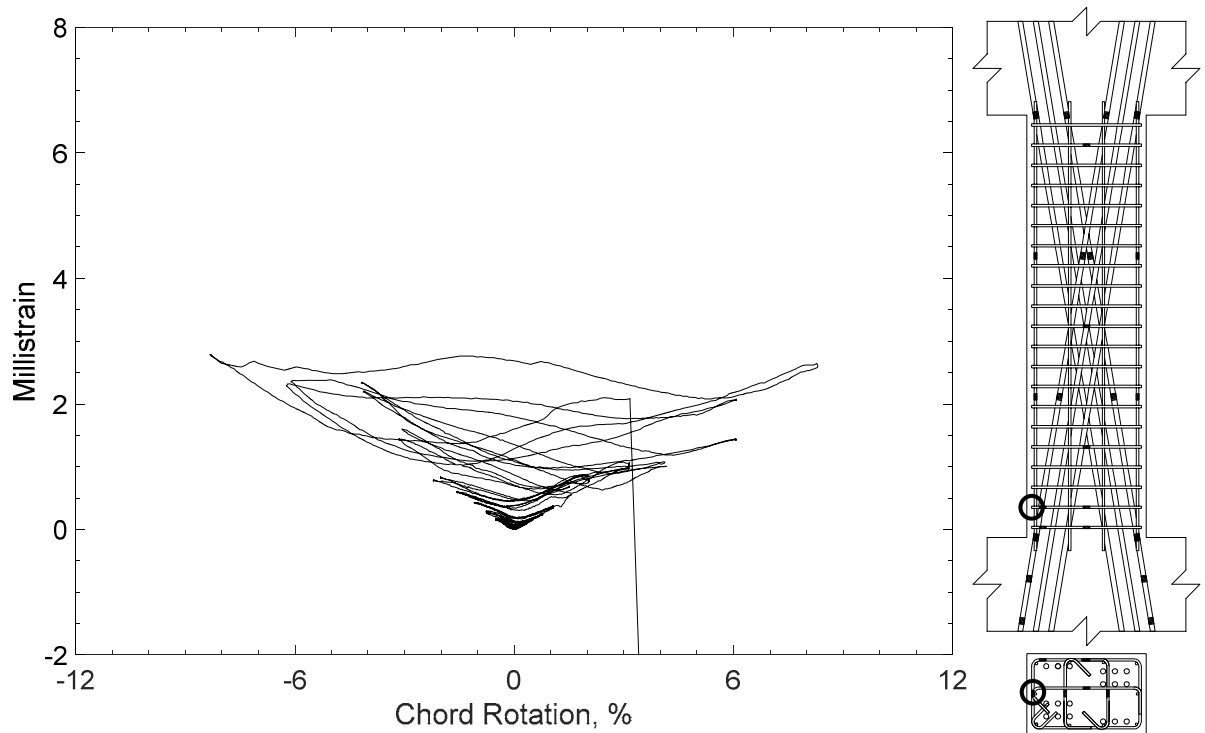


Figure 324 – Measured strain in closed stirrup of D80-3.5, strain gauge S6

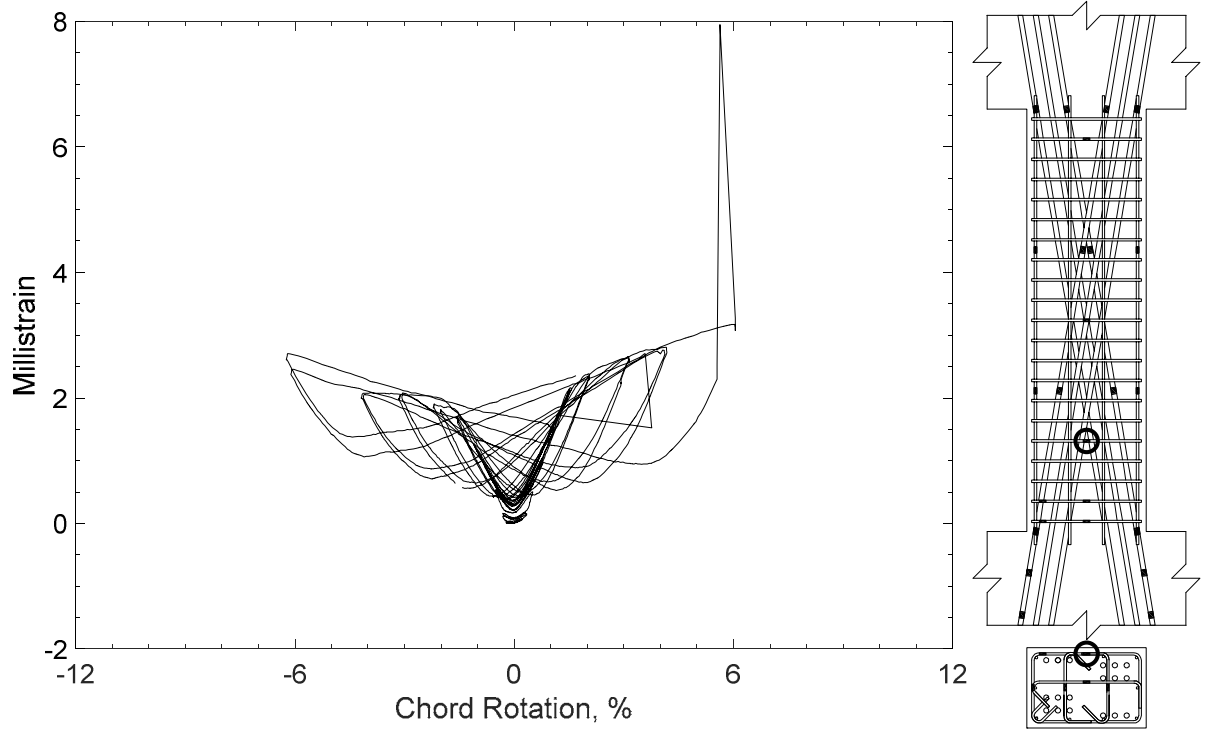


Figure 325 – Measured strain in closed stirrup of D80-3.5, strain gauge S7

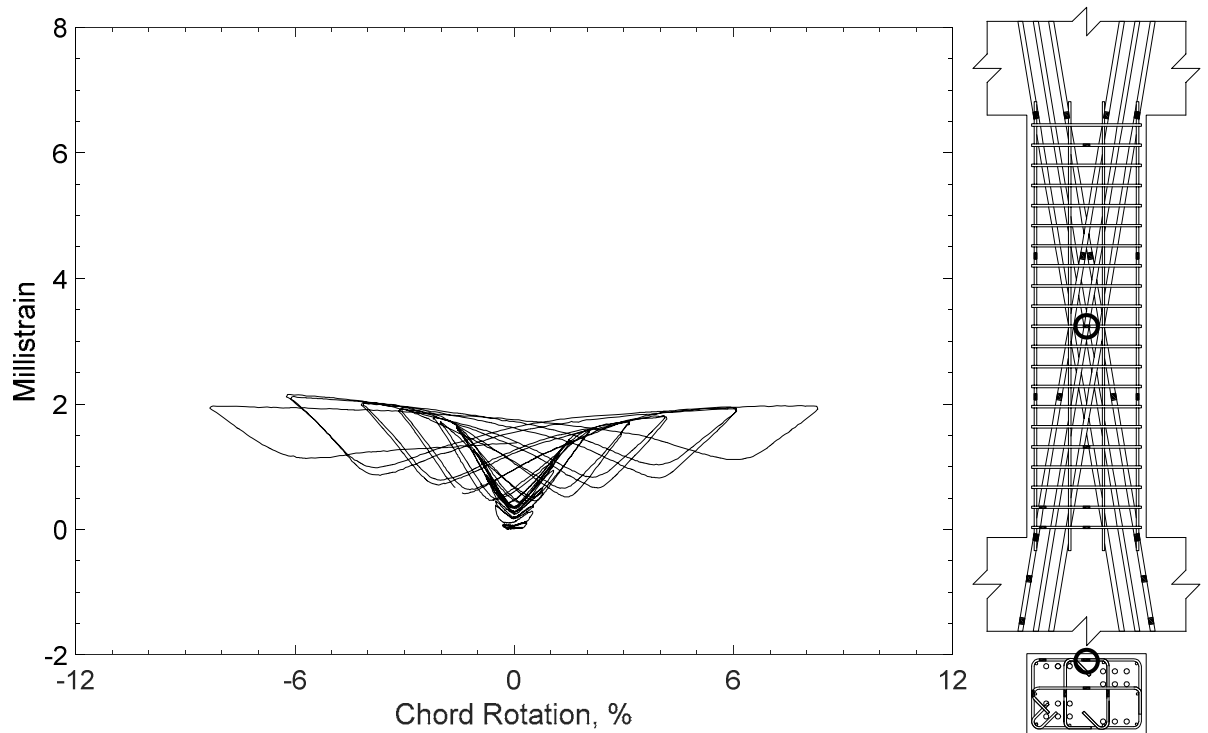


Figure 326 – Measured strain in closed stirrup of D80-3.5, strain gauge S8

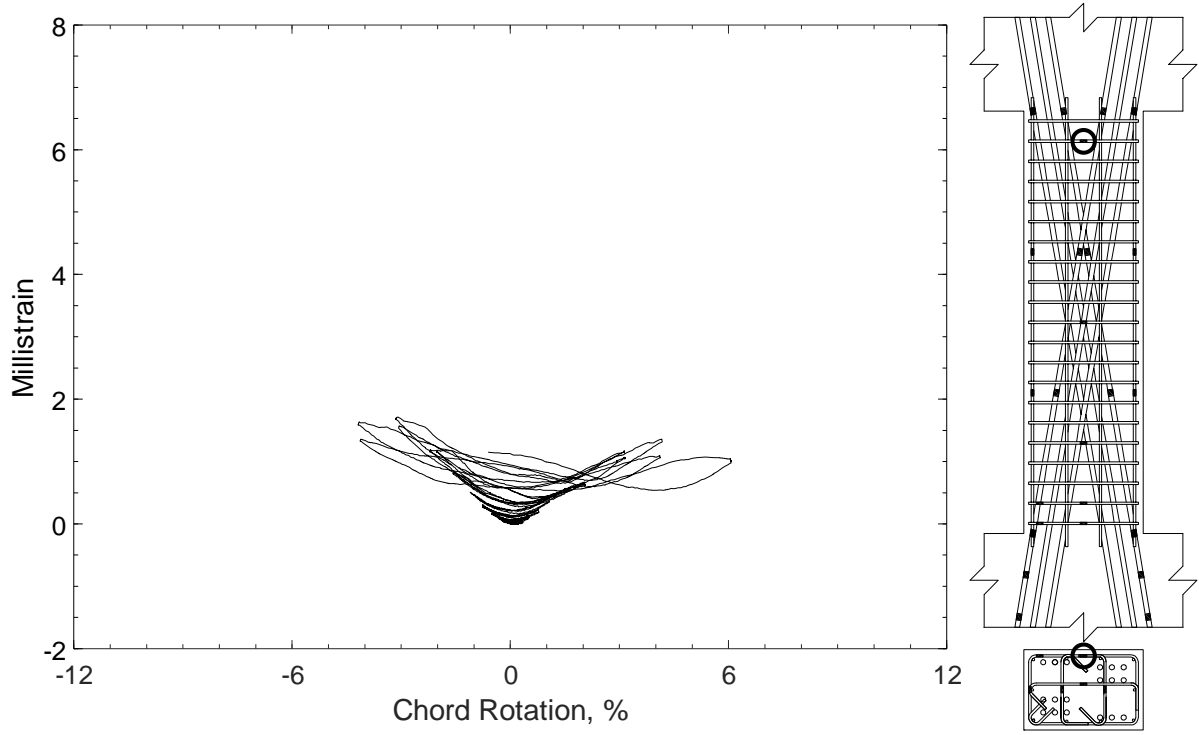


Figure 327 – Measured strain in closed stirrup of D80-3.5, strain gauge S9

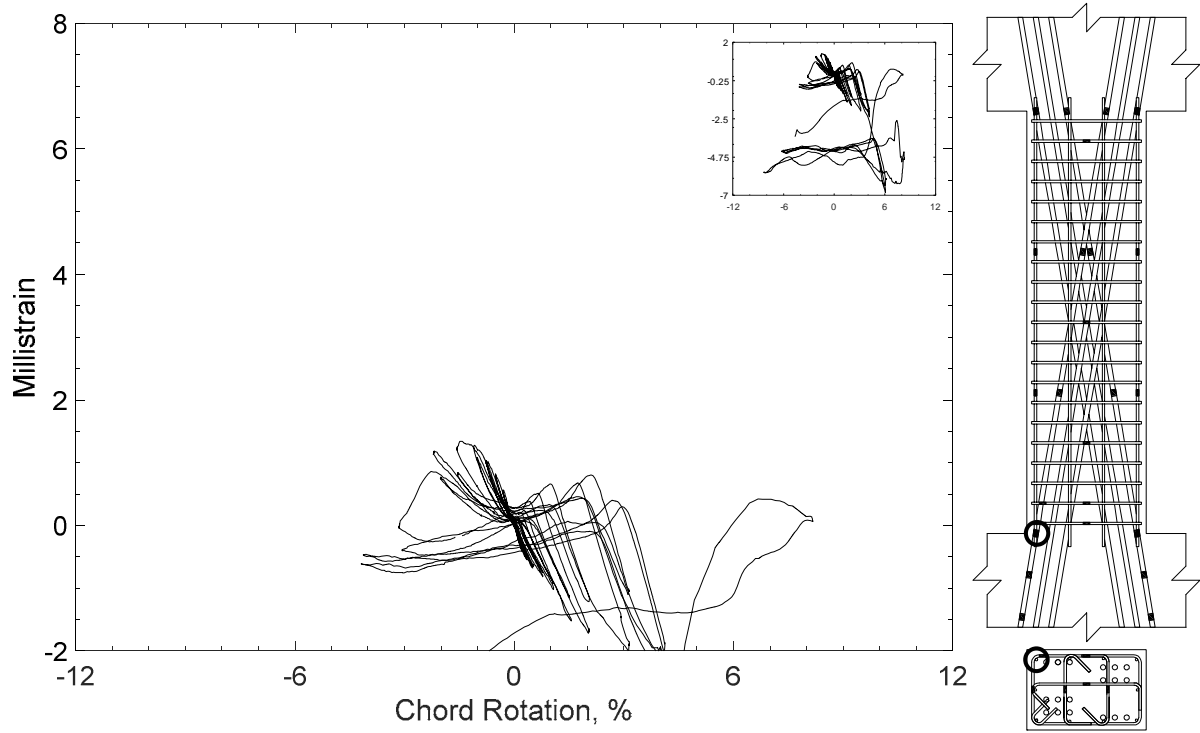


Figure 328 – Measured strain in parallel bar of D80-3.5, strain gauge H1

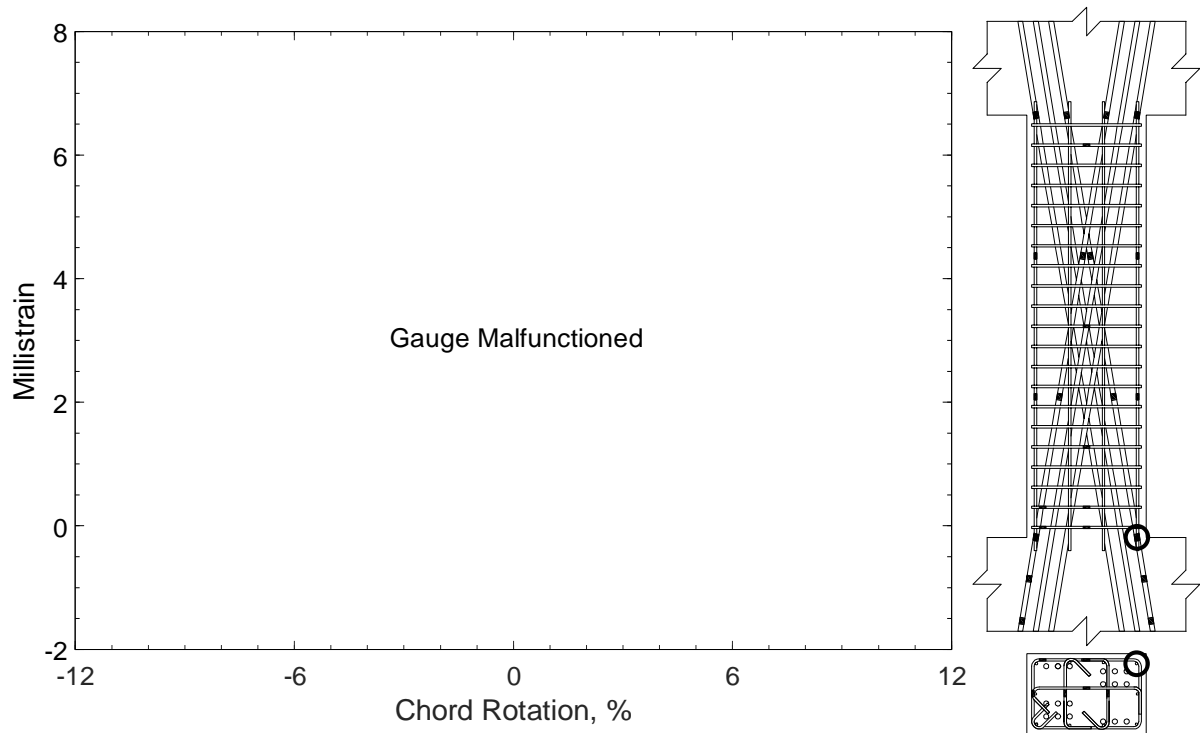


Figure 329 – Measured strain in parallel bar of D80-3.5, strain gauge H2

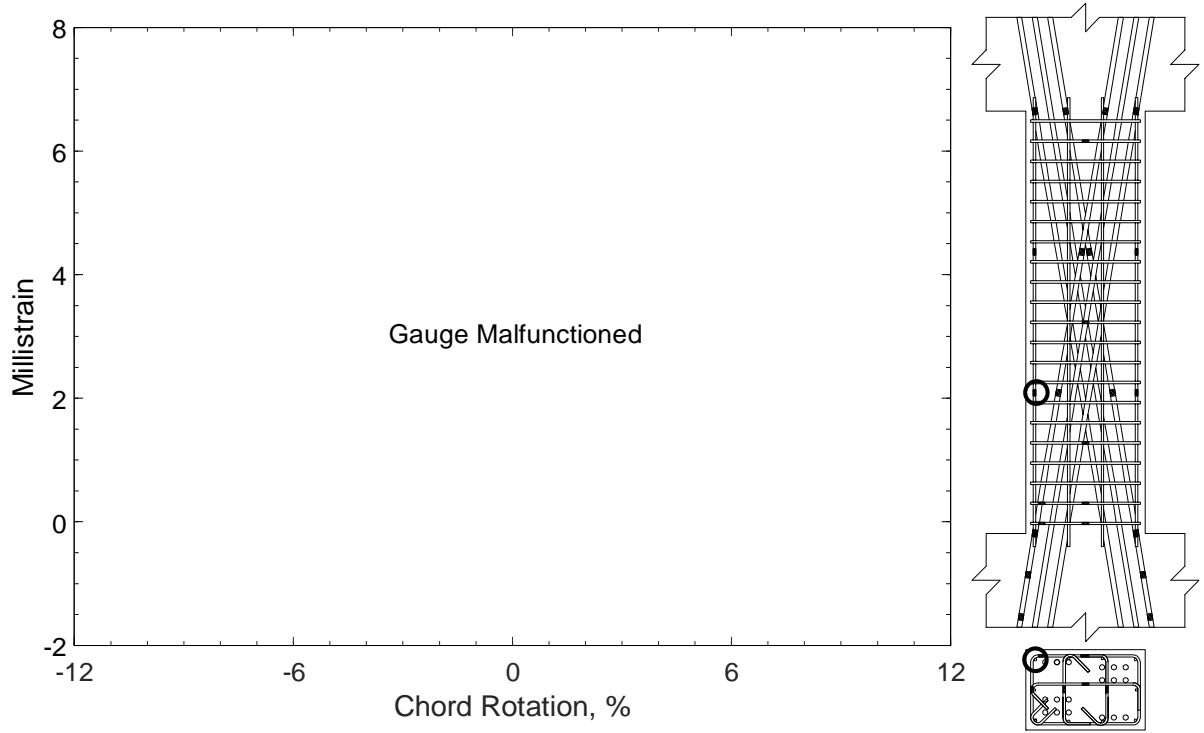


Figure 330 – Measured strain in parallel bar of D80-3.5, strain gauge H3

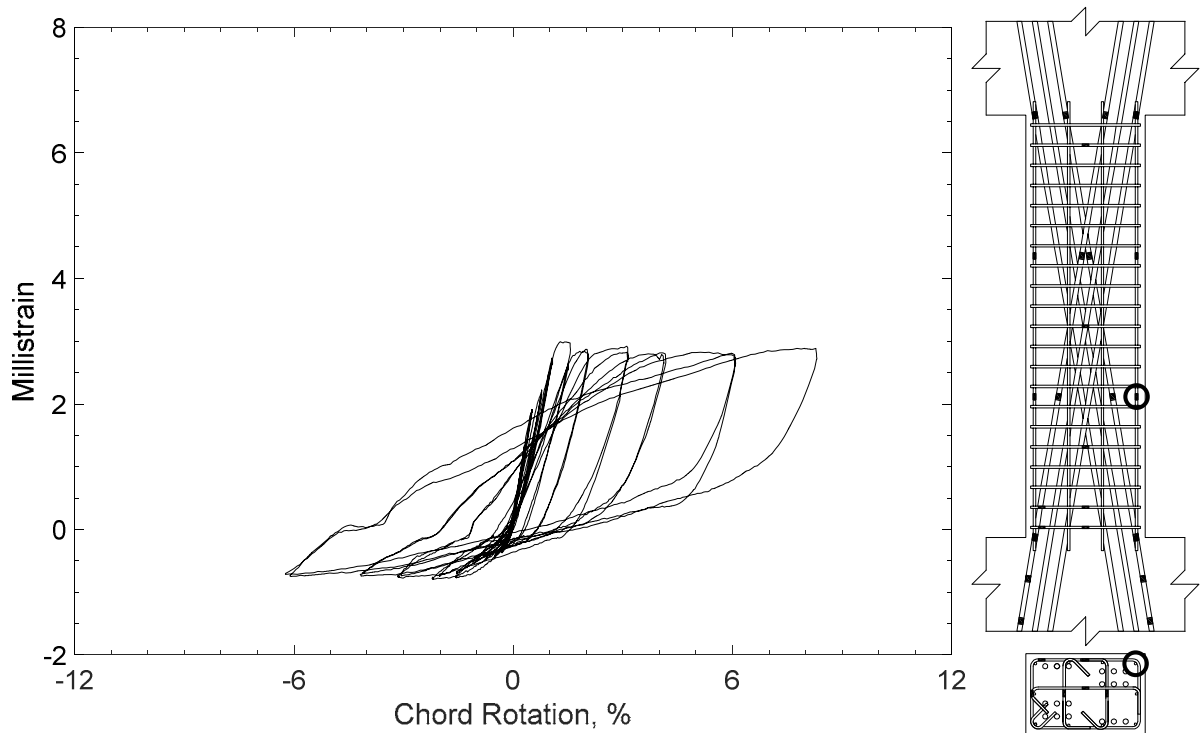


Figure 331 – Measured strain in parallel bar of D80-3.5, strain gauge H4

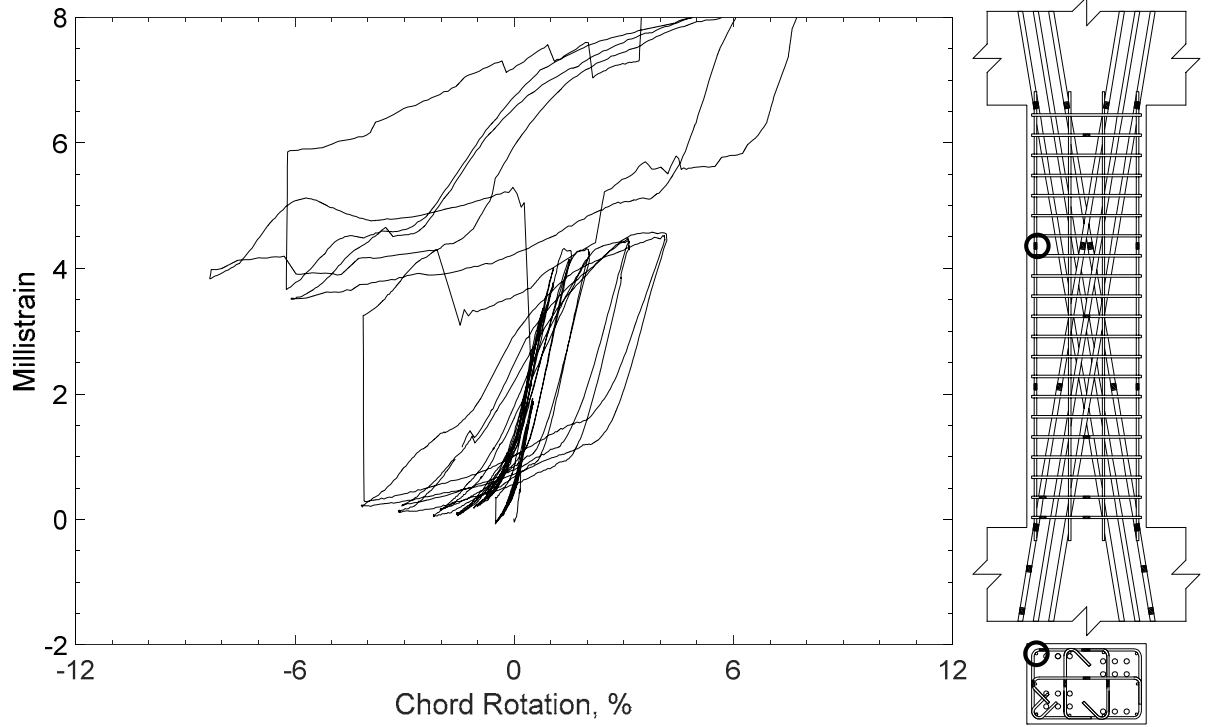


Figure 332 – Measured strain in parallel bar of D80-3.5, strain gauge H5

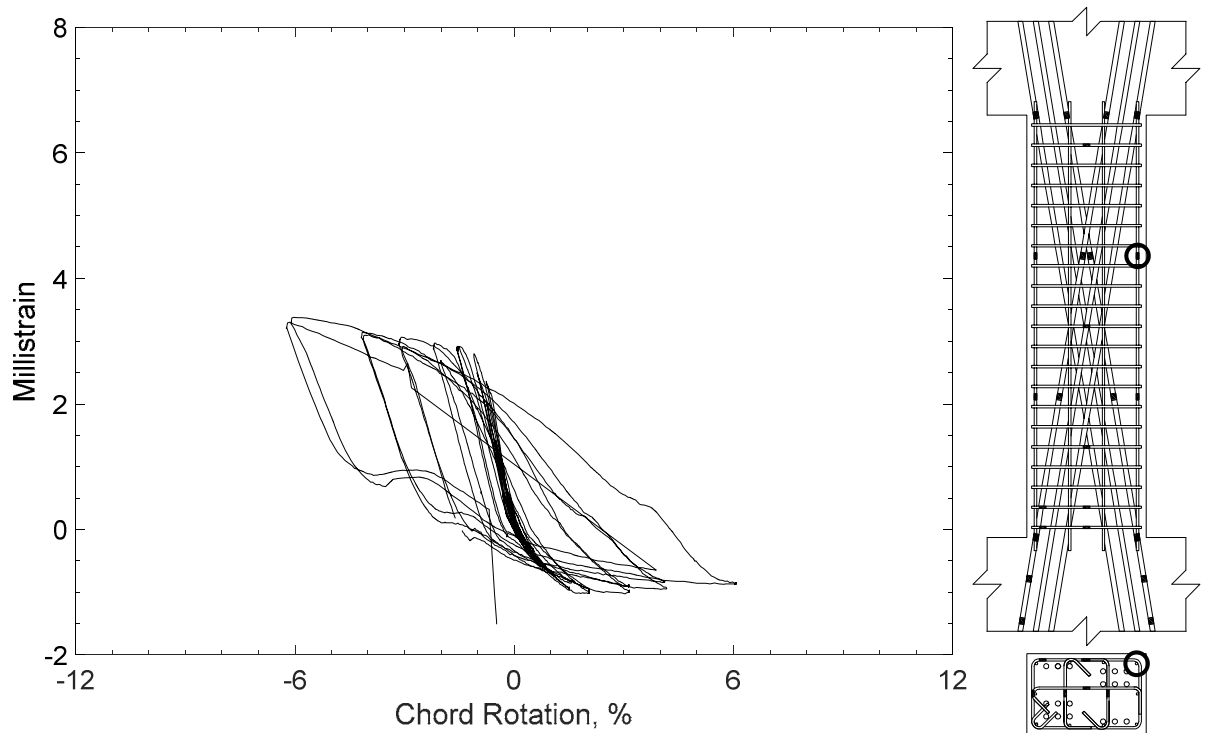


Figure 333 – Measured strain in parallel bar of D80-3.5, strain gauge H6

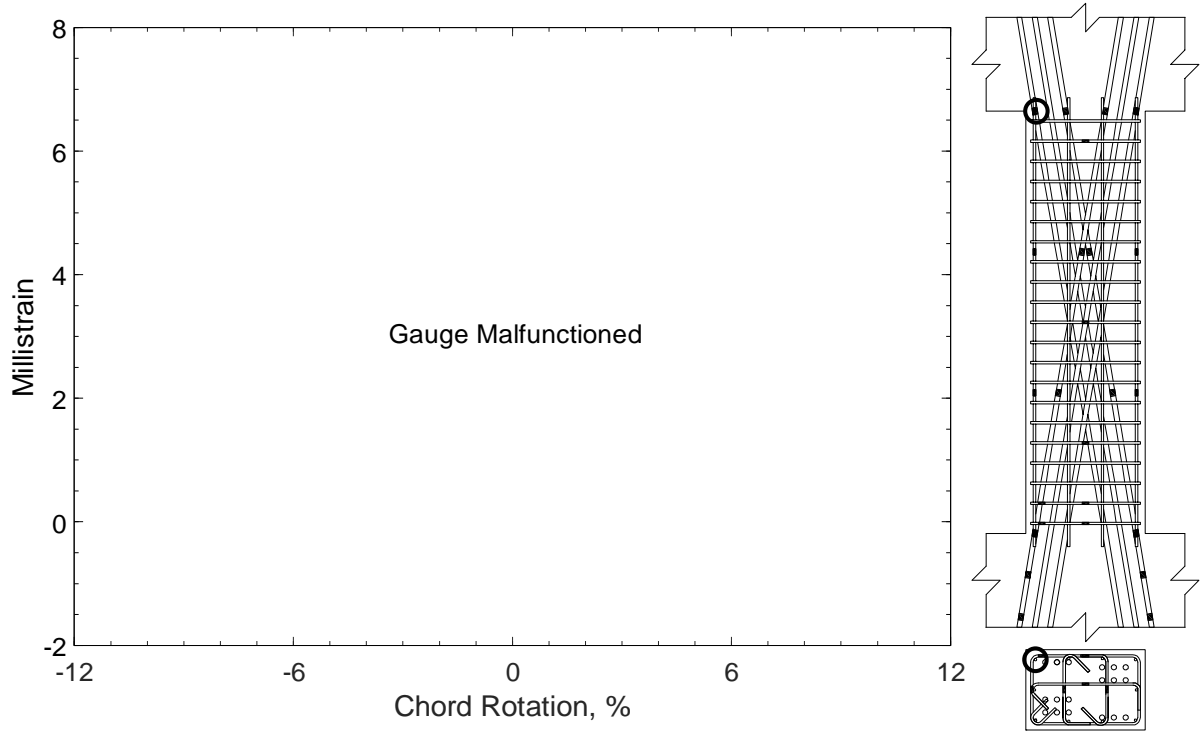


Figure 334 – Measured strain in parallel bar of D80-3.5, strain gauge H7

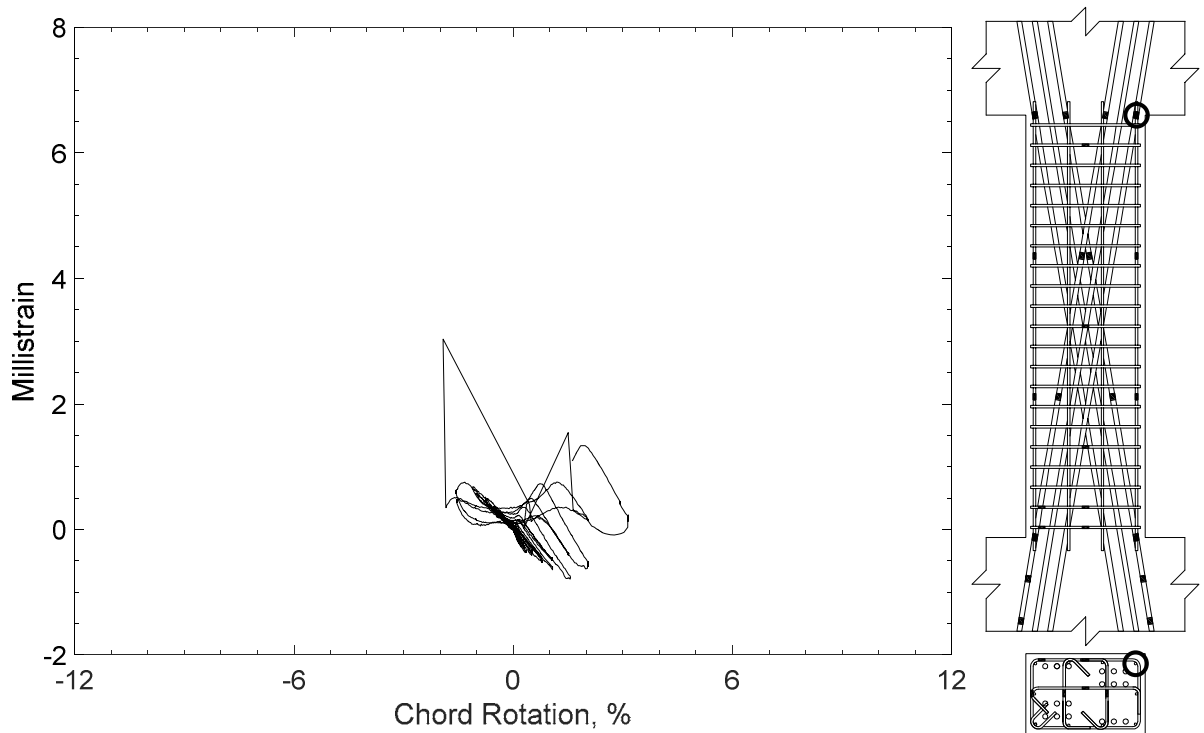


Figure 335 – Measured strain in parallel bar of D80-3.5, strain gauge H8

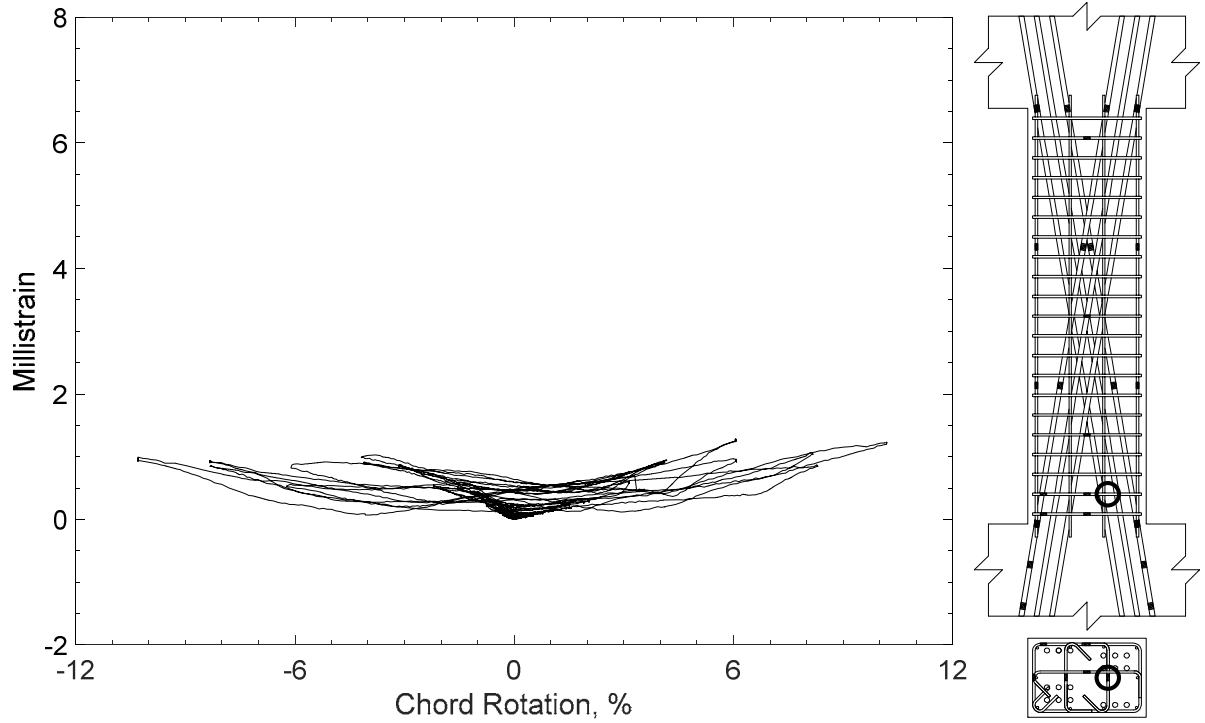


Figure 336 – Measured strain in crosstie of D80-3.5, strain gauge T1

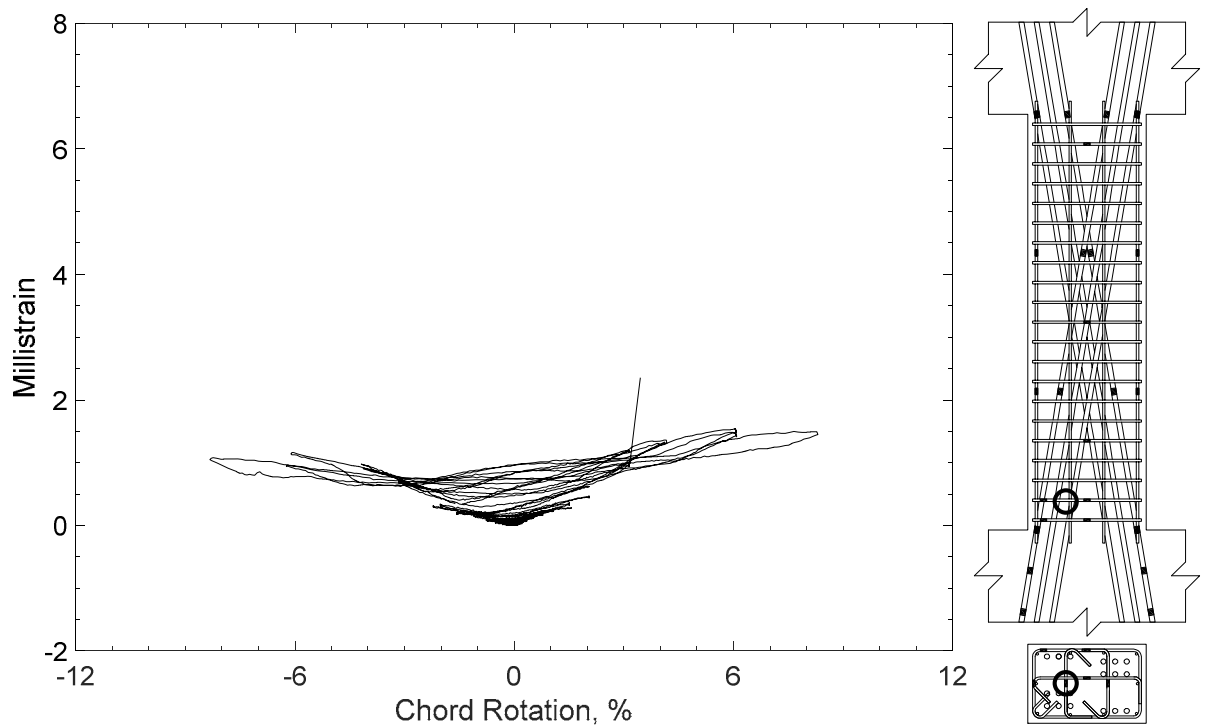


Figure 337 – Measured strain in crosstie of D80-3.5, strain gauge T2

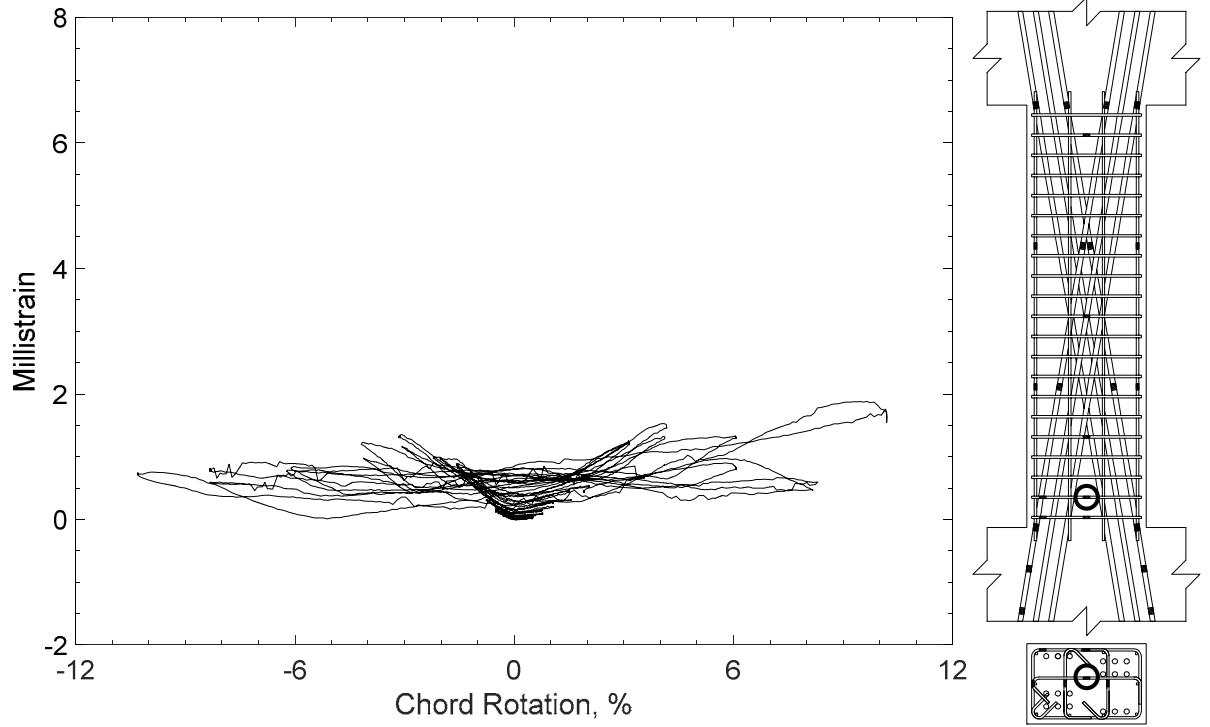


Figure 338 – Measured strain in crosstie of D80-3.5, strain gauge T3

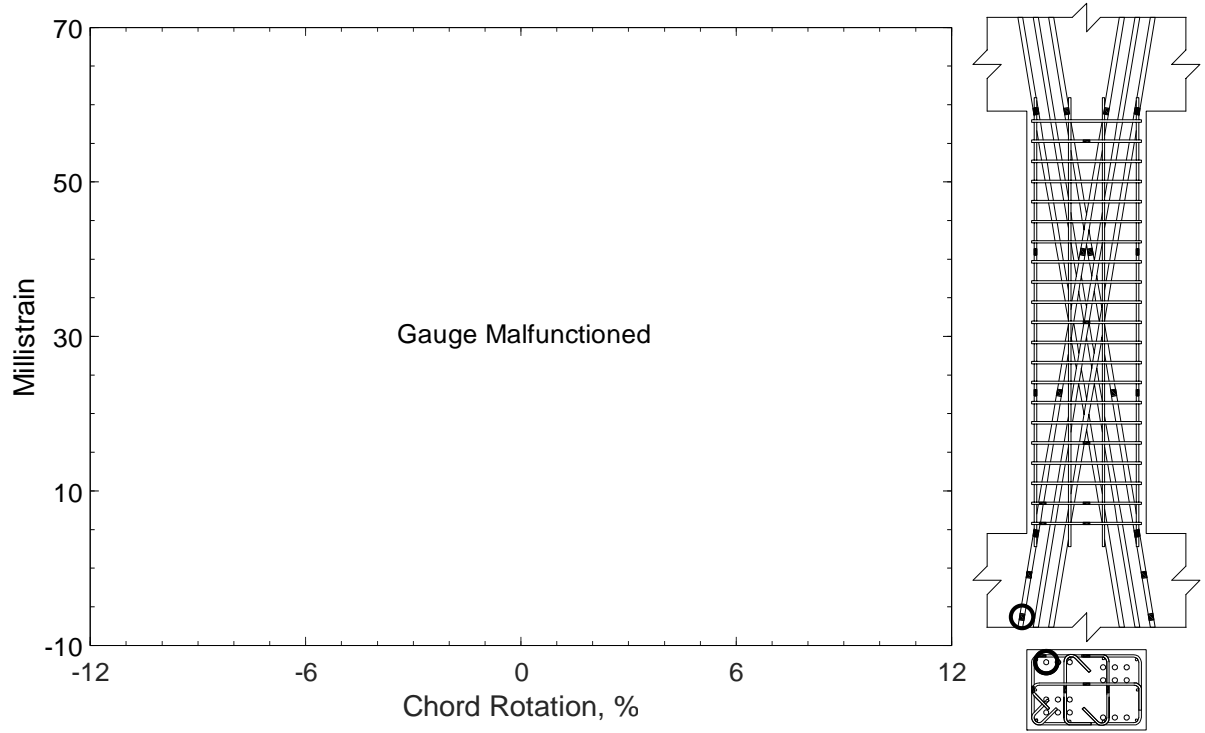


Figure 339 – Measured strain in diagonal bar of D100-3.5, strain gauge D1

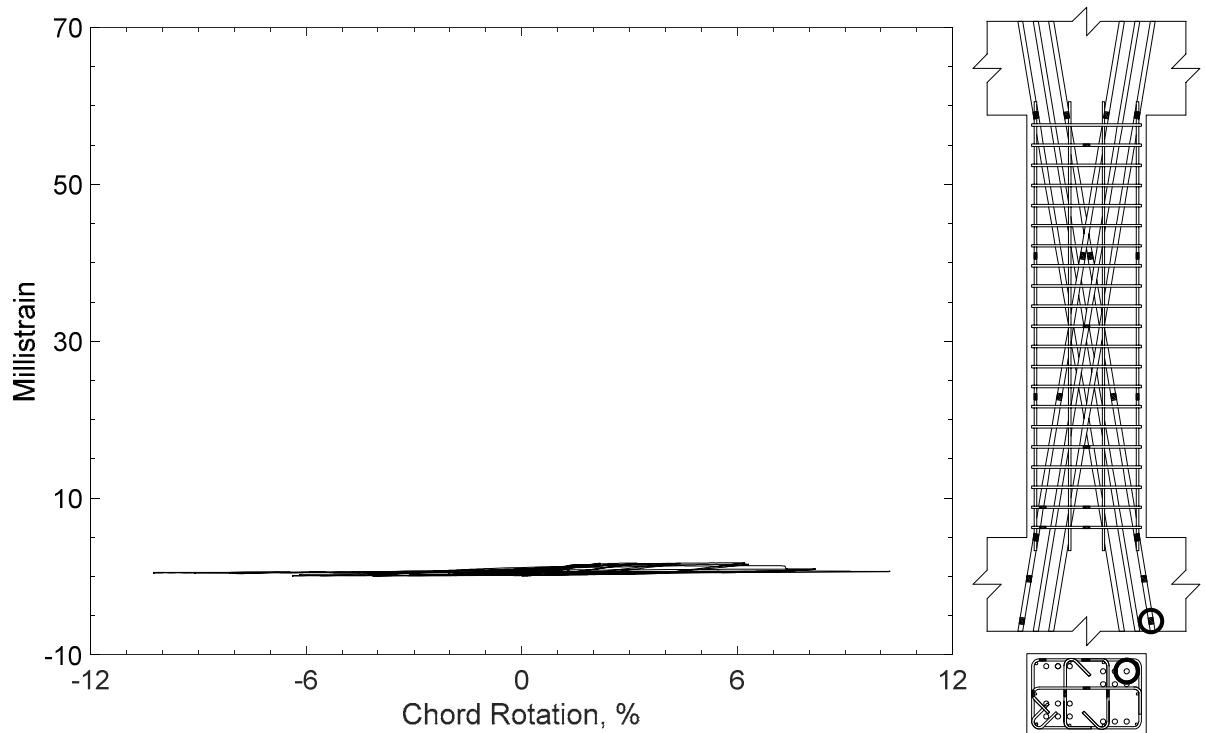


Figure 340 – Measured strain in diagonal bar of D100-3.5, strain gauge D2

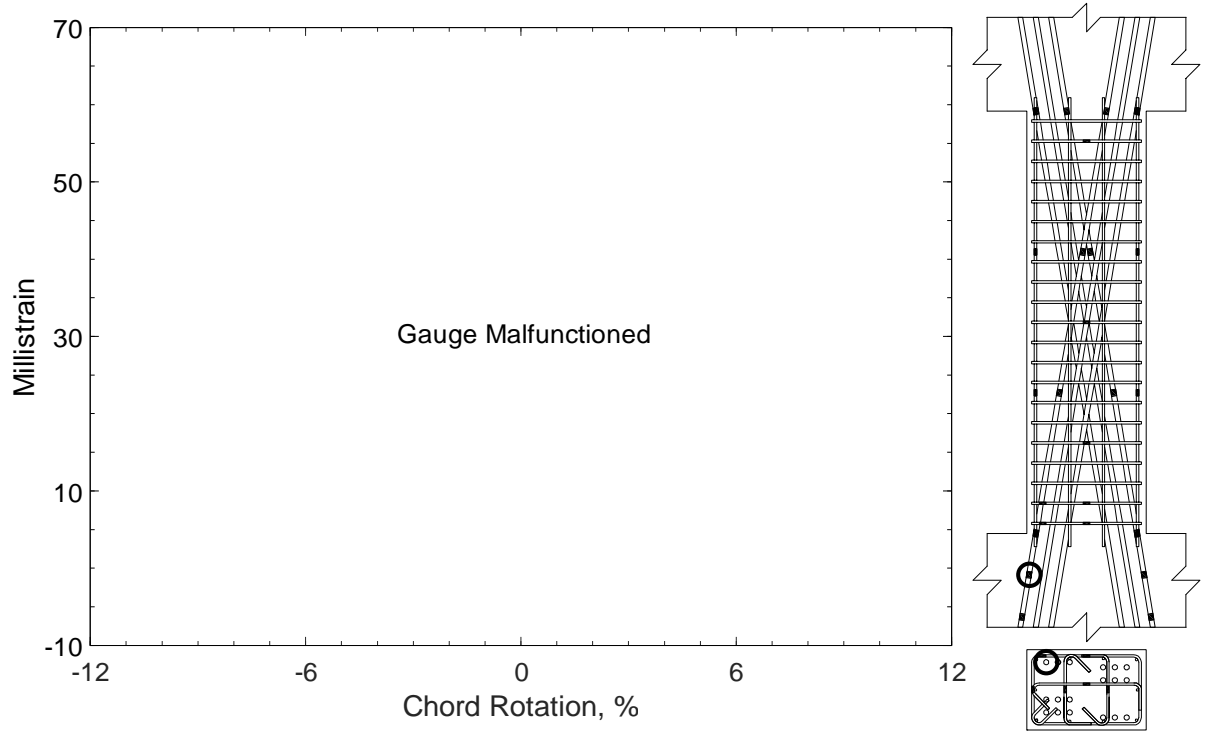


Figure 341 – Measured strain in diagonal bar of D100-3.5, strain gauge D3

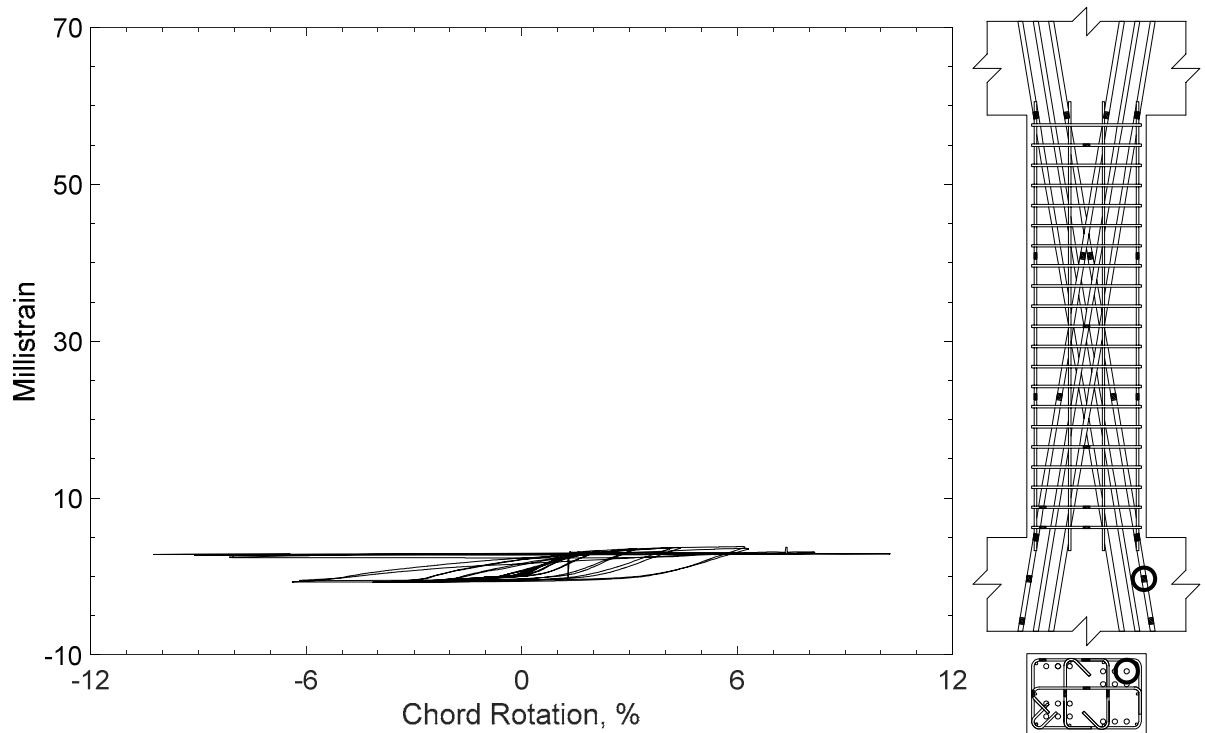


Figure 342 – Measured strain in diagonal bar of D100-3.5, strain gauge D4

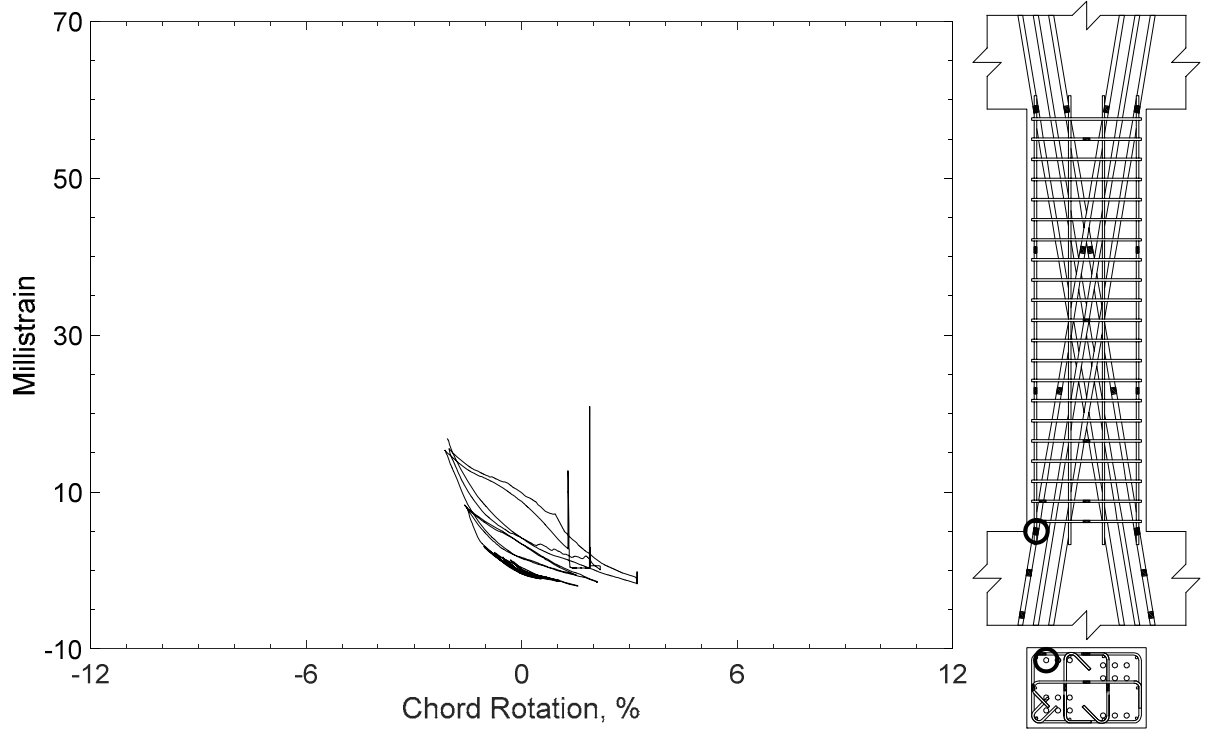


Figure 343 – Measured strain in diagonal bar of D100-3.5, strain gauge D5

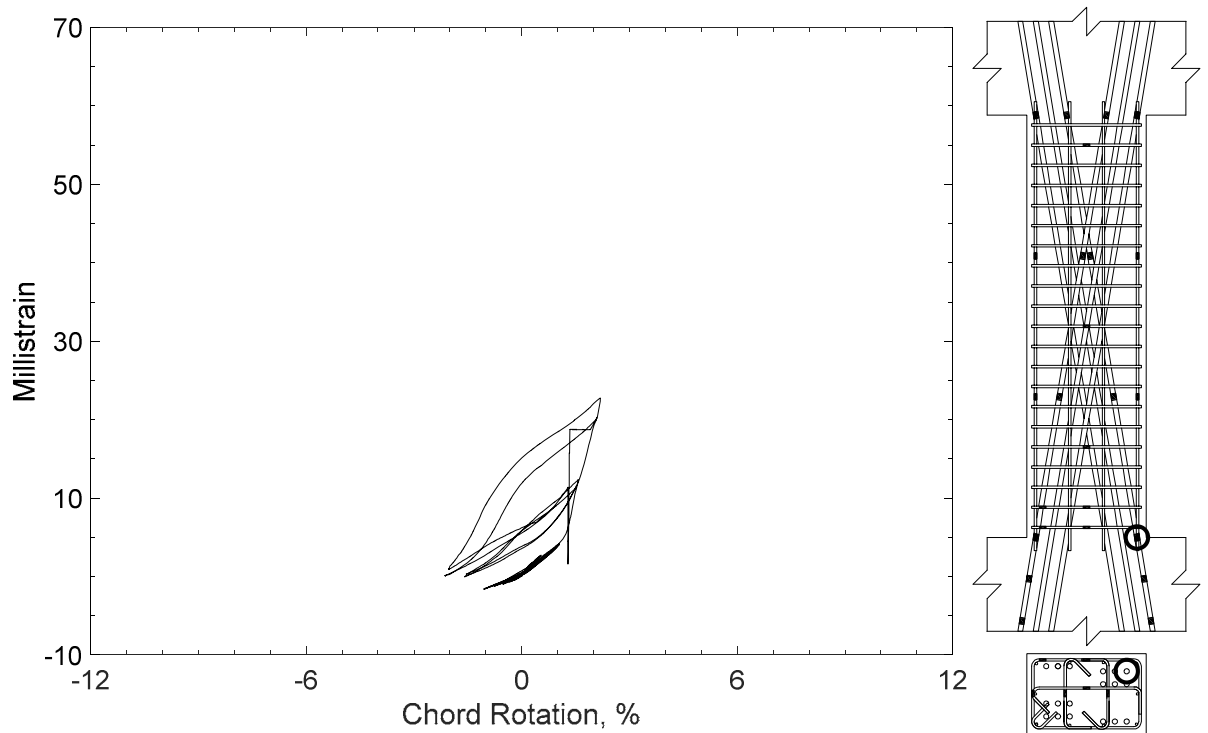


Figure 344 – Measured strain in diagonal bar of D100-3.5, strain gauge D6

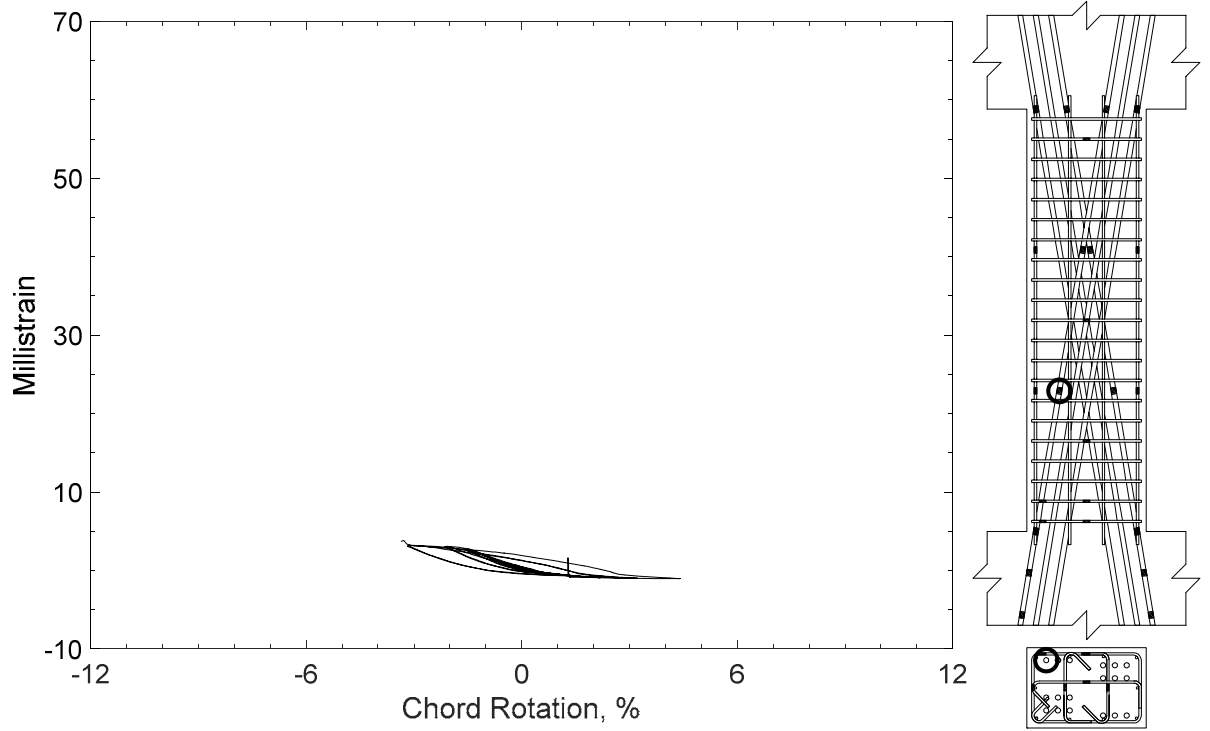


Figure 345 – Measured strain in diagonal bar of D100-3.5, strain gauge D7

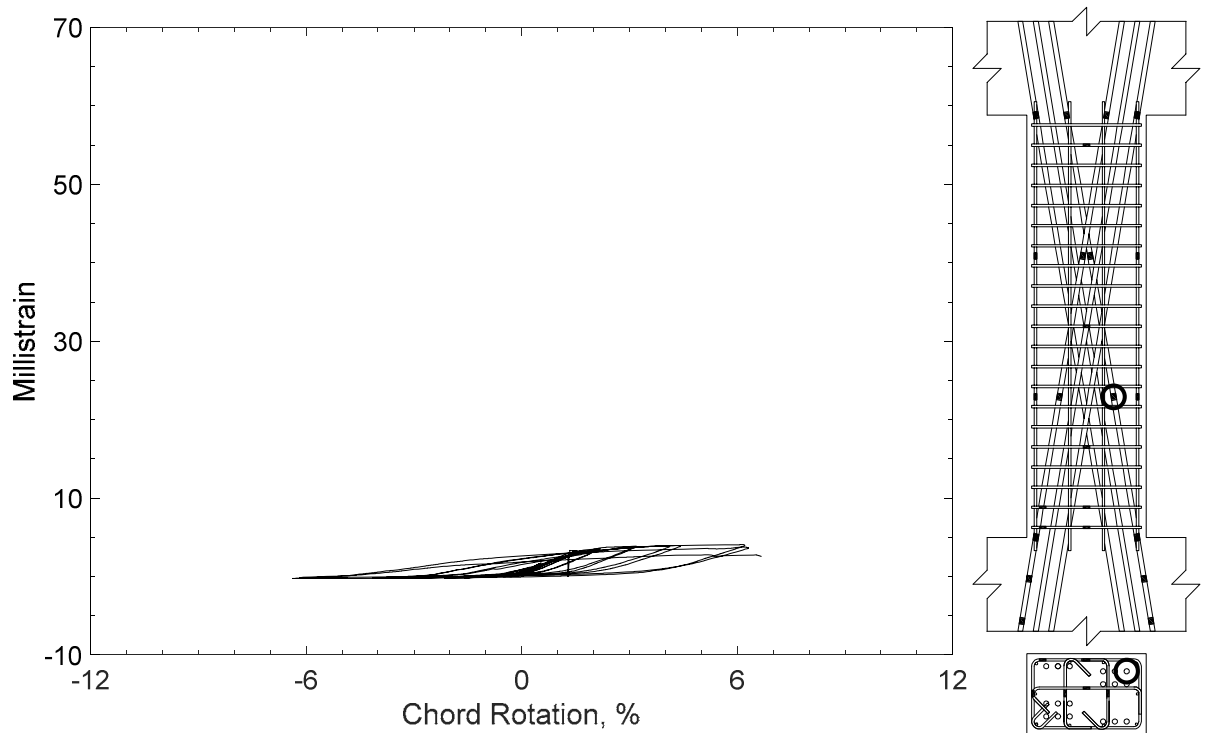


Figure 346 – Measured strain in diagonal bar of D100-3.5, strain gauge D8

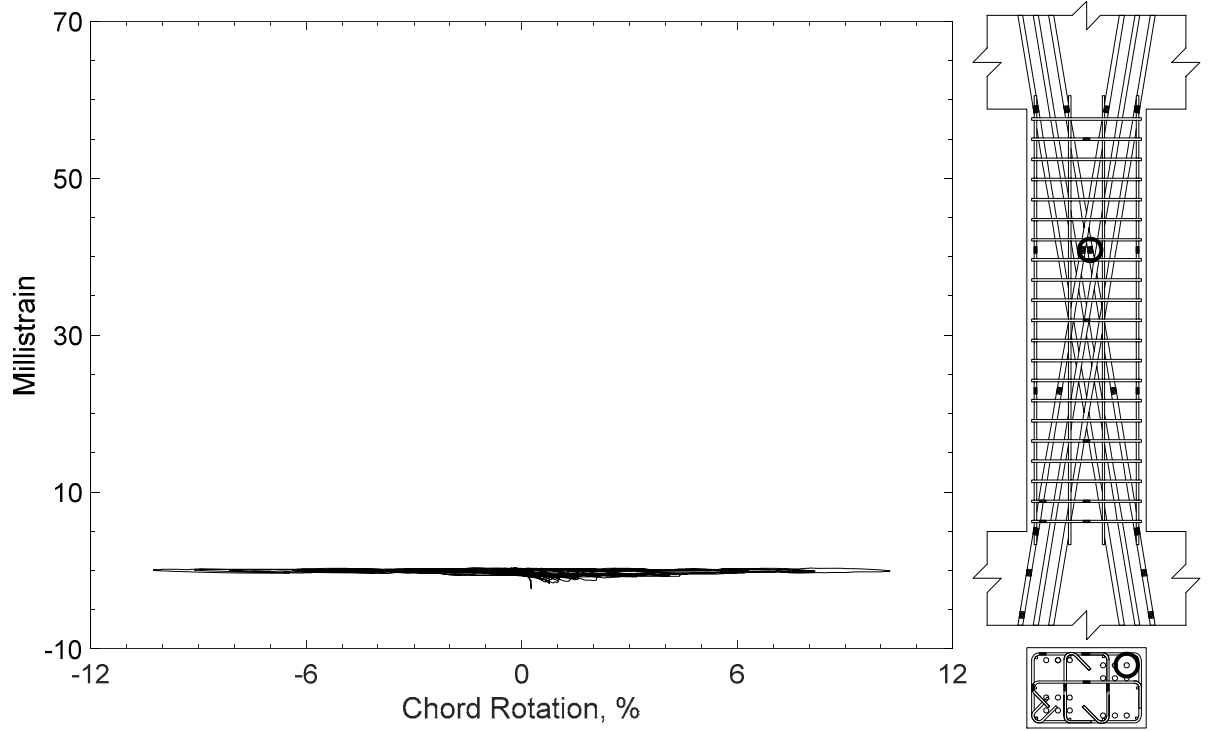


Figure 347 – Measured strain in diagonal bar of D100-3.5, strain gauge D9

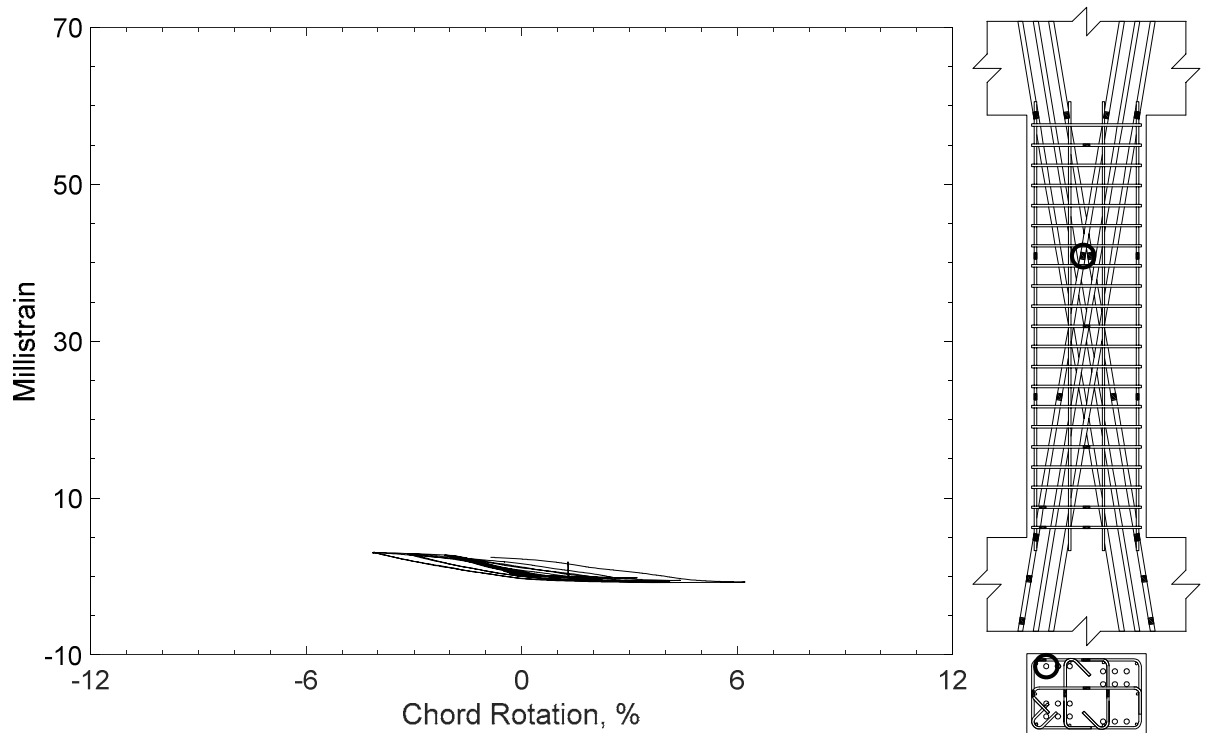


Figure 348 – Measured strain in diagonal bar of D100-3.5, strain gauge D10

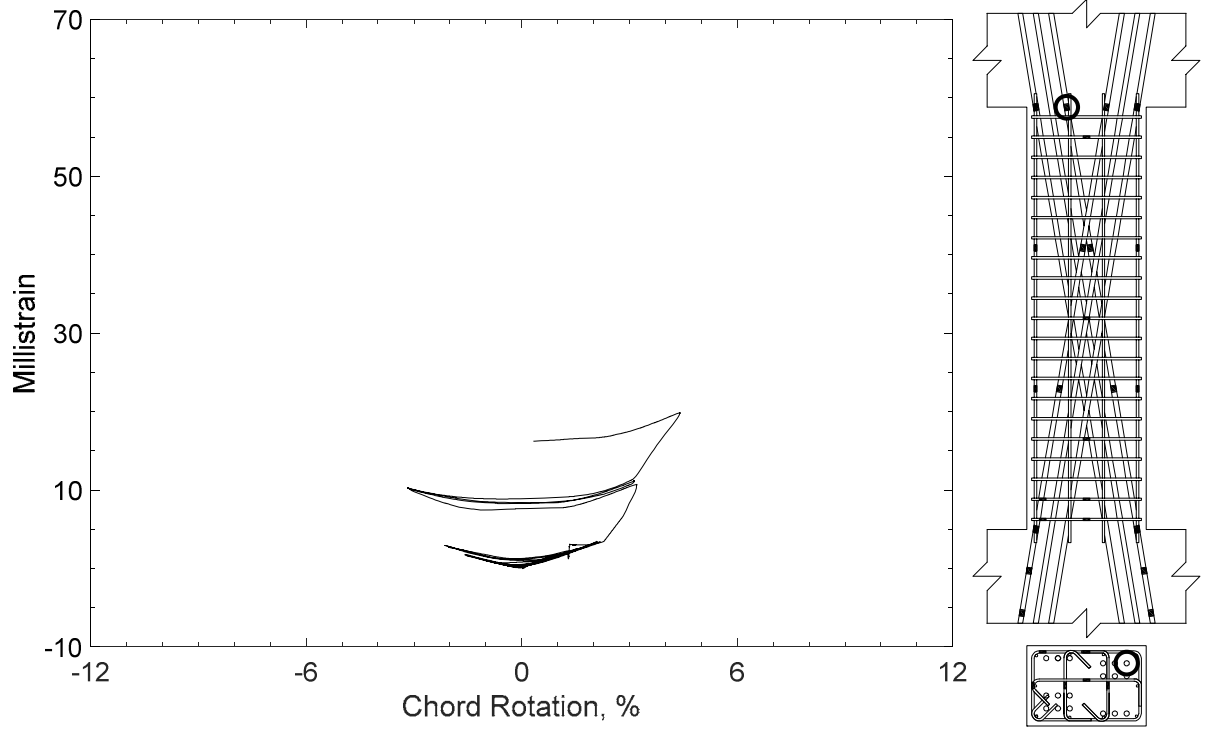


Figure 349 – Measured strain in diagonal bar of D100-3.5, strain gauge D11

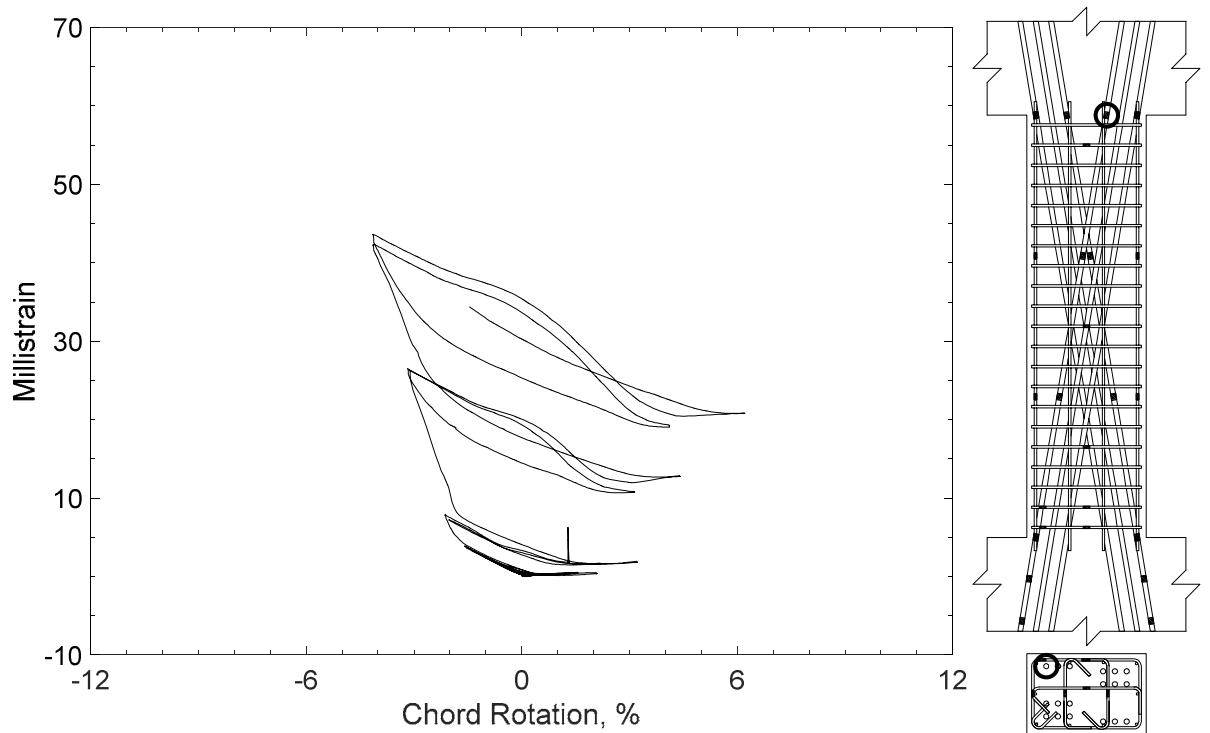


Figure 350 – Measured strain in diagonal bar of D100-3.5, strain gauge D12

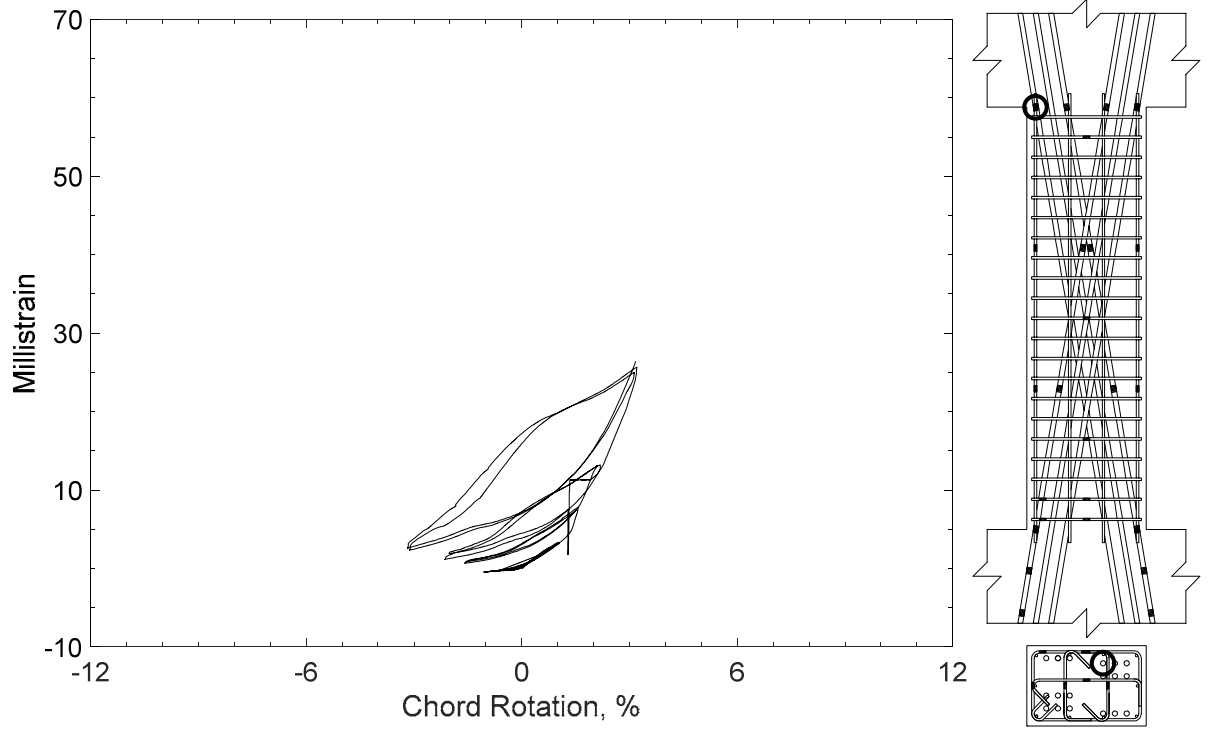


Figure 351 – Measured strain in diagonal bar of D100-3.5, strain gauge D13

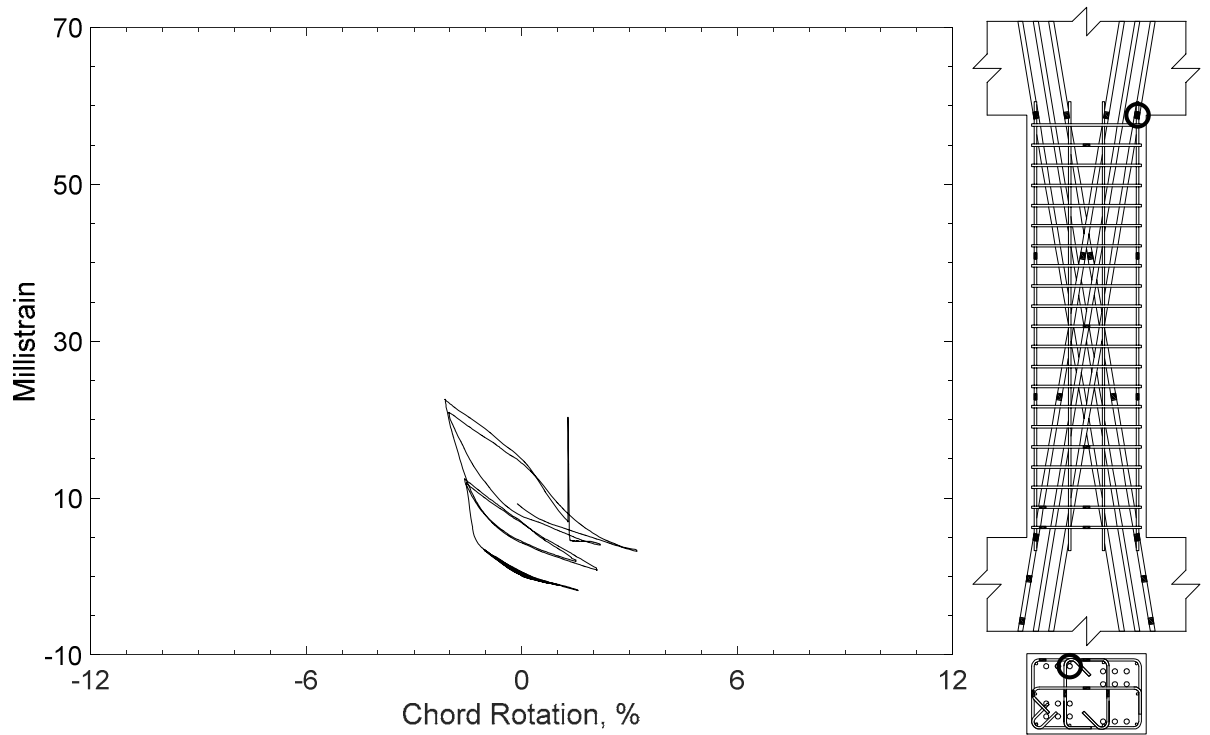


Figure 352 – Measured strain in diagonal bar of D100-3.5, strain gauge D14

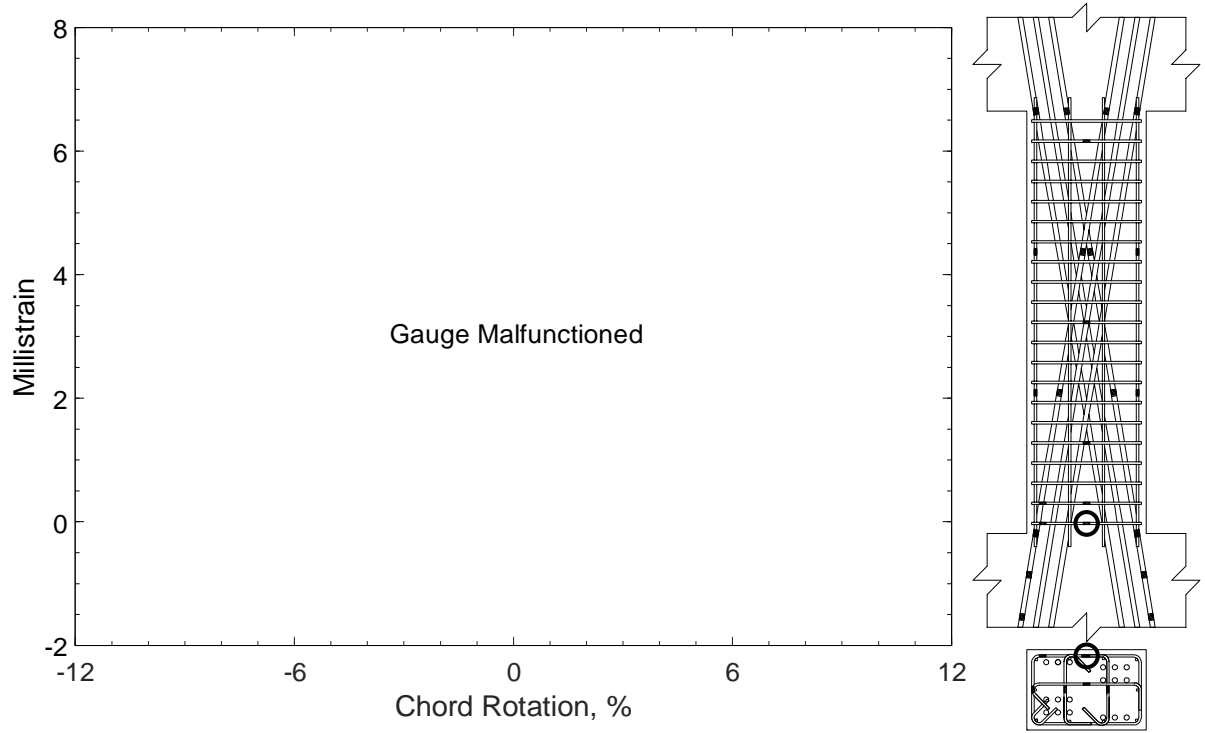


Figure 353 – Measured strain in closed stirrup of D100-3.5, strain gauge S1

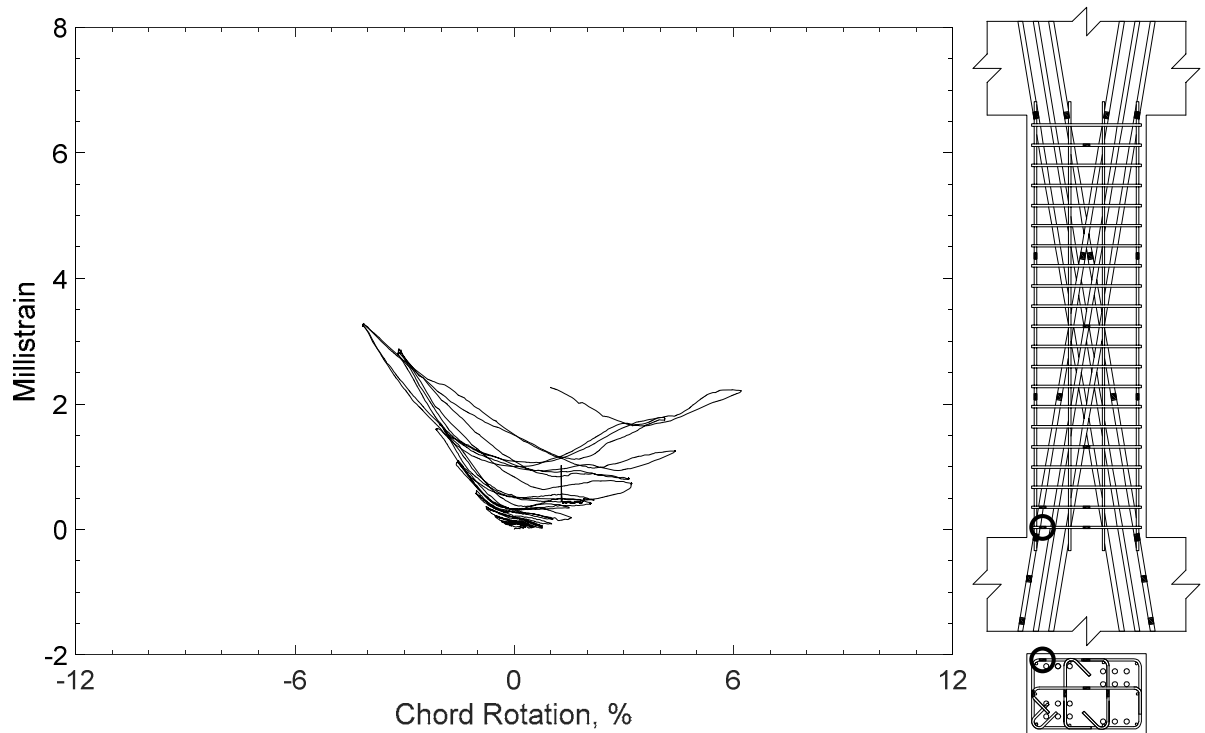


Figure 354 – Measured strain in closed stirrup of D100-3.5, strain gauge S2

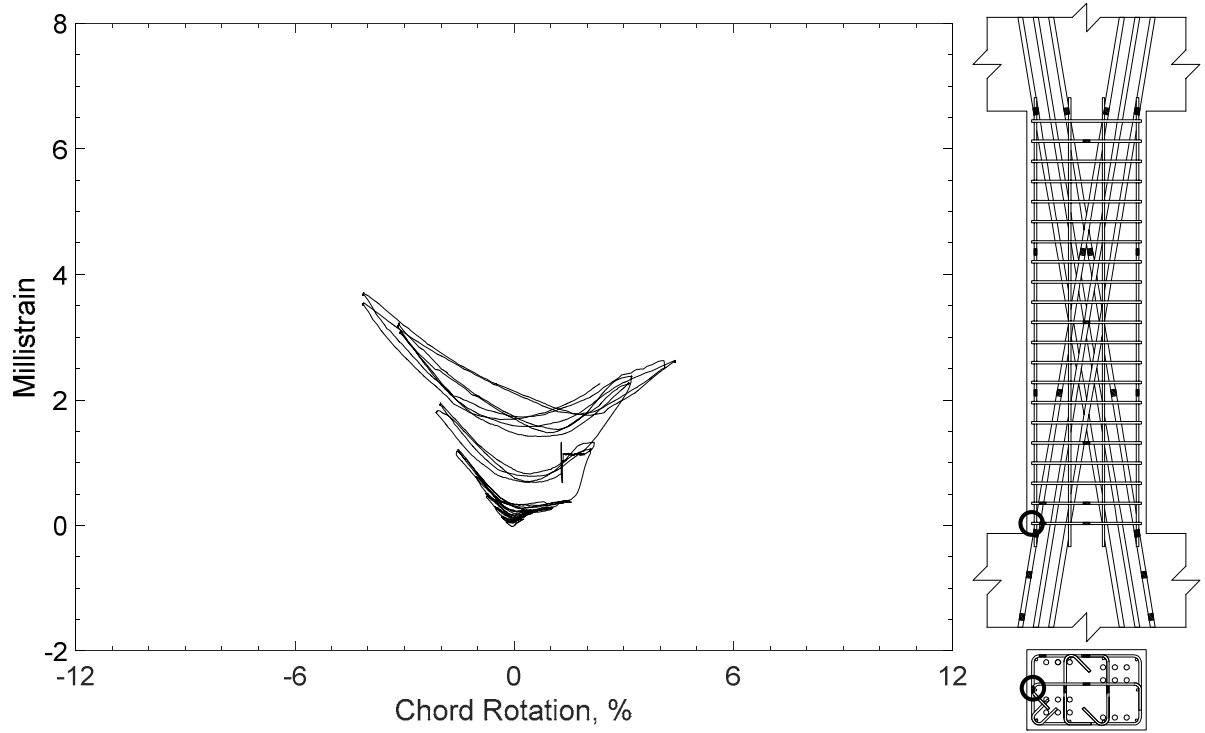


Figure 355 – Measured strain in closed stirrup of D100-3.5, strain gauge S3

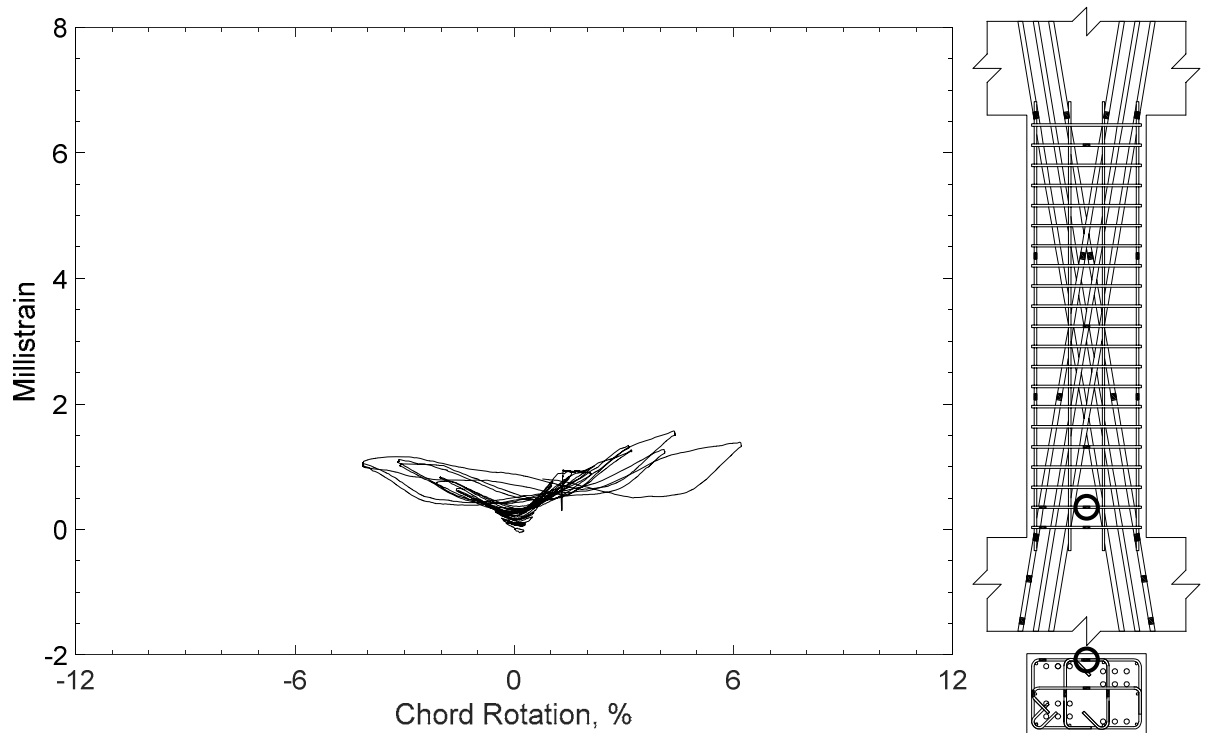


Figure 356 – Measured strain in closed stirrup of D100-3.5, strain gauge S4

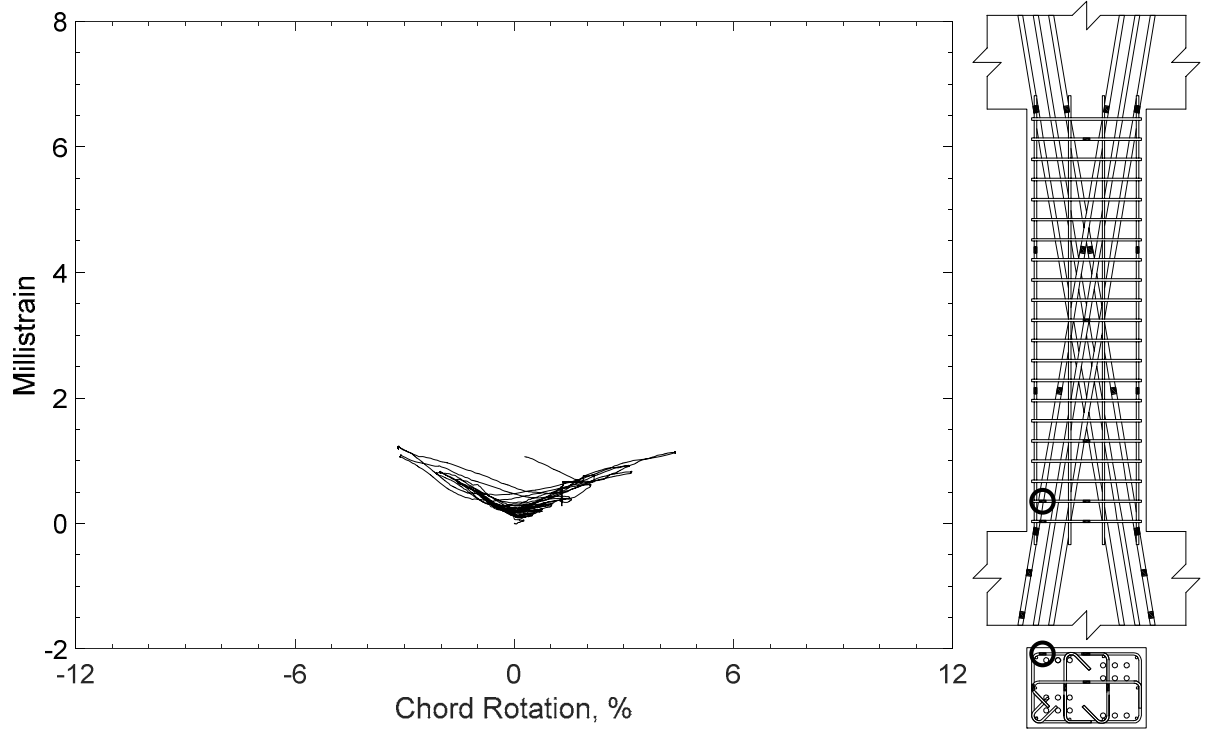


Figure 357 – Measured strain in closed stirrup of D100-3.5, strain gauge S5

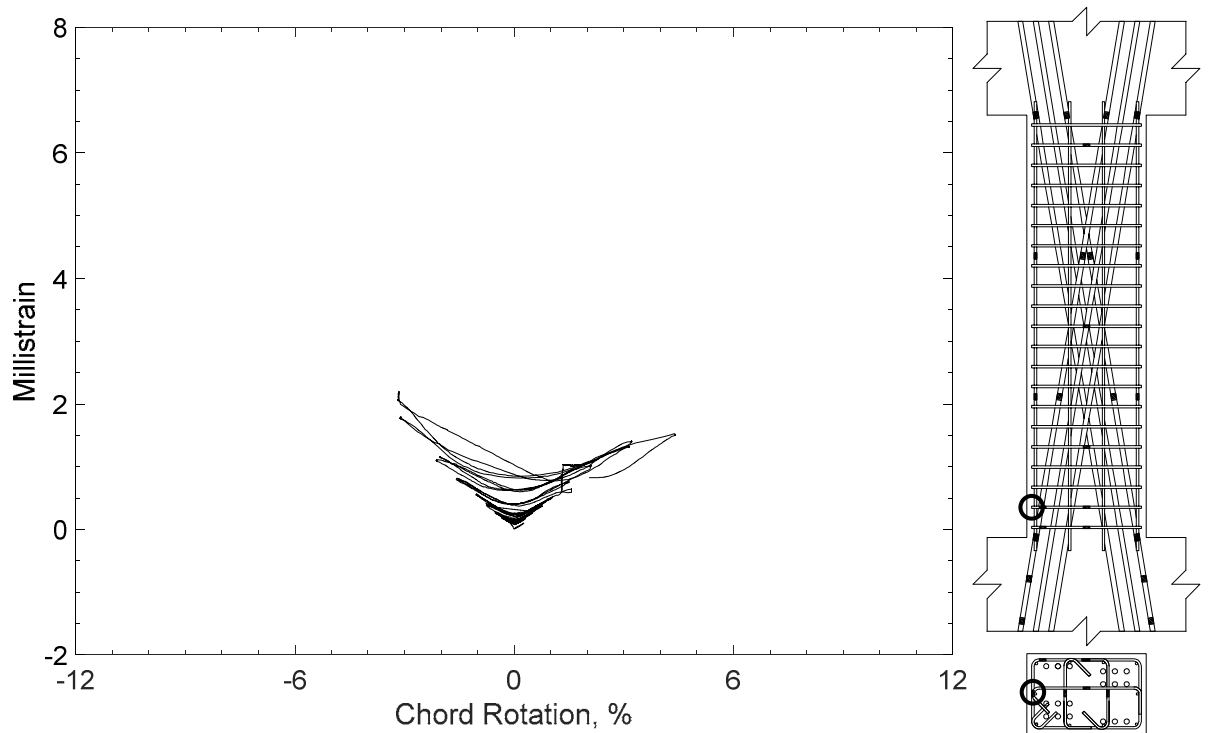


Figure 358 – Measured strain in closed stirrup of D100-3.5, strain gauge S6

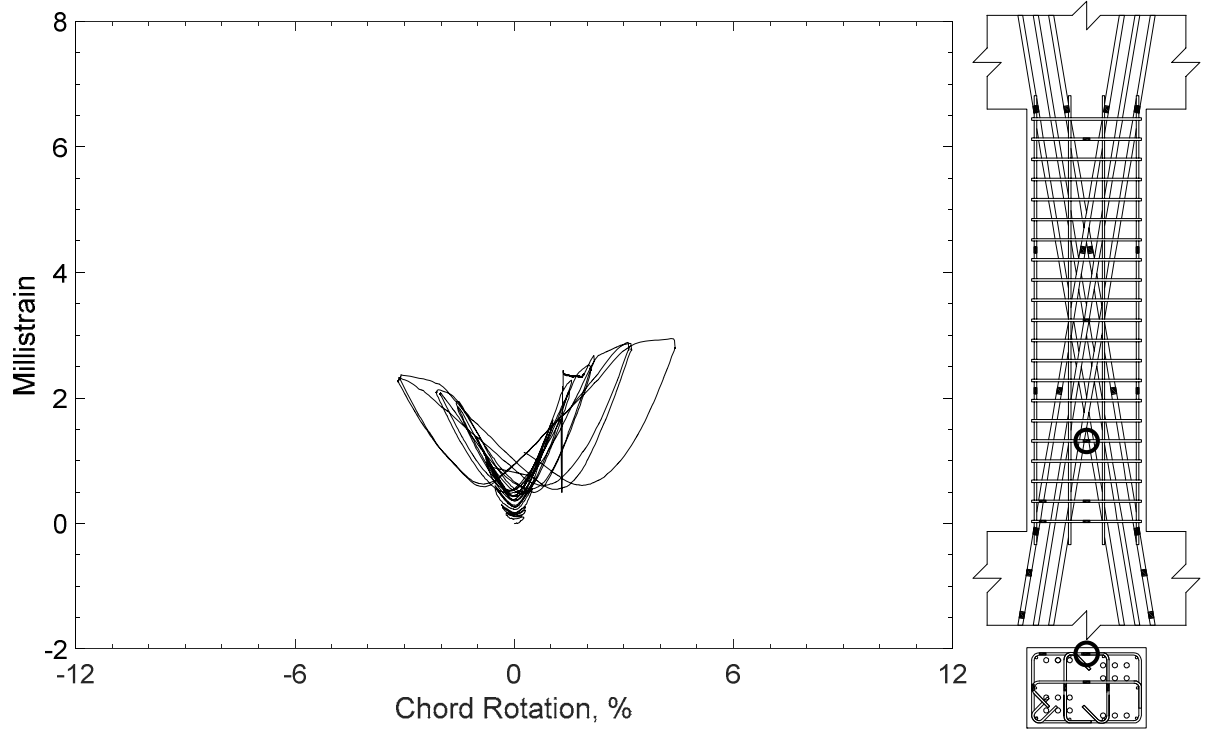


Figure 359 – Measured strain in closed stirrup of D100-3.5, strain gauge S7

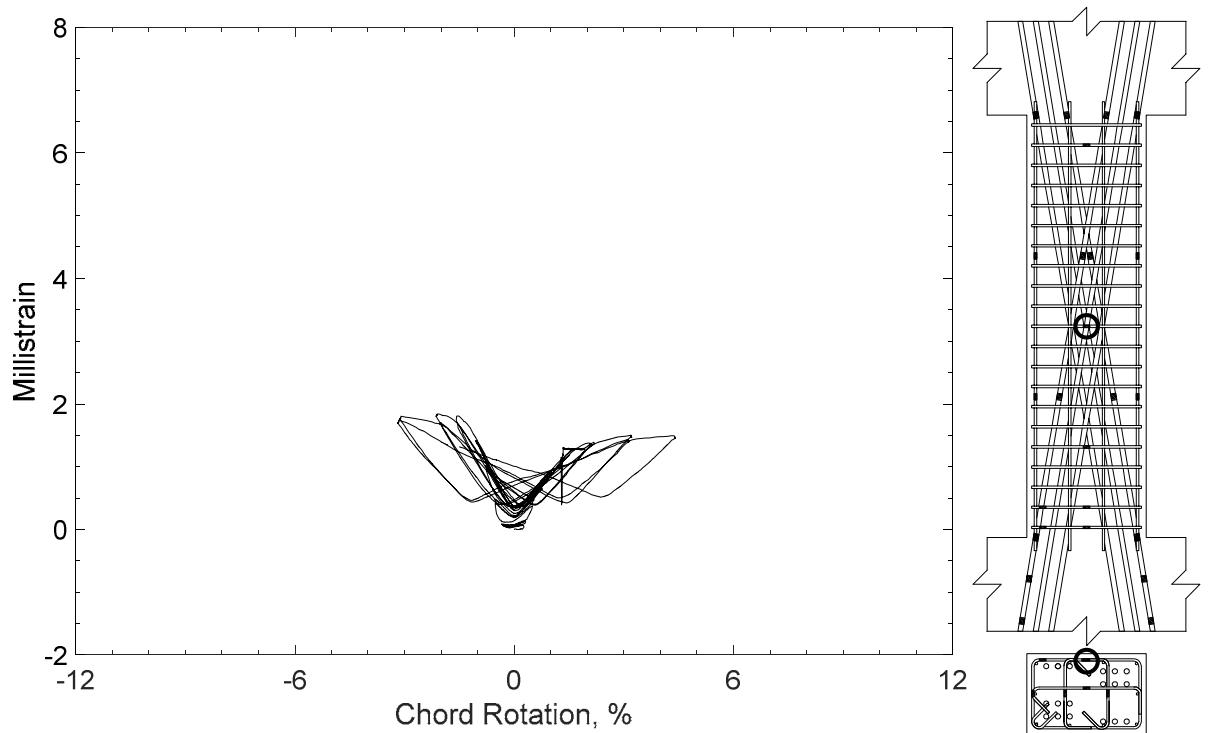


Figure 360 – Measured strain in closed stirrup of D100-3.5, strain gauge S8

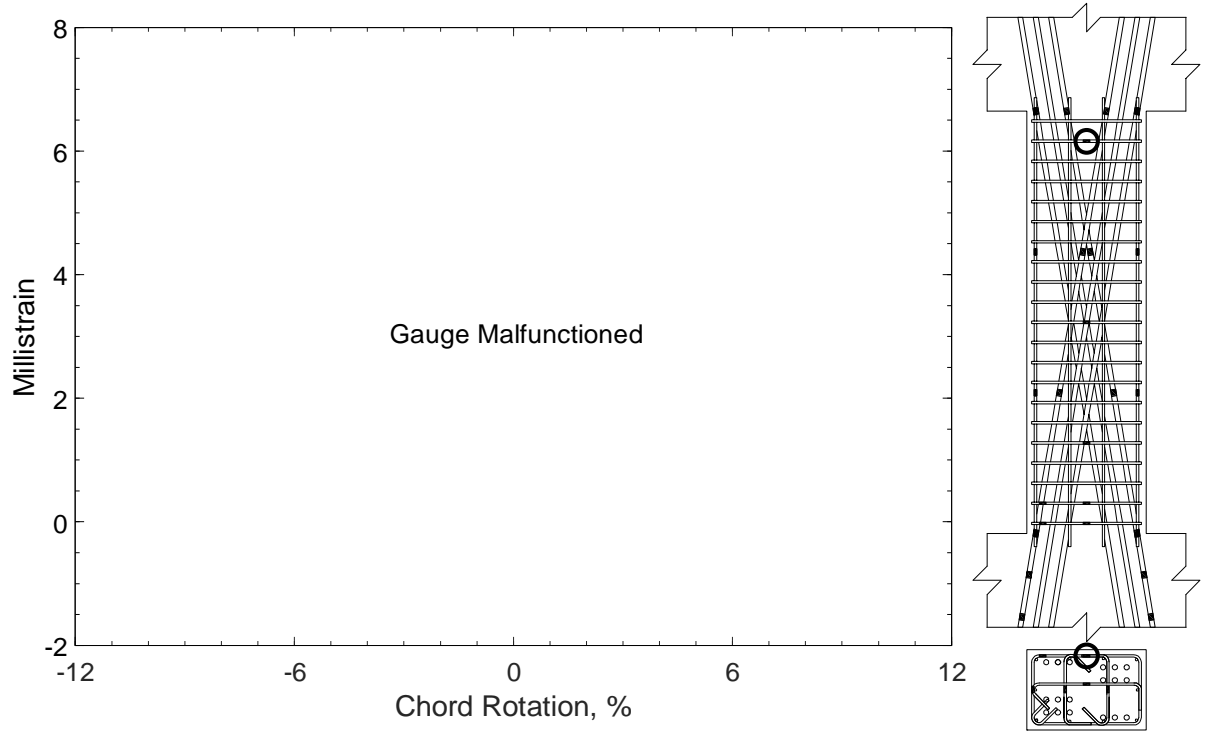


Figure 361 – Measured strain in closed stirrup of D100-3.5, strain gauge S9

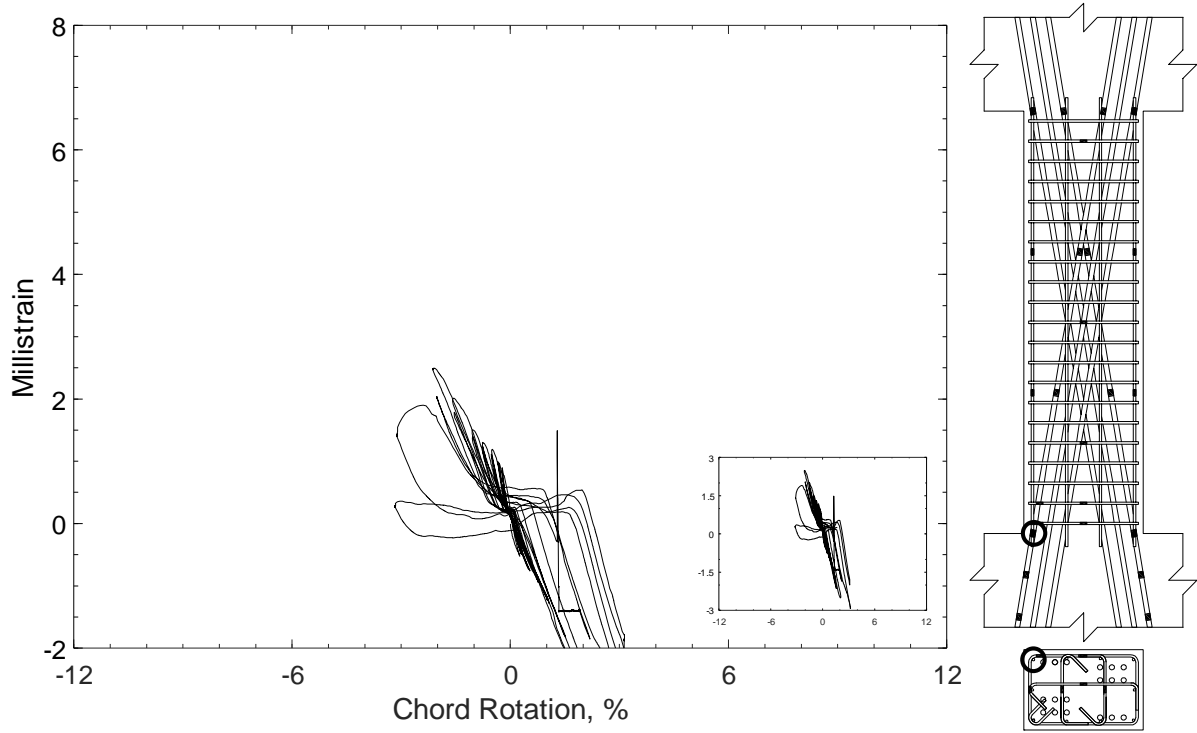


Figure 362 – Measured strain in parallel bar of D100-3.5, strain gauge H1

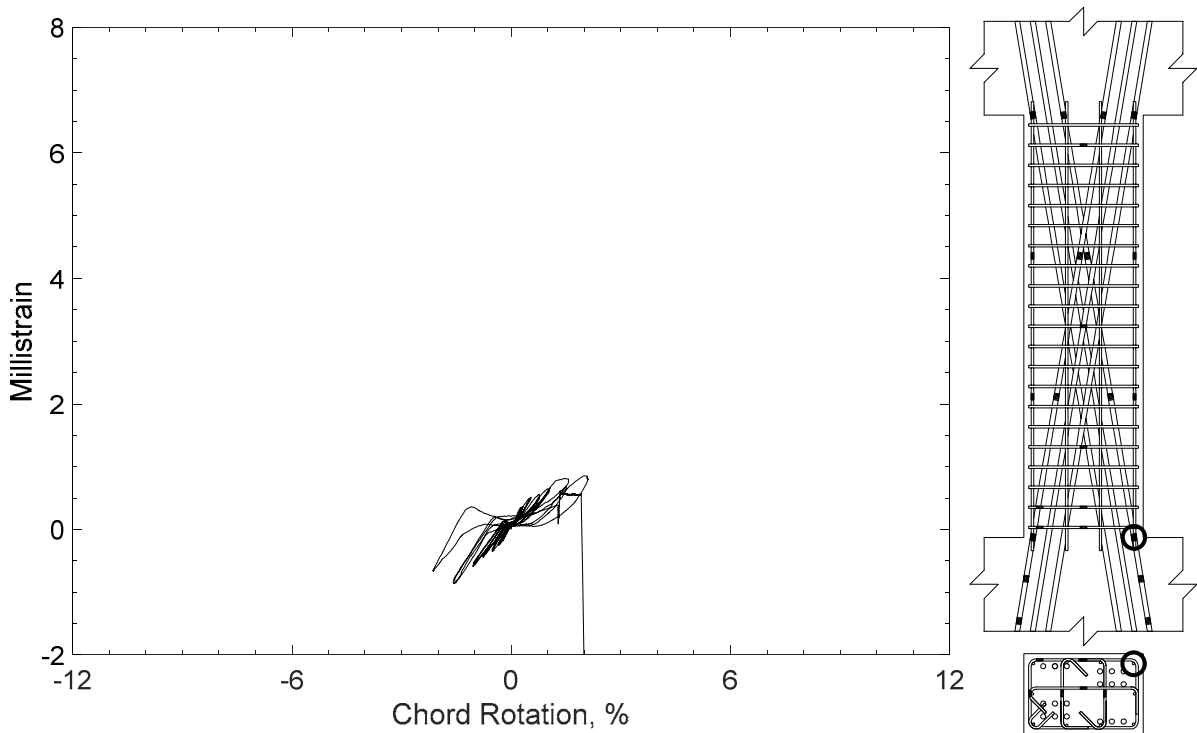


Figure 363 – Measured strain in parallel bar of D100-3.5, strain gauge H2

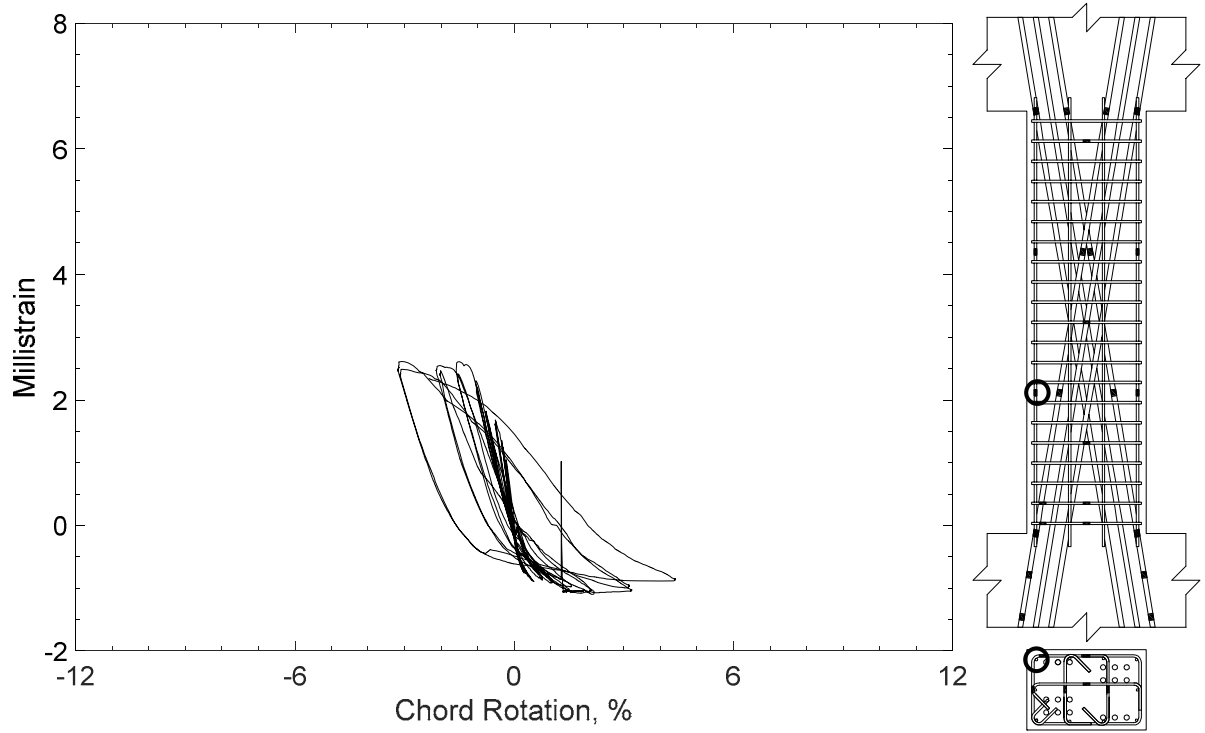


Figure 364 – Measured strain in parallel bar of D100-3.5, strain gauge H3

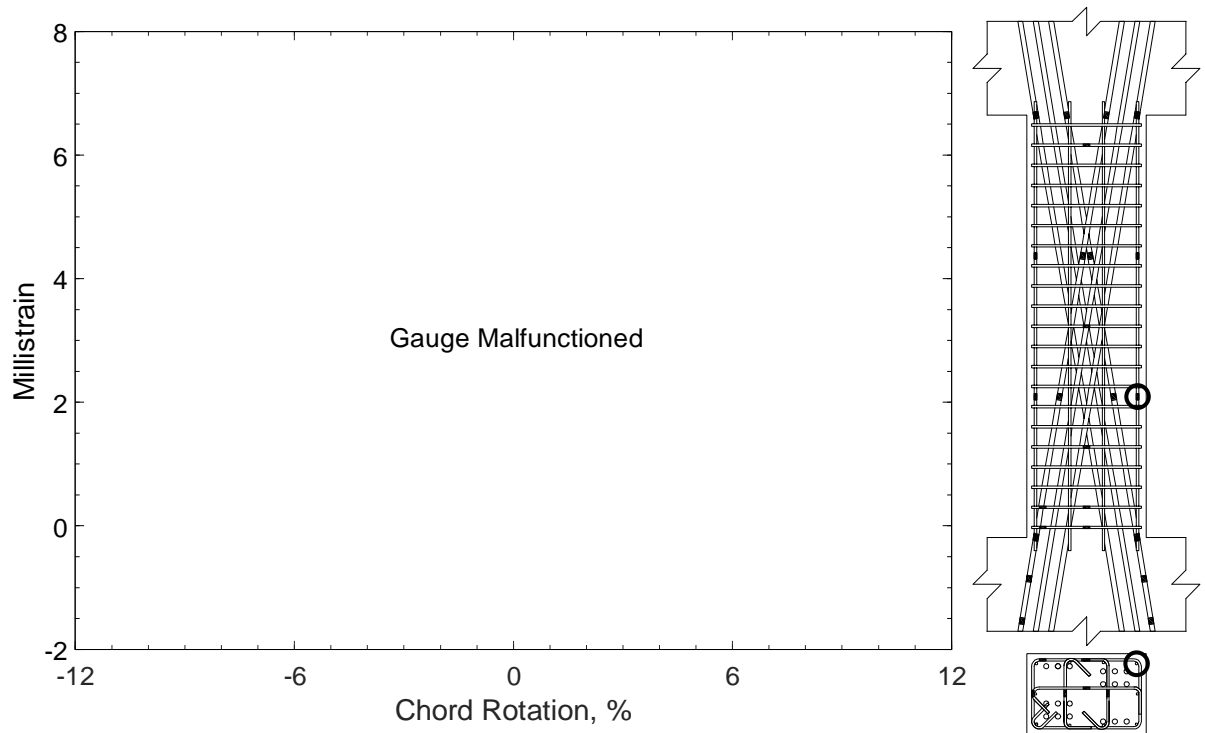


Figure 365 – Measured strain in parallel bar of D100-3.5, strain gauge H4

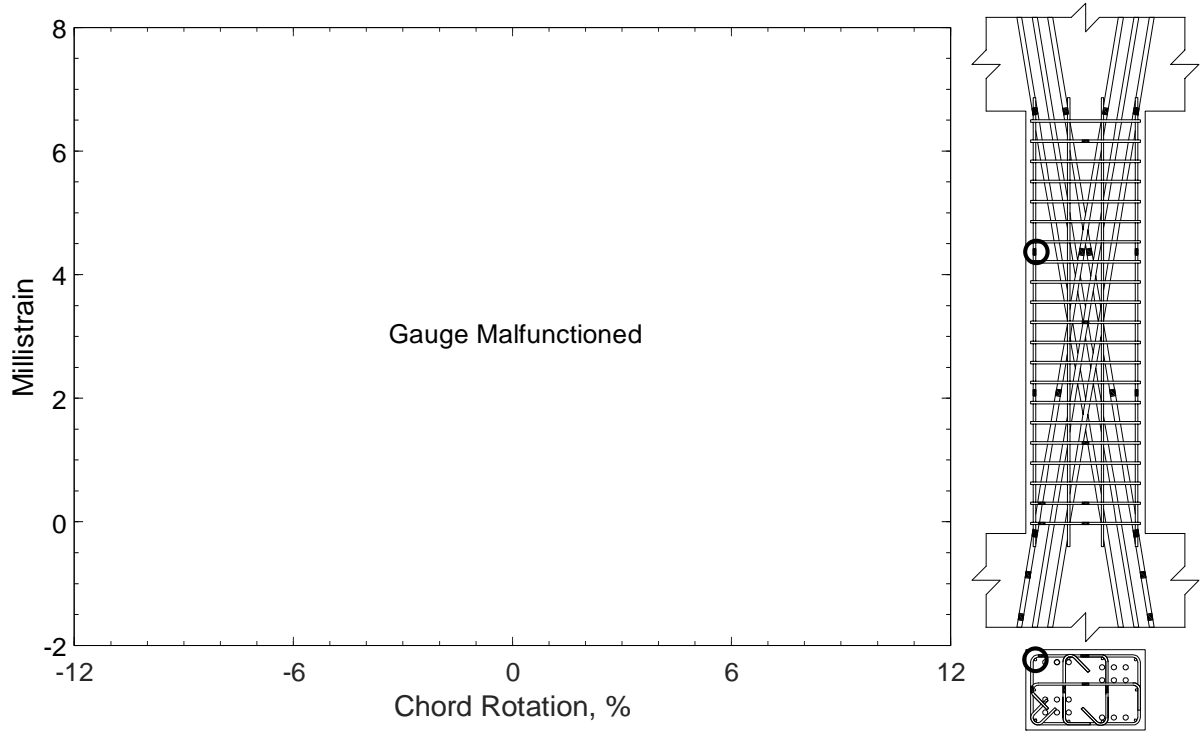


Figure 366 – Measured strain in parallel bar of D100-3.5, strain gauge H5

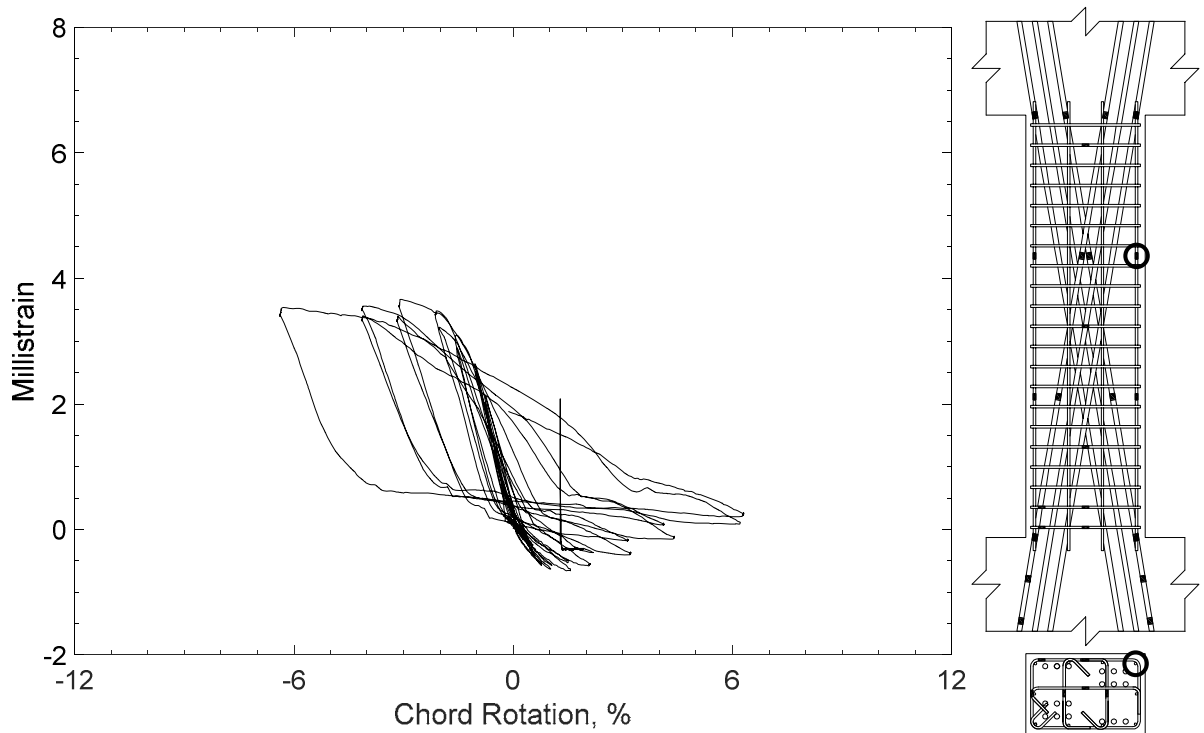


Figure 367 – Measured strain in parallel bar of D100-3.5, strain gauge H6

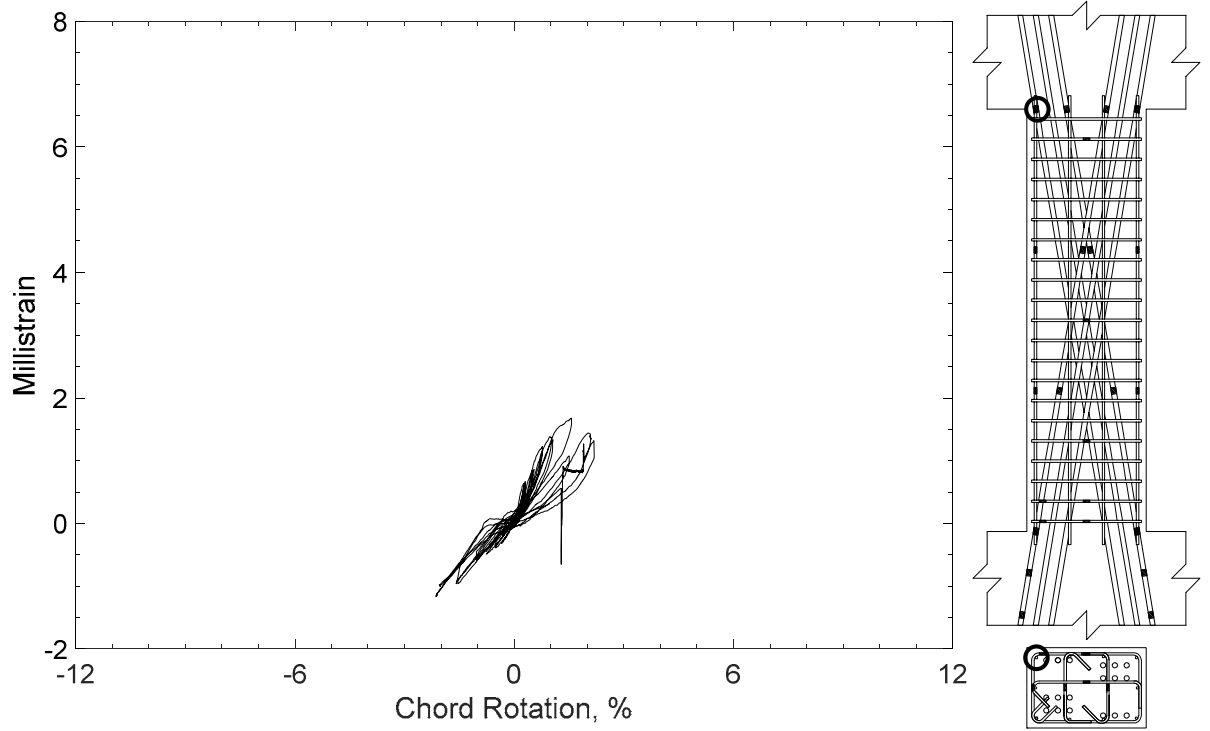


Figure 368 – Measured strain in parallel bar of D100-3.5, strain gauge H7

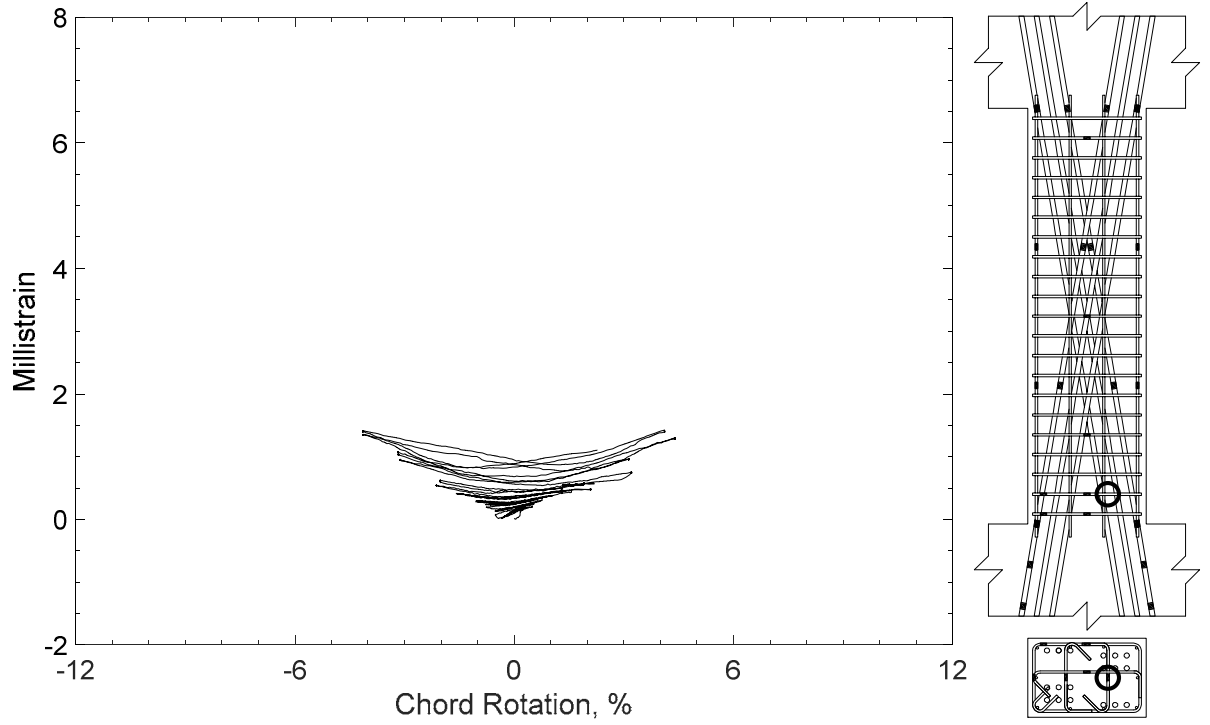


Figure 369 – Measured strain in crosstie of D100-3.5, strain gauge T1

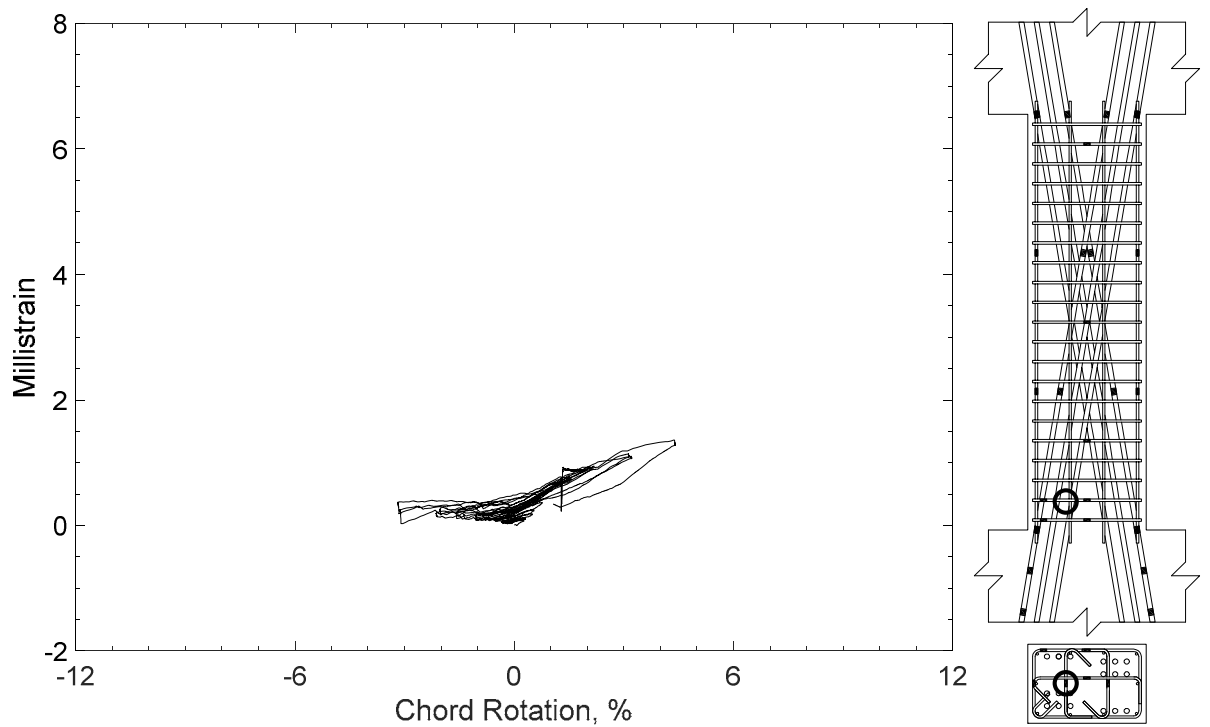


Figure 370 – Measured strain in crosstie of D100-3.5, strain gauge T2

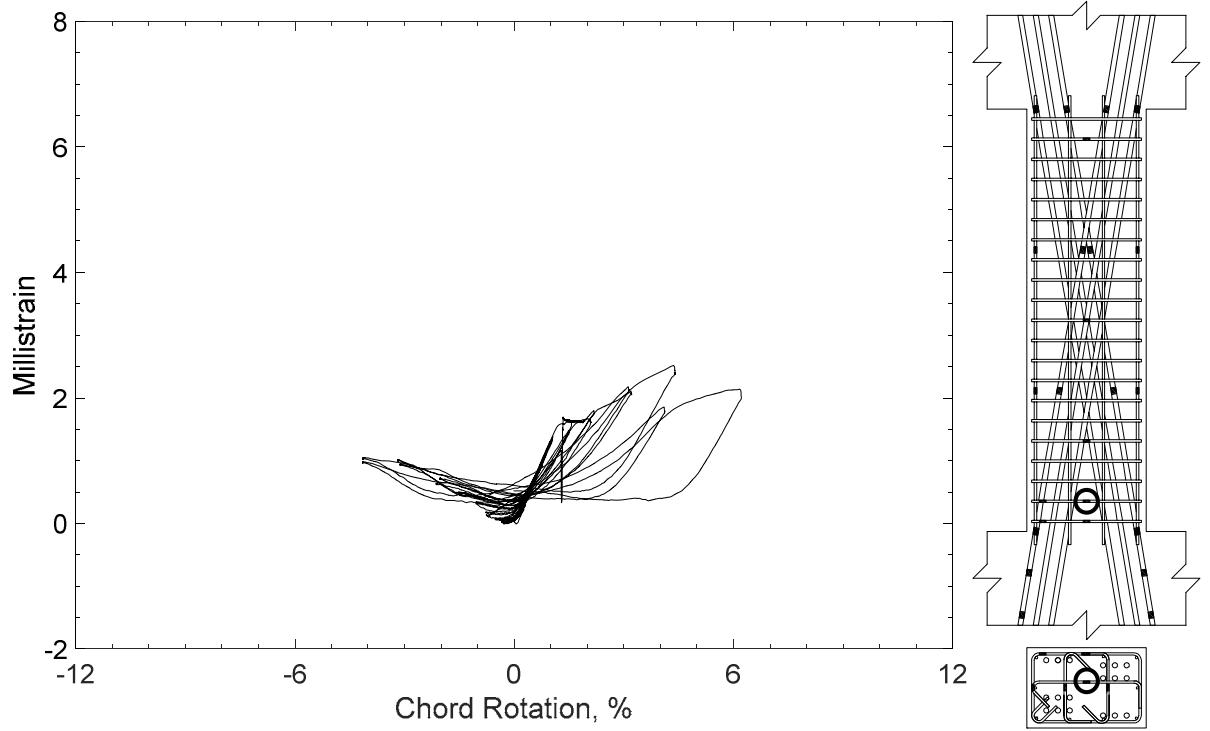


Figure 371 – Measured strain in crosstie of D100-3.5, strain gauge T3

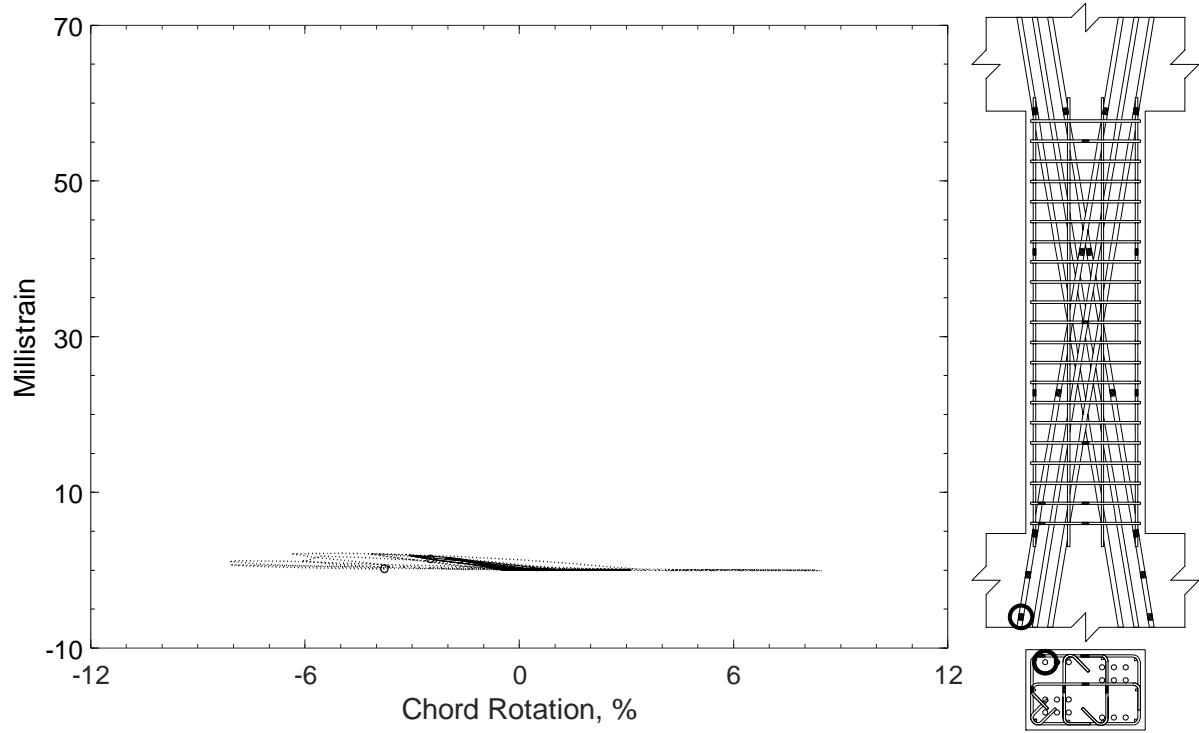


Figure 372 – Measured strain in diagonal bar of D120-3.5, strain gauge D1

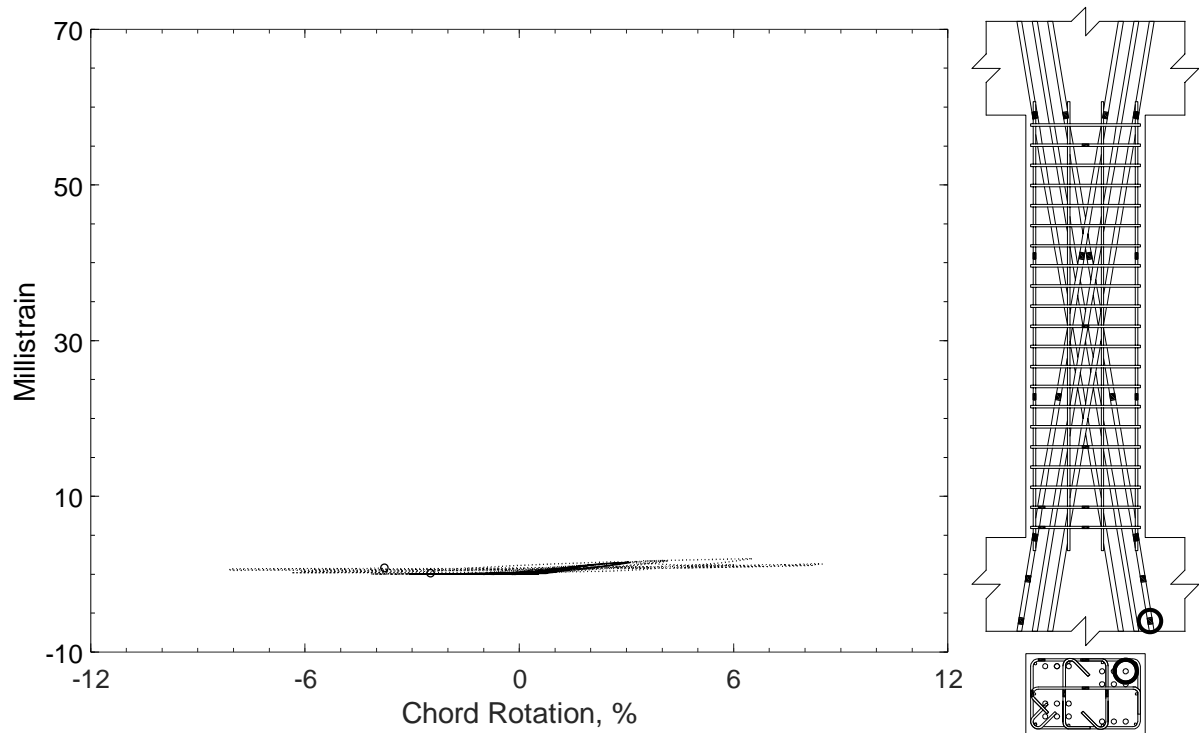


Figure 373 – Measured strain in diagonal bar of D120-3.5, strain gauge D2

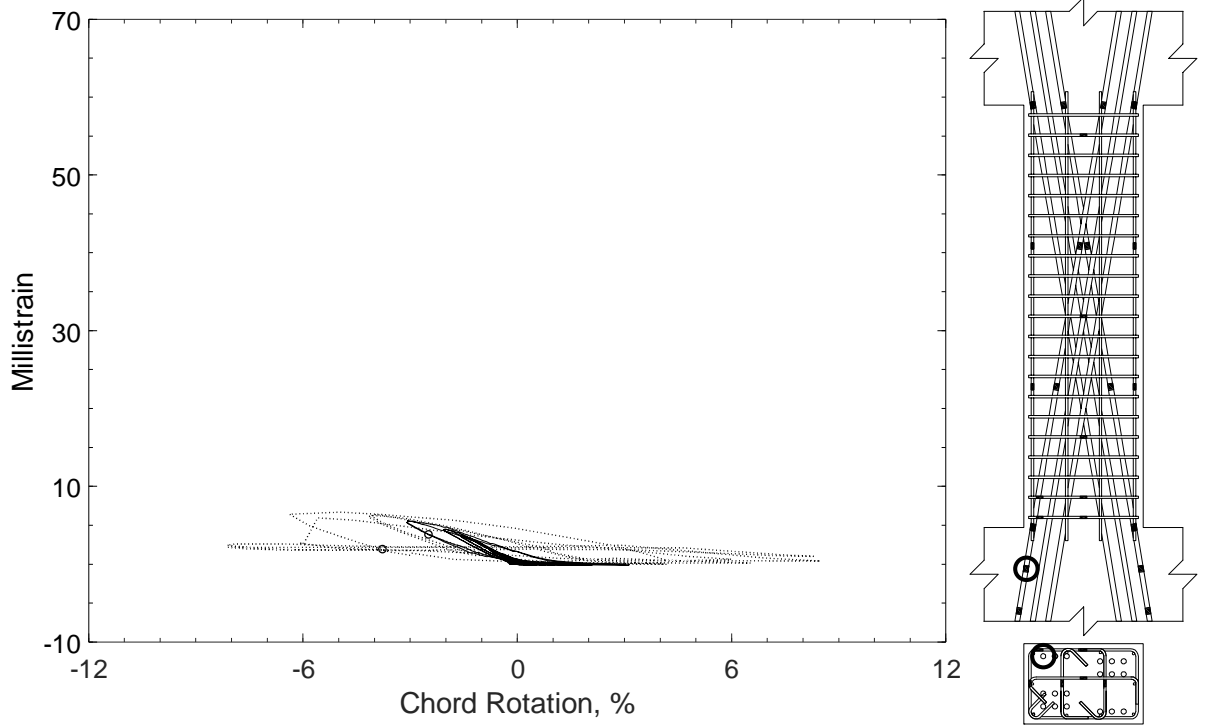


Figure 374 – Measured strain in diagonal bar of D120-3.5, strain gauge D3

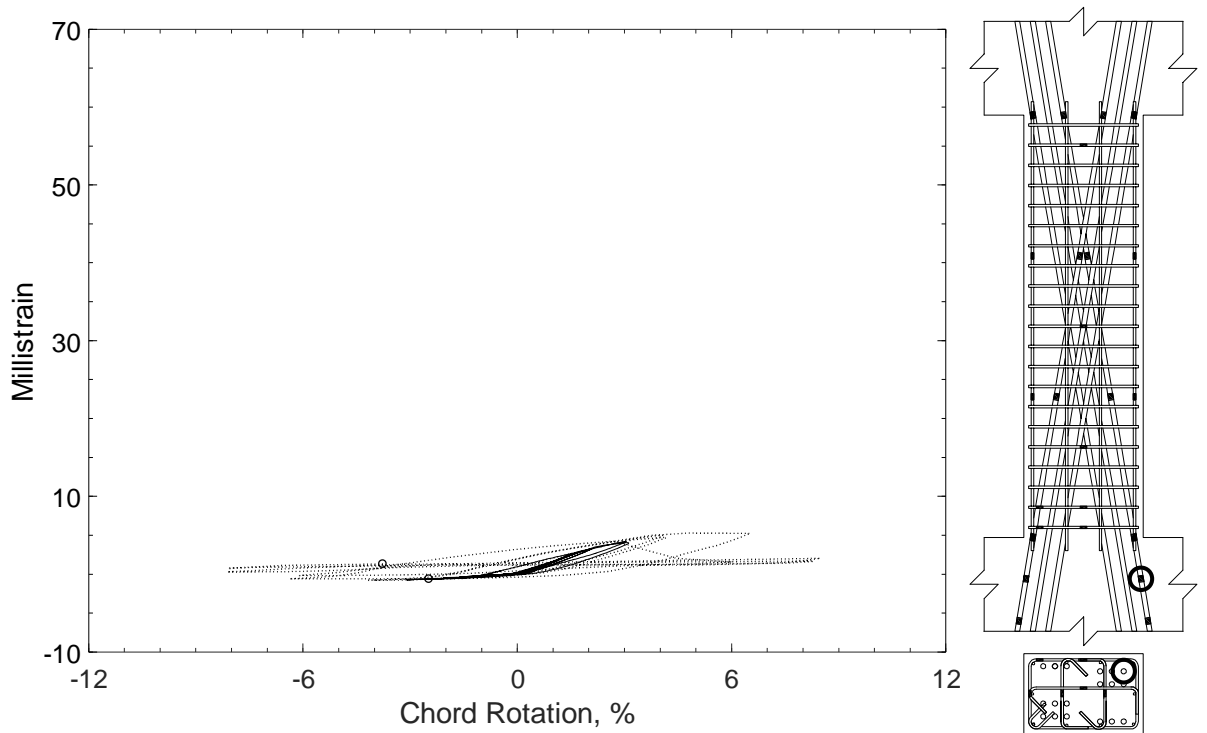


Figure 375 – Measured strain in diagonal bar of D120-3.5, strain gauge D4

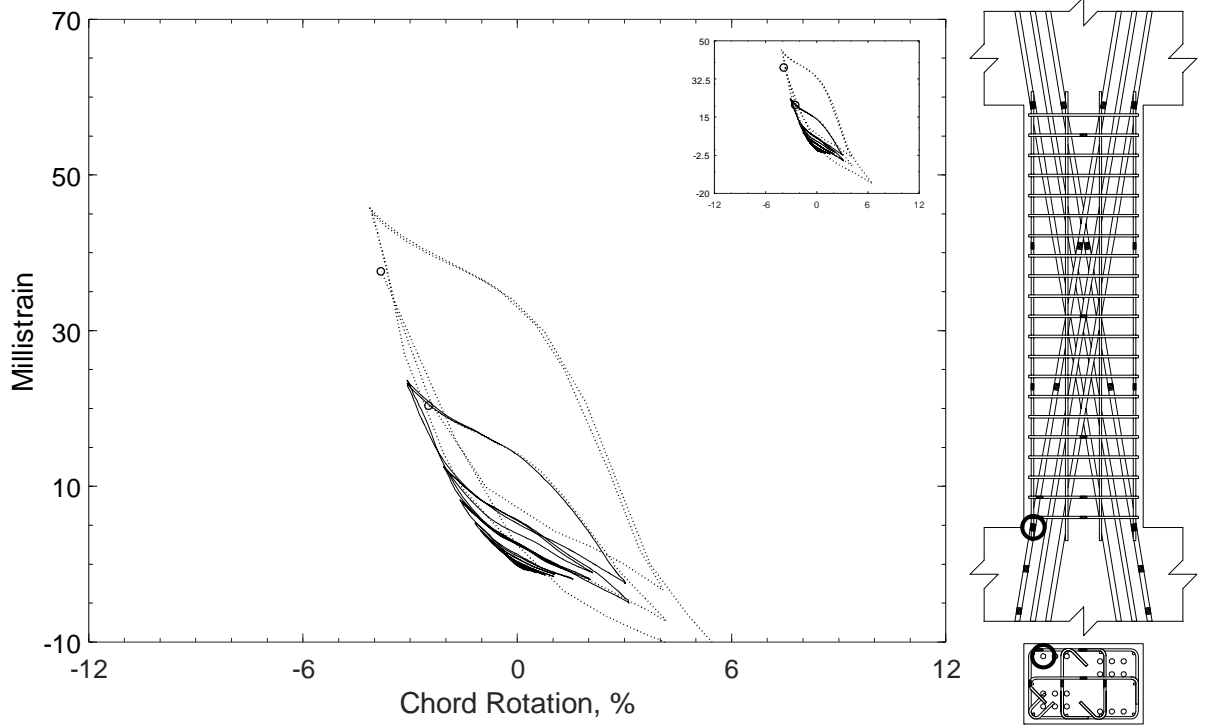


Figure 376 – Measured strain in diagonal bar of D120-3.5, strain gauge D5

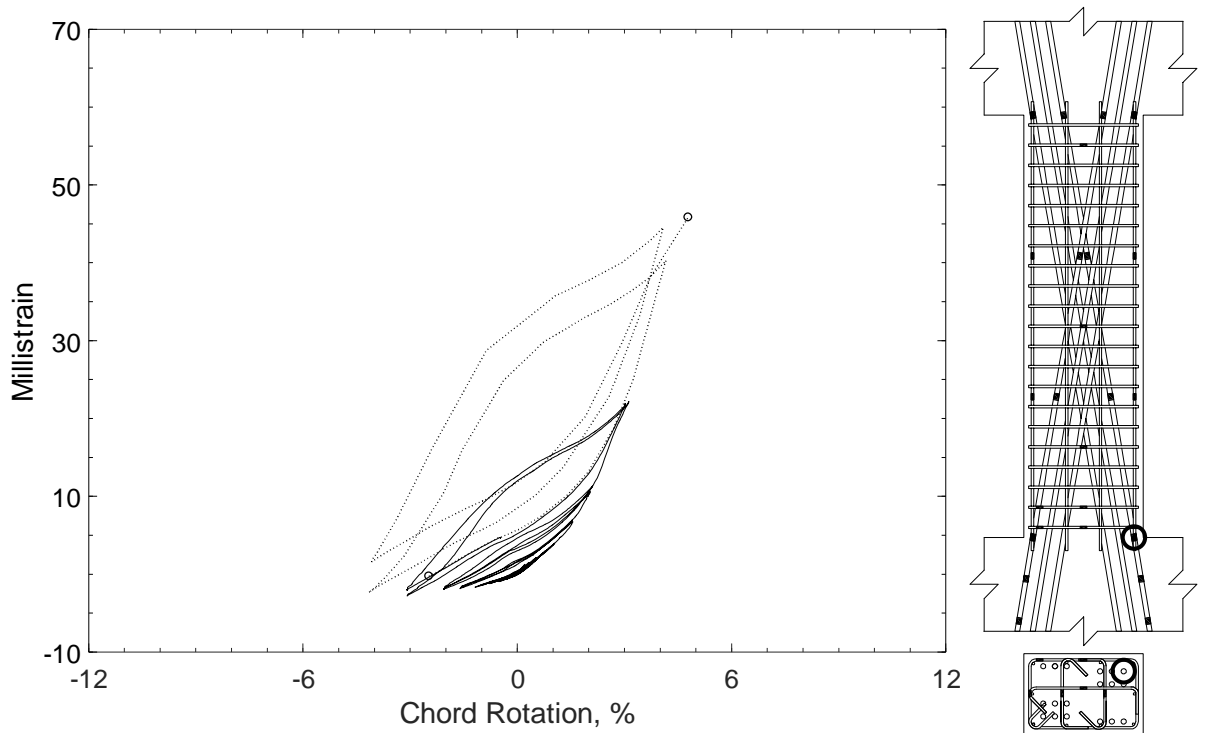


Figure 377 – Measured strain in diagonal bar of D120-3.5, strain gauge D6

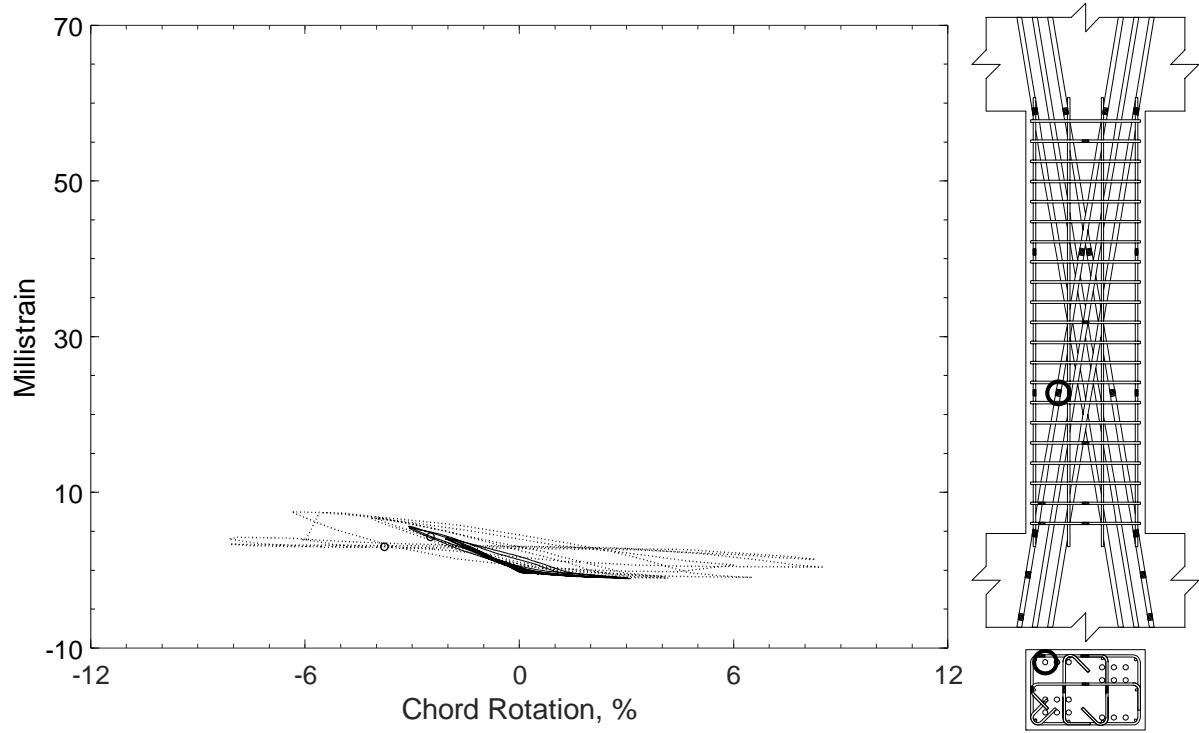


Figure 378 – Measured strain in diagonal bar of D120-3.5, strain gauge D7

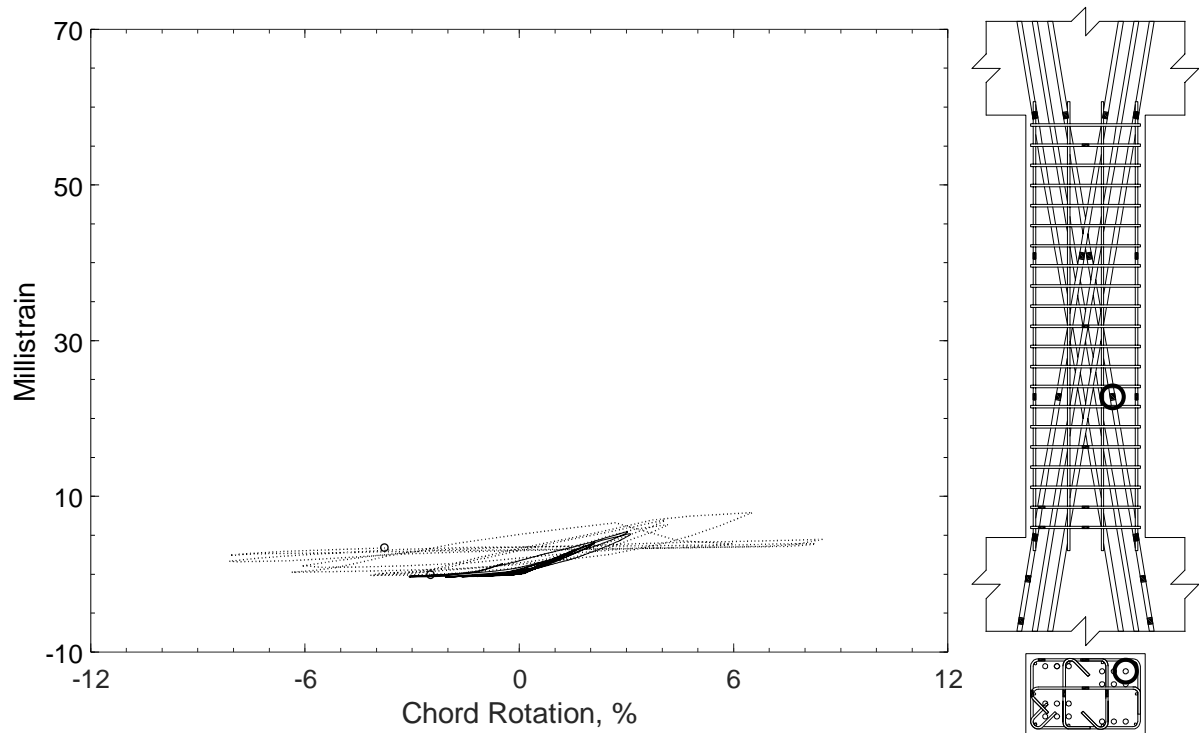


Figure 379 – Measured strain in diagonal bar of D120-3.5, strain gauge D8

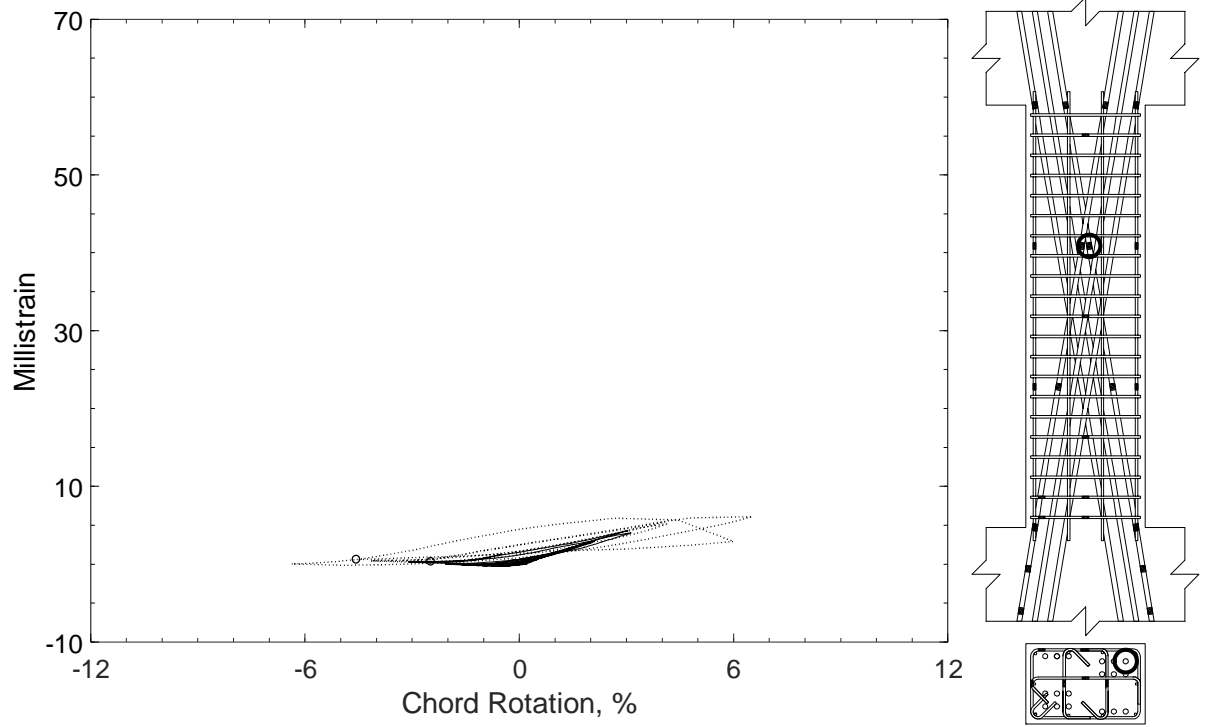


Figure 380 – Measured strain in diagonal bar of D120-3.5, strain gauge D9

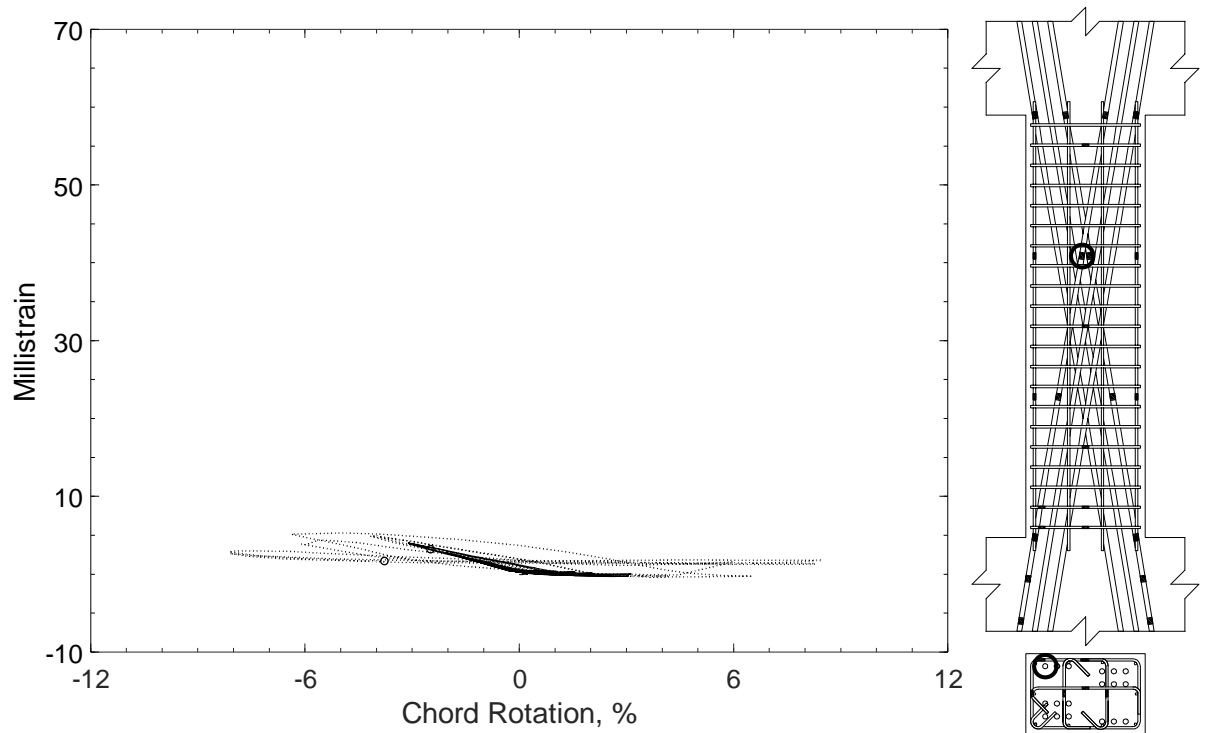


Figure 381 – Measured strain in diagonal bar of D120-3.5, strain gauge D10

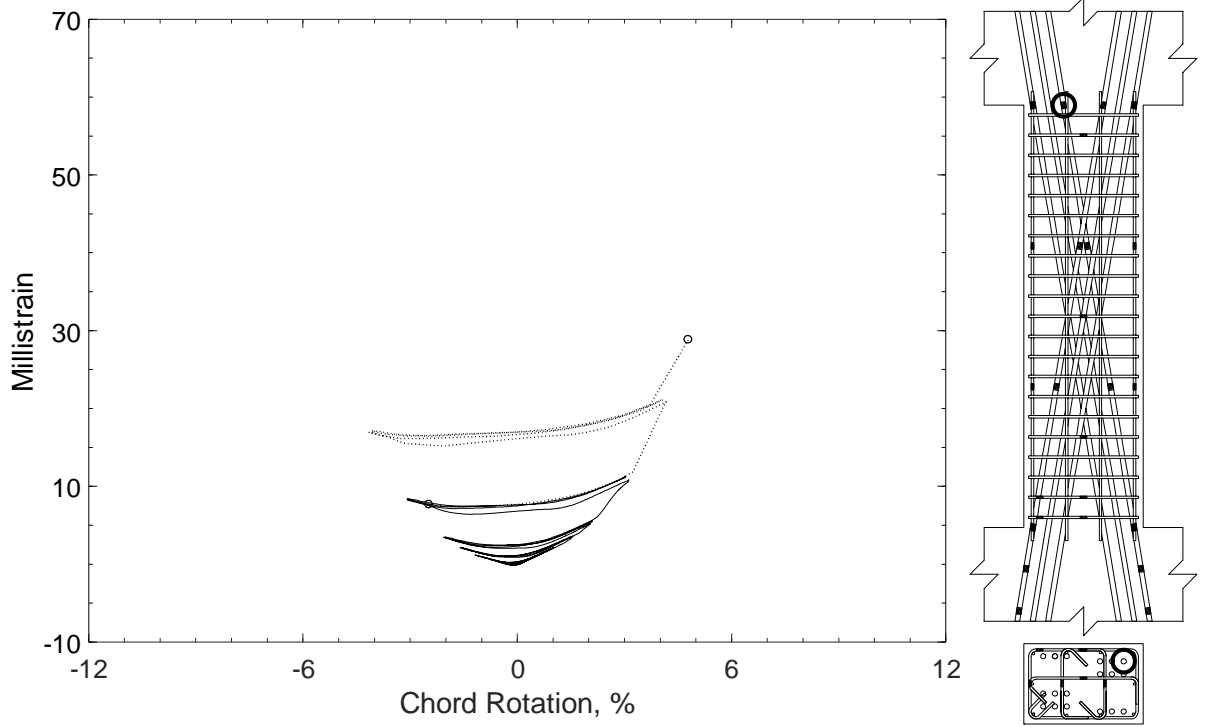


Figure 382 – Measured strain in diagonal bar of D120-3.5, strain gauge D11

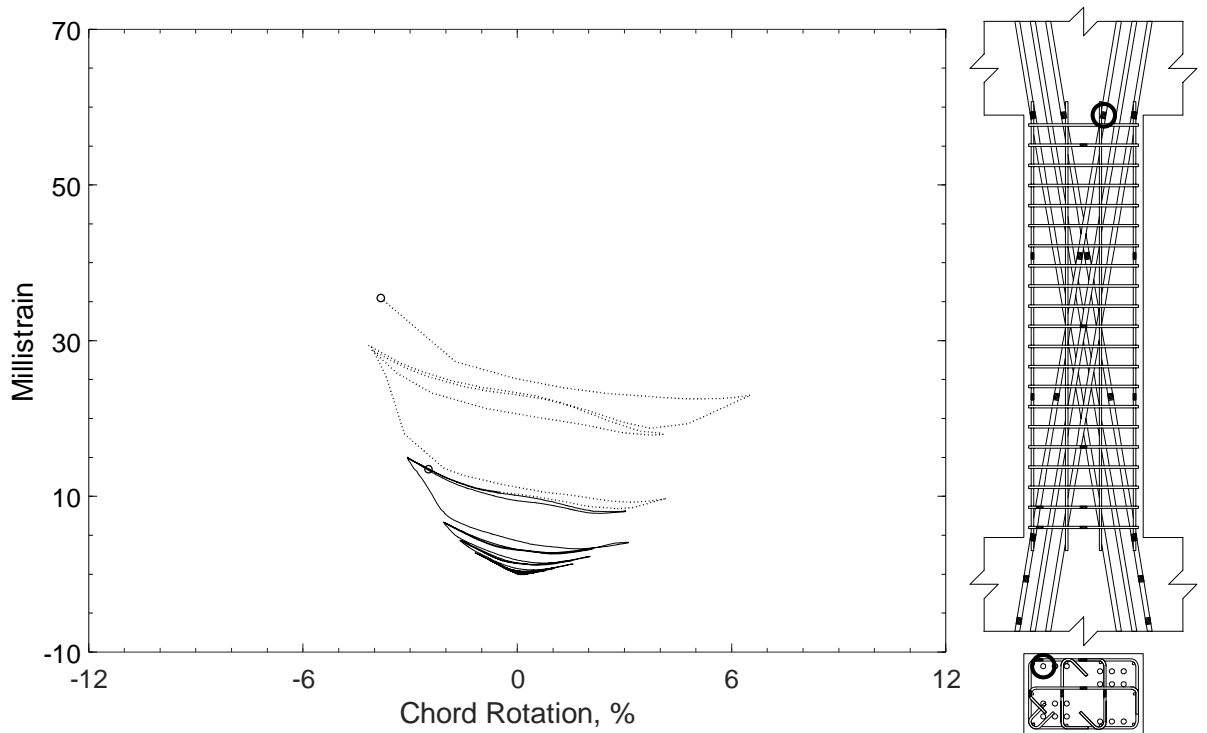


Figure 383 – Measured strain in diagonal bar of D120-3.5, strain gauge D12

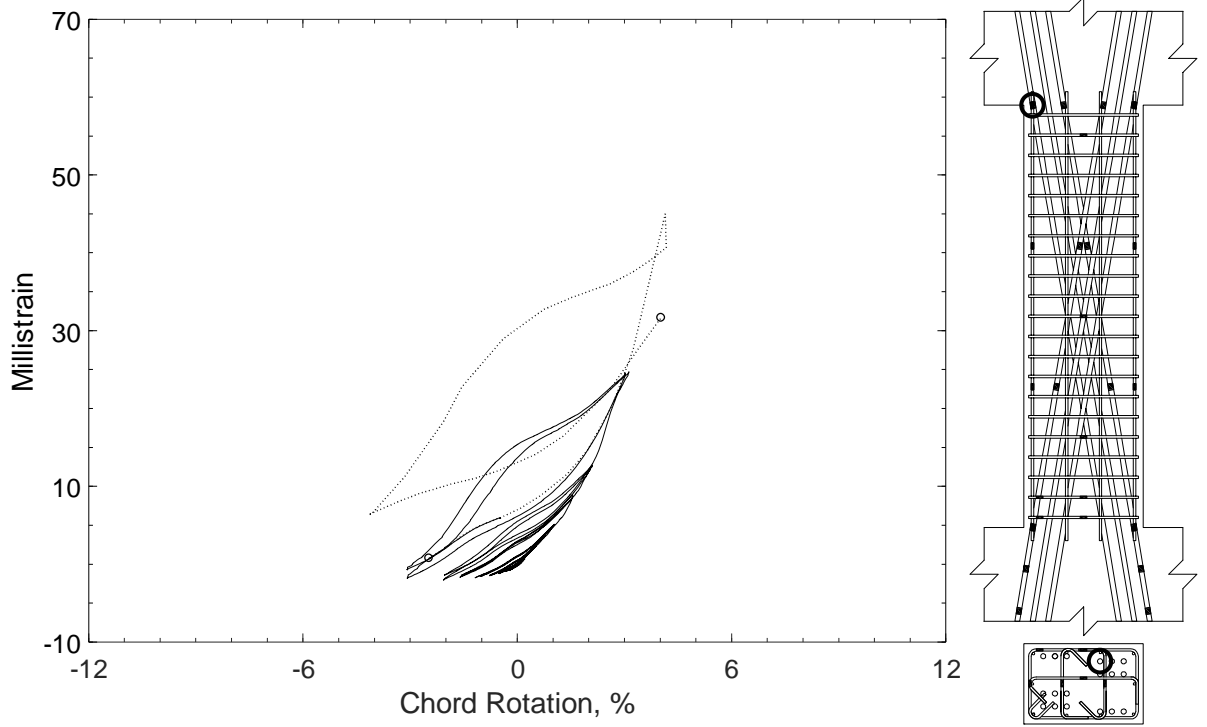


Figure 384 – Measured strain in diagonal bar of D120-3.5, strain gauge D13

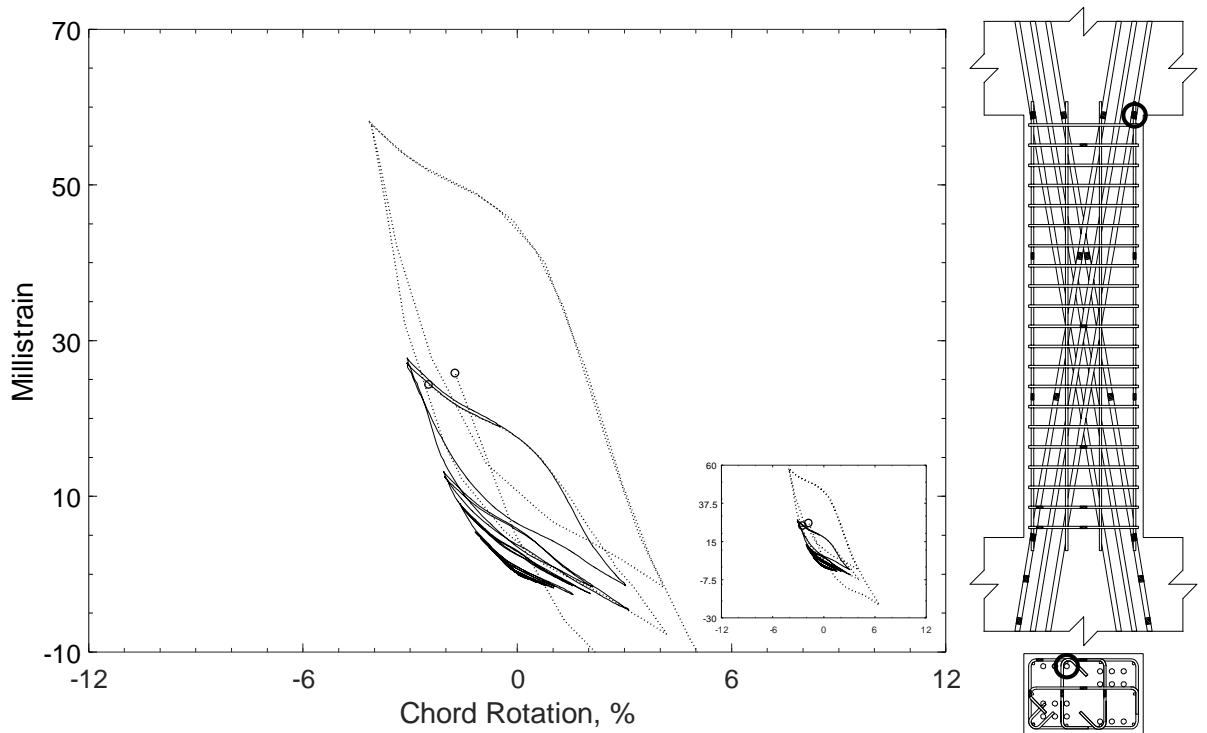


Figure 385 – Measured strain in diagonal bar of D120-3.5, strain gauge D14

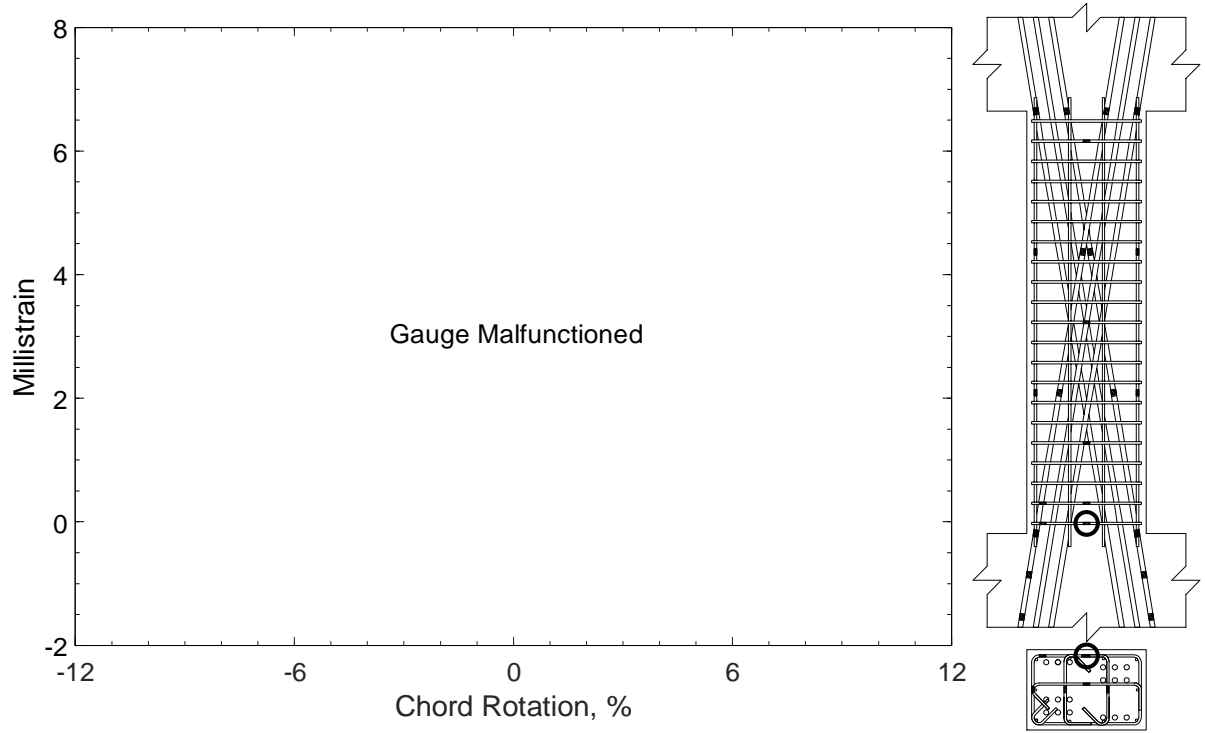


Figure 386 – Measured strain in closed stirrup of D120-3.5, strain gauge S1

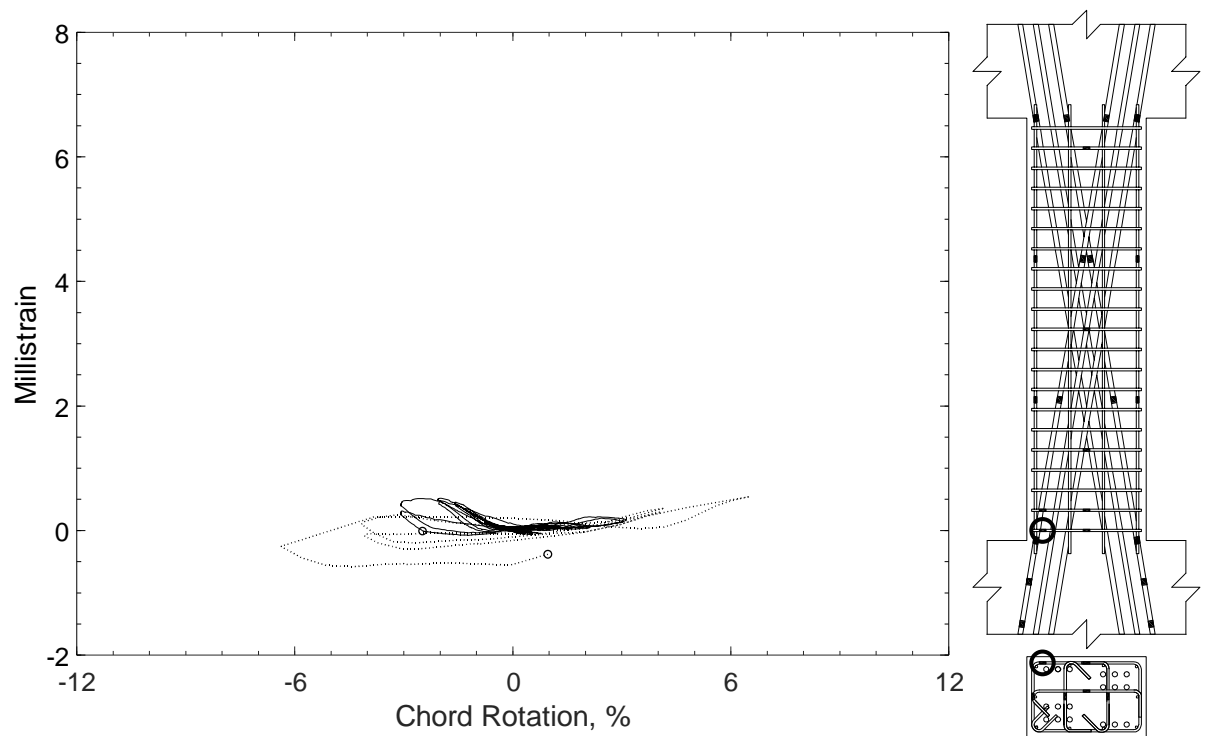


Figure 387 – Measured strain in closed stirrup of D120-3.5, strain gauge S2

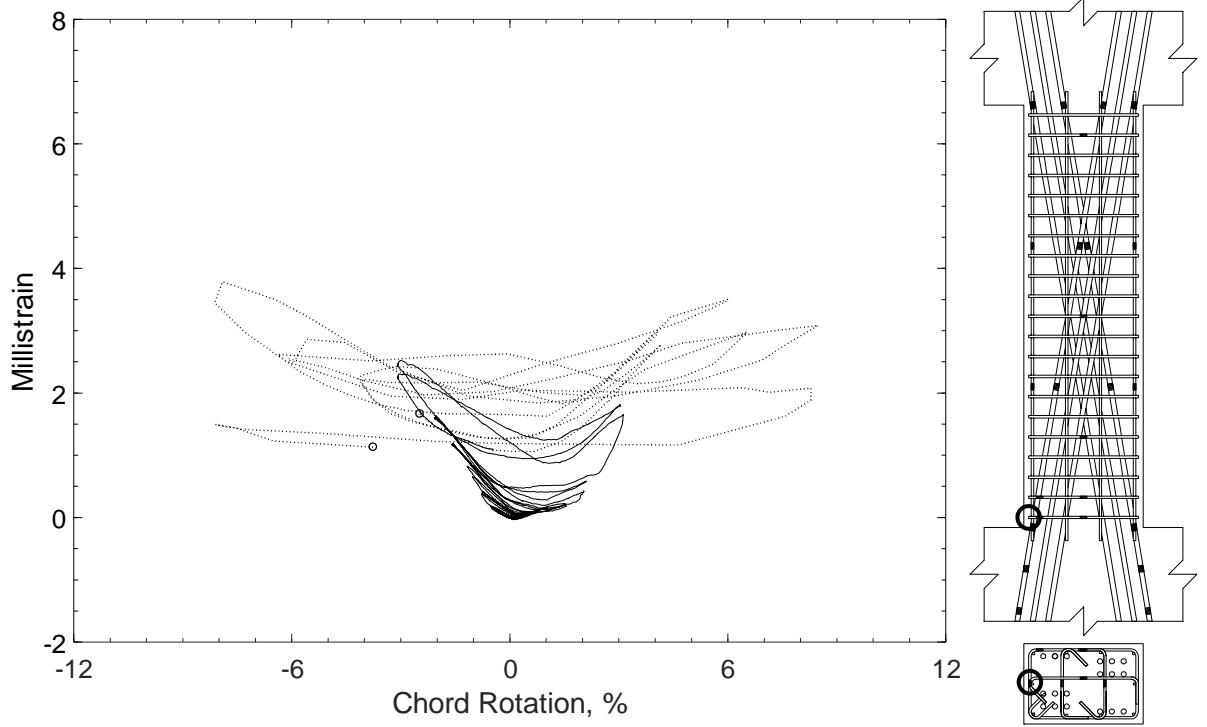


Figure 388 – Measured strain in closed stirrup of D120-3.5, strain gauge S3

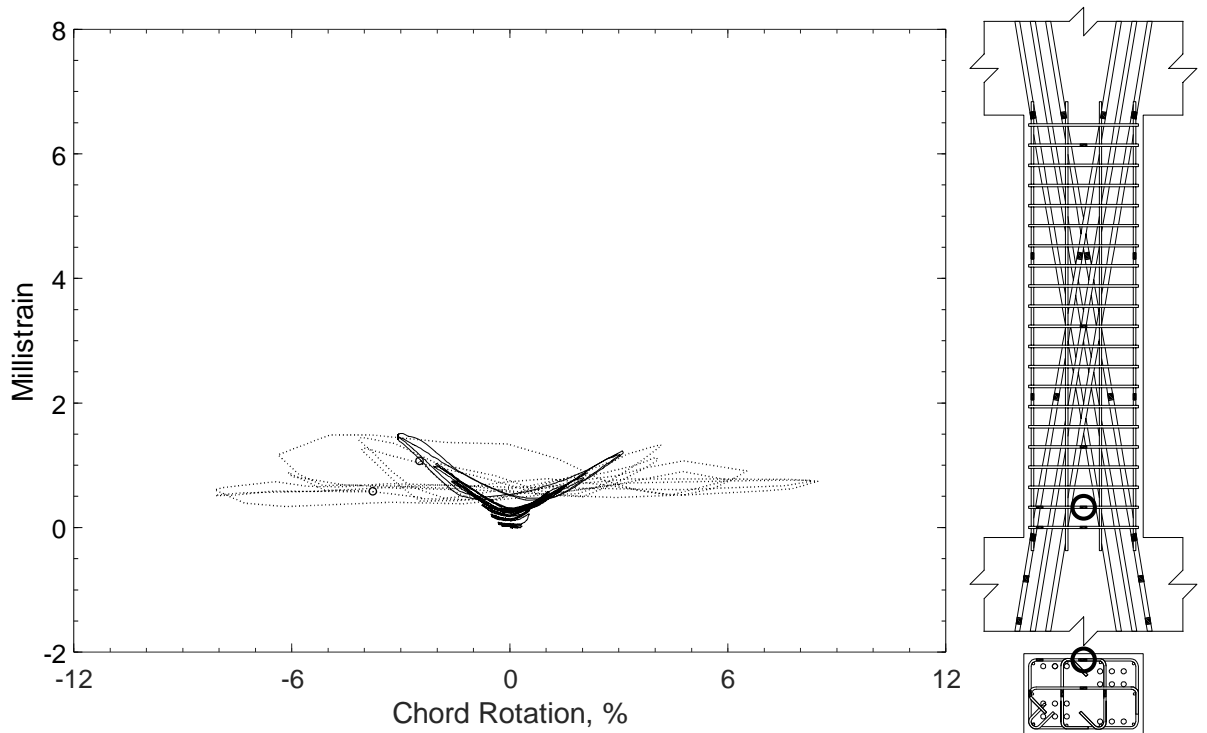


Figure 389 – Measured strain in closed stirrup of D120-3.5, strain gauge S4

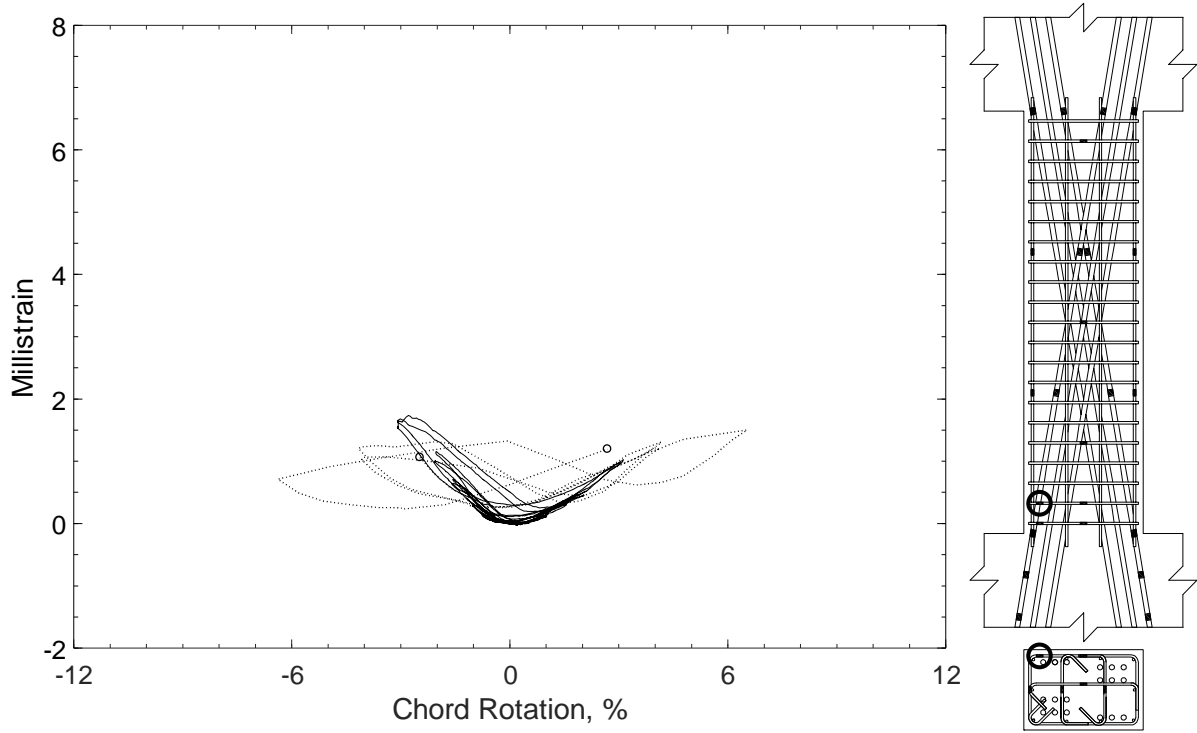


Figure 390 – Measured strain in closed stirrup of D120-3.5, strain gauge S5

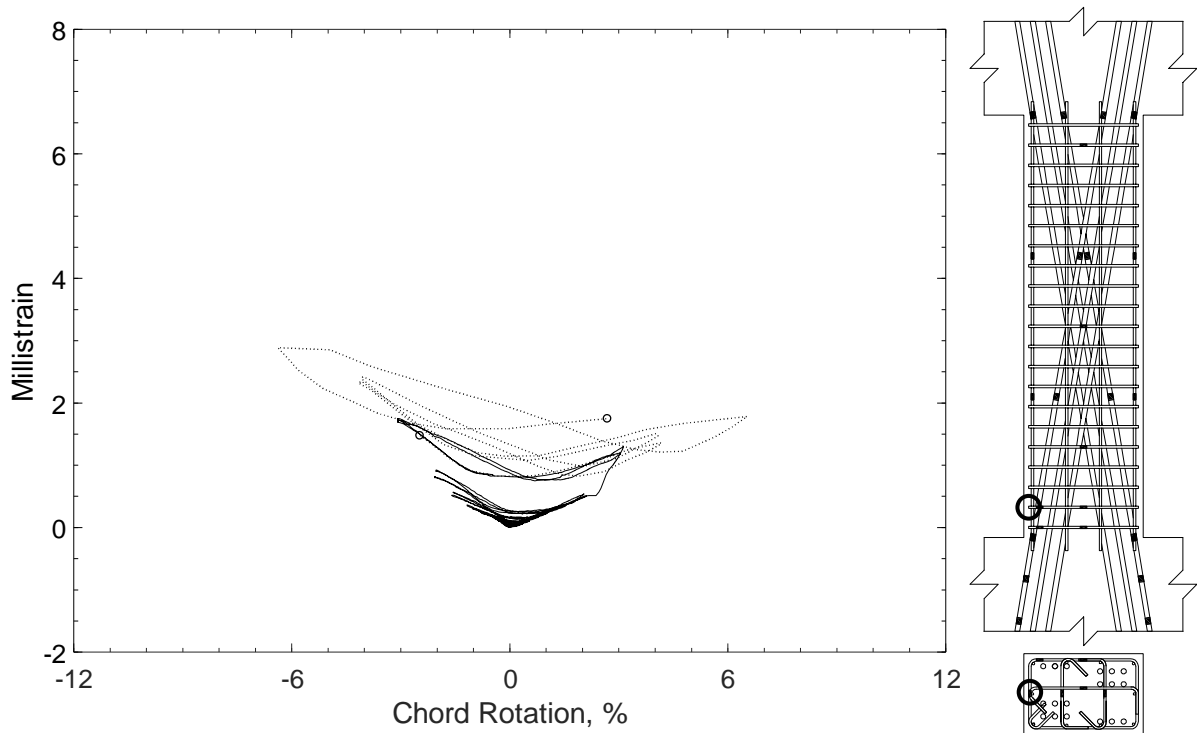


Figure 391 – Measured strain in closed stirrup of D120-3.5, strain gauge S6

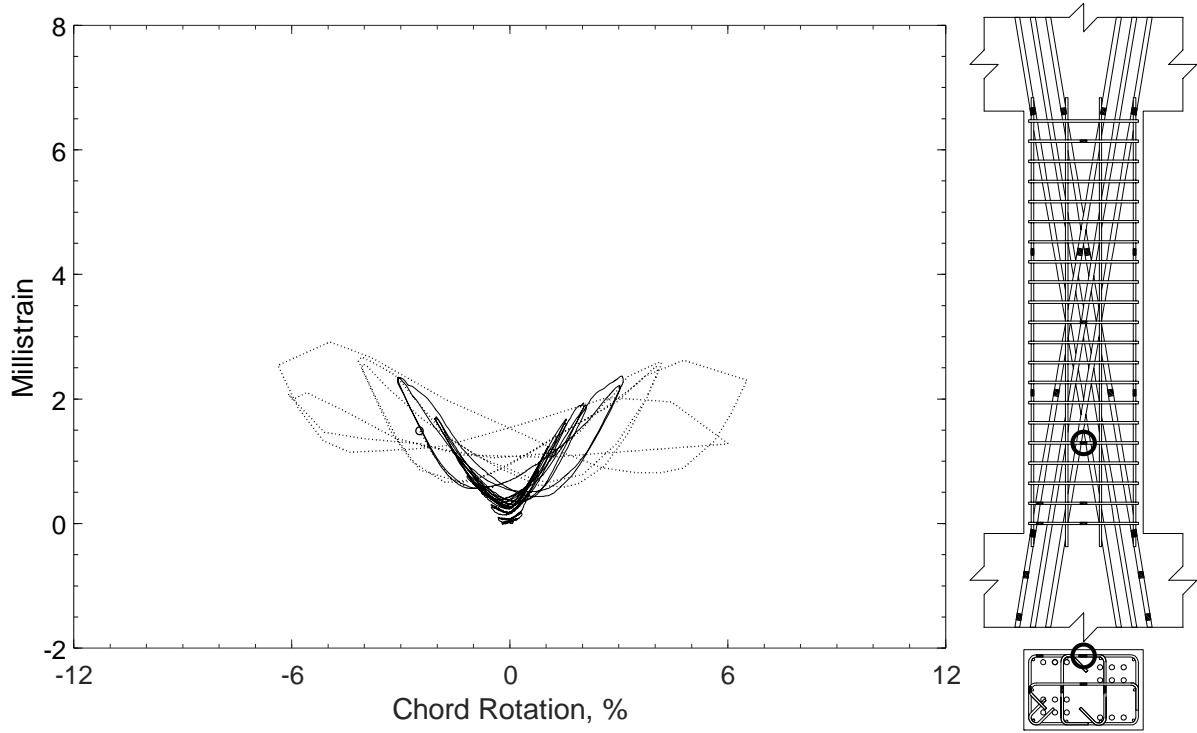


Figure 392 – Measured strain in closed stirrup of D120-3.5, strain gauge S7

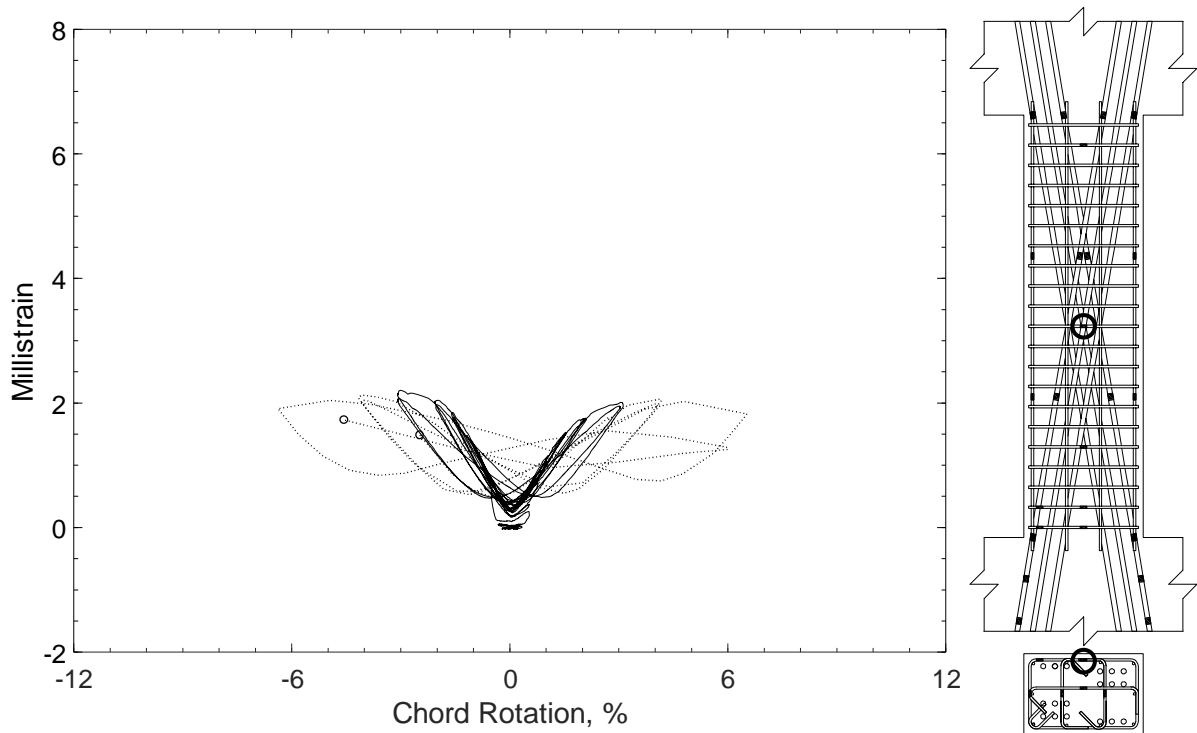


Figure 393 – Measured strain in closed stirrup of D120-3.5, strain gauge S8

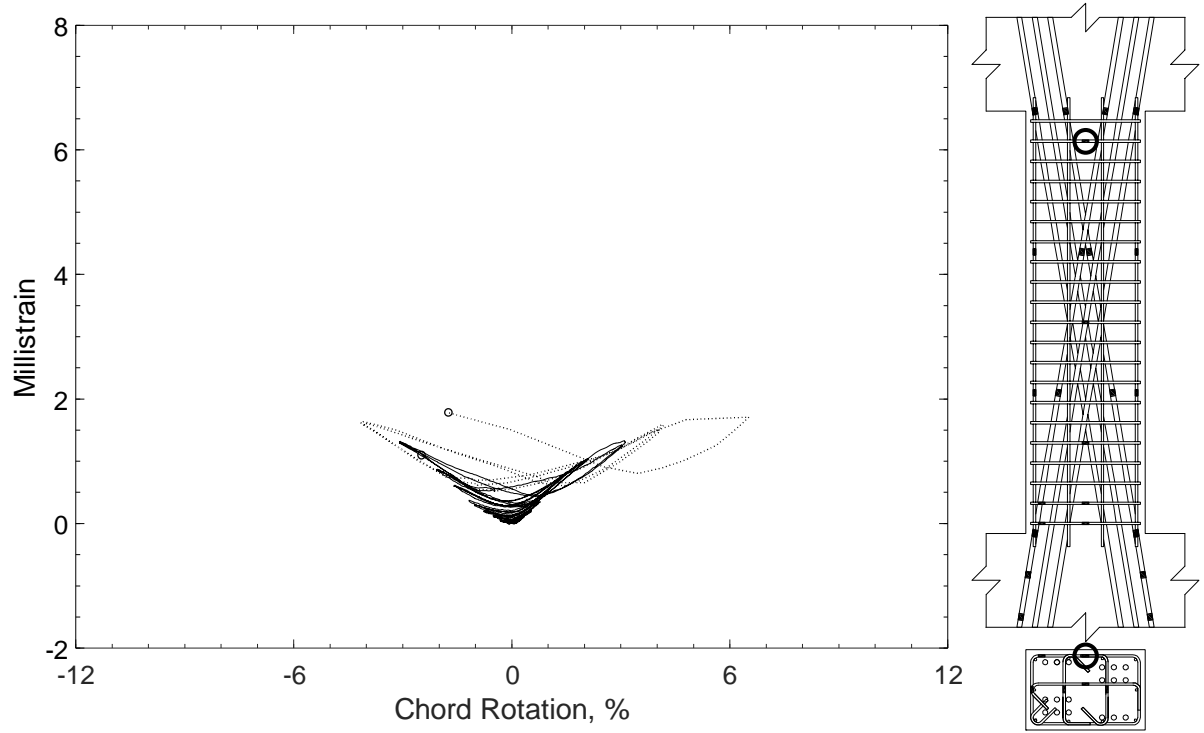


Figure 394 – Measured strain in closed stirrup of D120-3.5, strain gauge S9

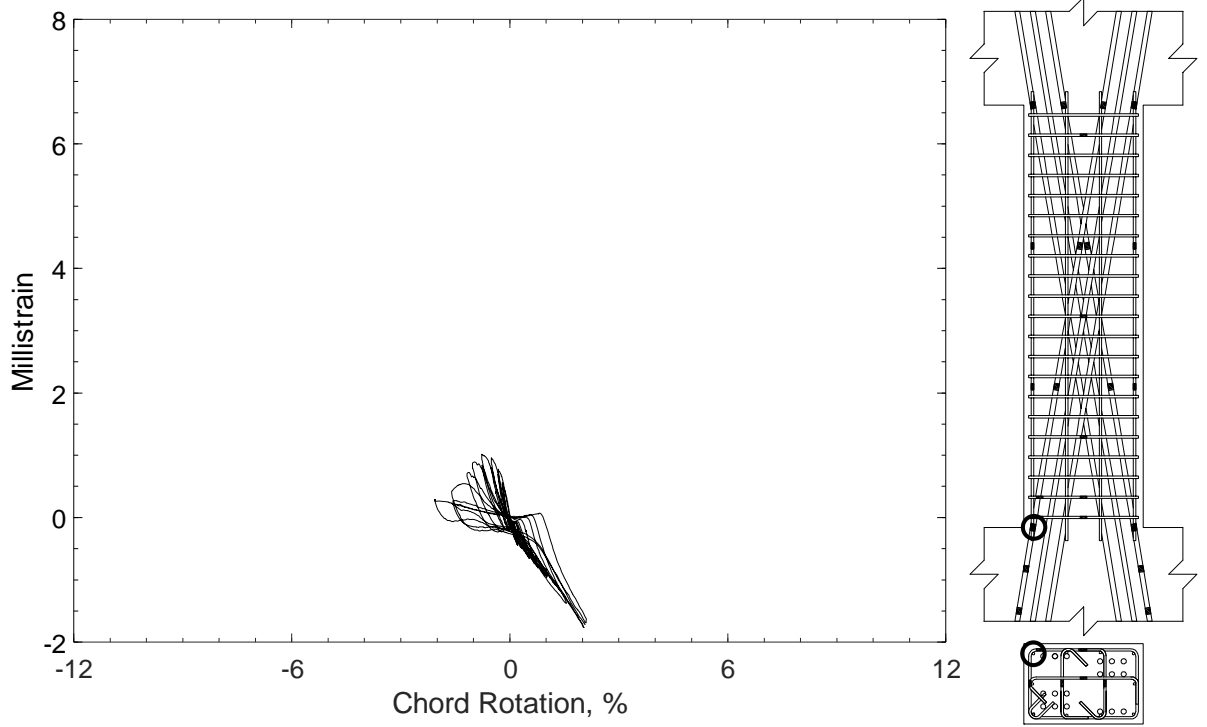


Figure 395 – Measured strain in parallel bar of D120-3.5, strain gauge H1

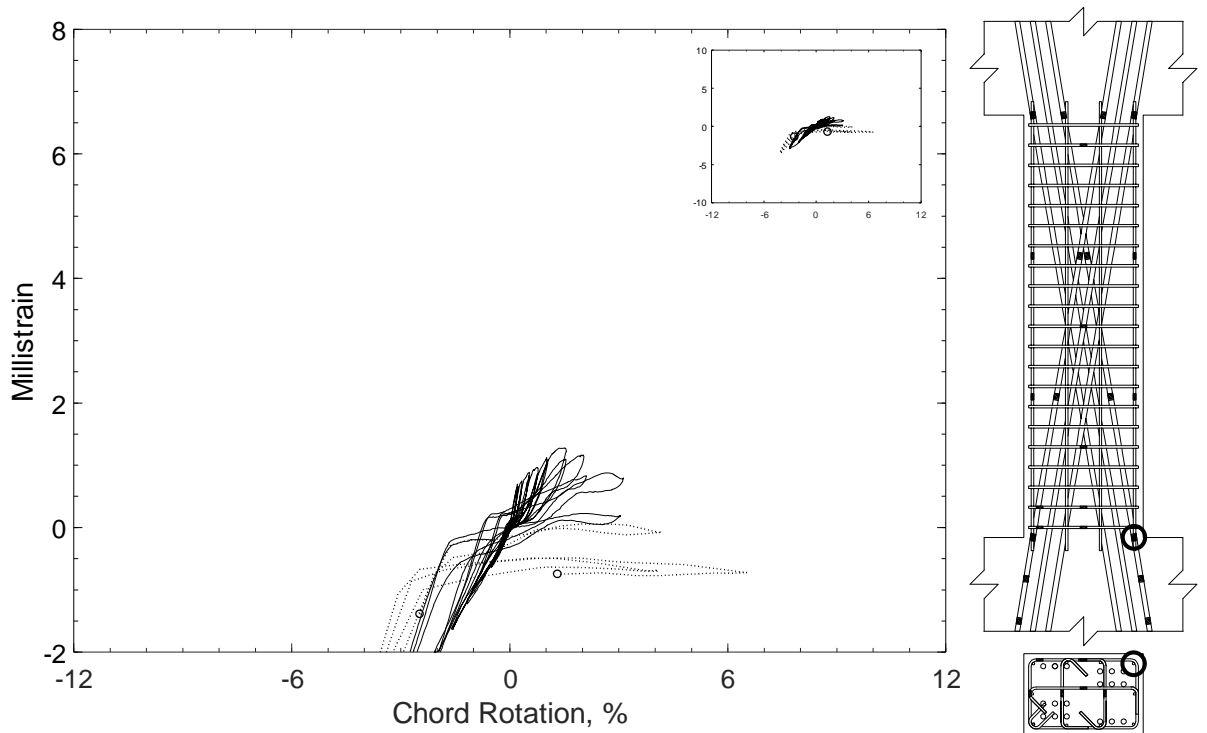


Figure 396 – Measured strain in parallel bar of D120-3.5, strain gauge H2

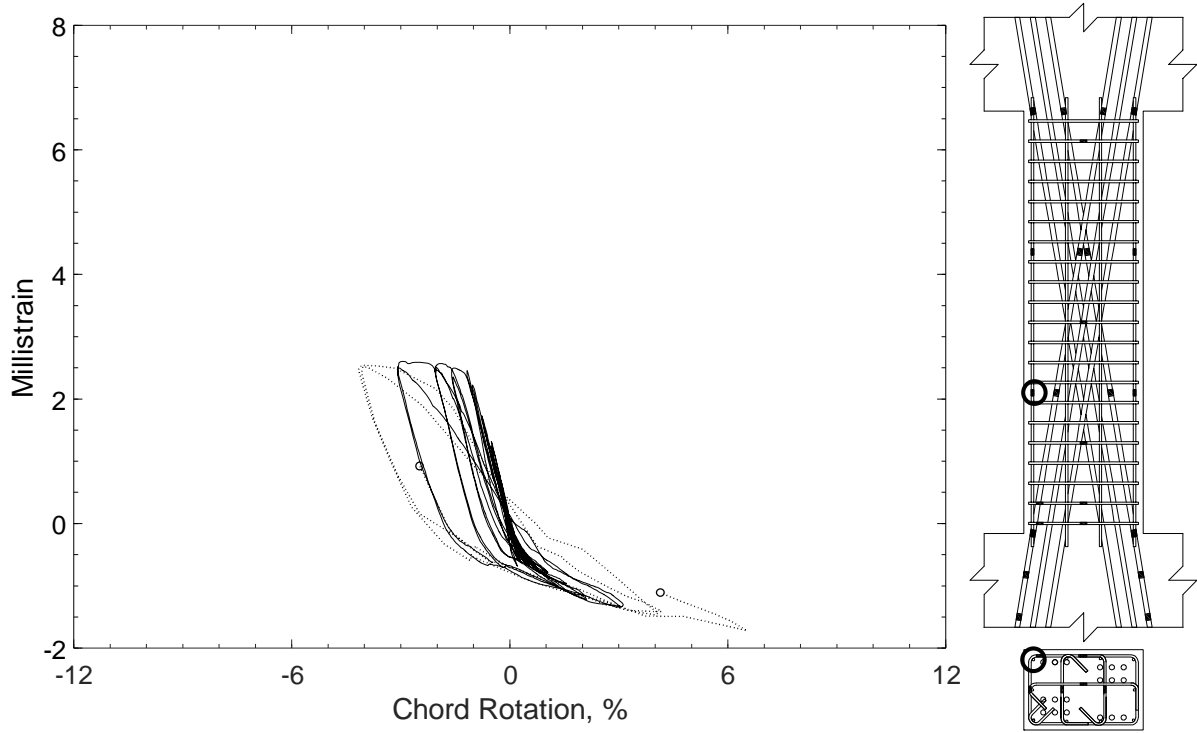


Figure 397 – Measured strain in parallel bar of D120-3.5, strain gauge H3

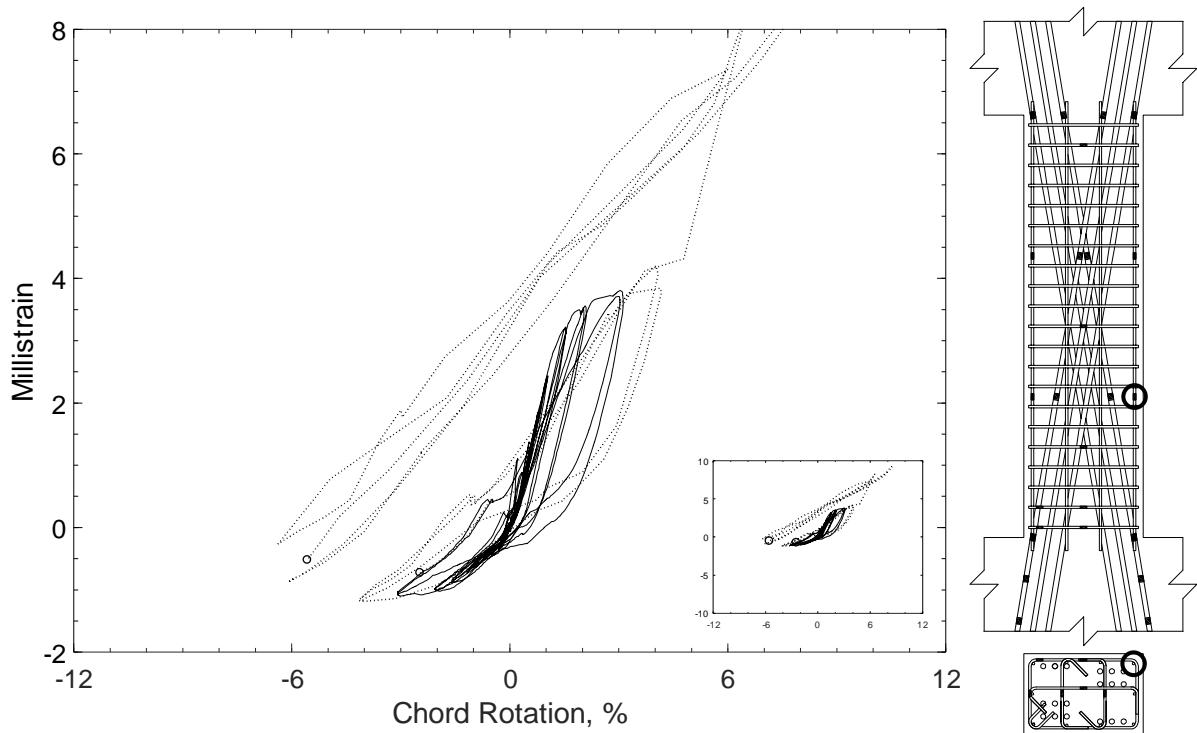


Figure 398 – Measured strain in parallel bar of D120-3.5, strain gauge H4

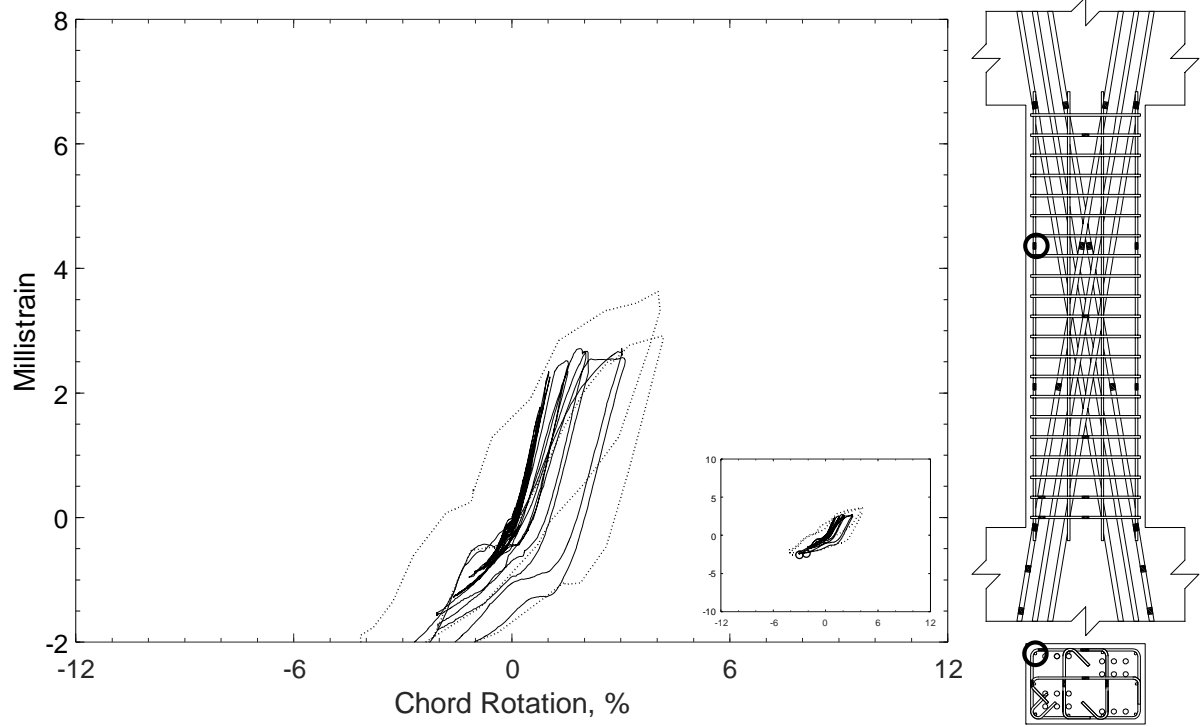


Figure 399 – Measured strain in parallel bar of D120-3.5, strain gauge H5

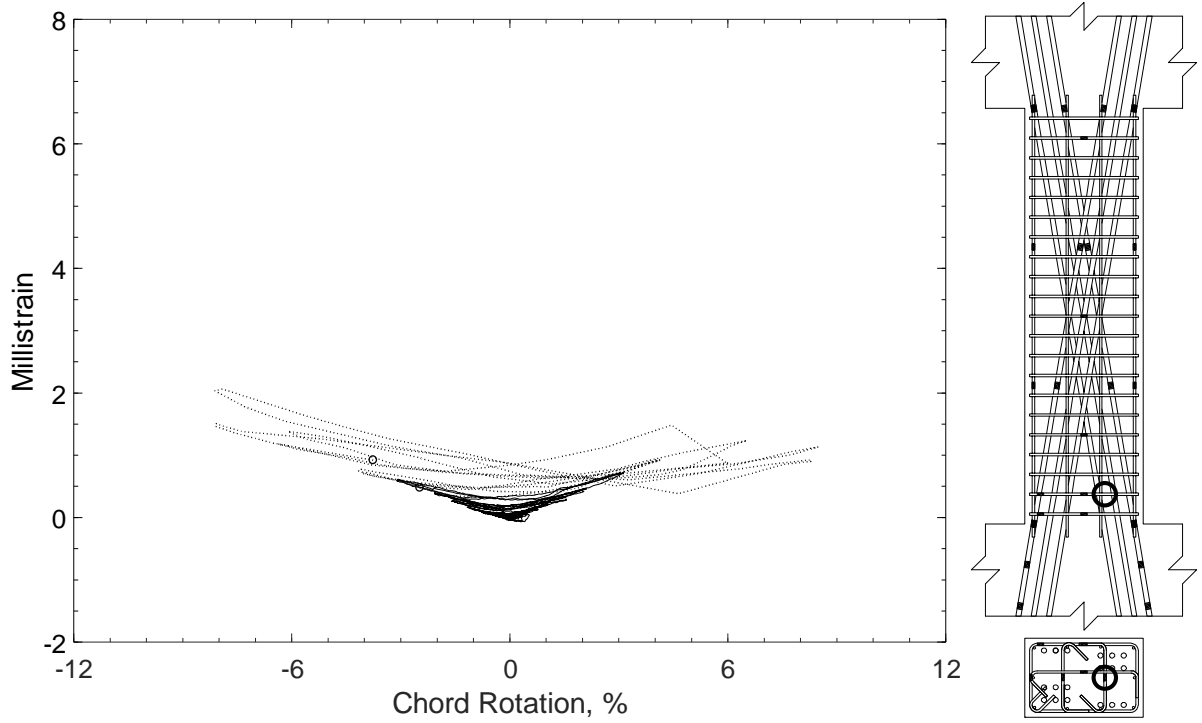


Figure 400 – Measured strain in crosstie of D120-3.5, strain gauge T1

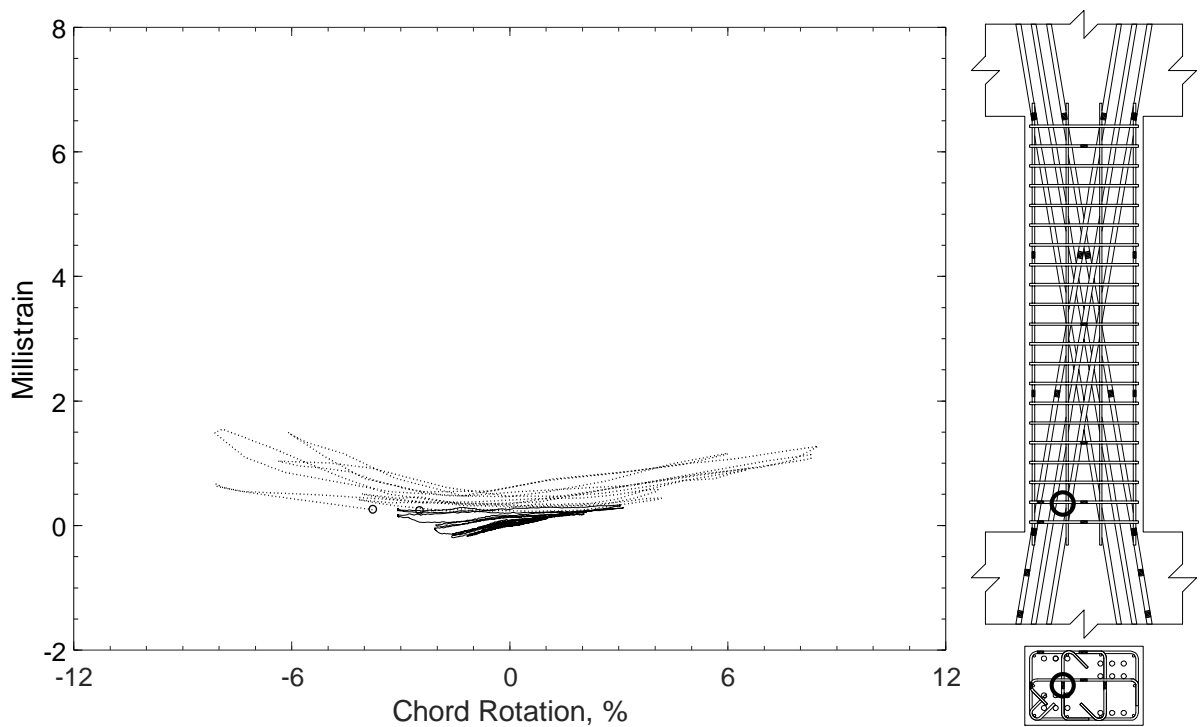


Figure 401 – Measured strain in crosstie of D120-3.5, strain gauge T2

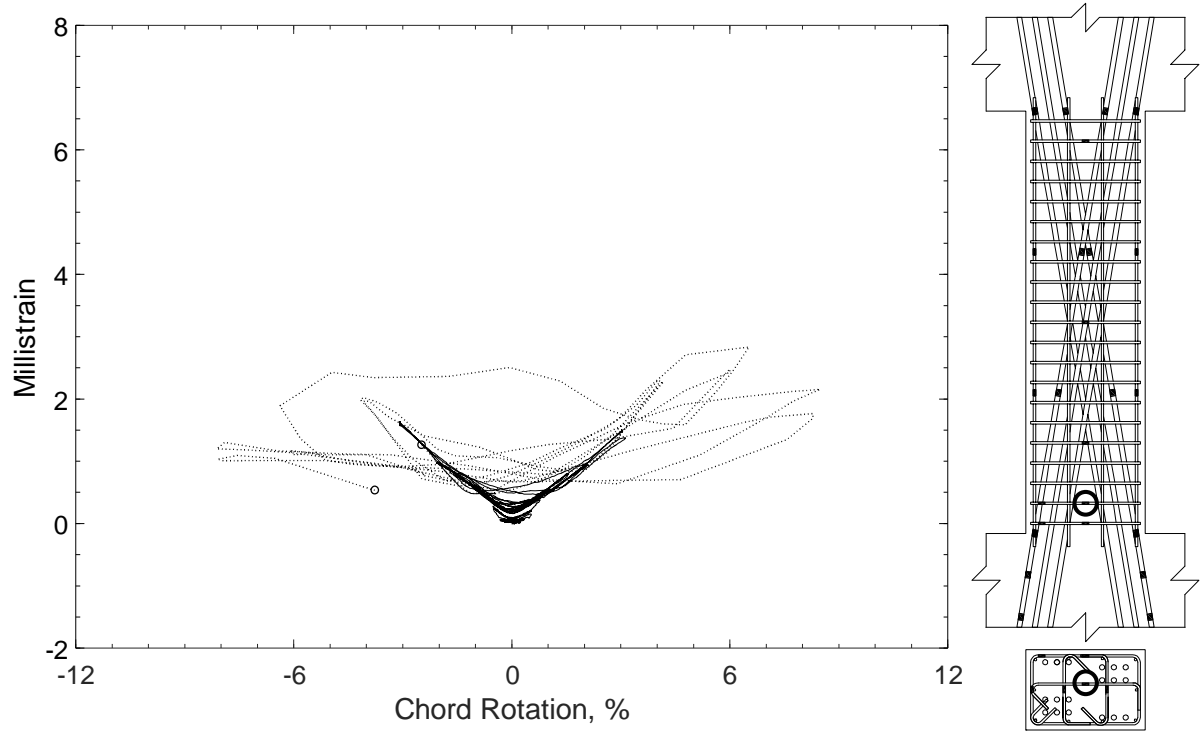


Figure 402 – Measured strain in crosstie of D120-3.5, strain gauge T3

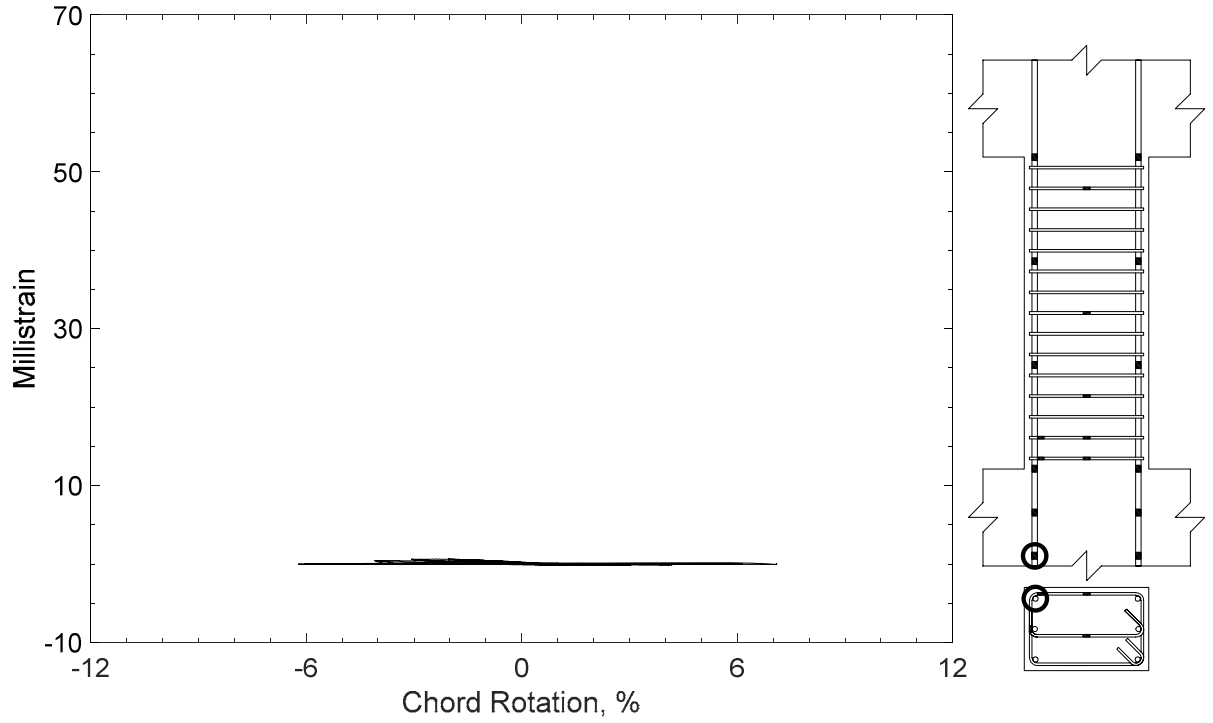


Figure 403 – Measured strain in parallel bar of P80-2.5, strain gauge P1

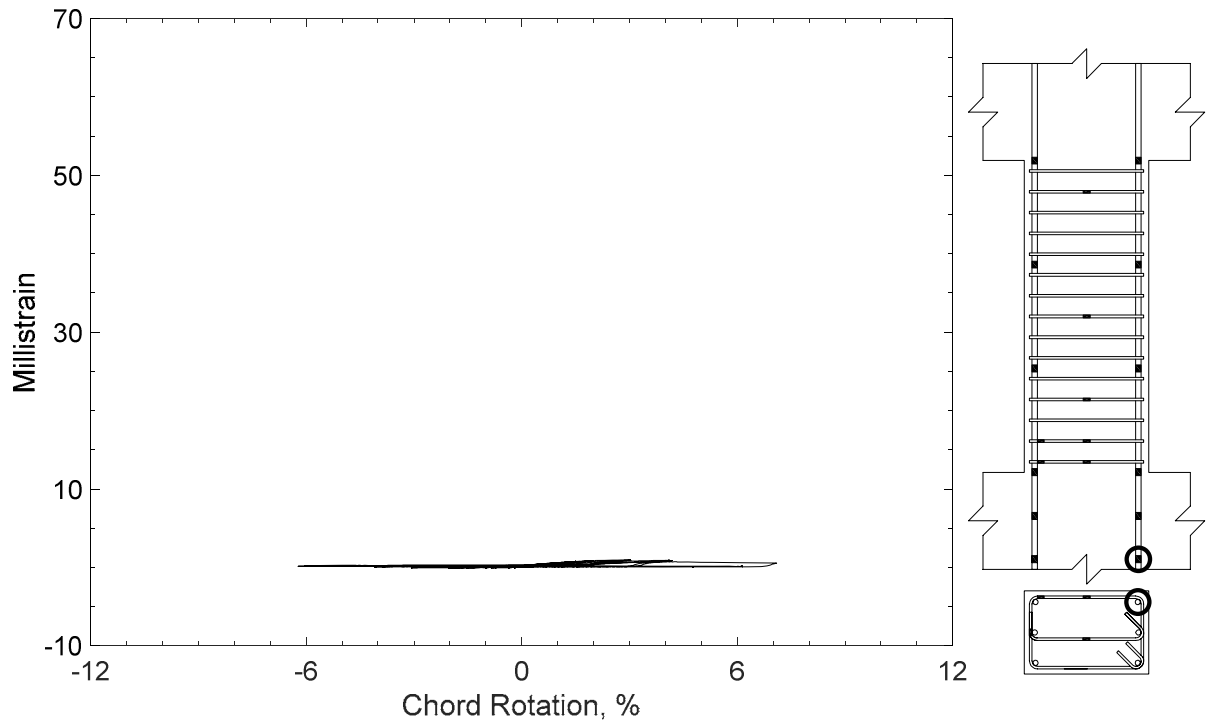


Figure 404 – Measured strain in parallel bar of P80-2.5, strain gauge P2

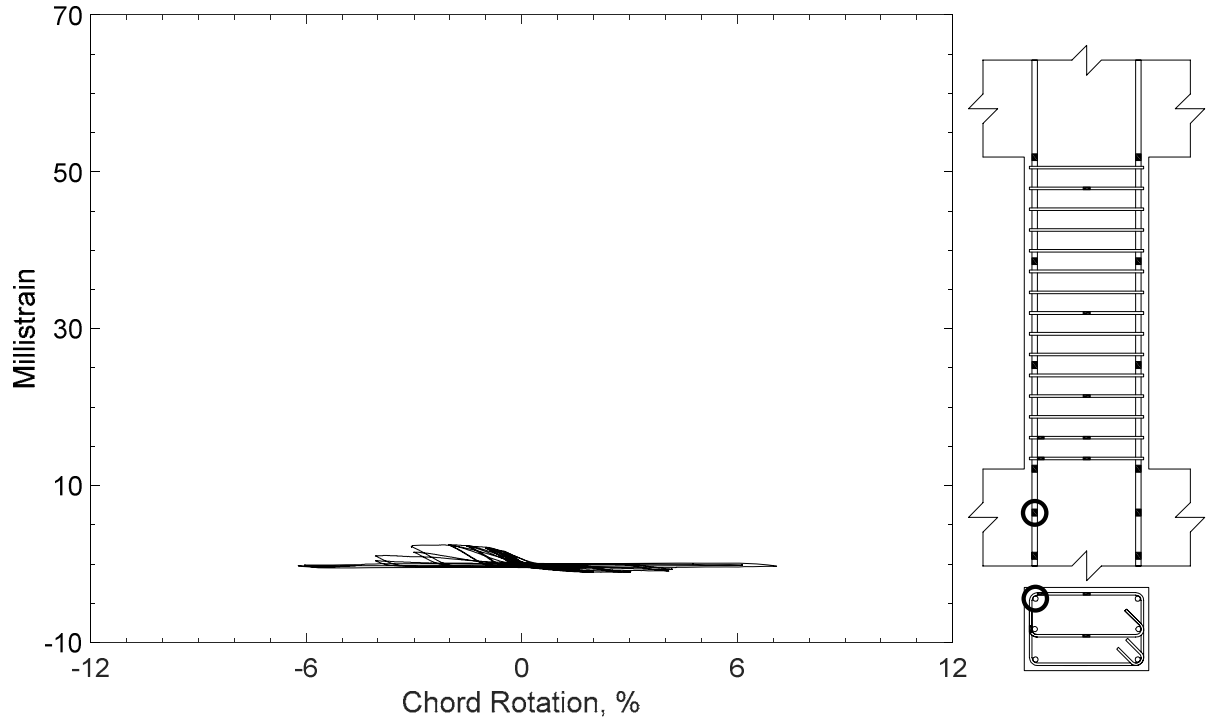


Figure 405 – Measured strain in parallel bar of P80-2.5, strain gauge P3

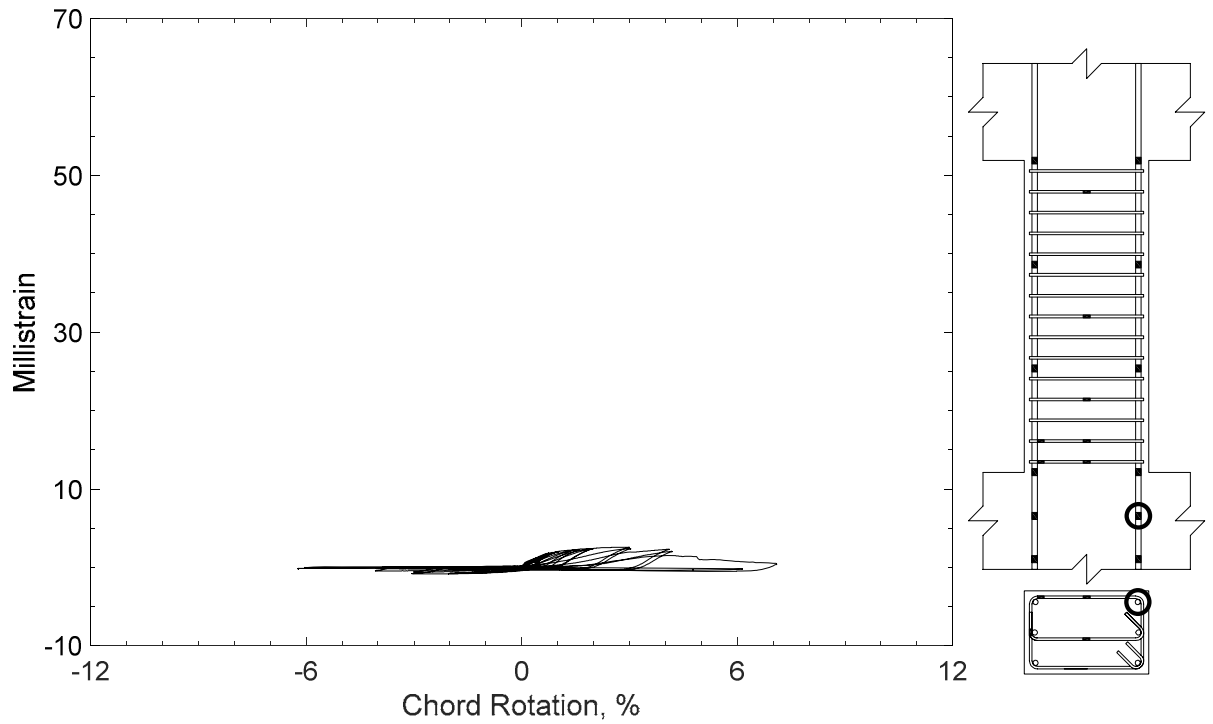


Figure 406 – Measured strain in parallel bar of P80-2.5, strain gauge P4

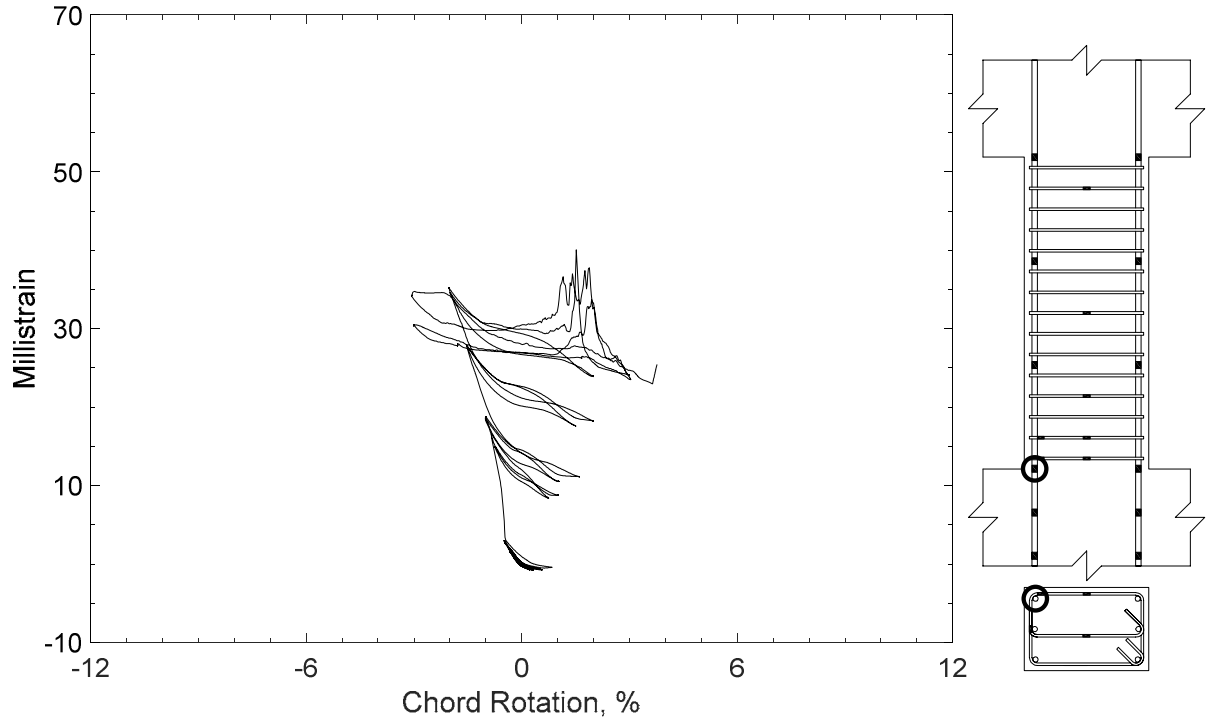


Figure 407 – Measured strain in parallel bar of P80-2.5, strain gauge P5

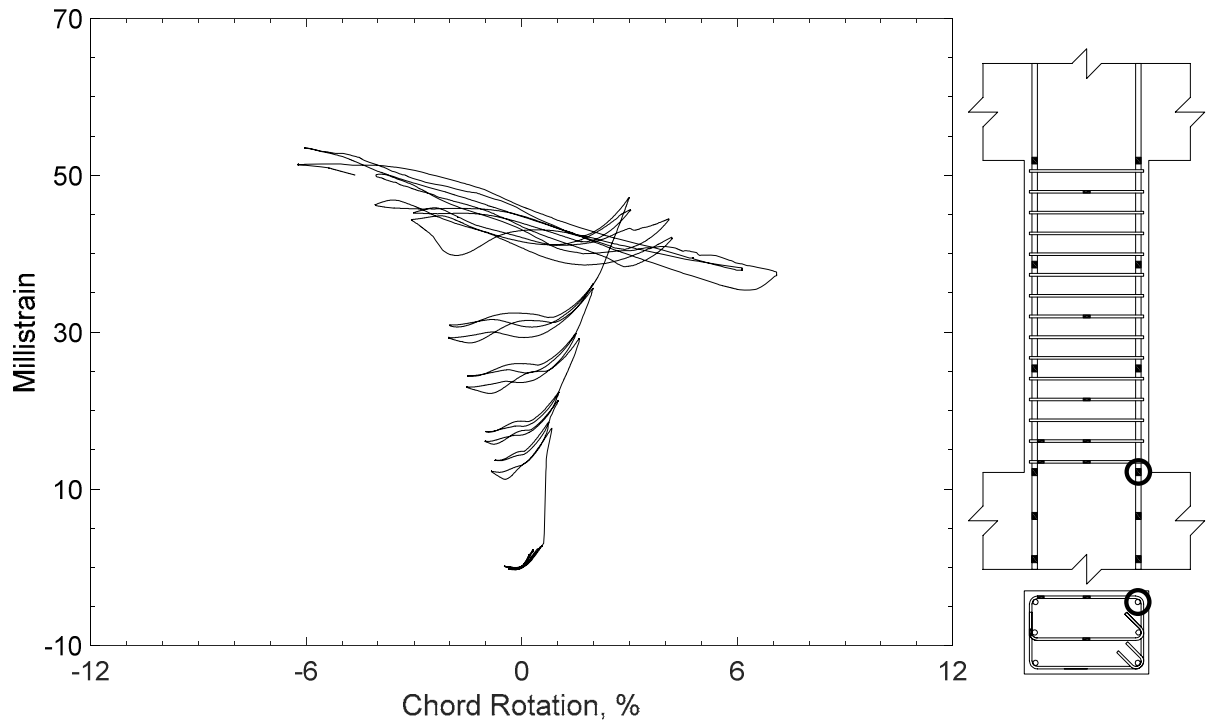


Figure 408 – Measured strain in parallel bar of P80-2.5, strain gauge P6

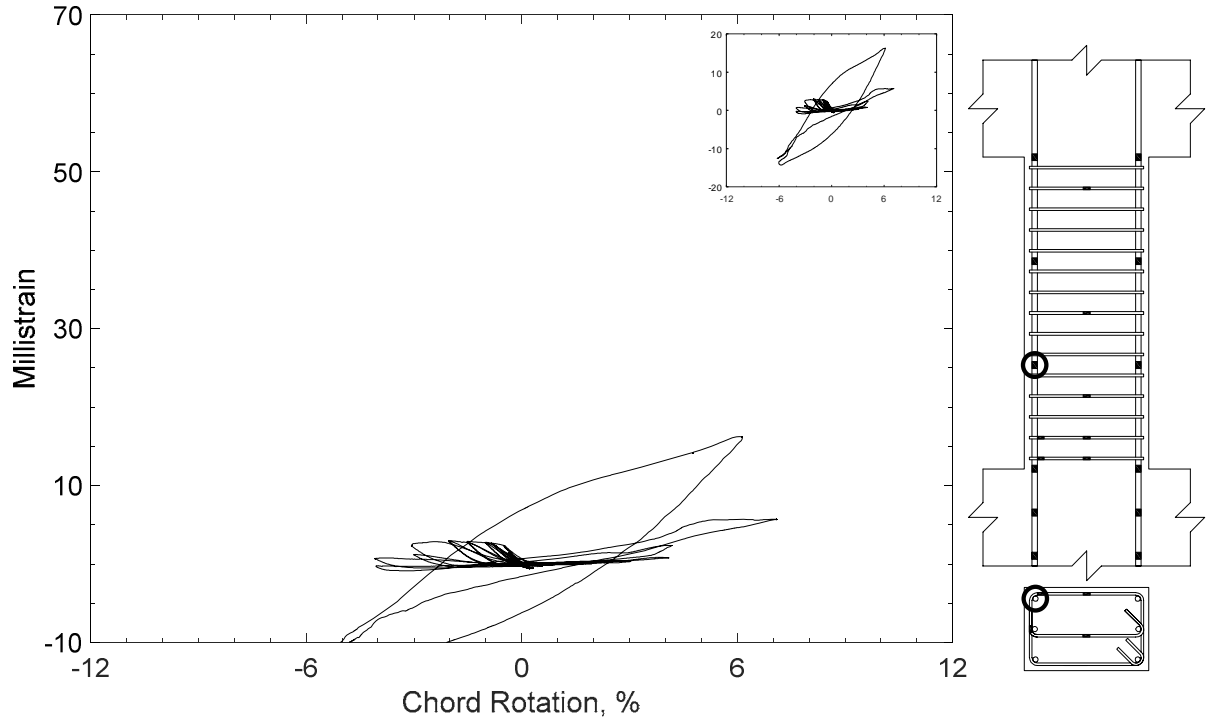


Figure 409 – Measured strain in parallel bar of P80-2.5, strain gauge P7

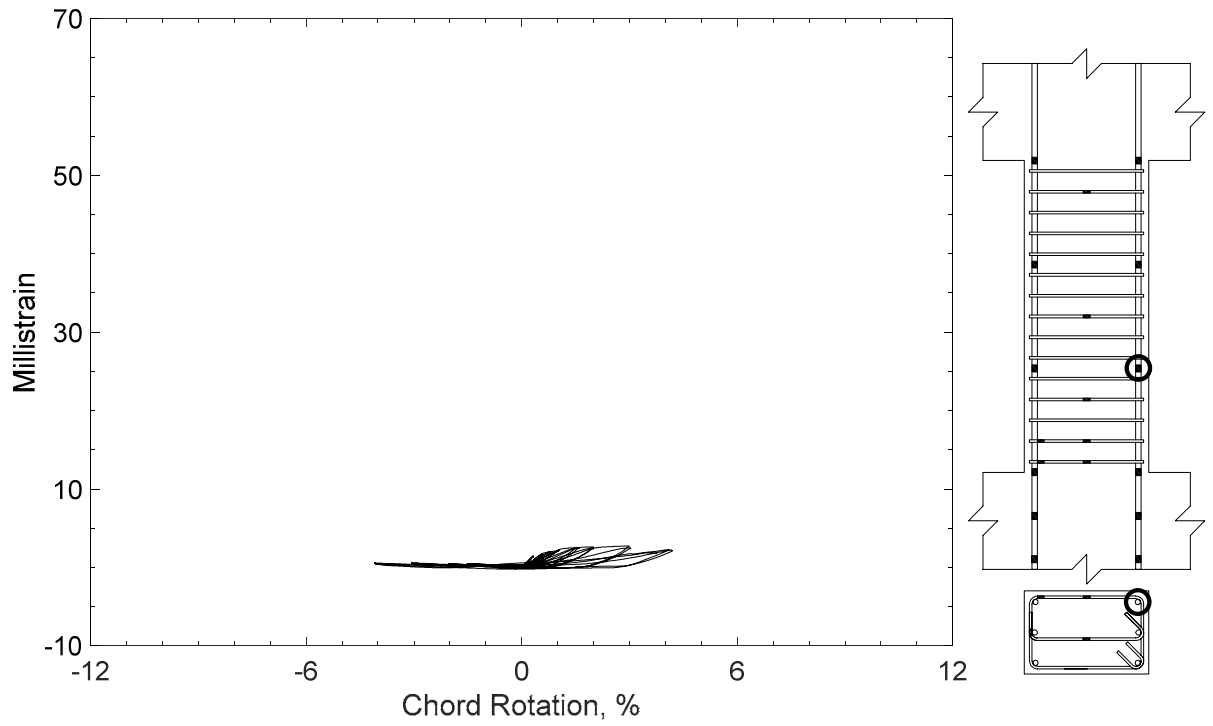


Figure 410 – Measured strain in parallel bar of P80-2.5, strain gauge P8

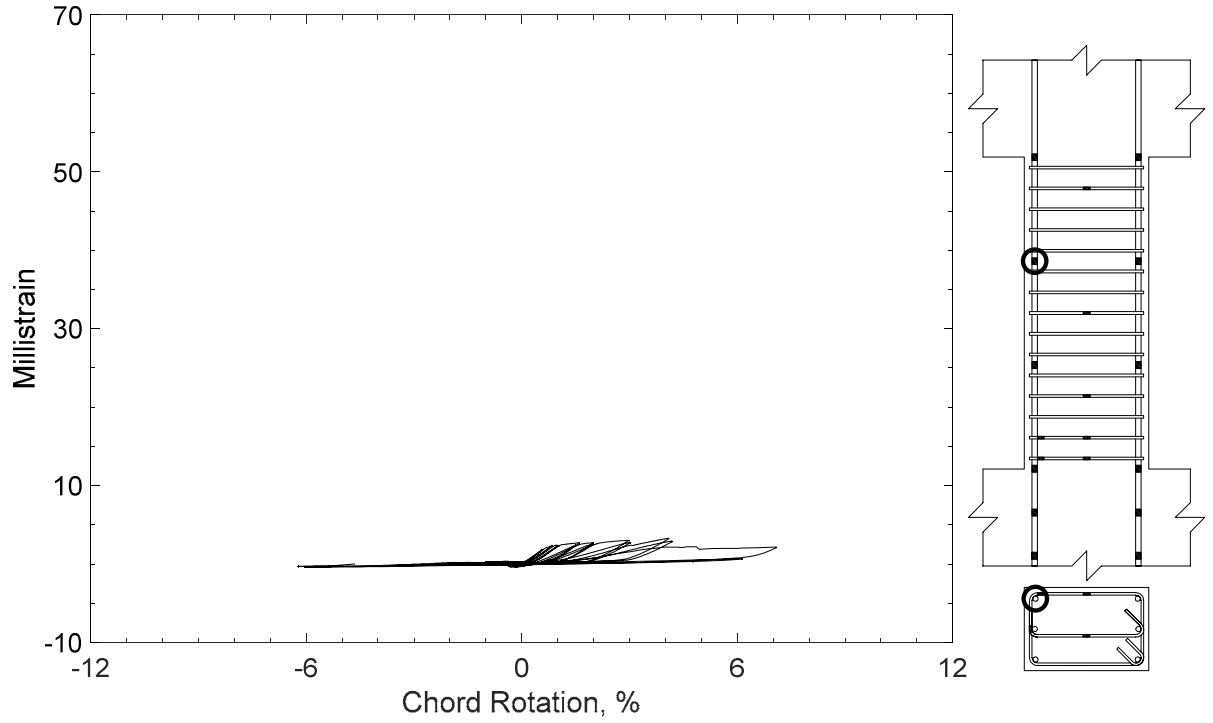


Figure 411 – Measured strain in parallel bar of P80-2.5, strain gauge P9

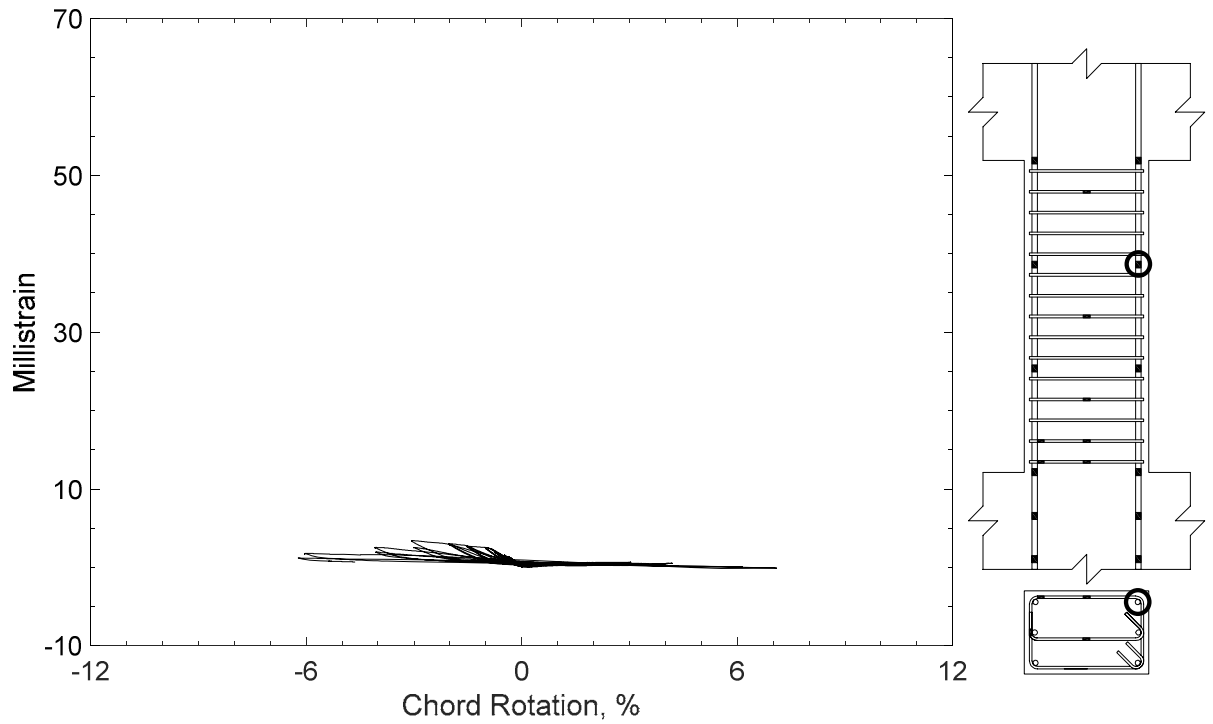


Figure 412 – Measured strain in parallel bar of P80-2.5, strain gauge P10

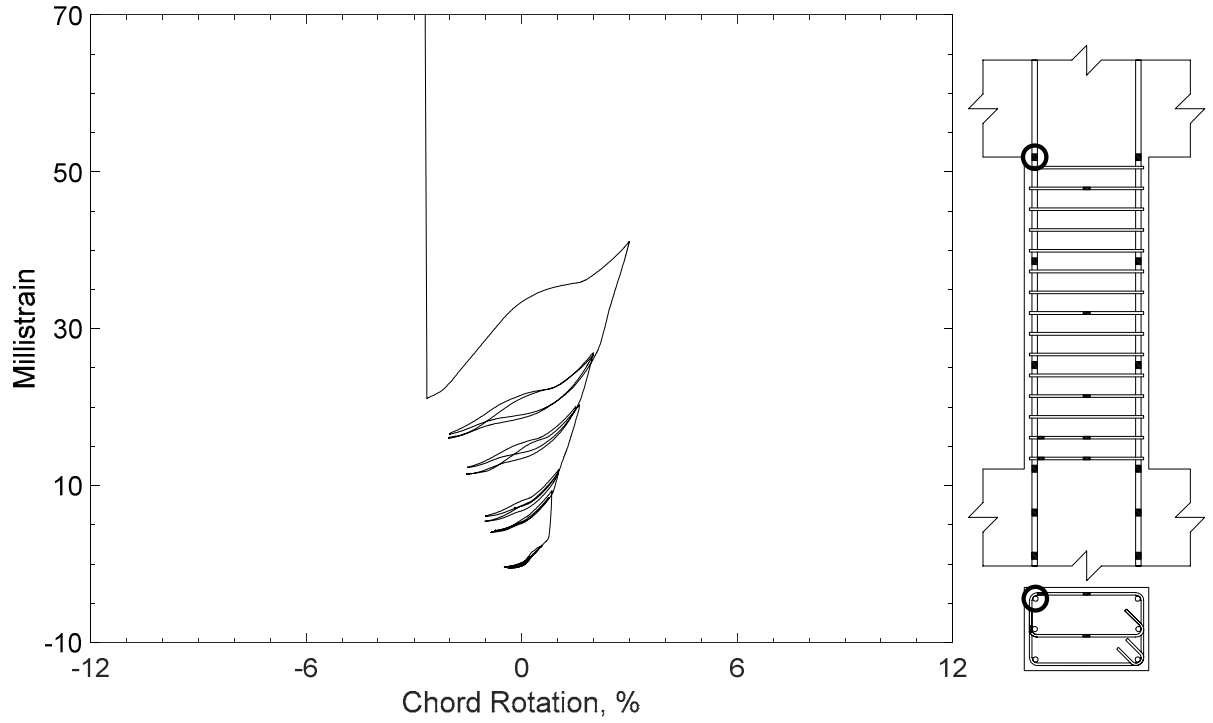


Figure 413 – Measured strain in parallel bar of P80-2.5, strain gauge P11

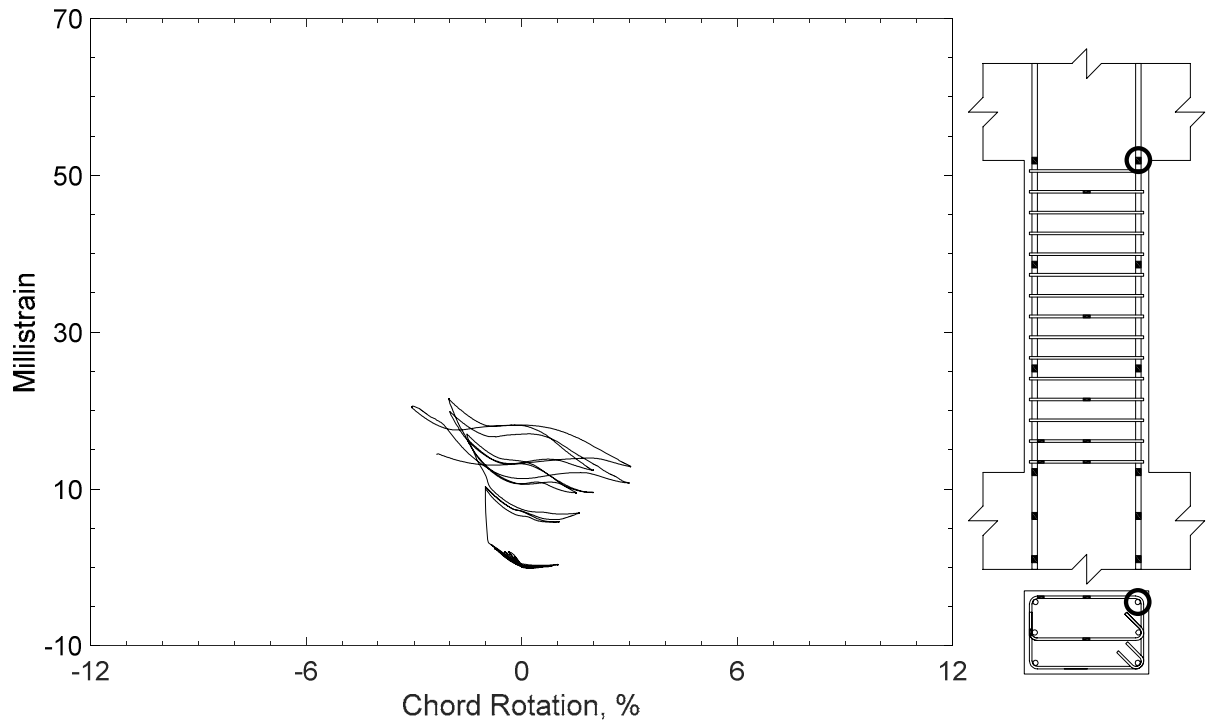


Figure 414 – Measured strain in parallel bar of P80-2.5, strain gauge P12

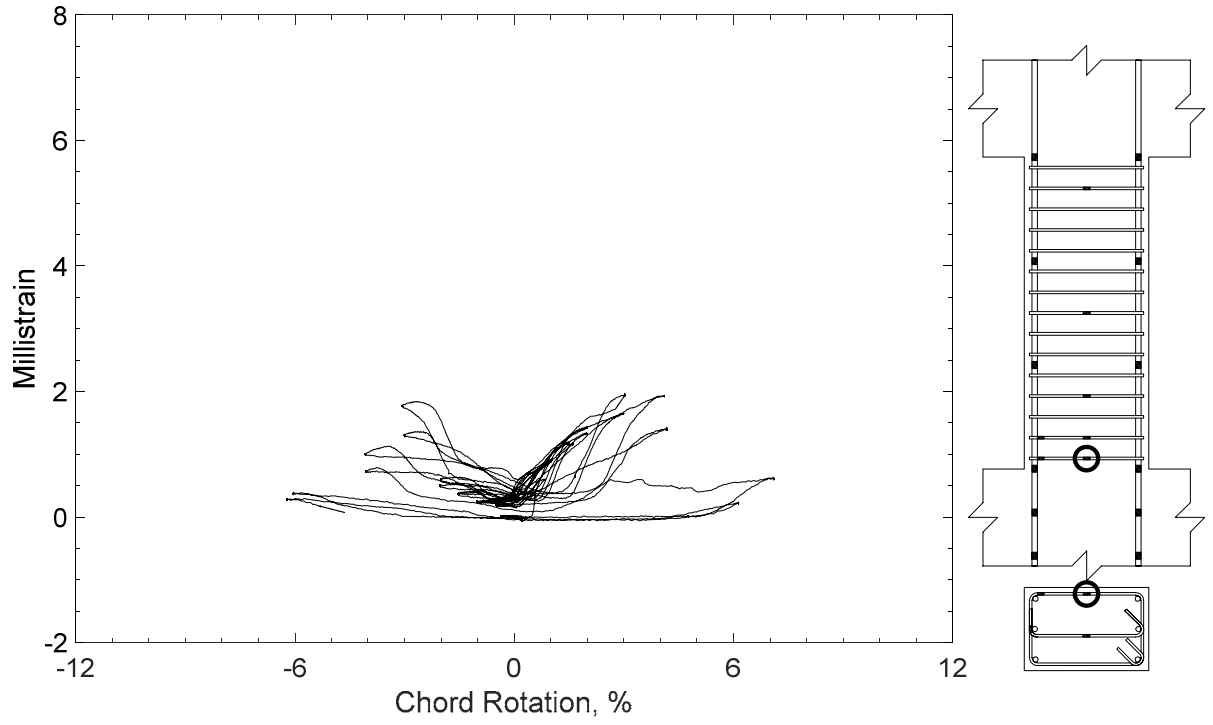


Figure 415 – Measured strain in closed stirrup of P80-2.5, strain gauge S1

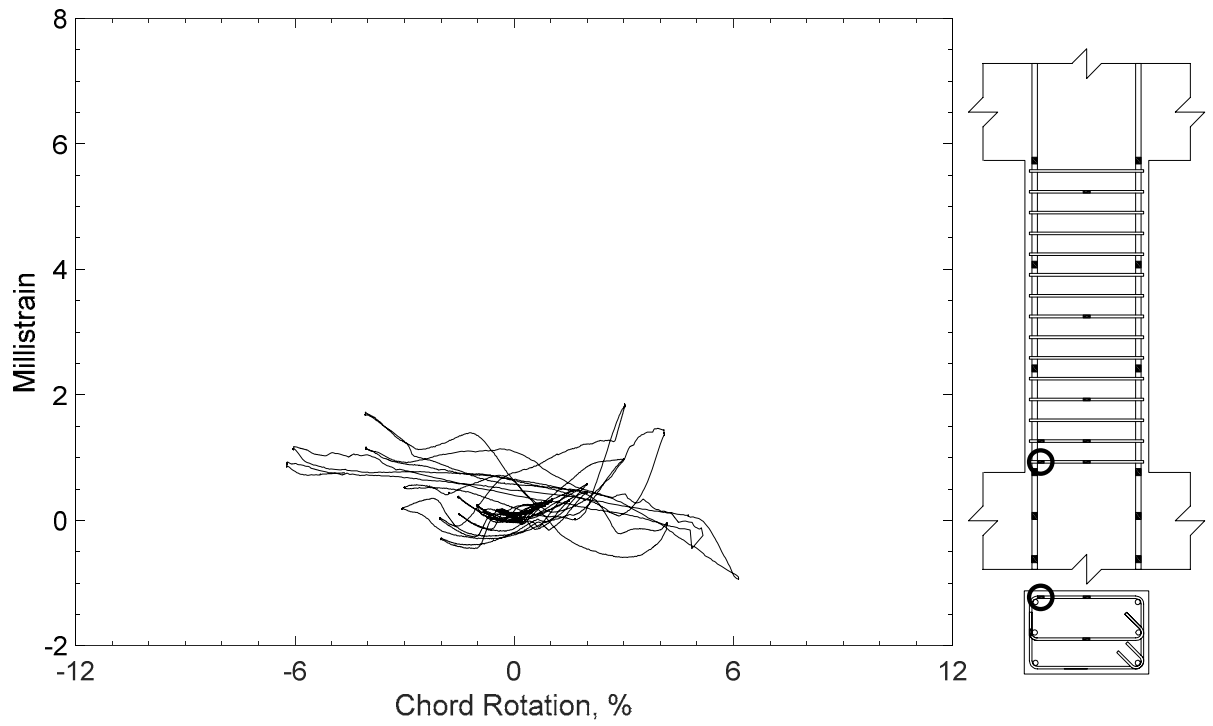


Figure 416 – Measured strain in closed stirrup of P80-2.5, strain gauge S2

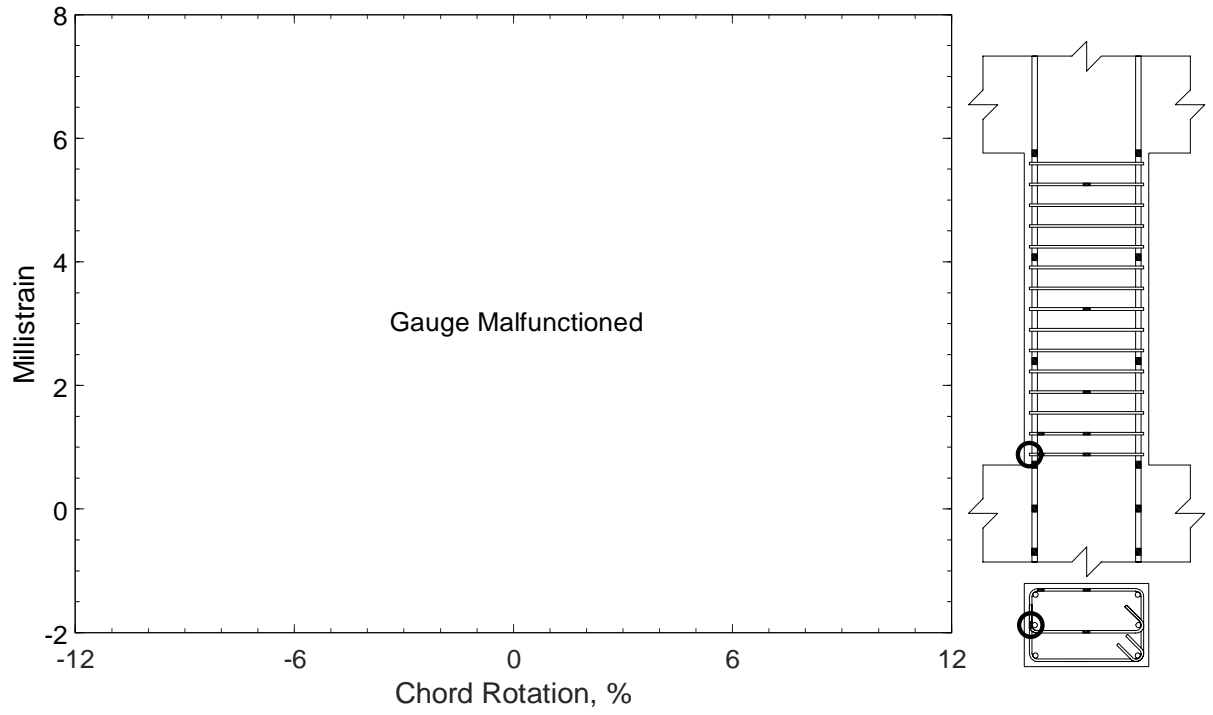


Figure 417 – Measured strain in closed stirrup of P80-2.5, strain gauge S3

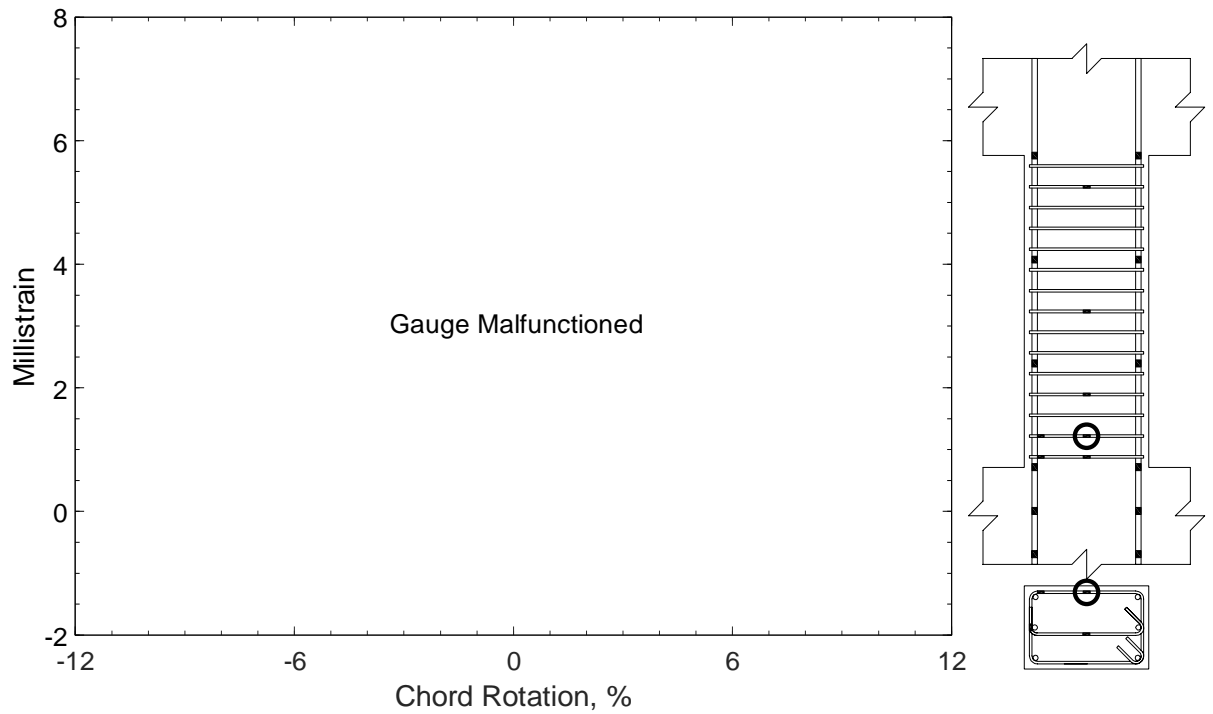


Figure 418 – Measured strain in closed stirrup of P80-2.5, strain gauge S4

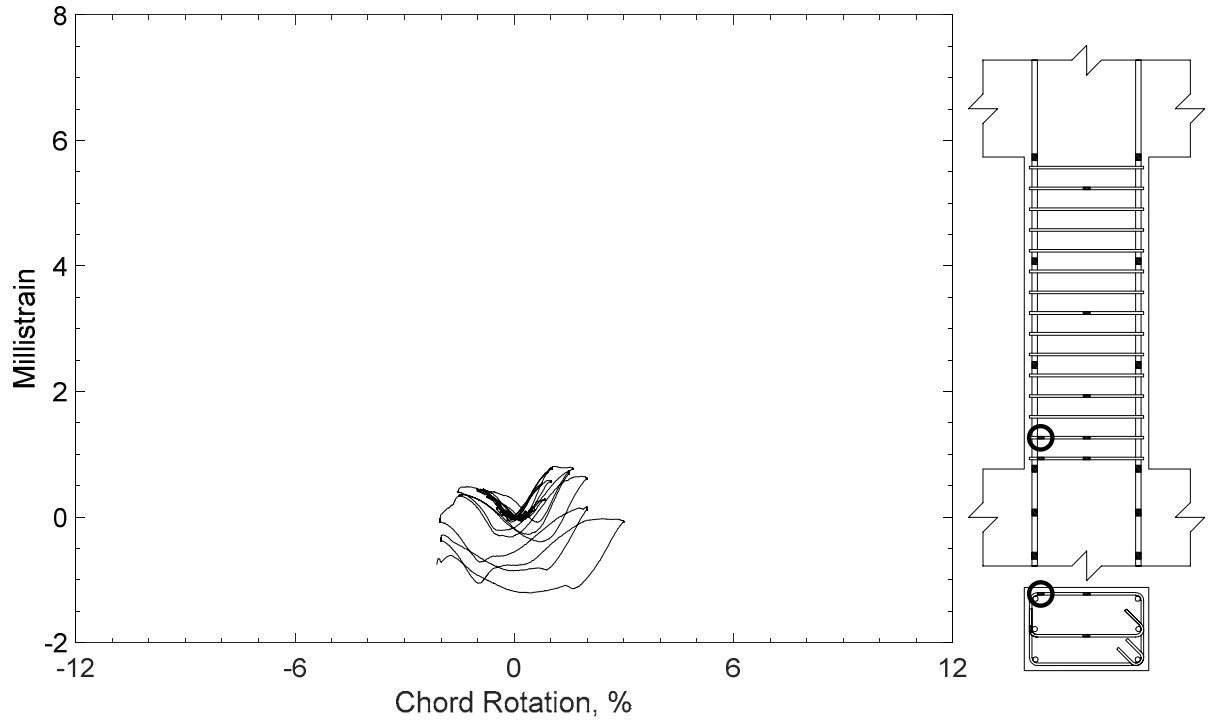


Figure 419 – Measured strain in closed stirrup of P80-2.5, strain gauge S5

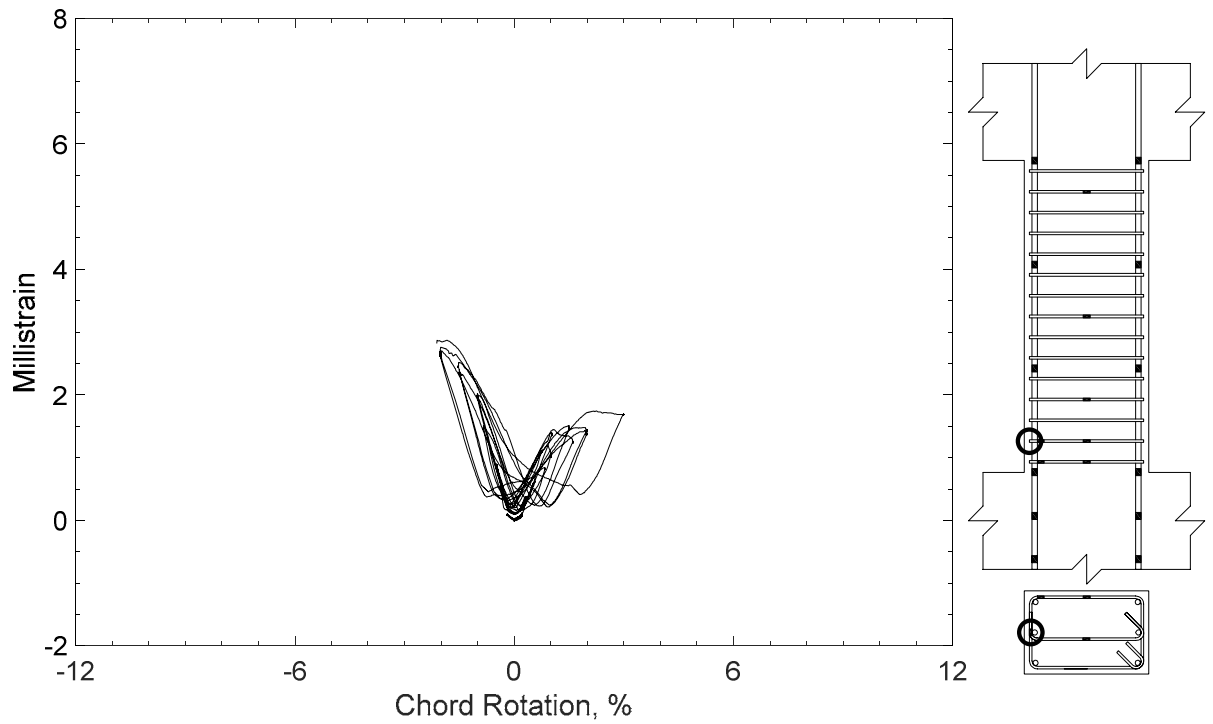


Figure 420 – Measured strain in closed stirrup of P80-2.5, strain gauge S6

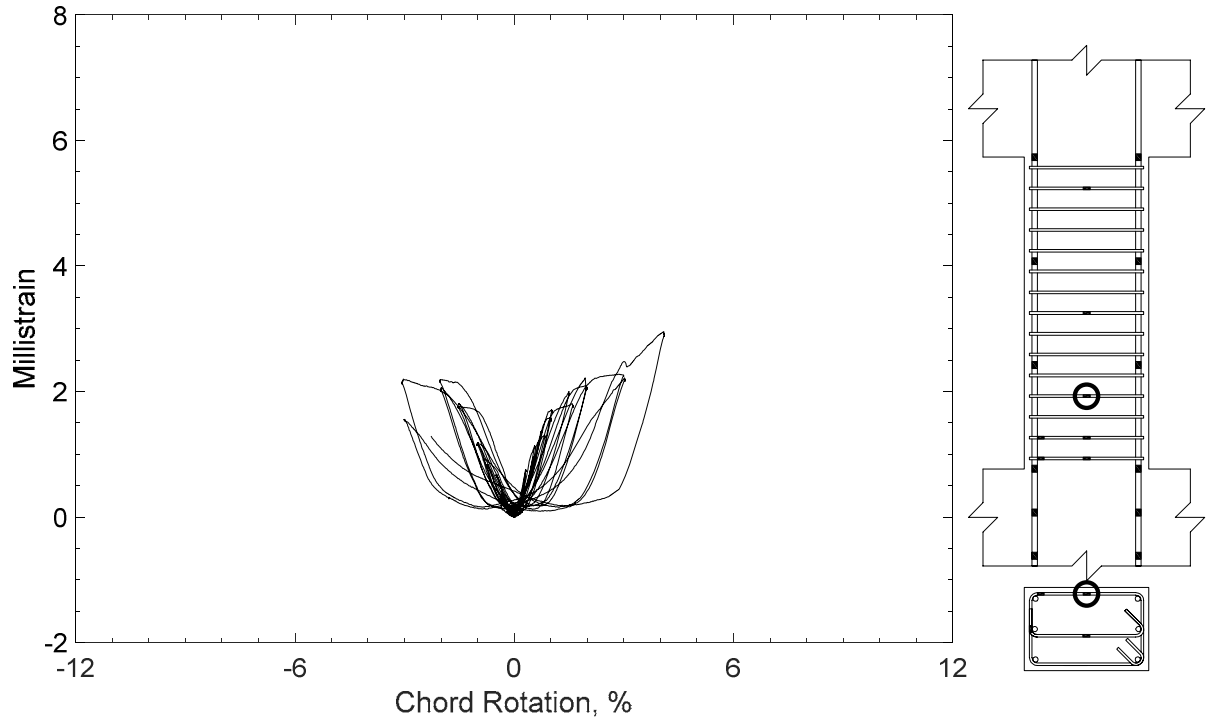


Figure 421 – Measured strain in closed stirrup of P80-2.5, strain gauge S7

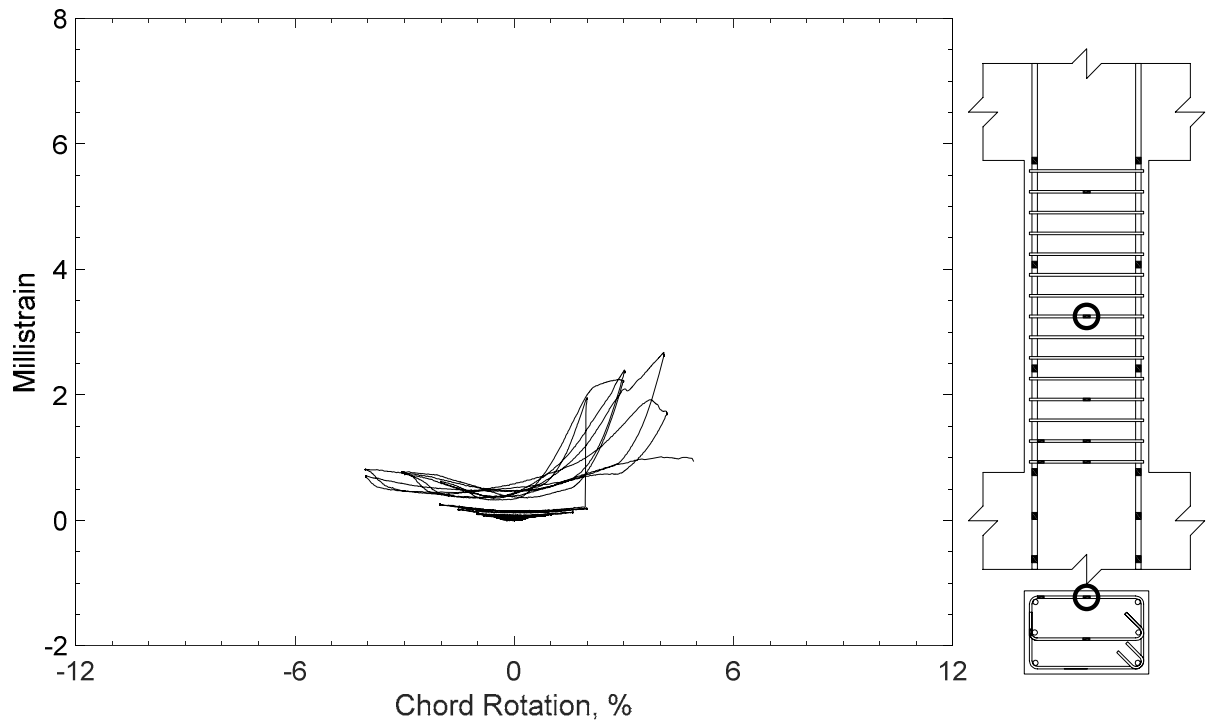


Figure 422 – Measured strain in closed stirrup of P80-2.5, strain gauge S8

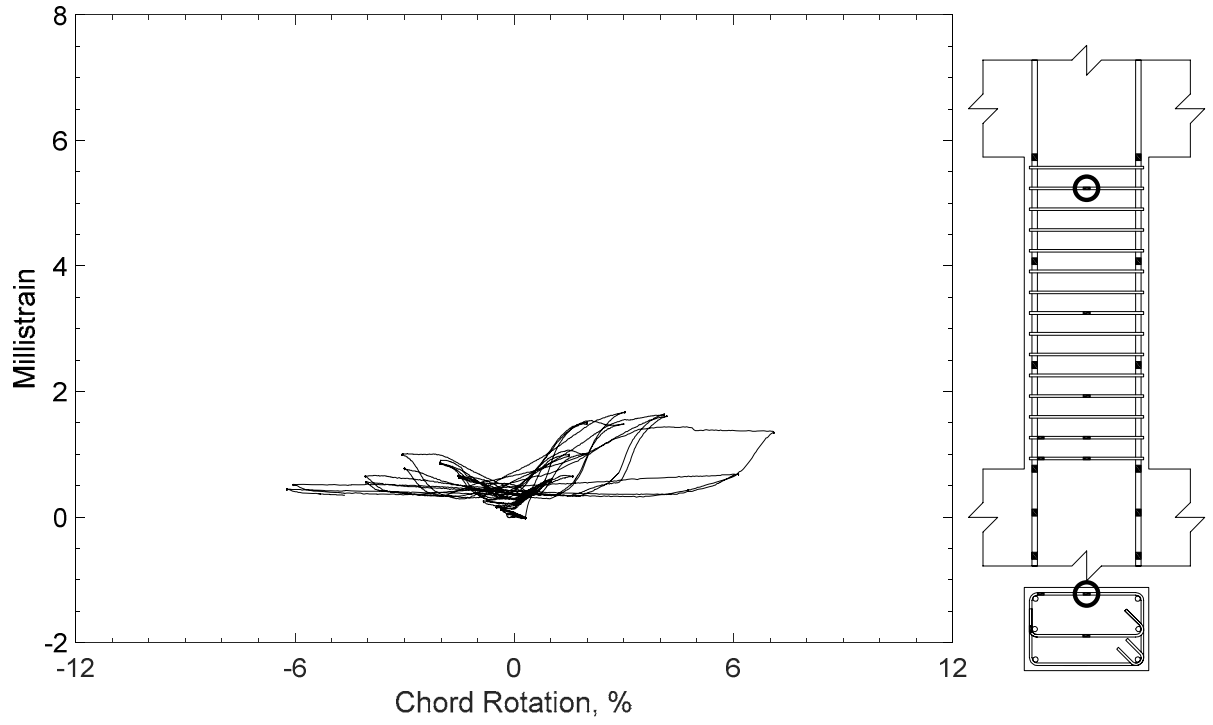


Figure 423 – Measured strain in closed stirrup of P80-2.5, strain gauge S9

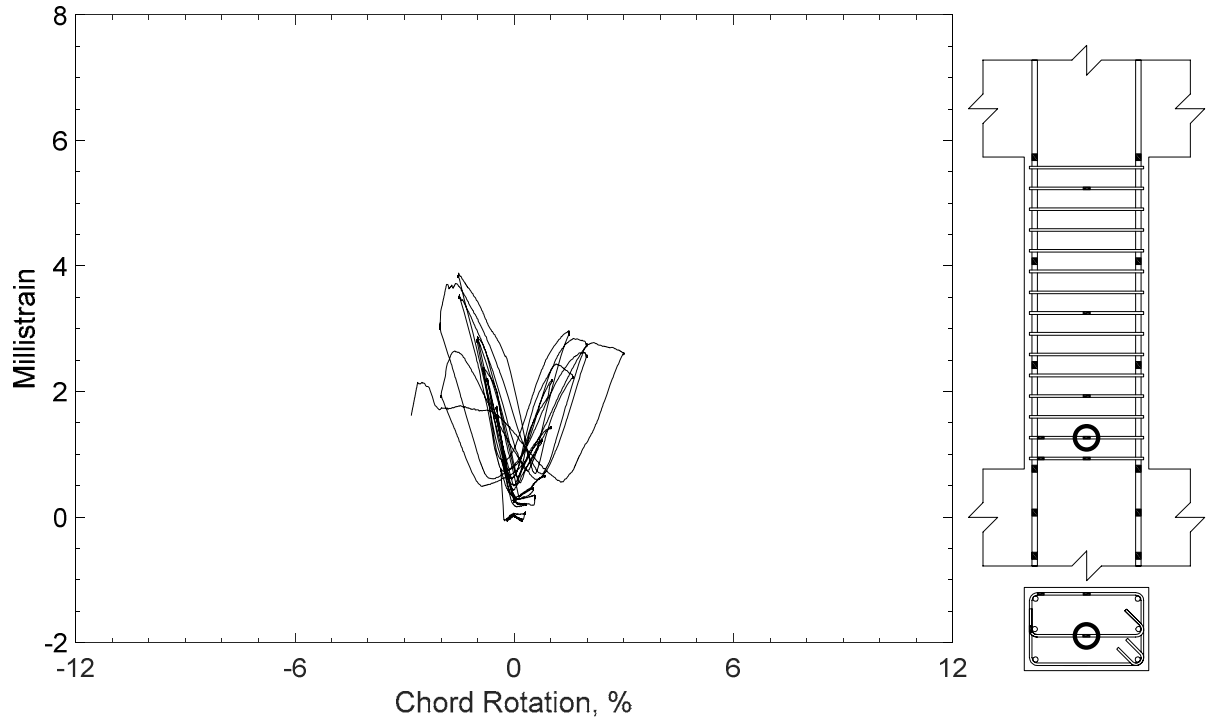


Figure 424 – Measured strain in cross-tie of P80-2.5, strain gauge T1

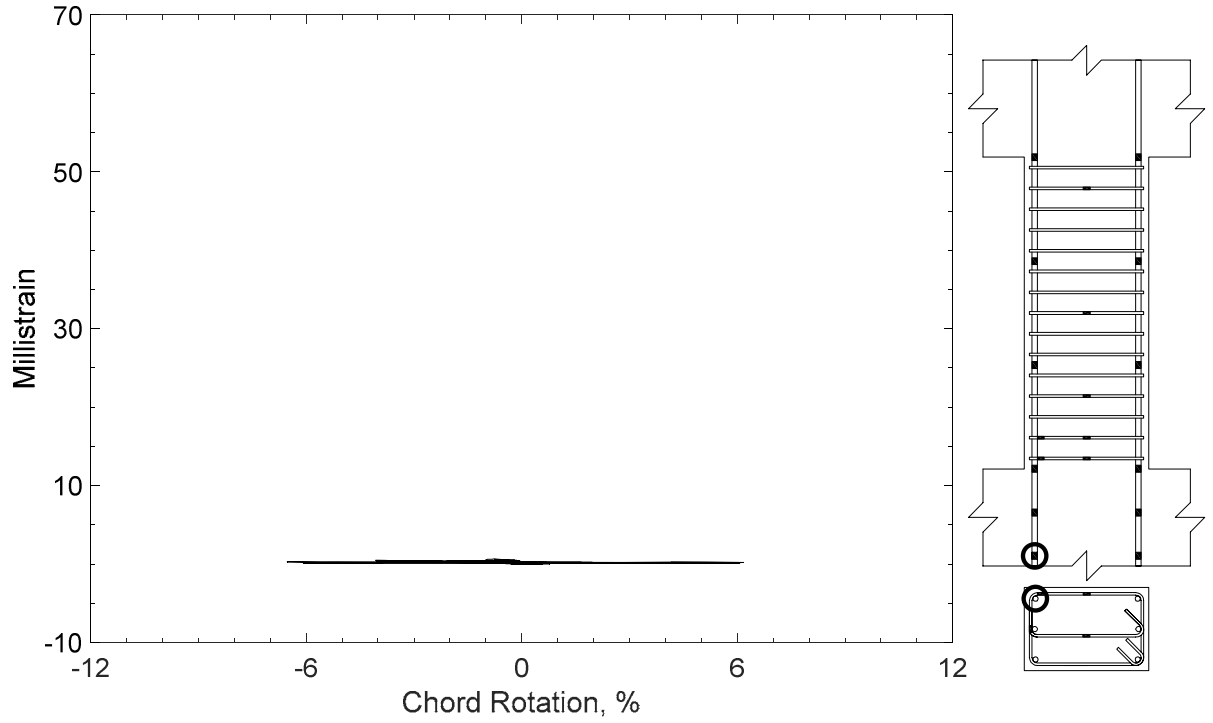


Figure 425 – Measured strain in parallel bar of P100-2.5, strain gauge P1

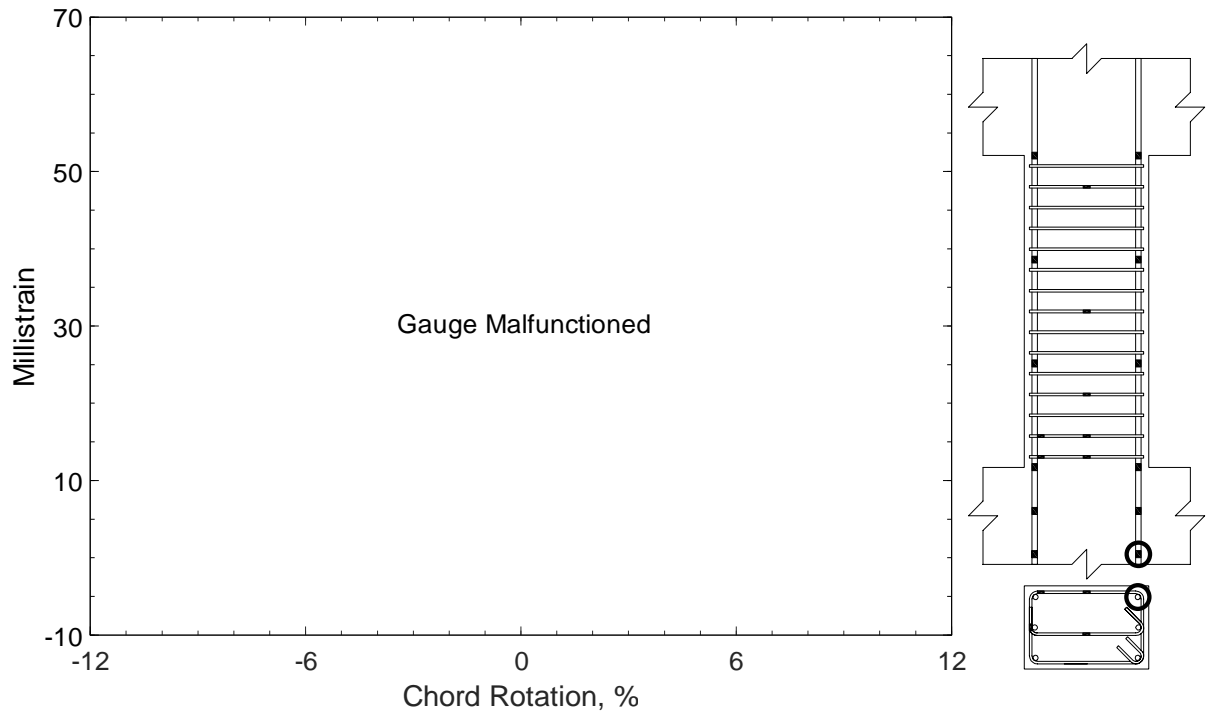


Figure 426 – Measured strain in parallel bar of P100-2.5, strain gauge P2

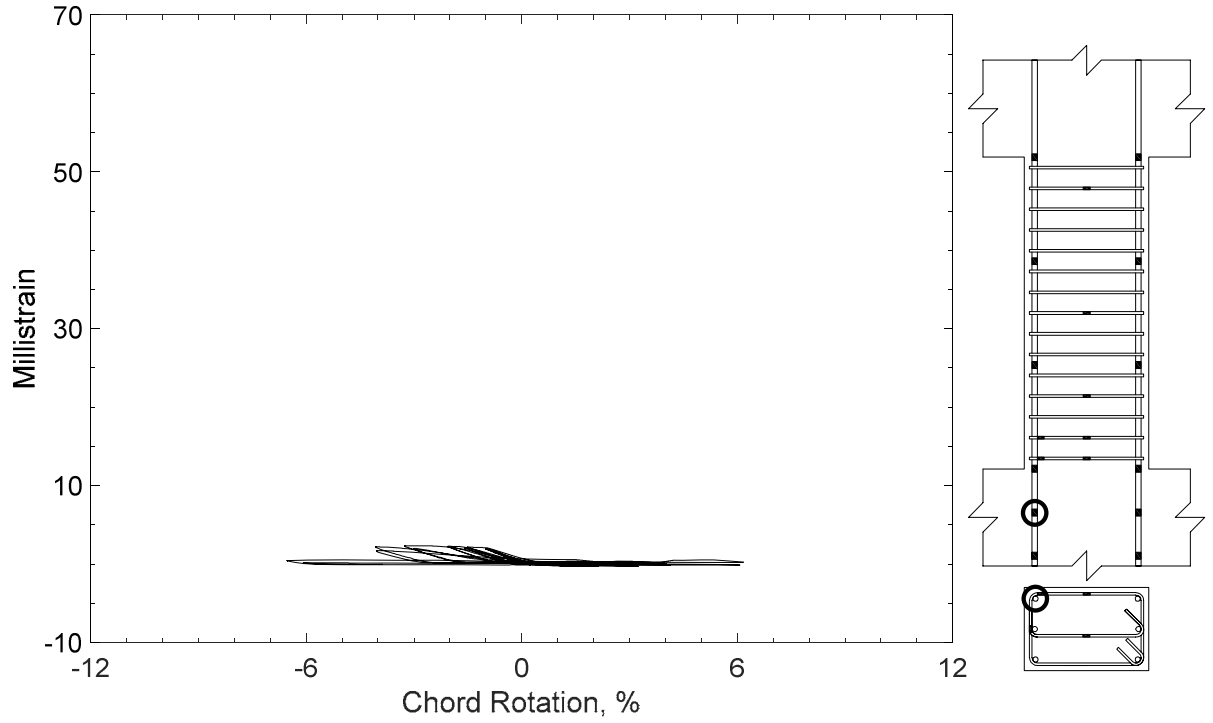


Figure 427 – Measured strain in parallel bar of P100-2.5, strain gauge P3

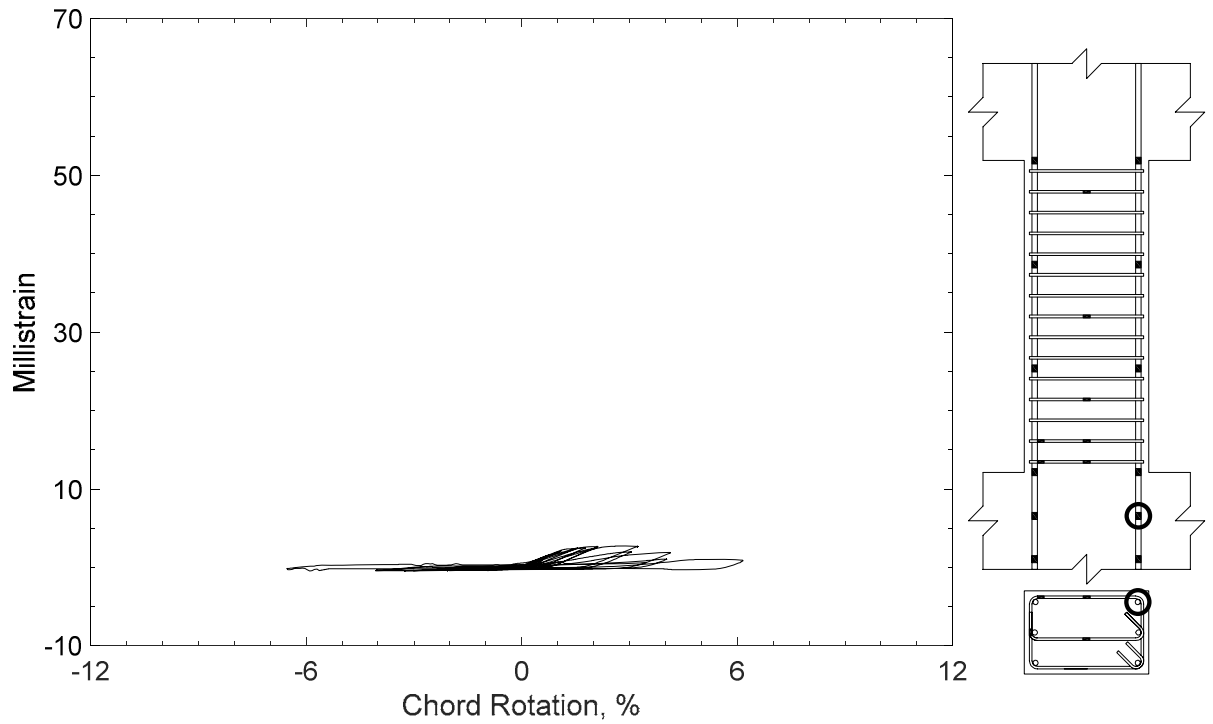


Figure 428 – Measured strain in parallel bar of P100-2.5, strain gauge P4

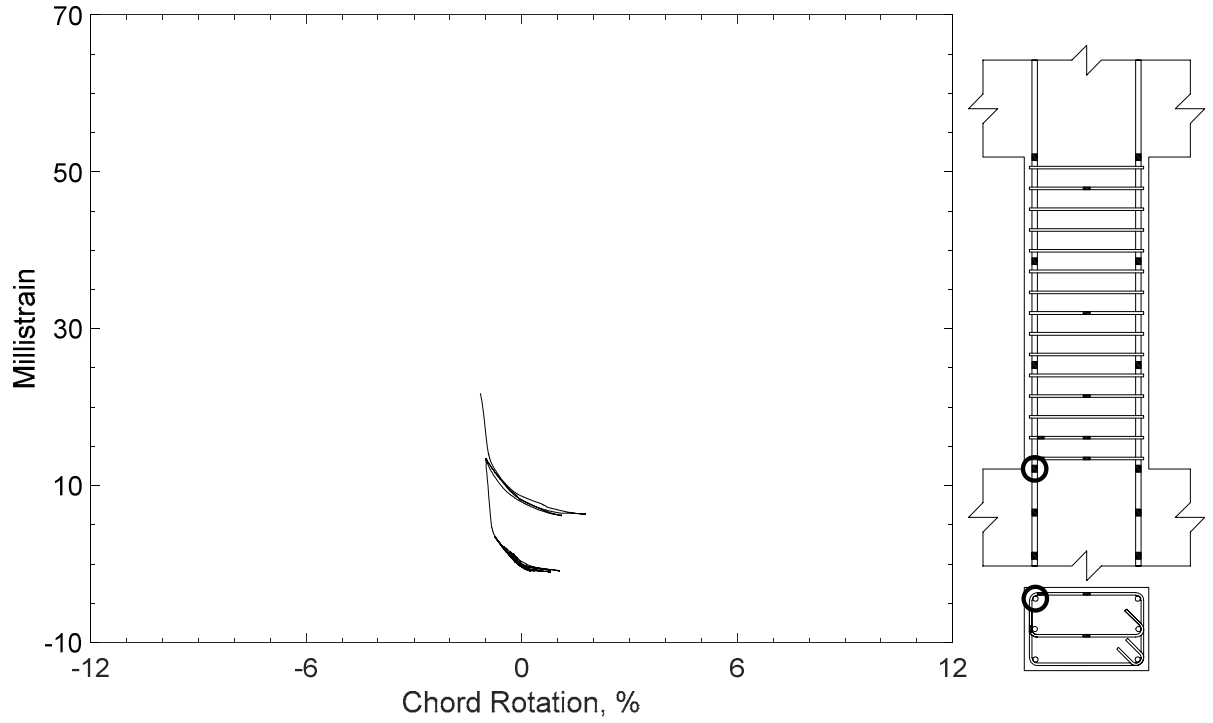


Figure 429 – Measured strain in parallel bar of P100-2.5, strain gauge P5

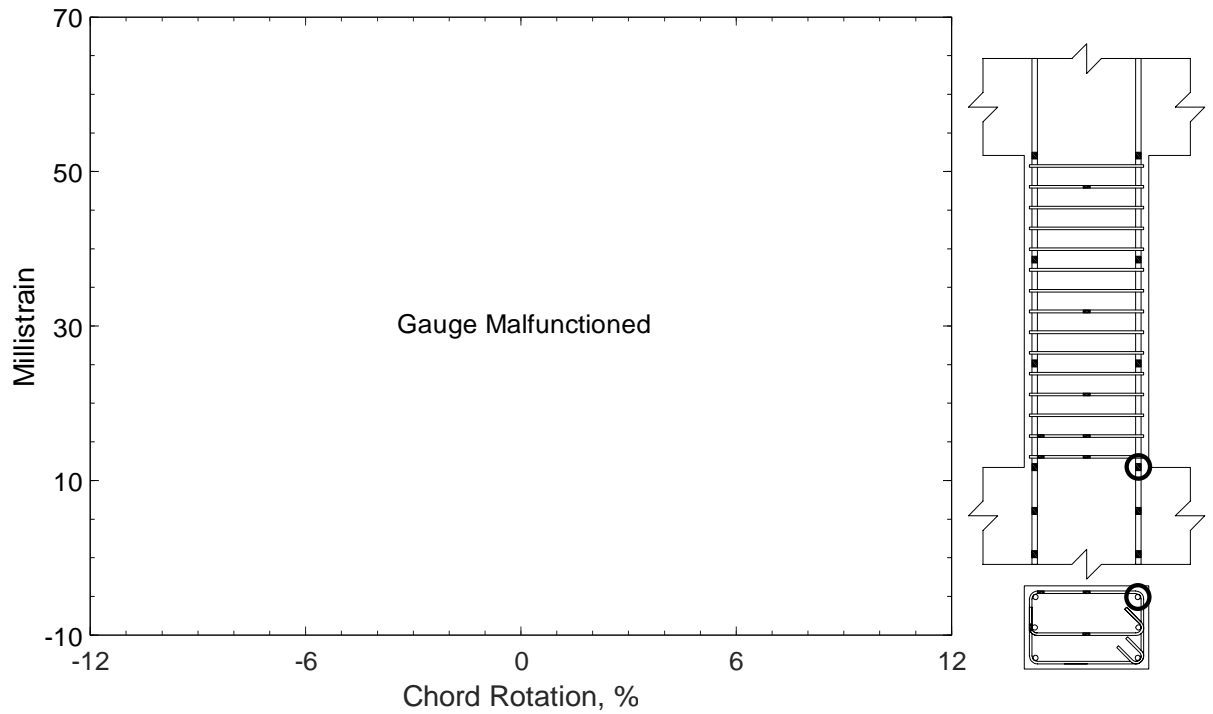


Figure 430 – Measured strain in parallel bar of P100-2.5, strain gauge P6

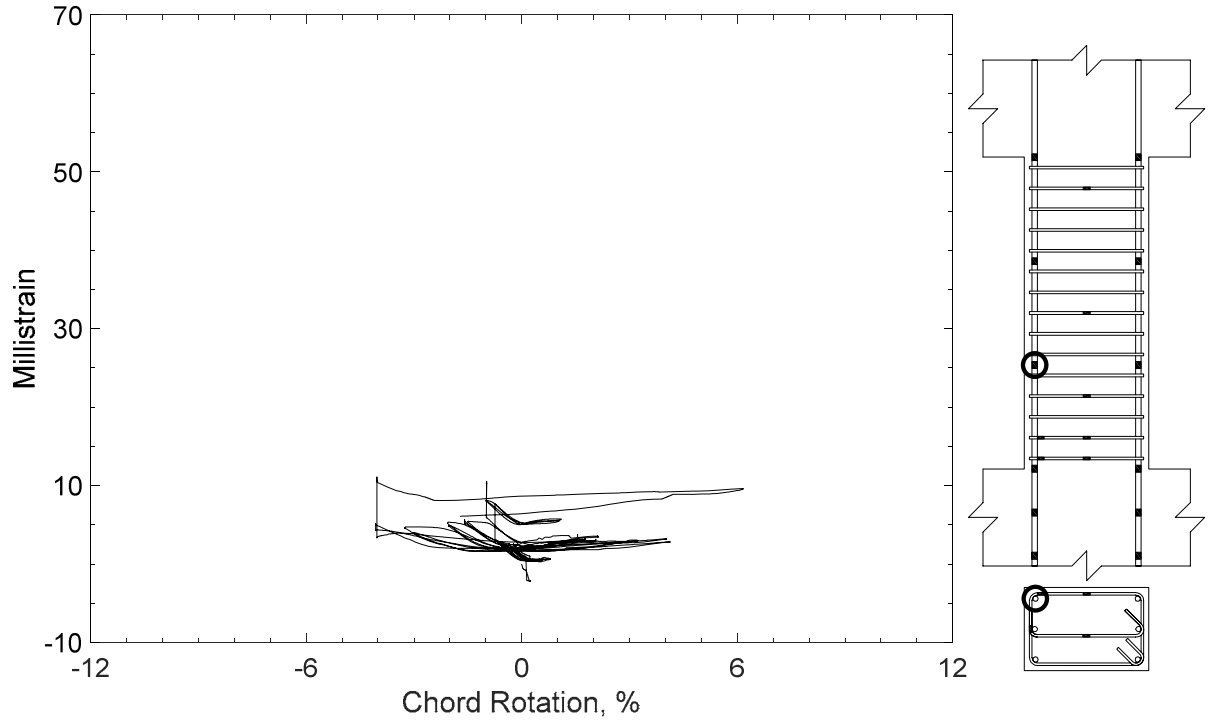


Figure 431 – Measured strain in parallel bar of P100-2.5, strain gauge P7

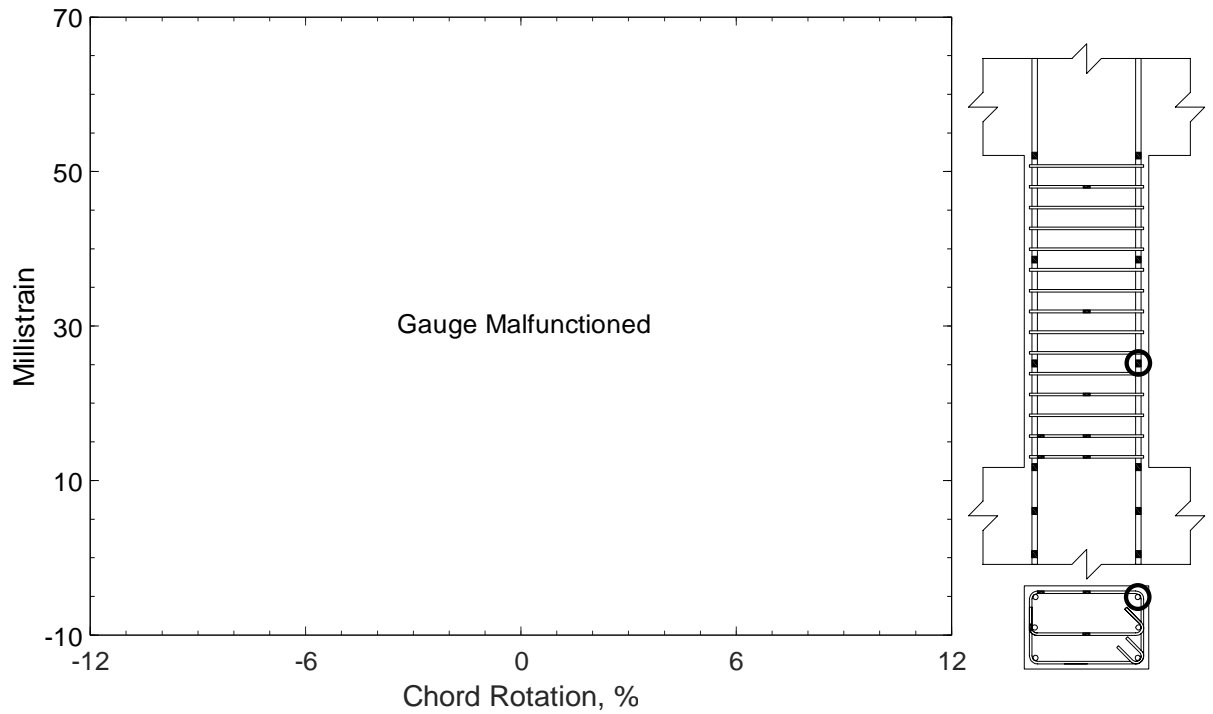


Figure 432 – Measured strain in parallel bar of P100-2.5, strain gauge P8

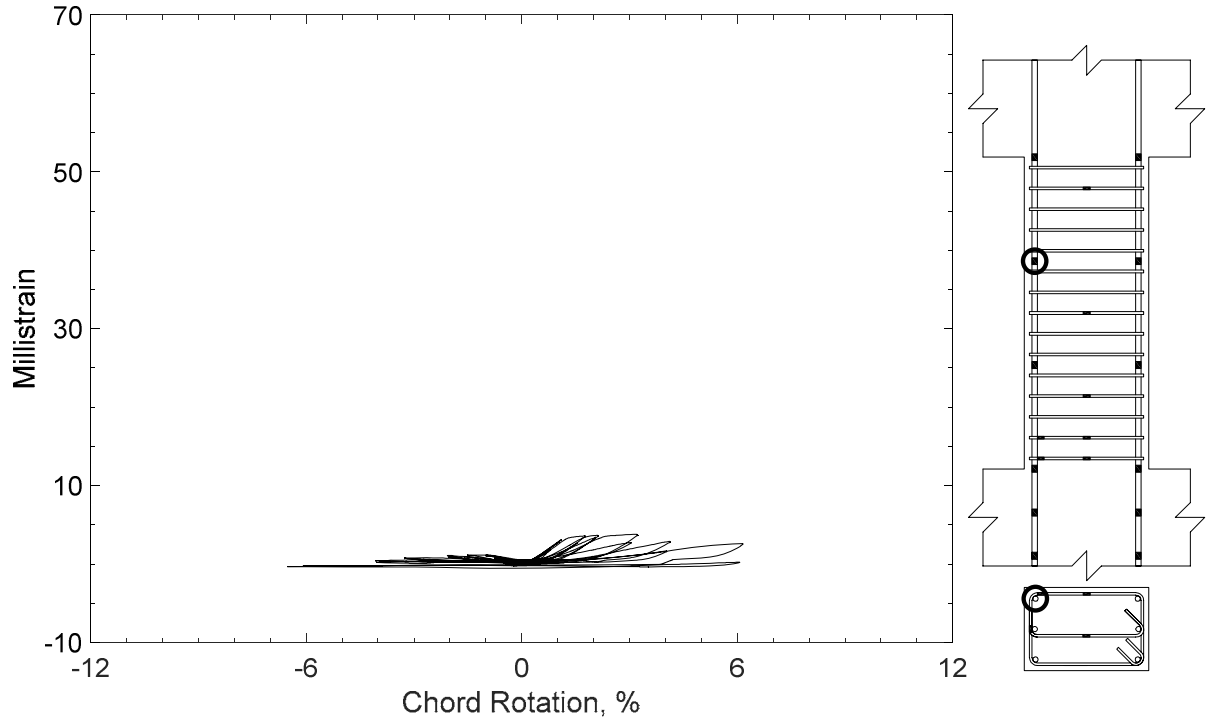


Figure 433 – Measured strain in parallel bar of P100-2.5, strain gauge P9

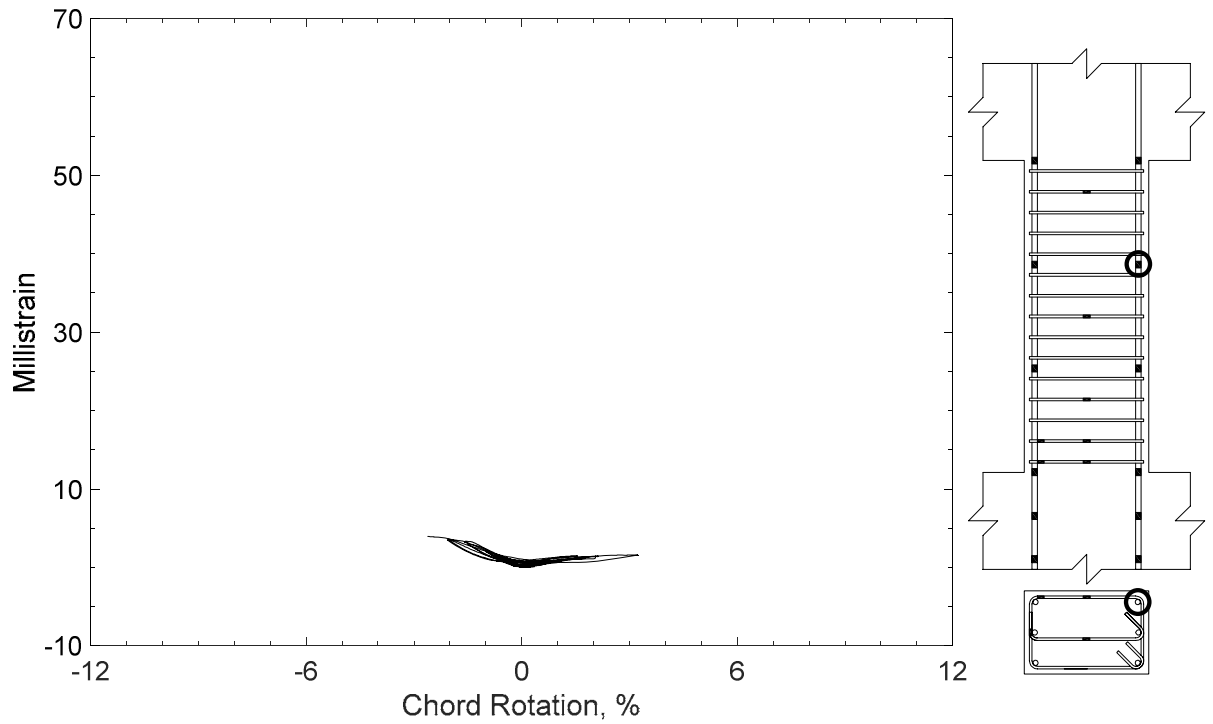


Figure 434 – Measured strain in parallel bar of P100-2.5, strain gauge P10

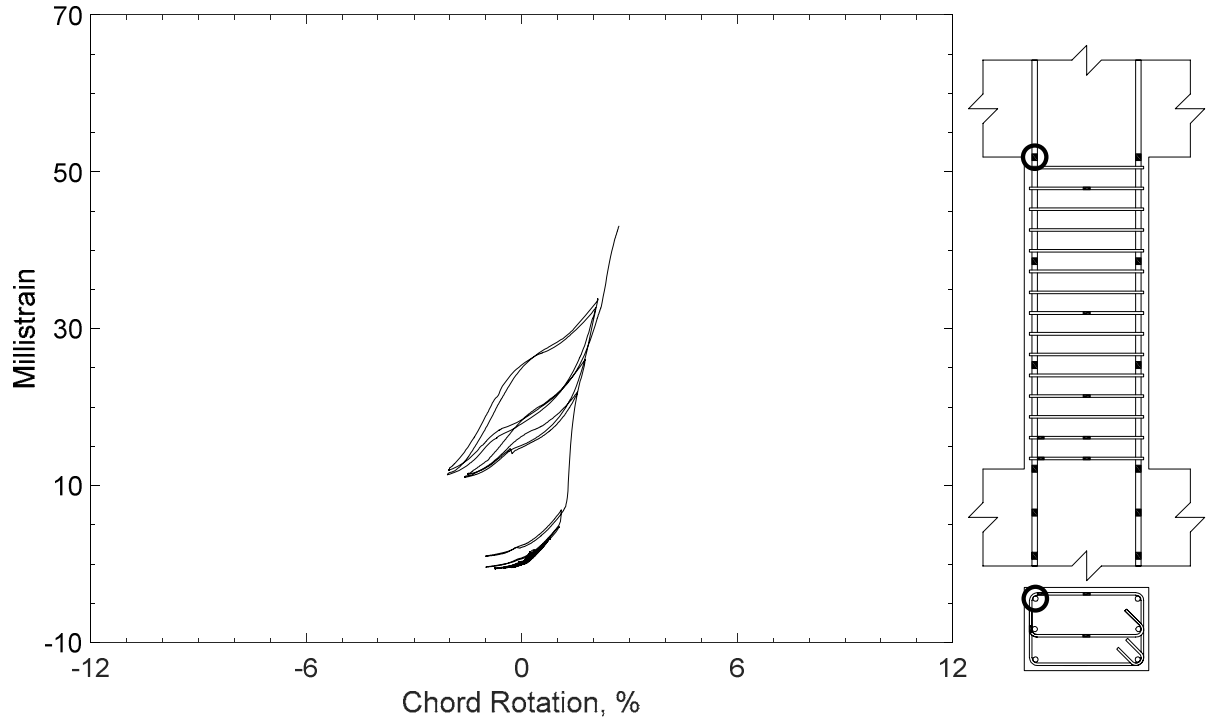


Figure 435 – Measured strain in parallel bar of P100-2.5, strain gauge P11

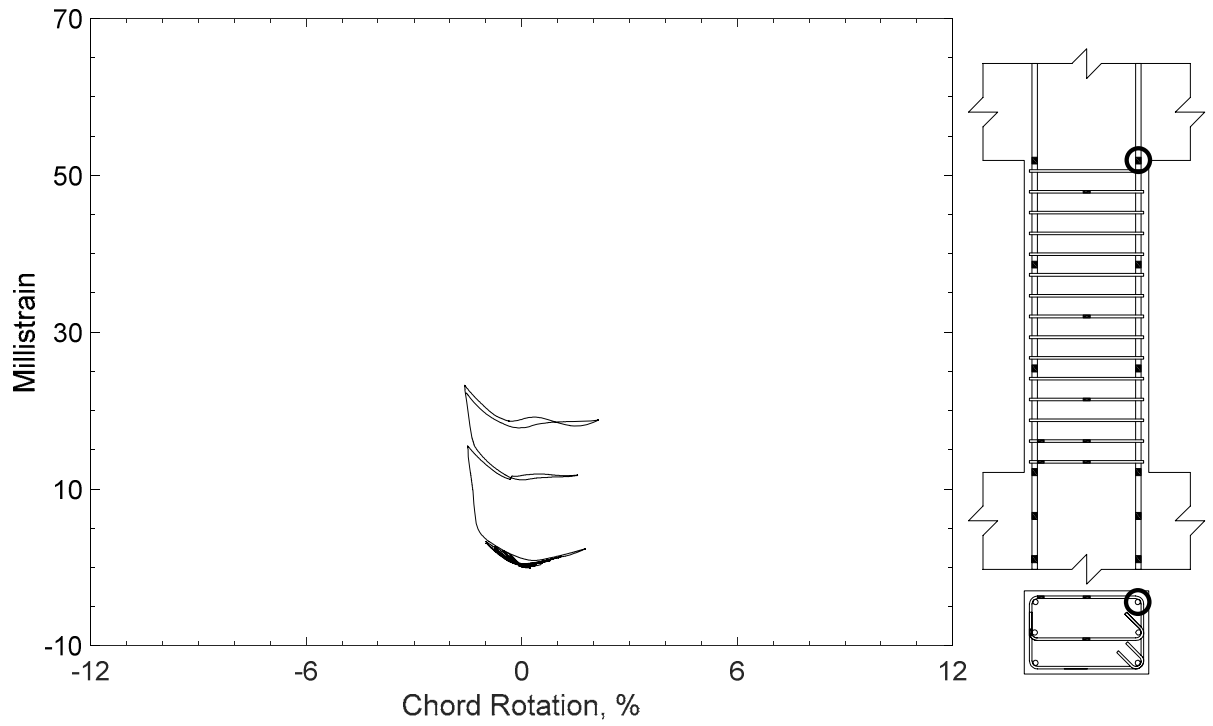


Figure 436 – Measured strain in parallel bar of P100-2.5, strain gauge P12

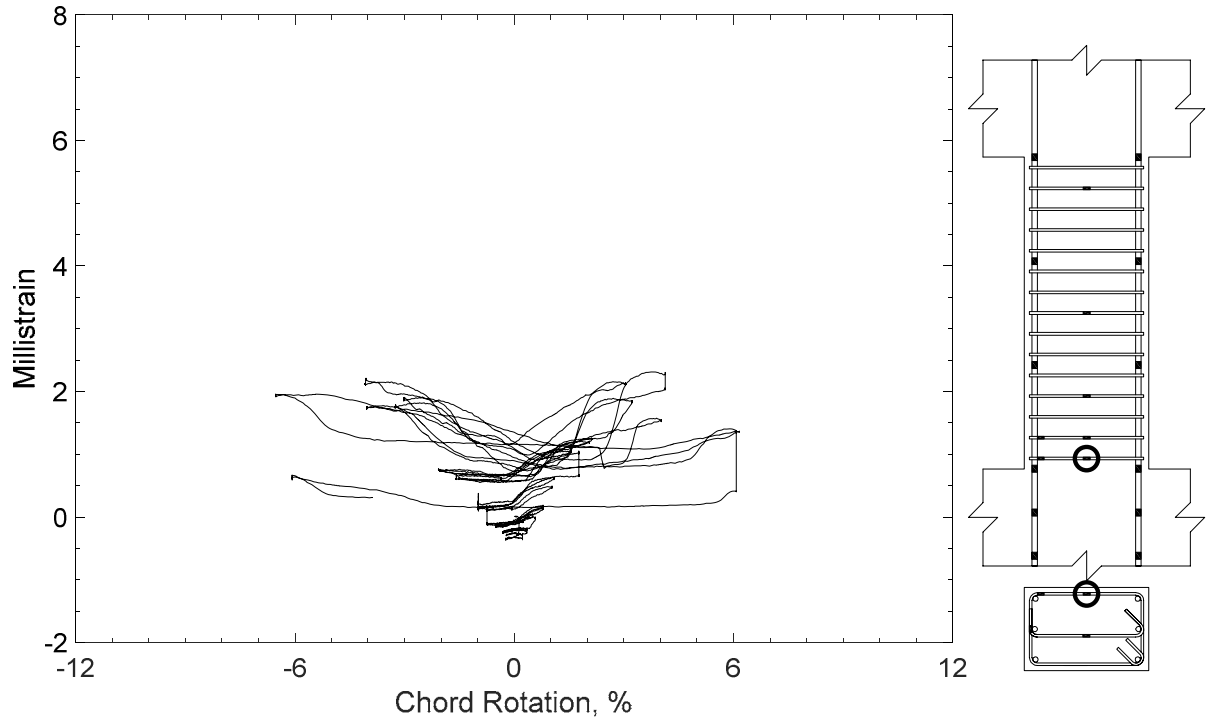


Figure 437 – Measured strain in closed stirrup of P100-2.5, strain gauge S1

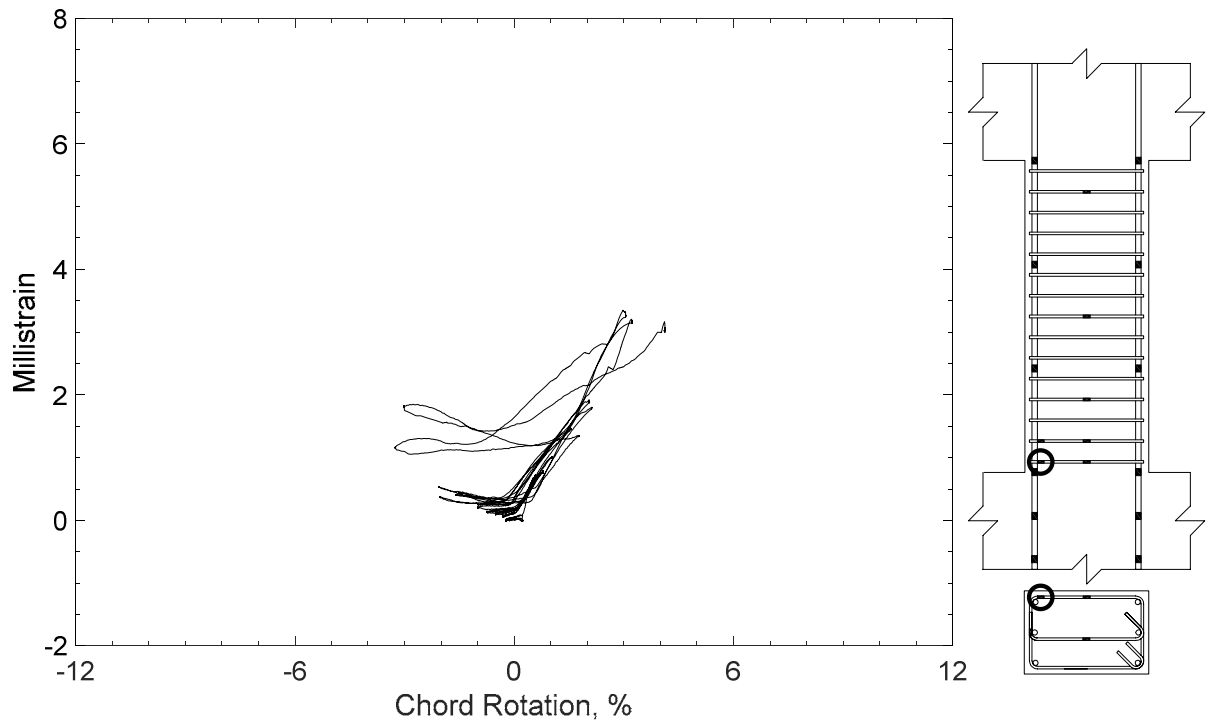


Figure 438 – Measured strain in closed stirrup of P100-2.5, strain gauge S2

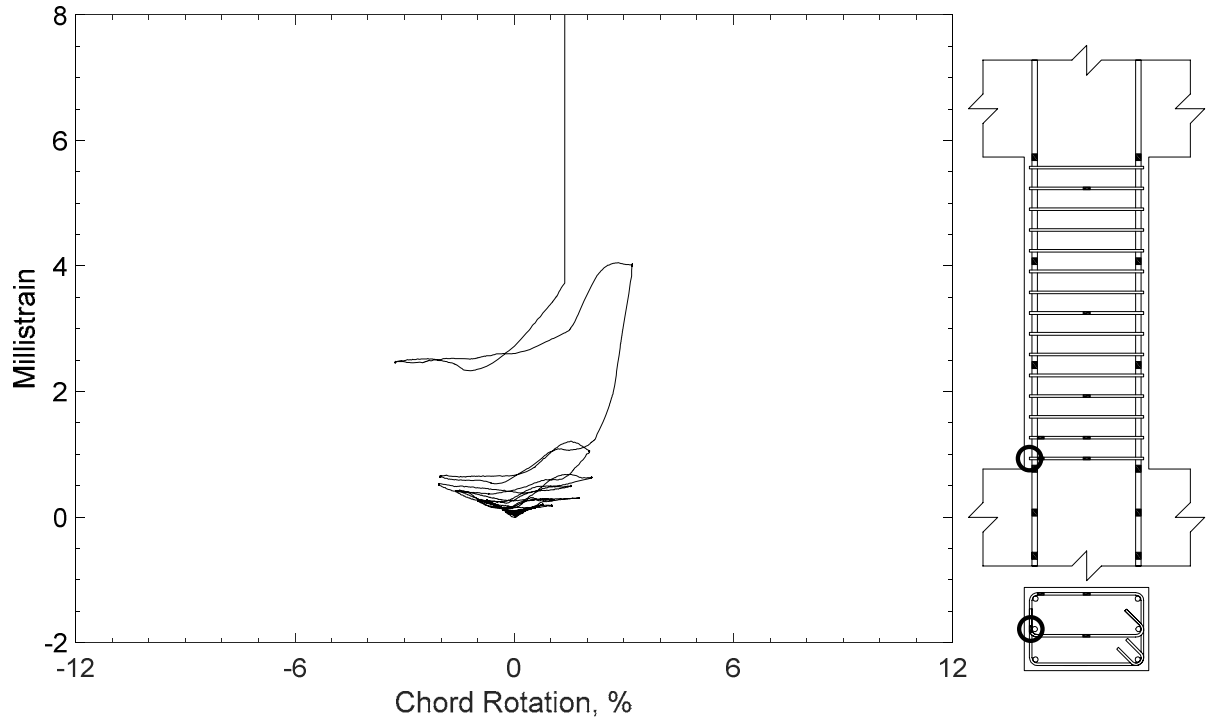


Figure 439 – Measured strain in closed stirrup of P100-2.5, strain gauge S3

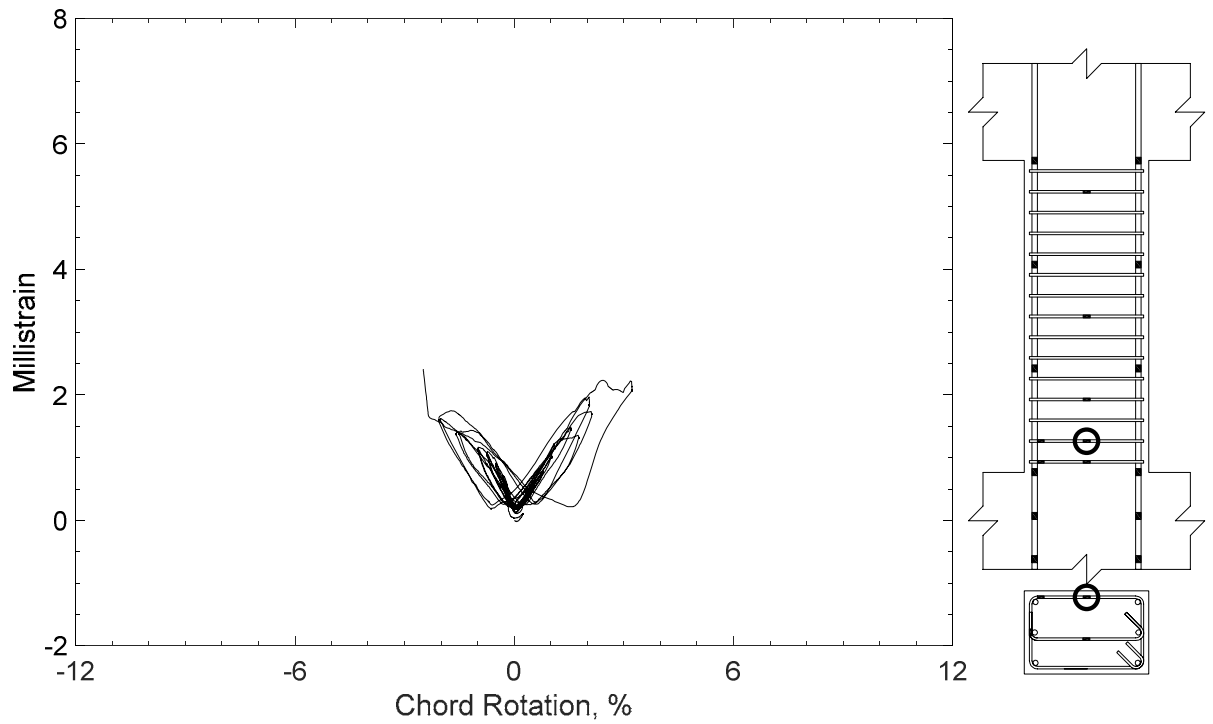


Figure 440 – Measured strain in closed stirrup of P100-2.5, strain gauge S4

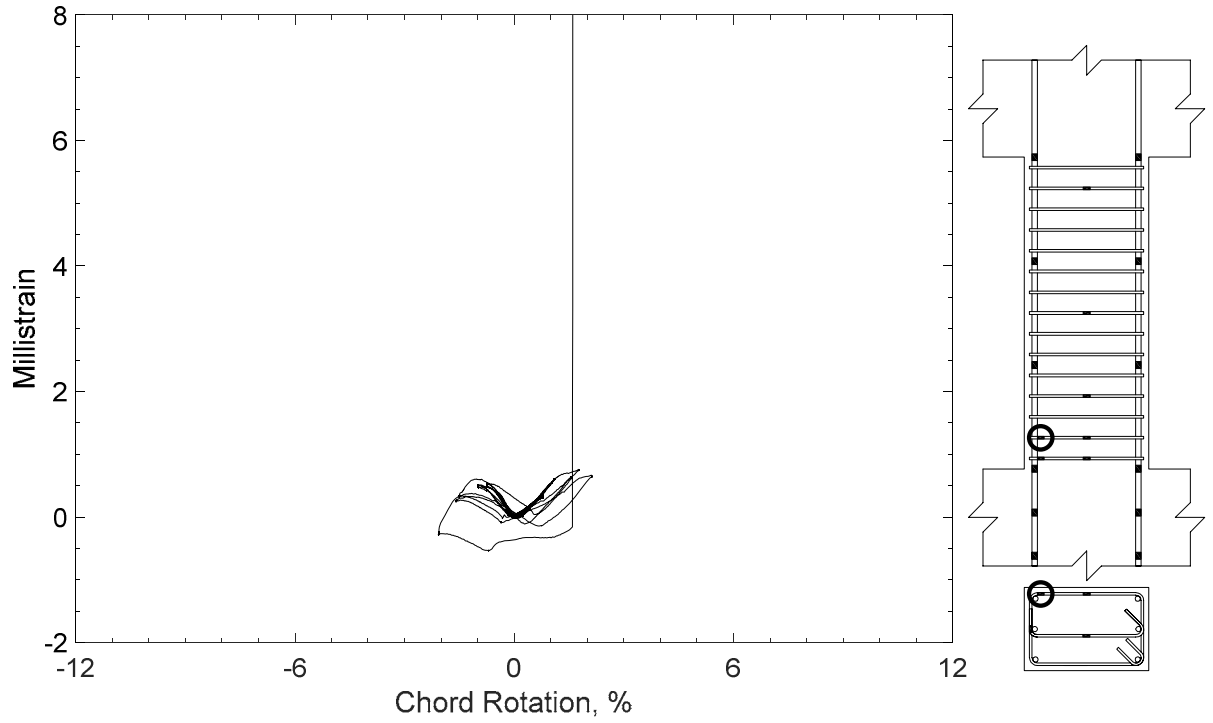


Figure 441 – Measured strain in closed stirrup of P100-2.5, strain gauge S5

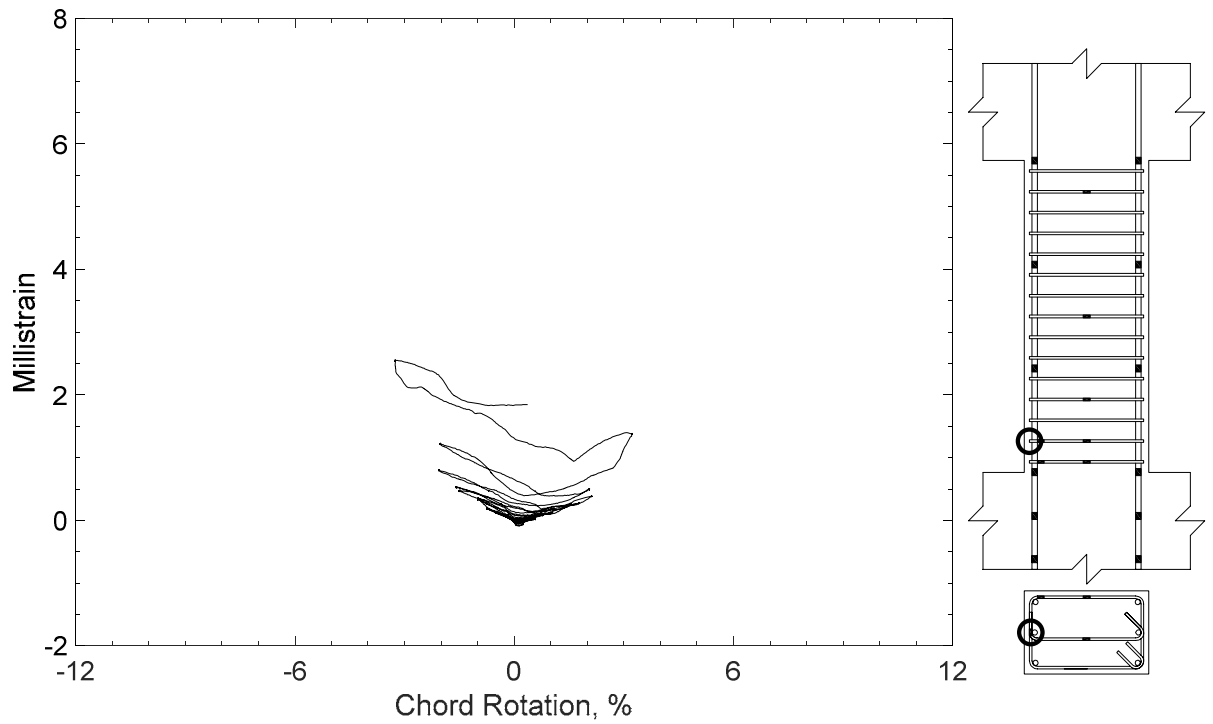


Figure 442 – Measured strain in closed stirrup of P100-2.5, strain gauge S6

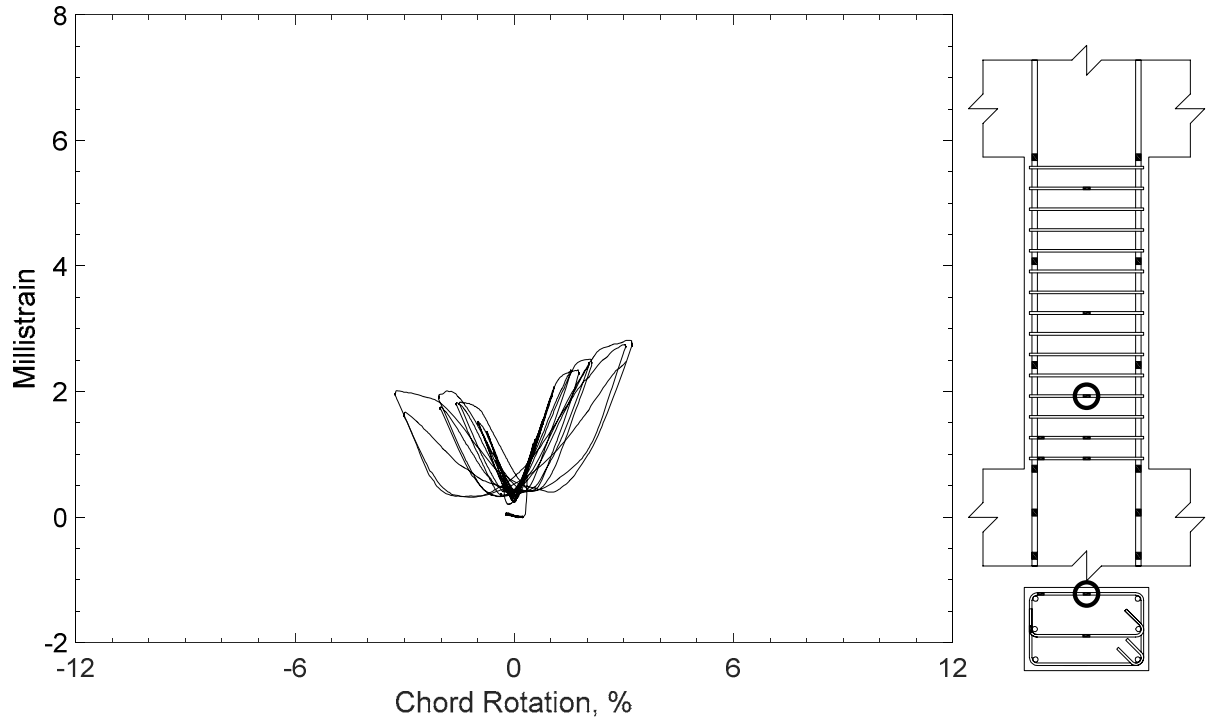


Figure 443 – Measured strain in closed stirrup of P100-2.5, strain gauge S7

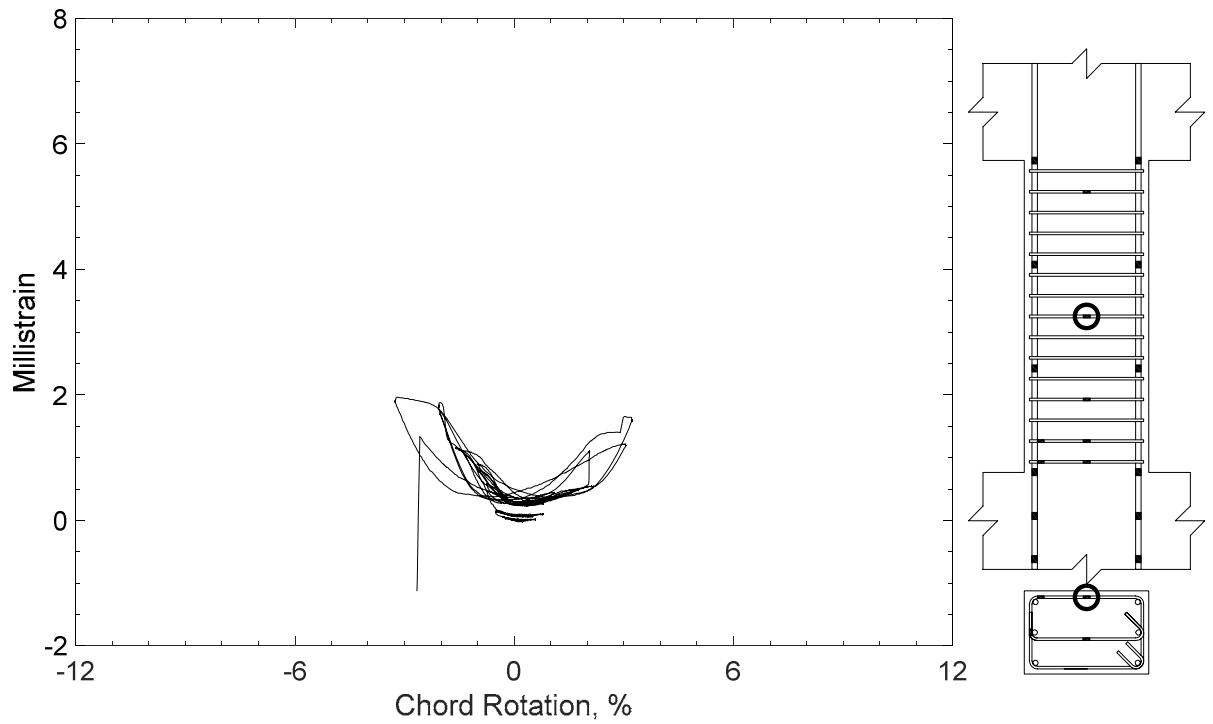


Figure 444 – Measured strain in closed stirrup of P100-2.5, strain gauge S8

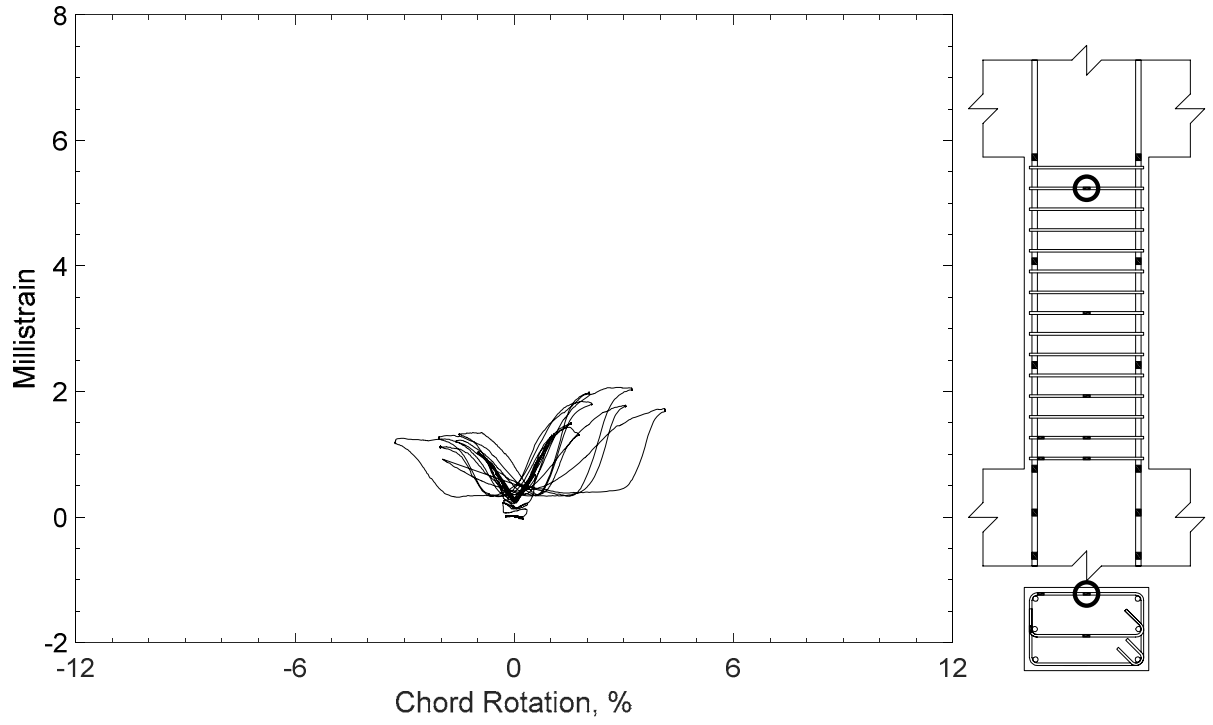


Figure 445 – Measured strain in closed stirrup of P100-2.5, strain gauge S9

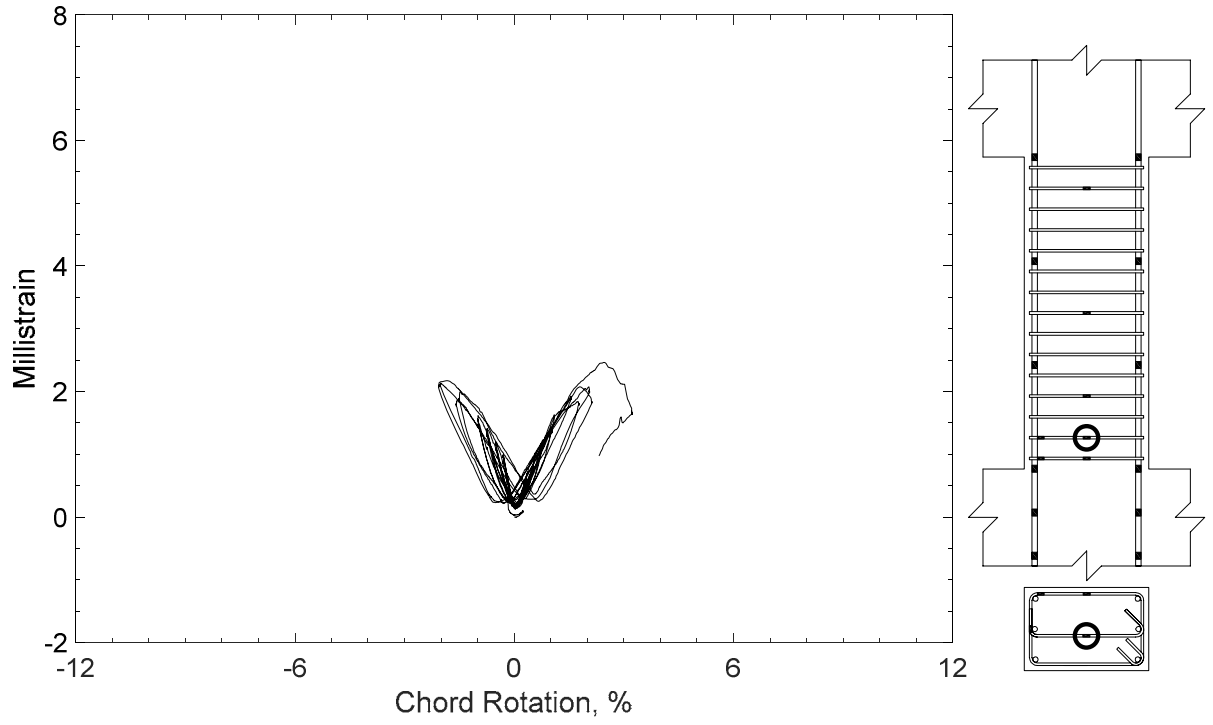


Figure 446 – Measured strain in cross-tie of P100-2.5, strain gauge T1

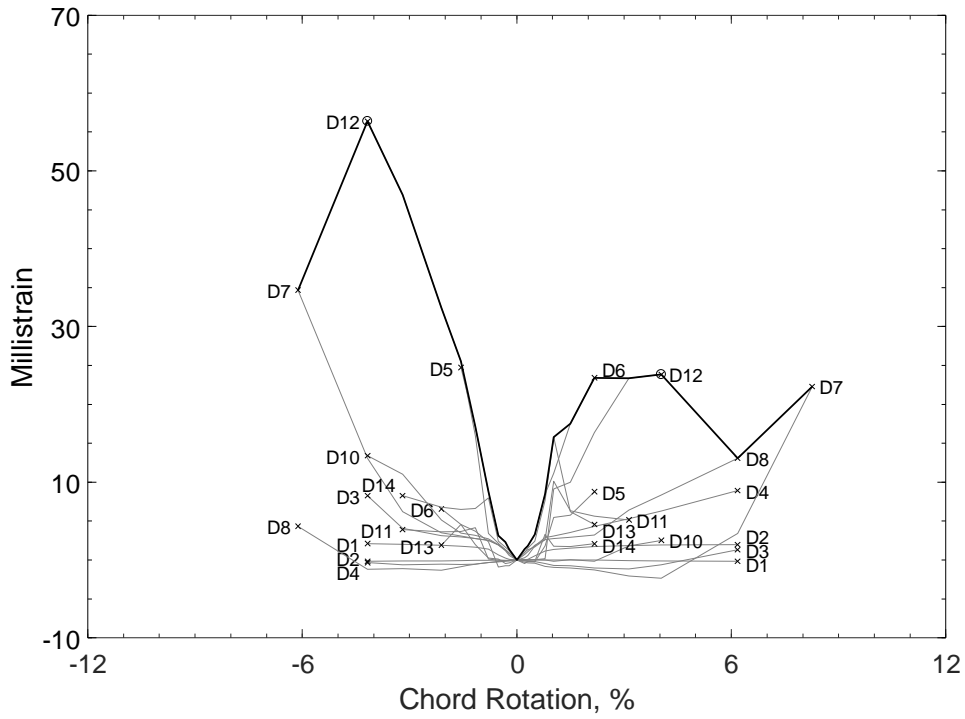


Figure 447 – Envelopes of measured strains in diagonal bars of D80-1.5, D strain gauges

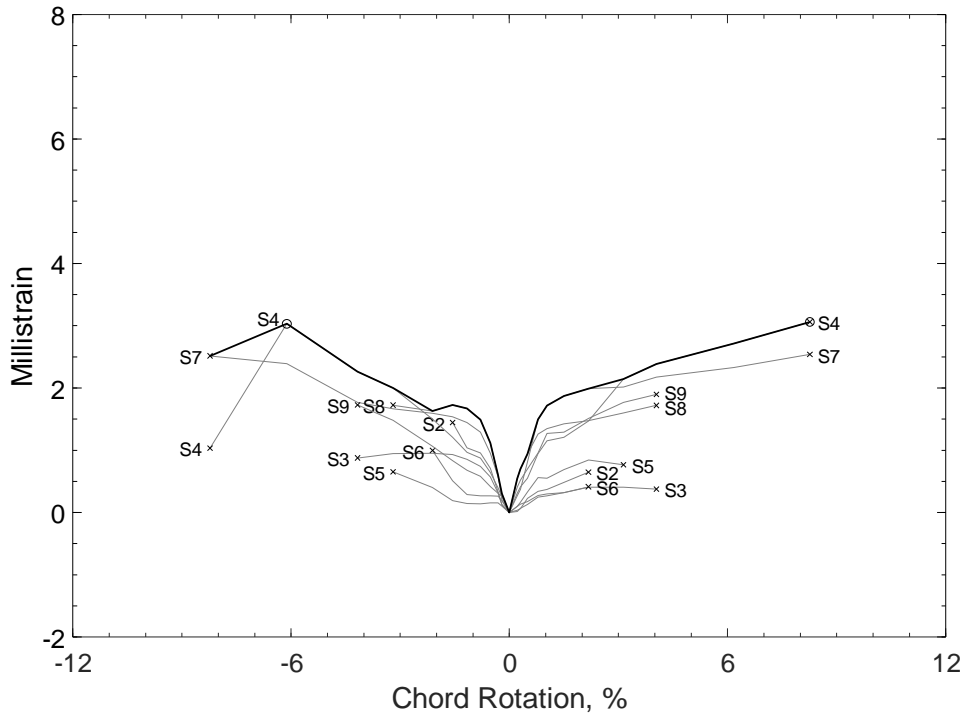


Figure 448 – Envelopes of measured strains in closed stirrups of D80-1.5, S strain gauges

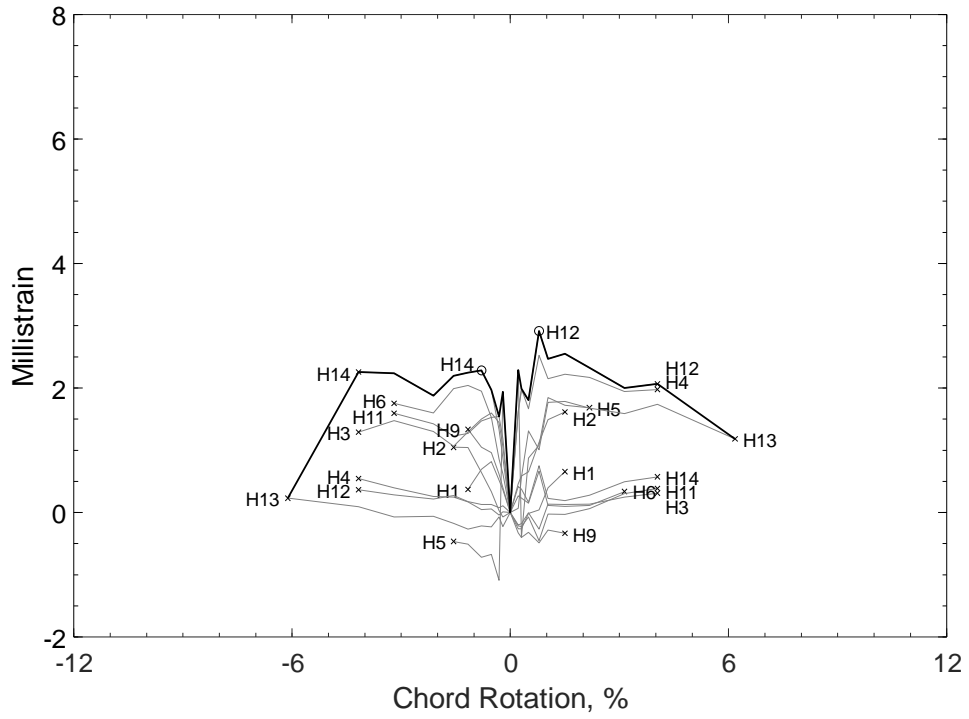


Figure 449 – Envelopes of measured strains in parallel bars of D80-1.5, H strain gauges

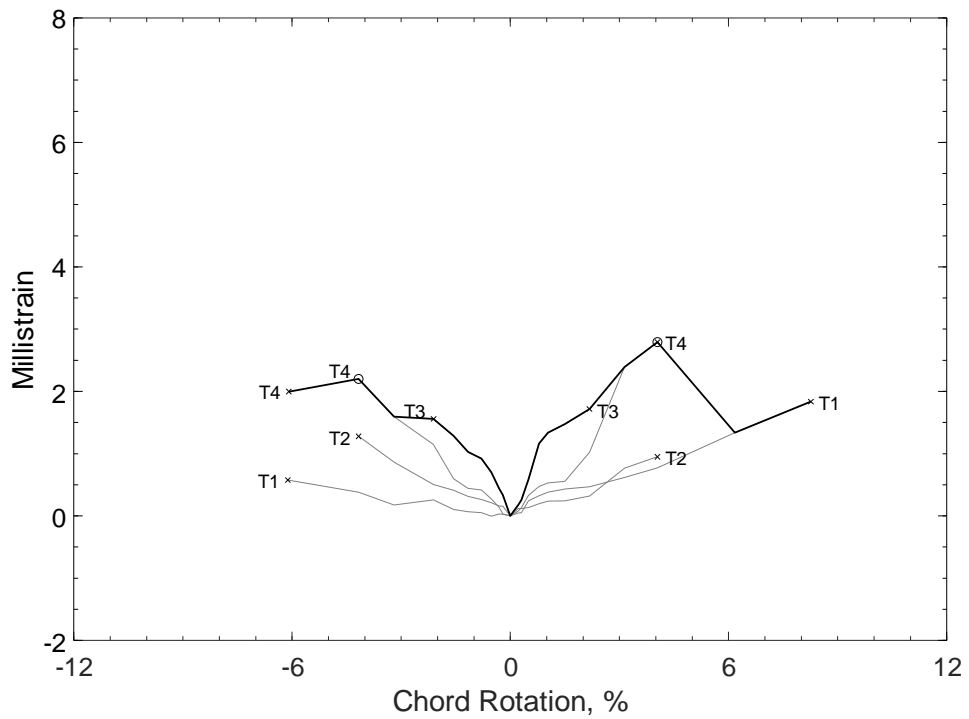


Figure 450 – Envelopes of measured strains in crosssties of D80-1.5, T strain gauges

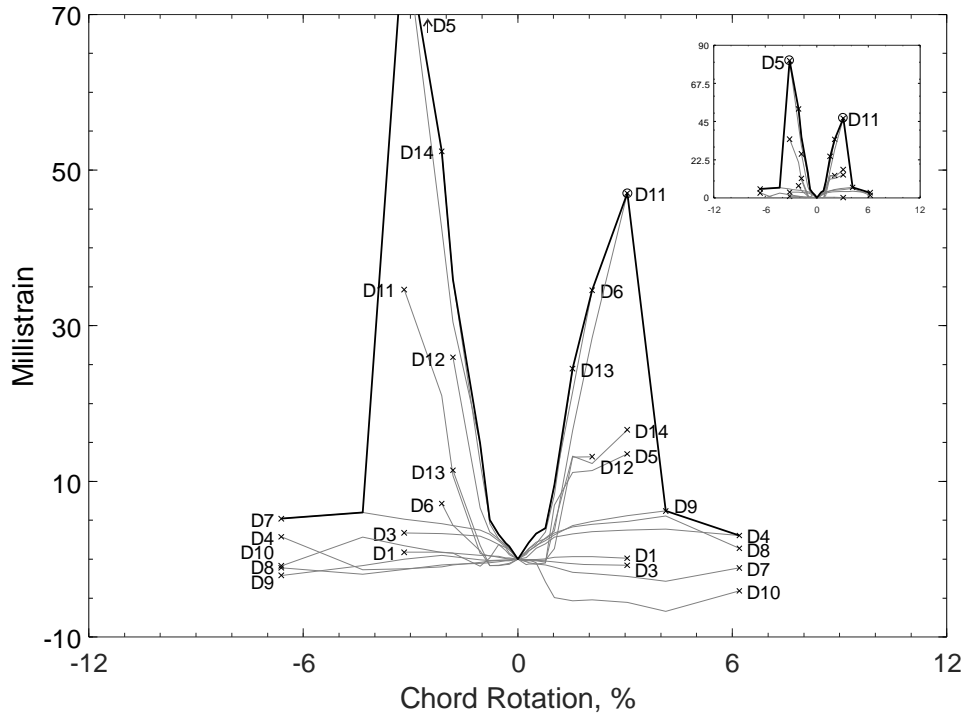


Figure 451 – Envelopes of measured strains in diagonal bars of D100-1.5, D strain gauges

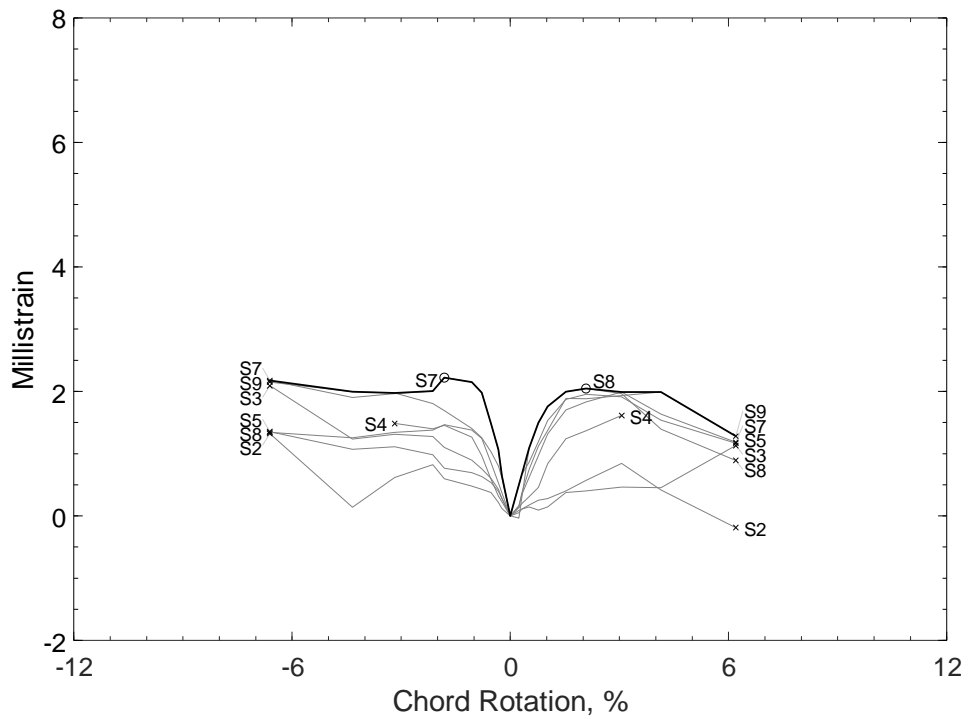


Figure 452 – Envelopes of measured strains in closed stirrups of D100-1.5, S strain gauges

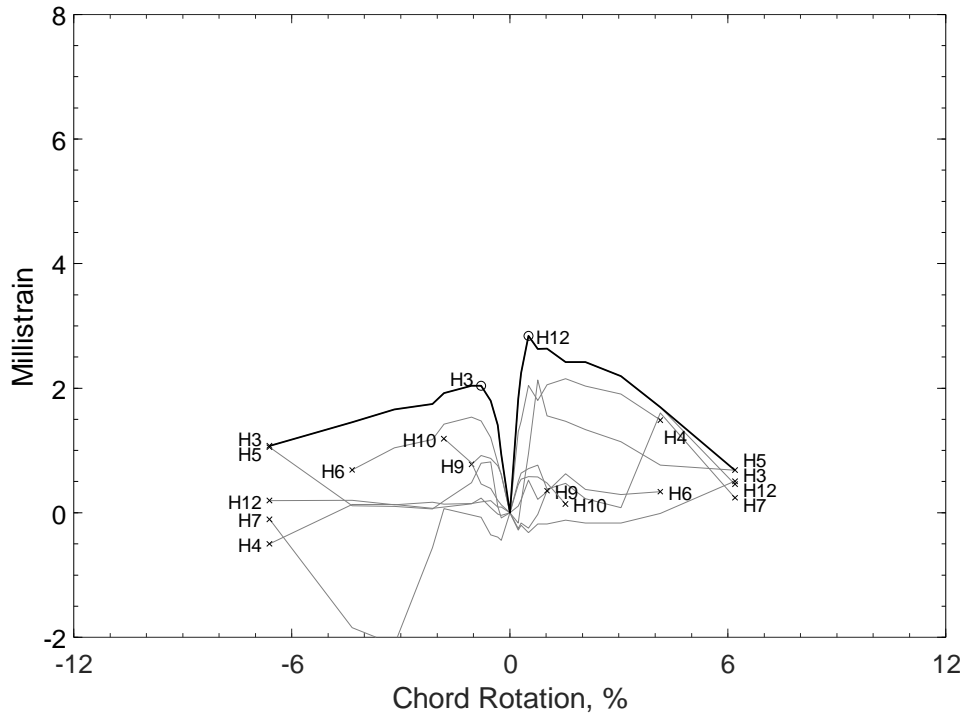


Figure 453 – Envelopes of measured strains in parallel bars of D100-1.5, H strain gauges

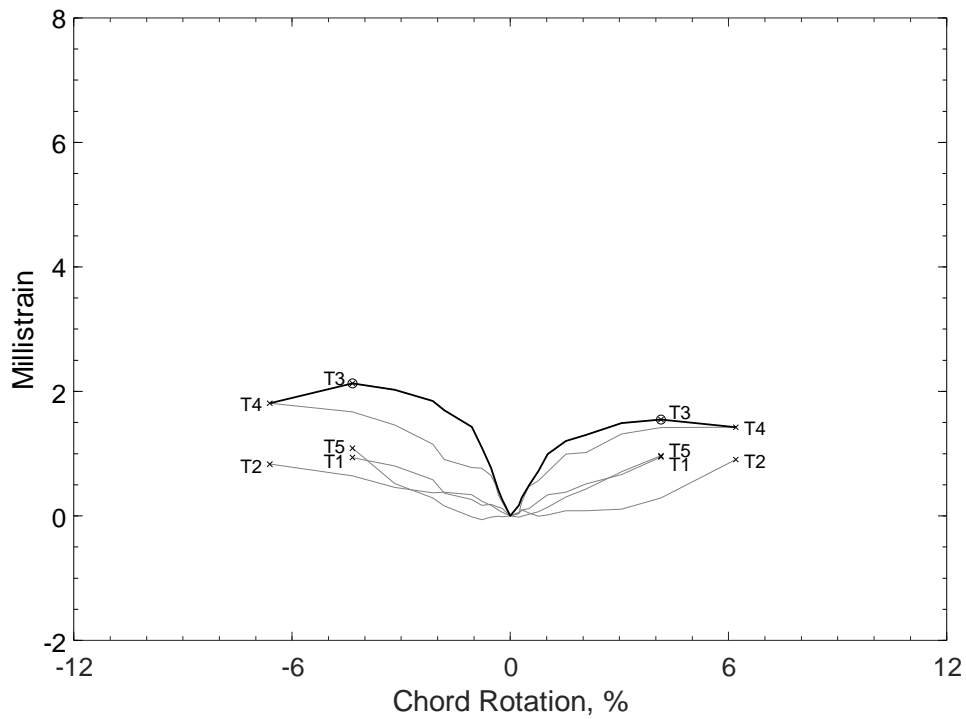


Figure 454 – Envelopes of measured strains in crosssties of D100-1.5, T strain gauges

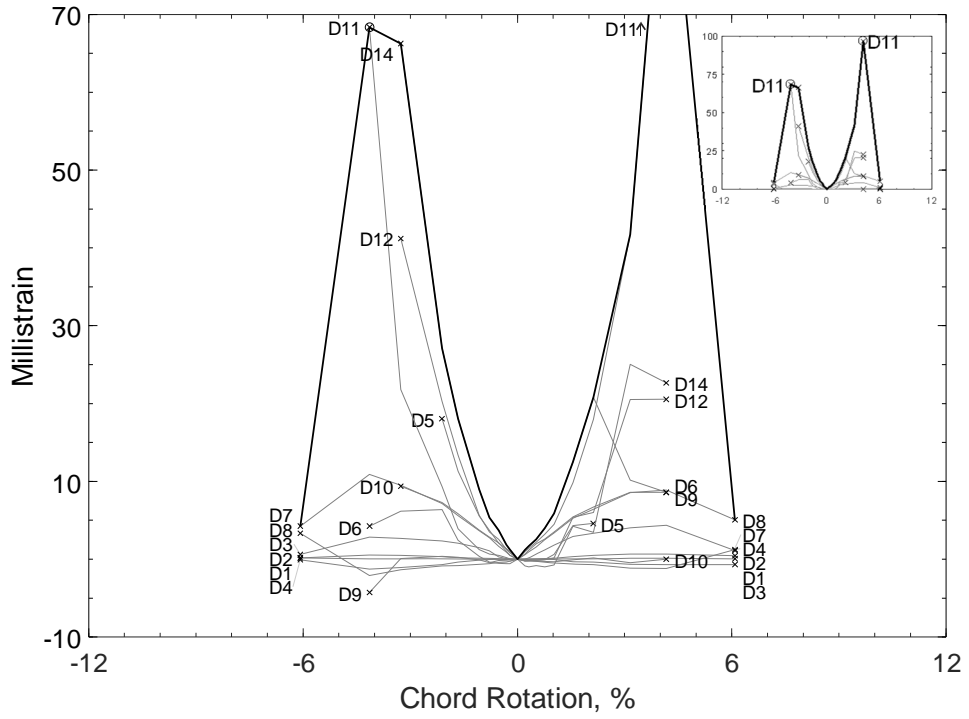


Figure 455 – Envelopes of measured strains in diagonal bars of D120-1.5, D strain gauges

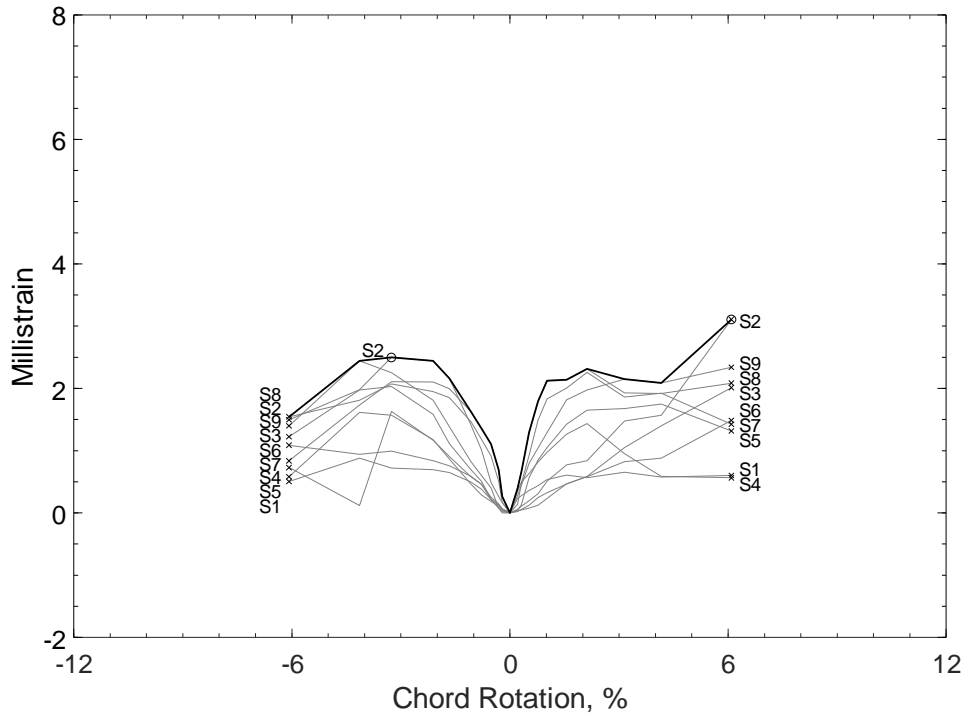


Figure 456 – Envelopes of measured strains in closed stirrups of D120-1.5, S strain gauges

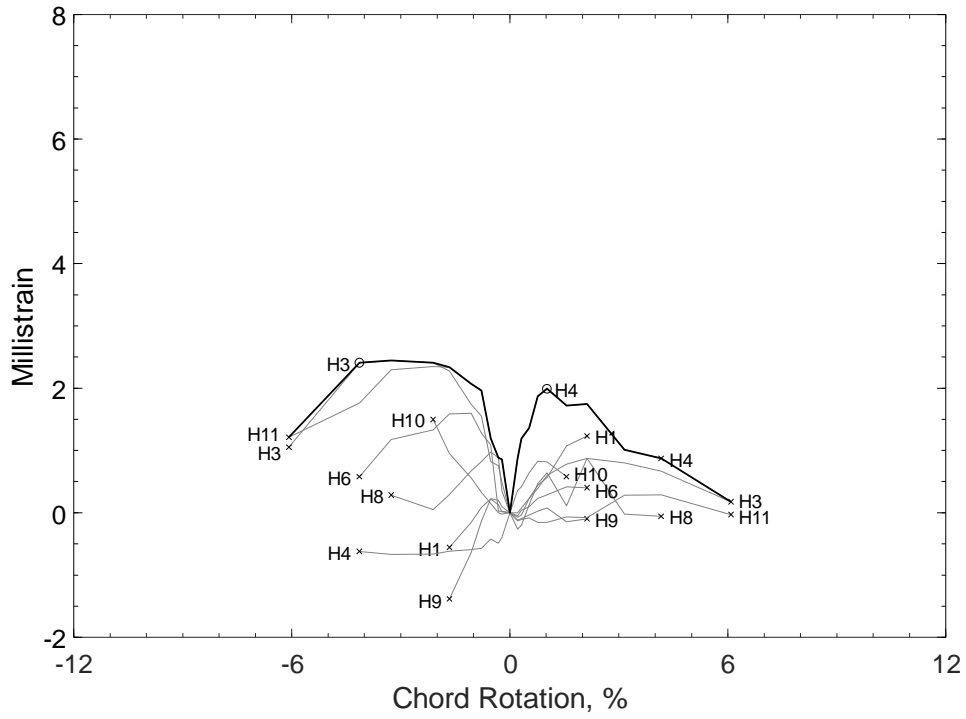


Figure 457 – Envelopes of measured strains in parallel bars of D120-1.5, H strain gauges

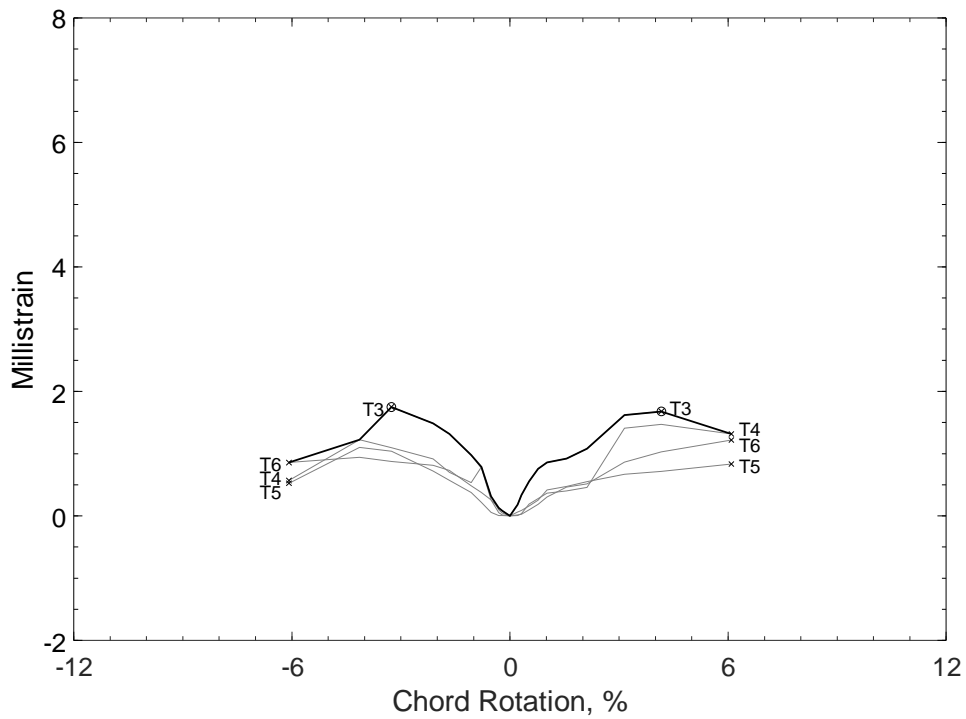


Figure 458 – Envelopes of measured strains in crosssties of D120-1.5, T strain gauges

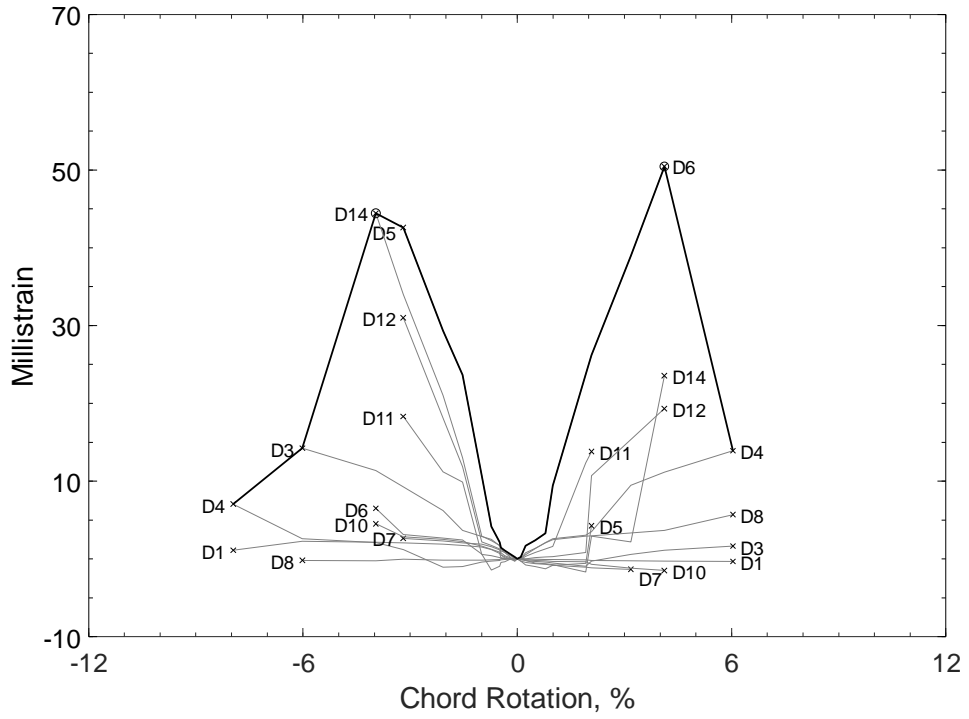


Figure 459 – Envelopes of measured strains in diagonal bars of D80-2.5, D strain gauges

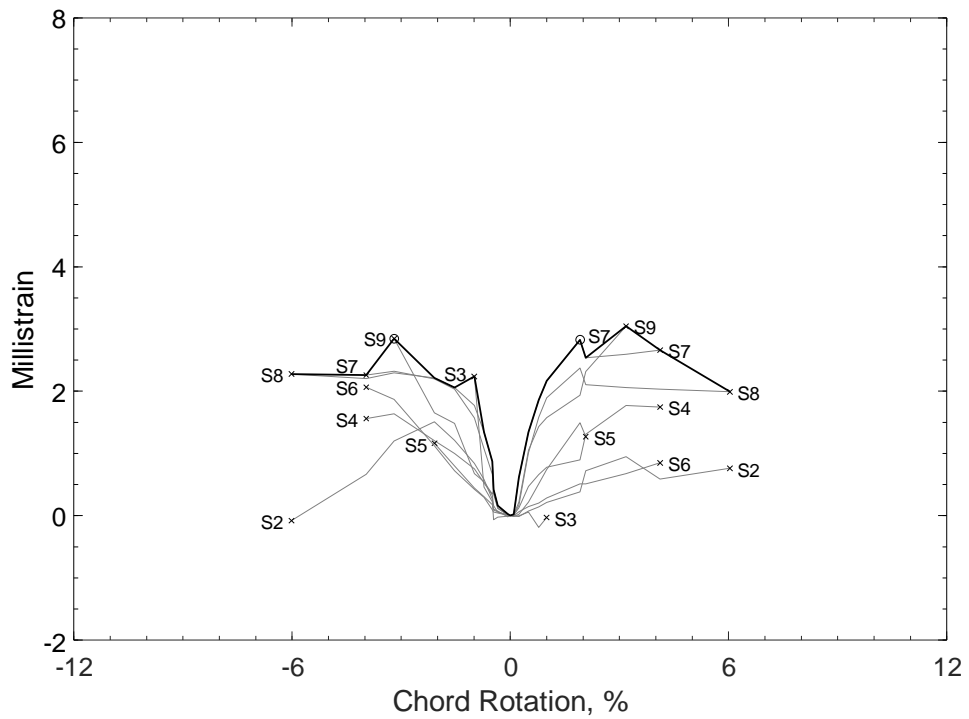


Figure 460 – Envelopes of measured strains in closed stirrups of D80-2.5, S strain gauges

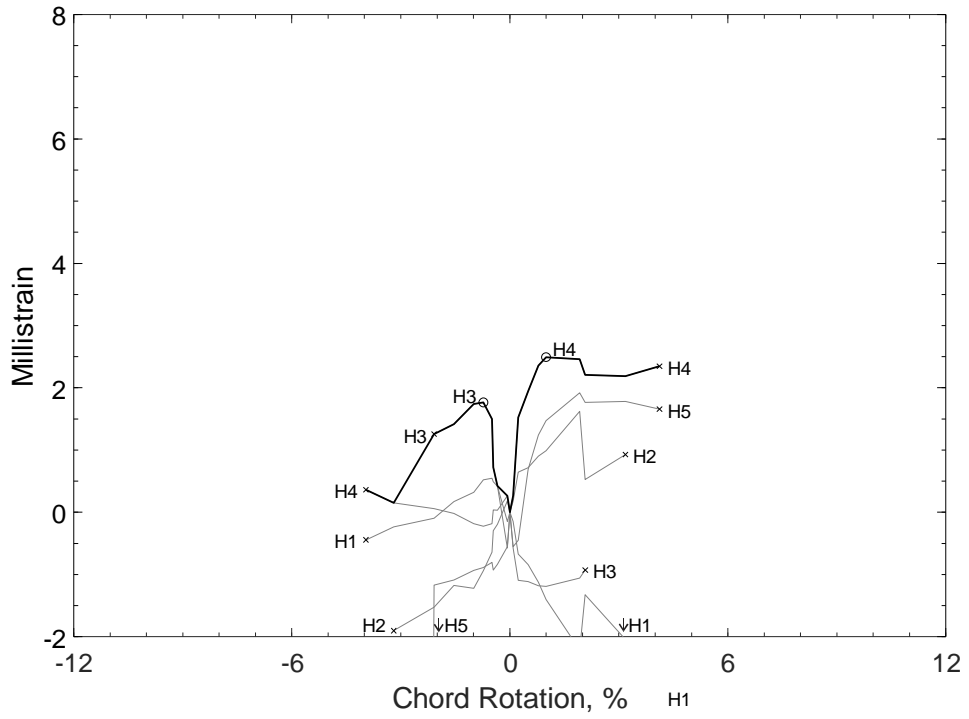


Figure 461 – Envelopes of measured strains in parallel bars of D80-2.5, H strain gauges

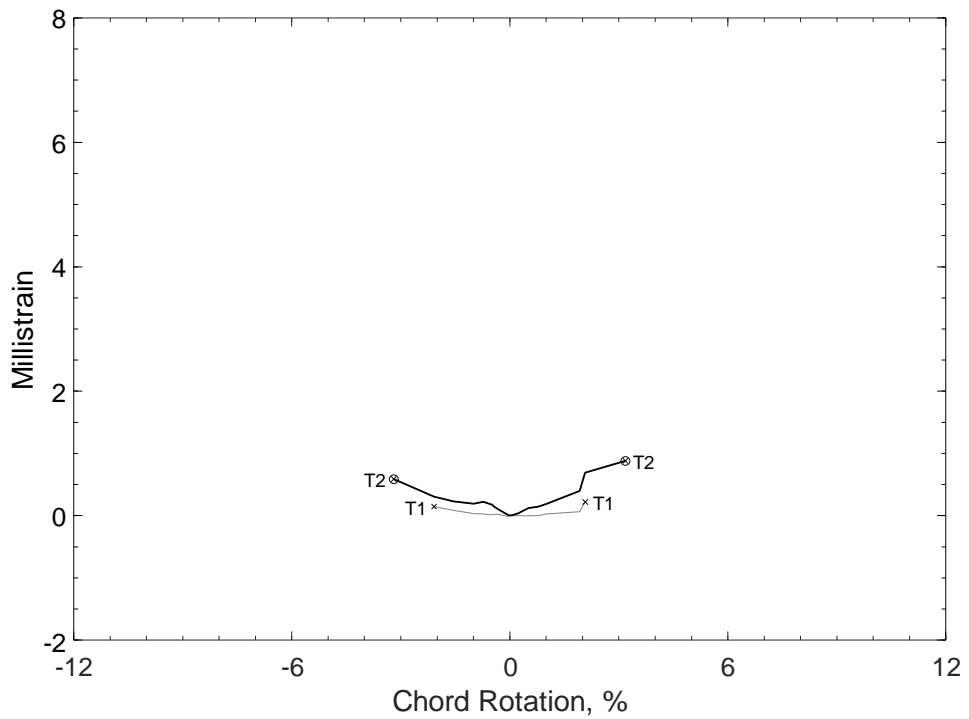


Figure 462 – Envelopes of measured strains in crosssties of D80-2.5, T strain gauges

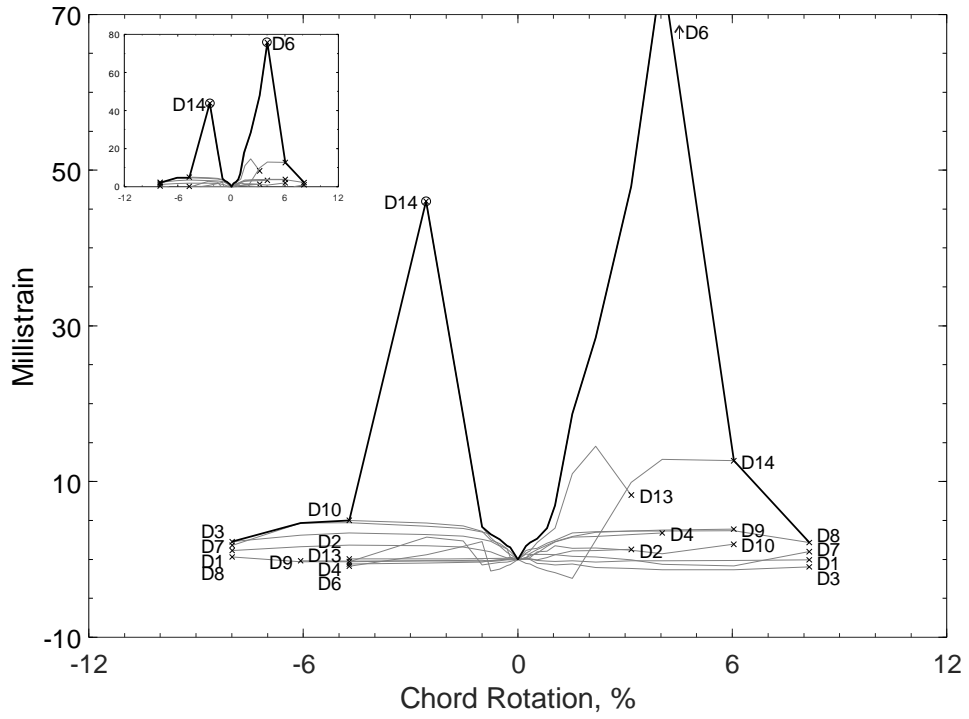


Figure 463 – Envelopes of measured strains in diagonal bars of D100-2.5, D strain gauges

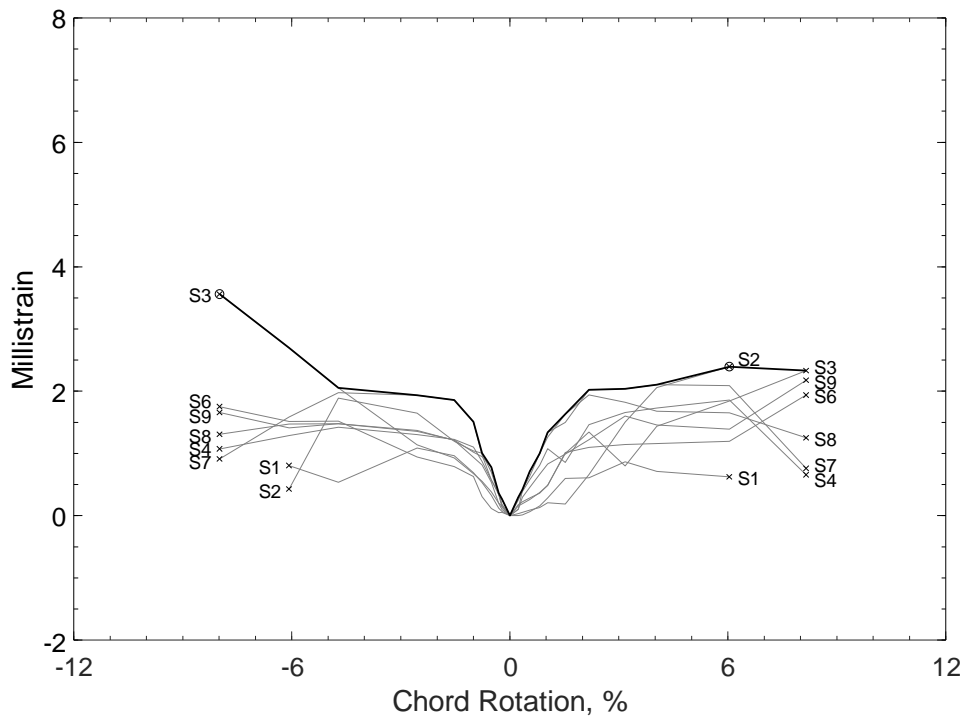


Figure 464 – Envelopes of measured strains in closed stirrups of D100-2.5, S strain gauges

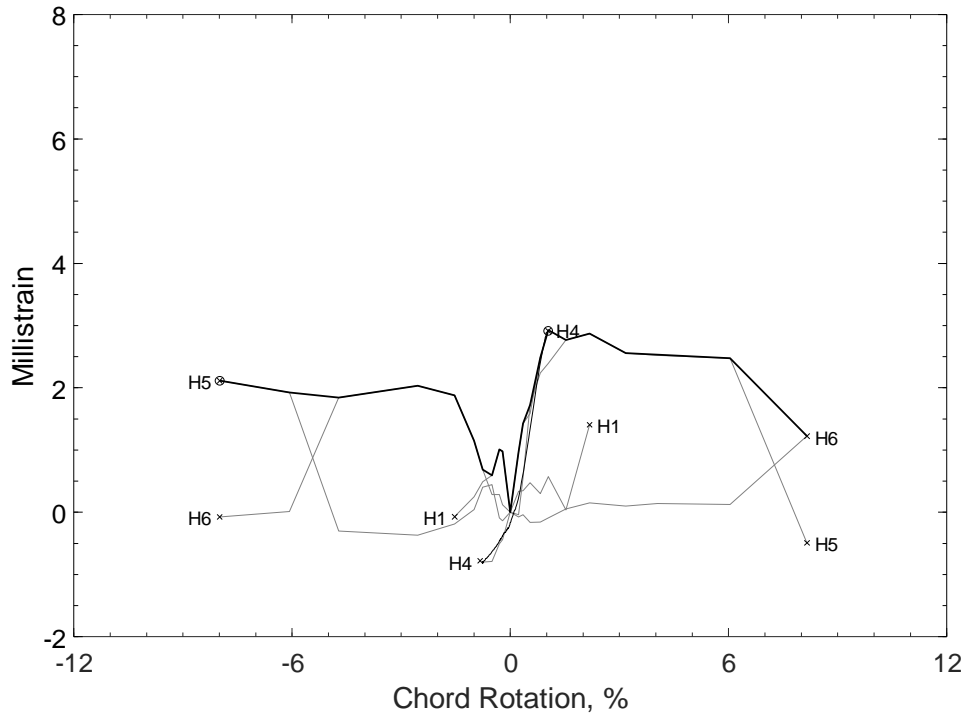


Figure 465 – Envelopes of measured strains in parallel bars of D100-2.5, H strain gauges

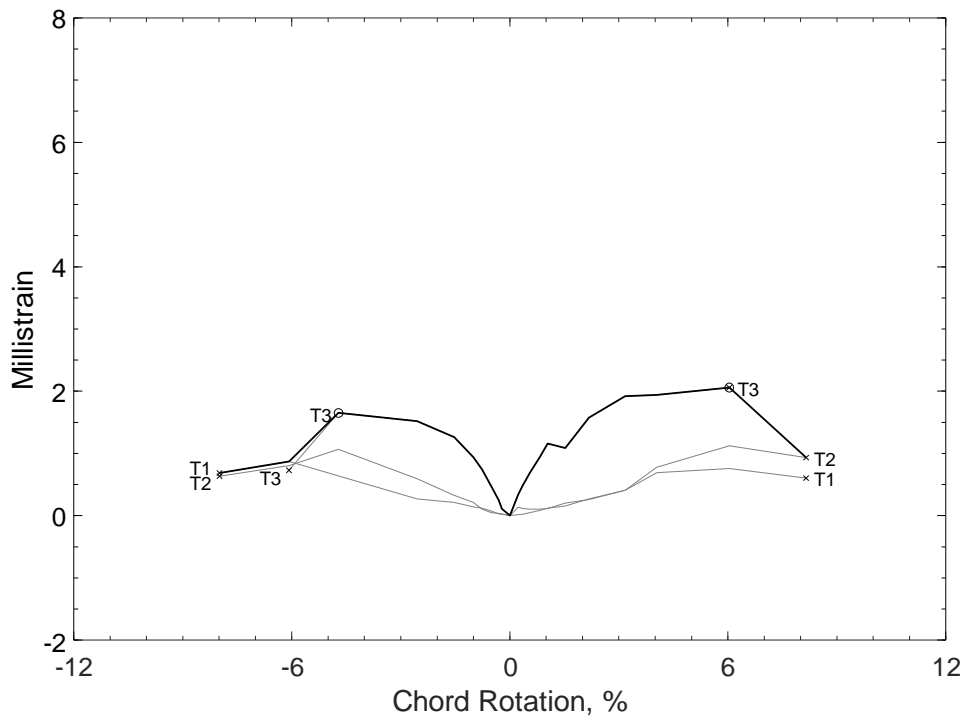


Figure 466 – Envelopes of measured strains in crosssties of D100-2.5, T strain gauges

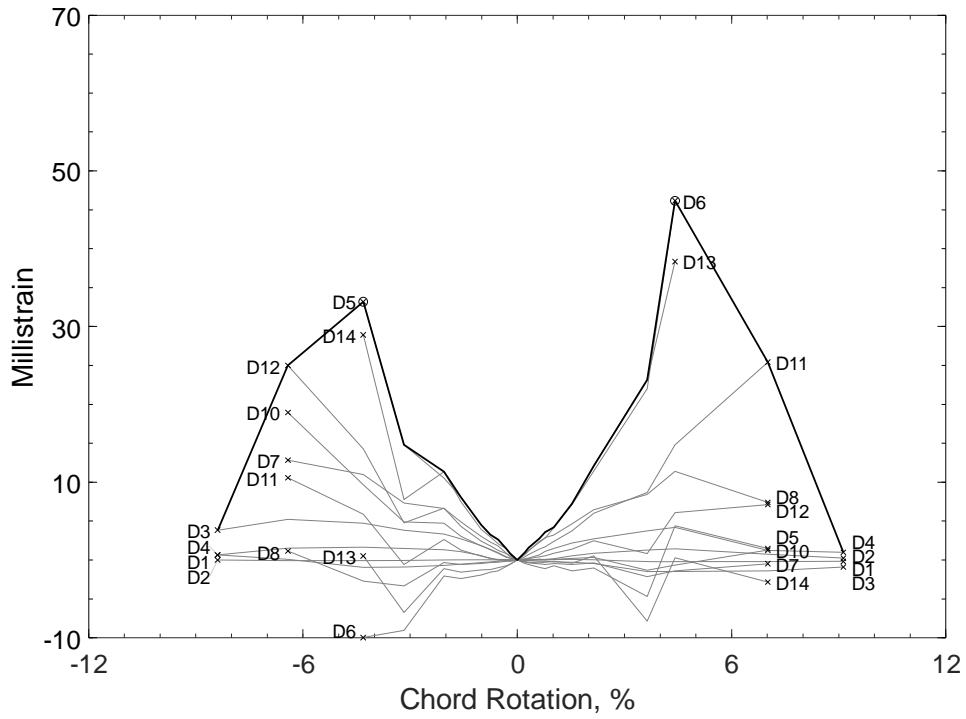


Figure 467 – Envelopes of measured strains in diagonal bars of D120-2.5, D strain gauges

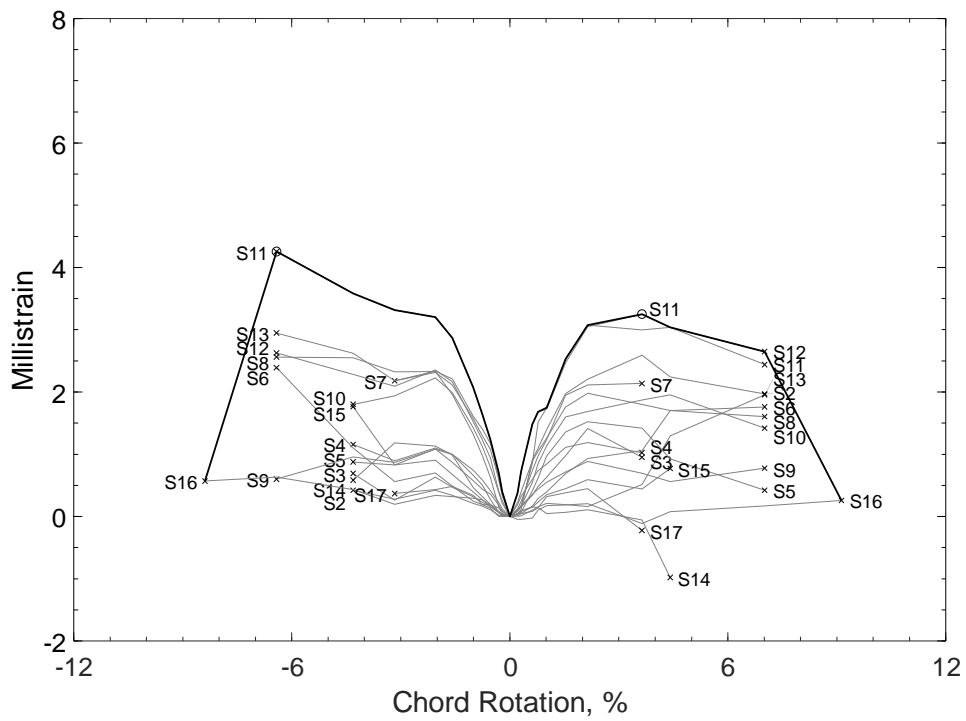


Figure 468 – Envelopes of measured strains in closed stirrups of D120-2.5, S strain gauges

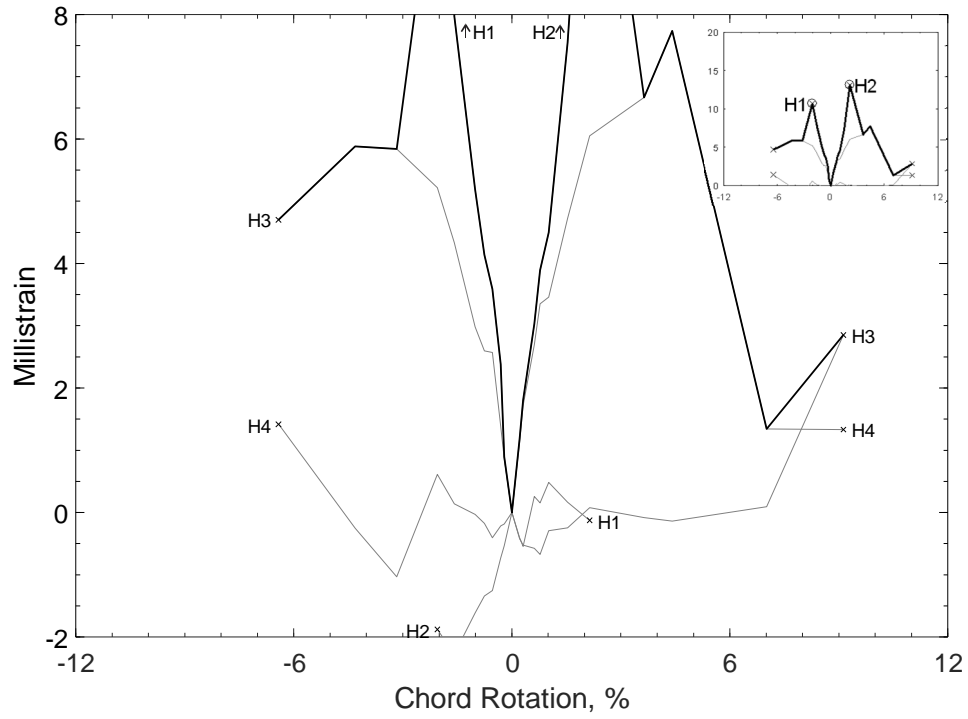


Figure 469 – Envelopes of measured strains in parallel bars of D120-2.5, H strain gauges

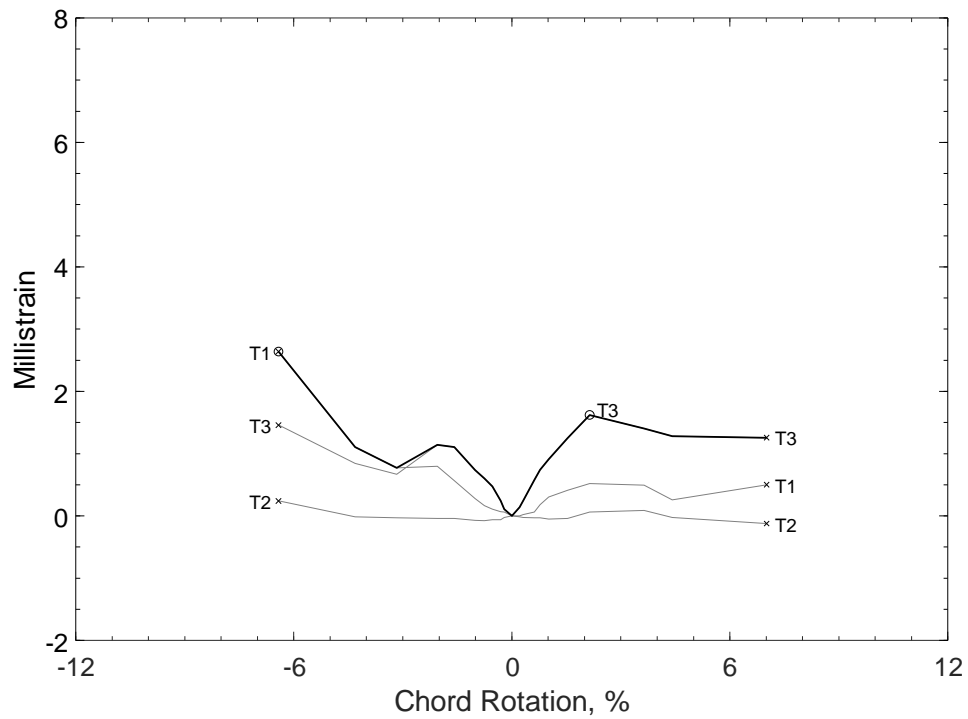


Figure 470 – Envelopes of measured strains in crosssties of D120-2.5, T strain gauges

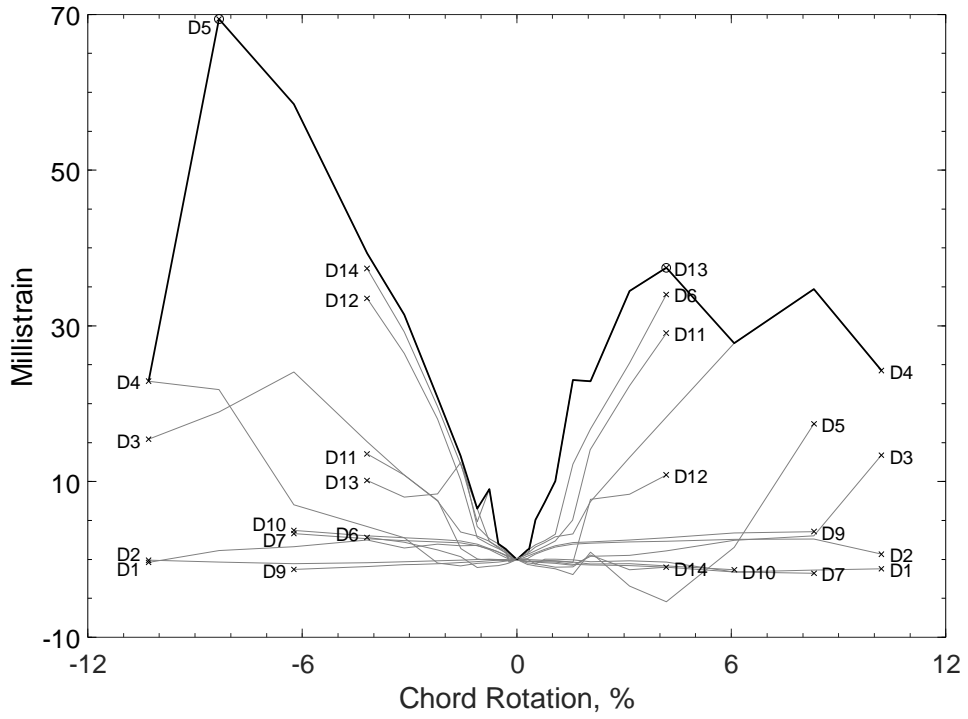


Figure 471 – Envelopes of measured strains in diagonal bars of D80-3.5, D strain gauges

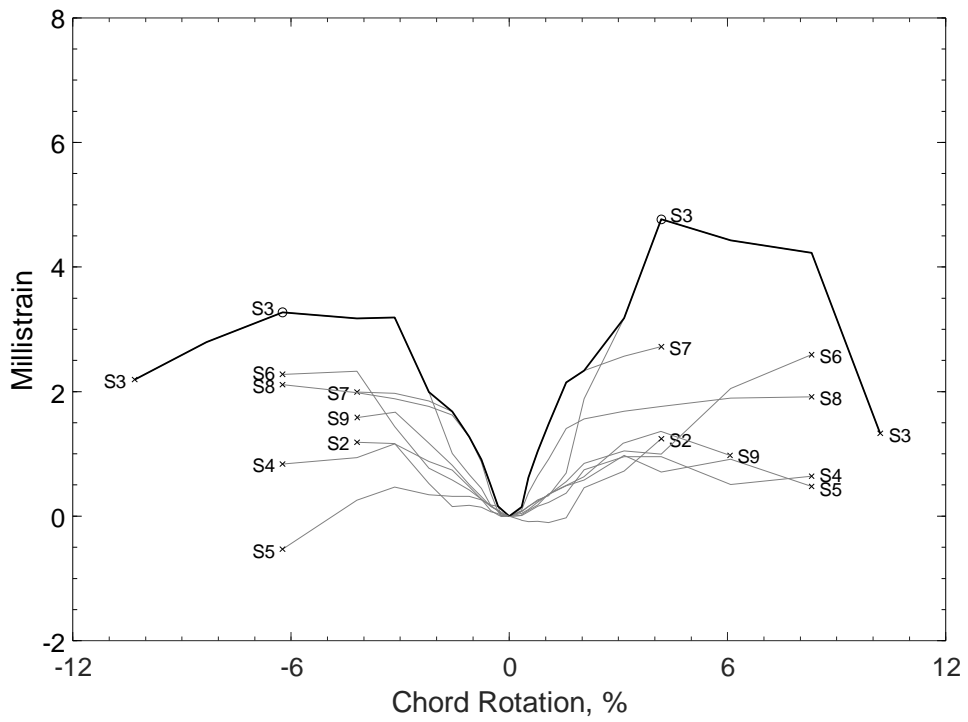


Figure 472 – Envelopes of measured strains in closed stirrups of D80-3.5, S strain gauges

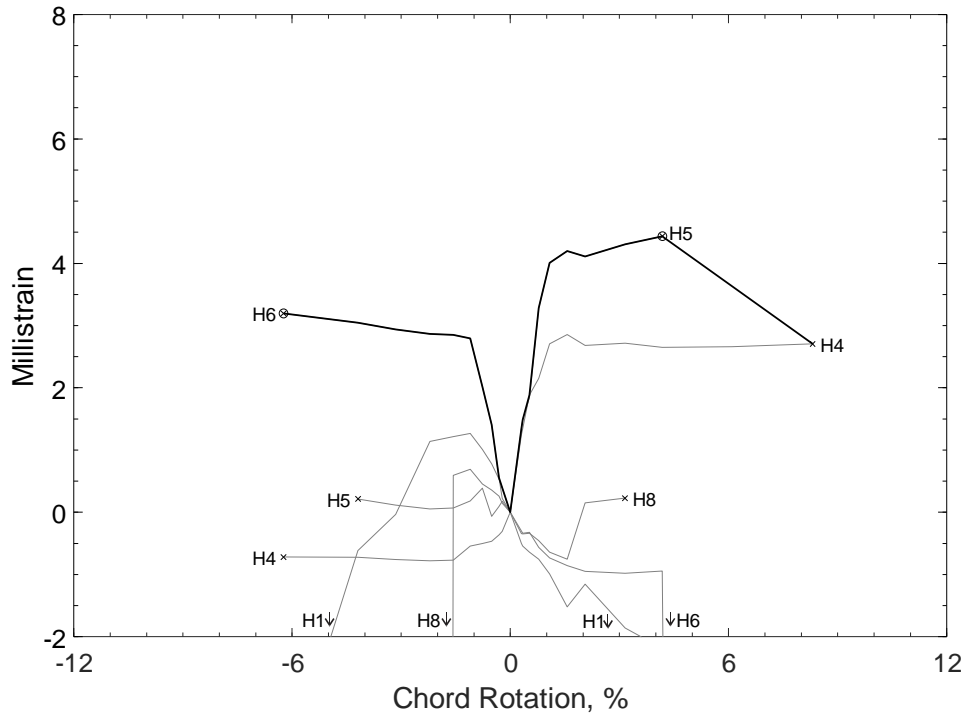


Figure 473 – Envelopes of measured strains in parallel bars of D80-3.5, H strain gauges

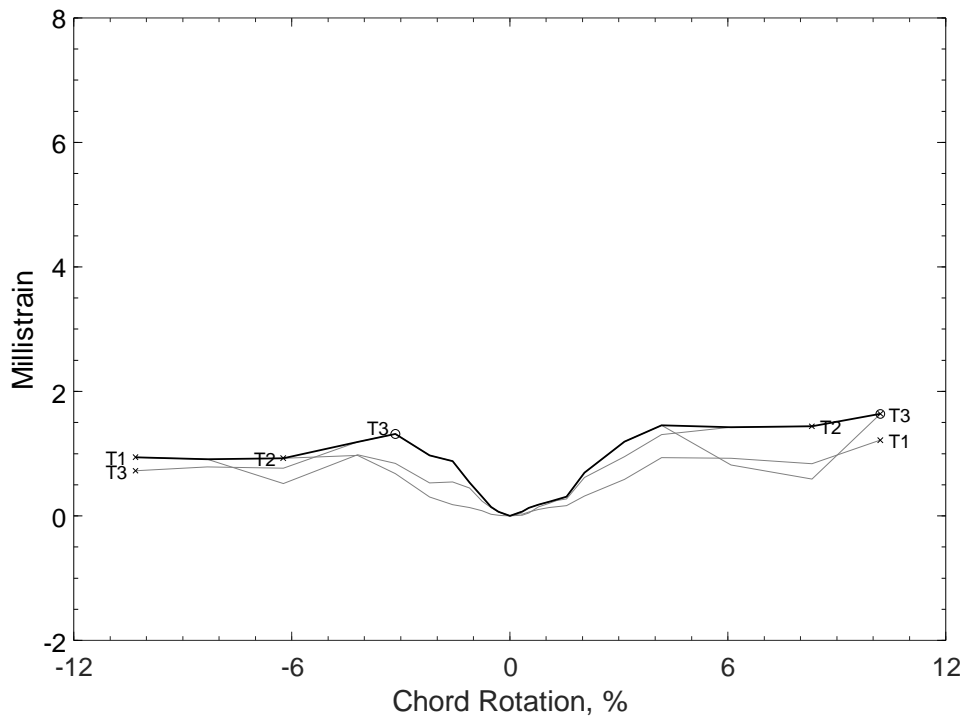


Figure 474 – Envelopes of measured strains in crosssties of D80-3.5, T strain gauges

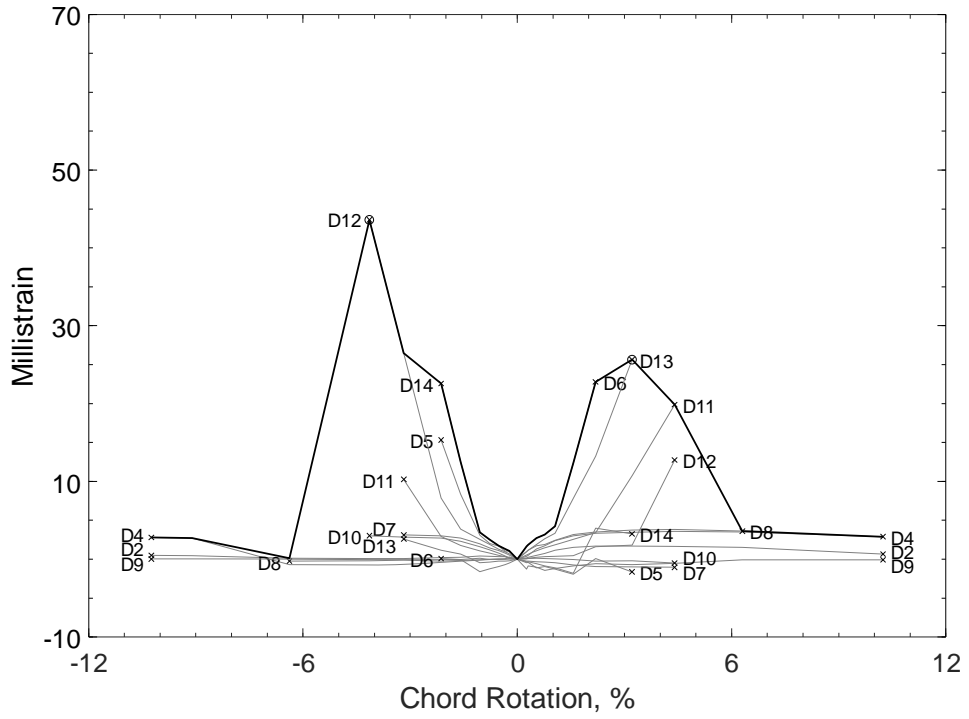


Figure 475 – Envelopes of measured strains in diagonal bars of D100-3.5, D strain gauges

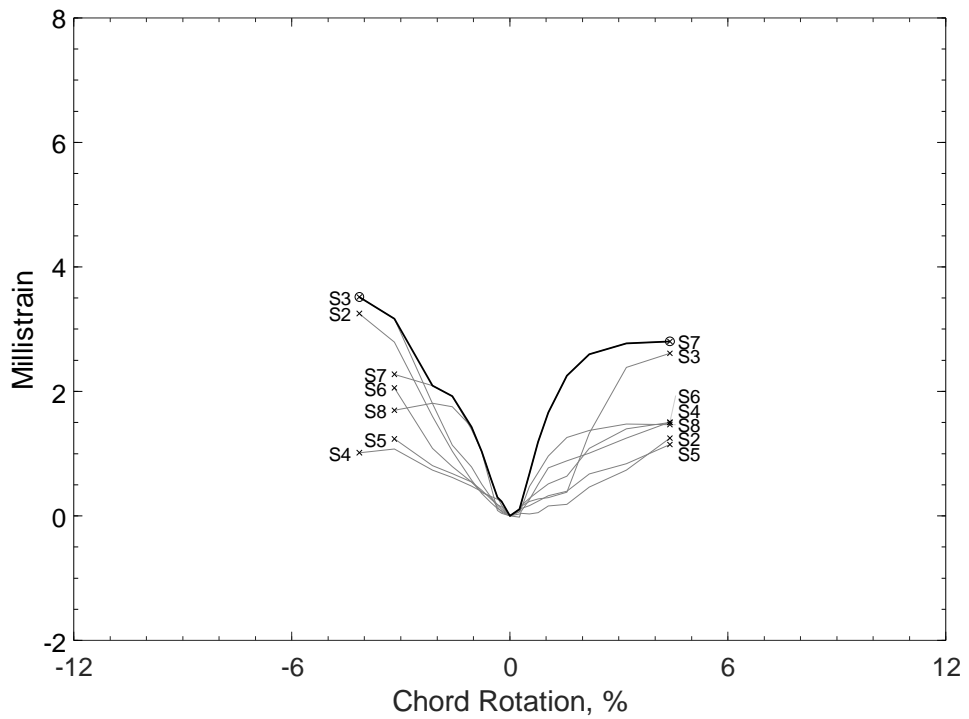


Figure 476 – Envelopes of measured strains in closed stirrups of D100-3.5, S strain gauges

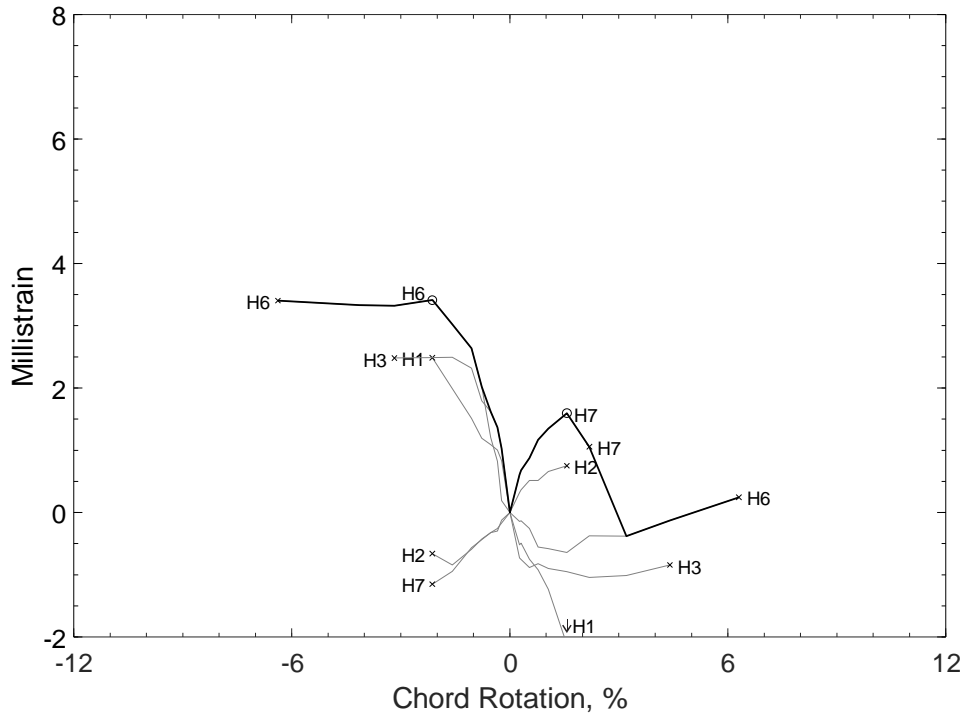


Figure 477 – Envelopes of measured strains in parallel bars of D100-3.5, H strain gauges

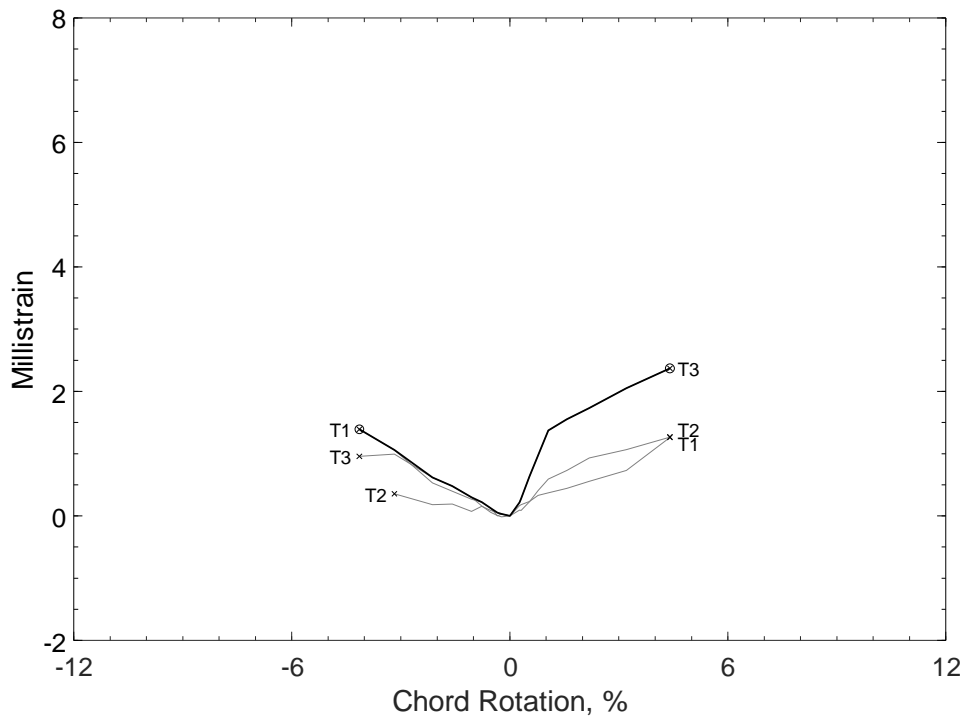


Figure 478 – Envelopes of measured strains in crosssties of D100-3.5, T strain gauges

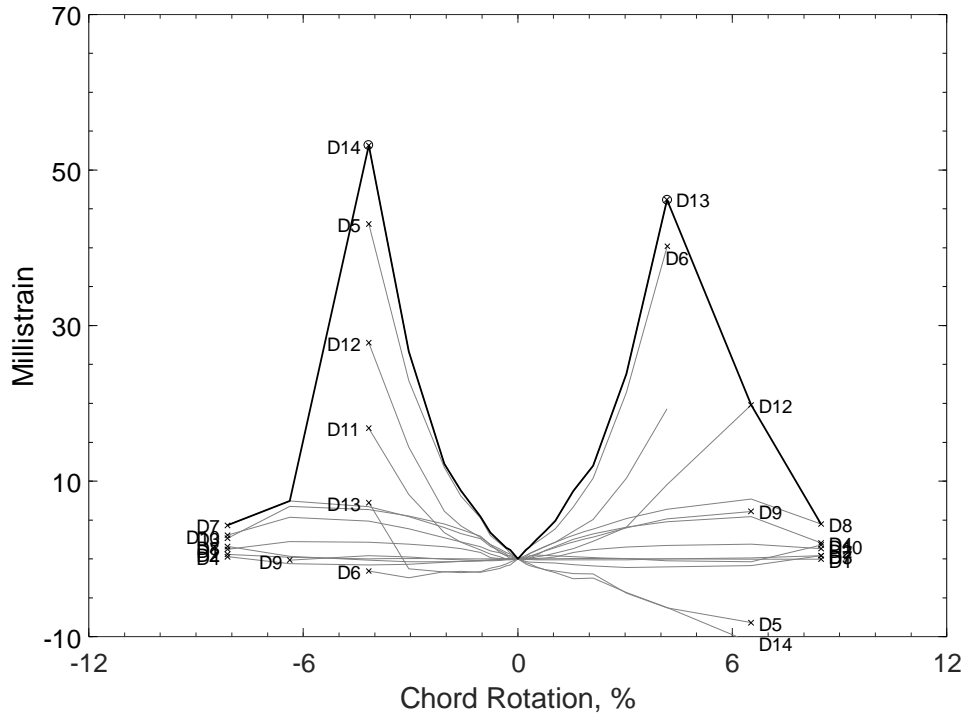


Figure 479 – Envelopes of measured strains in diagonal bars of D120-3.5, D strain gauges

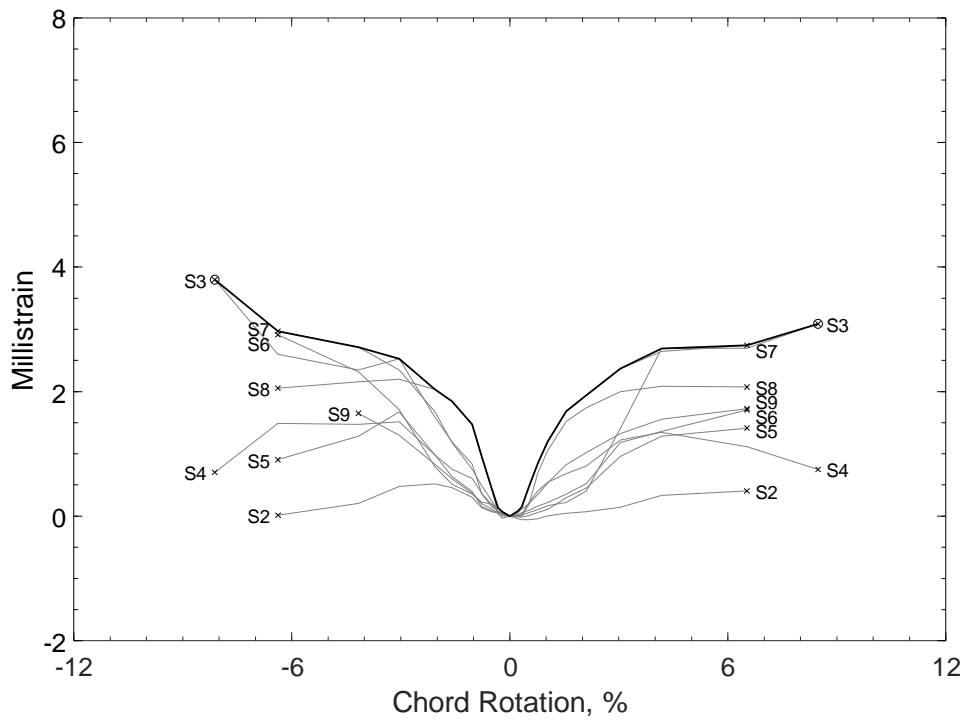


Figure 480 – Envelopes of measured strains in closed stirrups of D120-3.5, S strain gauges

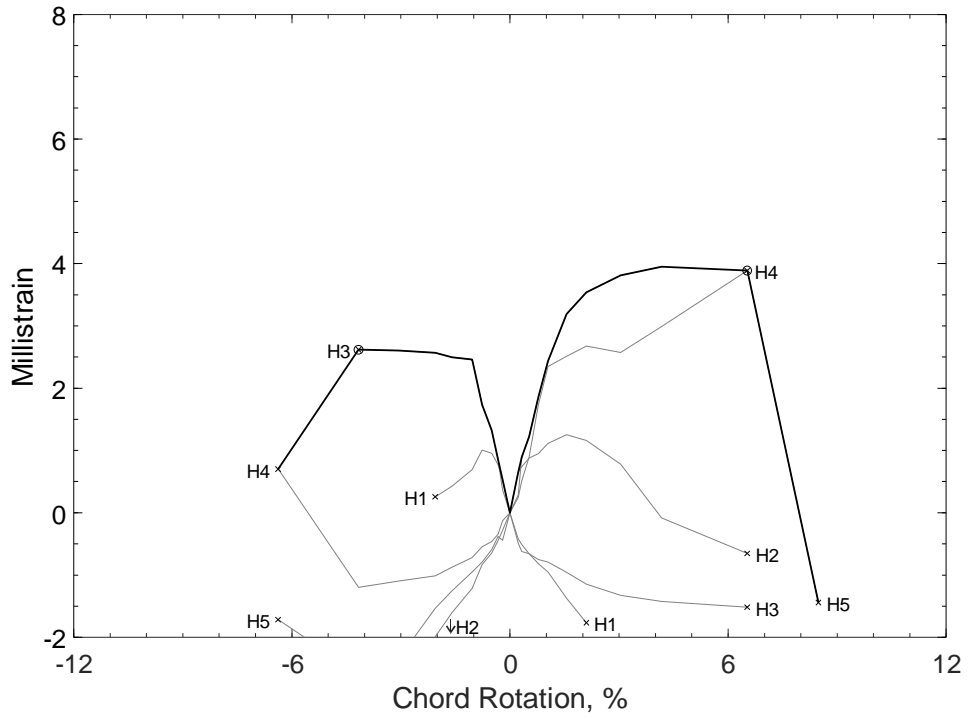


Figure 481 – Envelopes of measured strains in parallel bars of D120-3.5, H strain gauges

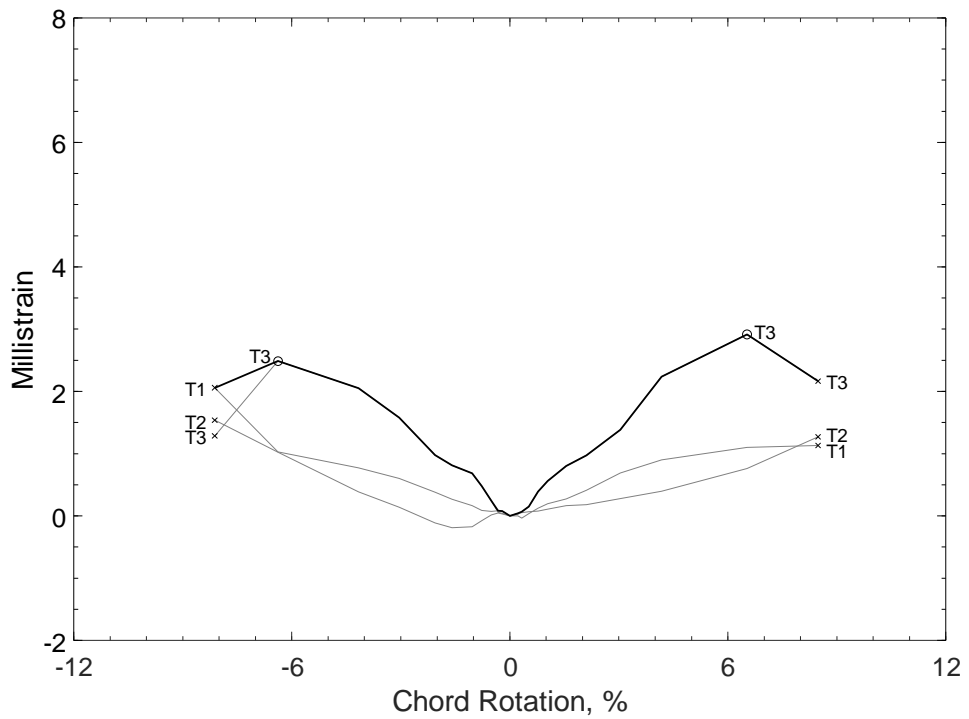


Figure 482 – Envelopes of measured strains in crosssties of D120-3.5, T strain gauges

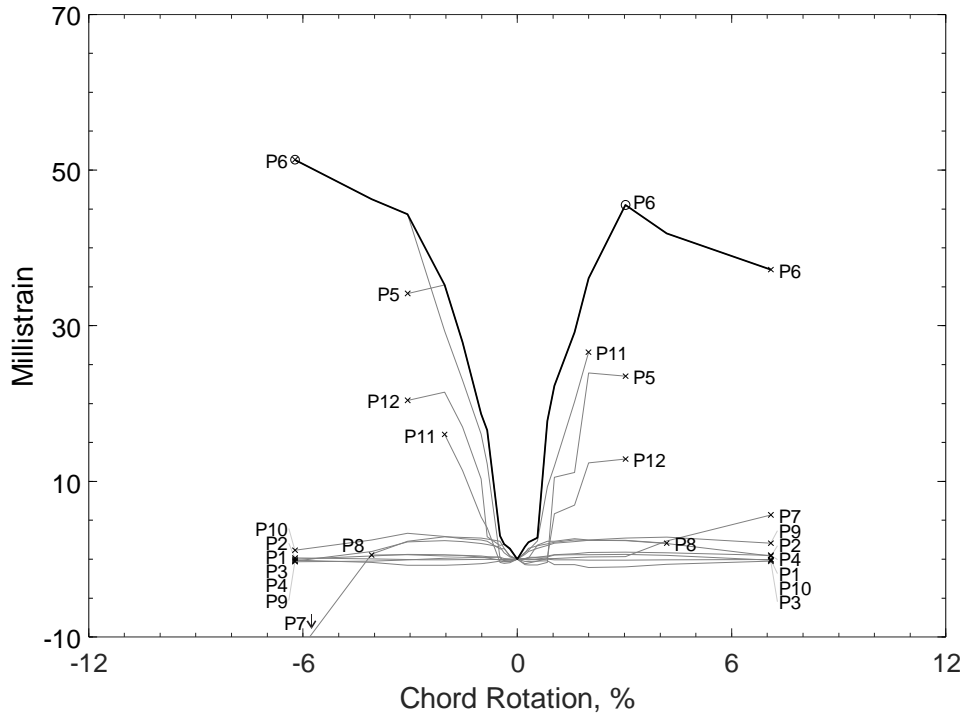


Figure 483 – Envelopes of measured strains in parallel bars of P80-2.5, P strain gauges

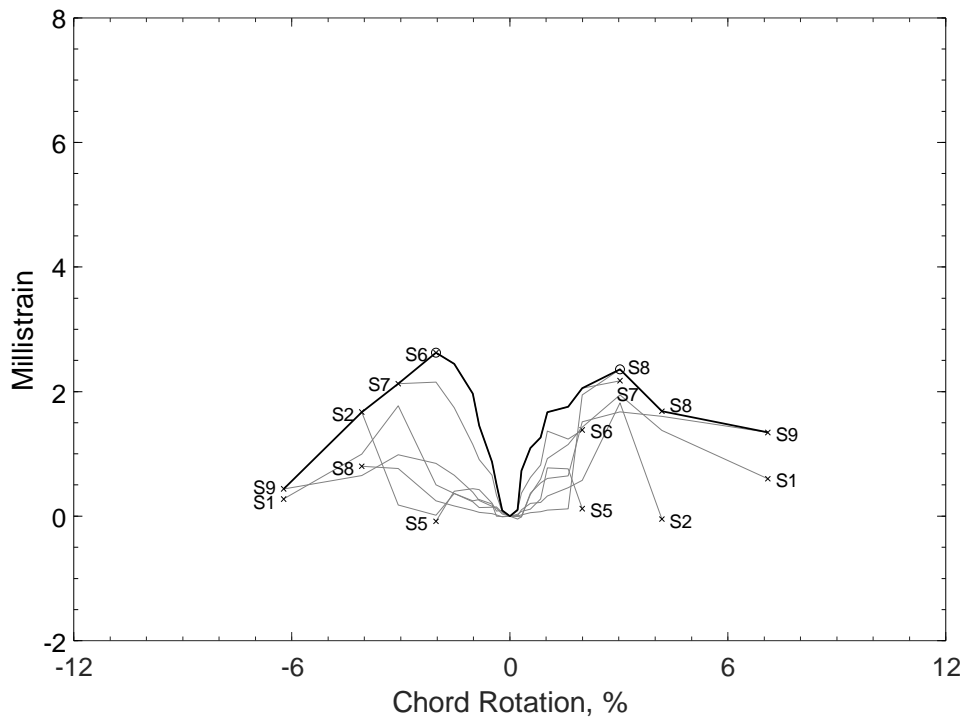


Figure 484 – Envelopes of measured strains in closed stirrups of P80-2.5, S strain gauges

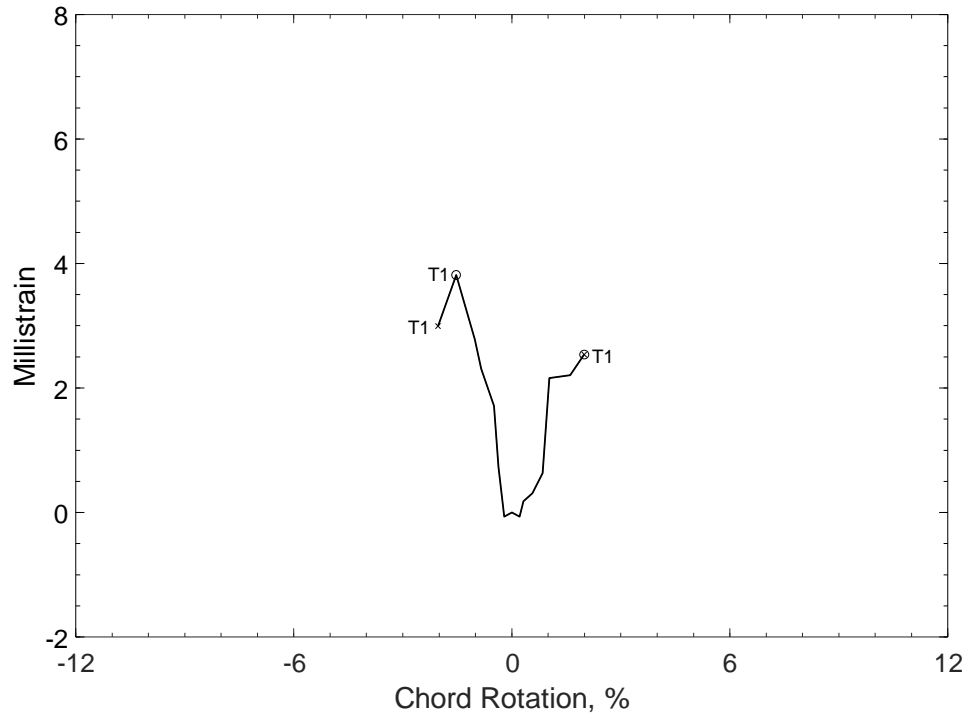


Figure 485 – Envelopes of measured strains in cross-ties of P80-2.5, T strain gauges

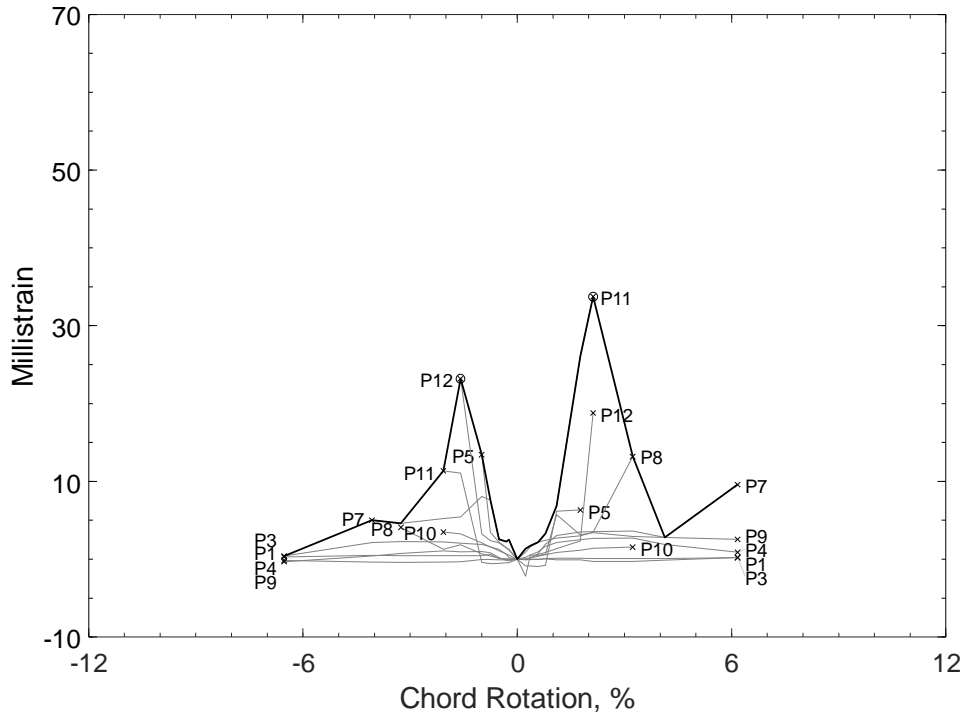


Figure 486 – Envelopes of measured strains in parallel bars of P100-2.5, P strain gauges

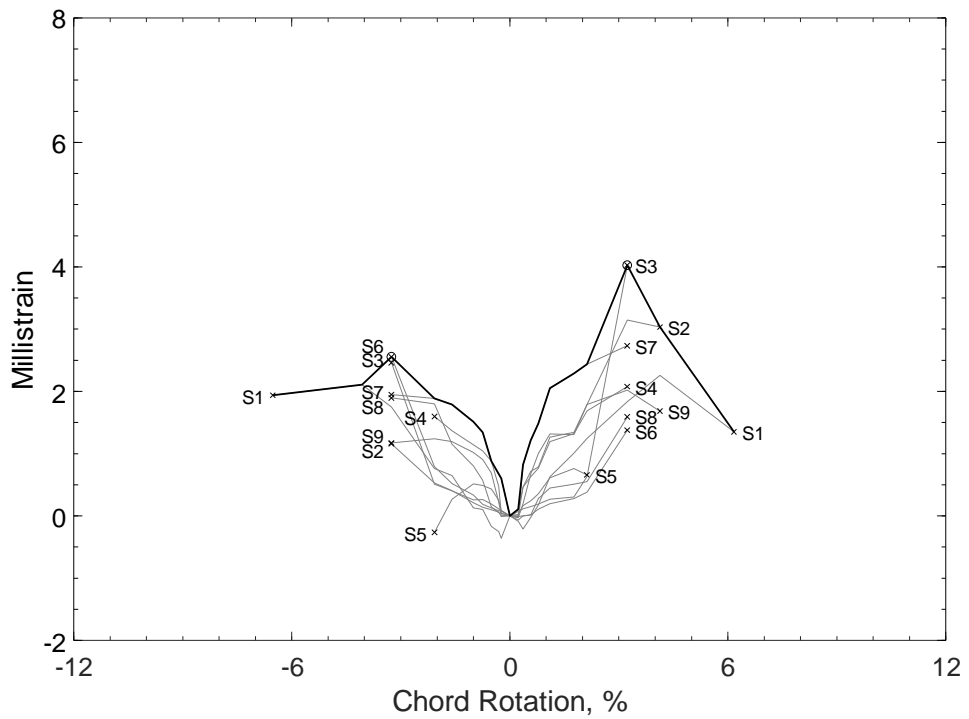


Figure 487 – Envelopes of measured strains in closed stirrups of P100-2.5, S strain gauges

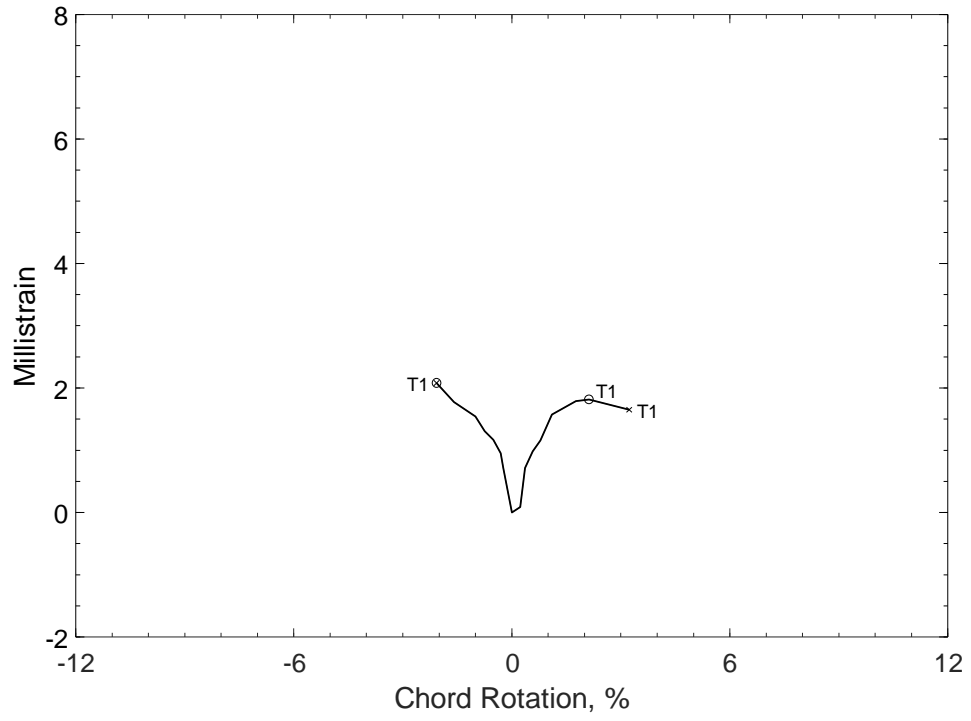


Figure 488 – Envelopes of measured strains in cross-ties of P100-2.5, T strain gauges

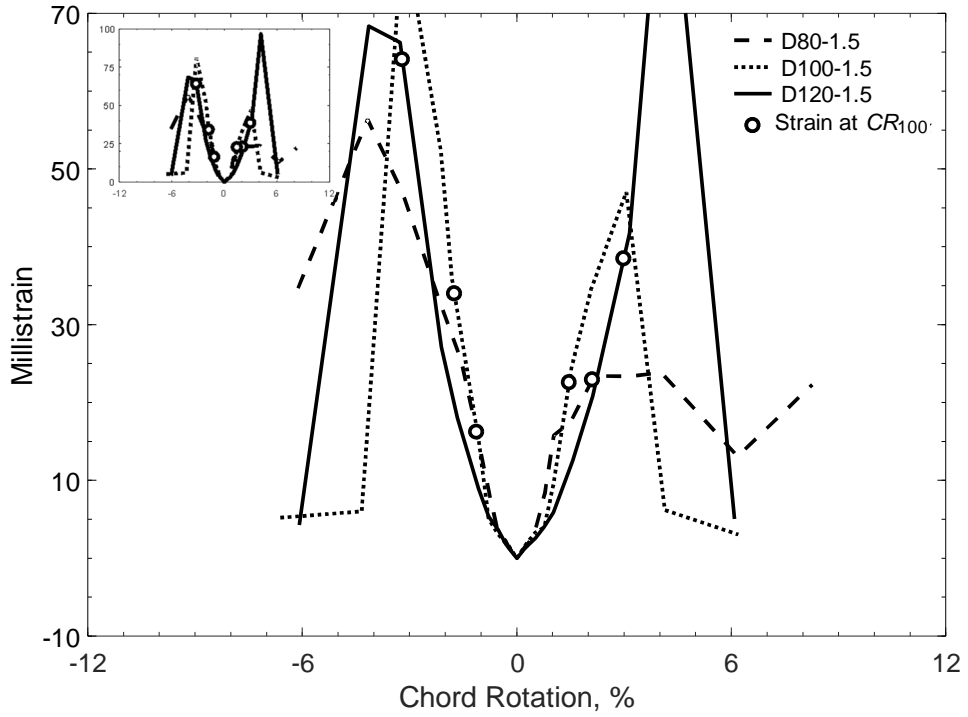


Figure 489 – Envelopes of measured strains in diagonal bars of D-type beams with an aspect ratio of 1.5, D strain gauges

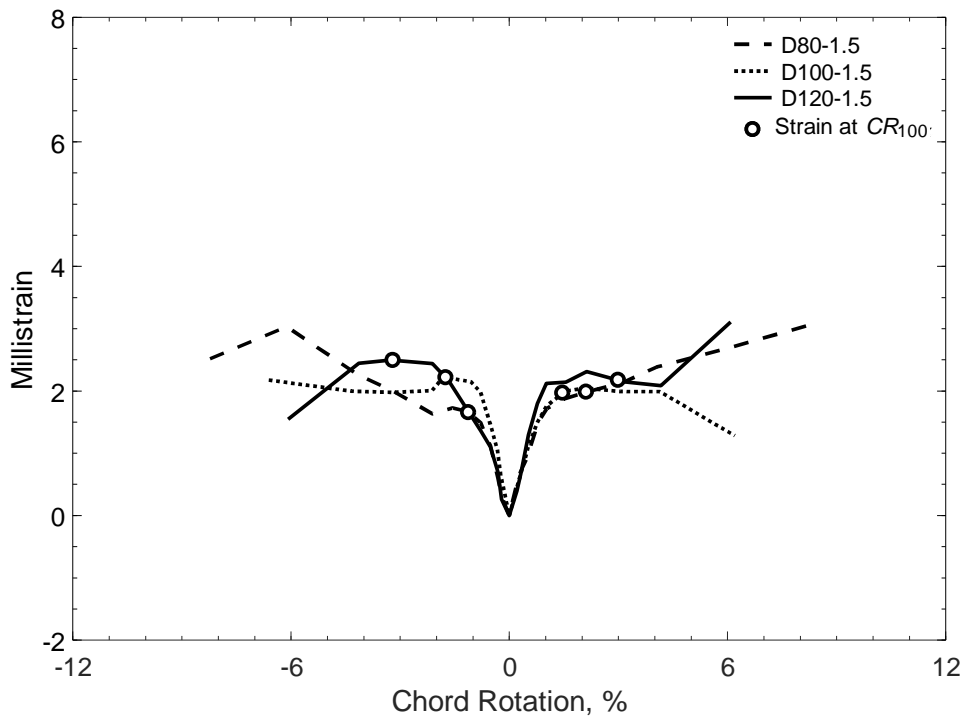


Figure 490 – Envelopes of measured strains in closed stirrups of D-type beams with an aspect ratio of 1.5, S strain gauges

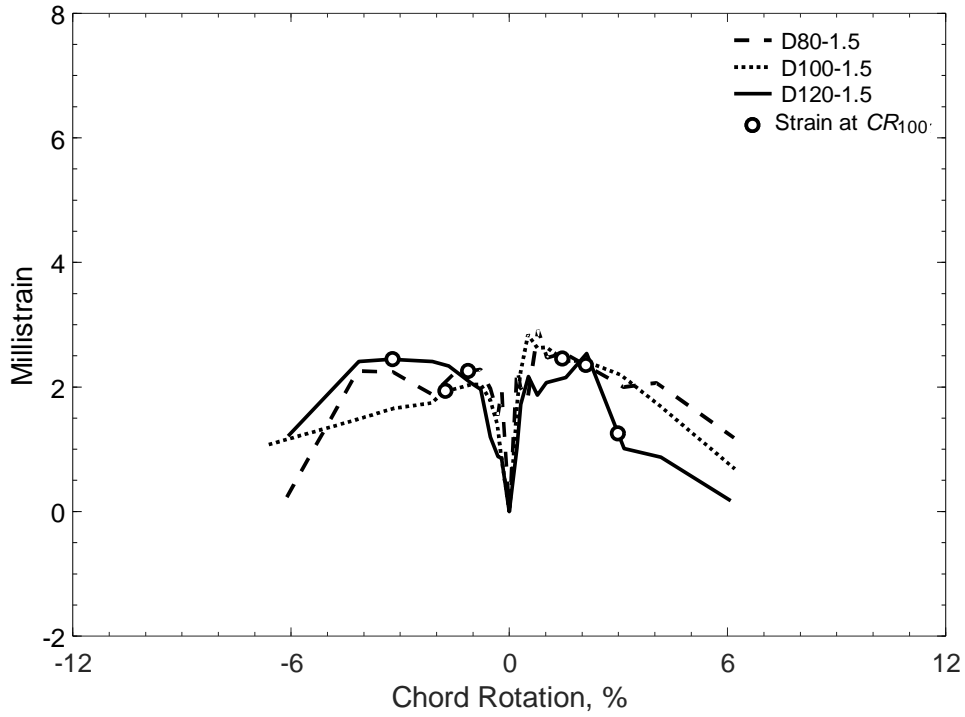


Figure 491 – Envelopes of measured strains in parallel bars of D-type beams with an aspect ratio of 1.5, H strain gauges

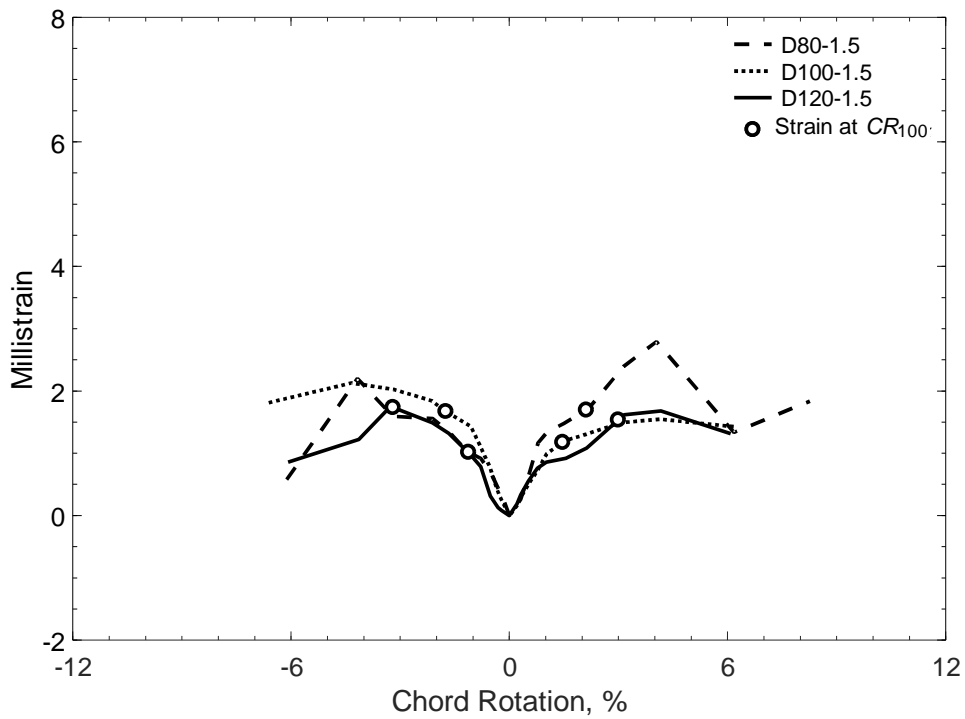


Figure 492 – Envelopes of measured strains in crosssties of D-type beams with an aspect ratio of 1.5, T strain gauges

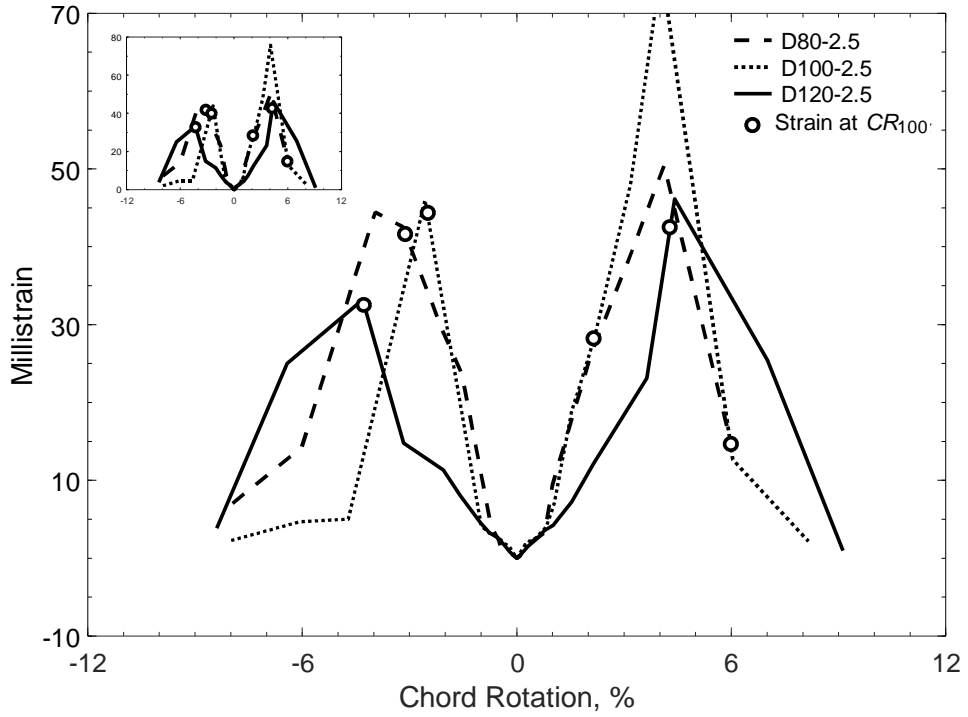


Figure 493 – Envelopes of measured strains in diagonal bars of D-type beams with an aspect ratio of 2.5, D strain gauges

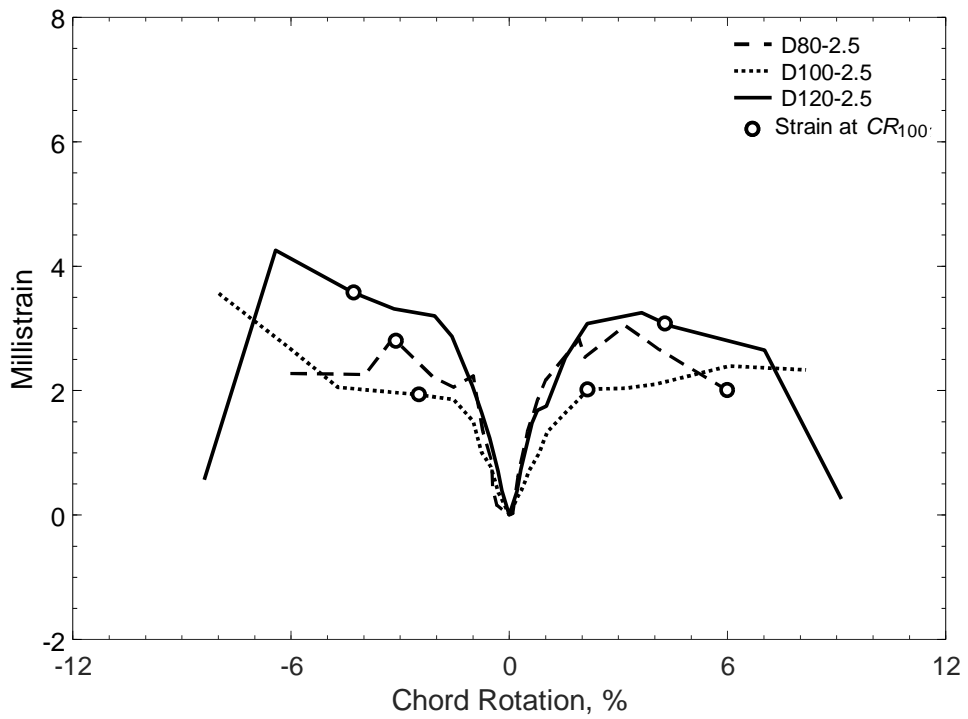


Figure 494 – Envelopes of measured strains in closed stirrups of D-type beams with an aspect ratio of 2.5, S strain gauges

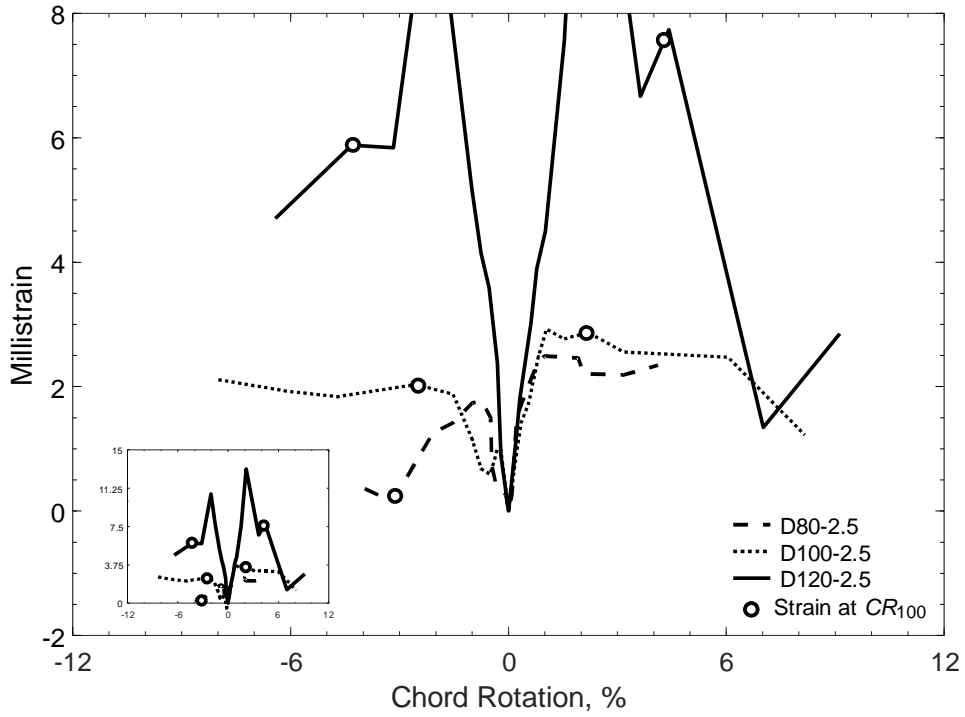


Figure 495 – Envelopes of measured strains in parallel bars of D-type beams with an aspect ratio of 2.5, H strain gauges

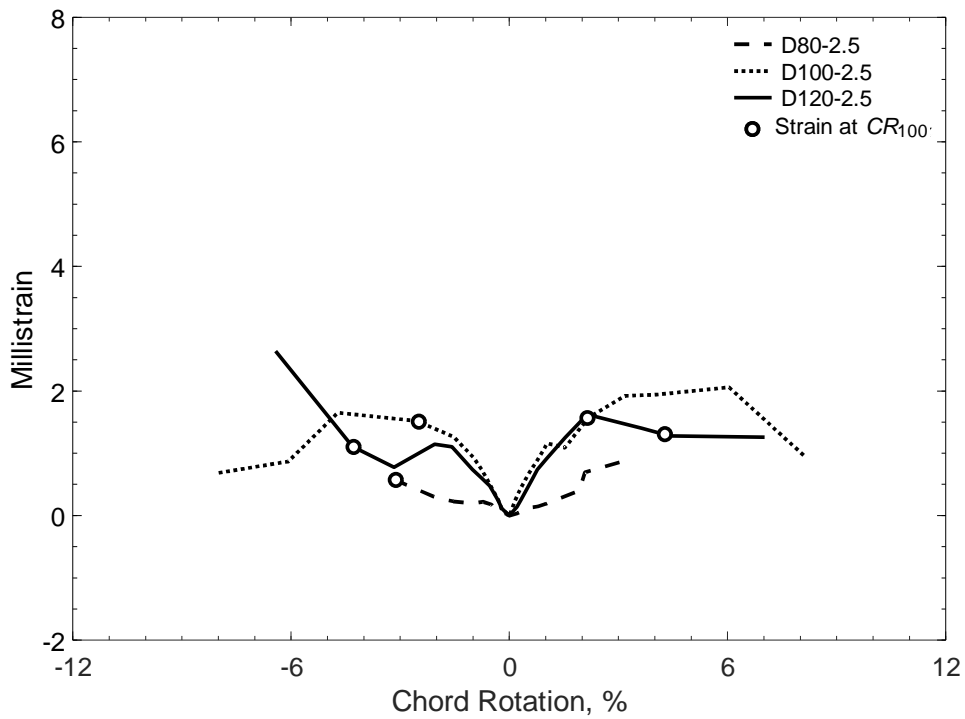


Figure 496 – Envelopes of measured strains in crosssties of D-type beams with an aspect ratio of 2.5, T strain gauges

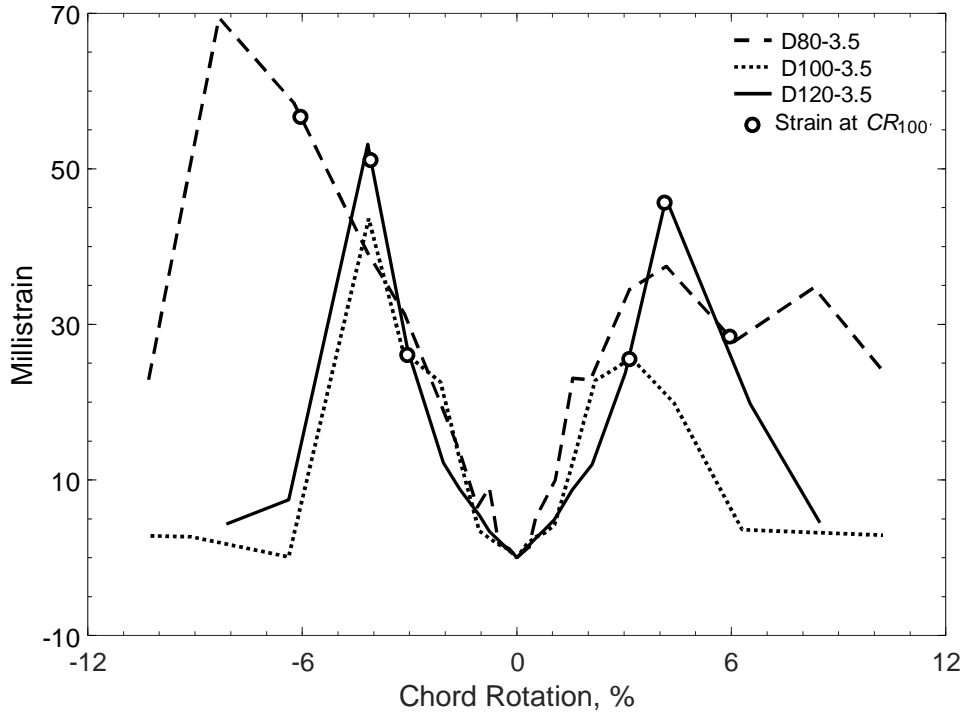


Figure 497 – Envelopes of measured strains in diagonal bars of D-type beams with an aspect ratio of 3.5, D strain gauges

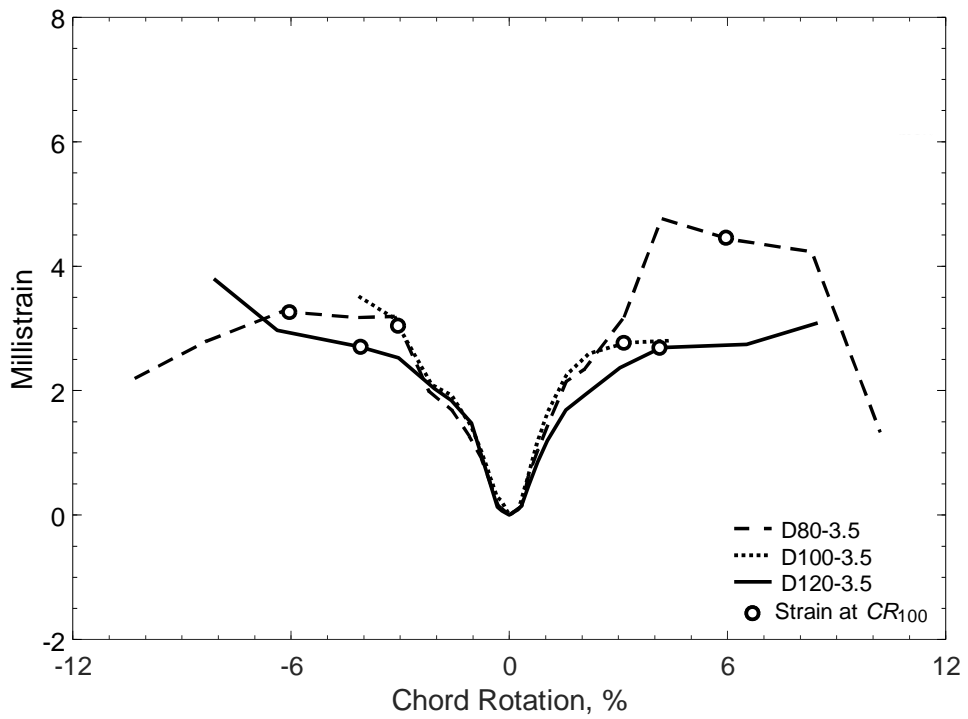


Figure 498 – Envelopes of measured strains in closed stirrups of D-type beams with an aspect ratio of 3.5, S strain gauges

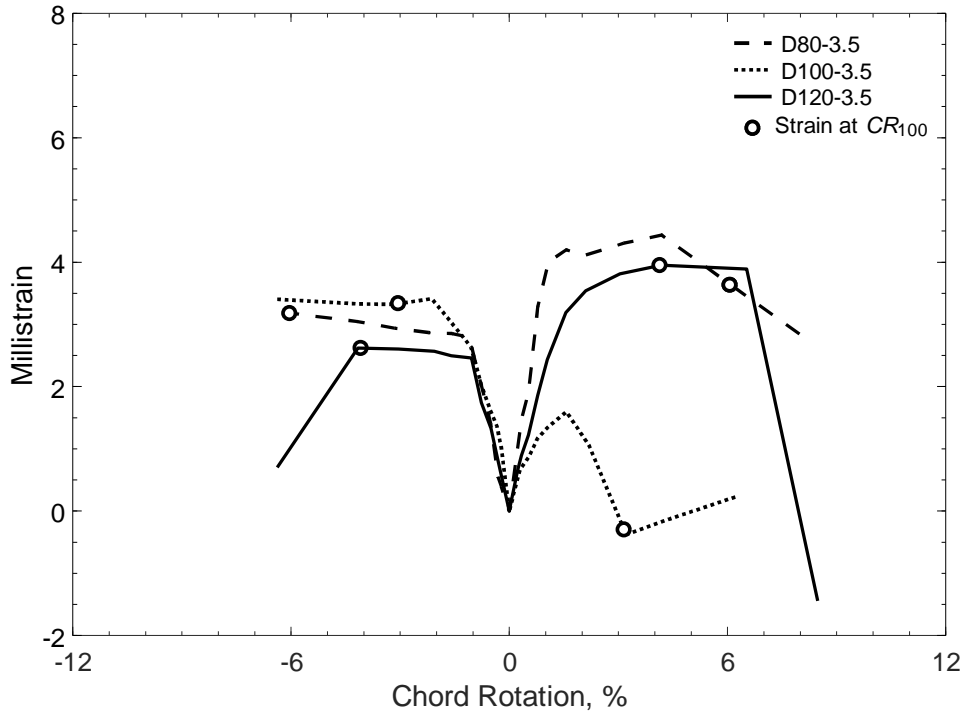


Figure 499 – Envelopes of measured strains in parallel bars of D-type beams with an aspect ratio of 3.5, H strain gauges

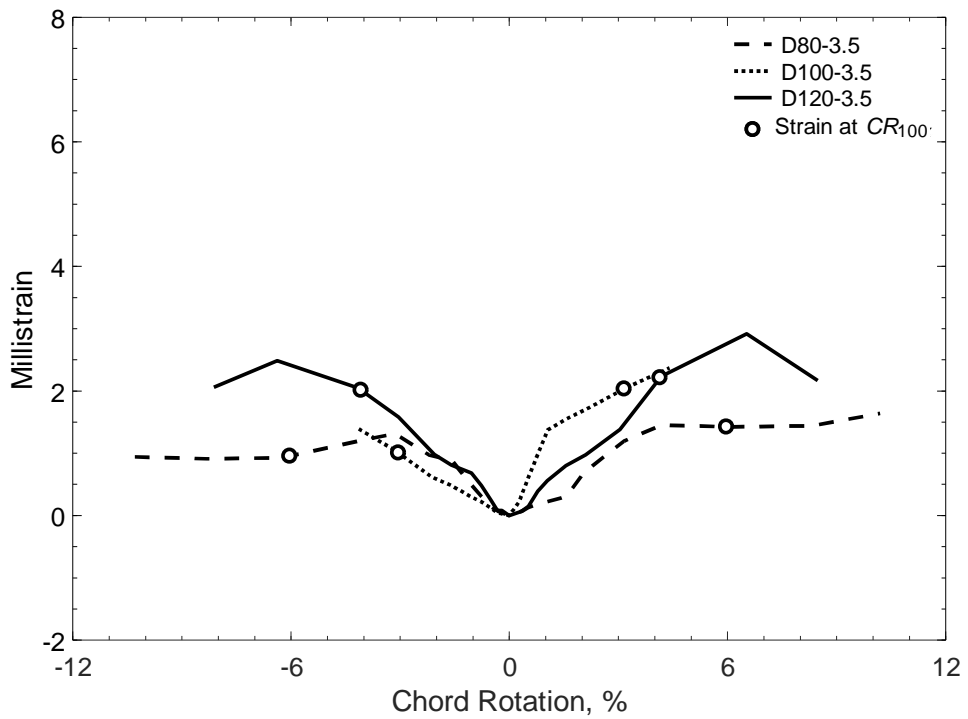


Figure 500 – Envelopes of measured strains in cross-ties of D-type beams with an aspect ratio of 3.5, T strain gauges

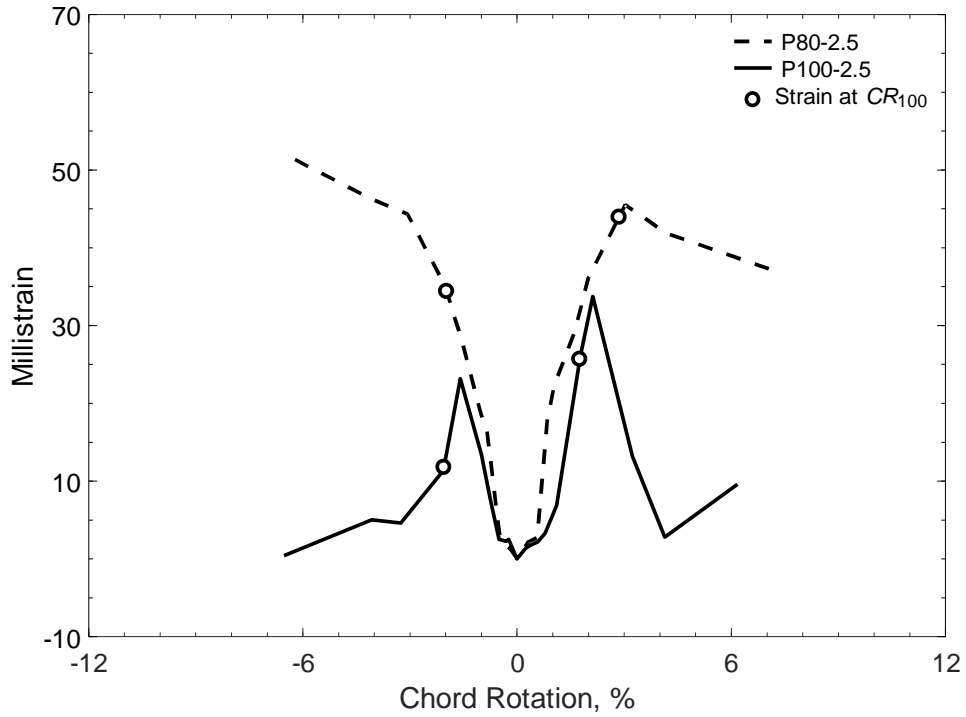


Figure 501 – Envelopes of measured strains in parallel bars of P-type beams with an aspect ratio of 2.5, P strain gauges

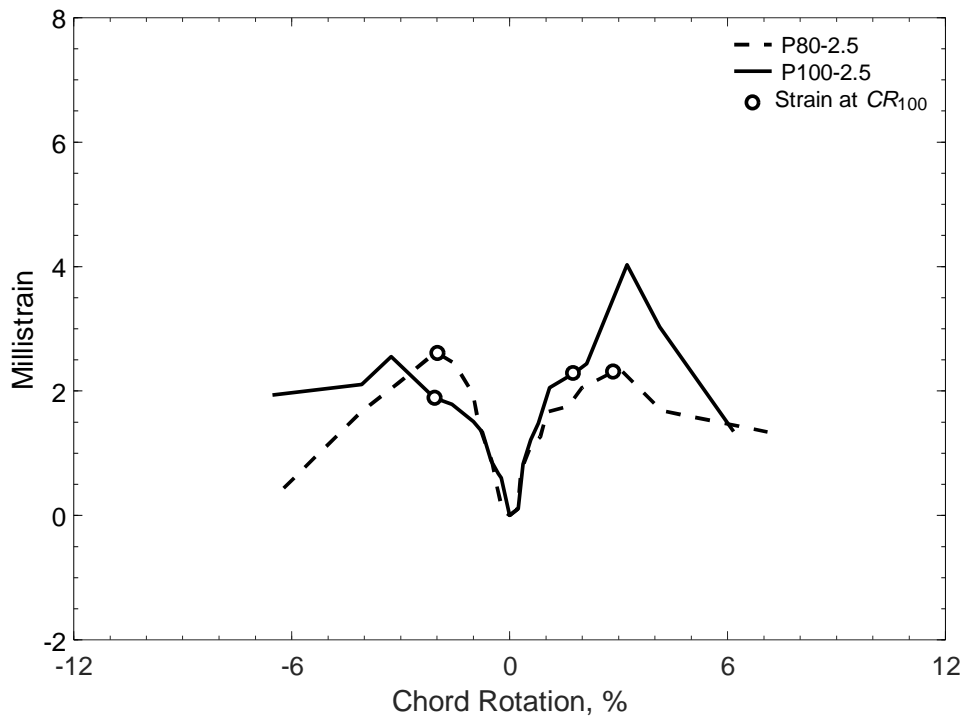


Figure 502 – Envelopes of measured strains in closed stirrups of P-type beams with an aspect ratio of 2.5, S strain gauges

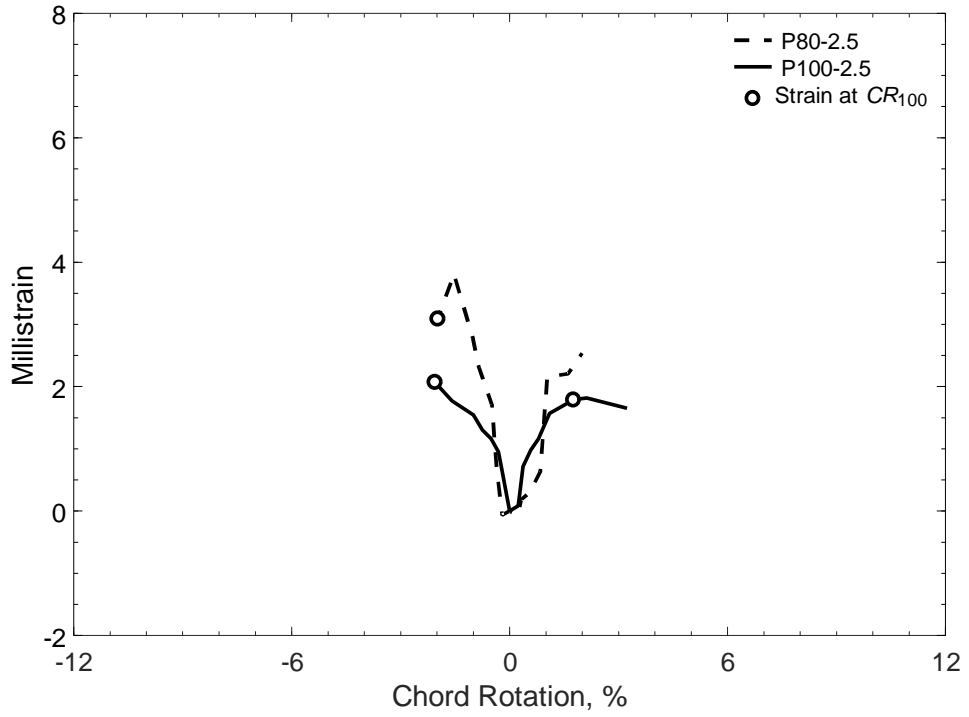


Figure 503 – Envelopes of measured strains in crossties of P-type beams with aspect ratio of 2.5, T strain gauges

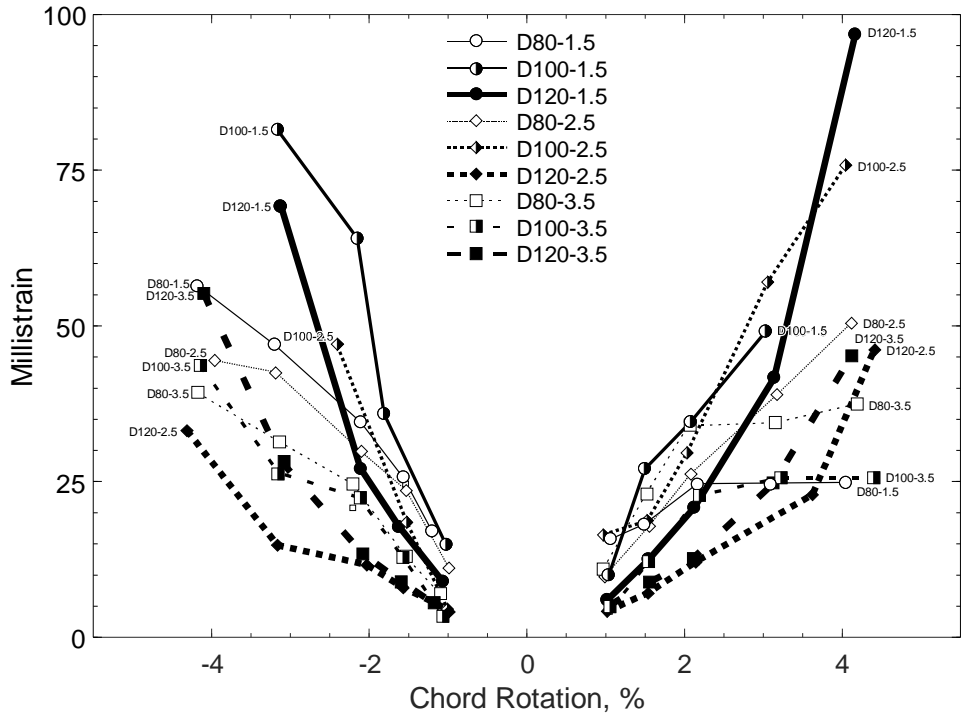


Figure 504 – Maximum strains in D-type beams during loading steps 5 through 9 (1% through 4% chord rotation), D strain gauges

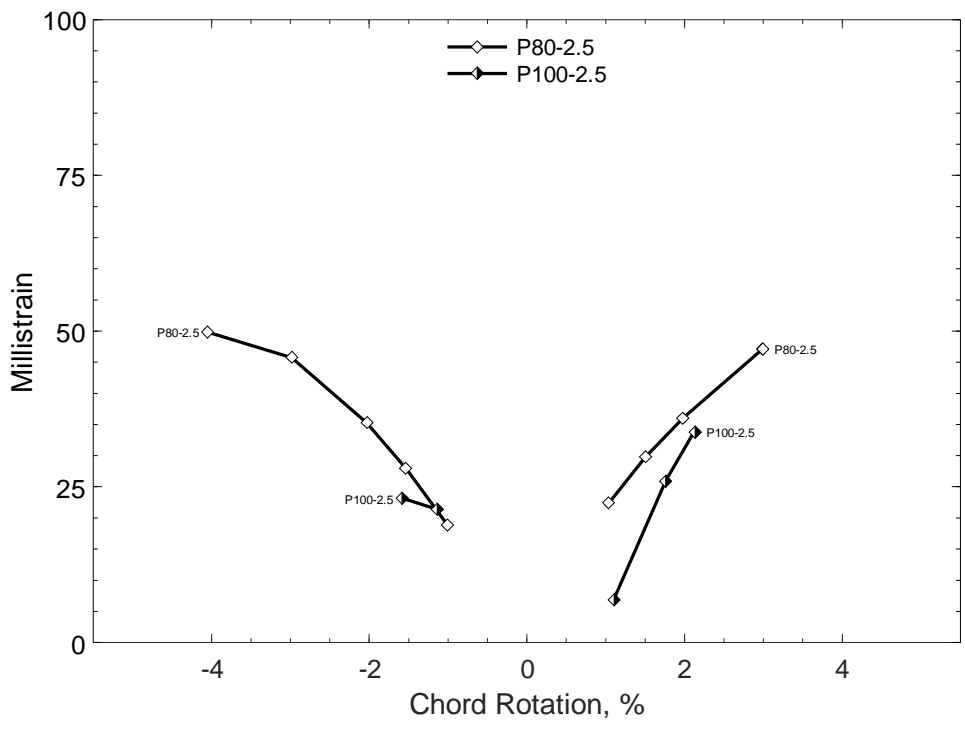


Figure 505 – Maximum strains in P-type beams during loading steps 5 through 9 (1% through 4% chord rotation), P strain gauges

APPENDIX A: NOTATION

A_{ch}	=	cross-sectional area of a member measured to the outside edges of transverse reinforcement, in. ²
A_{eff}	=	effective shear area, in. ²
A_g	=	gross area of concrete section, in. ²
A_s	=	total area of primary longitudinal reinforcement along the top or bottom face of a coupling beam with parallel reinforcement layout, in. ²
A_{sh}	=	total cross-sectional area of transverse reinforcement, including crossies, within spacing s and perpendicular to dimension b_c , in. ²
A_{vd}	=	total area of reinforcement in each group of diagonal bars in a diagonally-reinforced coupling beam, in. ²
A_w	=	shear area, $A_w = b_w h / 1.2$ (for rectangular sections), in. ²
b_c	=	cross-sectional dimension of member core measured to the outside edges of the transverse reinforcement composing area A_{sh} , in.
b_w	=	beam width, in.
c_c	=	clear cover of reinforcement, in.
CR	=	chord rotation of the coupling beam, corrected for sliding and relative rotation between the top and bottom block, rad
CR_{75}	=	chord rotation corresponding to $V = 0.75V_{max}$ on the V versus CR envelope curve (before V_{max} and for a given loading direction), rad
CR_{100}	=	chord rotation corresponding to V_{max} , rad
d	=	distance from extreme compression fiber to centroid of longitudinal tension reinforcement, in.
d_b	=	nominal diameter of the primary longitudinal reinforcing bar, in.
E_s	=	modulus of elasticity of steel reinforcement, 29,000 ksi (200,000 MPa)
E_c	=	modulus of elasticity of concrete, psi
f'_c	=	specified compressive strength of concrete, psi
f_{cm}	=	measured average compressive strength of concrete, psi

f_{ct}	=	measured average splitting tensile strength of concrete, psi
f_t	=	measured peak stress or tensile strength of reinforcement, ksi
f_y	=	specified yield stress of longitudinal reinforcement, ksi
f_{ym}	=	measured yield stress of longitudinal reinforcement, ksi
f_{yt}	=	specified yield stress of transverse reinforcement, ksi
f_{ytm}	=	measured yield stress of transverse reinforcement, ksi
G_c	=	shear modulus of concrete, $G_c = 0.4E_c$, ksi
h	=	beam height, in.
i	=	index referring to layer of reinforcement
I_{eff}	=	effective moment of inertia, in. ⁴
I_g	=	gross moment of inertia, in. ⁴
I_{tr}	=	uncracked moment of inertia of the transformed section, in. ⁴
K	=	stiffness calculated using ASCE 41-17 Table 10-19 ^[4] , kips/in.
K_e	=	secant stiffness associated with CR_{75} , kips/in.
K_S	=	secant stiffness associated with the peak force of a loading step (Tables 10 through 13), kips/in.
ℓ_e	=	minimum straight embedment length to develop a tension stress of $1.25f_y$, in.
ℓ_n	=	length of clear span measured face-to-face of supports, in.
M_{nm}	=	calculated flexural strength corresponding to a stress of f_{ym} in the primary longitudinal reinforcement, lb-in.
M_{pr}	=	calculated flexural strength corresponding to a stress of $1.25f_y$ in the primary longitudinal reinforcement, lb-in.
n	=	total number of primary longitudinal reinforcing bars For a D-type beam, number of bars in each group of diagonal bars For a P-type beam, number of bars along the top or bottom face
s	=	spacing of transverse reinforcement, center-to-center, in.
v_e	=	calculated shear stress based on specified material properties, psi

- for a D-type beam, $v_e = 2A_{vd} f_y \sin \alpha / (b_w h)$, psi
- for a P-type beam, $v_e = (2M_{pr} / \ell_n) / (b_w d)$, psi
- v_{max} = shear stress associated with V_{max} , psi
- for a D-type beam, $v_{max} = V_{max} / (b_w h)$, psi
- for a P-type beam, $v_{max} = V_{max} / (b_w d)$, psi
- v_{nm} = shear stress associated with V_{nm} , psi
- for a D-type beam, $v_{nm} = V_{nm} / (b_w h)$, psi
- for a P-type beam, $v_{nm} = V_{nm} / (b_w d)$, psi
- V = applied shear, kips
- V_{max} = maximum applied shear, kips
- V_{nm} = calculated shear strength based on measured material properties, kips
- for a D-type beam, $V_{nm} = 2A_{vd} f_{ym} \sin \alpha$
- for a P-type beam, $V_{nm} = 2M_{nm} / \ell_n$
- α = angle of inclination of diagonal reinforcement relative to beam longitudinal axis, degrees
- δ_{bot} = displacement of the bottom block top surface, in.
- δ_{top} = displacement of the top block bottom surface, in.
- ϵ_{sf} = fracture elongation of reinforcement, in./in.
- ϵ_{su} = uniform elongation of reinforcement or strain corresponding to f_t , in./in.
- θ_{bot} = rotation of the bottom block (in the loading plane), rad
- θ_{top} = rotation of the top block (in the loading plane), rad
- ρ = ratio of A_s to $b_w d$

**APPENDIX B: SELECTED PHOTOS
OF SPECIMENS DURING CONSTRUCTION**

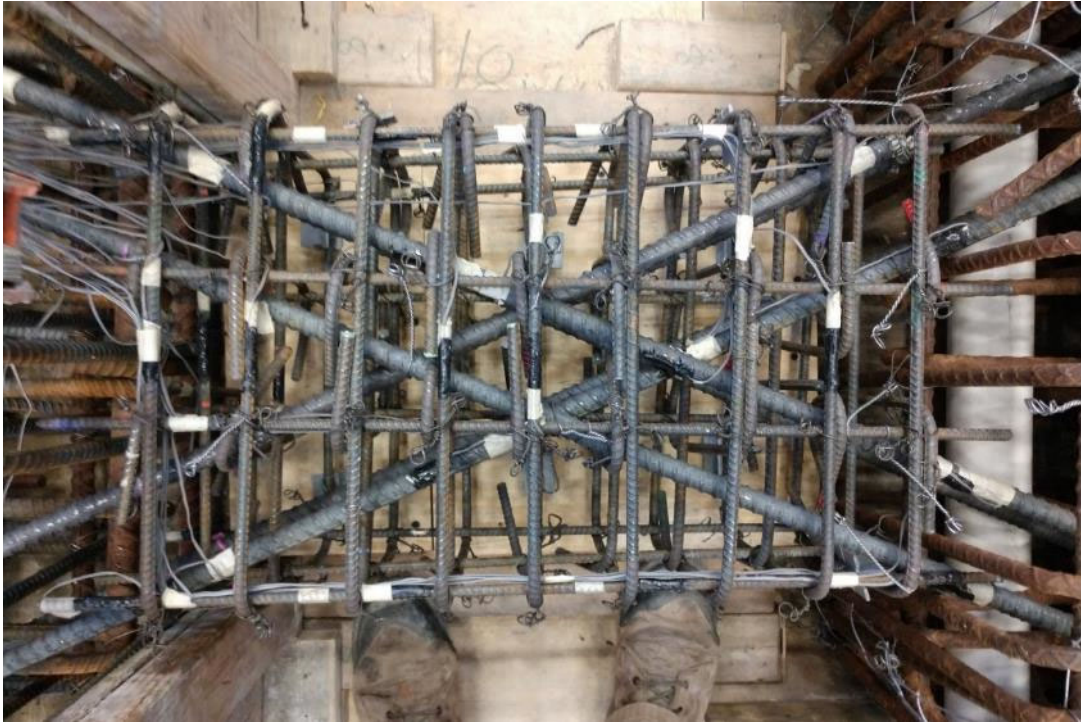


Figure B.1 – Coupling beam reinforcement, D120-1.5



Figure B.2 – Coupling beam reinforcement, D120-2.5



Figure B.3 – Coupling beam reinforcement, D120-3.5



Figure B.4 – Coupling beam reinforcement, P100-2.5



Figure B.5 – Base block reinforcement,
typical of beams with aspect ratios of 2.5 and 3.5

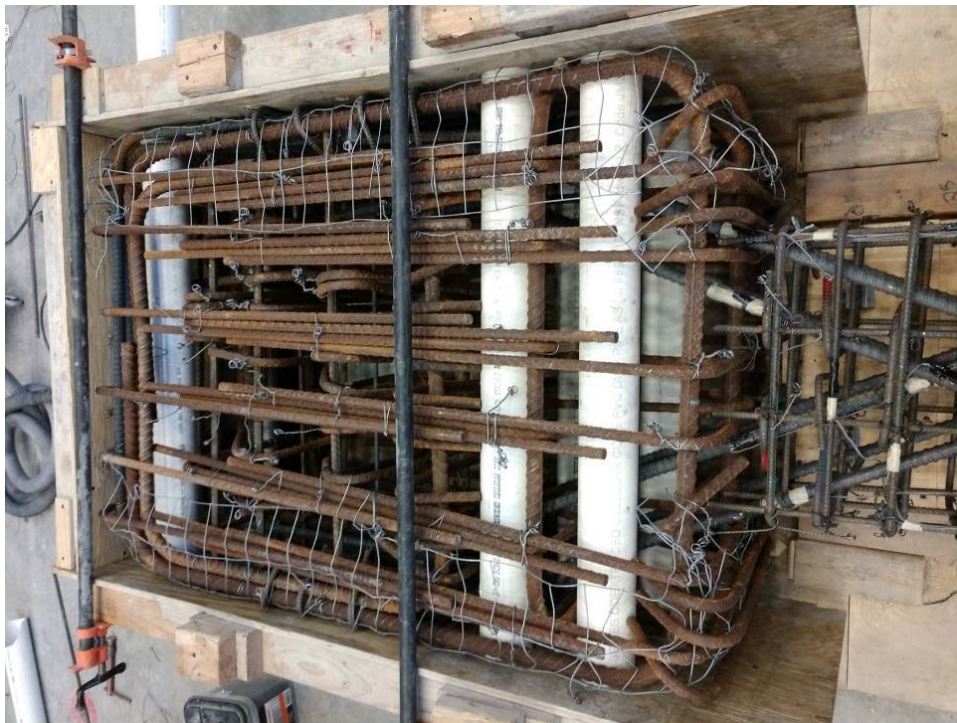


Figure B.6 –Top block reinforcement
typical of beams with aspect ratios of 2.5 and 3.5



Figure B.7 – Specimens before casting, D80-1.5, D100-1.5, and D120-1.5 (from left to right)



Figure B.8 – Specimens after formwork removal, D100-3.5, D80-3.5, P100-2.5, P80-2.5, D100-2.5, and D80-2.5 (from left to right)

**APPENDIX C: SELECTED PHOTOS
OF SPECIMENS DURING TESTING**

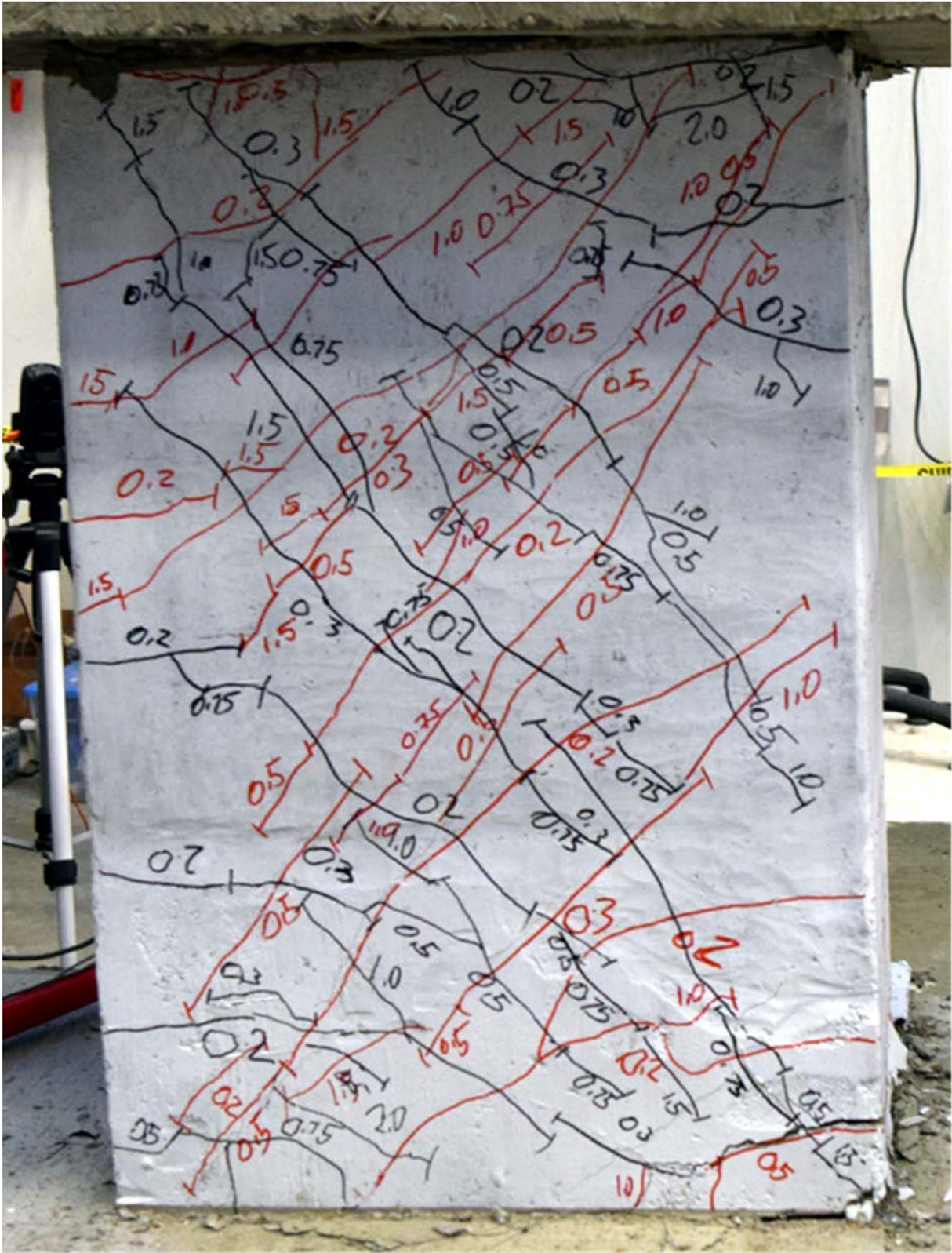


Figure C.1 – D80-1.5 during second cycle to 2% chord rotation

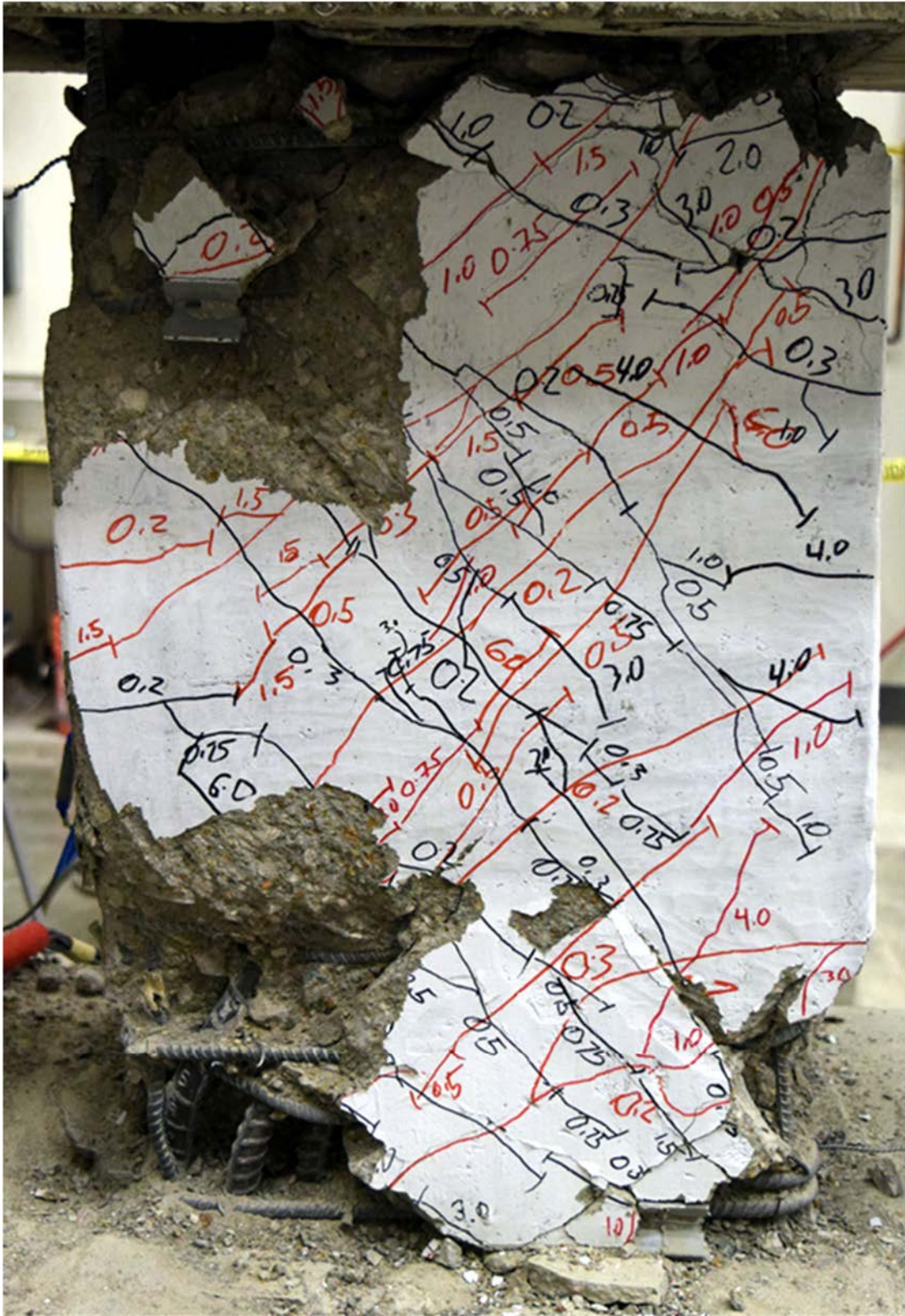


Figure C.2 – D80-1.5 during second cycle to 6% chord rotation



Figure C.3 – D80-1.5 at +2% chord rotation, second cycle



Figure C.4 – D80-1.5 at -2% chord rotation, second cycle



Figure C.5 – D80-1.5 at +4% chord rotation, second cycle



Figure C.6 – D80-1.5 at -4% chord rotation, second cycle



Figure C.7 – D80-1.5 at +6% chord rotation, second cycle



Figure C.8 – D80-1.5 at -6% chord rotation, second cycle



Figure C.9 – D80-1.5 at +8% chord rotation, first cycle



Figure C.10 – D80-1.5 at -8% chord rotation, first cycle

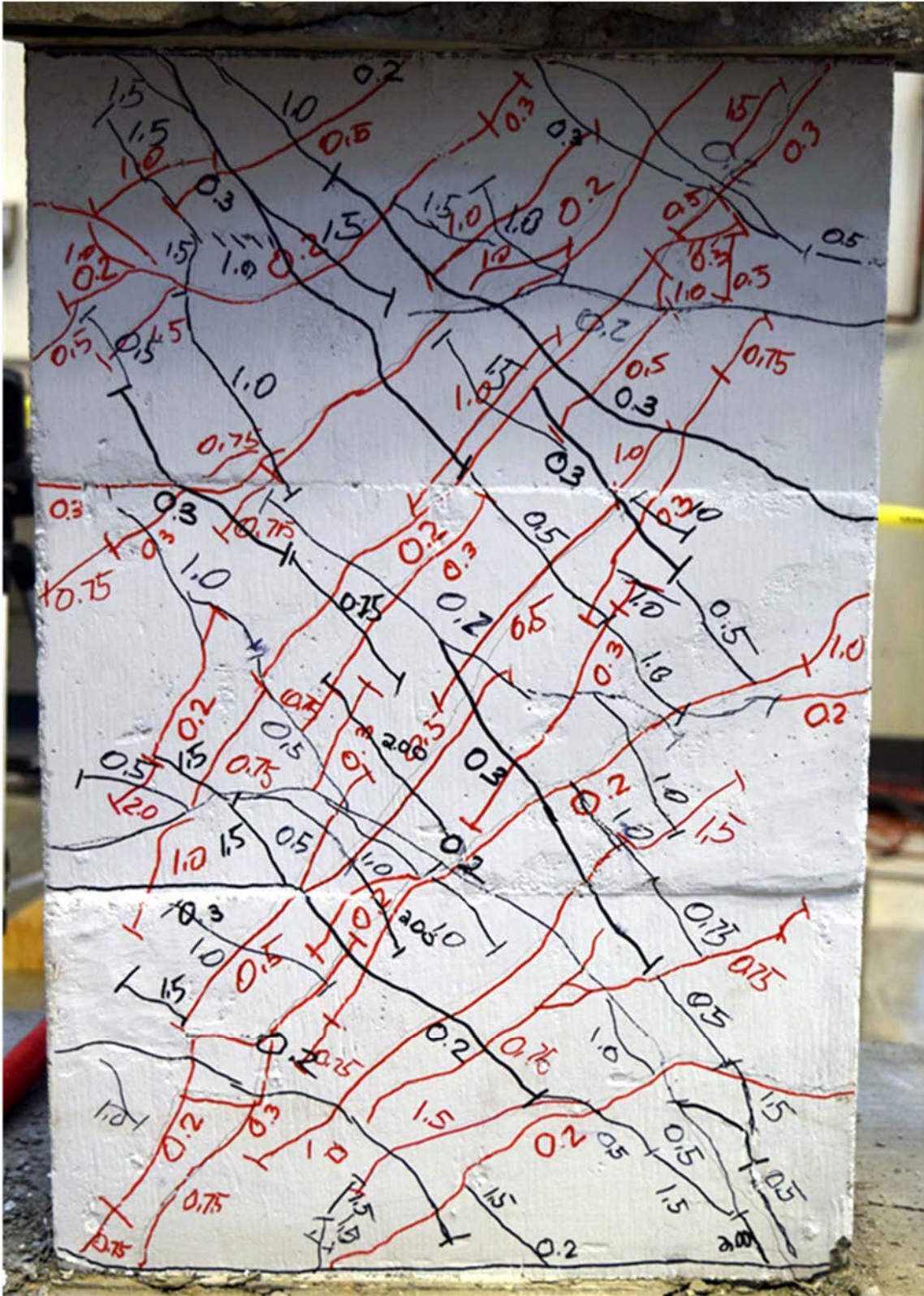


Figure C.11 – D100-1.5 during second cycle to 2% chord rotation

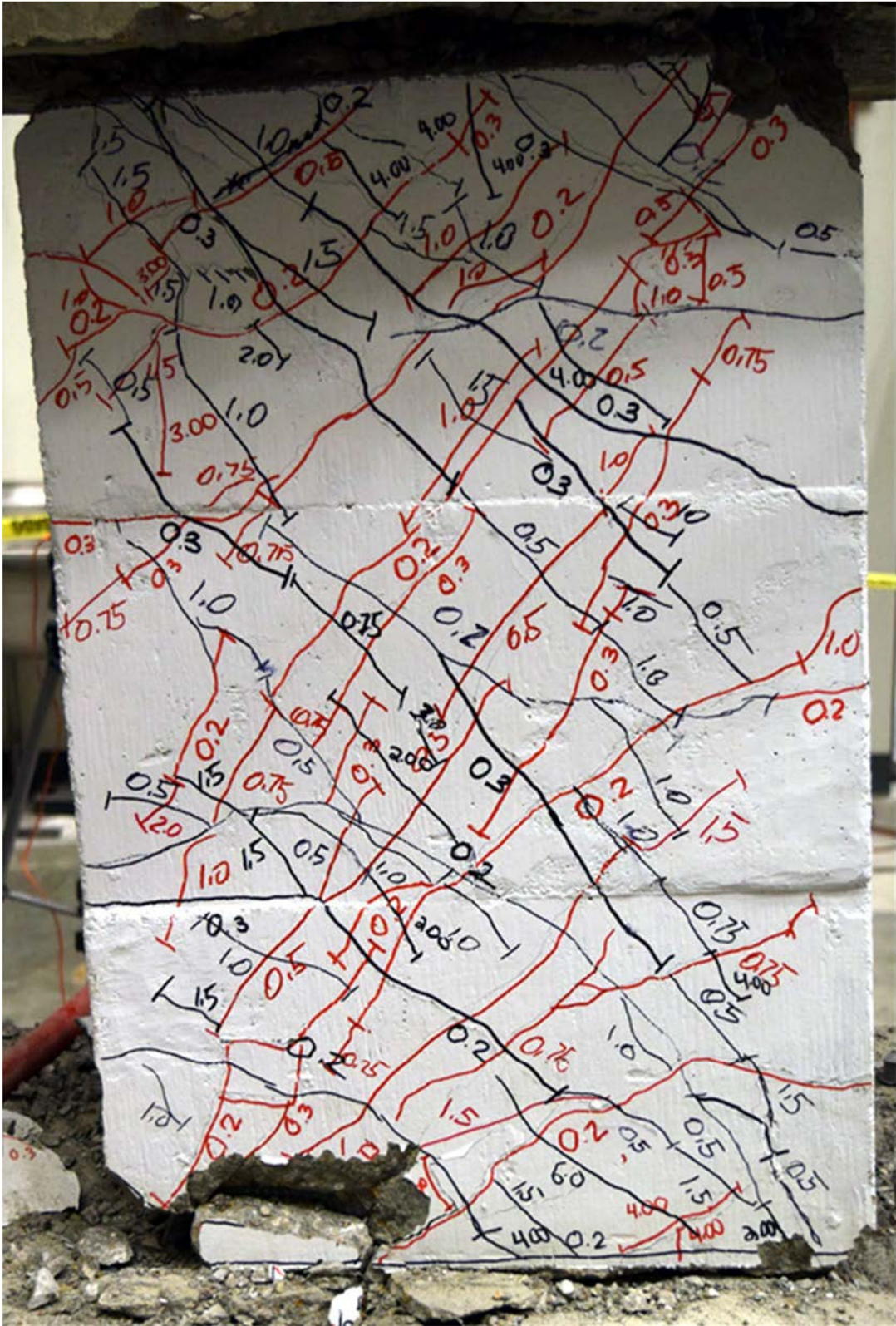


Figure C.12 – D100-1.5 during second cycle to 6% chord rotation



Figure C.13 – D100-1.5 at +2% chord rotation, second cycle



Figure C.14 – D100-1.5 at -2% chord rotation, second cycle



Figure C.15 – D100-1.5 at +4% chord rotation, second cycle



Figure C.16 – D100-1.5 at -4% chord rotation, second cycle



Figure C.17 – D100-1.5 at +6% chord rotation, second cycle



Figure C.18 – D100-1.5 at -6% chord rotation, second cycle



Figure C.19 – D100-1.5 at +8% chord rotation, first cycle

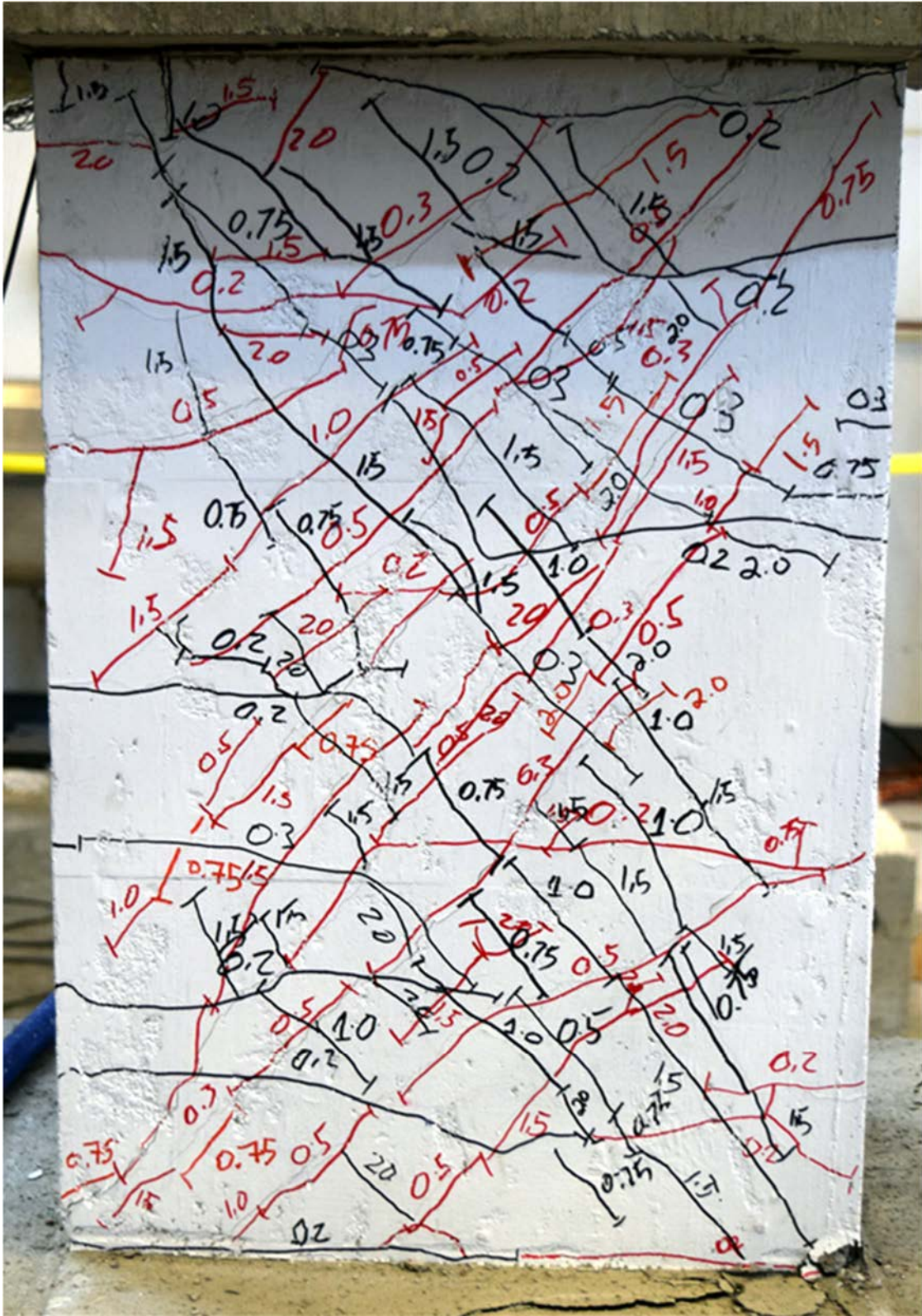


Figure C.20 – D120-1.5 during second cycle to 2% chord rotation

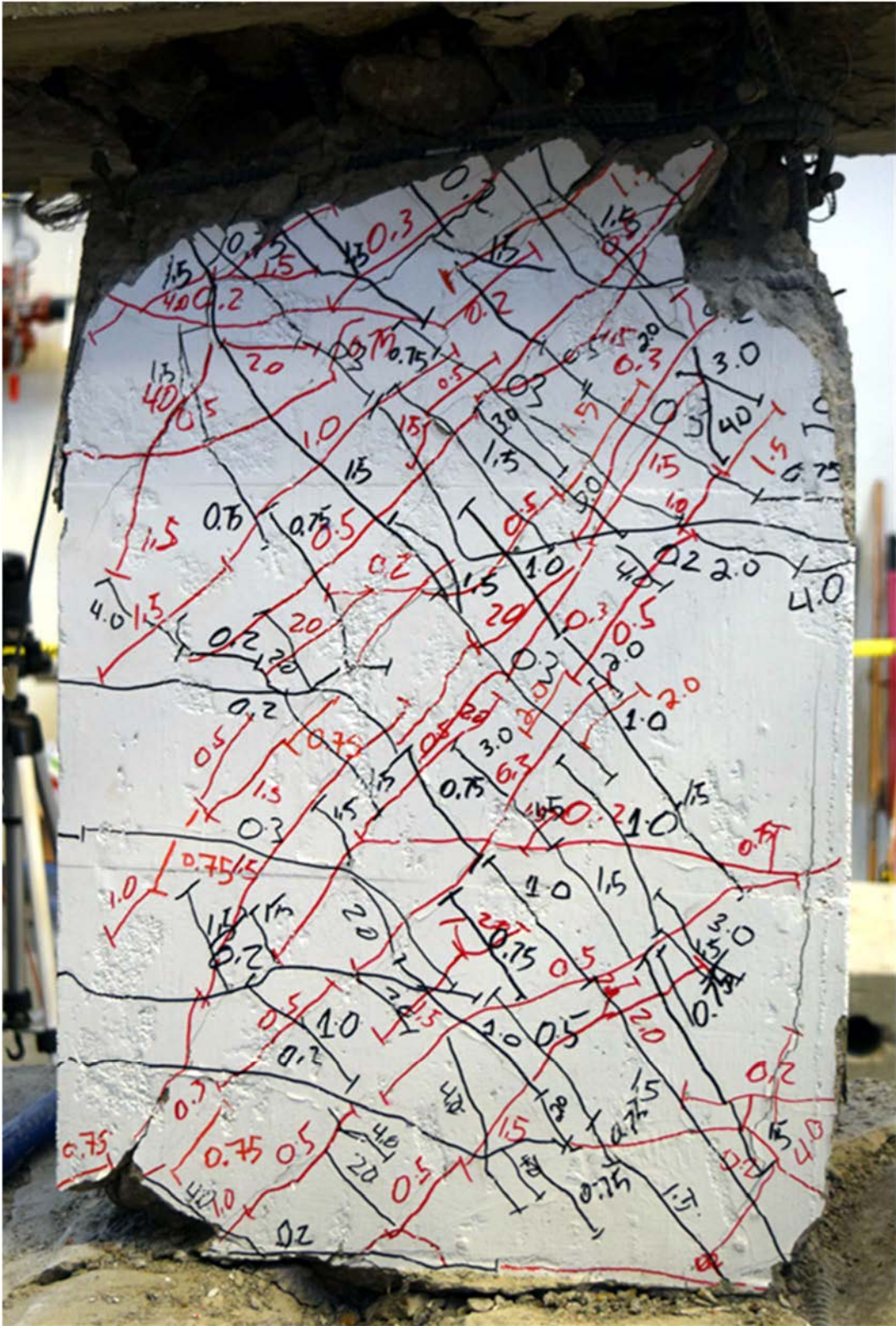


Figure C.21 – D120-1.5 during first cycle to 6% chord rotation



Figure C.22 – D120-1.5 at +2% chord rotation, second cycle

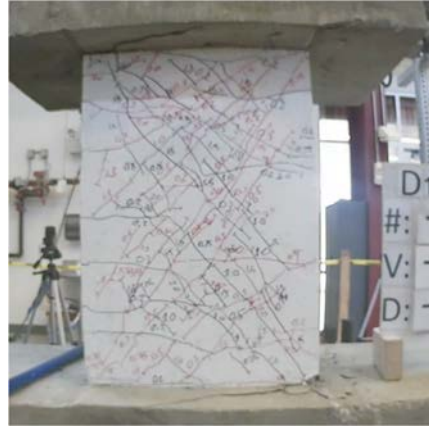


Figure C.23 – D120-1.5 at -2% chord rotation, second cycle



Figure C.24 – D120-1.5 at +4% chord rotation, second cycle



Figure C.25 – D120-1.5 at -4% chord rotation, second cycle



Figure C.26 – D120-1.5 at +6% chord rotation, first cycle



Figure C.27 – D120-1.5 at -6% chord rotation, first cycle

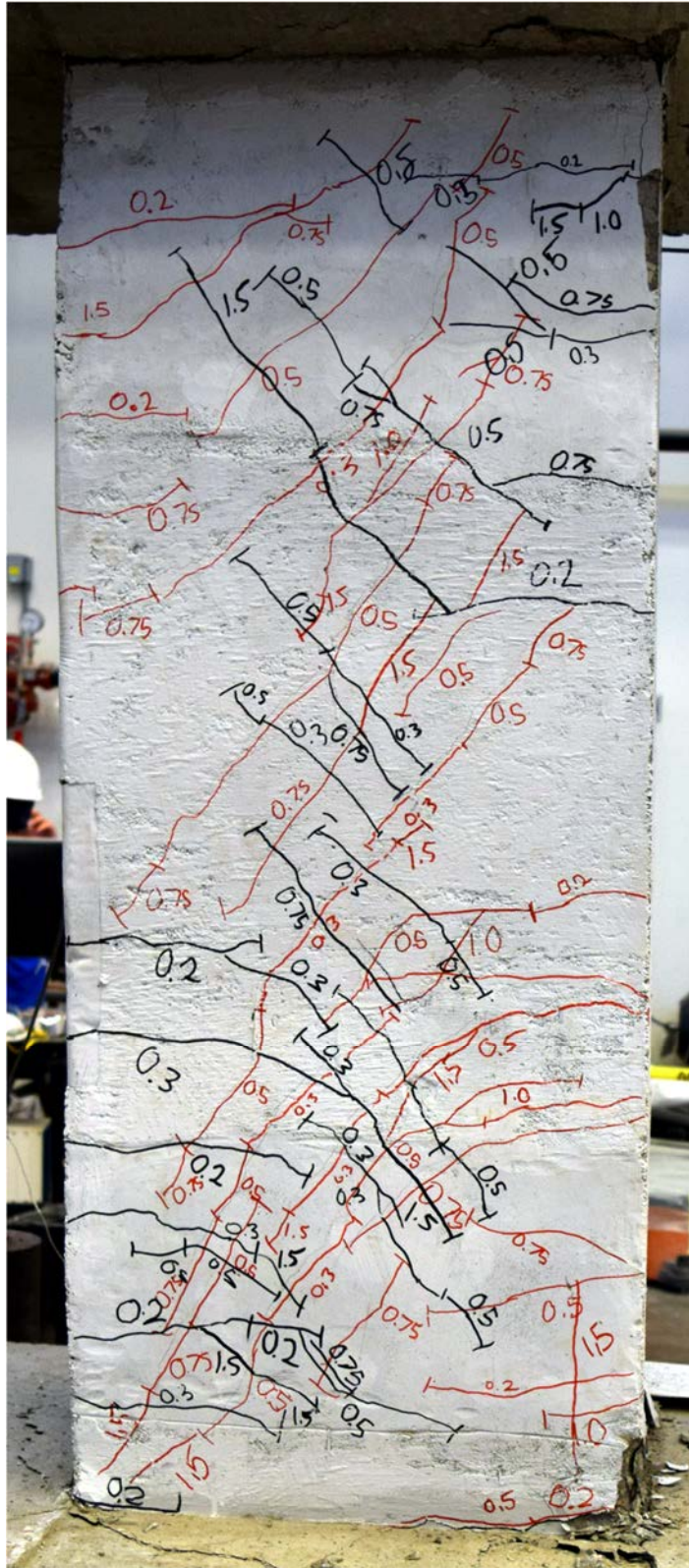


Figure C.28 – D80-2.5 during second cycle to 2% chord rotation

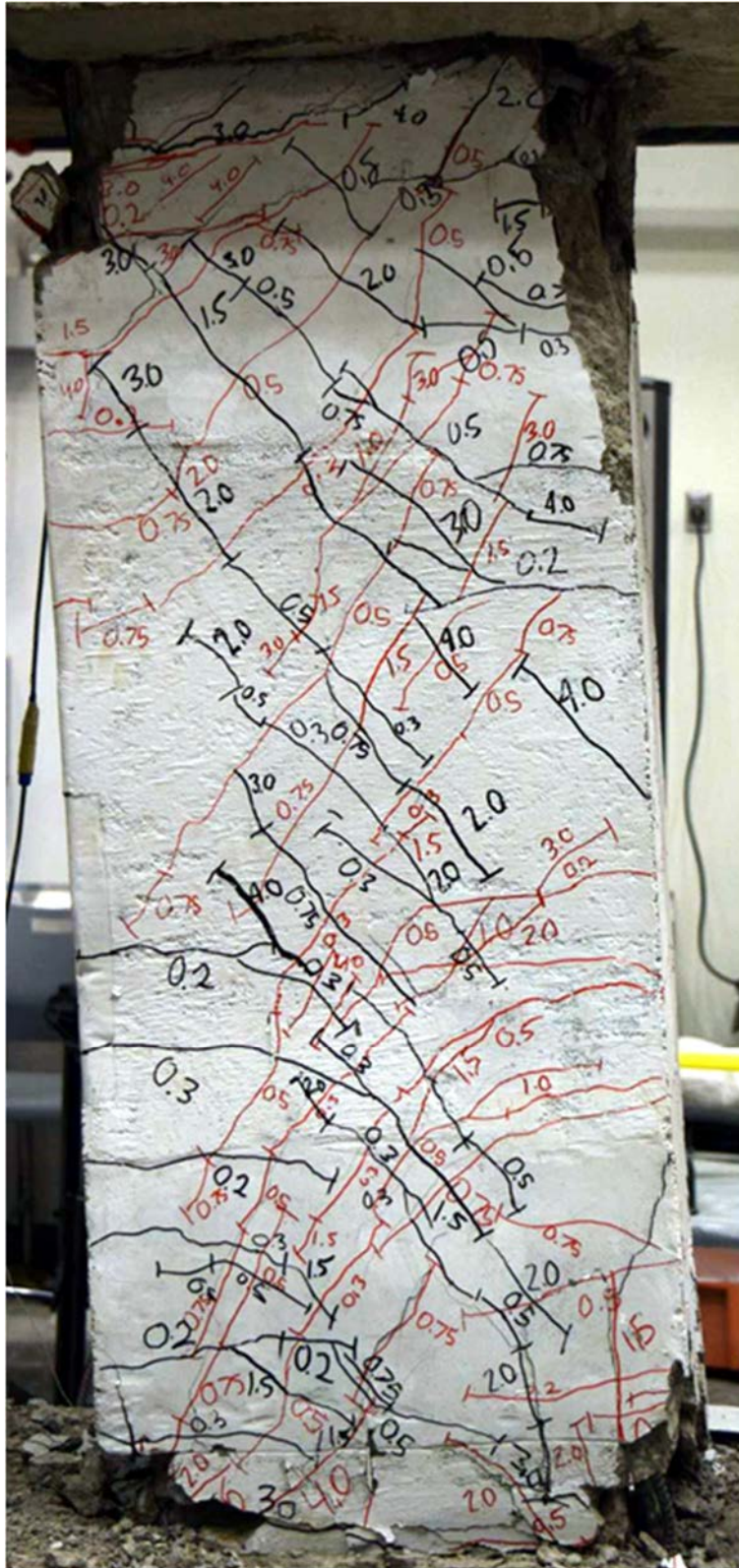


Figure C.29 – D80-2.5 during second cycle to 6% chord rotation



Figure C.30 – D80-2.5 at +2% chord rotation, second cycle

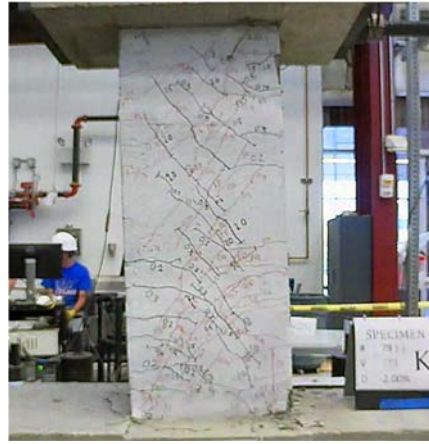


Figure C.31 – D80-2.5 at -2% chord rotation, second cycle



Figure C.32 – D80-2.5 at +4% chord rotation, second cycle



Figure C.33 – D80-2.5 at -4% chord rotation, second cycle



Figure C.34 – D80-2.5 at +6% chord rotation, second cycle



Figure C.35 – D80-2.5 at -6% chord rotation, second cycle



Figure C.36 – D80-2.5 at +8% chord rotation, second cycle



Figure C.37 – D80-2.5 at -8% chord rotation, second cycle



Figure C.38 – D80-2.5 at +10% chord rotation, first cycle



Figure C.39 – D80-2.5 at -10% chord rotation, first cycle

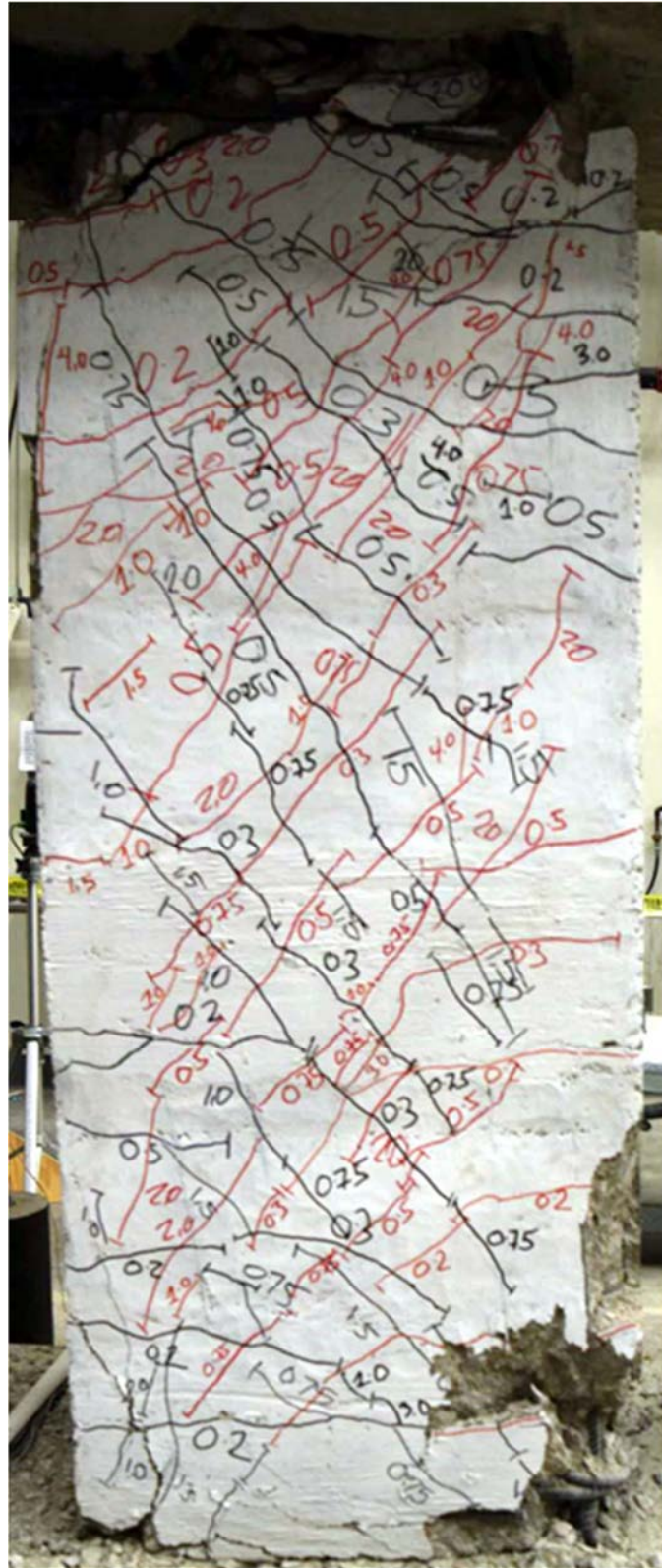


Figure C.41 – D100-2.5 during second cycle to 6% chord rotation

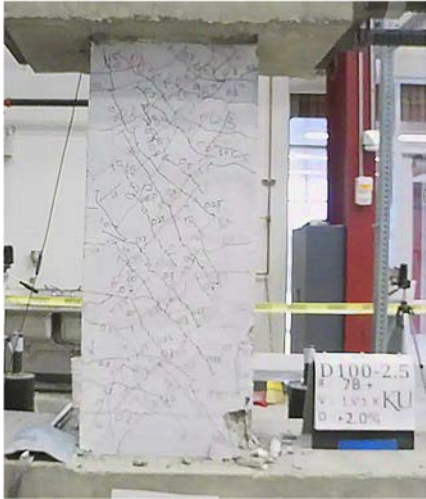


Figure C.42 – D100-2.5
at +2% chord rotation, second cycle

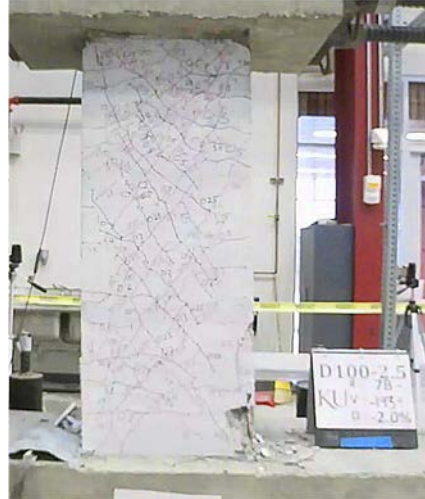


Figure C.43 – D100-2.5
at -2% chord rotation, second cycle

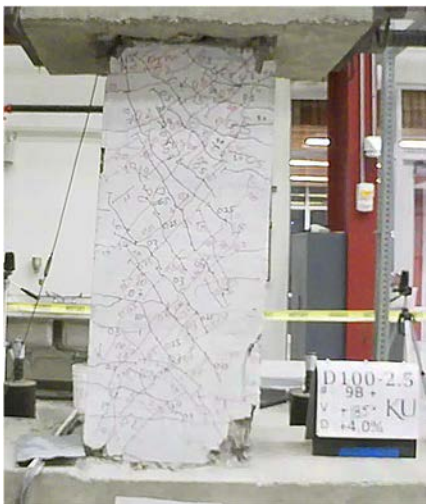


Figure C.44 – D100-2.5 at
+4% chord rotation, second cycle



Figure C.45 – D100-2.5 at
-4% chord rotation, second cycle

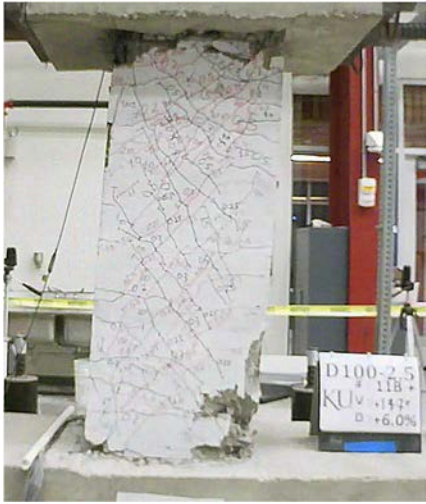


Figure C.46 – D100-2.5 at +6% chord rotation, second cycle



Figure C.47 – D100-2.5 at -6% chord rotation, second cycle



Figure C.48 – D100-2.5 at +8% chord rotation, first cycle



Figure C.49 – D100-2.5 at -8% chord rotation, first cycle

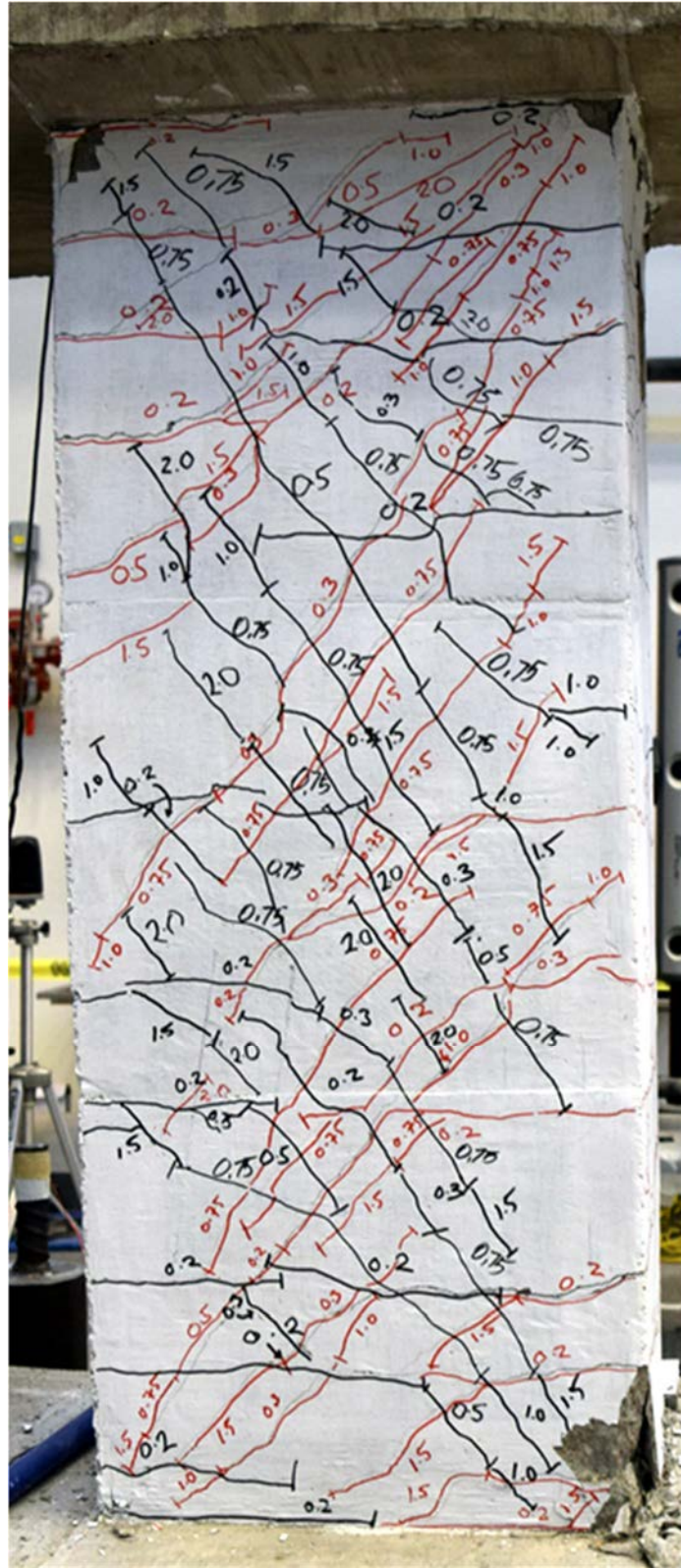


Figure C.50 – D120-2.5 during second cycle to 2% chord rotation

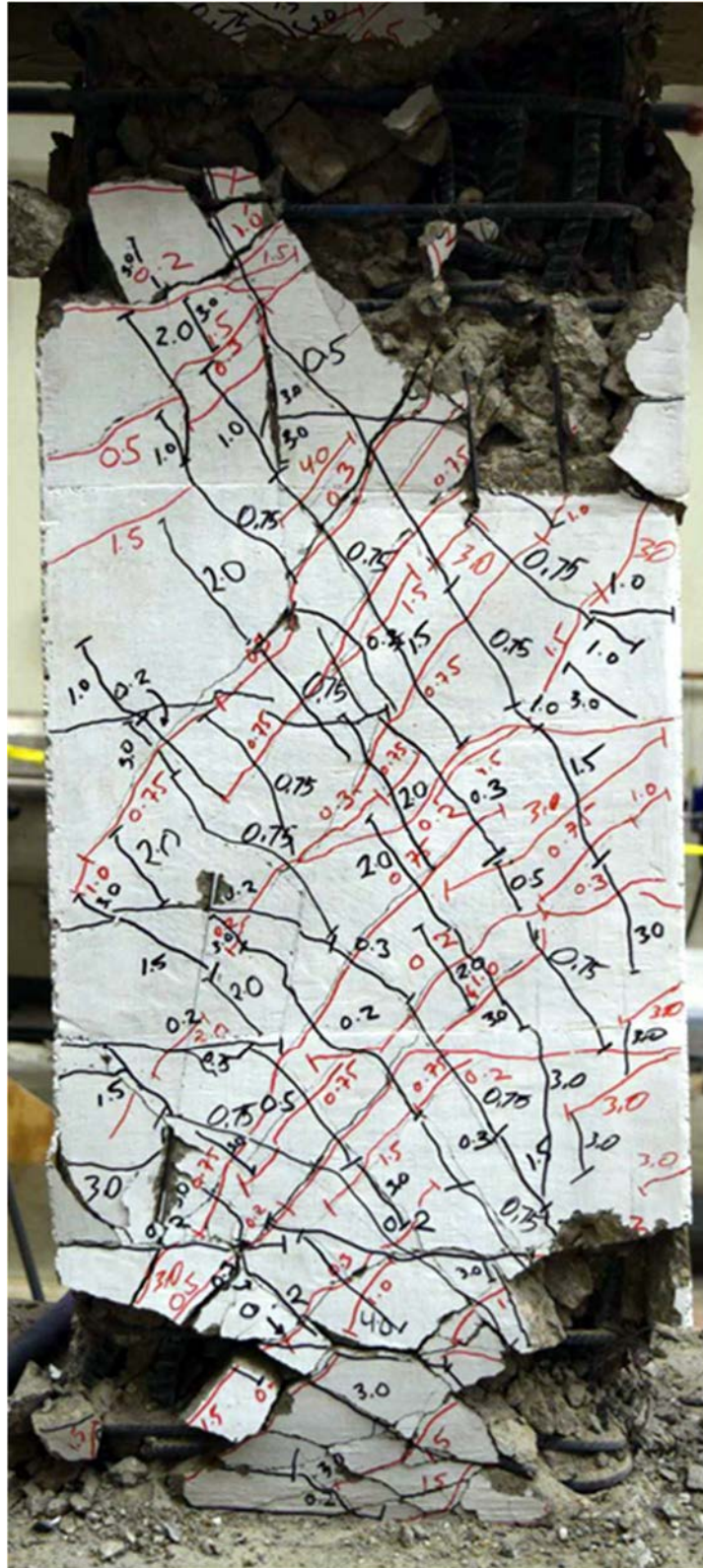


Figure C.51 – D120-2.5 during second cycle to 6% chord rotation

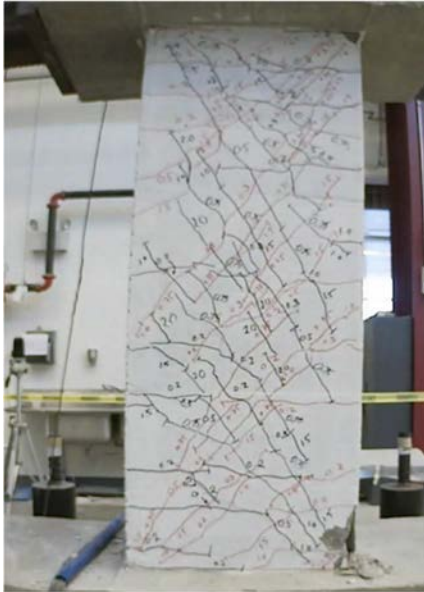


Figure C.52 – D120-2.5 at +2% chord rotation, second cycle

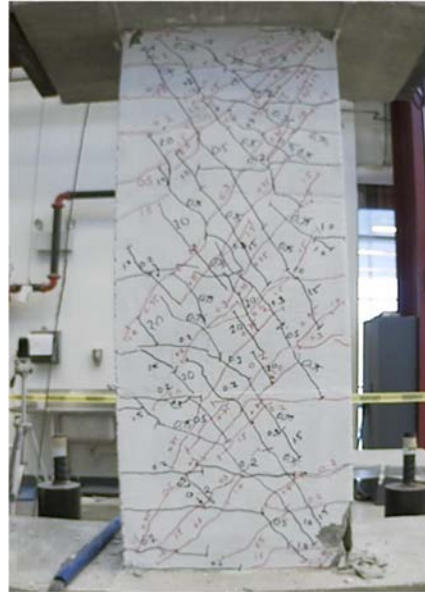


Figure C.53 – D120-2.5 at -2% chord rotation, second cycle

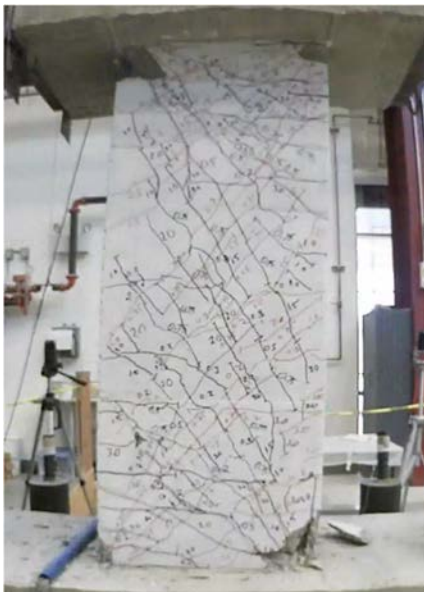


Figure C.54 – D120-2.5 at +4% chord rotation, second cycle

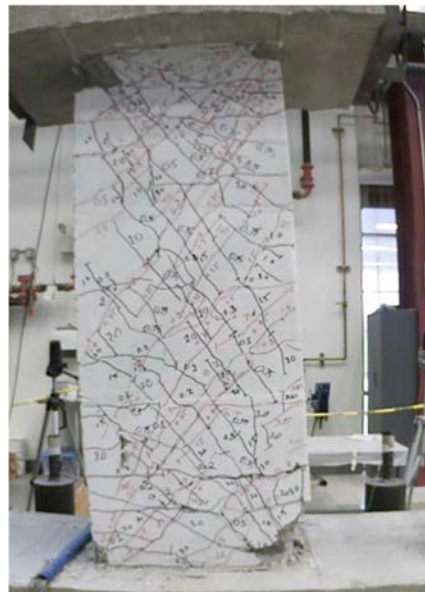


Figure C.55 – D120-2.5 at -4% chord rotation, second cycle

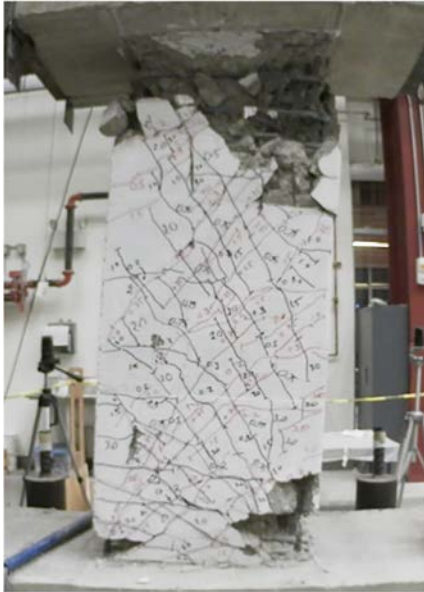


Figure C.56 – D120-2.5 at +6% chord rotation, second cycle

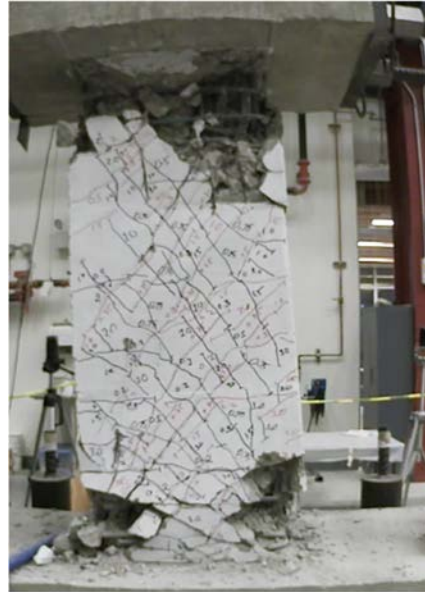


Figure C.57 – D120-2.5 at -6% chord rotation, second cycle

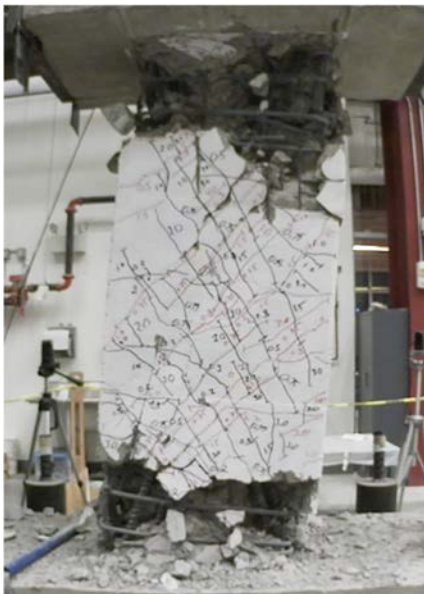


Figure C.58 – D120-2.5 at +8% chord rotation, second cycle

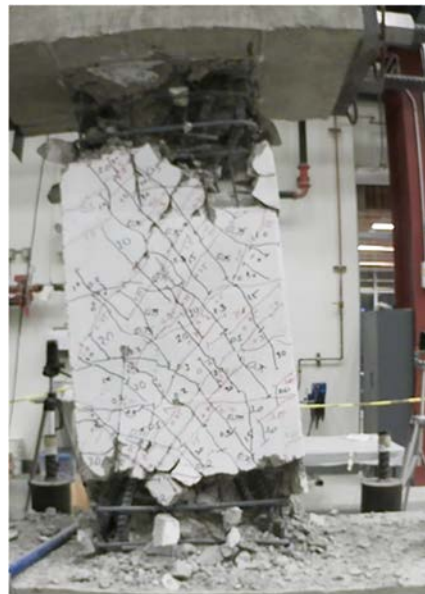


Figure C.59 – D120-2.5 at -8% chord rotation, second cycle

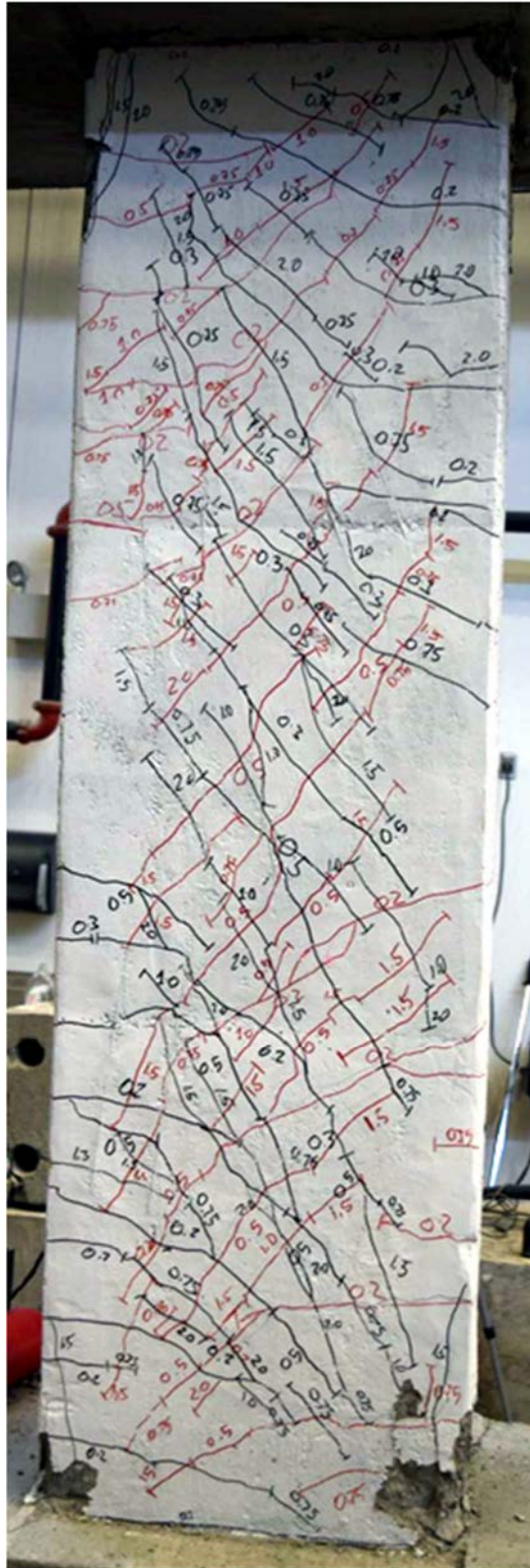


Figure C.60 – D80-3.5 during second cycle to 2% chord rotation

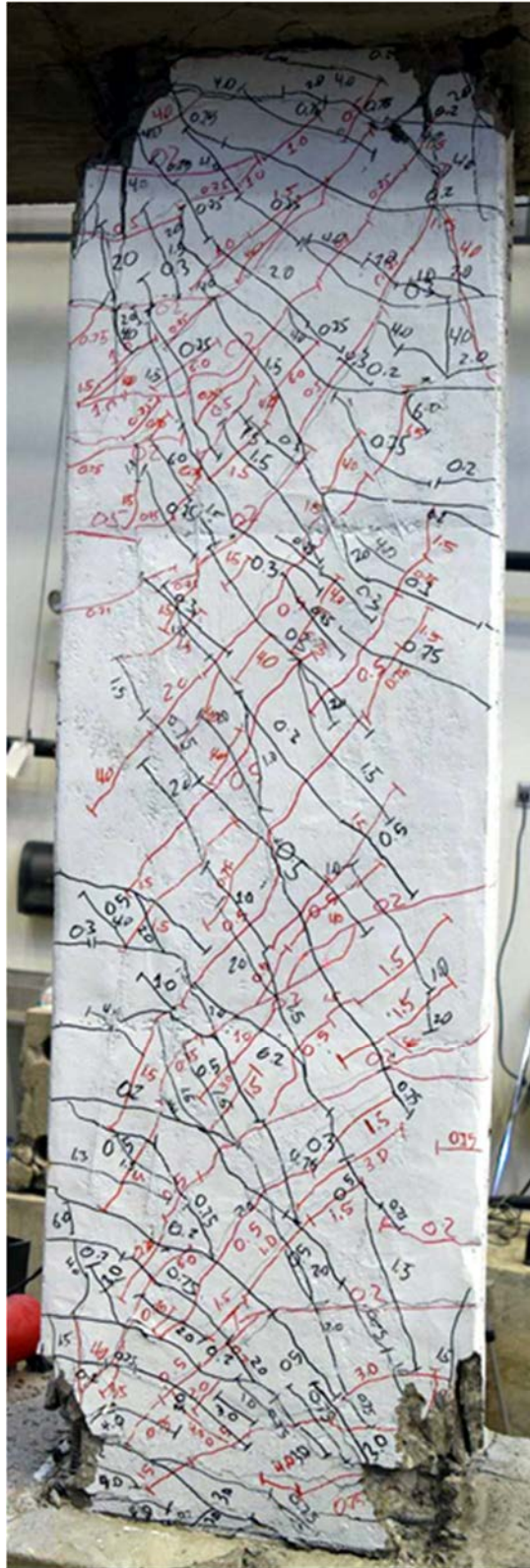


Figure C.61 – D80-3.5 during second cycle to 6% chord rotation



Figure C.62 – D80-3.5 at +2% chord rotation, second cycle



Figure C.63 – D80-3.5 at -2% chord rotation, second cycle

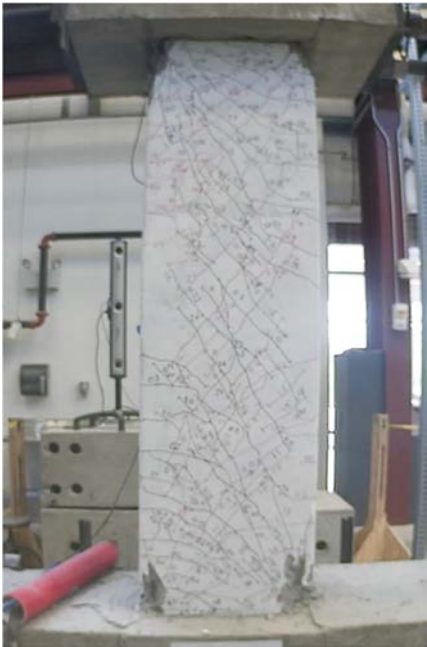


Figure C.64 – D80-3.5 at +4% chord rotation, second cycle



Figure C.65 – D80-3.5 at -4% chord rotation, second cycle



Figure C.66 – D80-3.5 at +6% chord rotation, second cycle



Figure C.67 – D80-3.5 at -6% chord rotation, second cycle



Figure C.68 – D80-3.5 at +8% chord rotation, second cycle



Figure C.69 – D80-3.5 at -8% chord rotation, second cycle



Figure C.70 – D80-3.5 at +10% chord rotation, first cycle



Figure C.71 – D80-3.5 at -10% chord rotation, first cycle

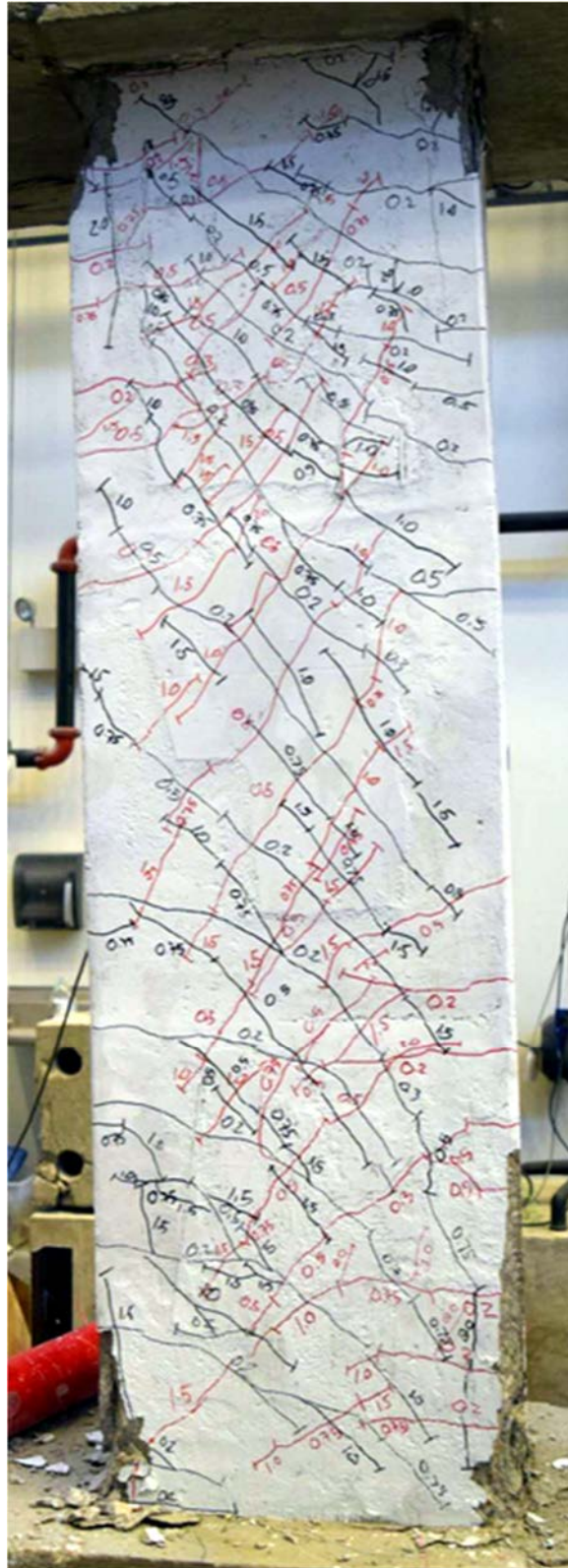


Figure C.72 – D100-3.5 during second cycle to 2% chord rotation

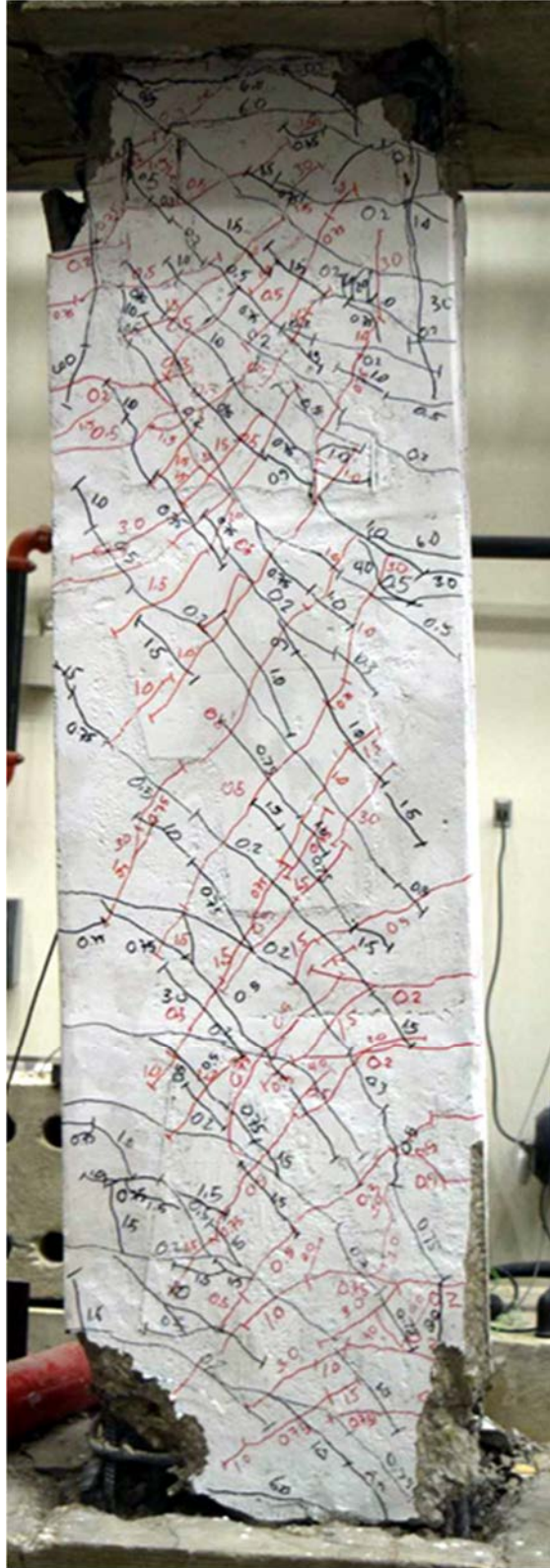


Figure C.73 – D100-3.5 during second cycle to 6% chord rotation



Figure C.74 – D100-3.5 at +2% chord rotation, second cycle

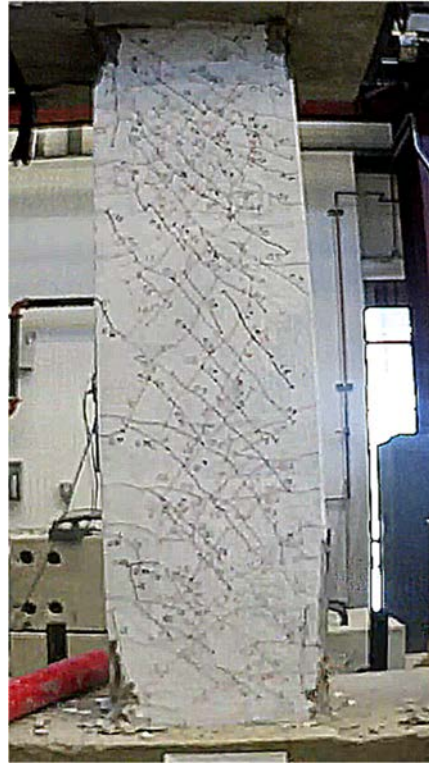


Figure C.75 – D100-3.5 at -2% chord rotation, second cycle



Figure C.76 – D100-3.5 at +4% chord rotation, second cycle

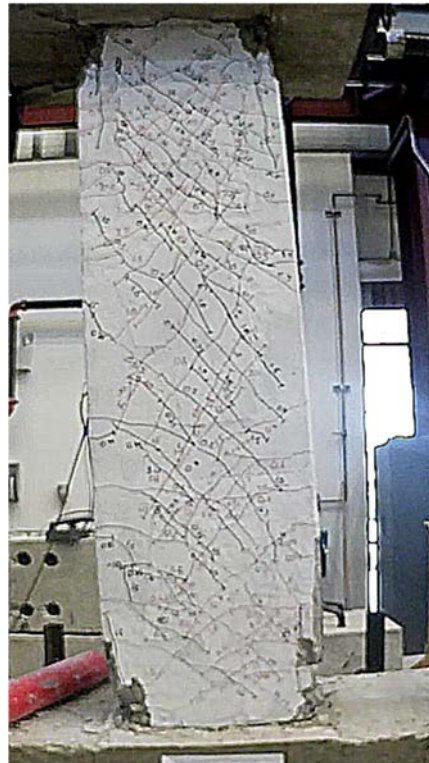


Figure C.77 – D100-3.5 at -4% chord rotation, second cycle



Figure C.78 – D100-3.5 at +6% chord rotation, second cycle

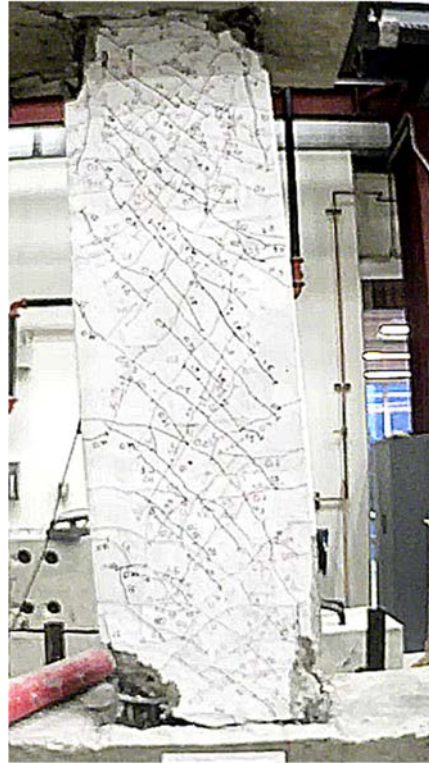


Figure C.79 – D100-3.5 at -6% chord rotation, second cycle



Figure C.80 – D100-3.5 at +8% chord rotation, second cycle



Figure C.81 – D100-3.5 at -8% chord rotation, second cycle



Figure C.82 – D100-3.5 at +10% chord rotation, first cycle



Figure C.83 – D100-3.5 at -10% chord rotation, first cycle

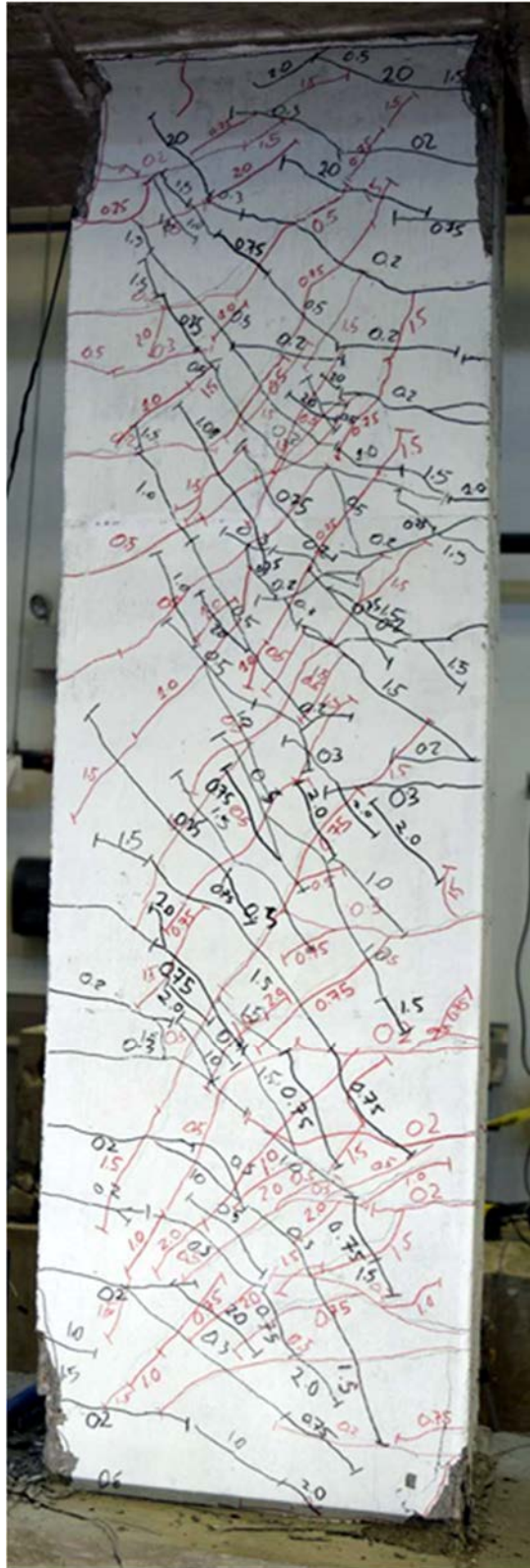


Figure C.84 – D120-3.5 during second cycle to 2% chord rotation

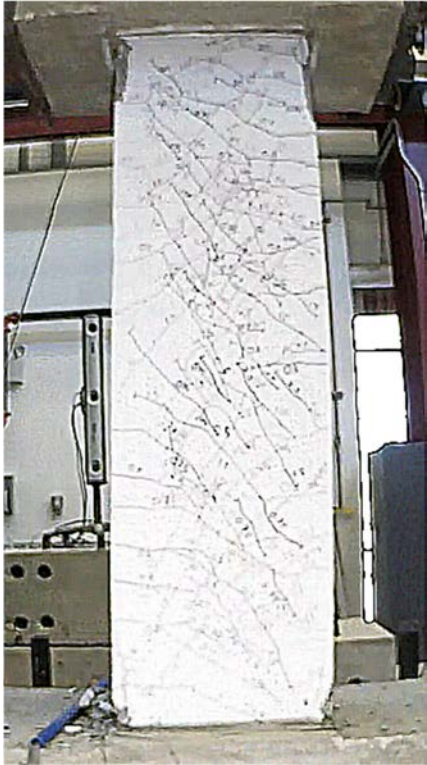


Figure C.86 – D120-3.5 at +2% chord rotation, second cycle

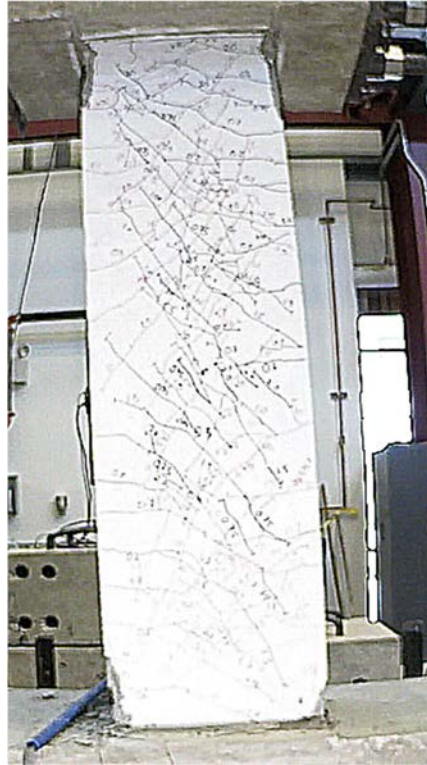


Figure C.87 – D120-3.5 at -2% chord rotation, second cycle

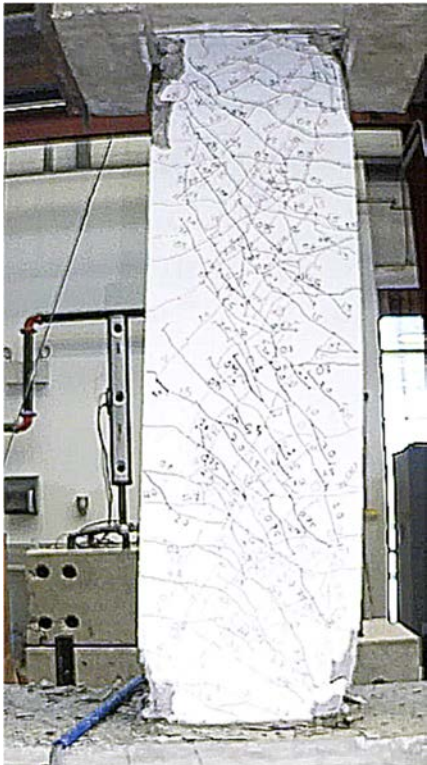


Figure C.88 – D120-3.5 at +4% chord rotation, second cycle

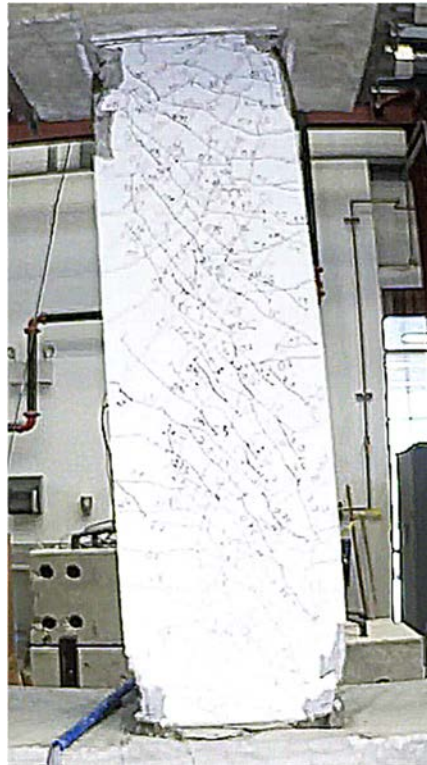


Figure C.89 – D120-3.5 at -4% chord rotation, second cycle



Figure C.90 – D120-3.5 at +6% chord rotation, second cycle

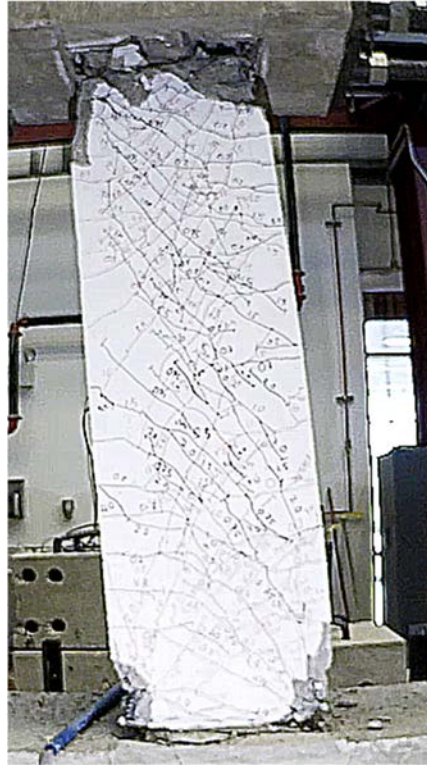


Figure C.91 – D120-3.5 at -6% chord rotation, second cycle

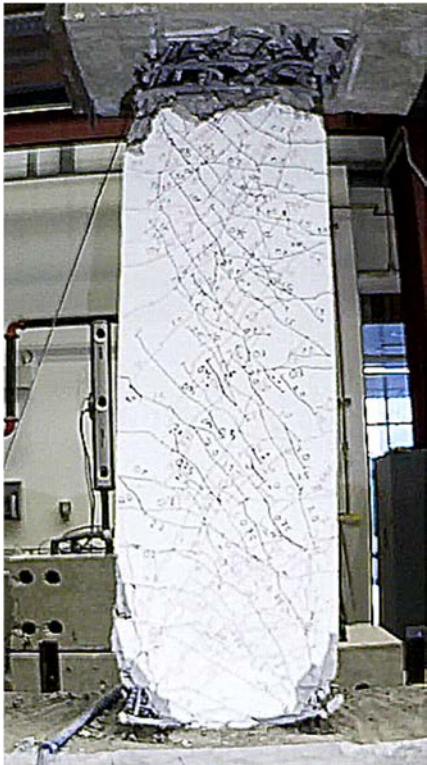


Figure C.92 – D120-3.5 at +8% chord rotation, second cycle

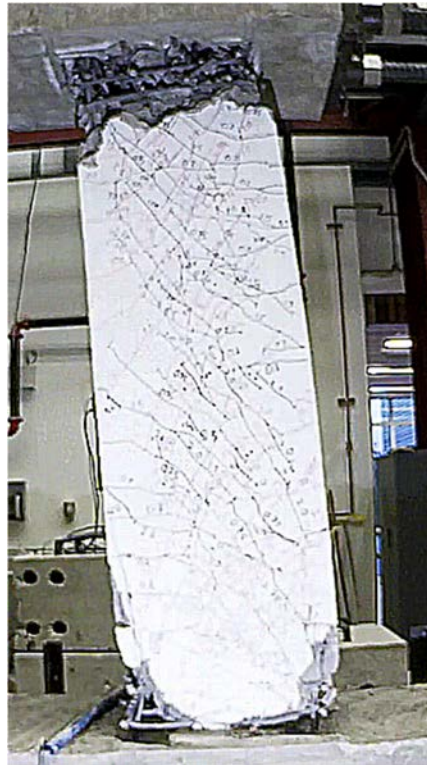


Figure C.93 – D120-3.5 at -8% chord rotation, second cycle

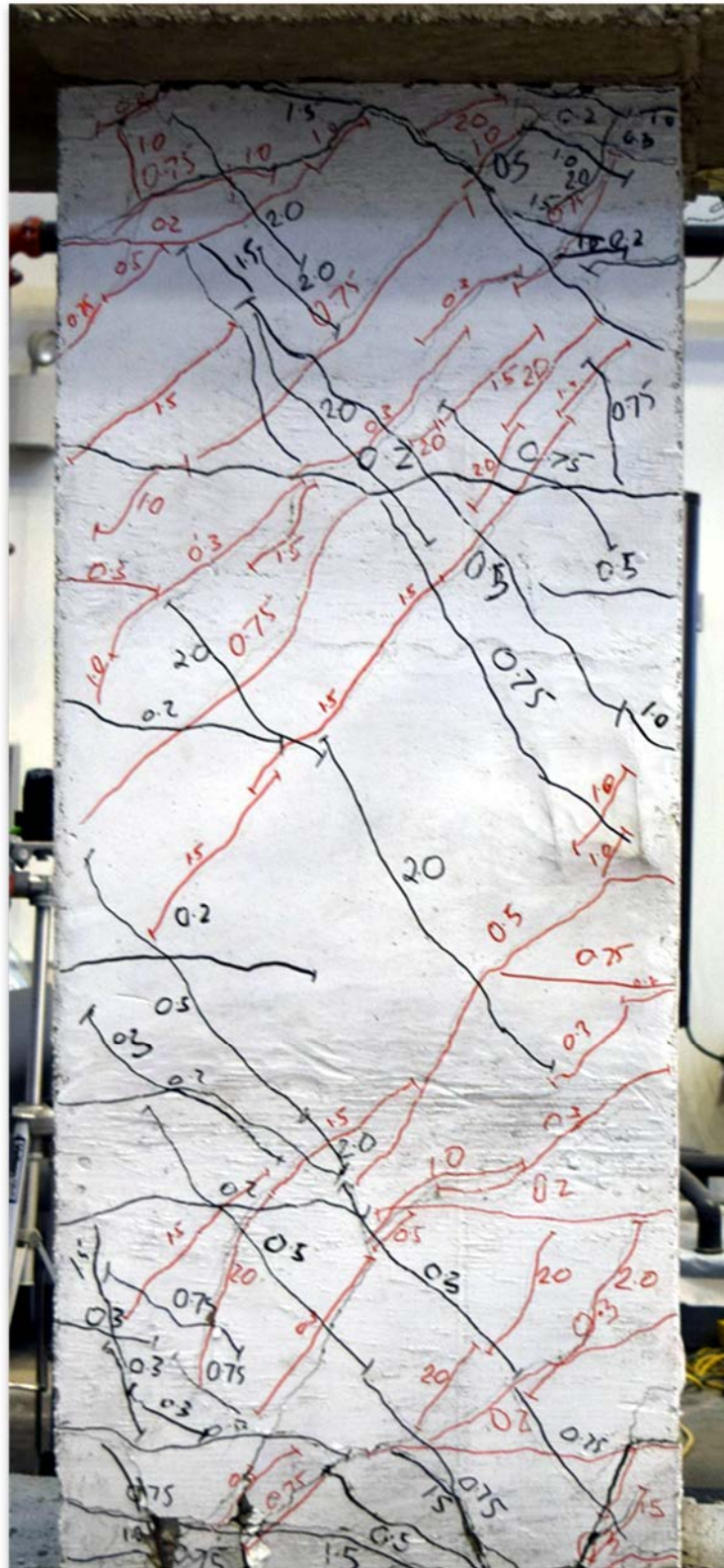


Figure C.94 – P80-2.5 during second cycle to 2% chord rotation

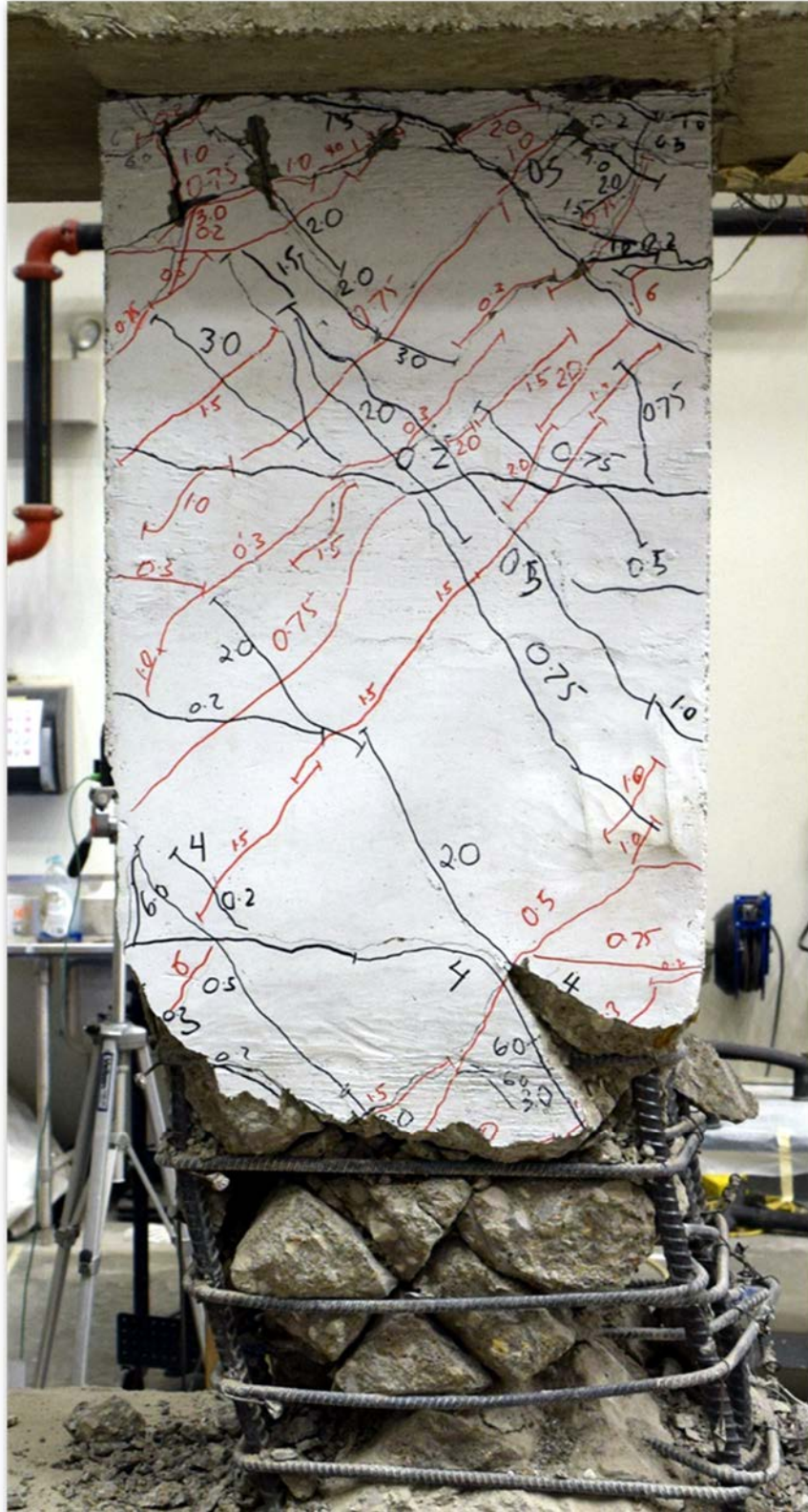


Figure C.95 – P80-2.5 during second cycle to 6% chord rotation



Figure C.96 – P80-2.5 at +2% chord rotation, second cycle



Figure C.97 – P80-2.5 at -2% chord rotation, second cycle



Figure C.98 – P80-2.5 at +4% chord rotation, second cycle



Figure C.99 – P80-2.5 at -4% chord rotation, second cycle



Figure C.100 – P80-2.5 at +6% chord rotation, second cycle



Figure C.101 – P80-2.5 at -6% chord rotation, second cycle

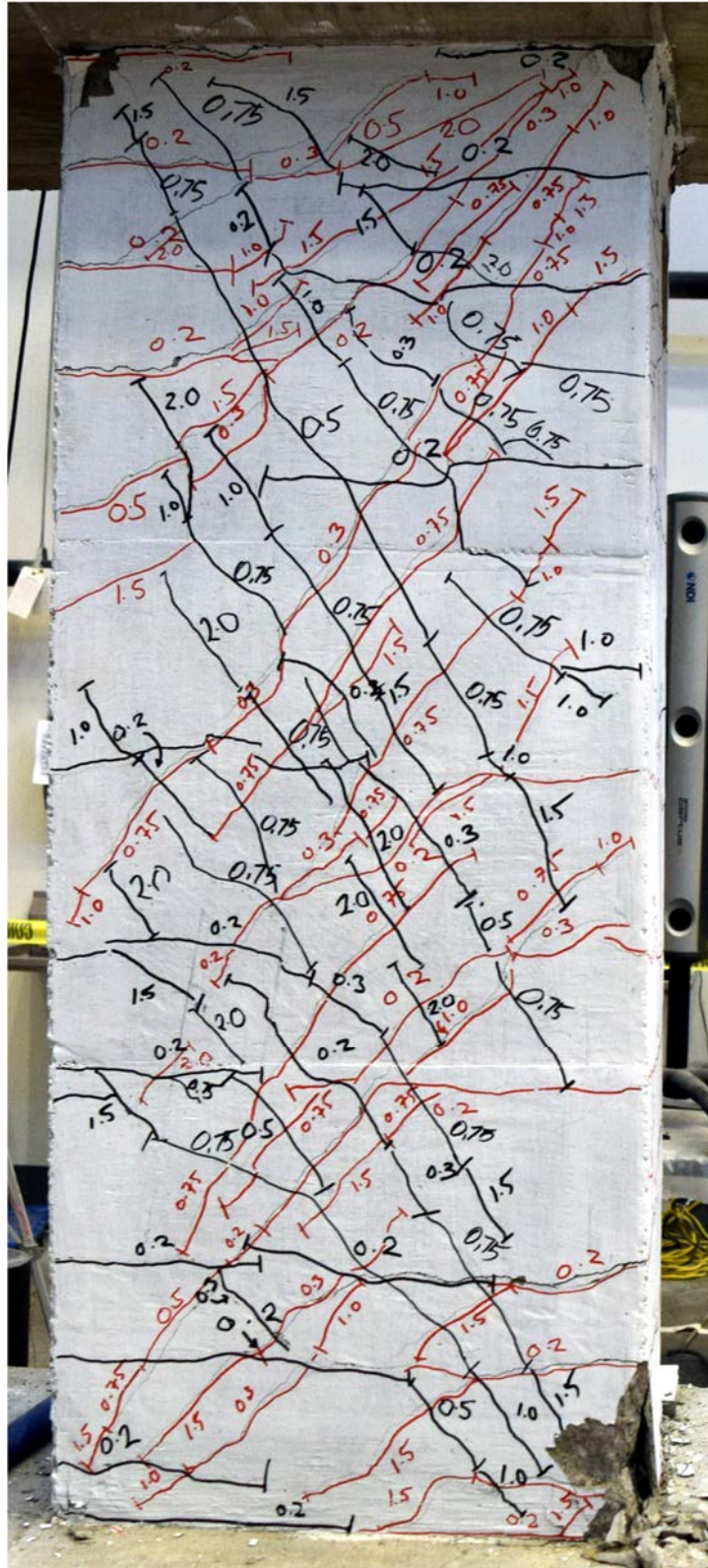


Figure C.102 – P100-2.5 during second cycle to 2% chord rotation

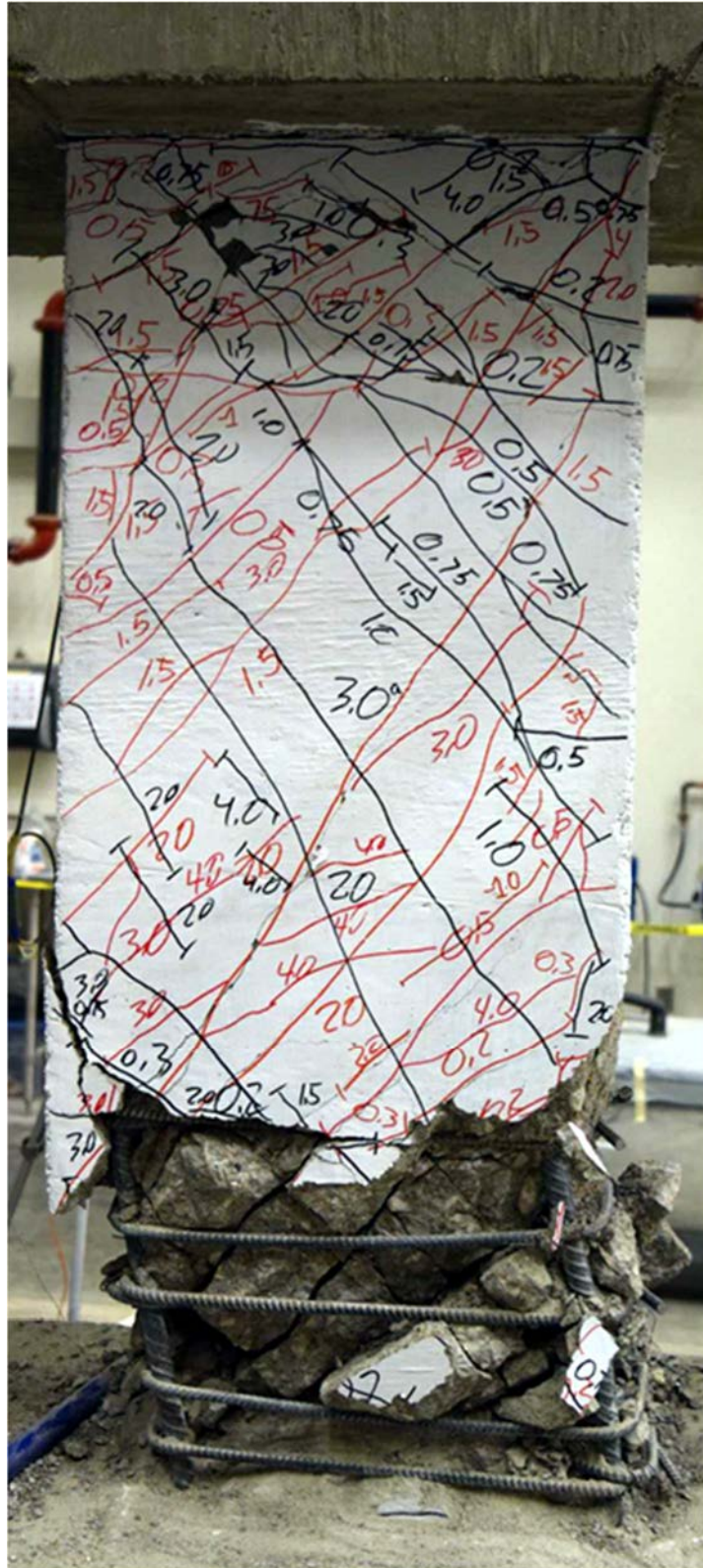


Figure C.103 – P100-2.5 during second cycle to 6% chord rotation

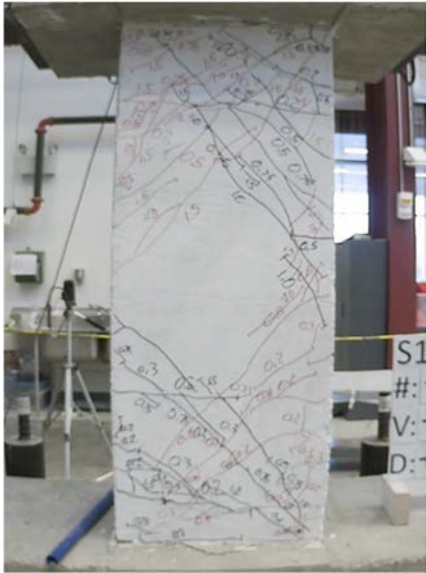


Figure C.104 – P100-2.5 at +2% chord rotation, second cycle

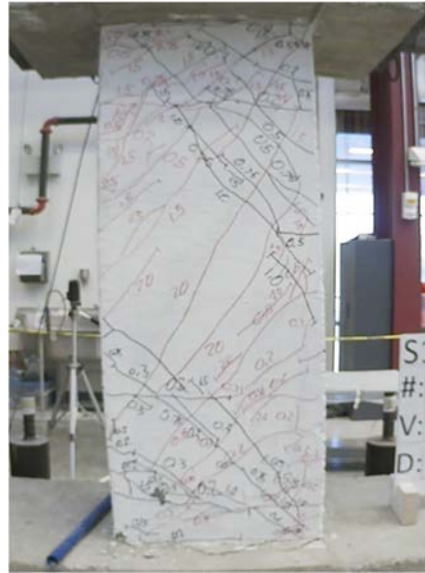


Figure C.105 – P100-2.5 at -2% chord rotation, second cycle



Figure C.106 – P100-2.5 at +4% chord rotation, second cycle



Figure C.107 – P100-2.5 at -4% chord rotation, second cycle



Figure C.108 – P100-2.5 at +6% chord rotation, second cycle



Figure C.109 – P100-2.5 at -6% chord rotation, second cycle